Université du Québec

Institut National de la Recherche Scientifique

Centre Eau Terre Environnement

Enlèvement de Carbamazépine de l'eau et des eaux usées en utilisant des systèmes nano imprégnés de biochar-enzyme (BENS)

Présenté par

Mitra Naghdi

Thèse présentée pour l'obtention du grade de

Philosophiae doctor (Ph.D.) en sciences de l'eau

Jury d'évaluation

Président du jury et examinateur interne	Antonio Avalos Ramirez
	Chercheur en bioprocédés environnementaux
	CNETE, Shawinigan, Québec, Canada
Examinateur externe	Serge Kaliaguine, Professeur
	Université Laval, Québec, Canada
Examinateur externe	Safia Hamoudi, Professeure
	Université Laval, Québec, Canada
Directrice de recherche	Satinder Kaur Brar, Professeure
	INRS-ETE, Québec, Canada

DEDICACE

This thesis is dedicated to my parents, my husband and my son for their endless love and support.

REMERCIEMENTS

Résumé

La carbamazépine (CBZ) est un composé pharmaceutique connu, utilisé comme antiépileptique et anticonvulsif pour diverses applications psychothérapeutiques. En raison du taux de consommation élevé et de la structure chimique stable du CBZ, ce composé persistant est libéré en continu dans l'environnement. La CBZ trouve son chemin à travers le système de collecte des eaux usées dans les usines de traitement des eaux usées (WWTPs) et malheureusement le processus de traitement à ce jour dans les WWTPs conventionnelles n'est pas efficace pour la dégradation de la CBZ (~10%). Ces dernières années, la plupart des procédés d'oxydation développés pour la dégradation du composé pharmaceutique sont coûteux, et nécessitent beaucoup d'énergie ou impliquent l'utilisation de produits chimiques dangereux. De plus, la plupart des études de dégradation de la CBZ ont été réalisées dans des solutions aqueuses enrichies où la concentration de CBZ n'était pas pertinente aux concentrations réelles dans l'environnement et il n'a donc pas été possible d'extrapoler les résultats aux conditions réelles. Par conséquent, le développement de nouvelles techniques de dégradation de la CBZ représente un grand intérêt.

Après avoir passé en revue les méthodes d'élimination actuelles, un nouveau système basé sur l'intégration de la dégradation enzymatique et de l'adsorption sur le nanobiochar est proposé. D'une part, les enzymes, en particulier les laccases, sont bien connues pour transformer les composés organiques en sous-produits moins nocifs par rapport aux processus d'oxydation, mais ils sont lents et sensibles aux changements de processus. D'autre part, le biochar, produit de la pyrolyse de la biomasse résiduaire, est capable d'adsorber et de retenir efficacement les micropolluants, notamment sous forme nanométrique grâce à un rapport surface / volume plus élevé, mais il ne dégrade pas les composés. L'incorporation de nanobiochar et l'immobilisation de la laccase peuvent simultanément augmenter la stabilité de l'enzyme et fournir suffisamment de temps pour la dégradation enzymatique.

Premièrement, le nanobiochar a été produit par broyage à billes et les propriétés physico-chimiques associées ont été évaluées. Ensuite, la capacité de la matière première et du nanobiochar pour l'adsorption de la CBZ a été étudiée. Plus tard, le nanobiochar produit a été fonctionnalisé par traitement avec des acides minéraux. De plus, la possibilité d'immobilisation de la laccase sur du nanobiochar fonctionnalisé a

été étudiée par des méthodes physiques et chimiques. Enfin, la performance de la laccase immobilisée sur nanobiochar pour la dégradation de la CBZ dans l'eau milli-Q et les effluents secondaires a été étudiée en mode discontinu et continu.

Le nanobiochar a été produit à partir de biochar de pin en utilisant un broyeur à billes planétaire qui a été considéré comme une méthode verte. Pour la production de nanobiochar, la méthodologie de surface de réponse (RSM) avec une conception composite centrale (CCD) a été utilisée pour étudier les effets de différents paramètres, y compris le rapport de la masse des billes à la masse de biochar, la vitesse de rotation et le temps. Les effets linéaires et quadratiques du temps et aussi l'effet d'interaction du temps et de la vitesse de rotation ont été des contributeurs importants par rapport à la taille des particules. Enfin, à des paramètres de broyage optimaux (100 min, 575 rpm et 4,5 g/g de bille à biochar) et de conditionnement à -80 °C, un nanobiochar avec la taille moyenne des particules de 60 nm a été atteint. De plus, la surface spécifique est passée de 3,12 m^2/g à 47,25 m^2/g.

L'élimination de la CBZ à une gamme de concentration pertinente pour l'environnement (0,5-20 ppb) a été étudiée par adsorption sur du nanobiochar de pin produit tel quel. Les résultats ont montré que le nanobiochar peut éliminer jusqu'à 74% et 95% de la CBZ après 1 et 6 heures de contact, respectivement. Parmi les isothermes et les modèles cinétiques examinés, l'adsorption de la CBZ sur nanobiochar a montré de meilleurs paramètres d'ajustement avec le modèle isotherme de Freundlich (R^2 = 0,9822) et le modèle cinétique de pseudo-deuxième ordre (R^2 = 0,9994).

Pour étudier la biodégradation de la CBZ en utilisant la laccase libre, un RSM avec un CCD a été utilisé pour étudier les effets de différents paramètres incluant le pH, la température, la concentration du médiateur et la concentration en laccase sur la biodégradation de la CBZ dans la phase aqueuse. Le coefficient de régression multiple (R^2 = 75,97%) indique un modèle raisonnable pour la mise en œuvre pratique. Parmi les paramètres examinés, les termes linéaires de la concentration du pH et du médiateur et les termes quadratiques de la température, du pH et de la concentration en laccase ont eu les effets les plus importants. Il a été observé que l'exécution de la biotransformation à 35 °C, pH 6, avec 60 U/L de concentration enzymatique et 18 µM de concentration médiateur a entraîné une élimination de 95% de la CBZ.

Pour l'immobilisation physique, la modification de surface du nanobiochar a été réalisée en utilisant le HCl, le H_2SO_4, le HNO_3 et leurs mélanges. La fonctionnalisation

chimique de la surface du nanobiochar a été étudiée pour former des groupes fonctionnels carboxyliques pour une liaison plus forte. Le mélange de H_2SO_4 et de HNO_3 (50:50, v/v) a montré la meilleure performance à la surface du carbone par formation de groupes carboxyliques de 4,7 mmol/g. Selon les résultats, le stockage, le pH et les stabilités thermiques de la laccase immobilisée sur la nanobiochar fonctionnalisé ont été améliorés par rapport à la laccase libre. Les tests de réversibilité pour l'oxydation de l'acide 2,2'-azino-di- (3-éthylbenzothiazoline sulfonique) (ABTS) ont montré que la laccase immobilisée maintenait 70% de l'activité initiale après 3 cycles. Enfin, l'utilisation de la laccase immobilisée pour la dégradation du CBZ a montré une élimination de 83% et 86% dans l'eau pure enrichie et l'effluent secondaire, respectivement.

Pour l'immobilisation covalente, d'abord, la modification de surface du nanobiochar a été réalisée en utilisant un mélange de H_2SO_4 et HNO_3 (3:1, v/v). Plus tard, la laccase brute a été immobilisée par covalence sur du nanobiochar fonctionnalisé en utilisant une méthode en deux étapes d'amidation par le diimide activé. L'effet de différents paramètres a été étudié, y compris la concentration en laccase, la concentration de nanobiochar, la concentration de l'agent de réticulation et le temps de contact. Les conditions optimales se sont révélées être 14 mg/mL de concentration de laccase, 5 mg/mL de nanobiochar, 8,2 mM de réticulant et 3 h de temps de contact. De plus, la laccase immobilisée a maintenu sa performance catalytique jusqu'à sept cycles d'utilisation et a montré plus de 50% de l'activité initiale après deux mois de stockage à température ambiante.

L'effet de différents paramètres incluant le pH, la température, la concentration de CBZ et le temps de contact lors de l'élimination de la CBZ par la laccase immobilisée par covalence a été étudié en mode discontinu. Les conditions optimales étaient pH 4, 20 °C, 5 µg/L de concentration de CBZ et 24 h de temps de contact. La contribution de l'efficacité d'élimination pour la CBZ dans l'eau pure a été atteinte à 33% et 63% pour l'adsorption et la dégradation en 24 h, respectivement. De plus, les performances d'élimination de la CBZ ont été étudiées sur sept cycles de traitement consécutifs utilisant le même biocatalyseur dans de l'eau milli-Q et l'efficacité d'élimination était comprise entre 84% et 31%. L'élimination de la CBZ en mode continu a montré plus de 45% et 60% dans l'eau pure et l'effluent secondaire, respectivement, après 24 heures de réaction. L'eau traitée n'a montré aucune toxicité selon l'essai de criblage d'oestrogène de levure (YES). L'incorporation de chitosane dans la matrice laccase-

nanobiochar a montré une activité antibactérienne vis-à-vis de la bactérie Gram-positive, *Bacillus subtilis*. L'eau traitée n'a montré aucune toxicité selon le test YES.

Abstract

Carbamazepine (CBZ) is a known pharmaceutical compound used as an antiepileptic and anticonvulsant medication for various psychotherapeutic applications. It is also used in combination with other drugs for treatment of alcohol withdrawal. Owing to the large consumption rate and stable chemical structure of CBZ, this persistent compound is continuously released into the environment. CBZ finds its way through sewage collection systems into wastewater treatment plants (WWTPs) and unfortunately the treatment process as of date in conventional WWTPs is not effective for degradation of CBZ (~10%). The residual CBZ in environment nevertheless may be exposed to light and as reported in studies, photo-degraded products of CBZ are more toxic than the CBZ itself. Furthermore, most of the oxidation processes developed for degradation of pharmaceutical compounds in recent years are costly, energy intensive or involve using hazardous chemicals. Moreover, most of the CBZ degradation studies were performed in spiked aqueous solutions where the concentration of CBZ was not relevant to real environmental concentrations and therefore it was not possible to extrapolate the results to real conditions. Therefore, developing new techniques for degradation of psychiatric drugs such as CBZ is of interest.

Therefore, developing new techniques for degradation of antidepressants, such as CBZ is of interest. In the present study, after reviewing the current removal methods, a new system based on integration of enzymatic degradation and adsorption onto nanobiochar is proposed. On one hand, enzymes, specifically laccases, are well known to transform organic compounds to less harmful by-products compared to oxidation processes, however they are slow and sensitive to process changes. On the other hand, biochar, a product of waste biomass pyrolysis, is able to adsorb and retain micropollutants efficiently, especially in nano form due to higher surface to volume ratio, however it does not degrade the compounds. Incorporation of nanobiochar and immobilization of laccase can simultaneously increase the stability of enzyme and provide enough time for enzymatic degradation.

Firstly, nanobiochar was produced through ball milling and the related physico-chemical properties were evaluated. Then, the capacity of raw and nanobiochar for adsorption of CBZ was studied. Later, the produced nanobiochar was functionalized through treatment with mineral acids. Furthermore, the possibility of immobilization of

laccase onto functionalized nanobiochar was studied through physical and chemical methods. Finally, the performance of laccase immobilized on nanobiochar for degradation of CBZ in milli-Q water and secondary effluents was investigated in batch and continuous modes.

Nanobiochar was produced from pine wood biochar using a planetary ball mill which has been considered as a green method. For production of nanobiochar, response surface methodology (RSM) with a central composite design (CCD) was utilized to investigate the effects of different parameters including ball to biochar mass ratio, rotational speed, and time. The linear and quadratic effects of time and also the interaction effect of time and rotational speed were significant contributors to particle size. Further studies showed that conditioning the samples at cryogenic temperatures prior to milling inhibited nanoparticles agglomeration. Finally, at optimum milling parameters (100 min, 575 rpm and 4.5 g/g ball to biochar ratio) and conditioning at -80 °C, nanobiochar with the average particle size of 60 nm was achieved. Moreover, the specific surface area was increased from 3.12 m^2/g to 47.25 m^2/g.

Removal of CBZ at environmentally relevant concentration range (0.5-20 ppb) was studied through adsorption on as-produced pinewood nanobiochar. The results showed that nanobiochar can remove up to 74% and 95% of CBZ after 1 and 6 hours contact time, respectively. Among examined isotherms and kinetic models, adsorption of CBZ on nanobiochar showed better fitting parameters with Freundlich isotherm model (R^2 = 0.9822) and pseudo-second order kinetic model (R^2 = 0.9994). Calculation of adsorption energy showed that adsorption of CBZ on nanobiochar is a physical process. Increasing pH from 3 to 6 enhanced the adsorption efficiency by 2.3 folds. The addition of Tween 80 as a model surfactant was studied in the range of 0 to 1 (Tween 80 to CBZ molar ratio) and the results showed that adsorption efficiency can be enhanced by 57%.

For studying the biodegradation of CBZ using free laccase, RSM with a CCD was utilized to investigate the effects of different parameters including pH, temperature, mediator concentration and laccase concentration on biodegradation of CBZ in the aqueous phase. A quadratic model was fitted to express the effects of each parameter including quadratic, linear and interaction terms. The adequacy of the developed model was confirmed by the coefficient of multiple regression (R^2 = 75.97%) indicating a reasonable model for practical implementation. Among the examined parameters, linear terms of pH and mediator concentration and quadratic terms of temperature, pH

and laccase concentration had the largest effects. It was observed that performing the biotransformation at 35 °C, pH 6, with 60 U/L of enzyme concentration and 18 µM of mediator concentration resulted in 95% removal of CBZ.

For physical immobilization, surface modification of nanobiochar was performed using HCl, H_2SO_4, HNO_3 and their mixtures. Chemical functionalization of the nanobiochar surface was investigated to form carboxylic functional groups for stronger bonding. The mixture of H_2SO_4 and HNO_3 (50:50, v/v) showed the best performance on the surface of carbon by formation of 4.7 mmol/g carboxylic groups. According to the results, the storage, pH and thermal stabilities of immobilized laccase on functionalized nanobiochar were improved compared to free laccase. The reusability tests toward oxidation of 2,2′-azino-di-(3-ethylbenzthiazoline sulfonic acid) (ABTS) showed that the immobilized laccase maintained 70% of its initial activity after 3 cycles. Finally, using immobilized laccase for degradation of CBZ exhibited 83% and 86% removal in spiked pure water and secondary effluent, respectively.

For covalent immobilization, first, the surface modification of nanobiochar was performed using a mixture of H_2SO_4 and HNO_3 (3:1, v/v). Later, crude laccase was covalently immobilized onto functionalized nanobiochar using a two-step method of diimide-activated amidation. The effect of different parameters were investigated including laccase concentration, nanobiochar concentration, cross-linker concentration and contact time. The optimal conditions were found to be 14 mg/mL of laccase concentration, 5 mg/mL of nanobiochar, 8.2 mM of cross-linker and 3 h of contact time. In addition, immobilized laccase maintained its catalytic performance up to seven cycles of utilization and showed more than 50% of initial activity after two months of room temperature storage.

The effect of different parameters including pH, temperature, CBZ concentration and contact time on removal of CBZ by covalently immobilized laccase was investigated in batch mode. The optimal conditions were pH 4, 20 °C, 5 µg/L of CBZ concentration and 24 h of contact time. The contribution of removal efficiency for CBZ in pure water was 33% and 63% for adsorption and degradation in 24 h, respectively. Furthermore, the performances of elimination of CBZ were investigated over seven consecutive treatment cycles using the same biocatalyst in milli-Q water and the removal efficiency was in the range 84% to 31%. The removal of CBZ in continuous mode exhibited more than 45% and 60% in pure water and secondary effluent, respectively, after 24 hours of reaction. The treated water showed no toxicity according to the Yeast Estrogen

Screen (YES) assay. The incorporation of chitosan into laccase-nanobiochar matrix showed antibacterial activity towards Gram-positive bacreia, *Bacillus subtilis*. The treated water showed no toxicity according to the Yeast Estrogen Screen (YES) assay.

Publications de cette thèse

1- **M. Naghdi**, M. Taheran, S. K. Brar, M. Verma, R.Y. Surampalli, J.R. Valero, Green and Energy Efficient Methods for Production of Metallic Nanoparticles. *Beilstein Journal of Nanotechnology*, 6 (2015) 2354-2376.

2- **M. Naghdi**, M. Taheran, S. J. Sarma, S. K. Brar, A. A. Ramirez, M. Verma. Nanotechnology for removal of Emerging Contaminants, In Sustainable Agriculture Reviews, Vol 20. Springer publication.

3- **M. Naghdi**, M. Taheran, T. Rouissi, S. K. Brar, M. Verma, R. Y. Surampalli, J. R. Valero, A green method for Production of Nanobiochar by Ball Milling, Optimization and Characterization. *Journal of Cleaner Production*, 164 (2017) 1394-1405.

4- **M. Naghdi**, M. Taheran, R. Pulicharla, S. K. Brar, M. Verma, R. Y. Surampalli, Pine-Wood derived Nanobiochar for Removal of Carbamazepine from Aqueous Media: Adsorption Behavior and Influential Parameters. *Arabian Journal of Chemistry*, (2017) DOI.org/10.1016/j.arabjc.2016.12.025 (In press).

5- **M. Naghdi**, M. Taheran, S. K. Brar, A. Kermanshahi-pour, M. Verma, R. Y. Surampalli, Removal of pharmaceutical compounds in water and wastewater using fungal oxidoreductase enzymes. *Environmental Pollution*, 234 (2018) 190-213.

6- **M. Naghdi**, M. Taheran, S. K. Brar, A. Kermanshahi-pour, M. Verma, R. Y. Surampalli, Biotransformation of Carbamazepine by Laccase-Mediator System: Kinetics, By-products and Toxicity Assessment. *Process Biochemistry*, 67 (2018) 147-154

7- **M. Naghdi**, M. Taheran, S. K. Brar, A. Kermanshahi-pour, M. Verma, R. Y. Surampalli, Immobilized laccase on oxygen functionalized nanobiochars through mineral acids treatment for removal of carbamazepine. *Science of the Total Environment*, 584 (**2017**) 393-401.

8- **M. Naghdi**, M. Taheran, S. K. Brar, A. Kermanshahi-pour, M. Verma, R. Y. Surampalli, Pinewood Nanobiochar: a Unique Carrier for the Immobilization of Crude Laccase by Covalent Bonding. *International Journal of Biological Macromolecules*, 115 (2018) 563-571.

9- **M. Naghdi**, M. Taheran, S. K. Brar, A. Kermanshahi-pour, M. Verma, R. Y. Surampalli, Fabrication of Nanobiocatalyst Using Encapsulated Laccase onto Chitosan-Nanobiochar composite. *Enzyme and Microbial Technology*, submitted.

10- **M. Naghdi**, A. Mateos, M. Taheran, S. K. Brar, M. Verma, R. Y. Surampalli, Biodegradation of Carbamazepine by Covalently Immobilized Enzyme Using Nanobiochar and Crude Laccase in Batch and Continuous Mode. *Biochemical Engineering Journal*, submitted.

11- **M. Naghdi**, M. Taheran, M. A. Laadila, S. K. Brar, R. Y. Surampalli, M. Verma, Antagonistic effects of divalent metal ions and humic acid on removal of carbamazepine. *Journal of environmental science*, submitted.

Publication en dehors de cette thèse

1. M. Chaali, **M. Naghdi**, S. K. Brar, A. Avalos-Ramirez, A review on the advances of nitrifying biofilm reactors and their removal rates in wastewater treatment. *Journal of Chemical Technology & Biotechnology,* (2018) doi.org/10.1002/jctb.5692 (In Press).

2. M. Taheran, **M. Naghdi**, S. K. Brar, E. J. Knystautas, M. Verma, R.Y. Surampalli, J.R. Valero, Biodegradation of Chlortetracycline by Trametes versicolor–Produced Laccase: By-Product Identification. *ASCE Journal of Environmental Engineering*, 144 (2018) 1-9.

3. M. Taheran, **M. Naghdi**, S. K. Brar, E. J. Knystautas, M. Verma, R.Y. Surampalli, J.R. Valero, Covalent Immobilization of laccase onto nanofibrous membrane for degradation of pharmaceutical residues in water. *ACS Sustainable Chemistry & Engineering*, 5 (2017) 10430-10438.

4. M. Taheran, **M. Naghdi**, S. K. Brar, E. J. Knystautas, M. Verma, R.Y. Surampalli, J.R. Valero, Degradation of chlortetracycline using immobilized laccase on Polyacrylonitrile-biochar composite nanofibrous membrane. *Science of the Total Environment*, 605 (2017) 315-321.

5. M. Taheran, **M. Naghdi**, S. K. Brar, E. J. Knystautas, M. Verma, A. A. Ramirez, R.Y. Surampalli, J.R. Valero, Adsorption Study of Environmentally relevant concentrations of Chlortetracycline on Pinewood Biochar, *Science of the Total Environment*, 571 (2016) 772-777.

6. M. Taheran, **M. Naghdi**, S. K. Brar, E. J. Knystautas, M. Verma, R.Y. Surampalli, J.R. Valero, Development of adsorptive membrane by confinement of activated biochar into electrospun nanofibers. *Beilstein Journal of Nanotechnology*, 7 (2016) 1556-1563.

7. M. Taheran, **M. Naghdi**, S. K. Brar, E. M. Verma, R.Y. Surampalli, Emerging contaminants: Here Today, There Tomorrow! *Environmental Nanotechnology, Monitoring & Management,* (**Accepted**).

8. W. Shuai, R. K. Das, **M. Naghdi**, S. K. Brar, M. Verma, a Review on the Important Aspects of Lipase Immobilization on Nanomaterials, *Biotechnology and Applied Biochemistry* 64 (2016) 496-508.

9. R. K. Das, V. L. Pachapur, L. Lonappan, R. Pulicharla, S. Maiti, **M. Naghdi**, M. Cledon, L. M. A. Dalila, S. J. Sarma, S. K. Brar, Biological Synthesis of Metallic Nanoparticles: Plants, Animals and Microbial Aspects. *Nanotechnology for Environmental Engineering*, 2 (2017) 1-21.

10. **M, Naghdi**, Y, Ouarda, S, Metahni, S. K. Brar and M, Cledon, Instrumental Approach towards Understanding Nano-Pollutants. *Nanotechnology for Environmental Engineering*, 2 (2017**)** 1-17.

11. **M. Naghdi**, M. Cledon, S. K. Brar, A. A. Ramirez, Nitrification of vegetable waste using nitrifying bacteria. *Ecological Engineering*, (2017) DOI.org/10.1016/j.ecoleng.2017.07.003 (In press).

Conférences

1. **M. Naghdi**, M. Taheran, S. K. Brar, M. Verma, R.Y. Surampalli, J.R. Valero, Functionalization of Nanobiochar for Laccase Immobilization*, 66th Canadian Chemical Engineering Conference*, October, 2016, Laval University, Quebec, Canada.

2. R. K. Das, S. Maiti, **M. Naghdi**, R. Pulicharla, V. Pachapur, S. K. Brar, Nanotechnology for Value-addition and Decontamination, *252nd ACS National Meeting*, August, 2016 Philadelphia, USA. (With my PhD supervisor among keynote speakers).

3. **M. Naghdi**, M. Taheran, S. K. Brar, A. A. Ramirez, M. Verma and R.Y. Surampalli, Pinewood Nanobiochar: a Unique Carrier for the Immobilization of Crude Laccase by Covalent Bonding, 32th conference of the Canadian Association on Water Quality in Eastern Canada (CAWQ), May, 2018, Université de Sherbrooke.

Table des matières

Liste des figures

Liste des tableaux

XXX

Liste des abréviations

ACT	Acetaminophen
ACE	Acetosyringone
AOPs	Advanced oxidation processes
AMP	Amitriptyline
ANOVA	Analysis of variance
ATL	Atenolol
ICP-AES	Atomic emission spectrometry -inductively coupled plasma
ATR	Attenuated total reflectance
ABTS	2,2'-azino-bis(3-ethylbenzothiazoline-6-sulphonic acid)
BS	*Bacillus Subtilis*
BFB	Bezafibrate
BOD_5	Biochemical oxygen demand
BET	Brunauer-Emmett-Teller
CAF	Caffeine
CBZ	Carbamazepine
CMS	Carboxymethyl cellulose sodium
CMC	Carboxymethyl chitosan
CEC	Cation Exchange Capacity
CCD	Central composite design
CET	Cetirizine
CTAC	Cetyltrimethylammonium chloride
COD	Chemical oxygen demand
CTS or Cs	Chitosan
CHIT-NH	Chitosan-ninhydrin
CTC	Chlortetracycline
CPF	Ciprofloxacine
CTL	Citalopram
CYP450	Cytochrome P450
K_d	Deactivation constant
DPS	Degraded pueraria starch
DAPHP	2, 6-diaminopyridinyl heparin

DZP	Diazepam
DCF	Diclofenac
DiOH-CBZ	10,11-dihydro-10,11-dihydroxy-CBZ
EP-CBZ	10,11-dihydro-10,11-epoxy-CBZ
DMF	Dimethyl formamide
DI-MS	Direct inlet-mass spectrometry
DC	Doxycycline
EC	Electrical conductivity
EDGs	Electron donating groups
EWGs	Electron withdrawing groups
EFC	Enrofloxacin
EA	*Enterobacter aerogenes*
EMR	Enzymatic membrane reactor
ETM	Erythromycin
EC	*Escherichia coli*
FEF	Fenofibrate
FEP	Fenoprofen
FLX	Fluoxetine
FTIR	Fourier transform infrared spectroscopy
E	Free energy
FNBC	Functionalized nanobiochar
GFZ	Gemfibrozil
Glu	Glutaraldehyde
GAC	Granular activated carbon
GNs	Graphene nano-sheets
GO	Graphene oxide
GK	Gum karaya
HPLC-DAD-MS	High-performance liquid chromatography-diode array detection-electrospray ionization mass spectrometry
^{1}H NMR	^{1}H nuclear magnetic resonance
HRP	Horseradish peroxidase
hER	Human estrogen receptor
HA	Hyaluronan

HBT	1-hydroxybenzotriazole
IBP	Ibuprofen
IDM	Indomethacin
KEP	Ketoprofen
Lac	Laccase
LOF	Lack of fit test
LF	Langmuir-Freundlich
LDTD-MS	Laser Diode Thermal Desorption-Mass Spectroscopy
LiP	Lignin peroxidase
LC-ESI-TOF-MS	Liquid chromatography electrospray time-of-flight mass spectrometry
LCQ	Liquid chromatography quadrupole
LOI	Loss on ignition
MnP	Manganese peroxidase
MFA	Mefenamic acid
MBR	Membrane bioreactor
MAA	Mercaptoacetic acid
MMT	Montmorillonite
MWCNTs	Multi-walled carbon nanotubes
MT	*Myceliophthora thermophila*
NLs	Nanolayers
NPs	Nanoparticles
NTs	Nanotubes
NPX	Naproxen
NRL	Natural rubber latex
EDAC	N-ethyl-N'-(3-dimethylaminopropyl) carbodiimide hydrochloride
NHS	N-hydroxysuccinimide
MES	2-(N-Morpholino) ethanesulfonic acid
NOR	Norfloxacin
K_{ow}	Octanol/water partition coefficient
OST	Oseltamivir
ORP	Oxidation-reduction potential
OTC	Oxytetracycline

PCT	Paracetamol
PC	Phanerochaete chrysosporium
PS	*Phanerochaete sordida*
PhACs	Pharmaceutically active compounds
BC-PW	Pinewood Biochar
PO	*Pleurotus ostreatus*
PMM	Polanyi-Manes model
PAHs	Polycyclic aromatic hydrocarbons
PEG	Polyethylene glycol
POMs	Polyoxometalates
PVA	Poly-vinyl alcohol
PPL	Propranolol
PPZ	Propyphenazone
CuO	Copper oxide
RSM	Response surface methodology
SEM	Scanning electron microscopy
SWCNTs	Single-walled carbon nanotubes
SDS	Sodium dodecyl sulfate
SDR	Spinning disk reactor
SDM	Sulfadimethoxine
SMZ	Sulfamethazine
SMX	Sulfamethoxazole
SMM	Sulfamonomethoxine
SPY	Sulfapyridine
STZ	Sulfathiazole
SAA	Sulfonamides sulfanilamide,
SERS	Surface-enhanced Raman scattering
SPR	Surface plasmon resonance
SS	Suspended solids
SA	Syringaldazine
TC	Tetracycline
TEMPO	2,2,6,6-tetramethylpiperidinyloxyl
TDS	Total dissolved solids

TKN	Total Kjeldahl nitrogen
TS	Total solids
TV	*Trametes versicolor*
TPs	Transformation products
TEM	Transmission electron microscopy
TMP	Trimethoprim
TPP	Tripolyphosphate
UV	Ultraviolet
VEA	Veratryl alcohol
VP	Versatile peroxidase
VLA	Violuric acid
VSS	Volatile suspended solids
WWTPs	Wastewater treatment plants
WHC	Water holding capacity
WRF	White-rot fungi
XRD	X-Ray diffraction
YES	Yeast Estrogen Screen assay
ZP	Zeta potential

Liste des équations

$$\text{Specific Gravity, G} = \frac{W_0}{W_0 + (W_A - W_B)}$$

$$Y = \beta_0 + \sum_{i=1} \beta_i X_i + \sum \beta_{ii} X_i^2 + \sum_{i=1} \sum_{j=i+1} \beta_{ij} X_i X_j$$

$$P_{cal} = \frac{1}{2} P^* m_b w_p^3 R_p^2 n_b$$

$$q_e = K_F C_e^{1/n}$$

$$\log q_e = \log K_F + {}^{1}/_{n} \, \log C_e$$

$$q_e = Q^0 C_e / (K_L + C_e)$$

$$\frac{1}{q_e} = \left(\frac{K_L}{Q^0}\right)\frac{1}{C_e} + \frac{1}{Q^0}$$

$$q_e = K_P C_e + Q^0 C_e / (K_L + C_e)$$

$$q_t = q_e (1 - \exp^{-k_1 t})$$

$$\log(q_e - q_t) = \log q_e - \frac{k_1}{2.303} t$$

$$q_t = \frac{k_2 q_e^2 t}{1 + k_2 q_e t}$$

$$\frac{t}{q_t} = \frac{1}{k_2 q_e^2} + \frac{1}{q_e} t$$

$$V_0 = k_2 q_e^2$$

$$q_t = k_p t^{0.5}$$

$$q_e = q_s \exp(-K_{ad} \varepsilon^2)$$

$$Ln \, q_e = Ln \, q_s - K_{ad} \varepsilon^2$$

$$\varepsilon = RT \, Ln \left(1 + \frac{1}{C_e}\right)$$

$$E = \frac{1}{\sqrt{2 \times K_{ad}}}$$

$$V = \frac{V_m [S]}{K_M + [S]}$$

CHAPITRE 1

SYNTHÈSE

Chapitre 1. Synthèse

Partie 1. Introduction

Les composés pharmaceutiques sont des matériaux biologiquement actifs connus pour avoir un effet particulier sur l'homme et les animaux. De grandes quantités de composés pharmaceutiques sont utilisées pour la prévention, le diagnostic et le traitement des maladies chez les humains et les animaux. La consommation moyenne par habitant de composés pharmaceutiques par an est estimée à environ 15 g et 50-150 g dans le monde et dans les pays industrialisés, respectivement. Ces composés sont en train de devenir un problème environnemental mondial en raison de leur présence dans l'environnement aquatique et des impacts potentiels sur la faune et les humains. Par conséquent, l'étude du devenir et des méthodes de traitement de ces composés a attiré l'attention de chercheurs du monde entier [1, 2].

La carbamazépine (5H-dibenzo[b,f]azépine-5-carboxamide) (CBZ) est un composé pharmaceutique connu utilisé comme antiépileptique et anticonvulsif pour diverses applications psychothérapeutiques. Elle est également utilisée en association avec d'autres médicaments pour le traitement du sevrage alcoolique [3]. La CBZ a été découverte par le chimiste Walter Schindler en Suisse en 1953 et approuvé au Royaume-Uni et aux États-Unis depuis 1965 et 1968, respectivement. La CBZ est ionisée dans le liquide intracellulaire, ce qui lui permet de se lier aux canaux sodiques sensibles à la tension activés et d'empêcher le déclenchement répétitif d'un potentiel d'action. Par conséquent, les cellules affectées restent moins excitables jusqu'à ce que la CBZ soit dissociée.

La CBZ est répertoriée pour le suivi de la directive-cadre sur l'eau de l'EU car elle est fréquemment détectée dans différentes sources d'eau (eaux usées, eaux souterraines, rivière ou surface) à des concentrations relativement élevées [4]. Le taux de consommation annuel de la CBZ a été estimé à 1014, 39 et 28 tonnes dans le monde (l'année 2008), aux États-Unis (l'année 2008) et au Canada (l'année 2001) respectivement [5]. En raison du taux de consommation élevé et de la structure chimique stable de la CBZ, ce composé persistant est libéré en continu dans l'environnement. Tel qu'indiqué, environ 30% de la CBZ prescrite est excrétée dans le système d'eaux usées sous forme inchangée après la consommation humaine et elle ne peut pas être éliminée efficacement par les stations d'épuration conventionnelles (WWTPs) <10% [6]. Néanmoins, certaines études ont même montré une concentration plus élevée de la CBZ dans les effluents que dans l'influent, ce qui est

dû à l'hydrolyse des produits de transformation de la CBZ au cours du processus de traitement biologique conventionnel. Ainsi, des études ont démontré que la CBZ est l'un des composés pharmaceutiquement actifs (PhACs) les plus fréquemment détectés dans les WWTPs et les eaux de surface dans le monde entier avec des concentrations allant jusqu'à plusieurs dizaines de ng/L dans l'eau potable et plusieurs µg/L dans les eaux de surface [7, 8]. Des études sur les eaux souterraines ont montré que la CBZ pouvait rester intacte après 8-10 ans de passage dans le sous-sol. De plus, les études ont montré que la CBZ n'était pas soumis à la dégradation ou à l'adsorption, ce qui est supposé être une des raisons de son omniprésence dans les eaux souterraines [9].

Récemment, des efforts de recherche remarquables ont été faits pour développer des stratégies optimales pour l'élimination de la CBZ des eaux usées. D'une part, l'élimination efficace de la CBZ dans les procédés de traitement physico-chimiques traditionnels n'est pas réalisable en raison de l'hydrophilicité et de la stabilité chimique de la CBZ. D'un autre côté, d'autres méthodes de traitement, telles que les procédés d'oxydation avancés (AOPs), la séparation par membrane, le processus d'adsorption, peuvent atteindre des niveaux élevés d'élimination de la CBZ. Cependant, il existe encore des défis avec ces technologies telles que l'élimination des rétentats membranaires, la capacité d'adsorption limitée et la formation de sous-produits plus toxiques au cours des processus d'oxydation avancés.

Au cours des 15 dernières années, des systèmes d'adsorption et des réacteurs enzymatiques ont été utilisés pour la dégradation ou l'élimination efficace de ces contaminants récalcitrants. Plus précisément, la dégradation des micropolluants à l'aide d'enzymes oxydoréductases telles que la laccase s'est révélée efficace en termes de dégradation et même de minéralisation. Cependant, le processus est lent et sensible aux conditions opératives. L'immobilisation de l'enzyme sur des supports de taille nanométrique ayant une capacité d'adsorption vis-à-vis des micropolluants peut améliorer la stabilité du nanobiocatalyseur obtenu dans des conditions opérationnelles et augmenter ses performances. Ce processus hybride peut être considéré comme une étape complémentaire dans le traitement tertiaire des WWTPs. La recherche actuelle vise à développer un système de nano-biocatalyseur pour une dégradation efficace de la CBZ à une concentration d'eaux usées pertinente du point de vue environnemental, sur la base d'une combinaison de système adsorbant de taille nanométrique et de dégradation enzymatique.

Référence

1. Tiwari, B., Sellamuthu, B., Ouarda, Y., Drogui, P., Tyagi, R.D., and Buelna, G., Review on fate and mechanism of removal of pharmaceutical pollutants from wastewater using biological approach. Bioresource Technology, 2017. 224: p. 1-12.

2. Mohapatra, D.P., Brar, S.K., Tyagi, R.D., Picard, P., and Surampalli, R.Y., Carbamazepine in municipal wastewater and wastewater sludge: Ultrafast quantification by laser diode thermal desorption-atmospheric pressure chemical ionization coupled with tandem mass spectrometry. Talanta, 2012. 99: p. 247-255.

3. Miao, X.S. and Metcalfe, C.D., Determination of carbamazepine and its metabolites in aqueous samples using liquid chromatography− electrospray tandem mass spectrometry. Analytical chemistry, 2003. 75(15): p. 3731-3738.

4. Stuart, M., Manamsa, K., Talbot, J., and Crane, E., Emerging contaminants in groundwater. 2011.

5. Zhang, Y., Geißen, S.U., and Gal, C., Carbamazepine and diclofenac: removal in wastewater treatment plants and occurrence in water bodies. Chemosphere, 2008. 73(8): p. 1151-1161.

6. Radjenović, J., Petrović, M., and Barceló, D., Fate and distribution of pharmaceuticals in wastewater and sewage sludge of the conventional activated sludge (CAS) and advanced membrane bioreactor (MBR) treatment. Water Research, 2009. 43(3): p. 831-841.

7. Carabin, A., Drogui, P., and Robert, D., Photo-degradation of carbamazepine using TiO 2 suspended photocatalysts. Journal of the Taiwan Institute of Chemical Engineers, 2015. 54: p. 109-117.

8. Tang, L., Wang, J.j., Jia, C.t., Lv, G.x., Xu, G., Li, W.t., Wang, L., Zhang, J.y., and Wu, M.-h., Simulated solar driven catalytic degradation of psychiatric drug carbamazepine with binary BiVO4 heterostructures sensitized by graphene quantum dots. Applied Catalysis B: Environmental, 2017. 205: p. 587-596.

9.   Sui, Q., Cao, X., Lu, S., Zhao, W., Qiu, Z., and Yu, G., Occurrence, sources and fate of pharmaceuticals and personal care products in the groundwater: a review. Emerging Contaminants, 2015. 1(1): p. 14-24.

Partie 2. Revue de littérature

2.1 Contaminants émergents - Produits pharmaceutiques

Les contaminants émergents (ECs) sont des composés polluants qui ont suscité beaucoup d'intérêt en raison de leurs effets sur la santé et l'environnement. Ces ECs ont été introduits dans l'environnement depuis leurs premières utilisations [1], mais à ce moment-là, ils étaient en-dessous des limites de détection des méthodes analytiques. Au cours des 20 dernières années, en utilisant des instruments analytiques sophistiqués, les chercheurs ont détecté des ECs dans différents compartiments environnementaux, y compris le sol, l'eau, l'air et les sédiments. Jusqu'à présent, il n'y a pas de mesures réglementaires pour la majorité des ECs et leurs métabolites [2, 3], mais leurs impacts sur la santé humaine et l'écosystème deviennent de plus en plus évidents suite aux récents travaux de recherche.

Un grand nombre de composés pharmaceutiques est utilisé pour la prévention, le diagnostic et le traitement de maladies chez les humains et les animaux. Une grande partie de ces composés thérapeutiques ne peuvent pas être métabolisés par le corps humain. Ils sont évacués donc par l'urine et les excréments et pénètrent dans les stations d'épuration municipales (WWTPs) et dans l'environnement [4]. Aussi les industries pharmaceutiques, les hôpitaux, les déchets des animaux et les centres de recherche libèrent des polluants pharmaceutiques dans l'environnement [5]. La présence de composés pharmaceutiquement actifs (PhACs) à de faibles concentrations dans l'environnement peut affecter la qualité de l'eau et avoir un impact potentiel sur l'approvisionnement en eau potable, les écosystèmes et la santé humaine [6, 7]. Par exemple, la féminisation des poissons mâles dans certains milieux aquatiques est attribuée aux hormones stéroïdes qui sont rejetées dans les rivières par les systèmes municipaux de traitement des eaux usées [8]. En outre, il existe des rapports sur la relation entre la prolifération du cancer et les diphényléthers polybromés [9].

Il a été démontré que l'exposition continue à des concentrations sub-toxiques de certains composés thérapeutiques peut avoir des effets inattendus sur les organismes non ciblés. En outre, elle peut induire des effets indésirables sur les écosystèmes et les humains. Ainsi, la présence de PhAC dans l'environnement peut entraîner des menaces pour la santé humaine et écologique. En raison de connaissances insuffisantes sur leur toxicité, leurs impacts et leur comportement, peu d'entre eux sont

surveillés dans l'environnement et beaucoup restent non réglementés [10]. Mais comme leur potentiel de risques à long terme est de plus en plus reconnu, des normes et réglementations pertinentes devraient être publiées au cours des prochaines décennies.

2.1.1 Les drogues psychoactives - Carbamazépine

La carbamazépine (5H-dibenzo[b,f]azépine-5-carboxamide) ou CBZ est l'un des résidus pharmaceutiques les plus fréquemment détectés dans les plans d'eau tels que les effluents des stations d'épuration et des rivières en Europe et en Amérique du Nord. De plus, la concentration de CBZ dans l'effluent était parfois plus élevée que dans l'influent. La raison a été attribuée à l'hydrolyse des conjugués de la CBZ au cours du processus de traitement biologique classique [11-13] et à la libération progressive de la CBZ dans les particules fécales en phase liquide lorsque les fèces sont décomposées par des microorganismes [14]. La CBZ a été découverte par le chimiste Walter Schindler en Suisse en 1953 et a été approuvé au Royaume-Uni depuis 1965 et aux États-Unis depuis 1968. En raison de son volume élevé de consommation, de sa présence dans l'environnement aquatique et de ses impacts possibles sur la faune et les humains, la CBZ devient une menace potentielle pour l'environnement [15, 16].

2.1.2 Application de la CBZ et ses propriétés

La CBZ est un acide organique et sa structure moléculaire est représentée à la figure 1.2.1. Elle appartient à une classe de médicaments appelés antiépileptiques/anticonvulsifs qui agissent sur la réduction de l'activité électrique anormale dans le cerveau. La CBZ peut être utilisée seule ou en association avec d'autres médicaments pour contrôler certains types de crises. La CBZ peut traiter la névralgie du trijumeau (une condition qui provoque la douleur du nerf facial), des incidents de manie ou des incidents mixtes chez les patients atteints de trouble bipolaire I [17]. La CBZ est également utilisée pour traiter le syndrome de stress post-traumatique, le sevrage médicamenteux et alcoolique, le syndrome des jambes sans repos, le diabète insipide, certains syndromes douloureux et une maladie chez les enfants appelée chorée [18].
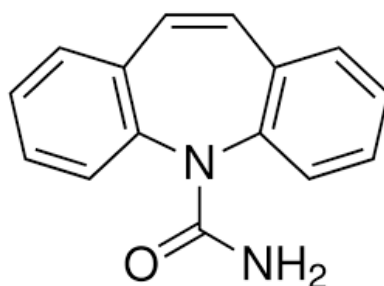
Figure 1.2.1 Structure de la carbamazépine

Les propriétés physicochimiques de la CBZ sont énumérées dans le Tableau 1.2.1. La concentration de CBZ dans le plasma sanguin atteint son pic 4 à 8 h après l'ingestion et il peut prendre jusqu'à 26 h pour que la CBZ exerce son effet [15, 19]. Après l'administration, une partie de la CBZ (72%) est ionisée dans les fluides intracellulaires, ce qui lui permet de se lier aux canaux sodiques sensibles à la tension activés et d'empêcher le déclenchement répétitif d'un potentiel d'action. Par conséquent, les cellules affectées restent moins excitables jusqu'à ce que la CBZ soit dissociée de ses métabolites par le système du cytochrome P450. Les métabolites peuvent inhiber la forme pharmaceutiquement active de la CBZ et finalement être excrétés dans l'urine. La demi-vie d'élimination de CBZ est généralement comprise entre 25 et 65 h [20]. La partie non métabolisée (28%) et certains métabolites sont ensuite excrétés du corps par l'urine et les fèces [7]. La Figure 1.2.2 montre les principaux métabolites de la CBZ.

Tableau 1.2.1 Propriétés physico-chimiques de la carbamazépine

Property	Detail
Molecular formula	$C_{15}H_{12}N_2O$
CAS Number	298-46-4
Molecular weight	236.27 g/mol
Usage	Analgesic, antiepileptic
Appearance	White, light yellowish powder
Water solubility	17.7 mg/L (25 °C)
Log K_{ow} (octanol-water)	2.45
Henry's Law Constant	1.09×10^{-5} Pa m^3/mol (25 °C)
pK_a	Neutral
Elimination half-life	25-65 h
Density	1.3±0.1 g/cm^3
Melting point	189-193 °C
Boiling point	411.0±48.0 °C at 760 mmHg
Vapor pressure	1.84×10^{-7} mmHg at 25 °C
Dosage	Maintenance usually 800-1200 mg daily
Solvent solubility	Soluble in alcohol and in acetone

2.1.3 Estimation de la consommation de la CBZ

Les quantités de produits pharmaceutiques consommés dans une région ou dans le monde permettent d'estimer leur occurrence et leur influence sur l'environnement aquatique [21]. Le Tableau 1.2.2 présente les volumes annuels consommés de la CBZ dans certaines régions. Actuellement, ces données de consommation globale ne peuvent pas être trouvées dans la littérature publiée puisque les gens peuvent obtenir des médicaments soit sur ordonnance ou en vente libre. En outre, la vente d'un certain médicament sous différentes marques obscurcit les données. Dans ce cas, la CBZ a les noms de marque suivants: Biston, Calepsine, Carbatrol, Epitol, Equetro, Finlepsine, Sirtal, Stazépine, Tegretol, Telesmin, Timonil, etc. La consommation annuelle mondiale de CBZ est estimée à 1014 tonnes et cela signifie que plus de 30 tonnes de CBZ doivent être retirées des effluents des WWTP [15]. Les valeurs estimées sont en accord avec Intercontinental Marketing Statistics qui a déclaré le commerce de 942 tonnes de CBZ en 2007 dans 76 grands pays qui représenteraient 96% du marché pharmaceutique mondial [7].

Tableau 1.2.2 Volumes annuels de la carbamazépine consommée dans certains pays [7]

Regions	Annual consumption Tons	Population 10^6	DPC mg	References
Australia	10	19	526	[22]
Austria	6 (in 1997)	8	750	[23]
Canada	28 (in 2001)	31	903	[24]
Finland	4.6 (in 2005)	5	920	[12]
France	40	59	678	[25]
Germany	87 (in 1999)	82	1061	[7]
England	40 (in 2000)	49	816	[26]
USA	43 (in 2000) 35 (in 2003)	284	151	[27]
World	1014			
DPC of developed countries, including USA			482	
DPC of developed countries, excluding USA			852	
DPC of developed countries, adopted			667	
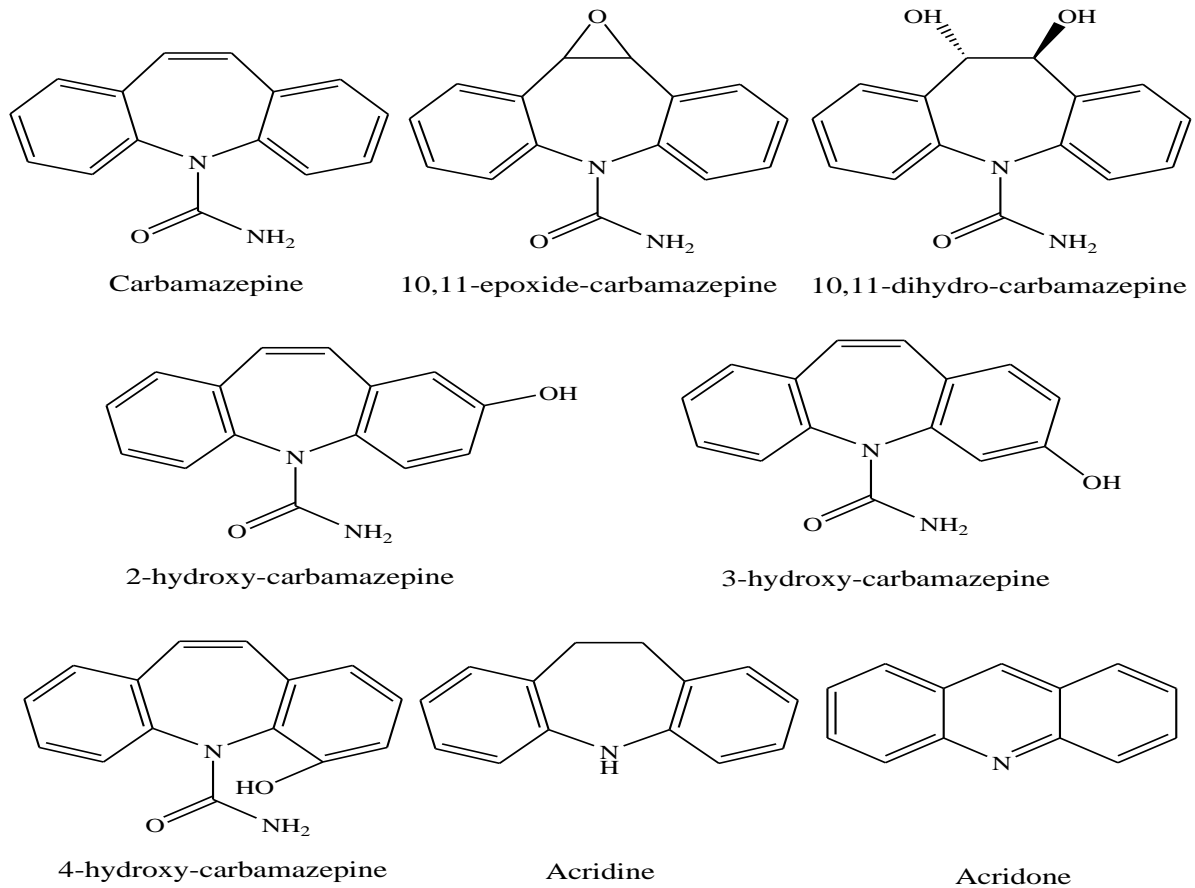
Figure 1.2.2 Carbamazépine et ses métabolites

2.2 Présence et devenir de la CBZ dans l'environnement

Les produits pharmaceutiques se retrouvent dans les usines WWTPs à travers les systèmes de collecte des eaux usées. Cependant, certains médicaments ne sont pas éliminés efficacement dans les usines de traitement des eaux usées et se retrouvent par la suite dans des plans d'eau. La CBZ est un exemple d'un produit pharmaceutique qui est mal éliminé par les WWTPs. Elle a été détectée dans les affluents et les boues d'épuration (WWS), dans les eaux de surface, les eaux souterraines et parfois dans l'eau potable, avec des concentrations décroissantes dues à la dilution et à certains processus d'élimination, comme la phototransformation et l'adsorption dans le sol. La CBZ a été détectée dans les masses d'eau à travers l'Europe, l'Amérique et l'Asie [28]. La moyenne de la concentration de la CBZ détectée dans les effluents des usines de traitement des eaux usées et dans les eaux de surface dans certains pays a été résumée à la Figure 1.2.3.
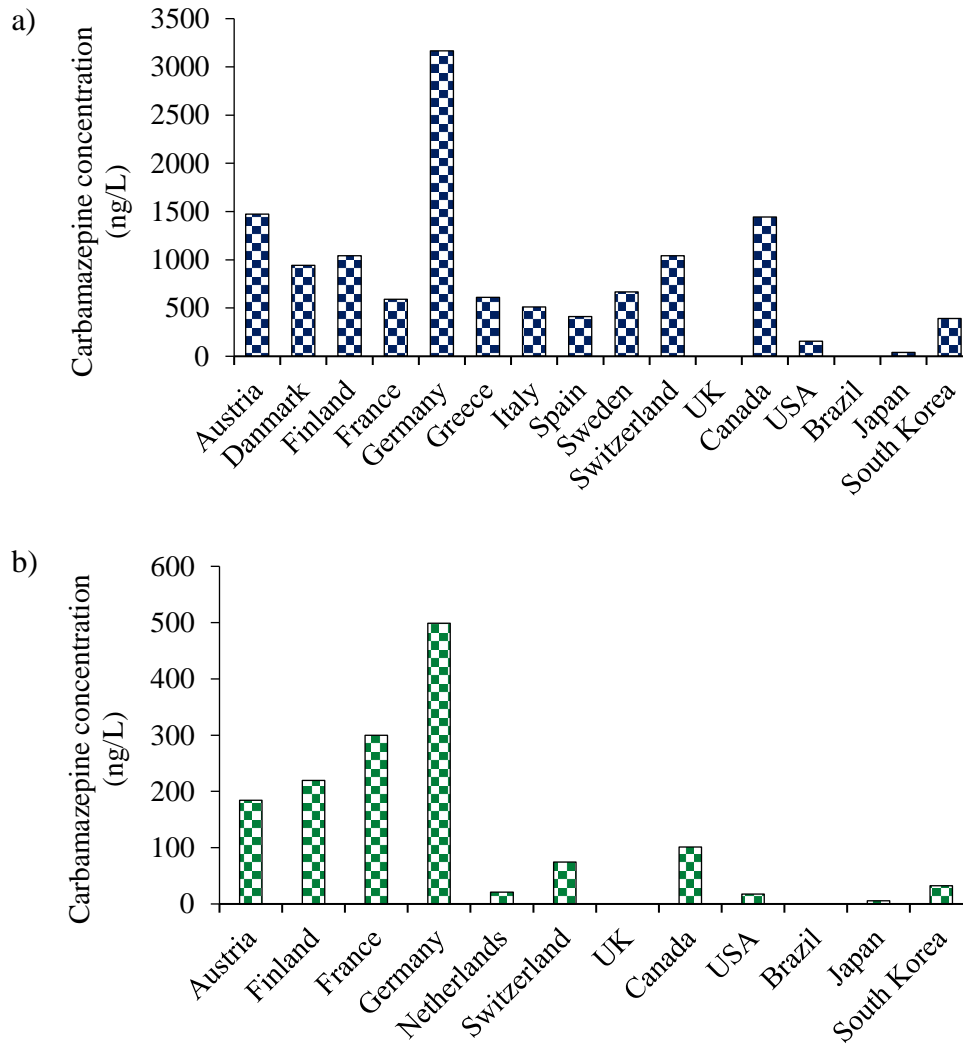
Figure 1.2.3 Concentrations moyennes détectées de la carbamazépine dans les effluents des usines de traitement des eaux usées (a) et des eaux de surface (b) dans certains pays [7]

Les WWTPs sont des passerelles importantes d'où la CBZ peut entrer dans le cycle de l'eau. La concentration maximale de la CBZ retrouvée dans les effluents des usines de traitement des eaux usées en Allemagne était de 6300 ng/L [29]. De plus, la CBZ a été trouvée dans la plupart des effluents des stations d'épuration municipales canadiennes à des concentrations allant jusqu'à 2,3 µg/L [30, 31]. Les eaux usées hospitalières sont une autre source de résidus pharmaceutiques en raison de la consommation élevée de certains médicaments à l'hôpital. Il a été rapporté que 26% de la CBZ totale provenaient des hôpitaux [32]. La Figure 1.2.4 présente le bilan massique de la CBZ observé dans les eaux usées (WW) et WWS des WWTPs.

Dans les eaux de surface, les concentrations de la CBZ sont relativement faibles et varient également selon les pays (Figure 1.2.3). La plus forte concentration déclarée de la CBZ dans les eaux de surface appartenait à Berlin (1075 ng/L) [33]. Dans une étude menée par l'US Geological Survey (USGS), une concentration moyenne de la CBZ de 60 ng/L dans l'eau et de 41,6 ng / mg dans les sédiments a été retrouvée dans 44 rivières à travers les États-Unis [27]. Après le déversement des effluents dans les eaux de surface, la CBZ est probablement capable d'atteindre un aquifère en traversant une zone souterraine insaturée sans être soumise à aucune adsorption ou dégradation au cours de son passage [34, 35]. La CBZ a été détectée à la concentration de 20 ng/L dans un puits d'eau potable abandonné situé à 100 m d'un lac où la CBZ a été détectée à 135 ng/L [36]. Au lieu d'être déchargés, les effluents sont de plus en plus réutilisés dans les pays arides et semi-arides, pour l'irrigation et / ou pour le réapprovisionnement des aquifères. Les chances de détecter la présence de la CBZ dans les eaux souterraines sont accrues dans les régions où les effluents des WWTP sont utilisés pour la recharge des eaux souterraines. La CBZ a été détectée dans l'effluent de la WWTP et dans le puits de surveillance avec une concentration de155 ng/L et 90 ng/L, respectivement [37].

L'utilisation de WW pour l'irrigation peut conduire au transfert de la CBZ et de ses métabolites dans le sol. Des études ont montré que la CBZ était présente dans les sols irrigués avec des concentrations allant de 0,02 à 15 ng/g de matière sèche [38, 39]. Le coefficient de distribution (K_d) de la CBZ est de 1,2L/kgss entre la boue secondaire et l'eau, ce qui est loin de la valeur de 500 L/kgss requise pour une sorption importante sur les boues [7]. On suppose que l'incinération de WWS peut minéraliser la CBZ et qu'elle sera absente des résidus de cendres. Cependant, si l'incinération était arrêtée pour une utilisation finale et bénéfique des boues, comme dans l'agriculture et l'épandage, la présence de la CBZ pourrait poser la question de la réutilisation des boues avec la possibilité de contamination du sol et des aquifères [28].
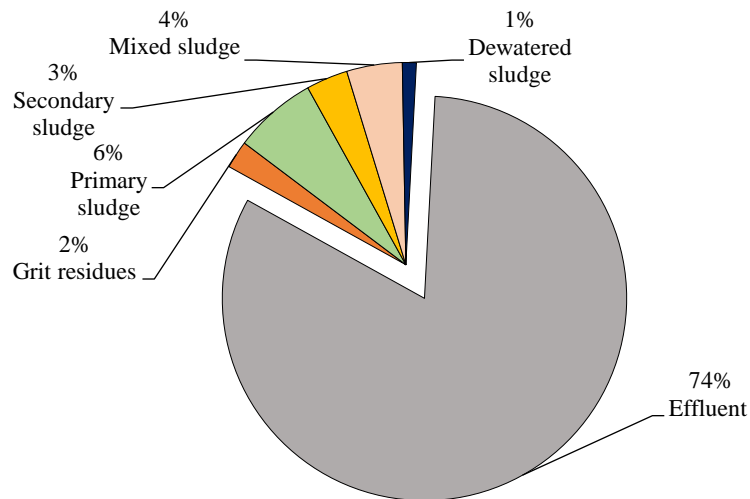
Figure 1.2.4 Flux massique quotidien de la carbamazépine dans différentes unités de traitement des eaux usées [15].

2.3 Écotoxicologie de la CBZ

Les inquiétudes pour la santé humaine et les impacts écologiques des PhACs, même à des concentrations aussi faibles que du ng/L, sont devenues une préoccupation majeure de la recherche scientifique [40]. La CBZ est largement présente dans les plans d'eau et il est donc nécessaire d'évaluer ses impacts sur les écosystèmes où elle est présente. Des bioessais ont généralement été utilisés pour étudier la toxicité de la CBZ en exposant les organismes d'essai à des concentrations spécifiques de la CBZ. Ces bioessais sont ensuite utilisés pour calculer les concentrations estimées sans effet (PNEC) et les résultats sont ensuite comparés aux concentrations environnementales mesurées (MEC) [25, 41]. Pour la caractérisation des risques, c'est une estimation de l'incidence de l'effet indésirable résultant de l'exposition réelle ou prévue à une substance, un quotient de risque est calculé entre la CME la plus élevée et la CSEP [25]. Le calcul de la caractérisation des risques (MEC/PNEC) pour la CBZ obtenue pour différents pays est présenté dans la Figure 1.2.5.
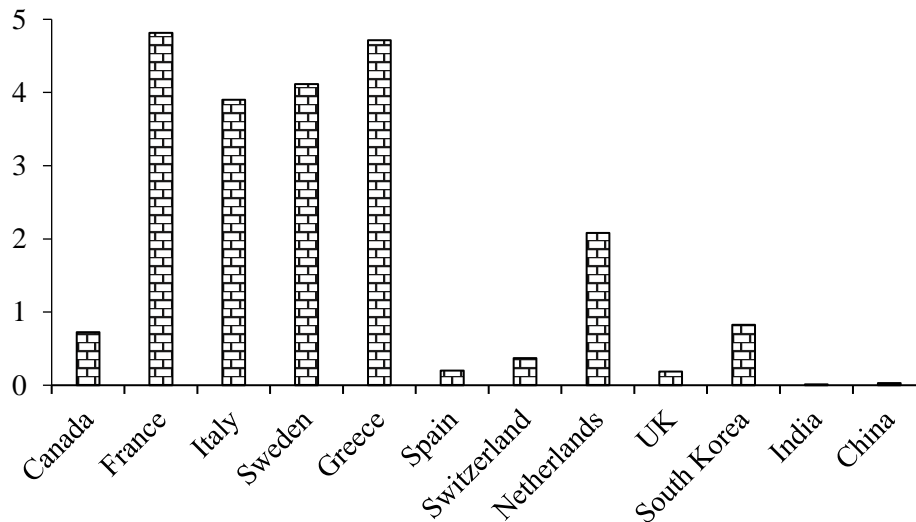
Figure 1.2.5 Quotient de risque ou rapport de risque de la carbamazépine rapportée dans la littérature. Le risque aquatique est suspecté lorsque le quotient de risque est ≥ 1 [15].

Selon les résultats, la CBZ a été classée comme "R52/53 Nocif pour les organismes aquatiques et peut entraîner des effets néfastes à long terme sur l'environnement aquatique" basé sur la législation européenne actuelle et sur la classification et l'étiquetage des produits chimiques (92/32/ EEC) [42]. Les expériences de toxicité aiguë de la CBZ utilisant des organismes aquatiques ont indiqué des concentrations de CE_{50} de l'ordre de mg/L, ce qui est beaucoup plus élevé que les concentrations de la CBZ pertinentes pour l'environnement et il semble donc que l'écotoxicité aiguë de la CBZ est plutôt improbable. Cependant, des études physiologiques avec des concentrations plus faibles et des paramètres sensibles ont montré que la CBZ peut nuire aux espèces exposées. Il existent des preuves d'impacts de la CBZ sur l'organisme non-cible à de très faibles concentrations, cependant, plus d'études basées sur les animaux sont nécessaires pour connaître l'effet toxique de la CBZ et de ses métabolites sur la santé humaine, et aussi sur des méthodes de retrait de la CBZ efficaces des milieux environnementaux, y compris l'eau, WW et WWS.

2.4 Retrait de la CBZ dans une station d'épuration des eaux usées (WWTP)

La CBZ et ses métabolites sont transportés avec les eaux usées vers les usines de traitement des eaux usées à travers le système de collecte des eaux usées et si elle n'est pas efficacement éliminée dans les WWTPs, elle trouvera son chemin dans l'écosystème. La plupart des usines de traitement des eaux usées utilisent des

procédés de boues activées dans lesquels des microorganismes sont appliqués pour dégrader les polluants à des formes acceptables ou les minéraliser en eau et en dioxyde de carbone. Les polluants peuvent être éliminés de l'eau par extraction à l'air, sorption sur les boues et dégradation par phototransformation. Par conséquent, l'élimination des résidus pharmaceutiques dans les procédés de boues activées comprend quatre mécanismes incluant la biotransformation, l'extraction à l'air, la sorption et la phototransformation. Cependant, un coefficient de Henry supérieur à 3×10^{-3} est nécessaire pour l'extraction significative d'un composé dans un bioréacteur à aération par bulle fine [43]. En conséquence, l'élimination de CBZ (coefficients Henry: $1,09\times10^{-5}$) par entraînement à l'air est limitée et est donc omise de la discussion suivante. Plusieurs études ont rapporté que des cultures pures isolées à partir de boues activées, de sédiments ou d'eaux usées peuvent être utilisées pour éliminer la CBZ dans la gamme de 30% à 50% [44, 45]. De plus, les résultats des chercheurs ont montré que la dégradation de la CBZ est indépendante du temps de rétention des boues (SRT) et dans la plupart des cas, elle est inférieure à 10% [23, 46, 47]. Les WWTPs sont généralement utilisées dans un environnement ouvert, ce qui permet aux eaux usées d'être exposées à la lumière du soleil. La CBZ peut être photolysée sous irradiation solaire, mais seulement à un taux relativement faible [48]. Ainsi, compte tenu du faible temps de rétention hydraulique des WWTPs, la phototransformation de la CBZ dans les WWTPs est négligeable.

2.5 Méthodes de traitement pour l'élimination des produits pharmaceutiques

Tel qu'indiqué précédemment, bien que les concentrations de PhACs dans l'environnement soient faibles, l'exposition continue à ces composés a soulevé des préoccupations au sujet des impacts inconnus à long terme. En conséquence, l'élimination des PhACs a attiré beaucoup d'attention. En général, les méthodes d'élimination des PhACs se répartissent en trois catégories: les méthodes physiques, chimiques et biologiques. Dans les paragraphes suivants, chaque catégorie est brièvement expliquée.

2.5.1 Méthodes physiques
2.5.1.1 Systèmes d'adsorption

Chapitre 1. Synthèse

L'adsorption est une technique efficace pour l'élimination des micropolluants dans l'eau. Pendant de nombreuses années, le charbon actif et les adsorbants naturels, tels que les bentonites et les zéolithes, ont été utilisées comme matériau d'adsorption efficace pour éliminer les polluants de l'eau potable et industrielle [49, 50]. Dans le cas des systèmes de traitement, la diminution de la capacité d'adsorption et la détérioration du charbon actif se sont produites avec le temps de fonctionnement [51]. Nguyen *et al.* ont étudié l'élimination de la CBZ par un bioréacteur à membrane (MBR) et un système de charbon actif granulaire (GAC) sur une période de 196 jours et ils ont observé que l'efficacité d'élimination a augmenté de 32% pour MBR à plus de 95% pour MBR-GAC [52]. Yu *et al.* ont rapporté qu'après 12 jours de contact, l'adsorption de 94% de la CBZ sur des CAG commercial et charbon à base de noix de coco a été réalisée [53]. Dickenson *et al.* ont étudié l'adsorption de la CBZ sur le PAC et ils ont observé qu'avec l'augmentation de la concentration de charbon actif en poudre (PAC) de 0 à 20 mg/L, l'efficacité d'élimination de CBZ est passée de 0 à 100% [54]. Aussi Snyder *et al.* ont réalisé l'adsorption de CBZ (100 ng/L) sur PAC (5 mg/L), et réalisé l'élimination de 70% de CBZ dans l'eau de surface [55].

Le graphène est un matériau carboné nanométrique avec une seule couche composée d'atomes de carbone. La structure de base du graphène est un réseau bidimensionnel d'atomes de carbone liés par covalence via des orbitales hybrides sp^2 pour former une feuille en nid d'abeille. L'oxyde de graphène (GO) est un précurseur du graphène qui est toujours préparé via l'oxydation du graphite. Le graphène et l'oxyde de graphène peuvent éliminer les PhACs grâce à leur surface spécifique plus élevée que celle du charbon actif. Par conséquent, le graphène a attiré l'attention des chercheurs en tant qu'adsorbant potentiellement prometteur pour éliminer les PhACs [56, 57]. Par exemple, Rizzo *et al.* ont atteint 97% d'élimination pour la CBZ (100 mg/L) dans de l'eau synthétique en utilisant du graphène [58]. Dans une étude similaire, *Cai et Larese-Casanova* ont appliqué trois types d'oxydes de graphène, à savoir GO-C, GO-M et GO-A pour l'adsorption de la CBZ et ils ont constaté que GO-C avait une capacité d'adsorption élevée pour la CBZ des sites de sorption de surface [59]. Liu *et al.* ont préparé deux oxydes de graphène réduit (rGO$_1$ et rGO$_2$ pour l'élimination de CBZ et ils ont atteint l'adsorption maximale de 120,0 mg/g (surface = 331 m^2/g) et 95,0 mg/g (surface = 325 m^2/g), l'adsorption de la CBZ était presque indépendante du pH sur une gamme de pH de 2,0-12,0 et la force ionique avait un effet négligeable sur l'adsorption de la CBZ [60]. L'adsorption de la CBZ peut être bien expliquée par

l'interaction π-π des électrons π dans la CBZ avec les électrons π de la surface du GO [61].

Outre le graphène, les nanotubes de carbone ont montré d'excellentes propriétés au cours des dernières décennies, ce qui en fait un candidat potentiel pour de nombreuses applications, telles que le stockage d'énergie, les dispositifs médicaux et la purification de l'eau. Oleszczuk *et al.* ont étudié l'adsorption de la CBZ sur des nanotubes de carbone multi-parois (MWCNTs) et ont observé jusqu'à 90,6% d'élimination de CBZ après 24 h en fonction du diamètre extérieur de MWCNT [62]. Wang *et al.* ont observé que les MWCNT peuvent éliminer la CBZ et que, lorsque la concentration d'alimentation diminue, l'élimination du composé augmente. Ils ont également comparé l'efficacité d'adsorption de la CBZ par le MWCNT immaculé et le MWCNT hydroxylé et leurs résultats ont montré que le MWCNT hydroxylé avait une efficacité d'adsorption supérieure (97% comparé à 32%) [63]. Lerman *et al.* ont utilisé des nanotubes de carbone à paroi unique (SWCNTs) pour l'élimination de la CBZ et leurs résultats ont montré une couverture monocouche incomplète des SWCNTs, ce qui indique que la CBZ pourrait interagir avec des sites de préférence polaires sur SWCNTs. Ils ont également montré que la matière organique dissoute (DOM) est en compétition avec la CBZ et réduit son efficacité d'élimination de telle sorte que les valeurs de K_d de la CBZ passent de 58,1 L/g (système sans DOM) à 14,5 en présence de DOM [64].

Récemment, les chercheurs se sont intéressés à l'utilisation de matériaux carbonés à faible coût issus de déchets agricoles en raison de leur capacité d'absorption et de sorption des micropolluants [65]. Le biochar, un produit de pyrolyse de la biomasse résiduaire, a suscité un grand intérêt pour la purification des sources d'eau en raison de ses propriétés, telles que la porosité et la capacité d'adsorber et d'échanger différents contaminants organiques et inorganiques [66-69]. Les avantages de l'utilisation du biochar pour le traitement des eaux usées ont déjà été rapportés [70-72]. Nielsen *et al.* ont utilisé du biochar produit à partir des boues d'épuration, les déchets de l'aquaculture et leurs mélanges, pour l'adsorption de la CBZ de l'eau. Leurs résultats ont montré que l'équilibre était atteint dans les 5 heures et que la capacité d'adsorption du matériau fait à partir de 90% de boues d'épuration et de 10% des déchets de l'aquaculture était de 37,2 mg/g à une concentration d'équilibre de 50 mg/L CBZ [73]. Jung *et al.* ont caractérisé chimiquement le biochar activé (copeaux de pin à encens) et ont montré une adsorption de 80% de la CBZ (2,3-11,8 mg/L).

L'adsorption de la CBZ non ionizable à pH varié a permis aux adsorbants d'interagir par interaction hydrophobe [74].

2.5.1.2 Séparations membranaires

Les technologies de filtration membranaire, notamment l'osmose inverse (RO), l'osmose directe (FO) et la nanofiltration (NF), ont démontré une grande capacité de séparation des micropolluants de l'eau et des eaux usées. Dans une étude, Sui *et al.* ont étudié l'élimination de la CBZ pendant le traitement par filtration sur sable (SF), ultrafiltration (UF), UF/ozonation et microfiltration/osmose inverse (MF/RO) dans les WWTPs. Leurs résultats ont montré que l'élimination par SF, UF et MF/RO étaient de 0-50%, 0% et > 90%, respectivement. La valeur de coupure de poids moléculaire des membranes UF était beaucoup plus élevée que 1000 Da, ainsi les membranes UF ont montré une mauvaise rétention de la CBZ. En outre, ils ont constaté que l'ozonation est efficace pour éliminer la CBZ avec des taux d'élimination dépassant les 95%. Cela peut être dû au fait que la double liaison dans l'anneau azépine de CBZ était sensible à l'attaque par l'ozone [75]. Xie *et al.* ont étudié les effets du pH de l'alimentation sur le rejet de la CBZ dans un système FO. Ils ont trouvé que le rejet de la CBZ était d'environ 90% et qu'il était indépendant du pH [76]. En outre, Jin *et al.* ont étudié le rejet de la CBZ par des membranes FO et ils ont observé que le comportement de rejet était lié aux propriétés interfaciales de la membrane et aussi aux caractéristiques physico-chimiques du composé cible. Dans leurs conditions d'essai, une élimination de CBZ jusqu'à 95% a été observée [77]. Nghiem *et al.* ont utilisé une membrane de composite NF à couche mince pour éliminer la CBZ (500 µg/L) et ils ont constaté que la concentration de la CBZ dans les deux courants de perméat est demeurée constante à pH 4,0 pendant le temps de filtration (500 min). Ils ont attribué ce comportement à la faible hydrophobicité de la CBZ qui empêche son adsorption sur la membrane [78]. Aussi, Vergili *et al.* ont étudié la performance d'une membrane de NF pour l'élimination de la CBZ incorporée dans une eau de surface et leurs résultats ont montré un rejet global d'environ 31 à 39% avec une concentration initiale de 0,025 µg/L. Ils ont indiqué que la répulsion électrostatique ne contribuait pas au rejet de la CBZ mais que l'exclusion stérique était probablement le mécanisme de rétention de la CBZ neutre [79]. Dans un travail similaire, Radjenovic *et al.* ont étudié l'élimination de la CBZ pendant la NF et la RO dans un système de traitement d'eau potable à grande échelle alimenté par des eaux souterraines. Ils ont signalé un rejet presque

complet de la CBZ avec la NF et la RO. Cependant, la libération du flotde l'eau salée de NF et de RO avec une concentration élevée de la CBZ, c'est-à-dire plusieurs centaines de nanogrammes par litre, dans la rivière voisine représente un risque possible de ce type de traitement [80].

2.5.2 Procédés d'oxydation avancés (AOPs)

Des technologies d'oxydation avancées pour l'élimination des produits pharmaceutiques comprennent une grande variété d'approches, par ex. irradiation aux ultraviolets (UV), sonolyse, radiolyse gamma, ozonation (O_3), UV/H_2O_2, oxydation de type Fenton et oxydation électrochimique et combinaisons telles que O_3/UV. Ces techniques éliminent efficacement les micropolluants, mais présentent encore certaines limites, telles que des coûts d'investissement et d'exploitation élevés et la formation de sous-produits toxiques [65].

Le mécanisme d'ozonation est principalement basé sur la production de radicaux hydroxyles. Kovalova *et al.* ont montré une élimination de la CBZ de plus de 97% en utilisant l'ozonation. Ils ont également signalé que l'élimination de la CBZ peut être significativement améliorée en ajoutant du peroxyde d'hydrogène [81]. De même, Tootchi *et al.* et Rosal *et al.* ont montré que l'ozonation pouvait éliminer 100% de la CBZ dans les premières minutes et minéraliser 50% de la CBZ dans les 10 à 20 premières minutes de réaction [82-84]. De plus, Schaar *et al.* ont constaté que l'ozone en tant que système de post-traitement entraînait une amélioration de l'élimination des produits pharmaceutiques tels que la CBZ [85]. Ternes *et al.* ont montré qu'en appliquant 5 mg/L d'ozone à l'effluent d'une station d'épuration municipale avec un temps de contact de 18 minutes, la CBZ était éliminée avec une efficacité de plus de 50% [86]. L'oxydation de Fenton en utilisant des sels de fer et du peroxyde d'hydrogène dans des conditions acides est un traitement d'oxydation important pour éliminer les polluants, et il est généralement utilisé pour le traitement des eaux usées industrielles. Similaire à l'ozonation, l'oxydation de Fenton dépend de la forte capacité d'oxydation des radicaux hydroxyles [50].

Le mécanisme de traitement par irradiation UV comprend l'attaque et la destruction des liaisons chimiques des polluants par lumière UV directe, appelée "photolyse". Cependant, la photolyse UV directe n'est pas toujours efficace pour l'élimination des micropolluants. Par exemple, des études antérieures ont montré que la photolyse par UV directe n'était pas efficace pour réduire la concentration de la CBZ [87]. D'autre

part, Keen *et al.* ont rapporté que les sous-produits de la CBZ contenant un groupe hydroxyle ou carbonyle peuvent être entièrement minéralisés par les UV/H_2O_2 après l'activation d'une culture bactérienne mixte [88]. En outre, Nguyen *et al.* ont étudié la combinaison du traitement MBR avec l'oxydation par UV pour l'élimination de la CBZ. L'efficacité d'élimination de la CBZ par MBR et UV était seulement de 32±17% et de 30±7%, respectivement, tandis que le traitement par UV (7,5 min) après MBR entraînait un retrait global de 96%. Cela est dû à moins de masse de composés organiques / contenus dans le perméat de MBR par rapport à l'alimentation du MBR qui peut rivaliser pour l'adsorption de la lumière UV [89].

L'irradiation gamma est un autre AOP efficace pour éliminer les polluants organiques persistants, tels que les produits pharmaceutiques. Par exemple, Kimura *et al.* ont montré que la CBZ à 5 mmol/L dans les eaux usées traitées biologiquement, pouvait être complètement dégradée à 2,0 kGy par irradiation gamma [90]. Wang *et al.* ont combiné l'irradiation gamma avec la biodégradation pour éliminer la CBZ des eaux usées. Ils ont étudié l'effet des doses d'irradiation (300, 600 et 800 Gy) sur l'élimination de la CBZ et ils ont observé que l'efficacité d'élimination de la CBZ augmentait avec la dose d'irradiation et que l'efficacité maximale était de 99,8% à 800 Gy [91].

2.5.3 Processus enzymatiques

Une alternative biologique prometteuse aux boues activées conventionnelles peut être basée sur l'utilisation de cultures de champignons de pourriture blanche (WRF) capables de produire des enzymes ligninolytiques telles que l'enzyme manganèse peroxydase (MnP), la lignine peroxydase (LiP), la peroxydase polyvalente (VP) et la laccase. La capacité de ces microorganismes à dégrader une large gamme de composés xénobiotiques a été étudiée intensivement. La MnP est une enzyme de l'hème glycoprotéine capable de catalyser l'oxydation des molécules organiques en présence de H_2O_2 [92]. Le LiP catalyse la dépolymérisation de la lignine dans un processus oxydant dépendant de H_2O_2 mais il est également capable d'éliminer plusieurs composés aromatiques récalcitrants tels que les composés phénoliques et les hydrocarbures aromatiques polycycliques (PAH) [93]. La VP est capable d'impliquer de multiples sites de liaison pour les substrats afin d'oxyder une large gamme de composés tels que les substrats phénoliques et non phénoliques, les colorants à faible et à haut potentiel redox et les hydroquinones [94]. Enfin, la laccase (benzène diol: oxygène oxydoréductase) est une enzyme oxydoréductase utilisant le

cuivre comme cofacteur et qui est de faible spécificité vis-à-vis des composés organiques. Elle catalyse généralement l'oxydation des substrats donneurs d'hydrogène tels que le phénol, la lignine ou les acrylamines par réduction à quatre électrons de O_2 à H_2O [95]. En dehors des enzymes mentionnées, des systèmes enzymatiques intracellulaires, tels que le cytochrome P450, ont été rapportés comme jouant un rôle dans l'élimination de certains micropolluants [96].

2.5.3.1 Culture de cellules fongiques entières

Dans le cas de l'utilisation de WRF en culture entière pour l'élimination des polluants, les mécanismes comprennent (i) la sorption sur la biomasse, (ii) la dégradation par des enzymes extracellulaires et (iii) la dégradation par des enzymes intercellulaires ou liées au mycélium. Cela peut conduire à faire des différences significatives dans l'élimination par WRF en culture entière et en enzyme isolée. Un résumé des différents travaux sur la dégradation de la CBZ en utilisant la cellule entière de WRF est présentée dans le Tableau 1.2.3. Marco-Urrea *et al.* ont utilisé quatre WRF (*Trametes versicolor*, *Irpex lacteus*, *Ganoderma lucidum* et *Phanerochaete chrysosporium*) pour la dégradation de 10 mg/L CBZ pendant 7 jours d'incubation. Parmi les souches, *Trametes versicolor* et *Ganoderma lucidum* ont montré une dégradation de la CBZ de ~58% et ~47%, respectivement [97]. Golan-Rozen *et al.* ont étudié les mécanismes par lesquels le WRF Pleurotus ostreatus métabolise la CBZ en culture liquide et ils ont découvert que lorsque les deux systèmes cytochrome P450 (CYP450) et MnP étaient actifs, 99% du CBZ ajouté était transformé en 10,11-époxy-CBZ. D'un autre côté, lorsque le CYP450 et le MnP étaient tous deux inactivés, seulement 10 à 30% de la CBZ ajoutée était transformée, ce qui pourrait être attribué à la peroxydase polyvalente [96].

Jelic *et al.* ont utilisé *T. versicolor* pour la dégradation de la CBZ et de ses métabolites dans un bioréacteur à lit fluidisé (FBR) fonctionnant en mode <<*fed-batch*>> et continu. Ils ont observé environ 96% d'élimination de la CBZ après 2 jours en mode <<*fed-batch*>>. Cependant, en mode continu avec un temps de rétention hydraulique de 3 jours, seulement 54% de la concentration d'entrée s'est dégradée après que le réacteur ait atteint un état stable (25 jours). Ceci correspond à un taux de dégradation de CBZ de 11,9 µg CBZ/g poids sec du culot/j [98]. *Zhang et Geissen* ont étudié l'élimination du CBZ dans un bioréacteur inoculé avec du *P. chrysosporium* cultivé sur de la mousse de polyéther dans des conditions non stériles. Ils ont réalisé une

élimination élevée de la CBZ (60-80%) en fonctionnement continu avec un apport de nutriments. Cependant, dans les expériences en batch, environ 80% de l'élimination a été réalisée après 4 h, ce qui était principalement dû à une adsorption sur la mousse. La proportion de biodégradation dans l'élimination de la CBZ au cours du processus discontinu varie entre 21 et 68% [99]. Dans une autre étude reliée à la précédente, *Rodarte-Morales et al.* ont travaillé sur l'élimination de la CBZ par des culots de *P. chrysosporium* pendant 50 jours dans un réacteur à cuve agitée et dans des réacteurs à lit fixe. Ils ont observé une élimination partielle de la CBZ jusqu'à 50% sous flux d'air continu ou d'impulsions d'oxygène dans le réacteur à cuve agitée [100].

Tableau 1.2.3 Efficacité d'élimination de la CBZ par différentes souches de WRF (cellule entière)

WRF species	Reactor type	Operating conditions	Initial concentration (mg/L)	Removal efficiency (%)	References
P. chrysosporium **(LiP, MnP)**	Stirred tank (Continuous)	Reactor volume: 1.5 L Temperature: 30 °C Electron donor: glucose Time: 50 days HRT: 24 h pH: 4.5	0.5	25-60	[100]
T. versicolor **(Laccase, LiP, MnP)**	Fluidized bed (Batch-fed)	Reactor volume: 1.5 L Temperature: 25 °C Electron donor: glucose Time: 15 days Inoculum: 3.8 g pH: 4.5	0.05-9	61-94	[98]
T. versicolor **(Laccase, LiP, MnP)**	Fluidized bed (Batch-fed)	Reactor volume: 10 L Non-sterile conditions Real hospital wastewater Electron donor: glucose Inoculum: 1.5 g/L Temperature: 25 °C Time: 8 days pH: 4.5	0	-50	[101]

T. versicolor (Laccase, LiP, MnP)	Fluidized bed (Continuous)	Reactor volume: 10 L Non-sterile conditions Real hospital wastewater Electron donor: glucose Inoculum: 1.4 g/L Temperature: 25 °C Time: 8 days pH: 4.5	0.056	0	[102]
T. versicolor (Laccase, LiP, MnP)	Membrane bioreactor (Continuous)	Reactor volume: 5.5 L Non-sterile conditions Inoculum: 3 g/L HRT: 2 day Temperature: 27 °C Time: 110 days pH: 4.5	0.005	20	[89]

2.5.3.2 Enzyme libre

L'élimination d'une gamme de polluants dans des expériences en mode discontinu et en mode continu a été étudiée aux enzymes extracellulaires individuelles. L'utilisation de l'enzyme isolée au lieu d'une préparation de cellules entières permet de séparer les étapes de croissance fongique et de dégradation des polluants, ce qui constitue une stratégie appropriée pour éviter les problèmes de contamination par les bactéries. Par exemple, *Zhang et Geißen* ont produit de la lignine peroxydase brute en utilisant *P. chrysosporium* pour la dégradation de la CBZ et ils ont rapporté une efficacité de dégradation inférieure à 10% en présence de 24 ppm de H_2O_2 [103]. Hata *et al.* ont suggéré que l'addition répétée de laccase et de la 1-hydroxybenzotriazole (HBT), qui est un médiateur de rédox, est efficace dans l'élimination de CBZ. Ils ont observé 22% d'élimination de la CBZ après 24 h en utilisant un seul traitement, et une élimination de 60% de la CBZ après 48 h en utilisant un traitement répété [104]. Bien que les échantillons d'enzymes purifiées et brutes se sont avérés efficaces dans la dégradation d'une gamme de polluants, l'enzyme brute a démontré une meilleure élimination de certains produits pharmaceutiques par rapport à l'enzyme purifiée, probablement due à la présence de médiateurs naturels dans l'enzyme brute [50].

2.5.3.3 Enzyme immobilisée

L'utilisation des enzymes dans leurs formes libres entraîne une perte continue de l'activité catalytique avec l'effluent traité, ce qui augmente le coût de fonctionnement. En outre, les enzymes libres sont plus sensibles aux conditions opératives, y compris le pH et la température. L'immobilisation de l'enzyme sur des supports solides tels que les microparticules, les nanoparticules et les membranes est une approche prometteuse pour surmonter ce défi. Il existe de nombreux travaux de recherche rapportant les avantages de l'immobilisation de l'enzyme, y compris la réutilisabilité, la stabilité au stockage, la température et la stabilité du pH sur les supports [105]. Ji *et al.* ont étudié l'effet de l'acide p-coumarique, du syringaldéhyde et de l'acétosyringone, en tant que médiateurs de rédox pour l'élimination enzymatique de la CBZ par la laccase libre et immobilisée sur des nanoparticules de TiO_2. Parmi ceux-ci, l'acide p-coumarique a donné les performances optimales d'élimination de la CBZ avec un taux d'élimination de 60% (CBZ initiale de 20 uM) après 96 heures avec la laccase immobilisée. Ils ont identifié la 10,11-dihydro-10,11-dihydroxy-CBZ, la 10,11-dihydro-10,11-époxy-CBZ et l'acridone comme principaux métabolites de l'oxydation de la CBZ par la laccase [106]. Ba *et al.* ont développé un bioréacteur hybride des agrégats d'enzymes réticulés de laccase et de la membrane de microfiltration à fibres creuses de polysulfone pour l'élimination de la CBZ et ils ont obtenu des éliminations de la solution aqueuse d'environ 85% pour la CBZ. En régime continu, l'hybride a démontré des taux d'élimination de la CBZ à partir des eaux usées filtrées jusqu'à 93% après 72 h [107]. Cependant, ils ont utilisé un processus d'adsorption simple pour l'immobilisation de l'enzyme, ce qui a entraîné une faible réutilisabilité des biocatalyseurs. Par conséquent, une recherche plus approfondie est nécessaire dans ce domaine, en particulier en essayant la liaison covalente comme méthode d'immobilisation et en utilisant des matériaux adsorbants économiques.

En conclusion, la combinaison et l'intégration de systèmes d'adsorption et de procédés biologiques peuvent permettre aux opérateurs de tirer parti de tous les composants, y compris la production de produits de transformation non toxiques, la haute qualité des effluents et la possibilité d'automatisation.

Référence

1.   Englert, B.C., Nanomaterials and the environment: uses, methods and measurement. Journal of Environmental Monitoring, 2007. 9(11): p. 1154-1161.

2.   Deblonde, T., Cossu-Leguille, C., and Hartemann, P., Emerging pollutants in wastewater: A review of the literature. International Journal of Hygiene and Environmental Health, 2011. 214(6): p. 442-448.

3.   USEPA. Contaminants of Emerging Concern including Pharmaceuticals and Personal Care Products. 2015   [cited 2016 20 August]; Available from: http://water.epa.gov/scitech/cec/.

4.   Ferrando-Climent, L., Rodriguez-Mozaz, S., and Barceló, D., Incidence of anticancer drugs in an aquatic urban system: from hospital effluents through urban wastewater to natural environment. Environmental Pollution, 2014. 193: p. 216-223.

5.   Tiwari, B., Sellamuthu, B., Ouarda, Y., Drogui, P., Tyagi, R.D., and Buelna, G., Review on fate and mechanism of removal of pharmaceutical pollutants from wastewater using biological approach. Bioresource Technology, 2017. 224: p. 1-12.

6.   Rivera-Utrilla, J., Sánchez-Polo, M., Ferro-García, M.Á., Prados-Joya, G., and Ocampo-Pérez, R., Pharmaceuticals as emerging contaminants and their removal from water. A review. Chemosphere, 2013. 93(7): p. 1268-1287.

7.   Zhang, Y., Geißen, S.U., and Gal, C., Carbamazepine and diclofenac: Removal in wastewater treatment plants and occurrence in water bodies. Chemosphere, 2008. 73(8): p. 1151-1161.

8.   Spina, F., Cordero, C., Sgorbini, B., Schiliro, T., Gilli, G., Bicchi, C., and Varese, G.C., Endocrine Disrupting Chemicals (EDCs) in Municipal Wastewaters: Effective Degradation and Detoxification by Fungal Laccases. Chemical Engineering Transactions, 2013. 32: p. 391-397.

9.   Siddiqi, M.A., Laessig, R.H., and Reed, K.D., Polybrominated Diphenyl Ethers (PBDEs): New Pollutants–Old Diseases. Clinical Medicine & Research, 2003. 1(4): p. 281-290.

10. Sui, Q., Cao, X., Lu, S., Zhao, W., Qiu, Z., and Yu, G., Occurrence, sources and fate of pharmaceuticals and personal care products in the groundwater: a review. Emerging Contaminants, 2015. 1(1): p. 14-24.

11. Verlicchi, P., Al Aukidy, M., and Zambello, E., Occurrence of pharmaceutical compounds in urban wastewater: removal, mass load and environmental risk after a secondary treatment-a review. Science of the total environment, 2012. 429: p. 123-155.

12. Vieno, N., Tuhkanen, T., and Kronberg, L., Elimination of pharmaceuticals in sewage treatment plants in Finland. Water research, 2007. 41(5): p. 1001-1012.

13. Blair, B., Nikolaus, A., Hedman, C., Klaper, R., and Grundl, T., Evaluating the degradation, sorption, and negative mass balances of pharmaceuticals and personal care products during wastewater treatment. Chemosphere, 2015. 134: p. 395-401.

14. Göbel, A., McArdell, C.S., Joss, A., Siegrist, H., and Giger, W., Fate of sulfonamides, macrolides, and trimethoprim in different wastewater treatment technologies. Science of the Total Environment, 2007. 372(2): p. 361-371.

15. Mohapatra, D., Brar, S., Tyagi, R., Picard, P., and Surampalli, R., Analysis and advanced oxidation treatment of a persistent pharmaceutical compound in wastewater and wastewater sludge-carbamazepine. Science of the Total Environment, 2014. 470: p. 58-75.

16. Evgenidou, E.N., Konstantinou, I.K., and Lambropoulou, D.A., Occurrence and removal of transformation products of PPCPs and illicit drugs in wastewaters: a review. Science of the Total Environment, 2015. 505: p. 905-926.

17. Prajapati, S., Gohel, M., and Patel, L., Studies to enhance dissolution properties of carbamazepine. Indian journal of pharmaceutical sciences, 2007. 69(3): p. 427.

18. Miao, X.-S. and Metcalfe, C.D., Determination of carbamazepine and its metabolites in aqueous samples using liquid chromatography− electrospray tandem mass spectrometry. Analytical chemistry, 2003. 75(15): p. 3731-3738.

19. Guneysel, O., Onur, O., Denizbasi, A., and Saritemur, M., Carbamazepine overdose after exposure to simethicone: a case report. Journal of medical case reports, 2008. 2(1): p. 242.

20. Wishart, D.S., Knox, C., Guo, A.C., Shrivastava, S., Hassanali, M., Stothard, P., Chang, Z., and Woolsey, J., DrugBank: a comprehensive resource for in silico drug discovery and exploration. Nucleic acids research, 2006. 34(suppl 1): p. D668-D672.

21. Cohen, J.C., Gyansa-Lutterodt, M., Torpey, K., Esmail, L., and Kurokawa, G., TRIPS, the Doha Declaration and increasing access to medicines: policy options for Ghana. Globalization and health, 2005. 1(1): p. 17.

22. Khan, S.J. and Ongerth, J.E., Modelling of pharmaceutical residues in Australian sewage by quantities of use and fugacity calculations. Chemosphere, 2004. 54(3): p. 355-367.

23. Strenn, B., Clara, M., Gans, O., and Kreuzinger, N., Carbamazepine, diclofenac, ibuprofen and bezafibrate-investigations on the behaviour of selected pharmaceuticals during wastewater treatment. Water Science and Technology, 2004. 50(5): p. 269-276.

24. Miao, X.S., Yang, J.J., and Metcalfe, C.D., Carbamazepine and its metabolites in wastewater and in biosolids in a municipal wastewater treatment plant. Environmental science & technology, 2005. 39(19): p. 7469-7475.

25. Ferrari, B.t., Paxeus, N., Giudice, R.L., Pollio, A., and Garric, J., Ecotoxicological impact of pharmaceuticals found in treated wastewaters: study of carbamazepine, clofibric acid, and diclofenac. Ecotoxicology and environmental safety, 2003. 55(3): p. 359-370.

26. Jones, O., Voulvoulis, N., and Lester, J., Aquatic environmental assessment of the top 25 English prescription pharmaceuticals. Water research, 2002. 36(20): p. 5013-5022.

27. Thacker, P., Pharmaceutical data elude researchers. Environmental science & technology, 2005. 39(9): p. 193A.

28. Mohapatra, D.P., Brar, S.K., Tyagi, R.D., Picard, P., and Surampalli, R.Y., Carbamazepine in municipal wastewater and wastewater sludge: Ultrafast quantification by laser diode thermal desorption-atmospheric pressure chemical ionization coupled with tandem mass spectrometry. Talanta, 2012. 99: p. 247-255.

29. Ternes, T.A., Occurrence of drugs in German sewage treatment plants and rivers. Water research, 1998. 32(11): p. 3245-3260.

30. Metcalfe, C.D., Miao, X.S., Koenig, B.G., and Struger, J., Distribution of acidic and neutral drugs in surface waters near sewage treatment plants in the lower Great Lakes, Canada. Environmental Toxicology and Chemistry, 2003. 22(12): p. 2881-2889.

31. Metcalfe, C.D., Koenig, B.G., Bennie, D.T., Servos, M., Ternes, T.A., and Hirsch, R., Occurrence of neutral and acidic drugs in the effluents of Canadian sewage treatment plants. Environmental toxicology and chemistry, 2003. 22(12): p. 2872-2880.

32. Heberer, T. and Feldmann, D., Contribution of effluents from hospitals and private households to the total loads of diclofenac and carbamazepine in municipal sewage effluents-modeling versus measurements. Journal of Hazardous materials, 2005. 122(3): p. 211-218.

33. Heberer, T., Reddersen, K., and Mechlinski, A., From municipal sewage to drinking water: fate and removal of pharmaceutical residues in the aquatic environment in urban areas. Water Science and Technology, 2002. 46(3): p. 81-88.

34. Clara, M., Strenn, B., and Kreuzinger, N., Carbamazepine as a possible anthropogenic marker in the aquatic environment: investigations on the behaviour of carbamazepine in wastewater treatment and during groundwater infiltration. Water research, 2004. 38(4): p. 947-954.

35. Scheytt, T.J., Mersmann, P., and Heberer, T., Mobility of pharmaceuticals carbamazepine, diclofenac, ibuprofen, and propyphenazone in miscible-

displacement experiments. Journal of Contaminant Hydrology, 2006. 83(1): p. 53-69.

36.   Heberer, T., Verstraeten, I.M., Meyer, M.T., Mechlinski, A., and Reddersen, K., Occurrence and fate of pharmaceuticals during bank filtration–preliminary results from investigations in Germany and the United States. Journal of Contemporary Water Research and Education, 2011. 120(1): p. 2.

37.   Drewes, J., Heberer, T., and Reddersen, K., Fate of pharmaceuticals during indirect potable reuse. Water Science and Technology, 2002. 46(3): p. 73-80.

38.   Kinney, C.A., Furlong, E.T., Zaugg, S.D., Burkhardt, M.R., Werner, S.L., Cahill, J.D., and Jorgensen, G.R., Survey of organic wastewater contaminants in biosolids destined for land application. Environmental science & technology, 2006. 40(23): p. 7207-7215.

39.   Köck-Schulmeyer, M., Ginebreda, A., Postigo, C., López-Serna, R., Pérez, S., Brix, R., Llorca, M., de Alda, M.L., Petrović, M., and Munné, A., Wastewater reuse in Mediterranean semi-arid areas: the impact of discharges of tertiary treated sewage on the load of polar micro pollutants in the Llobregat river (NE Spain). Chemosphere, 2011. 82(5): p. 670-678.

40.   Cunningham, V.L., Perino, C., Vincent, J., Hartmann, A., and Bechter, R., Human health risk assessment of carbamazepine in surface waters of North America and Europe. Regulatory Toxicology and Pharmacology, 2010. 56(3): p. 343-351.

41.   Kim, Y., Choi, K., Jung, J., Park, S., Kim, P.-G., and Park, J., Aquatic toxicity of acetaminophen, carbamazepine, cimetidine, diltiazem and six major sulfonamides, and their potential ecological risks in Korea. Environment International, 2007. 33(3): p. 370-375.

42.   Jos, A., Repetto, G., Rios, J., Hazen, M., Molero, M., Del Peso, A., Salguero, M., Fernández-Freire, P., Pérez-Martın, J., and Cameán, A., Ecotoxicological evaluation of carbamazepine using six different model systems with eighteen endpoints. Toxicology in Vitro, 2003. 17(5): p. 525-532.

43.   Poseidon, Poseidon Final Report: Assessment of Technologies for the Removal of Pharmaceuticals and Personal Care Products in Sewage and Drinking Water Facilities to Improve the Indirect Potable Water Reuse. Contract No. EVK1-CT-2000-00047, 2006.

44.   Popa Ungureanu, C., Favier, L., Bahrim, G., and Amrane, A., Response surface optimization of experimental conditions for carbamazepine biodegradation by Streptomyces MIUG 4.89. New Biotechnology, 2015. 32(3): p. 347-357.

45.   Li, A., Cai, R., Cui, D., Qiu, T., Pang, C., Yang, J., Ma, F., and Ren, N., Characterization and biodegradation kinetics of a new cold-adapted carbamazepine-degrading bacterium, Pseudomonas sp. CBZ-4. Journal of Environmental Sciences, 2013. 25(11): p. 2281-2290.

46.   Clara, M., Strenn, B., Ausserleitner, M., and Kreuzinger, N., Comparison of the behaviour of selected micropollutants in a membrane bioreactor and a conventional wastewater treatment plant. Water Science and Technology, 2004. 50(5): p. 29-36.

47.   Clara, M., Kreuzinger, N., Strenn, B., Gans, O., and Kroiss, H., The solids retention time-a suitable design parameter to evaluate the capacity of wastewater treatment plants to remove micropollutants. Water research, 2005. 39(1): p. 97-106.

48.   Andreozzi, R., Marotta, R., Pinto, G., and Pollio, A., Carbamazepine in water: persistence in the environment, ozonation treatment and preliminary assessment on algal toxicity. Water Research, 2002. 36(11): p. 2869-2877.

49.   Martucci, A., Pasti, L., Marchetti, N., Cavazzini, A., Dondi, F., and Alberti, A., Adsorption of pharmaceuticals from aqueous solutions on synthetic zeolites. Microporous and Mesoporous Materials, 2012. 148(1): p. 174-183.

50.   Wang, J. and Wang, S., Removal of pharmaceuticals and personal care products (PPCPs) from wastewater: A review. Journal of Environmental Management, 2016. 182: p. 620-640.

51.   Liu, Z.H., Kanjo, Y., and Mizutani, S., Removal mechanisms for endocrine disrupting compounds (EDCs) in wastewater treatment-physical means, biodegradation, and chemical advanced oxidation: a review. Science of the Total Environment, 2009. 407(2): p. 731-748.

52.   Nguyen, L.N., Hai, F.I., Kang, J., Price, W.E., and Nghiem, L.D., Coupling granular activated carbon adsorption with membrane bioreactor treatment for trace organic contaminant removal: Breakthrough behaviour of persistent and hydrophilic compounds. Journal of environmental management, 2013. 119: p. 173-181.

53.   Yu, Z., Peldszus, S., Anderson, W.B., and Huck, P.M. Adsorption of selected pharmaceuticals and endocrine disrupting substances by GAC at low concentration levels. in Proceedings of AWWA Water Quality and Technology Conference 2005. 2005.

54.   Dickenson, E.R.V. and Drewes, J.E., Quantitative structure property relationships for the adsorption of pharmaceuticals onto activated carbon. Water Science and Technology, 2010. 62(10): p. 2270-2276.

55.   Snyder, S.A., Adham, S., Redding, A.M., Cannon, F.S., DeCarolis, J., Oppenheimer, J., Wert, E.C., and Yoon, Y., Role of membranes and activated carbon in the removal of endocrine disruptors and pharmaceuticals. Desalination, 2007. 202(1-3): p. 156-181.

56.   Altmann, J., Ruhl, A.S., Zietzschmann, F., and Jekel, M., Direct comparison of ozonation and adsorption onto powdered activated carbon for micropollutant removal in advanced wastewater treatment. Water Research, 2014. 55: p. 185-193.

57.   Yu, Z., Peldszus, S., and Huck, P.M., Adsorption characteristics of selected pharmaceuticals and an endocrine disrupting compound—Naproxen, carbamazepine and nonylphenol-on activated carbon. Water Research, 2008. 42(12): p. 2873-2882.

58. Rizzo, L., Fiorentino, A., Grassi, M., Attanasio, D., and Guida, M., Advanced treatment of urban wastewater by sand filtration and graphene adsorption for wastewater reuse: Effect on a mixture of pharmaceuticals and toxicity. Journal of environmental chemical engineering, 2015. 3(1): p. 122-128.

59. Cai, N. and Larese-Casanova, P., Sorption of carbamazepine by commercial graphene oxides: A comparative study with granular activated carbon and multiwalled carbon nanotubes. Journal of Colloid and Interface Science, 2014. 426: p. 152-161.

60. Liu, F.F., Zhao, J., Wang, S., Du, P., and Xing, B., Effects of Solution Chemistry on Adsorption of Selected Pharmaceuticals and Personal Care Products (PPCPs) by Graphenes and Carbon Nanotubes. Environmental Science & Technology, 2014. 48(22): p. 13197-13206.

61. Khan, A., Wang, J., Li, J., Wang, X., Chen, Z., Alsaedi, A., Hayat, T., Chen, Y., and Wang, X., The role of graphene oxide and graphene oxide-based nanomaterials in the removal of pharmaceuticals from aqueous media: a review. Environmental Science and Pollution Research, 2017: p. 1-21.

62. Oleszczuk, P., Pan, B., and Xing, B., Adsorption and Desorption of Oxytetracycline and Carbamazepine by Multiwalled Carbon Nanotubes. Environmental Science & Technology, 2009. 43(24): p. 9167-9173.

63. Wang, Y., Ma, J., Zhu, J., Ye, N., Zhang, X., and Huang, H., Multi-walled carbon nanotubes with selected properties for dynamic filtration of pharmaceuticals and personal care products. Water research, 2016. 92: p. 104-112.

64. Lerman, I., Chen, Y., Xing, B., and Chefetz, B., Adsorption of carbamazepine by carbon nanotubes: Effects of DOM introduction and competition with phenanthrene and bisphenol A. Environmental Pollution, 2013. 182: p. 169-176.

65. Tapia-Orozco, N., Ibarra-Cabrera, R., Tecante, A., Gimeno, M., Parra, R., and Garcia-Arrazola, R., Removal strategies for endocrine disrupting chemicals

using cellulose-based materials as adsorbents: A review. Journal of Environmental Chemical Engineering, 2016. 4(3): p. 3122-3142.

66.   Yargicoglu, E.N., Sadasivam, B.Y., Reddy, K.R., and Spokas, K., Physical and chemical characterization of waste wood derived biochars. Waste Management, 2015. 36: p. 256-268.

67.   Reddy, K., Xie, T., and Dastgheibi, S., Evaluation of Biochar as a Potential Filter Media for the Removal of Mixed Contaminants from Urban Storm Water Runoff. Journal of Environmental Engineering, 2014. 140(12): p. 04014043.

68.   Krika, F., Azzouz, N., and Ncibi, M.C., Adsorptive removal of cadmium from aqueous solution by cork biomass: Equilibrium, dynamic and thermodynamic studies. Arabian Journal of Chemistry, 2011.

69.   Aljeboree, A.M., Alshirifi, A.N., and Alkaim, A.F., Kinetics and equilibrium study for the adsorption of textile dyes on coconut shell activated carbon. Arabian Journal of Chemistry, 2014.

70.   Inyang, M., Gao, B., Zimmerman, A., Zhang, M., and Chen, H., Synthesis, characterization, and dye sorption ability of carbon nanotube–biochar nanocomposites. Chemical Engineering Journal, 2014. 236: p. 39-46.

71.   Inyang, M., Gao, B., Yao, Y., Xue, Y., Zimmerman, A.R., Pullammanappallil, P., and Cao, X., Removal of heavy metals from aqueous solution by biochars derived from anaerobically digested biomass. Bioresource Technology, 2012. 110: p. 50-56.

72.   Zhang, M., Gao, B., Yao, Y., and Inyang, M., Phosphate removal ability of biochar/MgAl-LDH ultra-fine composites prepared by liquid-phase deposition. Chemosphere, 2013. 92(8): p. 1042-1047.

73.   Nielsen, L., Zhang, P., and Bandosz, T.J., Adsorption of carbamazepine on sludge/fish waste derived adsorbents: Effect of surface chemistry and texture. Chemical Engineering Journal, 2015. 267: p. 170-181.

74. Jung, C., Park, J., Lim, K.H., Park, S., Heo, J., Her, N., Oh, J., Yun, S., and Yoon, Y., Adsorption of selected endocrine disrupting compounds and pharmaceuticals on activated biochars. Journal of hazardous materials, 2013. 263: p. 702-710.

75. Sui, Q., Huang, J., Deng, S., Yu, G., and Fan, Q., Occurrence and removal of pharmaceuticals, caffeine and DEET in wastewater treatment plants of Beijing, China. Water Research, 2010. 44(2): p. 417-426.

76. Xie, M., Price, W.E., and Nghiem, L.D., Rejection of pharmaceutically active compounds by forward osmosis: Role of solution pH and membrane orientation. Separation and Purification Technology, 2012. 93: p. 107-114.

77. Jin, X., Shan, J., Wang, C., Wei, J., and Tang, C.Y., Rejection of pharmaceuticals by forward osmosis membranes. Journal of Hazardous Materials, 2012. 227–228: p. 55-61.

78. Nghiem, L.D., Schäfer, A.I., and Elimelech, M., Role of electrostatic interactions in the retention of pharmaceutically active contaminants by a loose nanofiltration membrane. Journal of Membrane Science, 2006. 286(1–2): p. 52-59.

79. Vergili, I., Application of nanofiltration for the removal of carbamazepine, diclofenac and ibuprofen from drinking water sources. Journal of Environmental Management, 2013. 127: p. 177-187.

80. Radjenović, J., Petrović, M., Ventura, F., and Barceló, D., Rejection of pharmaceuticals in nanofiltration and reverse osmosis membrane drinking water treatment. Water Research, 2008. 42(14): p. 3601-3610.

81. Kovalova, L., Siegrist, H., von Gunten, U., Eugster, J., Hagenbuch, M., Wittmer, A., Moser, R., and McArdell, C.S., Elimination of Micropollutants during Post-Treatment of Hospital Wastewater with Powdered Activated Carbon, Ozone, and UV. Environmental Science & Technology, 2013. 47(14): p. 7899-7908.

82. Tootchi, L., Seth, R., Tabe, S., and Yang, P., Transformation products of pharmaceutically active compounds during drinking water ozonation. Water Science and Technology: Water Supply, 2013. 13(6): p. 1576-1582.

83. Rosal, R., Rodríguez, A., Gonzalo, M.S., and García-Calvo, E., Catalytic ozonation of naproxen and carbamazepine on titanium dioxide. Applied Catalysis B: Environmental, 2008. 84(1–2): p. 48-57.

84. Antoniou, M.G. and Andersen, H.R., Evaluation of pretreatments for inhibiting bromate formation during ozonation. Environmental technology, 2012. 33(15): p. 1747-1753.

85. Schaar, H., Clara, M., Gans, O., and Kreuzinger, N., Micropollutant removal during biological wastewater treatment and a subsequent ozonation step. Environmental Pollution, 2010. 158(5): p. 1399-1404.

86. Ternes, T.A., Stüber, J., Herrmann, N., McDowell, D., Ried, A., Kampmann, M., and Teiser, B., Ozonation: a tool for removal of pharmaceuticals, contrast media and musk fragrances from wastewater? Water research, 2003. 37(8): p. 1976-1982.

87. Vogna, D., Marotta, R., Napolitano, A., Andreozzi, R., and d'Ischia, M., Advanced oxidation of the pharmaceutical drug diclofenac with UV/H 2 O 2 and ozone. Water Research, 2004. 38(2): p. 414-422.

88. Keen, O.S., Baik, S., Linden, K.G., Aga, D.S., and Love, N.G., Enhanced Biodegradation of Carbamazepine after UV/H2O2 Advanced Oxidation. Environmental Science & Technology, 2012. 46(11): p. 6222-6227.

89. Nguyen, L.N., Hai, F.I., Kang, J., Price, W.E., and Nghiem, L.D., Removal of emerging trace organic contaminants by MBR-based hybrid treatment processes. International Biodeterioration & Biodegradation, 2013. 85: p. 474-482.

90. Kimura, A., Osawa, M., and Taguchi, M., Decomposition of persistent pharmaceuticals in wastewater by ionizing radiation. Radiation Physics and Chemistry, 2012. 81(9): p. 1508-1512.

91.   Wang, S. and Wang, J., Carbamazepine degradation by gamma irradiation coupled to biological treatment. Journal of Hazardous Materials, 2017. 321: p. 639-646.

92.   Wong, D.W., Structure and action mechanism of ligninolytic enzymes. Applied biochemistry and biotechnology, 2009. 157(2): p. 174-209.

93.   Christian, V., Shrivastava, R., Shukla, D., Modi, H., and Vyas, B., Degradation of xenobiotic compounds by lignin-degrading white-rot fungi: enzymology and mechanisms involved. 2005.

94.   Camarero, S., Sarkar, S., Ruiz-Dueñas, F.J., Martínez, M.a.J., and Martínez, Á.T., Description of a versatile peroxidase involved in the natural degradation of lignin that has both manganese peroxidase and lignin peroxidase substrate interaction sites. Journal of Biological Chemistry, 1999. 274(15): p. 10324-10330.

95.   Yang, S., Hai, F.I., Nghiem, L.D., Price, W.E., Roddick, F., Moreira, M.T., and Magram, S.F., Understanding the factors controlling the removal of trace organic contaminants by white-rot fungi and their lignin modifying enzymes: a critical review. Bioresource technology, 2013. 141: p. 97-108.

96.   Golan-Rozen, N., Chefetz, B., Ben-Ari, J., Geva, J., and Hadar, Y., Transformation of the recalcitrant pharmaceutical compound carbamazepine by Pleurotus ostreatus: role of cytochrome P450 monooxygenase and manganese peroxidase. Environmental science & technology, 2011. 45(16): p. 6800-6805.

97.   Marco-Urrea, E., Pérez-Trujillo, M., Vicent, T., and Caminal, G., Ability of white-rot fungi to remove selected pharmaceuticals and identification of degradation products of ibuprofen by Trametes versicolor. Chemosphere, 2009. 74(6): p. 765-772.

98.   Jelic, A., Cruz-Morató, C., Marco-Urrea, E., Sarrà, M., Perez, S., Vicent, T., Petrović, M., and Barcelo, D., Degradation of carbamazepine by Trametes

versicolor in an air pulsed fluidized bed bioreactor and identification of intermediates. Water Research, 2012. 46(4): p. 955-964.

99.   Zhang, Y. and Geißen, S.-U., Elimination of carbamazepine in a non-sterile fungal bioreactor. Bioresource technology, 2012. 112: p. 221-227.

100.   Rodarte-Morales, A.I., Feijoo, G., Moreira, M.T., and Lema, J.M., Operation of stirred tank reactors (STRs) and fixed-bed reactors (FBRs) with free and immobilized Phanerochaete chrysosporium for the continuous removal of pharmaceutical compounds. Biochemical Engineering Journal, 2012. 66: p. 38-45.

101.   Cruz-Morató, C., Ferrando-Climent, L., Rodriguez-Mozaz, S., Barceló, D., Marco-Urrea, E., Vicent, T., and Sarrà, M., Degradation of pharmaceuticals in non-sterile urban wastewater by Trametes versicolor in a fluidized bed bioreactor. Water Research, 2013. 47(14): p. 5200-5210.

102.   Cruz-Morató, C., Lucas, D., Llorca, M., Rodriguez-Mozaz, S., Gorga, M., Petrovic, M., Barceló, D., Vicent, T., Sarrà, M., and Marco-Urrea, E., Hospital wastewater treatment by fungal bioreactor: Removal efficiency for pharmaceuticals and endocrine disruptor compounds. Science of The Total Environment, 2014. 493: p. 365-376.

103.   Zhang, Y. and Geißen, S.-U., In vitro degradation of carbamazepine and diclofenac by crude lignin peroxidase. Journal of Hazardous Materials, 2010. 176(1–3): p. 1089-1092.

104.   Hata, T., Shintate, H., Kawai, S., Okamura, H., and Nishida, T., Elimination of carbamazepine by repeated treatment with laccase in the presence of 1-hydroxybenzotriazole. Journal of Hazardous Materials, 2010. 181(1–3): p. 1175-1178.

105.   Ansari, S.A. and Husain, Q., Potential applications of enzymes immobilized on/in nano materials: A review. Biotechnology Advances, 2012. 30(3): p. 512-523.

106. Ji, C., Hou, J., Wang, K., Zhang, Y., and Chen, V., Biocatalytic degradation of carbamazepine with immobilized laccase-mediator membrane hybrid reactor. Journal of Membrane Science, 2016. 502: p. 11-20.

107. Ba, S., Jones, J.P., and Cabana, H., Hybrid bioreactor (HBR) of hollow fiber microfilter membrane and cross-linked laccase aggregates eliminate aromatic pharmaceuticals in wastewaters. Journal of Hazardous Materials, 2014. 280: p. 662-670.

Partie 3. Problématique

D'après la littérature sur le devenir de la carbamazépine (CBZ) dans les usines de traitement des eaux usées (WWTPs) et l'environnement, les problèmes suivants ont été soulevés.

➢ Environ 1014 tonnes de la CBZ sont consommées dans le monde entier sur une base annuelle et la CBZ est le 8ème des médicaments psychoactifs les plus vendus dans le monde. En tant que substance psychotrope, la CBZ est classée comme composé nocif pour les organismes aquatiques et peut entraîner des effets néfastes à long terme sur l'environnement aquatique. De même, les résidus de la CBZ dans l'environnement ont un impact négatif sur les écosystèmes et les humains. Cependant, les mesures réglementaires/législatives visant à contrôler la CBZ dans l'environnement sont minimes.

➢ La CBZ a été détectée dans les boues d'influent, les effluents et les eaux usées des WWTP, des eaux de surface, des eaux souterraines et parfois dans l'eau potable. Étant le principal puits de la CBZ, la WWTP devrait jouer un rôle important dans l'élimination de la CBZ des eaux usées et empêcher son rejet dans l'environnement. Le coefficient de distribution de la CBZ entre l'eau et la boue secondaire est de 1,2 L/Kg_{ss}, par conséquent, la majeure partie de la CBZ reste associée à la phase aqueuse. Cependant, le système de traitement conventionnel n'est pas capable d'éliminer efficacement la CBZ des eaux usées (1-10%). De plus, la phototransformation de la CBZ dans les stations d'épuration est négligeable et des études supplémentaires ont prouvé que l'efficacité d'élimination de la CBZ est indépendante du temps de rétention des boues.

➢ Au cours des dernières décennies, l'adsorption est apparue comme une méthode de traitement efficace pour l'élimination des composés organiques, y compris la CBZ. Les nanomatériaux carbonés, tels que l'oxyde de graphène et les nanotubes de carbone, ont été largement étudiés et utilisés comme adsorbants pour les micropolluants. Cependant, ils sont très chers et leur production n'implique pas de méthodes respectueuses de l'environnement. Récemment, en tant qu'alternative à la gestion des déchets, le biochar, qui est un produit de pyrolyse de la biomasse des déchets, a suscité un grand intérêt pour la purification des sources d'eau. Les propriétés spécifiques du biochar, telles que le faible coût, la structure poreuse, la grande surface et les groupes fonctionnels de surface font des biochars des candidats potentiels pour l'élimination des micropolluants. La réduction de la taille des particules de biochar à une gamme de « nano », c'est-à-dire inférieure à 100 nm, peut encore améliorer ses propriétés, en particulier le rapport surface/volume et

le potentiel d'adsorption par rapport au biochar brut. Les considérations environnementales et les défis technologiques ont conduit à la recherche de procédés écologiques et économes en énergie pour les matériaux nanostructurés avancés. Une méthode respectueuse de l'environnement pour la production de biochar nanométrique doit donc être étudiée. *De plus, la synthèse, les propriétés physiques et chimiques du nanobiochar produit et son application pour l'adsorption doivent être étudiées. Cependant, en raison de l'interaction des polluants avec la surface du nanobiochar, les conditions d'adsorption doivent être étudiées.*

➢ La dégradation enzymatique des micropolluants est un domaine de recherche émergent. Les enzymes ligninolytiques, telles que la laccase, ont montré une excellente capacité de dégradation vis-à-vis des micropolluants, tels que les produits pharmaceutiques. Il existe peu d'études de dégradation dans lesquelles la concentration de la CBZ est pertinente par rapport à la concentration réelle dans l'environnement ou dans les eaux usées. Par conséquent, on a besoin de plus d'expériences et de données pour extrapoler les résultats aux conditions réelles. *Cependant, pour une réhabilitation à grande échelle, de grandes quantités de l'enzyme sont nécessaires et le coût de production peut être très élevé par les méthodes conventionnelles. Par conséquent, d'autres substrats efficaces et rentables pour la production d'enzymes doivent être étudiés.*

➢ Dans les traitements enzymatiques, la réutilisabilité et la stabilité de l'enzyme libre sont les deux principaux inconvénients qui peuvent être surmontés par l'immobilisation enzymatique sur une variété de supports. Par conséquent, l'utilisation de matériaux de support pour l'immobilisation sera une approche efficace. L'immobilisation d'une enzyme améliorera sa stabilité et la protégera de la dénaturation par une gamme de co-solvants organiques. Malgré ces avantages, l'immobilisation peut entraîner une diminution de l'activité de l'enzyme. *Par conséquent, différents processus d'immobilisation doivent être étudiés et optimisés.*

➢ Dans l'immobilisation physique, la faible liaison entre le support et l'enzyme entraîne la lixiviation de l'enzyme. Par conséquent, la surface des supports doit être correctement modifiée pour former des groupes fonctionnels avec une liaison protéique plus forte. Il existe de nombreux rapports sur l'utilisation de matériaux carbonés fonctionnalisés pour différentes applications industrielles, mais seulement quelques-uns d'entre eux sont liés à l'immobilisation des enzymes. Les acides minéraux tels que HCl, H_2SO_4, HNO_3 et leurs mélanges sont les produits chimiques courants utilisés pour former des groupes carboxyliques (COOR) et phénoliques (C-OR), ce qui entraîne une augmentation de

l'affinité des matériaux carbonés avec les composés organiques. La fonctionnalisation du nanobiochar à travers différents acides minéraux et organiques doit donc être étudiée.

➢ L'utilisation de nanobiochar fonctionnalisé comme support solide pour l'immobilisation enzymatique doit être étudiée. Cette méthode aura l'avantage supplémentaire de l'adsorption des contaminants par le biochar avec la dégradation induite par l'enzyme. *De plus, l'adsorption fournira suffisamment de temps pour l'action des enzymes.*

➢ Le CBZ et certains de ses métabolites tels que l'acridine et l'acridone démontrent une toxicité vis-à-vis de plusieurs organismes. Toutes les méthodes de traitement qui impliquent la dégradation de la CBZ produiront des produits de transformation. Par conséquent, le traitement enzymatique de la CBZ produira également des produits de transformation. *Par conséquent, le devenir et les niveaux de toxicité des produits de transformation de la CBZ doivent être étudiés.*

Partie 4. Hypothèse

"Le développement du nanosystème imprégné de biochar-enzyme (BENS) pour la dégradation des contaminants émergents-carbamazépine" repose sur les hypothèses suivantes:

1- Selon la littérature, la CBZ est continuellement libérée dans l'environnement et, en raison de sa tendance à la consommation en constante augmentation, sa concentration devrait augmenter à l'avenir. De plus, les mesures réglementaires/législatives visant à contrôler le rejet de CBZ dans l'environnement sont minimes. La CBZ n'est pas complètement supprimée dans *les WWTPs et par conséquent la modification des méthodes conventionnelles ou le développement de nouvelles stratégies de suppression peuvent aider à prévenir les problèmes à l'avenir.*

2- Le biochar est une nouvelle classe de matériaux carbonés produits par la pyrolyse de la biomasse et possède des propriétés supérieures, telles que la structure poreuse, la surface spécifique élevée et les groupes fonctionnels de surface, ainsi qu'un faible coût de production. La production de nanobiochar par des **méthodes vertes** peut améliorer son rapport entre la surface et le volume et la capacité d'adsorption et simultanément répondre aux préoccupations environnementales sur les méthodes complexes pour la production de nanomatériaux. En outre, *le nanobiochar produit peut être un adsorbant prometteur ou un support pour l'immobilisation enzymatique pour l'élimination des micropolluants.*

3- L'application du nanobiochar produit dans différentes méthodes d'élimination dépend de plusieurs facteurs, tels que les propriétés physico-chimiques du nanobiochar et les conditions opérationnelles. Par conséquent, tout en étudiant l'application potentielle de nanobiochar pour l'élimination de la CBZ, *la caractérisation correcte de nanobiochar est la clé dans la prise de décision pour ses applications.*

4- L'étude de l'adsorption de la CBZ sur le nanobiochar produit montre le potentiel d'adsorption du nanobiochar par rapport au biochar brut ou à d'autres matériaux carbonés. Il peut révéler les interactions entre la CBZ et la surface du nanobiochar et vérifier si le nanobiochar est efficace dans l'adsorption rapide de la CBZ. La réalisation d'études d'adsorption à des concentrations pertinentes pour l'environnement est importante pour la CBZ. Plusieurs autres paramètres, tels que le pH et la dose d'adsorbant peuvent affecter le processus d'adsorption et lors de la réalisation d'expériences, ces paramètres doivent être pris en compte. *De plus, les études sur*

l'isotherme d'adsorption et les modèles cinétiques sont importantes pour comprendre les mécanismes impliqués dans l'adsorption.

5- L'utilisation de marc de pomme comme substrat résiduel unique peut réduire considérablement le coût de production des enzymes. Les enzymes ligninolytiques, par ex. laccase, sont capables de dégrader des composés organiques d'une manière non spécifique. L'utilisation de médiateurs redox, tels que ABTS peut augmenter l'efficacité de la laccase. L'étude de la dégradation de la CBZ en utilisant le système laccase-médiateur dans différentes conditions de température et de pH peut aider à développer une méthode de traitement efficace. De plus, *les produits de transformation de la dégradation de la CBZ doivent être identifiés et la toxicité de la CBZ et de ses produits de transformation doit être analysée, ce qui peut révéler un traitement complet de la CBZ.*

6- La fonctionnalisation du nanobiochar par traitement oxydatif forme des groupes fonctionnels carboxyliques sur la surface du nanobiochar et fournit des points d'ancrage idéaux pour la fixation physique et la liaison covalente des enzymes sur la surface du nanobiochar traité. Par conséquent, la surface modifiée peut subir une variété de réactions. *La formation du groupe carboxylique sur la surface du nanobiochar par le biais de différents traitements d'acides minéraux doit donc être étudiée.*

7- L'immobilisation de la laccase sur le nanobiochar fonctionnel peut intégrer les avantages du système d'adsorption et du traitement enzymatique. En outre, le processus d'immobilisation peut augmenter la stabilité de l'enzyme. **Dans ce système, il y a suffisamment de temps pour la dégradation des composés organiques par l'enzyme**. *Cette approche peut être efficace pour le traitement de CBZ dans l'eau et les eaux usées.*

8- Le traitement du CBZ dans l'eau et les eaux usées en utilisant une enzyme immobilisée sur du nanobiochar fonctionnalisé produira des produits de transformation non toxiques qui peuvent être minéralisés avec une oxydation supplémentaire. *Ce type de nano-biocatalyseur peut être étendu pour le stade tertiaire des applications de WWTP et la production de biochar et d'enzymes à partir de déchets peut effectivement réduire le coût.*

Partie 5. Objectifs

L'objectif global de ce travail est de "développer un nanosystème de biochar imprégné d'enzymes pour l'élimination du CBZ dans les eaux usées". Le présent projet de recherche comprend les objectifs de recherche spécifiques suivants:

1- Production de nanobiochar écologique et économique en énergie et l'optimisation des paramètres production de particules de taille inférieure à 100 nanomètres.

2- Caractérisation des propriétés physico-chimiques du nanobiochar produit.

3- Investigation de l'adsorption de la CBZ sur le nanobiochar brut et produit.

4- Production de laccase à partir de substrat à faible coût et étude de la dégradation de la CBZ à l'aide de laccase libre et estimation de la toxicité de la CBZ et de ses produits de transformation.

5- Fonctionnalisation du nanobiochar par traitement acide.

6- Immobilisation physique de la laccase sur le nanobiochar fonctionnalisé et étude de l'efficacité de l'immobilisation, de la réutilisabilité et de la stabilité opérationnelle.

7- L'immobilisation covalente de la laccase sur le nanobiochar fonctionnalisé et l'étude de l'efficacité de l'immobilisation, de la réutilisabilité et de la stabilité thermique.

8- Utilisation de la laccase immobilisée physique et covalente pour la dégradation de la CBZ dans l'effluent pur et secondaire de traitement des WWTPs dans des conditions réelles et comparaison des résultats.

Partie 6. Originalité

D'après les hypothèses et les objectifs précédents, cette étude englobe l'originalité en raison des points suivants:

1. Production de nanobiochar de pin et caractérisation de ses propriétés physicochimiques.

2. Étude du comportement d'adsorption de la CBZ sur le nanobiochar produit à différentes valeurs de pH et de concentration.

3. Étudier les effets des paramètres opérationnels sur l'efficacité de la dégradation de la laccase vis-à-vis de la CBZ en utilisant la méthodologie de surface de réponse.

4. Études de toxicité de la CBZ et de ses sous-produits après dégradation avec la laccase.

5. Fonctionnalisation du nanobiochar par traitement acide.

6. Étude de la dégradation par batch de la CBZ en utilisant une laccase physiquement immobilisée sur le nanobiochar fonctionnalisé.

7. Étude de la dégradation discontinue et continue de la CBZ en utilisant une laccase immobilisée par covalence sur le nanobiochar fonctionnalisé.

En se basant sur les hypothèses et les objectifs, l'originalité de la présente étude est la suivante:

"Développement d'un nouveau nano-biocatalyseur comprenant du nanobiochar et de l'enzyme pour la dégradation de la carbamazépine dans les eaux et les eaux usées"

Partie 7. Sommaire des différents volets de recherche effectués dans cette étude

1. Étude de la production de nanobiochar et de son interaction avec la carbamazépine

Titre: Une méthode verte pour la production de nanobiochar par broyage à billes - optimisation et caractérisation

Le nanobiochar a été produit à partir de biochar de pin en utilisant un broyeur à billes planétaire. Une méthodologie de conception expérimentale composite et de surface de réponse a été utilisée pour optimiser les paramètres de broyage à billes, y compris le temps, la vitesse de rotation et le rapport bille-biochar pour obtenir des nanoparticules en peu de temps et à faible consommation d'énergie. Les résultats de l'ANOVA ont montré que les estimations de l'effet linéaire et quadratique du temps et de l'effet d'interaction du temps et de la vitesse de rotation étaient des facteurs significatifs de la taille des particules pendant la moulure ($p < 0,05$). Aux paramètres de broyage optimaux (1,6 h, 575 rpm et 4,5 g/g) et conditionnés pendant 24 h à -80 °C, on a obtenu du nanobiochar de taille moyenne d'environ 60 nm. Le test d'adsorption a prouvé que le nanobiochar produit en utilisant la méthode verte est prometteur dans l'élimination des micropolluants des milieux aqueux en éliminant jusqu'à 95% de la carbamazépine de l'eau.

Titre: Nanobiochar dérivé du bois de pin pour l'élimination de la carbamazépine des milieux aqueux: Comportement d'adsorption et paramètres influents

L'efficacité d'adsorption de la carbamazépine (CBZ) à de très faibles concentrations (0,5-20 ppb) sur du nanobiochar produit à partir de pin avec une taille moyenne de particule de 60 nm a été étudiée. Les résultats ont montré que le nanobiochar peut éliminer jusqu'à 95% de CBZ (74 µg CBZ/g de nanobiochar) après 3 h de contact. L'adsorption de CBZ sur nanobiochar a suivi le modèle isotherme de Freundlich ($R^2 = 0,9822$) et le modèle cinétique de pseudo-deuxième ordre ($R^2 = 0,9994$). Il a été trouvé qu'une augmentation du pH de 3 à 8 peut améliorer l'efficacité d'adsorption de 2,3 fois. En outre, en raison de la présence de surfactant dans les eaux usées, l'addition de Tween 80 comme tensioactif modèle a été étudiée dans la plage de 0 à 1 (rapport molaire Tween 80 à CBZ) et les résultats ont montré 57% d'efficacité d'adsorption.

Ainsi, le nanobiochar obtenu à partir de résidus de pin peut être un sorbant prometteur pour les micropolluants.

2. Étudier la performance de la laccase libre pour l'élimination de la carbamazépine.

Titre: Biotransformation de la carbamazépine par le système laccase-médiateur: cinétique, sous-produits et évaluation de la toxicité

Les effets de la température, du pH, de la concentration enzymatique et de la concentration du médiateur sur l'efficacité de la dégradation de la CBZ ont été étudiés à l'aide d'une méthodologie de conception composite et de surface de réponse centrale. L'adéquation du modèle développé a été confirmée par le coefficient de régression multiple (R^2 = 75,97%) indiquant un modèle raisonnable pour la mise en œuvre pratique. Les résultats ont montré que l'exécution de la biotransformation à 35 °C, pH 6, avec 60 U/L de concentration enzymatique et 18 µM de concentration médiateur a entraîné une élimination de 95% de CBZ. La 10,11-dihydro-10,11-dihydroxy-CBZ et la 10,11-dihydro-10,11-époxy-CBZ ont été identifiées comme les principaux métabolites de l'oxydation du CBZ par la laccase. Les tests d'œstrogénicité ont indiqué que la CBZ avec une concentration initiale de 4 µM et ses produits de biotransformation n'avaient aucun effet œstrogénique. La transformation réussie de CBZ a démontré le potentiel du système de laccase-médiateur pour l'élimination des micro-contaminants récalcitrants.

Titre: Effets antagonistes des ions métalliques divalents et de l'acide humique sur l'élimination de la carbamazépine

Dans cette étude, la dégradation de la carbamazépine (CBZ) en présence de différentes concentrations d'ions métalliques divalents, y compris Fe^{2+}, Cu^{2+}, Mg^{2+} et Ca^{2+} et l'acide humique a été étudiée. Les résultats ont montré que par rapport à l'échantillon témoin, Cu^{2+} et Ca^{2+} peuvent augmenter l'efficacité de dégradation de la CBZ de 18%, mais Fe^{2+} et Mg^{2+} peuvent diminuer l'efficacité de la dégradation de 40%. En outre, la présence d'acide humique a diminué de 42% l'efficacité de dégradation de la CBZ en raison de la liaison covalente / non covalente avec les polluants. La présence d'ions métalliques et d'acide humique a diminué l'efficacité de la dégradation de 15%. Ces connaissances ne sont pas seulement importantes pour évaluer l'importance des facteurs clés sur l'oxydation des polluants, mais elles

comprennents également des valeurs dans la conception de bioprocédés basés sur l'oxydation de la laccase puisque les ingénieurs doivent identifier ces effets synergiques et antagonistes pour concevoir un système de traitement stable.

3. Recherche de différentes techniques d'immobilisation de la laccase sur le nanobiochar

Titre: Nanobiochar de pin: un support unique pour l'immobilisation de la laccase brute par liaison covalente

La laccase brute a été immobilisée de manière covalente sur du nanobiochar fonctionnalisé en utilisant une méthode en deux étapes d'amidation activée par le diimide. L'effet de différents paramètres a été étudié. Les conditions optimales se sont révélées être 14 mg/mL de concentration de laccase, 5 mg/mL de nanobiochar, 8,2 mM d'agent de liaison et 3 h de temps de contact. Pour étudier le pH, la température, le stockage et la stabilité opérationnelle, l'échantillon obtenu à partir des conditions optimisées a été utilisé. Les résultats ont montré la plus grande stabilité de la laccase immobilisée par rapport à la variation de température et de pH par rapport à la laccase libre. De plus, la laccase immobilisée a maintenu sa performance catalytique jusqu'à sept cycles d'utilisation et a montré plus de 50% de l'activité initiale après deux mois de stockage à température ambiante.

Titre: Fabrication d'un nanobiocatalyseur utilisant une laccase encapsulée sur un composite chitosane-nanobiochar

L'enzyme laccase de *Trametes versicolor* a été encapsulée pour la première fois dans une matrice de chitosane-nanobiochar. La technique de formation de gel de chitosane-tripolyphosphate a été utilisée pour produire des nanoparticules de biocatalyseur homogènes, avec 35% d'efficacité de liaison efficace et 3,5 unités/g d'activité apparente dans la meilleure configuration. La réutilisabilité de la laccase encapsulée a été démontrée vers l'oxydation du 2,2'-azinobis-(3-éthylbenzothiazoline-6-sulfonate) (ABTS) pendant plusieurs cycles consécutifs, présentant 30% de l'activité initiale après 5 cycles. La laccase encapsulée a montré une augmentation modérée de la stabilité de l'enzyme vis-à-vis du pH et de la variation de température par rapport à l'enzyme libre. De plus, la stabilité au stockage de la laccase à 4 °C et 25 °C a augmenté après l'immobilisation. Seulement 2% de la laccase a fui pendant une période de 5 jours à partir du biocatalyseur. La laccase sous sa forme libre n'a montré

aucune activité antibactérienne contre les micro-organismes modèles Gram positif et Gram négatif, tandis que la laccase encapsulée a montré une activité antibactérienne vis-à-vis des bactéries Gram-positives. Ainsi, l'encapsulation de la laccase est une méthode efficace pour maintenir l'enzyme active et stable pour différentes applications.

4. Étudier la dégradation de la carbamazépine par la laccase immobilisée.

Titre: Laccase immobilisée sur nanobiochars fonctionnalisés par oxygène grâce au traitement aux acides minéraux pour l'élimination de la carbamazépine

L'effet de l'oxydation du nanobiochar en utilisant HCl, H_2SO_4, HNO_3 et leurs mélanges sur l'immobilisation de la laccase a été étudié. La microscopie électronique à balayage a indiqué que la structure des nanobiochars restait intacte après oxydation et que la spectroscopie infrarouge à transformée de Fourier confirmait la formation de groupes carboxyliques en raison du traitement à l'acide. Les mesures de titrage ont montré que l'échantillon traité avec H_2SO_4 / HNO_3 (50:50, v/v) avait le plus grand nombre de groupes carboxyliques (4,7 mmol/g) et par conséquent l'efficacité la plus élevée pour l'immobilisation de la laccase. De plus, il a été observé que le stockage, le pH et la stabilité thermique de la laccase immobilisée sur le nanobiochar fonctionnalisé étaient améliorés par rapport à la laccase libre, montrant son potentiel pour des applications continues. Les essais de réversibilité vis-à-vis de l'oxydation de l'acide 2, 2'-azino-bis-(3-éthylbenzothiazoline-6-sulfonique) (ABTS) ont montré que la laccase immobilisée conservait 70% de l'activité initiale après 3 cycles. Enfin, l'utilisation de laccase immobilisée pour la dégradation de la carbamazépine a montré une élimination de 83% et 86% dans l'eau enrichie et l'effluent secondaire, respectivement.

5. Dégradation de la CBZ en mode discontinu et continu par laccase immobilisée par covalence

Titre: Biodégradation de la carbamazépine par une enzyme immobilisée par covalence en utilisant du nanobiochar et de la laccase brute en mode discontinu et continu

La laccase brute de *Trametes versicolor* a été immobilisée sur FNBC et utilisée pour l'élimination de la CBZ en mode discontinu et continu. L'effet des paramètres opérationnels (pH, température, concentration de la CBZ et temps de contact) pour l'élimination de la CBZ a été étudié par des tests en batch et les résultats ont montré

que l'élimination la plus élevée peut être obtenue à pH 4, 20 °C, concentration de la CBZ de 5 µg/L et temps de contact de 24 h. Une colonne à lit fixe remplie de laccase immobilisée sur FNBC a été alimentée en continu avec de l'eau pure enrichie et un effluent secondaire de traitement des eaux usées pendant deux jours. Les résultats ont montré que l'adsorption jouait un rôle important au début mais que la biodégradation avec l'enzyme restait le principal mécanisme d'élimination de la CBZ. Plus de 45% et 60% d'élimination de la CBZ ont été obtenus le premier jour dans l'eau pure et l'effluent secondaire, respectivement. Cependant, les efficacités d'élimination de CBZ dans l'eau pure et dans l'effluent secondaire ont chuté à 25% et 45% au bout de deux jours. En général, le nanobiochar dans ce travail a montré un potentiel significatif pour immobiliser les extraits d'enzymes brutes pour des applications pratiques rentables.

CHAPTER 2

Study of the green production of nanoparticles and their use for the removal of contaminants

Part 1

A Review: Green and Energy Efficient Methods for Production of Metallic Nanoparticles

Mitra Naghdi[1], Mehrdad Taheran[1], Satinder K. Brar[1*], M. Verma[2], R.Y. Surampalli[3], J.R. Valero[1]

[1]INRS-ETE, Université du Québec, 490, Rue de la Couronne, Québec, Canada G1K 9A9

[2]CO$_2$ Solutions Inc., 2300, rue Jean-Perrin, Québec, Québec G2C 1T9 Canada

[3]Department of Civil Engineering, University of Nebraska-Lincoln, N104 SEC PO Box 886105, Lincoln, NE 68588-6105, US

(*Phone: 1 418 654 3116; Fax: 1 418 654 2600; E-mail: satinder.brar@ete.inrs.ca)

Résumé

Au cours des dernières décennies, les chercheurs ont accordé une grande attention au concept de "chimie verte", qui vise à développer des méthodes efficaces pour la synthèse des nanoparticules (NPs) en termes de moindre impact sur la vie humaine et l'environnement. Généralement, plusieurs réactifs, y compris des précurseurs, des agents réducteurs, des agents stabilisants et des solvants sont utilisés pour la production de NP et, dans certains cas, de l'énergie est nécessaire pour atteindre la température optimale de réduction. Par conséquent, pour développer une approche écologique, les chercheurs ont eu l'opportunité d'étudier des réactifs respectueux de l'environnement et de nouvelles techniques de transfert d'énergie. Afin de remplacer les réactifs nocifs par des réactifs verts, les chercheurs ont travaillé sur différents types de saccharides, de polyols, d'acides carboxyliques, de polyoxométallates et d'extraits de diverses plantes pouvant jouer le rôle de réducteurs, de stabilisants ou de solvants. En outre, il existe des rapports sur l'utilisation des rayons ultraviolets (UV), gamma et de micro-ondes qui sont capables de réduire et de fournir un chauffage uniforme. Selon la littérature, il est possible d'utiliser des réactifs verts et de nouvelles techniques de transfert d'énergie pour la production de NPs. Cependant, ces nouvelles voies de synthèse doivent être optimisées en termes de performance, de coût, de qualité du produit (distribution de la forme et de la taille) et de capacité de mise à l'échelle. Cet article présente une revue de la plupart des réactifs verts employés et de nouvelles techniques de transfert d'énergie pour la production de NP métalliques.

Mots clés

Méthodes écologiques, Chimie verte, Réactifs verts, Nanoparticules

Abstract

In the last decade, researchers paid great attention to the concept of "Green Chemistry", which aims at the development of efficient methods for the synthesis of nanoparticles (NPs) in terms of the least possible impact on human life and environment. Generally, several reagents including precursors, reducing agents, stabilizing agents and solvents are used for the production of NPs and in some cases, energy is needed to reach the optimum temperature for reduction. Therefore, to develop a green approach, researchers had the opportunity to investigate eco-friendly reagents and new energy transfer techniques. In order to substitute the harmful reagents with green ones, researchers worked on different types of saccharides, polyols, carboxylic acids, polyoxometalates and extracts of various plants that can play the role of reducers, stabilizers or solvents. Also, there are some reports on using ultraviolet (UV), gamma and microwave irradiation that are capable of reducing and provide uniform heating. According to the literature, it is possible to use green reagents and novel energy transfer techniques for the production of NPs. However, these new synthesis routes should be optimized in terms of performance, cost, product quality (shape and size distribution) and scale-up capability. This paper presents a review of most of the employed green reagents and new energy transfer techniques for the production of metallic NPs.

Keywords

Introduction

Nanoscience and nanotechnology are defined in several ways. According to the strictest definition, nanotechnology is production or use of materials and structures so that at least one of their dimensions is in the range of 1-100 nm [1-3]. The properties of nanostructured materials differ remarkably from those of bulk materials due to variation in specific characteristics, such assize, morphology and distribution [4, 5]. By decreasing the size of nanomaterials, they exhibit higher surface to volume ratio that consequently increase their surface energy and biological effectiveness [6, 7]. Therefore, nanotechnology attracted the attentions of many researchers in different research areas, such as physics, chemistry, biology, and engineering [8]. Their investigations resulted in development of newly-structured materials, such as nanoparticles (NPs), nanolayers (NLs) and nanotubes (NTs) that have greatly influenced all aspects of human life [9-11]. Currently, a vast number of nanostructured materials with different properties are produced in lab-scale that may be implemented in different applications. It is highly predictable that NPs with proven applicability will be taken forward to large-scale production [12].

Among different nanostructured materials, metal NPs have a variety of potential applications in versatile areas, such as electronics, chemistry, energy, and medicine [13]. There are many methods for production of NPs, such as lithography, laser ablation, aerosol techniques radiolysis, and photochemical reduction. Generally, these methods are costly, energy intensive or they can be harmful to human and environment [14, 15]. For example, production of nanomaterials through chemical methods involve using dispersant, surfactants or chelating agents to prevent agglomeration of particles, while most of these reagents can be considered environmental pollutant, if they are going to be used in large scale production [16]. As a consequence, there have been growing concerns about the environmental issues of large-scale production of nanomaterials. Therefore, environmentally-friendly procedures should be developed that leads to the reduction of cost, energy, product loss and the emission of pollutants [6, 8, 17, 18]. However, production of monodispersed nanomaterials by using cheap and non-toxic reagents remains a challenge for researchers and more studies are needed to achieve high quality products with sustainable commercial viability [6, 13, 14, 19, 20]. Recently, biological systems including microbes and fungi as reactors and plant extracts as precursors

have been intensively explored [14]. In another approach, green reagents, such as saccharides, polyols and protein and new energy transfer techniques can be substituted for harmful reagents and conventional heating systems in a typical chemical reaction. In this review, the recent investigations in the past decade on the substitution of green reagents and energy transfer techniques for production of metallic NPs are reviewed.

Applications of nanotechnology

Due to smaller size and large specific area, NPs exhibit great properties and applications in different fields including chemistry (catalysis, sensors, and polymers), physics (optics and electronics), biotechnology (detection and control of micro-organism), and medicine (drug development and immunoassays) [4, 21-23]. For example, NPs made from platinum, palladium, gold, silver, and copper have applications in several areas, such as biological labeling, optoelectronics, photography, photonics, surface-enhanced Raman scattering (SERS) detection and catalysis of chemical reactions. Furthermore, biocompatible and functionalized NPs have applications in diagnosis and treatment of cancers. For these two purposes, fluorescent and magnetic nanocrystals for detection of tumors and also nanosystems for delivery of anticancer drugs to affected cells have been demonstrated [24-34]. In Table 2.1.1, the application of different metallic NPs is summarized.

Green chemistry metrics

"Green chemistry" and chemical processes are gradually integrating with new scientific and industrial developments to be aligned with the global demand to reduce the emission of toxic waste into environment. These sustainable processes should consider 12 major principles of green chemistry before putting them into practical effect. These principles are set to minimize the use of toxic reagents and maximize the yield of products [34, 116].

1. Inhibition of waste generation

Prevention of the generation of wastes is preferred to their purification. The formation of any priceless by-products or the loss of consumed energy can be taken into account as waste. Each form of wastes has its own impacts on the environment depending on its nature, toxicity, quantity, or the way it is released [117, 118]. Different strategies,

such as controlling the morphology can be taken into consideration to prevent generation of undesirable products during NPs fabrication.

2. Atom economy

Atom economy addresses the maximization of product yield in terms of raw materials consumption, so that the product employs the maximum number of atoms of the precursors. The ideal reaction would contain all the atoms of raw materials [119, 120]. Employing fewer number of reactants through selection of reagents capable of playing multiple roles (e.g. polysaccharides as reducing and capping agents) for production of metallic NPs is a common strategy that increases the atom economy of reactions [121].

3. Less harmful chemical process

Synthesis procedures should be designed to be capable of consuming and producing materials that have little or no toxicity to the environment and human health [11]. Using biologically produced compounds, such as coffee and tea extract for reduction of Ag and Pd precursors to NPs is reported as the example of green methods with non-hazardous reactants [51].

4. Designing safer materials

Gathering information about the properties and impacts of molecules on the environment and their transport and fate in the biosphere is necessary to achieve sustainability. By understanding their properties, scientists can design safer molecules for the environment and humans [122, 123]. For example, one of the problems with NMs is the impurities that they carry and which could have toxic effects on the environment. To prevent such a problem, using modern purification strategies can be useful whereby the impurities can be retained [18].

5. Less toxic solvents and auxiliaries

In Green Chemistry, solvents are considered a bigger challenge since their loss is more than other materials in different syntheses and processes [124, 125]. In addition, most of the conventional solvents have problems, such as toxicity, flammability, and corrosion. Their solubility and volatility may result in contamination of air, water and soil and also can increase the risk of exposure to workers. The recovery of these solvents through conventional distillation process is often energy-intensive. Therefore, in case of NPs synthesis, scientists focused on safer solutions, such as solventless systems or non-toxic solvents i.e. water/glycerol system. [92, 126, 127].

6. Energy efficiency

Reducing the activation energy of the chemical processes by selecting appropriate precursors in a way that the conversion can take place at ambient temperature is an important target to reduce energy consumption [128]. Enhancing the energy efficiency of a chemical process and using alternative energies, such as solar and wind power are considered to be important components of the solution [118]. Incorporation of starch as a reducing agent for synthesis of Ag-Au bimetallic NPs at room temperature is a good example of energy efficient process since there is no need to increase the temperature of the reaction medium [104].

7. Renewable feedstock

Increasing the share of renewable sources either for raw material and energy are very important. The largest renewable source for energy is biomass that is obtained from dead microorganisms and also includes wood, crops, agricultural residues, among others [129]. There are also many examples for using renewable material in synthesis of NPs including cellulose, chitin, starch and glycerol [130-133].

8. Reduce Derivatives

Derivatization processes, such as blocking, protection, and temporary physical or chemical alteration should be refrained, since they introduce additional chemicals and increase energy consumption and waste generation [116, 118]. In synthesis of metallic NPs, using biopolymers such as chitosan can eliminate the need to use capping agents [56, 86, 99].

9. Catalysis

Selecting proper catalytic reaction can enhance the overall efficiency of the process by decreasing the activation energy and increasing product selectivity. These advantages can result in less energy and raw material consumption, and also less waste generation [118]. For example, Polyoxometalates (POMs) can act as a photocatalysts in synthesis of metallic NPs so that the reactions can take place at room temperature within several minutes [134].

10. Degradability

Chemical products should not be long-standing in the environment and therefore chemists should design them so that at the end of their life span, they can easily cleave into simpler and non-toxic molecules [135]. For example, using edible and

58

biodegradable polymers, such as gum ghatti for stabilizing NPs ensures the short life span of product after releasing in to the environment [66].

11. Real-time analysis of pollutants

The monitoring of the concentrations of different chemicals and taking the required actions upon right time is so crucial for preventing undesirable events. This approach can save energy and prevent accidents and also unwanted production of by-products that may need further degradation steps. Conventional analytical methods involve pretreatment steps that generate wastes and therefore, green analytical chemistry can be defined as the use of determination steps that generate less waste and are safer to the environment and human health [136, 137]. In the field of nanotechnology, real time monitoring of size and shapes of nanostructures is of high importance though it is very sophisticated. There are reports on developing innovative systems, such as grazing-incidence small-angle x-ray scattering setup that showed high sensitivity to control the required parameters of NPs production [138].

12. Inherently safer chemistry

All types of required substances for a chemical process should be selected so that the all hazards and risks of the system, such as toxicity, flammability and explosivity are minimized to prevent accidents [116]. In recent years, researchers tried to get rid of toxic and flammable reagents, such as hydrazine, sodium borohydride, carbon monoxide, and dimethyl formamide (DMF) in the synthesis of NPs [90].

Green synthesis of NPs

Metal NPs can be produced and stabilized by various physical and chemical approaches. Among them, reduction of precursor and capping the produced NPs with various stabilization agents is of interest because of robustness and feasibility. In this process, the properties of NPs including size, shape and stability strongly depend on the reaction conditions, interaction of precursor with reducing agents, and adsorption of stabilizer with NPs. Therefore, researchers worked on different precursors, solvents, reducing agents, stabilizers and also reaction conditions to control the properties of NPs. However, the synthesis processes can exert serious problems to environment. In most of the recent reported synthesis processes, organic solvents like dimethylformamide (DMF) and toxic reducing agents, such as sodium borohydride are

heavily employed. Most of these solvents and reagents can exhibit potential risks to environment and organisms [34, 87].

In the recent 10 years, the awareness about the environmental issues of chemical processes has increased and led scientists to focus on 'green chemistry' for synthesis of nanostructured materials [32, 51]. Using safer reagents, less harmful solvents and renewable feedstock and energy are among the major issues that deserve attention in a green chemistry approach [4, 87]. For green synthesis of NPs, three major principles of green chemistry should be considered including the selection of: (I) green solvents, (II) non-toxic reducing agents, and (III) harmless stabilizer [21, 26, 32, 51, 112, 139].

Biochemical, biological and biomimetic processes are attracting the attention of researchers due to their viability and potential in minimization of waste [62, 92]. For example, synthesis of NPs in bio-directed systems and using bio-molecules as templates for production of inorganic molecules has attracted biologists and chemists [81].

Synthesis and stabilization of NPs from bio-compatible materials is of high importance for their applications in medical diagnosis and therapeutics [87]. Among the vast number of available natural raw materials, polysaccharides and biologically active products extracted from plants provide largest feedstock for this process [78]. The hydroxyl and other functional groups in polysaccharides can play major role in reduction and stabilization steps of metallic NPs production. Also, phytochemical compounds have biological activities and can be considered as a renewable resource for synthesis of metallic NPs [62].

Natural polymers form the other major category of organic materials that are used for stabilization of metal nanoparticle. For this purpose, the repeating unit of the polymer should have functional groups to bind the metal atoms. The size of metallic NPs can be logically controlled by using polymers as soft support [21].

Using microwave irradiation can reduce energy requirement and provides more environmentally friendly approach in comparison to conventional methods. Furthermore, microwave irradiation provides uniform nucleation and growth conditions for nanomaterials, since it offers rapid and uniform heating of constituents [112].

Green Reagents

Saccharides

Potara *et al.* found that chitosan (CTS) is not only capable of reduction and stabilization, but also it can act as a scaffold for the formation of Au NPs. Their results indicated that the formation, size, shape and crystalline structure of Au NPs in a polymeric matrix are strongly influenced by reaction temperature. At T=100 °C and T=20-50 °C, Au NPs were in the range of 18 nm and 27 nm respectively, while at lower temperatures (4-10 °C), they observed anisotropic nanosheets of different shapes within the range of 40-200 nm [86]. Also, Wei *et al.* used CTS in aqueous solution of $AgNO_3$ and $HAuCl_4$ to act as reducing agent and scaffold for the formation of Au and Ag NPs. They used surface plasmon resonance (SPR) analysis to confirm the formation of NPs [29]. In related reports, they used TEM analysis and observed that their Ag NPs have spherical shape with diameters of 6-8 nm [56, 99]. An *et al.* prepared Ag NPs using CTS as stabilizer agent after stirring the aqueous solution for 30 min at 30 °C. Their SEM micrographs showed a regular spherical shape with less than 20 nm in size and also their TGA analysis exhibited higher thermal stability of Ag-CTS in comparison to CTS. Their microbial experiments showed that the antibacterial performance of Ag-CTS is more than either Ag NPs or CTS [72]. Also, Sun *et al.* prepared Au NPs using $HAuCl_4$ as precursor and CTS as the reducing agent and stabilizer in a 30 h reaction at 55 °C. According to TEM images, the sizes of Au NPs were in the range of 10 and 50 nm. During the synthesis, they observed a decreasing trend in intrinsic viscosity [η] of chitosan that implied degradation of chitosan chains due to the reaction with $HAuCl_4$ [140]. Also, several researchers worked on derivatives of CTS. For example, Wang *et al.* produced biocompatible chitosan-ninhydrin (CHIT-NH) bio-conjugate for using as reducing agent of Au precursor at 37 °C. They claimed that this new reducing agent can overcome the non-uniform spatial distribution of stabilizers to form organized one-dimensional assemblies of Au NPs with average diameter of about 18 nm [114]. Long *et al.* used oligo-chitosan [$(GlcN)_x$] as stabilizer to prepare biocompatible Ag NPs from $AgNO_3$ at room temperature. Their NPs were stable at pH range of 1.8-9.0 and their average sizes were between 5 and 15 nm. They found that Ag NPs can be stable in NaCl solution; however, they are aggregated in the presence of $NaNO_3$ or NaH_2PO_4 [141]. Laudenslager *et al.* used CTS and carboxymethyl chitosan (CMC) as stabilizing agent for production of Pt, Au and Ag NPs. These two biopolymers gave similar size distributions, while CMC showed higher

aggregation due to lower availability of amines and the reduced cross-linking ability. The average sizes of Pt, Au, and Ag NPs were about 3.5, 23, and 7.5 nm respectively. According to their FTIR data, the amine and amide functionalities had the most interaction in CTS, while in CMC, the alcohol functionalities played this role [142]. Although CTS is a green reagent, using $NaBH_4$ as reducing agent indicates that the process is not totally green. Huang and Yang utilized CTS and heparin as reducing and stabilizing agents at 55 °C in synthesis of Au and Ag NPs respectively. Their results suggested that amino groups in chitosan and sulfonic groups in heparin can provide enough electrostatic attractive force for the formation and stabilization of the Au and Ag NPs. They observed an increasing trend in the size of the Ag NPs while increasing the concentration of Ag^+ or heparin. The particle sizes of CTS stabilized Au NPs and heparin stabilized Ag NPs were in the range of 7-20 nm and 9-29 nm, respectively [143].

Raveendran *et al.* reported a method for the synthesis of Au, Ag, and Au-Ag NPs in aqueous media, using glucose as the reductant and starch as stabilizer. The prepared bimetallic NPs were uniform and their sizes were within the quantum size domain (less than10 nm), where their electronic properties are size-dependent. They observed no signs of aggregation even after several months of storage [26, 108]. He *et al.* reduced $[Ag(NH_3)_2]^+$ ions by glucose in aqueous solution and then they added $Al(NO_3)_3$ into solution to synthesize Ag nanosheets. They claimed that the in situ generated $Al(OH)_3$ influenced the formation of Ag nanosheets. The produced nanosheets in 60 min reaction had a thickness of 20-30 nm [111]. Sun and Li produced colloidal carbon micro and nanospheres from glucose in a hydrothermal process (at 160-180 °C for 4-20 h) and used this functionalized carbon for in situ encapsulation of Ag and Au NPs. The size of the produced NPs with this method could be controlled in the range of 8-50 nm [144]. In a similar work, Yu and Yam used D-glucose in a hydrothermal process for synthesis of Ag NPs. As depicted in Figure 2.1.1 and Figure 2.1.2, they achieved interesting assembles of particles, such as cube, triangle, wire and spheres [145].

Soukupova *et al.* reduced the complex cation of $[Ag(NH_3)_2]^+$ by D-glucose to achieve Ag NPs in a single-step process. They studied the influence of different surfactants i.e. cationic (Cetyltrimethylammonium chloride: CTAC), anionic (sodium dodecylsuphate: SDS) and non-ionic (Tween 80) at 20 °C on fundamental characteristics of Ag NPs. They found that in comparison to unmodified NPs, non-ionic

surfactants can improve the polydispersity from 8.5% to 2.5%, and ionic surfactant can reduce the zeta potential of Ag NPs from -20 to -50 mV that is favorable to stabilization. They concluded that non-ionic surfactants can form a layer with inhibition function to prevent the formation of other nuclei and consequently lead to production of monodisperse NPs [100]. Lu *et al.* prepared super-paramagnetic Fe_3O_4 NPs utilizing gluconic acid as stabilizing agent and α-D-glucose as reducing agent at mild temperature (80 and 60 °C) in aqueous media. They obtained spherical NPs with comparable size (~12.5 nm) and polydispersity to conventional methods [90]. Darroudi *et al.* produced Ag NPs with gelatin and glucose as reducing and stabilizing agent for Ag^+ ions in aqueous media. They investigated the effect of temperature (28, 40 and 60 °C) on particle size and found that the size of NPs decrease with increasing temperature. They also observed that using gelatin solutions resulted in smaller particle size compared to gelatin-glucose solutions, due to the rate of reduction reaction. Their instrumental analysis including XRD, UV-Vis spectrometry, TEM, and AFM confirmed the formation of NPs with a quite narrow distribution of particle size. The size of their NPs was less than 15 nm [21]. Kvıtek *et al.* compared the performances of four different sugars including xylose, glucose, fructose and maltose in reduction of $AgNO_3$ in the presence of ammonia and production of spherical Ag NPs in a single-step reduction process at 20 °C. They found that decreasing the ammonia content from 0.2 M to 0.005 M can decrease the particle size from 380 down to 45 nm. For higher concentration of ammonia (0.2 M) there are slight differences in the particle sizes of Ag NPs produced by the four sugars (352-380 nm). But at low ammonia concentration (0.005 M), the average size of particles in the case of fructose (161 nm) are three times more than other sugars (47-57 nm) [57]. In a similar study, they used galactose and lactose as reducing agents and achieved Ag NPs with the average particle size of 50 and 35 nm at 0.005 M ammonia concentrations [65]. In another work, they produced spherical Ag NPs with an average diameter of 26 nm, and polydispersity of 2.3%. They also investigated the capability of different ionic and non-ionic surfactants and also polyethylene glycol (PEG) and polyvinylpyrrolidone (PVP) in surface modification and stabilization of Ag NPs produced by reaction of $AgNO_3$ and D-maltose. According to their results, sodium dodecyl sulfate (SDS), polyoxyethylenesorbitan monooleate (Tween-80) and PVP (MW: 360000) were superior stabilizers for aggregation of Ag NPs [64].

Tai *et al.* used starch and glucose to reduce $AgNO_3$ to Ag NPs in a spinning disk reactor (SDR). Their reaction at room temperature took place in 10 min and the sizes of their NPs were less than 10 nm. They observed that high $AgNO_3$/starch ratio or high glucose concentration can increase the yield up to 70%. They also found that the selection of pH and dispersing agent are highly influential in size measurement [146]. Deka *et al.* prepared starch-Au NPs composite by ultra-sonication for 20 min at 25 °C and used α-amylase for enzymatic release of Au NPs. Their TEM analysis showed well-dispersed spherical NPs with 10-30 nm diameter [83]. Vigneshwaran *et al.* utilized soluble starch as reduction and stabilization agent in synthesis of Ag NPs at 121 °C and 15 psi for 5 min. The sizes of prepared NPs were in the range of 10-34 nm. They observed no aggregation in aqueous solution over three months at ambient temperature. They confirmed the entrapment of Ag NPs inside the helical chains of amylose by iodometric titration method [87]. Li *et al.* produced Cd-Se bimetallic NPs using sodium selenosulfate (Na_2SeSO_3) as precursor and soluble starch as stabilizer at ambient temperature and pressure within 2 h. Their NPs were of the cubic structure with the average particle size of 3 nm according to XRD analysis and Debye-Scherrer equation [147]. Xia *et al.* used renewable degraded pueraria starch (DPS) as reducing and capping agent for the synthesis of Au-Ag bimetallic NPs at room temperature within ~24 h. They claimed that most of the synthesized particles had uniform spherical morphology with average diameter of 32 nm [104].

Kemp *et al.* synthesized Au and Ag NPs using 2, 6-diaminopyridinyl heparin (DAPHP) and hyaluronan (HA) as both reducing and stabilizing agents and $HAuCl_4$ and $AgNO_3$ as precursors at 70 °C. Both reducing agents resulted in high stability under physiological conditions, though the particles size distribution for heparin was narrower (7 nm for Ag and 10 nm for Au) than that of hyaluronan (5-30 nm for both Au and Ag NPs) since diaminopyridine group in heparin formed stronger bonds with NPs. According to their study, Au- and Ag-heparin NPs show considerable anticoagulant and inflammatory properties which is promising for various applications [70]. In a similar report, they used DAPHP and HA for production of Ag NPs from $AgNO_3$ and studied their antimicrobial properties. According to this study, Ag-HA and Ag-DAPHP are more stable at physiological salt concentrations than metallic NPs and they show remarkable antimicrobial activity [55]. In another study, they found that Ag- and Au-

DAPHP have potential applications in treatment of angiogenesis accelerated disorders, such as cancer and inflammatory diseases [71].

Cai *et al.* used the nanoporous structure of cellulose hydrogels to synthesize and stabilize Ag, Au, and Pt NPs through hydrothermal process. They found that by increasing $AgNO_3$ concentration, the particles size increases gradually from 8 to 11.4 nm at 80 °C and 24 h. Also, reaction time and temperature had direct influence on particle size. The average sizes of Ag, Au and Pt NPs, calculated by Scherrer equation, were 12.3, 6.5, and 4.4 nm respectively. The particle sizes, obtained by TEM analysis, were in good agreement with Scherrer equation [37]. Chen *et al.* employed carboxymethyl cellulose sodium (CMS) both as reducing and stabilizing agent for production of Ag NPs from $AgNO_3$. They employed microwave with the heating power of 0.4 kW to enhance the hydrolysis of CMS in the absence of catalyst in aqueous solution and used CMS hydrolyzate to reduce Ag ion. They found that decreasing $AgNO_3$ and increasing CMS concentration (0.04% for 0.1 mM $AgNO_3$) will lead to smaller NPs. According to their results, the concentration of CMS has very small effect on distribution of particle size, while an increase in the concentration of $AgNO_3$ results in broader size distribution. The NPs produced in this method had an average size of about 15 nm [17].

Jang *et al.* used dextran, a readily available polysaccharide, both as reducing and stabilizing agents to synthesize dex-Au NPs from $HAuCl_4$. The stability of Au NPs is enhanced due to cross-linking of aminated dextran chains on the surface of NPs using epichlorohydrin (C_3H_5ClO). The average diameters of their NPs were 80 nm [82]. Morrow *et al.* used diethylaminoethyl-dextran as reducing and stabilizing agents to produce Au NPs from Au^{3+} solution at 50 °C for 7.5 h. They found that the performance of dextran is strongly dependent on pH so that in alkaline solutions, the Au^{3+} ions are rapidly reduced to spherical NPs and their sizes range from 18 to 40 nm depending on pH, temperature, and the Au^{3+}/dextran ratio. However, in acidic conditions, the reduction is very slow and large Au NPs with different shapes are formed [35].

Saha *et al.* utilized calcium alginate gel beads as a template for Ag and Au NPs through a green photochemical process using UV light source (365 nm wavelength) for 40 min. In this process, alginate can serve as both reducing and stabilizing agents. The particles had spherical morphology and their sizes were less than 10 nm for both

Ag and Au. Their sorption experiment showed that the loading of Au on calcium alginate is more compared to Ag [98].

Venkatpurwar and Pokharkar mentioned a single step method for synthesis of Ag NPs by using sulfated polysaccharide extracted from marine red algae (*Porphyra vietnamensis*) in a 15 min reaction at 70 °C. The produced NPs showed SPR centered at 404 nm with average particle size measured to fall within the range of 13 nm. Their FTIR study admitted the role of sulfate groups of polysaccharide in reduction of $AgNO_3$. Also, the zeta potential measurement (-35.05 mV) confirmed the capping of anionic polysaccharide on the surface of NPs which is responsible for the electrostatic repulsion and consequently stability at wide range of pH (2-10) and electrolyte concentration (up to 10^{-2} M of NaCl) [63].

Thekkae Padil and Cernik used gum karaya (GK) to produce Copper oxide (CuO) NPs from $CuCl_2$ at 75 °C for 60 min. According to their FTIR results, different sugars, amino acids and fatty acids are responsible for reduction and stabilization processes. They also observed that by changing the concentration of precursor, one can obtain NPs with average particle diameter from 7.8 nm to 4.8 nm [89].

Polyols

Shameli *et al.* used polyethylene glycol (PEG) and β-D-glucose as stabilizing and reducing agents respectively to produce colloidal Ag NPs from $AgNO_3$ at 60 °C. They studied the properties of Ag NPs at different reaction times and found that the average particle sizes were 10.60, 11.23, 15.30 and 25.31 nm for different mixing times of 3, 6, 24 and 48 h, respectively. According to zeta potential of 54.5 mV, they concluded that the synthesized Ag NPs has acceptable stability [4]. In another study, they studied the antibacterial activity of different sizes of Ag NPs against two different bacteria and observed that Ag NPs with smaller size have more antibacterial activities [62]. Li *et al.* synthesized Ag NPs using PEG-200 as reducing and stabilizing agent and $AgNO_3$ as precursor at ambient temperature within 6 h. Their analysis showed that the Ag NPs are spherical and stable for several weeks and the particle sizes are less than 5 nm. PEG can also act as environmentally-friendly solvent and its hydroxyl groups can form complexes with metallic ions and consequently reduce them to NPs [110]. Likewise, Yan *et al.* used PEG-400 to produce Ag NPs at room temperature from $AgNO_3$ in 10 h. Relatively narrow size distributions were apparent for the products. Similarly, the

NPs were in the size range from 8 to 10 nm [148]. In another study, Roy and Lahiri tried to synthesize radioactive ^{198}Au NPs using PEG-4000 as reducing agent without any other organic solvent. Their particle sizes ranged from 15 nm to 20 nm [149]. Chin *et al.* used PEG as the solvent and stabilizer for producing Fe_3O_4 NPs by thermal decomposition of iron acetylacetonate ($Fe(acac)_3$) that is a non-toxic precursor. They found that by changing reaction time and concentrations of precursor and surfactants, one can control the shape and size of Fe_3O_4 NPs. According to them, the average size of Fe_3O_4 NPs increases from 2 nm to 7 nm when the concentration of precursor increases from 0.1 mmol to 8 mmol [91].

Zhang *et al.* used tannic acid (TA), a water-soluble polyphenol, as the reducing agent to prepare Ag NPs supported on graphene (Ag NPs-GN) in a single-step process for 90 min. They reacted $AgNO_3$ and graphene oxide (GO) with TA simultaneously and observed that GO sheets were impregnated with many Ag NPs with the diameters of several nanometers to 20 nm [73].

Kasthuri *et al.* synthesized anisotropic Au and quasi-spherical Ag NPs using apiin to reduce $AgNO_3$ and $HAuCl_4$ at room temperature within 60 sec. Apiin, an extracted compound from parsley and celery, has eight OH groups and can act also as stabilizing agent. They observed that the size and morphology of the synthesized NPs can be controlled by changing the precursor/apiin ratio. According to their TEM micrographs, the average sizes of the Au and Ag NPs were 21 and 39 nm respectively [38].

Carboxylic acids

Lai *et al.* produced superparamagnetic Fe_3O_4 NPs from $FeCl_3$ using mixture of water/glycerol as solvent and L-arginine as stabilizing agent. L-arginine is an amino acid that is naturally produced and therefore it is considered as a green reagent. The average size of the synthesized Fe_3O_4 NPs is reported to be 13 nm [92]. Although they employed the green reagents for production of NPs, using autoclave at 200 °C and for 6 h increased the energy requirement of the whole process. In another study, Hu *et al.* reduced Ag^+ to Ag NPs using L-lysine or L-arginine, and stabilized it with soluble starch. In comparison to Lai *et al.* they reduced the energy requirement using microwave irradiation for 10 sec at 150 °C. According to the TEM micrographs, the average particle size of the produced Ag NPs was 26.3 nm. They found that increasing the

microwave power from 30 to 120 W can reduce the heating time and particle size from 23 to 28 nm [112].

Kora *et al.* synthesized Ag NPs from $AgNO_3$ in an autoclave at 120 °C and 15 psi. In their reaction, gum kondagogu (*Cochlospermum gossypium*), a natural biopolymer with several hydroxyl and carboxylate groups, was used as a reducing and stabilizing agent. They studied the influence of gum particle size, gum concentration, $AgNO_3$ concentration and reaction time on the synthesis of Ag NPs and found that by increasing gum and $AgNO_3$ concentration, the efficiency of NP production is enhanced. Likewise, by increasing the autoclaving time, more hydroxyl groups are converted to carbonyl groups which in turn increase the reduction of Ag ions. The average size of the synthesized spherical NPs was around 3 nm [54]. In another study, they used gum ghatti (*Anogeissus latifolia*) as a reducing and stabilizing agent for synthesis of spherical Ag NPs from $AgNO_3$. They observed that by increasing reaction time, the efficiency of NP synthesis increases and it is attributed to the higher reduction capacity of the gum. They concluded that hydroxyl and carboxylate groups of the gum help the complexation of Ag ions during process [66].

Kumar *et al.* used amino acid based phenolic compounds as reducer and stabilizer for production of Ag NPs from $AgNO_3$ at room temperature. They stated that amino acids have reactive OH groups and their structural variations can result in production of spherical and prism-like NPs [22].

Polyoxometalates

Polyoxometalates (POMs) are kinds of anionic structures with transition metal atoms in their highest oxidation state. These materials can exhibit tremendous structural variety and interesting properties such as reversible electron exchange behavior that make them ideal candidates for homogeneous-phase electron transfer processes [150, 151]. POMs, can be used in synthesis of metallic NPs, since their solubility in water and capability for participating in multi-electron redox reactions without structural changes [152].

Zhang *et al.* studied the capability of the mixed-valence polyoxometalate β-$H_3[H_4P(Mo^V)_4(Mo^{VI})_8O_{40}]^{3-}$ (POM) both as a reducer and a stabilizer at room-temperature. They found that the morphology of the Au NPs can be modified by manipulating the initial concentrations of the POM and $HAuCl_4$. For C^0_{POM} = 0.5 mM

and [metallic salt]/[POM]=1, the size of NPs were less than 10 nm it decreased with reducing C^0_{POM} [151]. Zhang *et al.* used $K_9[H_4PV^{IV}W_{17}O_{62}]$ (HPV^{IV}) clusters as the reducer and stabilizer for production of Pd NPs from K_2PdCl_4 in acidic aqueous solutions. They also admitted that the starting molar ratio of precursor to POM has influence on formation of Pd NPs and reported different size (15-50 nm) for NPs in different precursor to POM ratios [150]. Also, Troupis *et al.* used $K_4[SiW_{12}O_{40}]$ as reducer, photo-catalyst, and stabilizer for production of Au, Ag, Pt and Pd NPs in aqueous solution at pH 5. They used a 1000 W Xenon arc lamp as illumination source to trigger the reaction. The Au and Ag particles were spherical with a diameter of 13.1 nm and 15.3 nm, respectively. However, Pd and Pt NPs had unclear morphology with the size of 5.0 nm and 2.7 nm [134]. Keita *et al.* used oxothiometalate, $Na_2[Mo_3(\mu_3$-$S)(\mu$-$S)_3(Hnta)_3]$, as reducer and stabilizer for production of Au NPs in aqueous medium at room temperature. The majority of their particles ranged from 9 to 10 nm. They also found that the ratio of Au precursor to POM governs the dispersion of shapes and sizes so that by increasing this ratio from 2 to 4, the size of particle increase from 5 to 54 nm [36]. In a related report, they used mixed valence POMs (Mo^V-Mo^{VI}) including $H_7[\beta$-$P(Mo^V)_4(Mo^{VI})_8O_{40}]$ (1), $(NH_4)_{10}[(Mo^V)_4$-$(Mo^{VI})_2O_{14}(O_3PCH_2PO_3)_2$ $(H_2OPCH_2PO_3)_2].15H_2O$ (2), and $[\in$ $P(Mo^V)_8(Mo^{VI})_4$ $O_{36}(OH)_4(La(H_2O)_{2.5}Cl_{1.25})_4].27H_2O$ (3), to produce Pt and Pd NPs from K_2PtCl_4, K_2PdCl_4, and $PdSO_4$ as precursors in aqueous media at room temperature. The stabilization capability of these mixtures followed the order of 1 > 2 >> 3. In the case of POM (1) and POM (2) the precursor to POM ratio did not affect the size of NPs but for POM (3) the average size of the NPs increases from 1.7-2 nm to 2.5-4 nm by increasing the precursor to POM ratio from 1 to 2 [153]. They also used α_2-$H_4PV^VW_{17}$ (POMs) to reduce $[PdCl_4]^{2-}$ to Pd NPs and reported a narrow distribution around 3 nm for NPs [154]. Dolbecq *et al.* used two POMs namely $(NH_4)_{18}[(Mo^V_2O_4)_6$-$(OH)_6(O_3PCH_2PO_3)_6].33H_2O$ (1) and $[(Mo^V_2O_4)_3(O_3PCH_2PO_3)_3(CH_3AsO_3)]$. $19H_2O$ (2) for synthesis of Pt and Pd NPs from K_2PtCl_4 and K_2PdCl_4. Similarly, they observed that the nature of POMs and the precursor to POM ratio can influence the size of NPs [155].

Alcohols

Chen *et al.* studied the fabrication of Pt-Pd bimetallic NPs using ethanol, as reducing agent under mild reaction conditions, and graphene nano-sheets (GNs), as supporting material. As it was expected, changing the molar ratio of the starting precursors, determine the shape of NPs on GNs. They also tried carbon black as support for NPs. According to their calculations, the particle sizes were 7.9 nm for Pt-Pd NPs supported on GNs, 10.2 nm for Pt-Pd NPs on carbon black, 17.3 nm for Pd NPs on GNs and 20.4 nm for flower-like Pt NPs supported on GNs [107]. Safaepour *et al.* studied the capability of geraniol for reduction of $AgNO_3$ to Ag NPs in aqueous solution of PEG-4000 using a microwave oven (with power of 850 W) for 40 sec. The sizes of produced NPs ranged from 1 to 10 nm with an average size of 6 nm [47].

Others reagents

Guidelli *et al.* studied the production of Ag NPs from $AgNO_3$ solution using natural rubber latex (NRL) extracted from *Hevea brasiliensis* at 100 °C for 60 min. Their NPs ranged from 2 nm to 100 nm and were spherical. According to their results, lower $AgNO_3$ concentration led to formation of smaller particles and higher $AgNO_3$ concentration can lead to formation of aggregates. Using FTIR spectra, they found that the ammonia which is used for conservation of the NRL, participate in the reduction of Ag ions and also the *cis*-isoprene moieties help stabilization of NPs [8]. Li *et al.* produced bimetallic Pd-Ag NPs from $AgNO_3$, K_2PdCl_4 using graphene oxide (GO) nanosheets as reducing agent, support and stabilizer. The synthesis process took place at 84 °C for 3 h for reduction of metallic ions and 200 °C for 24 h for reduction of GO. The produced bimetallic NPs were smaller than 10 nm [105]. Different green reagents that researchers tested for synthesis of NPs, are listed in Table 2.1.2. The molecular structures of different green reagents are depicted in Figure 2.1.3.

Phytochemicals

Phytochemicals are compounds that occur in plants and have disease preventive or protective capabilities for human. They are not essential for human body to survive but they can act as antioxidant, enzyme stimulator, antibacterial and they can interfere with DNA to prevent from multiplication of cancer cells. In recent years, researchers found that several phytochemicals, such as terpenoids and flavonoids can be employed in reduction of metal precursors to NPs [67, 156]. This synthesis method

has the advantages of other biological methods including low cost and being environmentally friendly [157]. However they should be thoroughly studied for specific applications.

Plant-derived components

Leela and Vivekanandan investigated the capability of leaf extracts of different plants including *Helianthus annus*, *Basella alba*, *Oryza sativa*, *Saccharum officinarum*, *Sorghum bicolour* and *Zea mays* for the reduction of Ag precursor. They found that *H. annus* has strong potential for reduction of Ag ions and therefore it is promising in the development of Ag NPs [50]. Also Song and Kim used five plant leaf extracts including *Pinus desiflora*, *Diopyros kaki*, *Ginko biloba*, *Magnolia kobus* and *Platanus orientalis* for synthesis of Ag NPs from $AgNO_3$. They found that the extract of *Magnolia kobus* was the best reducing agent for synthesis of Ag NPs. They observed that for *Magnolia Kobus*, the final conversions were 60% and 100% at 25 and 55 °C respectively and the average particle size ranged from 15 to 500 nm [7].

Begum *et al.* investigated the performances of three different aqueous extracts from Black Tea leaf in the formation of Ag and Au NPs from $AgNO_3$ and $HAuCl_4$. They used water soluble, water-ethyl acetate ($C_4H_8O_2$) soluble and water-dichloromethane (CH_2Cl_2) soluble compounds of black tea for reduction of precursors and stabilization of NPs. They observed that the first two extracts can efficiently lead to rapid formation of stable NPs with different shapes including spheres, trapezoids, prisms and rods. While, in the case of the third extract, no NP generation was detected under similar reaction conditions. Therefore, they concluded that polyphenols, such as flavonoids that are soluble in water and ethyl acetate, but are insoluble in dichloromethane are responsible for metallic ion reduction [24]. In another investigation, Moulton *et al.* used aqueous tea extract at different concentrations to reduce $AgNO_3$ to Ag NPs at room temperature and obtained spherical NPs with controllable size (11 nm to 30 nm). According to their microscopy analysis, they suggested that keratinocytes are responsible for stabilization of NPs [32]. Also, Nadagouda *et al.* used coffee and tea extracts to produce Ag and Pd NPs from $AgNO_3$ and $PdCl_2$ at room temperature. They obtained NPs in the size range of 20-60 nm and suggested that the Ag and Pd NPs were capped and stabilized by organic molecules such as polyphenols and caffeine [51]. In another study, Nune *et al.* used aqueous tea extract to reduce $NaAuCl_4$ to Au

NPs within 10 min. Their particles were spherical and in the size range of 15-45 nm [79].

Awwad and Salem worked on several phytochemicals with reducing capability to produce Ag NPs from AgNO$_3$ at room temperature. They used aqueous extract of *mulberry* leaves in the reduction process of AgNO$_3$ for 60 min. The produced NPs in this process were spherical and ranged from 20 to 40 nm [58]. In another work, Awwad *et al.* used the aqueous extract of carob leaf (*Ceratonia siliqua*) as reducing and stabilizing agents in a 2 min reaction. The polydispersed NPs were spherical, and their sizes ranged from 5 to 40 nm with an average size of 18 nm. Their FTIR study showed that the carboxyl, hydroxyl, and amine groups in the both leaf extracts are accountable for reduction of Ag$^+$ ions to Ag NPs and the protein portion of leaf extract can play the role of both reducing agent and stabilizer for Ag NPs [45].

Ravindra *et al.* used aqueous extracts of *Eucalyptus citriodora* and *Ficus bengalensis* to produce Ag NPs with the size of around 20 nm at room temperature within 2-5 min. They conducted two different experiments under sunlight and in dark and observed that sunlight does not have any significant effect on the formation of Ag NPs [67].

In the same work, Saxena *et al.* employed the leaf extract of *Ficus benghalensis* as reducing and stabilizing agent and for production of Ag NPs in 5 min at 50-60 °C. Their analysis showed that phenolic compounds with hydroxyl and ketonic groups are responsible for reduction of Ag ions. The synthesized particles were mono-dispersed and spherical with a diameter range of 16 nm [13].

Philip used aqueous leaf extract of fresh/dry *Mangifera indica* as a reducing agent for synthesis of nearly monodispersed spherical Au NPs from HAuCl$_4$ at ambient conditions. The reaction time was 2 min and they obtained NPs with an average size of around 18 nm. He found that the colloidal product was stable for more than 5 months. He also observed that dried leaf extract lead to smaller and more uniformly distributed particles in comparison to fresh ones [158]. He also used this extract for synthesis of Ag NPs from AgNO$_3$ at two different temperatures and pH and found that increasing pH and temperature accelerated the reaction and influenced the morphology of particles. According to the results, at pH 8, there are well-dispersed triangular, hexagonal and nearly spherical NPs with the average size of 20 nm. He also identified flavonoids, terpenoids and thiamine as the reducing compounds present in *Mangifera Indica* [43]. In another work, he used the leaf extract of *Hibiscus Rosa*

sinensis as a reducing agent for synthesis of Ag and Au NPs. The ratio of metal salt to extract influenced the size and shape of Au NPs. He observed triangular, hexagonal, dodecahedral and spherical shapes for Au NPs. In case of Ag NPs, he found that changing the reaction medium pH in the range of 6.8 to 8.5 resulted in different shapes. The FTIR spectra showed that Au NPs had interaction with amine groups and the Ag NPs with carboxylate ion groups [84].

Noruzi *et al.* used the aqueous extract of rose petals as reducing agent for production of $HAuCl_4$ to Au NPs within 5 min at room temperature and investigated the effects of concentrations of Au precursor and extract. Their TEM micrographs and XRD patterns showed that the synthesized NPs had various shapes with average size of 10 nm. FTIR study showed that primary amine ($-NH_2$), carbonyl, -OH and other functional groups involved in reduction of precursor and stabilization of NPs [20]. Nagajyothi *et al.* synthesized Ag and Au NPs from $AgNO_3$ and $HAuCl_4$ by using the aqueous extract of *Lonicera japonica* flower as a reducer and a stabilizer at 70 °C for 30-60 min. They obtained spherical, triangular and hexagonal Ag and Au NPs with average size of 7.8 and 8.02 nm respectively [25].

Sulaiman *et al.* prepared the leaf extract of *Eucalyptus chapmaniana* (*E. chapmaniana*) to produce Ag NPs from $AgNO_3$ at 50 °C for 60 min. The average sizes of produced NPs were estimated to be around 60 nm determined using Scherrer's formula [6]. Smitha *et al.* used leaf broth of *Cinnamomum zeylanicum* to reduce $HAuCl_4$ to Au NPs in 60 min reaction. Within this reaction, a mixture of Au nano prisms and spheres were formed so that lower concentrations of the extract resulted in more prism shaped particles, while higher concentrations favored formation of spherical particles. The average particle size was around 25 nm at higher concentrations of the extract. According to the FTIR study, they concluded that enzyme or proteins of leaf broth can reduce the Au ions [39].

Gnanasangeetha and SaralaThambavani investigated the effect of aqueous leaf extract of *Corriandrum sativum* in the production of ZnO NPs through reduction of $Zn(CH_3COO)_2$ with NaOH at room temperature for 2 h. According to their results, using this phytochemical compound can stabilize the NPs and reduce the particle size from 81 to 66 nm [46]. Zhan *et al.* simultaneously reduced $HAuCl_4$ and $PdCl_2$ by aqueous leaf extract of *Cacumen Platycladi* to produce Au-Pd bimetallic NPs with average size of 7 nm. The reaction took place in 2 h and the C=O and C-O groups in the extract

stabilized NPs. They also concluded that the water-soluble polyhydroxy biomolecules, such as flavonoid and sugar, are accountable for the reduction of metallic ions [106]. Swamy *et al.* reduced $AgNO_3$ to Ag NPs using methanolic leaf extract of *Leptadenia reticulata* (*L. reticulata*) at room temperature for 8 h. The produced NPs were spherical and their sizes ranged from 50 to 70 nm. They attributed the reduction of Ag ions to phenolics, terpenoids, polysaccharides, and flavone compounds [49]. Dipankar and Murugan synthesized Ag NPs from $AgNO_3$ by utilizing the aqueous leaf extracts of *Iresine herbstii* as reducing agent. The process was carried out in dark and at room temperature but it took 7 days to complete. The produced NPs were poly dispersed and their sizes ranged from 44 to 64 nm [48].

Shameli *et al.* extracted the tuber-powder of *Curcuma longa* (*C. longa*) into water for reducing $AgNO_3$ to Ag NPs at room temperature (25 °C) for 24 h. The produced NPs had an average diameter of 6.30 nm. From FTIR spectra, they concluded that the aldehyde groups in *C. longa* involved in Ag ions reduction and other groups, such as hydroxyl (-OH), amine (-NH) and aliphatic C-H involved in the capping of the NPs [42]. In another study, they extracted the stem bark of *Callicarpa maingayi* into methanol/water solution to use as reducing and stabilizing agents. This time, Ag NPs were spherical with the average diameter of 12.40 nm and same functional groups were identified to be involved in reduction and stabilization processes [115]. Zargar *et al.* synthesized spherical Ag NPs with an average size of 18.2 nm using methanolic leaf extract of *Vitex negundo* (*V. negundo*) as a reducing agent for $AgNO_3$ in a 48 h reaction at room temperature. Their results showed that *V. negundo* played an important role in the reduction and stabilization of Ag ions to Ag NPs [5]. In comparison to other investigations, it seems that the reaction rate of these two procedures at room temperature is not quite enough to implement in practical applications.

Kumar *et al.* studied the effect of pH on reduction of $AuCl_3$ to Au NPs in the presence of aqueous leaf extract of *Cassia auriculata* within 10 min at room temperature (28 °C). They found that changing pH in the range of 3.4-10.2 had no effect on the stability of the Au NPs. The produced NPs in pH 3.4 were a mixture of triangular and spherical shape with size of 15-25 nm. [74]. Also Mata *et al.* investigated the effect of pH on the reduction performance of biomass of the brown algae *Fucus vesiculosus* in the solution of $HAuCl_4$ at room temperature (23 °C). They found that maximum uptake

were obtained at pH 7 and hydroxyl groups in the algal polysaccharides were accountable for Au reduction [113].

Singh *et al.* synthesized Ag NPs from $AgNO_3$ using the aqueous leaf extract of *Argemone maxicana* as reducing and stabilizing agent at room temperature for 4 h. The XRD study showed that the produced Ag NPs has a mixture of cubic and hexagonal structures with the average size of 30 nm [9]. Das *et al.* used ethanolic leaf extract of *Centella asiatica* as reducing and stabilizing agent to synthesize Au NPs by reduction of $HAuCl_4$ at room temperature (25 °C). TEM studies showed the particles to be of various shapes and sizes. They observed that Au NPs had an average size range of 9.3-10.9 nm and they were stabilized by a coating of phenolic compounds [88].

Bar *et al.* synthesized Ag NPs from $AgNO_3$ by using the water dispersion of extract of *Jatropha curcas* as reducing and stabilizing agents. This reaction is completed in 15 min at 80 °C. They observed that the particles had diameter of 20-40 nm and were stabilized by the cyclic peptides present within the dispersion. FTIR showed peaks for carbonyl groups of the acid groups of different fatty acids, amide I and II which are responsible for reduction of Ag ions and stabilization of Ag NPs [76]. In another work, they carried out same experiment using aqueous seed extract of *Jatropha curcas* as reducing and stabilizing agents. They observed that by changing $AgNO_3$ particles with diameter ranging from 15 to 50 nm can be produced. Similarly, they identified same functional groups in *Jatropha curcas* for reduction of Ag ions [102].

Banerjee *et al.* used the leaf extracts of three different plants including *Musa balbisiana* (banana), *Azadirachta indica* (neem) and *Ocimum tenuiflorum* (black tulsi) to reduce $AgNO_3$ to Ag NPs in microwave oven for 4 min discontinuously. The smallest NPs were obtained using banana leaf extracts (80.2 nm). According to their FTIR study, compounds, such as flavonoids and terpenoids are responsible for stabilization of Ag NPs [109]. Basha *et al.* synthesized spherical Au NPs with the size of 4-24 nm using the extract of *Psidium guajava* (*P. guajava*). They used UV-vis spectra, FTIR, NMR and GC-MS techniques to analyze the extract of *P. guajava* and found that guavanoic acid is a responsible compound for reduction of $HAuCl_4$ to Au NPs [75].

Jha *et al.* investigated three different plant extracts including *Bryophyllum sp.*, *Cyprus sp.* and *Hydrilla sp.* to reduce $AgNO_3$ to Ag NPs at 40 °C in a 10 min reaction. The produced NPs ranged from 2 to 5 nm. They concluded that the reduction of Ag ions

were carried out by water soluble compounds, such as flavones, quinones and organic acids including oxalic, malic, tartaric and protocatechuic [159]. They also used *Eclipta* leaves to reduce the same Ag precursor and produced spherical particles in the range of 2-6 nm [160].

Krpetic *et al.* extracted two components from Cape aloe, namely aloin A and aloesin, to act as stabilizers in the synthesis of Au and Ag NPs from $NaAuCl_4$ and $AgNO_3$. They studied the effects of temperature, reaction time, and reducing agent concentration on particles size and shape of NPs. By changing the concentration of reducing agent ($NaBH_4$) from 0.1 to 0.01 M, and temperature from 25 to 55 °C, the average size of Au NPs increased from 4 to 45 nm for aloesin from 6 to 35 nm for aloin A [161]. Wang *et al.* used the aqueous extract of *Scutellaria barbata* as the reducing agent for $HAuCl_4$ and observed that 3 h is required for conversion of most of Au ions to Au NPs in the size range of 5-30 nm at the room temperature [77]. Xie *et al.* used aqueous extract of algae *Chlorella vulgaris* for reduction of $AgNO_3$ to Ag nanoplates in a 12 h reaction at room temperature. The thickness of the Ag nanoplates was 20 nm and the algal proteins were found to be responsible for the reduction of Ag ions to Ag nanoplates [59].

Chandran *et al.* used aqueous leaf extract of *Aloe Vera* to reduce $HAuCl_4$ to triangular Au NPs. They claimed that the employed procedure has control over the size of the triangular Au NPs in the range of 50 to 350 nm, by adjusting the concentration of *Aloe Vera* extract, which is favored for tuning their optical properties. Size of Au NPs can be controlled [41]. Also, Shankar *et al.* produced triangular Au NPs from $HAuCl_4$ using the extract of the lemongrass plant as reducing agent and observed that the produced NPs have considerable absorption in the near-infrared (NIR) region [40]. They also used the proteins/enzymes extracted from leaves of Geranium (*Pelargonium graveolens*) to reduce Ag ions to Ag NPs with an average size of 27 nm [162]. Gardea-Torresdey *et al.* studied the reducing capability of alfalfa biomass for production of Au NPs from solutions of $K(AuCl_4)$. The microscopic analysis showed five different types of Au NPs including FCC tetrahedral, hexagonal platelet, icosahedral multiple twinned, decahedral multiple twinned and irregular shaped particles. They also observed that smaller NPs were formed in low pH ($\approx$ 2) [163]. Aromal and Philip fabricated Au NPs from $HAuCl_4$ using the aqueous extract of fenugreek seeds (*Trigonella foenum-graecum*) as reducer and stabilizer. In their process, NPs with different sizes from 15

to 25 nm can be produced by adjusting the dominant parameters, such as pH and extract amount. The FTIR study showed that flavonoids are accountable for reduction of Au ions and proteins are involved in stabilization of NPs [19]. In a similar study, they used the extract of *Macrotyloma uniflorum* (*M. uniflorum*) as a reducing agent for production of Au NPs and studied the effects of extract concentration, temperature and pH on the formation of NPs. According to their results, the reduction rate is very high at 100 °C and the product is more stable at pH 6 in comparison to other conditions. The FTIR study showed that phenolic compounds involved in reduction and the proteins stabilized the NPs [14]. Summary of different plants used for NPs synthesis is presented in Table 2.1.3.

Food-derived reagents

Rastogi and Arunachalam used the aqueous extract of garlic (*Allium sativum*) for production of Ag NPs from $[Ag(NH_3)_2]^+$ within 15 min. They performed their experiment under bright sunlight and claimed that it can act as catalyst. The produced NPs were poly-dispersed and spherical with the average size of 7.3 nm. They suggested that the proteins of garlic are involved in stabilization of Ag NPs [164]. Also, Ahamed *et al.* used garlic clove extract for synthesis of Ag NPs from $AgNO_3$ at 50-60 °C within 30 min. Their Ag NPs were spherical with an average diameter of 12 nm [15]. Li *et al.* extracted *Capsicum annuum* L. for its use as reductant for synthesis of Ag NPs from $AgNO_3$. They obtained spherical NPs with mean size of 10 nm. The FTIR study showed that the proteins, which contain amine groups, act as reducing agent in the production of Ag NPs. Also they found that with increasing reaction time, the sizes of the NPs increase [30]. Amin *et al.* prepared methanolic extract of *Solanum xanthocarpum berry* (*S. xanthocarpum berry*) to use as the reducing and stabilizing agents for the production of Ag NPs from $AgNO_3$. The size and shape of Ag NPs can be controlled by selecting the proper values for reaction parameters including reaction time, temperature and the volume ratio of *S. xanthocarpum berry* to $AgNO_3$ solution. They could produce mono-dispersed and spherical NPs with 10 nm in size at *S. xanthocarpum berry* to $AgNO_3$ ratio of 2:1 within 25 min at 45 °C [69]. Philip investigated the capability of honey for reduction of $HAuCl_4$ at room temperature and stabilizing the produced NPs. According to these results, anisotropic and spherical nanocrystals with the average size of 15 nm can be produced within 3 h. The FTIR

study revealed that fructose acts as the reducing agent protein that can bind with Au surface through the amine groups to stabilize the NPs [81]. In another study, the aqueous extract of *Volvariella volvacea* was prepared to act as reducing and stabilizing agent in the synthesis process of Au, Ag and Au-Ag NPs from $HAuCl_4$ and $AgNO_3$. The reaction time for Au and Ag were reported to be 2.5h and 6 h respectively. Au NPs ranged from 20-150 nm in size and had different shapes while Ag NPs were spherical with average size of 15 nm. Au NPs are bound to proteins through free amino groups and Ag NPs through the carboxylate group of the residue of amino acids [31]. Jain *et al.* prepared the aqueous extract of papaya fruit for synthesis of polydispersed Ag NPs from $AgNO_3$ at room temperature for 5 h. The produced NPs had hexagonal shape with the average particle size of 15 nm. FTIR analysis showed ethers and polyols groups which are considered to be responsible for the reduction of Ag ions [60]. Shukla *et al.* produce Au NPs by reduction of $NaAuCl_4$ with aqueous soybean extracts at 25 °C for 4 h. Their TEM analysis showed that the average size of the Soy-Au NPs were 15 nm. Akin to many researchers, they identified amino acids as the reducing groups in the formation of Au NPs [78]. Kumar *et al.* extracted the water soluble portion of *Terminalia chebula* (*T. chebula*) fruit and employed it for synthesis of several metals and metal oxide NPs. In first study, they produced Ag NPs from Ag_2SO_4 within 20 min. TEM study showed anisotropic NPs with less than 100 nm in size. They found that the hydrolysable tannins such as di/tri-galloyl-glucose can be hydrolyzed to gallic acid and glucose that consequently act as reducing agent. Furthermore, oxidized polyphenols are responsible for stabilizing the NPs [61]. In the second study, they reduced $HAuCl_4$ to Au NPs using aqueous seed extract of *T. chebula*. The reaction time was 20 sec and NPs were anisotropic with the size range of 6 to 60 nm. This time, they identified hydrolysable tannins as the responsible agent for reductions and stabilization [85]. In their third work, they used $FeSO_4$ and $PdCl_2$ as precursor of FeO and Pd NPs in pH around 2. The reaction time for FeO and Pd formation were 5 min and 40 min respectively. The TEM study showed amorphous iron NPs with less than 80 nm in size and cubic Pd NPs with less than 100 nm in size. They concluded that phytochemicals/polyphenols are responsible for reducing and stabilizing processes [16]. Singh *et al.* used the aqueous extract of *Dillenia indica* (*D. indica*) for producing Ag NPs from $AgNO_3$. The particles size of these Ag NPs ranges from 40 to 100 nm. This fruit is a potent source of ascorbic acid, α-tocopherol, β-

carotene and phenolic components [52]. These components may be accountable for reduction of Ag ions; however, the researchers did not study the reduction mechanism. Armendariz *et al.* investigated the binding trend of Au^{3+} ions to Oat (*Avena sativa*) biomass in a 60 min reaction at different pH from 2 to 6. They observed that at pH 3 (optimum condition) about 80 % of Au ions were adsorbed to biomass and Au NPs with average size of 20 nm and different shapes such as tetrahedral, decahedral and hexagonal were produced. They also found that the NPs produced at pH 2 are larger than NPs produced in pH 3 and 4. According to their analysis, functional groups such as carboxyl, amino and sulfhydryl that are present in the cell walls of the inactivated tissues of the plant, ca be accountable for reduction of Au ions [165]. Lu *et al.* used pomelo peel as a source for production of carbon NPs in a hydrothermal process at 200 °C for 3 h. The obtained NPs ranged from 2 to 4 nm and the quantum yield was 6.9% [93].

Energy saving processes

Energy transfer

Generally, there is some energy consumption in NPs synthesis either for obtaining required temperature or for direct reduction of metallic ions. Each synthesis route should be optimized in terms of energy consumption, reaction time and quality of NPs. In recent years, researchers have been working on new energy transfer techniques such as microwave, ultrasonic, gamma, ultraviolet (UV), and ion radiation to simultaneously reduce the reaction time and energy requirement and enhance the control on size and shape of NPs due to uniform heating of these techniques [10, 27]. Sudeep and Kamat used thionine as a sensitizing dye for Photoinduced reduction of $AgNO_3$ by visible light. They produced NPs in less than 60 min with 20 nm in size. They found that NPs were stabilized by thionine [28]. In another study, Dubas and Pimpan employed a low power ultraviolet (UV) irradiation source (8 W) as a reducing system to produce Ag NPs from $AgNO_3$. They also used poly methacrylic acid (PMA) as reducing and stabilizing agent and the reaction was completed within 60 min at room temperature. The TEM images showed spherical NPs with the average particle size of 8 nm [166]. Also, Shameli *et al.* reduced $AgNO_3$ to Ag NPs by UV irradiation and they used Montmorillonite (MMT) and CTS as template and stabilizer respectively. They investigated the effect of UV irradiation time and according to their results, the

average size decreases from 10.97 nm to 3.16 nm by changing irradiation time from 3 h to 96 h [10]. Although they did not use any chemical reducer or heat treatment, no information was provided about energy consumption rate for this process. Bogle *et al.* used electron beam with the fluence of 2×10^{13} to 3×10^{15} e cm^{-2} and energy level of 6 MeV to reduce $AgNO_3$ in water and poly-vinyl alcohol (PVA). They found that the size of the Ag NPs could be tuned from 60 to 10 nm in PVA solution, and from 100 to 200 nm in aqueous solution by changing the electron fluence from 2×10^{13} to 3×10^{15} e cm^{-2} [167]. Abid *et al.* employed direct laser irradiation of $AgNO_3$ aqueous solution with the average energy of 12-14 mJ per pulse. They also used sodium dodecyl sulfate (SDS) to stabilize the particles. According to the proposed mechanism, the reaction starts with formation of radicals in the solution by multiphoton excitation and the growth of particles are terminated depending on the concentration of SDS. Therefore, increasing the SDS concentration can accelerate the termination process and consequently reduce the size of NPs. However by changing the [SDS]/[AgNO$_3$] ratio from 0.2 to 40, the average size will change in the range of 13 to 16 nm [27].

Bensebaa *et al.* produced two different NPs namely $CuInS_2$ and $CuInSe_2$ using microwave irradiation of aqueous solution for 30 min that increase the temperature to 90 °C. They employed mercaptoacetic acid (MAA) as stabilizing agent. Their TEM images showed particles with less than 5 nm in size. They claimed that low temperature and uniform heating with microwave are important parameters for production of high quality $CuInS_2$ [139]. Although they did not use any harmful solvent or reducer, the stabilizing agent seems to be poisonous.

Darroudi *et al.* reduced $AgNO_3$ to Ag NPs using ultrasonic waves at room temperature in the presence of gelatin that act as a stabilizer. They investigated the effects of Ag$^+$ concentrations, ultrasonication time, and ultrasonic amplitude on the size of NPs. They observed that smaller particle size can be obtained with higher ultrasonic amplitude and shorter ultrasonication time. Spherical Ag NPs with an average size of 3.5 nm were produced by 45 min sonication with the amplitude of 50 [33].

Ramnani *et al.* employed ^{60}Co gamma radiation as reducing agent for production of Ag nanoclusters on SiO_2 support in aqueous suspension containing isopropanol. According to their explanation, radical OH is produced as a result of water radiolysis and this radical can react with isopropanol to form isopropyl radical. The new radical will reduce Ag ions to Ag nanoclusters. They observed that the nanoclusters ranged

10-20 nm and were stable in the pH range of 2-9 [44]. In another study, Chen *et al.* produced Ag NPs by ^{60}Co gamma radiation of $AgNO_3$ solution in the presence of CTS as stabilizing agent and isopropanol as free radical scavenger. They obtained NPs with the average diameter of 4-5 nm under the fixed radiation dose of 40.9 Gy/min [168].

Other approaches

Yang *et al.* produced ZnO_2 NPs from natural ore containing hydrozincite $(Zn_5(CO_3)_2(OH)_6)$ using H_2O_2 as reducer in ambient temperature and pressure. The obtained NPs were in the size range of 3.1-4.2 nm. Although their reducing agent is not a green reagent, using the ore can reduce the energy consumption and costs [169]. Wang *et al.* applied ionic liquid 1-(3-aminopropyl)-3-methylimidazolium bromide (IL-NH_2), to reduce aqueous $HAuCl_4$ to Au NPs with average diameter of 1.7 nm. The reaction took place at room temperature and they observed that IL-NH_2 was also involved in stabilizing Au NPs through a weak interaction between Au and N groups [103]. Zhang *et al.* reduced $[Ag(NH_3)_2]^+$ in ethanol to Ag NPs using triblock copolymer of poly(ethylene oxide)-poly(propylene oxide)-poly(ethylene oxide) to induce reduction under ambient light illumination. They observed that higher concentrations of Ag precursor result in the narrower size distribution (10-20 nm) in comparison to lower concentrations (5-30 nm) [170].

Summary and Future Outlook

Green Chemistry is aimed to ensure that the scientists would consider the health of the whole planet as a design criterion for manufacturing of different products. NPs are among emerging products that can revolutionize the human life and therefore it is of great interest to produce them through green routes before proceeding to large scale production. In this paper, the recent investigations of different researchers on green synthesis of NPs are reviewed. To sum up, there are many green options to prevent from using harmful reagents such as reducers, stabilizers and solvents. Also there are new techniques for transferring of energy to reacting molecules, such as microwave and UV irradiation to decrease energy and time requirement as well as enhancing the control over particle size.

However, many of the proposed methods suffer from non-uniformity in shape and polydispersity in particle size. Therefore further study is required to carry out the following research activities:

1- Investigating the performance of other environmentally-friendly materials e.g. other plant extracts and food-derived compounds for use as reagents for NPs production.

2- Optimizing the process parameters including temperature, pH, mixing speed, concentration of each reactants to achieve the best results for size distribution and uniform shape. In the case of plant extracts, the purification of effective compounds can also be useful.

3- Finally, the repeatability, efficiency and scale-up capability of the selected methods should be evaluated.

Acknowledgements

References

1.   Albrecht, M.A., Evans, C.W., and Raston, C.L., Green chemistry and the health implications of nanoparticles. Green Chemistry, 2006. 8(5): p. 417-432.

2.   Masciangioli, T. and Zhang, W.X., Environmental Technologies at the Nanoscale. Environmental science & technology, 2003. 37(5): p. 102A-108A.

3.   Farokhzad, O.C. and Langer, R., Impact of Nanotechnology on Drug Delivery. ACS Nano, 2009. 3(1): p. 16-20.

4.   Shameli, K., Ahmad, M.B., Jazayeri, S.D., Sedaghat, S., Shabanzadeh, P., Jahangirian, H., Mahdavi, M., and Abdollahi, Y., Synthesis and Characterization of Polyethylene Glycol Mediated Silver Nanoparticles by the Green Method. International Journal of Molecular Sciences, 2012. 13(6): p. 6639-6650.

5.   Zargar, M., Hamid, A.A., Bakar, F.A., Shamsudin, M.N., Shameli, K., Jahanshiri, F., and Farahani, F., Green Synthesis and Antibacterial Effect of Silver Nanoparticles Using Vitex Negundo L. Molecules, 2011. 16(8): p. 6667-6676.

6.   Sulaiman, G.M., Mohammed, W.H., Marzoog, T.R., Al-Amiery, A.A., and Kadhum, A.H., Green synthesis, antimicrobial and cytotoxic effects of silver nanoparticles using Eucalyptus chapmaniana leaves extract. Asian Pacific Journal of Tropical Biomedicine, 2013. 3(1): p. 58-63.

7.   Song, J.Y. and Kim, B.S., Rapid biological synthesis of silver nanoparticles using plant leaf extracts. Bioprocess and Biosystems Engineering 2009. 32(1): p. 79-84.

8.   Guidelli, E.J., Ramos, A.P., Zaniquelli, M.E.D., and Baffa, O., Green synthesis of colloidal silver nanoparticles using natural rubber latex extracted from Hevea brasiliensis. Spectrochimica Acta Part A: Molecular and Biomolecular Spectroscopy, 2011. 82(1): p. 140-145.

9.   Singh, A., Jain, D., Upadhyay, M.K., Khandelwal, N., and Verma, H.N., Green synthesis of silver nanoparticles using argemone mexicana leaf extract and evaluation of their antimicrobial activities. Digest Journal of Nanomaterials and Biostructures, 2010. 5(2): p. 483-489.

10.   Shameli, K., Ahmad, M.B., Wan Yunus, W.M.Z., Rustaiyan, A., Ibrahim, N.A., Zargar, M., and Abdollahi, Y., Green synthesis of silver/montmorillonite/chitosan bionanocomposites using the UV irradiation method and evaluation of antibacterial activity. International Journal of Nanomedicine, 2010. 5: p. 875-887.

11.   Dahl, J.A., Maddux, B.L.S., and Hutchison, J.E., Toward Greener Nanosynthesis. Chemical Reviews, 2007. 107(6): p. 2228-2269.

12.   Donaldson, K. and Stone, V., Nanoscience Fact versus Fiction. Communications of the acm, 2004. 47(11): p. 113-115.

13. Saxena, A., Tripathi, R.M., Zafar, F., and Singh, P., Green synthesis of silver nanoparticles using aqueous solution of Ficus benghalensis leaf extract and characterization of their antibacterial activity. Materials Letters, 2012. 67(1): p. 91-94.

14. Aromal, S.A., Vidhu, V.K., and Philip, D., Green synthesis of well-dispersed gold nanoparticles using Macrotyloma uniflorum. Spectrochimica Acta Part A: Molecular and Biomolecular Spectroscopy, 2012. 85(1): p. 99-104.

15. Ahamed, M., Majeed Khan, M.A., Siddiqui, M.K.J., AlSalhi, M.S., and Alrokayan, S.A., Green synthesis, characterizationan devaluation of biocompatibility of silver nanoparticles. Physica E, 2011. 43(6): p. 1266-1271.

16. Kumar, K.M., Mandal, B.K., Kumar, K.S., Reddy, P.S., and Sreedhar, B., Biobased green method to synthesise palladium and iron nanoparticles using Terminalia chebula aqueous extract. Spectrochimica Acta Part A: Molecular and Biomolecular Spectroscopy, 2013. 102: p. 128-133.

17. Chen, J., Wang, J., Zhang, X., and Jin, Y., Microwave-assisted green synthesis of silver nanoparticles by carboxymethyl cellulose sodium and silver nitrate. Materials Chemistry and Physics, 2008. 108(2-3): p. 421-424.

18. Hutchison, J.E., Greener Nanoscience: A Proactive Approach to Advancing Applications and Reducing Implications of Nanotechnology. ACS Nano, 2008. 2(3): p. 395-402.

19. Aromal, S.A. and Philip, D., Green synthesis of gold nanoparticles using Trigonella foenum-graecum and its size-dependent catalytic activity. Spectrochimica Acta Part A: Molecular and Biomolecular Spectroscopy, 2012. 97: p. 1-5.

20. Noruzi, M., Zare, D., Khoshnevisan, K., and Davoodi, D., Rapid green synthesis of gold nanoparticles using Rosa hybrida petal extract at room temperature. Spectrochimica Acta Part A: Molecular and Biomolecular Spectroscopy, 2011. 79(5): p. 1461- 1465.

21. Darroudi, M., Ahmad, M.B., Abdullah, A.H., and Ibrahim, N.A., Green synthesis and characterization of gelatin-based and sugar-reduced silver nanoparticles. International Journal of Nanomedicine, 2011. 6: p. 569-574.

22. Kumar, V.V., Nithya, S., Shyam, A., Subramanian, N.S., Anthuvan, J.T., and Anthony, S.P., Natural Amino Acid Based Phenolic Derivatives for Synthesizing Silver Nanoparticles with Tunable Morphology and Antibacterial Studies. Bulletin of the Korean Chemical Society, 2013. 34(9): p. 2702-2706.

23. Kesavan, A. and Venkatraman, G., Nanotechnology and its Applications. The Scitech Journal, 2014. 1(6): p. 1-2.

24. Beguma, N.A., Mondal, S., Basu, S., Laskar, R.A., and Mandal, D., Biogenic synthesis of Au and Ag nanoparticles using aqueous solutions of Black Tea leaf extracts. Colloids and Surfaces B: Biointerfaces, 2009. 71(1): p. 113-118.

25. Nagajyothi, P.C., Lee, S.E., An, M., and Lee, K.D., Green Synthesis of Silver and Gold Nanoparticles Using Lonicera Japonica Flower Extract. The Bulletin of the Korean Chemical Society, 2012. 33(8): p. 2609-2612.

26. Raveendran, P., Fu, J., and Wallen, S.L., Completely "Green" Synthesis and Stabilization of Metal Nanoparticles. Journal of the American Chemical Society, 2003. 125(46): p. 13940-13941.

27. Abid, J.P., Wark, A.W., Brevet, P.F., and Girault, H.H., Preparation of silver nanoparticles in solution from a silver salt by laser irradiation. Chemical Communications, 2002(7): p. 792-793.

28. Sudeep, P.K. and Kamat, P.V., Photosensitized Growth of Silver Nanoparticles under Visible Light Irradiation: A Mechanistic Investigation. Chemistry of Materials, 2005. 17(22): p. 5404-5410.

29. Wei, D., Ye, Y., Jia, X., Yuan, C., and Qian, W., Chitosan as an active support for assembly of metal nanoparticles and application of the resultant bioconjugates in catalysis. Carbohydrate Research, 2010. 345(1): p. 74-81.

30.   Li, S., Shen, Y., Xie, A., Yu, X., Qiu, L., Zhang, L., and Zhang, Q., Green synthesis of silver nanoparticles using Capsicum annuum L. extract. Green Chemistry, 2007. 9(8): p. 852-858.

31.   Philip, D., Biosynthesis of Au, Ag and Au-Ag nanoparticles using edible mushroom extract. Spectrochimica Acta Part A: Molecular and Biomolecular Spectroscopy, 2009. 73(2): p. 374-381.

32.   Moulton, M.C., Braydich-Stolle, L.K., Nadagouda, M.N., Kunzelman, S., Hussain, S.M., and Varma, R.S., Synthesis, characterization and biocompatibility of ''green'' synthesized silver nanoparticles using tea polyphenols. Nanoscale, 2010. 2(5): p. 763-770.

33.   Darroudi, M., Zak, A.K., Muhamad, M.R., Huang, N.M., and Hakimi, M., Green synthesis of colloidal silver nanoparticles by sonochemical method. Materials Letters, 2012. 66(1): p. 117-120.

34.   Sharma, V.K., Yngard, R.A., and Lin, Y., Silver nanoparticles: Green synthesis and their antimicrobial activities. Advances in Colloid and Interface Science, 2009. 145(1-2): p. 83-96.

35.   Morrow, B.J., Matijevic´, E., and Goia, D.V., Preparation and stabilization of monodisperse colloidal gold by reduction with aminodextran. Journal of Colloid and Interface Science, 2009. 335(1): p. 62-69.

36.   Keita, B., Biboum, R.N., Mbomekalle´, I.M., Floquet, S., Simonnet-Je´gat, C., Cadot, E., Miserque, F., Berthet, P., and Nadjo, L., One-step synthesis and stabilization of gold nanoparticles in water with the simple oxothiometalate Na2[Mo3(m3-S)(m-S)3(Hnta)3]. Journal of Materials Chemistry, 2008. 18(27): p. 3196-3199.

37.   Cai, J., Kimura, S., Wada, M., and Kuga, S., Nanoporous Cellulose as Metal Nanoparticles Support. Biomacromolecules, 2009. 10(1): p. 87-94.

38.   Kasthuri, J., Veerapandian, S., and Rajendiran, N., Biological synthesis of silver and gold nanoparticles using apiin as reducing agent. Colloids and Surfaces B: Biointerfaces, 2009. 68(1): p. 55-60.

39.   Smitha, S.L., Philip, D., and Gopchandran, K.G., Green synthesis of gold nanoparticles using Cinnamomum zeylanicum leaf broth. Spectrochimica Acta Part A: Molecular and Biomolecular Spectroscopy, 2009. 74(3): p. 735-739.

40.   Shankar, S.S., Rai, A., Ahmad, A., and Sastry, M., Controlling the Optical Properties of Lemongrass Extract Synthesized Gold Nanotriangles and Potential Application in Infrared-Absorbing Optical Coatings. Chemistry of Materials, 2005. 17(3): p. 566-572.

41.   Chandran, S.P., Chaudhary, M., Pasricha, R., Ahmad, A., and Sastry, M., Synthesis of Gold Nanotriangles and Silver Nanoparticles Using Aloe Wera Plant Extract. Biotechnology Progress, 2006. 22(2): p. 577-583.

42.   Shameli, K., Ahmad, M.B., Zamanian, A., Sangpour, P., Shabanzadeh, P., Abdollahi, Y., and Zargar, M., Green biosynthesis of silver nanoparticles using Curcuma longa tuber powder. International Journal of Nanomedicine, 2012(7): p. 5603-5610.

43.   Philip, D., Mangifera Indica leaf-assisted biosynthesis of well-dispersed silver nanoparticles. Spectrochimica Acta Part A: Molecular and Biomolecular Spectroscopy, 2011. 78(1): p. 327-331.

44.   Ramnani, S.P., Biswal, J., and Sabharwal, S., Synthesis of silver nanoparticles supported on silica aerogel using gamma radiolysis. Radiation Physics and Chemistry, 2007. 76(8-9): p. 1290-1294.

45.   Awwad, A.M., Salem, N.M., and Abdeen, A.O., Green synthesis of silver nanoparticles using carob leaf extract and its antibacterial activity. International Journal of Industrial Chemistry, 2013. 4(1): p. 1-6.

46.   Gnanasangeetha, D. and SaralaThambavani, D., One Pot Synthesis of Zinc Oxide Nanoparticles via Chemical and Green Method. Research Journal of Material Sciences, 2013. 1(7): p. 1-8.

47.   Safaepour, M., Shahverdi, A.R., Shahverdi, H.R., Khorramizadeh, M.R., and Gohari, A.R., Green Synthesis of Small Silver Nanoparticles Using Geraniol and Its Cytotoxicity against Fibrosarcoma-Wehi 164. Avicenna Journal of Medical Biotechnology, 2009. 1(2): p. 111-115.

48.   Dipankar, C. and Murugan, S., The green synthesis, characterization and evaluation of the biological activities of silver nanoparticles synthesized from Iresine herbstii leaf aqueous extracts. Colloids and Surfaces B: Biointerfaces, 2012. 98: p. 112-119.

49.   Swamy, M.K., Sudipta, K.M., Jayanta, K., and Balasubramanya, S., The green synthesis, characterization, and evaluation of the biological activities of silver nanoparticles synthesized from Leptadenia reticulata leaf extract. Applied Nanoscience, 2014. 5(1): p. 73-81.

50.   Leela, A. and Vivekanandan, M., Tapping the unexploited plant resources for the synthesis of silver nanoparticles. African Journal of Biotechnology, 2008. 7(17): p. 3162-3165.

51.   Nadagouda, M.N. and Varma, R.S., Green synthesis of silver and palladium nanoparticles at room temperature using coffee and tea extract. Green Chemistry, 2008. 10(8): p. 859-862.

52.   Singh, S., Saikia, J.P., and Buragohain, A.K., A novel 'green' synthesis of colloidal silver nanoparticles (SNP) using Dillenia indica fruit extract. Colloids and Surfaces B: Biointerfaces, 2013. 102: p. 83-85.

53.   Zhang, L., Shen, Y., Xie, A., Li, S., Jin, B., and Zhang, Q., One-Step Synthesis of Monodisperse Silver Nanoparticles beneath Vitamin E Langmuir Monolayers. The Journal of Physical Chemistry B, 2006. 110(13): p. 6615-6620.

54.   Kora, A.J., Sashidhar, R.B., and Arunachalam, J., Gum kondagogu (Cochlospermum gossypium): A template for the green synthesis and stabilization of silver nanoparticles with antibacterial application. Carbohydrate Polymers, 2010. 82(3): p. 670-679.

55.   Kemp, M.M., Kumar, A., Clement, D., Ajayan, P., Mousa, S., and Linhardt, R.J., Hyaluronan- and heparin- reduced silver nanoparticles with antimicrobial properties. Nanomedicine, 2009. 4(4): p. 421-429.

56.   Wei, D. and Qian, W., Facile synthesis of Ag and Au nanoparticles utilizing chitosan as a mediator agent. Colloids and Surfaces B: Biointerfaces, 2008. 62(1): p. 136-142.

57.   Kvítek, L., Prucek, R., Panacek, A., Novotny, R., Hrbac, J., and Zboril, R., The influence of complexing agent concentration on particle size in the process of SERS active silver colloid synthesis. Journal of Materials Chemistry, 2005. 15(10): p. 1099-1105.

58.   Awwad, A.M. and Salem, N.M., Green Synthesis of Silver Nanoparticles by Mulberry Leaves Extract. Nanoscience and Nanotechnology, 2012. 2(4): p. 125-128.

59.   Xie, J., Lee, J.Y., Wang, D.I.C., and Ting, Y.P., Silver Nanoplates: From Biological to Biomimetic Synthesis. ACS Nano, 2007. 1(5): p. 429-439.

60.   Jain, D., Daima, H.K., Kachhwaha, S., and Kothari, S.L., Synthesis of plant-mediated silver nanoparticles using papaya fruit extract and evaluation of their anti microbial activities. Digest Journal of Nanomaterials and Biostructures, 2009. 4(3): p. 557-563.

61.   Kumar, K.M., Sinha, M., Mandal, B.K., Ghosh, A.R., Kumar, K.S., and Reddy, P.S., Green synthesis of silver nanoparticles using Terminalia chebula extract at room temperature and their antimicrobial studies. Spectrochimica Acta Part A: Molecular and Biomolecular Spectroscopy, 2012. 91: p. 228-233.

62.   Shameli, K., Ahmad, M.B., Jazayeri, S.D., Shabanzadeh, P., Sangpour, P., Jahangirian, H., and Gharayebi, Y., Investigation of antibacterial properties silver nanoparticles prepared via green method. Chemistry Central Journal, 2012(6): p. 1-10.

63.   Venkatpurwar, V. and Pokharkar, V., Green synthesis of silver nanoparticles using marine polysaccharide: Study of in-vitro antibacterial activity. Materials Letters, 2011. 65(6): p. 999-1002.

64.   Kvıtek, L., Panacek, A., Soukupova, J., Kolar, M., Vecerova, R., Prucek, R., Holecova, M., and Zboril, R., Effect of Surfactants and Polymers on Stability and Antibacterial Activity of Silver Nanoparticles (NPs). The Journal of Physical Chemistry C 2008. 112(25): p. 5825-5834.

65.   Panacek, A., Kvıtek, L., Prucek, R., Kolar, M., Vecerova, R., Pizurova, N., Sharma, V.K., Nevecna, T., and Zboril, R., Silver Colloid Nanoparticles: Synthesis, Characterization, and Their Antibacterial Activity. The Journal of Physical Chemistry B, 2006. 110(33): p. 16248-16253.

66.   Kora, A.J., Beedu, S.R., and Jayaraman, A., Size-controlled green synthesis of silver nanoparticles mediated by gum ghatti (Anogeissus latifolia) and its biological activity. Organic and Medicinal Chemistry Letters, 2012: p. 1-10.

67.   Ravindra, S., Murali Mohan, Y., Narayana Reddy, N., and Mohana Raju, K., Fabrication of antibacterial cotton fibres loaded with silver nanoparticles via "Green Approach". Colloids and Surfaces A: Physicochemical and Engineering Aspects, 2010. 367(13): p. 31-40.

68.   Vaseeharan, B., Ramasamy, P., and Chen, J.C., Antibacterial activity of silver nanoparticles (Ag Nps) synthesized by tea leaf extracts against pathogenic Vibrio harveyi and its protective efficacy on juvenile Feneropenaeus indicus. Applied Microbiology, 2010. 50(4): p. 352-356.

69.   Amin, M., Anwar, F., Janjua, M.R.S.A., Iqbal, M.A., and Rashid, U., Green Synthesis of Silver Nanoparticles through Reduction with Solanum xanthocarpum L. Berry Extract: Characterization, Antimicrobial and Urease

Inhibitory Activities against Helicobacter pylori. International Journal of Molecular Sciences, 2012. 13(8): p. 9923-9941.

70. Kemp, M.M., Kumar, A., Mousa, S., Park, T.J., Ajayan, P., Kubotera, N., Mousa, S.A., and Linhardt, R.J., Synthesis of Gold and Silver Nanoparticles Stabilized with Glycosaminoglycans Having Distinctive Biological Activities. Biomacromolecules, 2009. 10(3): p. 589-595.

71. Kemp, M.M., Kumar, A., Mousa, S., Dyskin, E., Yalcin, M., Ajayan, P., Linhardt, R.J., and Mousa, S.A., Gold and silver nanoparticles conjugated with heparin derivative possess anti-angiogenesis properties. Nanotechnology, 2009. 20(45): p. 455104-455110.

72. An, J., Luo, Q., Yuan, X., Wang, D., and Li, X., Preparation and Characterization of Silver-Chitosan Nanocomposite Particles with Antimicrobial Activity. Journal of Applied Polymer Science, 2011. 120(6): p. 3180-3189.

73. Zhang, Y., Liu, S., Wang, L., Qin, X., Tian, J., Lu, W., Chang, G., and Sun, X., One-pot green synthesis of Ag nanoparticles-graphene nanocomposites and their applications in SERS, H2O2, and glucose sensing. RSC Advances, 2012. 2(2): p. 538-545.

74. Kumar, V.G., Gokavarapu, S.D., Rajeswari, A., Dhas, T.S., Karthick, V., Kapadia, Z., Shrestha, T., Barathy, I.A., Roy, A., and Sinha, S., Facile green synthesis of gold nanoparticles using leaf extract of antidiabetic potent Cassia auriculata. Colloids and Surfaces B: Biointerfaces, 2011. 87(1): p. 159-163.

75. Basha, S.K., Govindaraju, K., Manikandan, R., Ahn, J.S., Bae, E.Y., and Singaravelu, G., Phytochemical mediated gold nanoparticles and their PTP 1B inhibitory activity. Colloids and Surfaces B: Biointerfaces, 2010. 75(2): p. 405-409.

76. Bar, H., Bhui, D.K., Sahoo, G.P., Sarkar, P., De, S.P., and Misra, A., Green synthesis of silver nanoparticles using latex of Jatropha curcas. Colloids and Surfaces A: Physicochemical and Engineering Aspects, 2009. 339(1-3): p. 134-139.

77.   Wang, Y., He, X., Wang, K., Zhang, X., and Tan, W., Barbated Skullcup herb extract-mediated biosynthesis of gold nanoparticles and its primary application in electrochemistry. Colloids and Surfaces B: Biointerfaces, 2009. 73(1): p. 75-79.

78.   Shukla, R., Nune, S.K., Chanda, N., Katti, K., Mekapothula, S., Kulkarni, R.R., Welshons, W.V., Kannan, R., and Katti, K.V., Soybeans as a Phytochemical Reservoir for the Production and Stabilization of Biocompatible Gold Nanoparticles. Green Nanoparticles by Using Green Chemistry, 2008. 4(9): p. 1425-1436.

79.   Nune, S.K., Chanda, N., Shukla, R., Katti, K., Kulkarni, R.R., Thilakavathy, S., Mekapothula, S., Kannan, R., and Katti, K.V., Green nanotechnology from tea: phytochemicals in tea as building blocks for production of biocompatible gold nanoparticles. Journal of Materials Chemistry, 2009. 19(19): p. 2912-2920.

80.   Armendariz, V., Parsons, J.G., Lopez, M.L., Peralta-Videa, J.R., Jose-Yacaman, M., and Gardea-Torresdey, J.L., The extraction of gold nanoparticles from oat and wheat biomasses using sodium citrate and cetyltrimethylammonium bromide, studied by x-ray absorption spectroscopy, high-resolution transmission electron microscopy, and UV-visible spectroscopy. Nanotechnology, 2009. 20(10): p. 105607-105614.

81.   Philip, D., Honey mediated green synthesis of gold nanoparticles. Spectrochimica Acta Part A: Molecular and Biomolecular Spectroscopy, 2009. 73(4): p. 650-653.

82.   Jang, H., Kim, Y.K., Ryoo, S.R., Kim, M.H., and Min, D.H., Facile synthesis of robust and biocompatible gold nanoparticles. Chemical Communications, 2010. 46(4): p. 583-585.

83.   Deka, J., Paul, A., Ramesh, A., and Chattopadhyay, A., Probing Au Nanoparticle Uptake by Enzyme Following the Digestion of a Starch-Au-Nanoparticle Composite. Langmuir, 2008. 24(18): p. 9945-9951.

84.   Philip, D., Green synthesis of gold and silver nanoparticles using Hibiscus rosa sinensis. Physica E, 2010. 42(5): p. 1417-1424.

85.   Kumar, K.M., Mandal, B.K., Sinha, M., and Krishnakumar, V., Terminalia chebula mediated green and rapid synthesis of gold nanoparticles. Spectrochimica Acta Part A: Molecular and Biomolecular Spectroscopy, 2012. 86: p. 490-494.

86.   Potara, M., Maniu, D., and Astilean, S., The synthesis of biocompatible and SERS-active gold nanoparticles using chitosan. Nanotechnology, 2009. 20(31): p. 315602-315608.

87.   Vigneshwaran, N., Nachane, R.P., Balasubramanya, R.H., and Varadarajan, P.V., A novel one-pot 'green' synthesis of stable silver nanoparticles using soluble starch. Carbohydrate Research, 2006. 341(12): p. 2012-2018.

88.   Das, R.K., Borthakur, B.B., and Bora, U., Green synthesis of gold nanoparticles using ethanolic leaf extract of Centella asiatica. Materials Letters, 2010. 64(13): p. 1445-1447.

89.   Thekkae Padil, V.V. and Cernik, M., Green synthesis of copper oxide nanoparticles using gum karaya as a biotemplate and their antibacterial application. International Journal of Nanomedicine, 2013. 8: p. 889-898.

90.   Lu, W., Shen, Y., Xie, A., and Zhang, W., Green synthesis and characterization of superparamagnetic Fe3O4 nanoparticles. Journal of Magnetism and Magnetic Materials, 2010. 322(13): p. 1828-1833.

91.   Chin, S.F., Pang, S.C., and Tan, C.H., Green Synthesis of Magnetite Nanoparticles (via Thermal Decomposition Method) with Controllable Size and Shape. Journal of Materials and Environmental Science, 2011. 2(3): p. 299-302.

92.   Lai, Y., Yin, W., Liu, J., Xi, R., and Zhan, J., One-Pot Green Synthesis and Bioapplication of L-Arginine-Capped Superparamagnetic Fe_3O_4 Nanoparticles. Nanoscale Research Letters, 2010. 5(2): p. 302-307.

93. Lu, W., Qin, X., Liu, S., Chang, G., Zhang, Y., Luo, Y., Asiri, A.M., Alyoubi, A.O., and Sun, X., Economical, Green Synthesis of Fluorescent Carbon Nanoparticles and Their Use as Probes for Rapid, Sensitive, and Selective Detection of Mercury(II) Ions. Analytical Chemistry, 2012. 84(12): p. 5351-5357.

94. Zhang, W.X., Nanoscale Iron Particles for Environmental Remediation: An Overview. Journal of Nanoparticle Research, 2003. 5(3-4): p. 323-332.

95. Noubactep, C., Caré, S., and Crane, R., Nanoscale Metallic Iron for Environmental Remediation: Prospects and Limitations. Water, Air, & Soil Pollution, 2012. 223(3): p. 1363-1382.

96. He, F., Zhao, D., Liu, J., and Roberts, C.B., Stabilization of Fe−Pd Nanoparticles with Sodium Carboxymethyl Cellulose for Enhanced Transport and Dechlorination of Trichloroethylene in Soil and Groundwater. Industrial & Engineering Chemistry Research, 2007. 46(1): p. 29-34.

97. Puddu, V., Choi, H., Dionysiou, D.D., and Puma, G.L., TiO2 photocatalyst for indoor air remediation: Influence of crystallinity, crystal phase, and UV radiation intensity on trichloroethylene degradation. Applied Catalysis B: Environmental, 2010. 94(3-4): p. 211-218.

98. Saha, S., Pal, A., Kundu, S., Basu, S., and Pal, T., Photochemical Green Synthesis of Calcium-Alginate-Stabilized Ag and Au Nanoparticles and Their Catalytic Application to 4-Nitrophenol Reduction. Langmuir, 2010. 26(4): p. 2885-2893.

99. Wei, D., Sun, W., Qian, W., Ye, Y., and Ma, X., The synthesis of chitosan-based silver nanoparticles and their antibacterial activity. Carbohydrate Research, 2009. 344(17): p. 2375-2382.

100. Soukupova, J., Kvítek, L., Panacek, A., Nevecna, T., and Zboril, R., Comprehensive study on surfactant role on silver nanoparticles (NPs) prepared via modified Tollens process. Materials Chemistry and Physics, 2008. 111(1): p. 77-81.

101.   Ghoreishi, S.M., Behpour, M., and Khayatkashani, M., Green synthesis of silver and gold nanoparticles using Rosa damascena and its primary application in electrochemistry. Physica E, 2011. 44(1): p. 97-104.

102.   Bar, H., Bhui, D.K., Sahoo, G.P., Sarkar, P., Pyne, S., and Misra, A., Green synthesis of silver nanoparticles using seed extract of Jatropha curcas. Colloids and Surfaces A: Physicochemical and Engineering Aspects, 2009. 348(1-3): p. 212-216.

103.   Wang, Z., Zhang, Q., Kuehner, D., Ivaska, A., and Niu, L., Green synthesis of 1-2 nm gold nanoparticles stabilized by amine-terminated ionic liquid and their electrocatalytic activity in oxygen reduction. Green Chemistry, 2008. 10(9): p. 907-909.

104.   Xia, B., He, F., and Li, L., Preparation of Bimetallic Nanoparticles Using a Facile Green Synthesis Method and Their Application. Langmuir, 2013. 29(15): p. 4901-4907.

105.   Li, L., Chen, M., Huang, G., Yang, N., Zhang, L., Wang, H., Liu, Y., Wang, W., and Gao, J., A green method to prepare Pd-Ag nanoparticles supported on reduced graphene oxide and their electrochemical catalysis of methanol and ethanol oxidation. Journal of Power Sources, 2014. 263: p. 13-21.

106.   Zhan, G., Huang, J., Du, M., Abdul-Rauf, I., Ma, Y., and Li, Q., Green synthesis of Au-Pd bimetallic nanoparticles: Single-step bioreduction method with plant extract. Materials Letters, 2011. 65(19-20): p. 2989-2991.

107.   Chen, X., Cai, Z., Chen, X., and Oyama, M., Green synthesis of graphene-PtPd alloy nanoparticles with high electrocatalytic performance for ethanol oxidation. Journal of Materials Chemistry A, 2014. 2(2): p. 315-320.

108.   Raveendran, P., Fu, J., and Wallen, S.L., A simple and ''green'' method for the synthesis of Au, Ag, and Au-Ag alloy nanoparticles. Green Chemistry, 2006. 8(1): p. 34-38.

109. Banerjee, P., Satapathy, M., Mukhopahayay, A., and Das, P., Leaf extract mediated green synthesis of silver nanoparticles from widely available Indian plants: synthesis, characterization, antimicrobial property and toxicity analysis. Bioresources and Bioprocessing, 2014. 1: p. 1-10.

110. Li, W., Guo, Y., and Zhang, P., SERS-Active Silver Nanoparticles Prepared by a Simple and Green Method. The Journal of Physical Chemistry 2010. 114(14): p. 6413-6417.

111. He, Y., Wu, X., Lu, G., and Shi, G., A facile route to silver nanosheets. Materials Chemistry and Physics, 2006. 98(1): p. 178-182.

112. Hu, B., Wang, S.B., Wang, K., Zhang, M., and Yu, S.H., Microwave-Assisted Rapid Facile "Green" Synthesis of Uniform Silver Nanoparticles: Self-Assembly into Multilayered Films and Their Optical Properties. The Journal of Physical Chemistry C, 2008. 112(30): p. 11169-11174.

113. Mata, Y.N., Torres, E., Blázquez, M.L., Ballester, A., González, F., and Mu˜noz, J.A., Gold (III) biosorption and bioreduction with the brown alga Fucus vesiculosus. Journal of Hazardous Materials, 2009. 166(2-3): p. 612-618.

114. Wang, Y., Li, Y.F., and Huang, C.Z., A One-Pot Green Method for One-Dimensional Assembly of Gold Nanoparticles with a Novel Chitosan-Ninhydrin Bioconjugate at Physiological Temperature. The Journal of Physical Chemistry C, 2009. 113(11): p. 4315-4320.

115. Shameli, K., Ahmad, M.B., Al-Mulla, E.A.J., Ibrahim, N.A., Shabanzadeh, P., Rustaiyan, A., Abdollahi, Y., Bagheri, S., Abdolmohammadi, S., Usman, M.S., and Zidan, M., Green Biosynthesis of Silver Nanoparticles Using Callicarpa maingayi Stem Bark Extraction. molecules, 2012. 17(7): p. 8506-8517.

116. Anastas, P.T. and Zimmerman, J.B., Peer Reviewed: Design Through the 12 Principles of Green Engineering. Environmental Science & Technology 2003. 37(5): p. 94A-101A.

117.   Sheldon, R.A., E factors, green chemistry and catalysis: an odyssey. Chemical Communications, 2008(29): p. 3352-3365.

118.   Anastas, P. and Eghbali, N., Green Chemistry: Principles and Practice. Chemical Society Reviews, 2010. 39(1): p. 301-312.

119.   Trost, B.M., Atom Economy-A Challenge for Organic Synthesis : Homogeneous Catalysis Leads the Way. Angewandte Chemie International Edition in English, 1995. 34(3): p. 259-281.

120.   Trost, B.M., The atom economy-a search for synthetic efficiency. Science, 1991. 254(5037): p. 1471-1477.

121.   Kalidindi, S.B., Sanyal, U., and Jagirdar, B.R., Metal Nanoparticles via the Atom-Economy Green Approach. Inorganic Chemistry, 2010. 49(9): p. 3965-3967.

122.   Dearden, J.C., In silico prediction of drug toxicity. Journal of Computer-Aided Molecular Design, 2003. 17(2-4): p. 119-127.

123.   Voutchkova, A.M., Ferris, L.A., Zimmerman, J.B., and Anastas, P.T., Toward molecular design for hazard reduction-fundamental relationships between chemical properties and toxicity. Tetrahedron, 2010. 66(5): p. 1031-1039.

124.   Constable, D.J.C., Curzons, A.D., and Cunningham, V.L., Metrics to 'green' chemistry-which are the best? Green Chemistry, 2002. 4(6): p. 521-527.

125.   Sheldon, R.A., Green solvents for sustainable organic synthesis: state of the art. Green Chemistry, 2005. 7(5): p. 267-278.

126.   Li, C.J. and Chen, L., Organic chemistry in water. Chemical Society Reviews, 2006. 35(1): p. 68-82.

127.   Hyde, J.R., Licence, P., Carter, D., and Poliakoff, M., Continuous catalytic reactions in supercritical fluids. Applied Catalysis A: General, 2001. 222(1-2): p. 119-131.

128. Horvath, I. and Anastas, P.T., Introduction: Green Chemistry. Chemical Reviews, 2007. 107(6): p. 2167-2168.

129. Gallezot, P., Process options for converting renewable feedstocks to bioproducts. Green Chemistry, 2007. 9(4): p. 295-302.

130. Gandini, A., Polymers from Renewable Resources: A Challenge for the Future of Macromolecular Materials. Macromolecules, 2008. 41(24): p. 9491-9504.

131. Meier, M.A.R., Metzger, J.O., and Schubert, U.S., Plant oil renewable resources as green alternatives in polymer science. Chemical Society Reviews, 2007. 36(11): p. 1788-1802.

132. Tokiwa, Y. and Calabia, B.P., Biological production of functional chemicals from renewable resources. Canadian Journal of Chemistry, 2008. 86(6): p. 548-555.

133. Pillai, C.K.S., Paul, W., and Sharma, C.P., Chitin and chitosan polymers: Chemistry, solubility and fiber formation. Progress in Polymer Science, 2009. 34(7): p. 641-678.

134. Troupis, A., Hiskia, A., and Papaconstantinou, E., Synthesis of Metal Nanoparticles by Using Polyoxometalates as Photocatalysts and Stabilizers. Angewandte Chemie International Edition, 2002. 41(11): p. 1911-1914.

135. Boethling, R.S., Sommer, E., and DiFiore, D., Designing Small Molecules for Biodegradability. Chemical Reviews 2007. 107: p. 2207-2227.

136. Rocha, F.R.P., Nobrega, J.A., and Filho, O.F., Flow analysis strategies to greener analytical chemistry. An overview. Green Chemistry, 2001. 3(5): p. 216-220.

137. Keith, L.H., Gron, L.U., and Young, J.L., Green Analytical Methodologies. Chemical Reviews, 2007. 107(6): p. 2695-2708.

138. Renaud, G., Lazzari, R., Revenant, C., Barbier, A., Noblet, M., Ulrich, O., Leroy, F., Jupille, J., Borensztein, Y., Henry, C.R., Deville, J.-P., Scheurer, F., Mane-

Mane, J., and Fruchart, O., Real-Time Monitoring of Growing Nanoparticles. Science, 2003. 300(5624): p. 1416-1419.

139. Bensebaa, F., Durand, C., Aouadou, A., Scoles, L., Du, X., Wang, D., and Le Page, Y., A new green synthesis method of CuInS2 and CuInSe2 nanoparticles and their integration into thin films. Journal of Nanoparticle Research, 2010. 12(5): p. 1897-1903.

140. Sun, C., Qu, R., Chen, H., Ji, C., Wang, C., Sun, Y., and Wang, B., Degradation behavior of chitosan chains in the 'green' synthesis of gold nanoparticles. Carbohydrate Research, 2008. 343(15): p. 2595-2599.

141. Long, D., Wu, G., and Chen, S., Preparation of oligochitosan stabilized silver nanoparticles by gamma irradiation. Radiation Physics and Chemistry, 2007. 76(7): p. 1126-1131.

142. Laudenslager, M.J., Schiffman, J.D., and Schauer, C.L., Carboxymethyl Chitosan as a Matrix Material for Platinum, Gold, and Silver Nanoparticles. Biomacromolecules, 2008. 9(10): p. 2682-2685.

143. Huang, H. and Yang, X., Synthesis of polysaccharide-stabilized gold and silver nanoparticles: a green method. Carbohydrate Research, 2004. 339(15): p. 2627-2631.

144. Sun, X. and Li, Y., Colloidal Carbon Spheres and Their Core/Shell Structures with Noble-Metal Nanoparticles. Angewandte Chemie International Edition, 2004. 43(5): p. 597-601.

145. Yu, D. and Yam, V.W.W., Hydrothermal-Induced Assembly of Colloidal Silver Spheres into Various Nanoparticles on the Basis of HTAB-Modified Silver Mirror Reaction. The Journal of Physical Chemistry B, 2005. 109(12): p. 5497-5503.

146. Tai, C.Y., Wang, Y.H., and Liu, H.S., A Green Process for Preparing Silver Nanoparticles Using Spinning Disk Reactor. AIChE Journal, 2008. 54(2): p. 445-452.

147. Li, J.H., Ren, C.L., Liu, X.Y., Hu, Z.D., and Xue, D.S., "Green" synthesis of starch capped CdSe nanoparticles at room temperature. Materials Science and Engineering A, 2007. 458(1-2): p. 319-322.

148. Yan, W., Wang, R., Xu, Z., Xu, J., Lin, L., Shen, Z., and Zhou, Y., A novel, practical and green synthesis of Ag nanoparticles catalyst and its application in three-component coupling of aldehyde, alkyne, and amine. Journal of Molecular Catalysis A: Chemical, 2006. 255(1-2): p. 81-85.

149. Roy, K. and Lahiri, S., A green method for synthesis of radioactive gold nanoparticles. Green Chemistry, 2006. 8(12): p. 1063-1066.

150. Zhang, J., Keita, B., Nadjo, L., Mbomekalle, I.M., and Liu, T., Self-Assembly of Polyoxometalate Macroanion-Capped Pd0 Nanoparticles in Aqueous Solution. Langmuir, 2008. 24(10): p. 5277-5283.

151. Zhang, G., Keita, B., Biboum, R.N., Miserque, F., Berthet, P., Dolbecq, A., Mialane, P., Catala, L., and Nadjo, L., Synthesis of various crystalline gold nanostructures in water: The polyoxometalate b-[H4PMo12O40]3- as the reducing and stabilizing agent. Journal of Materials Chemistry, 2009. 19(45): p. 8639-8644.

152. Weinstock, L.A., Homogeneous-Phase Electron-Transfer Reactions of Polyoxometalates. Chemical Reviews, 1998. 98(1): p. 113-170.

153. Keita, B., Zhang, G., Dolbecq, A., Mialane, P., Secheresse, F., Miserque, F., and Nadjo, L., MoV-MoVI Mixed Valence Polyoxometalates for Facile Synthesis of Stabilized Metal Nanoparticles: Electrocatalytic Oxidation of Alcohols. The Journal of Physical Chemistry C, 2007. 111(23): p. 8145-8148.

154. Keita, B., Mbomekalle, I.M., Nadjo, L., and Haut, C., Tuning the formal potentials of new VIV-substituted Dawson-type polyoxometalates for facile synthesis of metal nanoparticles. Electrochemistry Communications, 2004. 6(10): p. 978-983.

155. Dolbecq, A., Compain, J.D., Mialane, P., Marrot, J., Scheresse, F., Keita, B., Holzle, L.R.B., Miserque, F., and Nadjo, L., Hexa- and Dodecanuclear Polyoxomolybdate Cyclic Compounds: Application toward the Facile Synthesis of Nanoparticles and Film Electrodeposition. Chemistry-A European Journal, 2009. 15(3): p. 733-741.

156. Romeilah, R.M., Fayed, S.A., and Mahmoud, G.I., Chemical Compositions, Antiviral and Antioxidant Activities of Seven Essential Oils,. Journal of Applied Sciences Research, 2010. 6(1): p. 50-62.

157. Nabikhan, A., Kandasamy, K., Raj, A., and Alikunhi, N.M., Synthesis of antimicrobial silver nanoparticles by callus and leaf extracts from saltmarsh plant, Sesuvium portulacastrum L. Colloids and Surfaces B: Biointerfaces, 2010. 79 (2): p. 488-493.

158. Philip, D., Rapid green synthesis of spherical gold nanoparticles using Mangifera indica leaf. Spectrochimica Acta Part A: Molecular and Biomolecular Spectroscopy, 2010. 77(4): p. 807-810.

159. Jha, A.K., Prasad, K., Prasad, K., and Kulkarni, A.R., Plant system: Nature's nanofactory. Colloids and Surfaces B: Biointerfaces, 2009. 73(2): p. 219-223.

160. Jha, A.K., Prasad, K., Kumar, V., and Prasad, K., Biosynthesis of Silver Nanoparticles Using Eclipta Leaf. Journal of Biotechnology, 2009. 25(5): p. 1476-1479.

161. Krpetic, Z., Scari, G., Caneva, E., Speranza, G., and Porta, F., Gold Nanoparticles Prepared Using Cape Aloe Active Components. Langmuir, 2009. 25(13): p. 7217-7221.

162. Shankar, S.S., Ahmad, A., and Sastry, M., Geranium Leaf Assisted Biosynthesis of Silver Nanoparticles. Biotechnology Progress, 2003. 19(6): p. 1627-1631.

163. Gardea-Torresdey, J.L., Tiemann, K.J., Gamez, G., Dokken, K., Tehuacanero, S., and Jose-Yacaman, M., Gold nanoparticles obtained by bio-precipitation

from gold (III) solutions. Journal of Nanoparticle Research, 1999. 1(3): p. 397-404.

164.   Rastogi, L. and Arunachalam, J., Sunlight based irradiation strategy for rapid green synthesis of highly stable silver nanoparticles using aqueous garlic (Allium sativum) extract and their antibacterial potential. Materials Chemistry and Physics, 2011. 129(1-2): p. 558-563.

165.   Armendariz, V., Herrera, I., Peralta-Videa, J.R., Jose-Yacaman, M., Troiani, H., Santiago, P., and Gardea-Torresdey, J.L., Size controlled gold nanoparticle formation by Avena sativa biomass: use of plants in nanobiotechnology. Journal of Nanoparticle Research, 2004. 6(4): p. 377-382.

166.   Dubas, S.T. and Pimpan, V., Green synthesis of silver nanoparticles for ammonia sensing. Talanta, 2008. 76(1): p. 29-33.

167.   Bogle, K.A., Dhole, S.D., and Bhoraskar, V.N., Silver nanoparticles: synthesis and size control by electron irradiation. Nanotechnology, 2006. 17(13): p. 3204-3208.

168.   Chen, P., Song, L., Liu, Y., and Fang, Y., Synthesis of silver nanoparticles by g-ray irradiation in acetic water solution containing chitosan. Radiation Physics and Chemistry, 2007. 76(7): p. 1165-1168.

169.   Yang, L.Y., Feng, G.P., and Wang, T.X., Green synthesis of ZnO2 nanoparticles from hydrozincite and hydrogen peroxide at room temperature. Materials Letters, 2010. 64(14): p. 1647-1649.

170.   Zhang, L., Yu, J.C., Yip, H.Y., Li, Q., Kwong, K.W., Xu, A.W., and Wong, P.K., Ambient Light Reduction Strategy to Synthesize Silver Nanoparticles and Silver-Coated TiO2 with Enhanced Photocatalytic and Bactericidal Activities. Langmuir, 2003. 19(24): p. 10372-10380.

Table 2.1.1 Applications of nanotechnology in different fields

Application	NPs	Reference
Technology		
Optics	Au	[5, 25, 35-44]
• **Optical and electro-optical devices**	Ag	[5, 25, 37, 41-43, 45]
• **Spectrally selective coatings**	ZnO	[46]
	Pt	[37]
Medicine		
Diagnosis and treatment	Ag	[5-7, 9, 10, 13, 22, 25, 37, 41-43, 45, 47-
• **Monitoring of cancer**	Au	73]
• **Development of new drugs (anticancer)**	Pd	[14, 20, 25, 35, 37, 39, 56, 70, 71, 74-88]
• **Drug delivery**	CuO	[51]
• **Fabrication of implants**	Pt	[89]
• **Healthcare product (glucose sensor, antimicrobial agent)**	CuO	[37]
	Fe_3O_4	[89]
	ZnO	[90-92]
	Carbon	[46]
		[93]
DNA study	ZnO	[46]
• **Labeling, Detection, Sequencing**	Au	[74]
	Ag	[53]
Organics Decontamination		
Water purification	ZnO	[46]
	Au	[14]
Site remediation	Fe	[94, 95]
• **Soil**	Fe-Pd	[96]
• **Air**	TiO_2	[97]
Industry		
Chemical reaction	Ag	[5, 9, 19, 25, 37, 42, 45, 58, 60, 73, 98-
• **Electrocatalysts**	Au	102]
• **Photocatalysts**	Pt	[14, 25, 35, 37, 74, 77, 79, 80, 98, 101,
• **Pigments**	Pd	103]
	Au-Ag	[37]
	Pd-Ag	[16]
	Au-Pd	[104]
	ZnO	[105]
	Pt-Pd	[106]
		[46]
		[107]
Energy systems	Ag	[5, 42, 43, 108]
• **Heat transfer devices**	Au	[108]
• **Energy storage (electrical batteries)**	Au-Ag	[108]
• **Solar energy absorption**	CuO	[89]
Electronics	ZnO	[46]
• **Microelectronics**	Au	[14, 35, 36, 39, 77, 80, 109]
• **Nanoelectronics**	Ag	[9, 44, 60, 100, 102, 109]
• **High-conductivity elements fabrication**	Pt	[109]
• **Optoelectronics**		
Analytical and Measuring Instrument		
Surface enhanced raman spectroscopy (SERS)	Ag	[41, 44, 53, 56, 57, 73, 99, 100, 110-112]
	Au	[14, 35, 41, 56]
Sensors	Ag	[5, 43]
	Au	[35, 39, 82, 113]
	CuO	[89]
	ZnO	[46]
Biology		

Biological study • **Biological labeling** • **Targeted biological interactions** • **Detection of reporter molecules** • **Diagnostic biological probes** • **Biosensing** • **Fluorescent Probe**	Ag Fe_3O_4 Au	[5, 42, 43, 54, 66] [90] [36, 114]
Consumer Products		
Household items **(detergents, soaps, shampoos, cosmetic products, and toothpaste)**	Ag Au Pt Pd	[7, 43, 52, 115] [115] [115] [115]
Food	Ag	[7, 43]

Table 2.1.2 Summary of synthesized NPs with different green reagents

NPs	Precursor	Reducing agent	Stabilizer	Support	Size (nm)	Reference
Au	$HAuCl_4$	Chitosan	Chitosan	--	10-50	[140]
Ag	$AgNO_3$	$NaBH_4$	Chitosan	--	< 20	[72]
Au	$HAuCl_4$	Chitosan	Chitosan	--	18-200	[86]
Ag and Au	$AgNO_3$ and $HAuCl_4$	Chitosan	--	Chitosan	ND	[56]
Ag	$AgNO_3$	Chitosan	--	Chitosan	6-8	[99]
Au	$HAuCl_4$	CHIT-NH[A]	--	CHIT-NH[A]	18	[114]
Ag, Au and Pt	$AgNO_3$, $AuCl_3$ and H_2PtCl_6	$NaBH_4$	CMC[B]	--	3.5 (Pt), 23 (Au), and 7.5 (Ag)	[142]
Au	$HAuCl_4$	Chitosan	Chitosan	--	7-20	[143]
Ag	$AgNO_3$	--	$(GlcN)_x$[C]	--	5-15	[141]
Ag	$AgNO_3$	Heparin	Heparin	--	9-29	[143]
Au, Ag and Au-Ag	$AgNO_3$ and $HAuCl_4$	Glucose	Starch	--	< 10	[26, 108]
Ag	$[Ag(NH_3)_2]^+$	Glucose	--	--	20-30	[111]
Ag	$[Ag(NH_3)_2]^+$	D-glucose	SDS[D], Tween 80[E] or CTAC[F]	--	50 (SDS), 65 (Tween 80) and 66 (CTAC)	[100]
Fe_3O_4	$FeCl_3.6H_2O$	α-D-glucose	Gluconic acid	--	12.5	[90]
Ag	$AgNO_3$	Gelatin	Gelatin	--	< 15	[21]
Ag	$[Ag(NH_3)_2]^+$	Four Sugars [G]	--	--	45-380	[57]
Ag	$[Ag(NH_3)_2]^+$	D-maltose	SDS[D], Tween 80[E] or PVP 360[H]	--	26	[64]
Ag	$AgNO_3$	Glucose	Starch	--	10	[146]
Au	$HAuCl_4$	H_2O_2	Starch	--	10-30	[83]
Ag	$AgNO_3$	Starch	Starch	--	10-34	[87]
CdSe	$CdCl_2.2.5H_2O$, Se powder and $Na_2SO_3.7H_2O$	--	Starch	--	3	[147]
Au-Ag	$AgNO_3$ and $HAuCl_4$	DPS[I]	DPS[I]	--	32	[104]
Ag and Au	$AgNO_3$ and $HAuCl_4$	HA[J]	HA[J]	--	5-30 for both	[70]
Ag	$AgNO_3$	DAPHP[K]	DAPHP[K]	--	11	[55]
Ag and Au	$AgNO_3$ and $HAuCl_4$	DAPHP[K]	DAPHP[K]	--	10 (Au) and 7 (Ag)	[70]
Ag and Au	$AgNO_3$ and $HAuCl_4$	DAPHP[K]	DAPHP[K]	--	14 (Au) and 10-30 (Ag)	[71]
Ag, Au and Pt	$AgNO_3$, $HAuCl_4.3H_2O$ and $PtCl_4$	--	Cellulose	Cellulose	11.4 (Ag), 7 (Au) and 5.6 (Pt)	[37]
Ag	$AgNO_3$	CMS[L]	CMS[L]	--	15	[17]
Au	$HAuCl_4.3H_2O$	Dextran	Dextran	--	80	[82]
Au	$HAuCl_4$	DEAE-Dextran[M]	DEAE-Dextran[M]	--	18-40	[35]
Ag and Au	$AgNO_3$ and $HAuCl_4$	CA[N]	CA[N]	--	< 10 for both	[98]
Ag	$AgNO_3$	SP[O]	SP[O]	--	13	[63]
Ag	$AgNO_3$	β-D-glucose	PEG[P]	--	10.6-25.31	[4]
Ag	$AgNO_3$	Sugar	PEG[P]	--	11.23	[62]
Ag	$AgNO_3$	PEG[P]	PEG[P]	--	< 5	[110]
Ag	$AgNO_3$	PEG[P]	PEG[P]	--	8-10	[148]
[198]Au	$H^{198}AuCl_4$	PEG[P]	PEG[P]	--	15-20	[149]
Fe_3O_4	$Fe(acac)_3$ [Q]	PEG[P]	PEG[P]	--	2-7	[91]
Ag/GN	$AgNO_3$	TA[R]	--	GN[S]	20	[73]

Ag and Au	AgNO$_3$ and HAuCl$_4$	Apiin	Apiin	--	21 (Au) and 39 (Ag)	[38]
Fe$_3$O$_4$	FeCl$_3$	--	L-Arginine	--	13	[92]
Ag	AgNO$_3$	L-Lysine or L-Arginine	Starch	--	26.3	[112]
Ag	AgNO$_3$	Gum kondagogu	Gum kondagogu	--	3	[54]
Ag	AgNO$_3$	Amino acid	Amino acid	--	ND	[22]
Au	HAuCl$_4$	POM^T	POM^T	--	10	[151]
Pd	K$_2$PdCl$_4$	POM^T	POM^T	--	15-50	[150]
Ag, Au, Pd and Pt	AgNO$_3$, HAuCl$_4$, PdCl$_2$ and H$_2$PtCl$_6$	POM^T	POM^T	--	13 (Au), 15 (Ag), 5 (Pd) and 2.7-24 (Pt)	[134]
Au	HAuCl$_4$	POM^T	POM^T	--	9.5	[36]
Pd and Pt	K$_2$PtCl$_4$, K$_2$PdCl$_4$, and PdSO$_4$	POM^T	POM^T	--	1.7-4	[153]
Pd	[PdCl$_4$]$^{2-}$	POM^T	POM^T	--	3	[154]
Pd and Pt	K$_2$PtCl$_4$ and K$_2$PdCl$_4$	POM^T	POM^T	--	9-14 (Pd) and 1.7-3 (Pt)	[155]
Pt-Pd/GNs	K$_2$PdCl$_4$ and K$_2$PtCl$_4$	Ethanol	--	GN^S	7.9	[107]
Ag	AgNO$_3$	Geraniol	PEG^P	--	1-10	[47]
Ag	AgNO$_3$	NRL^U	NRL^U	--	2-100	[8]
Pd-Ag/RGO	AgNO$_3$ and K$_2$PdCl$_4$	GO^V	GO^V	GO^V	< 10	[105]

A) Chitosan-ninhydrin: CHIT-NH, B) Carboxymethyl chitosan: CMC, C) Oligochitosan: (GlcN)x, D) Sodium dodecyl sulfate: SDS, E) Polyoxyethylenesorbitan monooleate: Tween 80, F) Cetyltrimethylammonium chloride: CTAC, G) Xylose, Glucose, Fructose and Maltose, H) Polyvinylpyrrolidon: PVP 360, I) Degraded Pueraria Starch: DPS, J) Hyaluronan acid: HA, K) 2, 6- diaminopyridinyl heparin: DAPHP, L) Carboxymethyl cellulose sodium: CMS, M) Diethylaminoethyl-Dextran: DEAE-Dextran, N) Calcium alginate: CA, O) Sulfated polysaccharide: SP, P) Polyethylene Glycol: PEG Q) Iron acetylacetonate: Fe(acac)$_3$, R) Tannic acid: TA, S) Graphene: GN, T) Polyoxometalates: POM, U) Natural rubber latex: NRL, V) Graphene Oxide: GO, ND: No Data

Table 2.1.3 Important examples of nanoparticle biosynthesis using plants

Plant origin	NPs	Size (nm)	Morphology	References
Alfalfa	Au	Up to 360	FCC Tetrahedral, Hexagonal platelet, Icosahedral, Decahedral and Irregular	[163]
Aloe Vera	Au	50-350	Spherical and Triangular	[41]
Aloin A and Aloesin	Au	4-45	Spherical	[161]
Aloin A and Aloesin	Ag	5	Spherical	[161]
Argemone maxicana	Ag	30	Cubic and Hexagonal	[9]
Azadirachta indica (neem)	Ag	Up to 200	Triangular	[109]
Black Tea leaf extracts	Ag and Au	~20	Spheres, Trapezoids, Prisms and Rods	[24]
Bryophyllum sp	Ag	2-5	FCC unit cell structure	[159]
Cacumen Platycladi	Au-Pd	7	Spherical	[106]
Callicarpa maingayi	Ag	12.4	Spherical	[115]
Cassia auriculata	Au	15-25	Triangular and Spherical	[74]
Centella asiatica	Au	9.3-10.9	Triangular, Hexagonal and Spherical	[88]
Ceratonia silique	Ag	5-40	Spherical	[45]
Chlorella vulgaris	Ag	20	Truncated triangular and Irregular	[59]
Cinnamomum zeylanicum	Au	25	Prisms and Spheres	[39]
Corriandrum sativum	ZnO	66-81	Cubic	[46]
Curcuma longa	Ag	6.3	Spherical	[42]
Cyprus sp.	Ag	2-5	FCC unit cell structure	[159]
Eclipta	Ag	2-6	Spherical	[160]
Eucalyptus chapmaniana	Ag	60	FCC unit cell structure	[6]
Eucalyptus citriodora	Ag	~20	Spherical	[67]
Ficus bengalensis	Ag	~20	Spherical	[67]
Ficus benghalensis	Ag	16	Spherical	[13]
Fucus vesiculosus	Au	NR	Spherical	[113]
Hibiscus Rosa sinensis	Au	~14	Triangular, Hexagonal, Dodecahedral and Spherical	[84]
Hibiscus Rosa sinensis	Ag	~13	Spherical	[84]
Hydrilla sp	Ag	2-5	FCC unit cell structure	[159]
Iresine herbstii	Ag	44-64	Spherical	[48]
Jatropha curcas (latex)	Ag	20-40	FCC unit cell structure	[76]
Jatropha curcas (seed extract)	Ag	15-50	Spherical	[102]
Lemongrass plant	Au	~25	Triangular	[40]
Leptadenia reticulate	Ag	50-70	Spherical	[49]
Lonicera japonica	Ag	7.8	Spherical, Triangular and Hexagonal	[25]
Lonicera japonica	Au	8.02	Spherical, Triangular and Hexagonal	[25]
Macrotyloma uniflorum	Au	14-17	Spherical	[14]
Mangifera indica	Au	18	Spherical	[158]
Mangifera indica	Ag	20	Triangular, Hexagonal and Spherical	[43]
Mulberry leaves	Ag	20-40	Spherical	[58]
Musa balbisiana (banana)	Ag	80.2	Spherical	[109]
Ocimum tenuiflorum (tulsi)	Ag	Up to 200	Cuboidal	[109]
Pelargonium graveolens	Ag	27	Spherical and Ellipsoidal	[162]
Psidium guajava	Au	4-24	Spherical	[75]
Rose petals	Au	10	Spherical, Triangular and Hexagonal	[20]
Scutellaria barbata	Au	5-30	Spherical and Triangular	[77]
Tea extract	Ag	11-30	Spherical	[32]
Tea and coffee extract	Ag and Pd	20-60	Spherical	[51]
Tea extract	Au	15-45	Spherical	[79]
Trigonella foenum-graecum	Au	15-25	Spherical	[19]
Vitex negundo	Ag	18.2	Spherical	[5]

FCC: face centered cubic
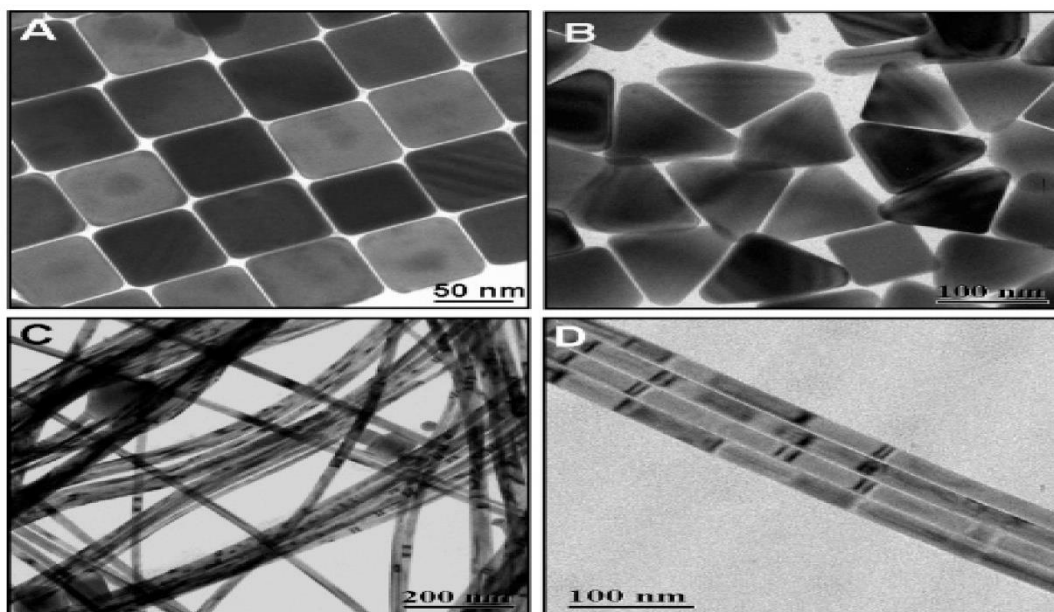
Figure 2.1.1 TEM images of Ag NPs: (a) cubes; (b) triangles; (c) wires; (d) an alignment of wires. Reproduced with permission from [145]; Copyright (2005) American Chemical Society.
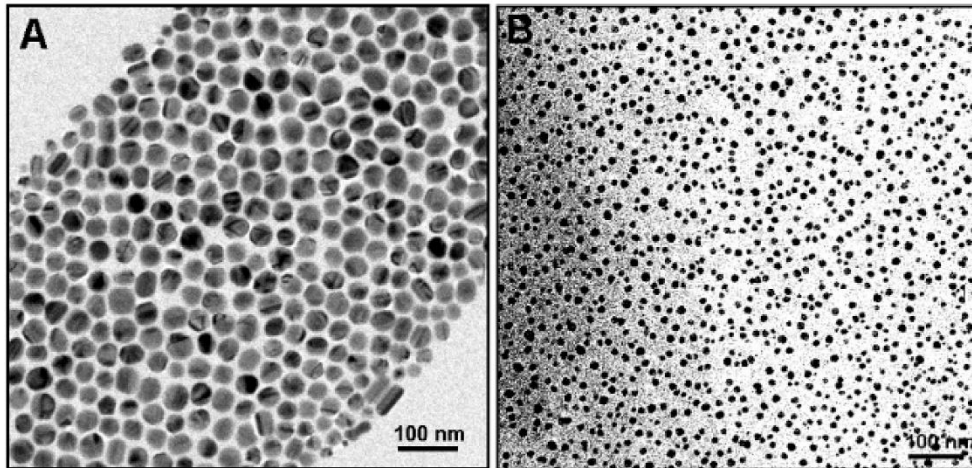
Figure 2.1.2 TEM images of Ag colloids synthesized at 120 °C for 8 h. Reproduced with permission from [145]; Copyright (2005) American Chemical Society.
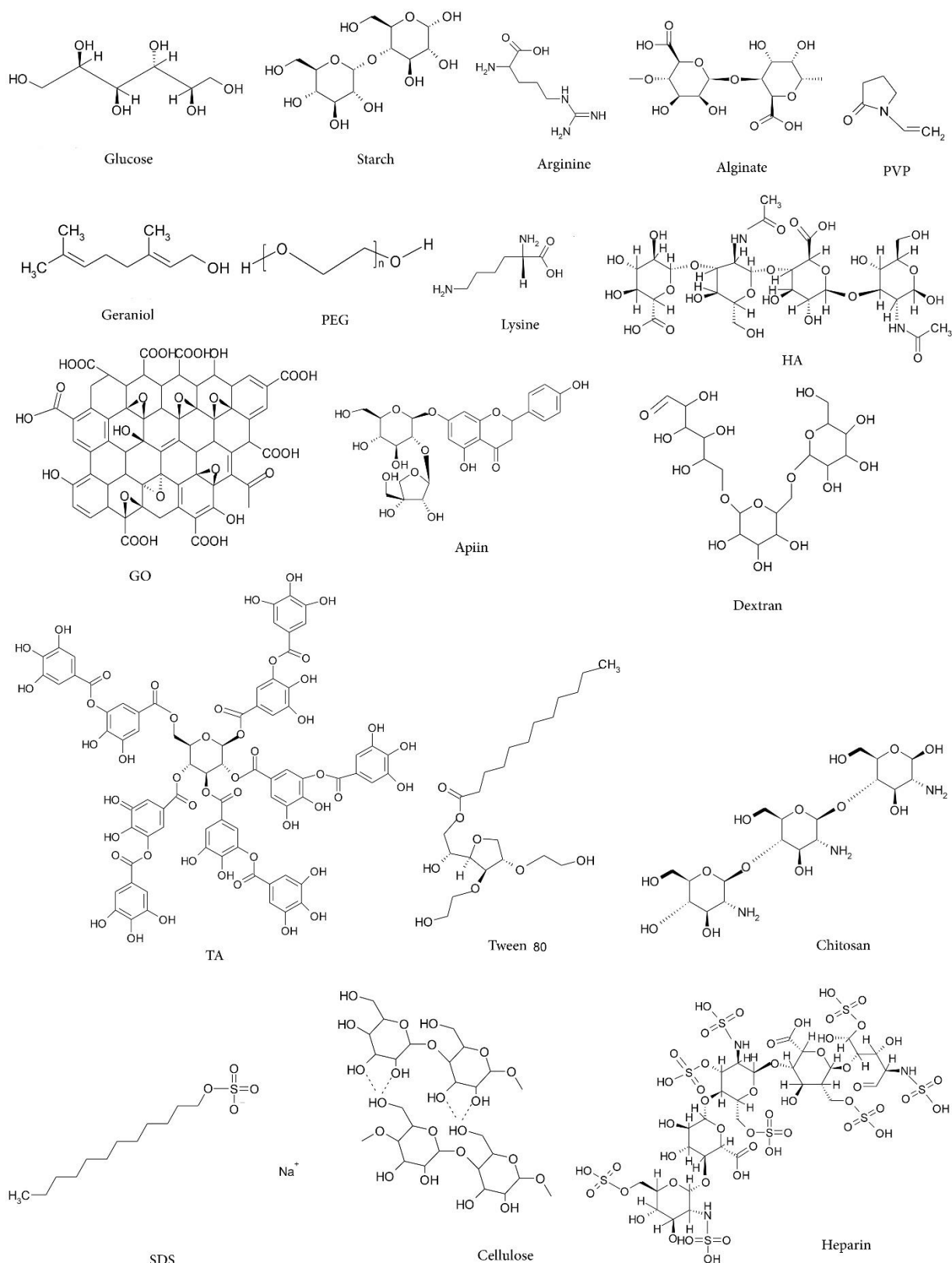
Figure 2.1.3 Molecular structures of different green reagents used for synthesis of NPs.

Part 2

Nanotechnology to Remove Contaminants

Mitra Naghdi[1], Mehrdad Taheran[1], Saurabh Jyoti Sarma[1], Satinder Kaur Brar[1], Antonio A. Ramirez[2], Mausam Verma[3]

[1]INRS-ETE, Université du Québec, 490, Rue de la Couronne, Québec, Canada G1K 9A9

[2]Centre National en Électrochimie et en Technologie Environnementales Inc., 2263, avenue du Collège, Shawinigan, Québec G9N 6V8 Canada

[3]CO$_2$ Solutions Inc., 2300, rue Jean-Perrin, Québec, Québec G2C 1T9 Canada

(*Phone: 1 418 654 3116; Fax: 1 418 654 2600; E-mail: satinder.brar@ete.inrs.ca)

Résumé

Les contaminants émergents constitueront un défi majeur pour la santé humaine et l'environnement puisque leurs concentrations sont en train d'augmenter. Les contaminants se retrouvent dans l'air, dans le sol et dans les milieux aquatiques avant de finir dans l'eau potable. Les contaminants causent de nombreux problèmes de santé aux organismes vivants, comme par exemple la perturbation des systèmes endocriniens et la féminisation des poissons mâles. . Par conséquent, la prévention de la libération de contaminants et le nettoyage des milieux contaminés sont nécessaires. De nombreux processus, y compris la séparation physique, le traitement biologique et la transformation chimique ont été mis en place pour éliminer les contaminants. Ici, nous passons en revue les méthodes d'élimination des contaminants à l'aide de nanomatériaux, tels que les nanoparticules, les nanotubes et les membranes nanostructurées. De nouveaux procédés basés sur des matériaux nanostructurés tels que les nanofils de TiO_2 ou la membrane de nanofiltration peuvent atteindre jusqu'à 95% d'élimination des contaminants.

Mots-clés

Nanotechnologie, Réhabilitation, Capteurs, Agriculture, Environnement

Abstract

Emerging contaminants will be a major challenge for human health and environment since their concentrations are increasing. Contaminants occur in air, soil and aquatic media, then finally end up in drinking water. Contaminants cause many health issues to living organisms, by disruption of endocrine systems and feminization of male fish, for instance. Therefore, prevention of contaminant release, and cleaning of contaminated media are needed. Many processes, including physical separation, biological treatment and chemical transformation have been set up to remove contaminants. Here we review methods to remove contaminants using nanomaterials, such as nanoparticles, nanotubes, and nanostructured membranes. New processes based on nanostructured materials such as TiO_2 nanowires or nanofiltration membrane can achieve up to 95% removal of contaminants.

Keywords

Introduction

Emerging contaminants are a number of polluting compounds, which are of emerging public interest due to potential health or environmental effects. These compounds have been released into environment since their use has commenced [1], but they might be beyond the detection limits of analytical methods. In the past 20 years, by developing sophisticated analytical instrument, researchers have detected them in different environmental compartment, including water, air, soil and sediments.

The possible routes for transport of emerging contaminants from point of use to drinking water have been illustrated in Figure 2.2.1. In the case of pharmaceutically active compounds, veterinary drugs find their ways into soil when manure is used on agricultural field. Later, they can go to groundwater or surface water through leaching or run-off from livestock slurries, respectively. Also, excess human pharmaceuticals and other chemical compounds in the customer products end up in wastewater treatment plants and afterwards, they can enter aquatic media through effluent or soil via biosolids [2]. It is noteworthy that compounds with higher volatility can go to air form soil or water.

Until date, there is no regulatory status for the majority of emerging contaminants and their metabolites [3] however their effects on ecosystem and human health is becoming more obvious as a result of recent research works. For example, the increased number of female fish in some aquatic media is attributed to steroid hormones that find their way into rivers from municipal wastewater treatment systems [4]. Also, there are reports on the relation of polybrominated diphenyl ethers and cancer proliferation [5]. Until now, three lists for emerging contaminants are published by the United States Environmental Protection Agency and the draft of fourth list is prepared. In Table 2.2.1, different classes of emerging contaminants with related examples have been presented.

To prevent adverse effects of emerging contaminants, capability of their efficient removal from different environmental compartments is of high importance. Different processes including filtration, adsorption, biodegradation and chemical oxidation are suggested to remove these compounds. However, they need much more research work to satisfy performance and economic requirements. Meanwhile, nanotechnology, with its impacts on scientific and technological breakthroughs, is the most likely tool to revolutionize the purification and remediation processes for contaminated media [6-

10]. Nanomaterials exhibit novel physical, chemical and biological properties due to their larger surface area per unit of volume and quantum effects. The potential capabilities of nanotechnology are divided into three classes, including treatment, detection, and prevention [11, 12]. In this chapter, thus, an overview on recent advances in nanotechnology for removing emerging contaminants from different media including water, wastewater and soil is provided. The applications of nanomaterials are critically reviewed based on their structures e.g. nanoparticles, nanotubes, among others and related challenges for their application in full-scale and the research needs for overcoming these challenges are also discussed.

Applications for water and wastewater treatment

At nanoscale, materials show size-dependent properties that are remarkably different from large particles. Several of these scalable properties including fast dissolution, high reactivity, and strong sorption are desirable for water treatment applications. Also, there are several discontinuous properties, such as superparamagnetism, localized surface plasmon resonance, and quantum confinement effect that can be used for specific applications. In Table 2.2.2, the application of nanomaterials in water treatment processes have been listed. Generally, there are physical separation methods, such as membrane filtration and adsorption system and chemical transformation processes, such as photocatalytic degradation and nanotechnology could enhance all these processes by novel well-structured materials, such as nanofibers, nanotubes, nanoplatelets, nanolayers, among others. In the following sections, the recent research on removal of emerging contaminants using important classes of nanostructured materials have been summarized.

Nanoscale TiO$_2$

Titanium dioxide (TiO$_2$), also known as Titania, is a well-known semiconductor with photocatalytic properties. This compound is widely used in advanced oxidation processes for water and air remediation. Nanoscale TiO$_2$ materials attracted the attention of researchers for their enhanced photocatalytic properties [14, 15]. As shown in Figure 2.2.2, the photocatalytic properties of TiO$_2$ originated from absorption of ultraviolet light that lead to the formation of charge carriers i.e. hole and electron. The generated holes in the valence band diffuse to the surface of TiO$_2$ and react with

water molecules to form hydroxyl radicals (OH$^\bullet$). On the other hand, oxygen molecule can be reduced by one of generated electrons to a superoxide radical (O$_2^{\bullet-}$) that can be further reduced by another electron or reacts with a hydroperoxyl radical (HO$_2^\bullet$) to form hydrogen peroxide (H$_2$O$_2$) [16]. Therefore, as a result of light absorption, reactive species, such as hydroxyl radicals and hydrogen peroxide are formed which reacts with contaminants in water and transform them into metabolites.

There are several challenges for commercialization of this process at large scale, such as high operational cost and lack of knowledge on the degradation mechanism. It is obvious that the metabolites of contaminants degradation should be much less toxic than the parent compounds, otherwise, only transforming the contaminants to another unfavorable species will be useless. Measuring the total organic carbon during the reaction is a good criterion to assess the performance of degradation system in transforming the contaminants to non-toxic species. Another challenge for using photooxidation process is the effect of solution chemistry and presence of other constituents in aqueous media, such as sulphate ions that can react with the reactive groups and impede the contaminant degradation.

In recent years, researchers have tried to thoroughly investigate the dominants parameters of this process in order to develop an efficient system for removal of all organic contaminants from water. For example, Mahmoodi and Arami immobilized TiO$_2$ nanoparticles on the walls of their reactor to act as nanophotocatalyst in the presence of ultraviolet irradiation for degradation of two agricultural organic pollutants including Alachlor and Fenitrothion. The results showed that after 180 min of reaction, both compounds degraded and after 240 min complete mineralization was achieved [17]. Hu *et al.* developed a dense TiO$_2$ membrane nanowire of 10-20 nm in diameter directly on Ti substrates at 180 ºC to prepare a nanophotocatalyst for degradation of trimethoprim, norfluoxetine and atorvastatin as a model pharmaceutical compounds in presence of ultraviolet light irradiation. Their results showed more than 95% degradation of model compound after 25 min of reaction [18].

To investigate the effect of pH and temperature, Liang *et al.* produced TiO$_2$ nanobelts with 30-100 nm in width and tens of um in length to use as nanophotocatalyst for degradation of persistent pharmaceutical compounds such as naproxen, carbamazepine and theophylline in water treatment effluents. According to their results, higher temperature and higher pH favors the photodegradation of theophylline

in presence of TiO_2 nanobelts and ultraviolet light. They also observed that after 90 min of reaction, more than 95% of three compounds were degraded [19]. Shirazi *et al.* used the TiO_2 nanoparticles with the average size of 21 nm to degrade carbamazepine from water in the presence of ultraviolet light. They achieved 85% degradation after 36 min for carbamazepine in distilled water, but they observed that the removal efficiency declined to 30% when the source of water was changed to groundwater. They attributed this reduction to the presence of divalent ions, such as SO_4^{2-} and CO_3^{2-} since these ions may adsorb onto the surface of the TiO_2 and prevent the generation of superoxide anion $O_2^{\cdot-}$ and hydroxyl radical $OH^\cdot$ [20]. In Table 2.2.3, the reaction constants and water matrices in different degradation systems, which follow the pseudo-first order reaction, are listed. According to this table, the value of K largely influences the economy of the systems. For example, when K is higher than 0.1 min^{-1}, more than 95% of the compound can be degraded within 30 min whereas for K less than 0.01 min^{-1}, only 16% of the contaminant can be degraded within the same time. Therefore, developing systems with higher K value can decrease the capital and operational costs to a remarkable extent.

Doped TiO_2

In order to increase the performance of TiO_2 nanophotocatalyst, researchers investigated the effect of doping TiO_2 with other elements such as iron, carbon and nitrogen. For example, Wang *et al.* synthesized anatase TiO_2 nanoparticles doped with iron and carbon (Fe/C-TiO_2) to degrade bisphenol A and clofibric acid in a photocatalytic process. They observed that Fe and C had synergistic effects on improving photocatalytic activities of Fe/C-TiO_2 as compared to C-TiO_2, Fe-TiO_2 and TiO_2 nanoparticles under simulated solar light and visible light irradiation. According to their results, no bisphenol A or clofibric acid could be detected after 4 h of irradiation with visible light by Fe/C TiO_2, and 61% and 71% of the total organic carbon were mineralized, respectively [27]. Hossaini *et al.* doped TiO_2 with a mixture of iron and non-metal elements i.e. N, S and F for use in light emitting diodes-activated photocatalysis process for degradation of diazinon pesticide. Their analysis showed that the nanophotocatalyst comprised of mesoporous nanocrystals with the average size of 6.7 nm. They observed that the new nanophotocatalyst can improve the degradation of diazinon by 52.3% compared to plain TiO_2 at neutral pH. Also, they

reported that diazinon degradation increased from 44.8% to 96.3% when the concentration of nanophotocatalyst increased from 25% to 300% at a reaction time of 100 min [21].

Pelaez *et al.* used nonionic fluorosurfactant as pore template material to dope TiO_2 nanoparticles with nitrogen and fluorine. The new material employed contained mesoporous structure with pore size of 2-10 nm in photocatalytic process under visible light with λ higher than 420 nm for destruction of microcystin. They achieved the highest degradation rate of 70% after 2 hours at pH 3, and the electrostatic interactions between compound and the TiO_2 nanoparticles with nitrogen and fluorine nanosystem favored photocatalytic degradation. They concluded that co-doping TiO_2 with nitrogen and fluorine increased photocatalytic activity compared to TiO_2 nanoparticles with only fluorine or nitrogen doping (less than 20% degradation) [14]. In a similar study, Barndok *et al.* synthesized a nanosystem of TiO_2 nanoparticles (50 nm) doped with nitrogen and fluorine to remove atrazine, carbamazepine, and caffeine from water through a photocatalytic process using solar light. They performed their tests in synthetic water and also in an effluent from a hybrid biological concentrator reactor. The results showed that after two hours of reaction, about 70, 75, and 80% removal in synthetic water and about 50, 70, and 70% removal in the biological concentrator reactor effluent was obtained for atrazine, carbamazepine, and caffeine [22]. The presence of various complex ions, such as sulfate and chloride compete with target compounds in the photocatalytic process and therefore the efficiency of such system under real conditions is less than the one obtained under controlled conditions in laboratory.

TiO_2 nanoparticles are also studied for their adsorption capacity for contaminants. For example, Hristovski *et al.* studied the capabilities of aggregated TiO_2 nanoparticles for adsorption of arsenate from four different water matrices in a packed bed column. In their batch tests, TiO_2 nanoparticles achieved 98% removal rate in all water matrices which is remarkable [28]. In another study, Hristovski *et al.* transformed TiO_2 into bundle-like titanate nanofibers of rectangular in shape with ~4um long and 30–100 nm thick in order to increase the adsorption capacity for arsenate. However, their experiment showed that commercial TiO_2 had 40 times more capacity in comparison to synthesized nanofibers and therefore they were less suitable for arsenate removal though they have unique surface chemistry and porosity [29]. In Table 2.2.4 and Table

2.2.5, a summary of nanostructured adsorbent with their related parameters are listed. In Freundlich model, there is no maximum adsorption capacity because adsorbates can form multilayers around adsorbent. But in Langmuir and Polanyi-Manes models, there are maximum values for adsorption or sorption. Many of the proposed nanostructured materials showed superior performance compared to their conventional counterparts. However the high cost of nanomaterials production and their limited life cycles are important challenges for their scale-up.

Magnetic nanoparticles

Magnetic nanoparticles consist of magnetic elements, such as iron, cobalt and nickel in their chemical structure. Since these nanomaterials combine high surface area with magnetic properties, they can be easily isolated from solution by applying a magnetic field. Because of these interesting properties, magnetic nanoparticles have been the focus of much research in recent years for their potential use in catalysis and adsorption. For example, Shen *et al.* synthesized magnetic Fe_3O_4-C18 composite nanoparticles with the size of 5-10 nm for using in the clean-up and enrichment procedures of measuring organophosphorous pesticides by gas chromatography technique. According to their results, the composite nanoparticles have comparable recovery of 80-93% to conventional C18 materials that is 82-94% recovery while clean-up and enrichment procedures are faster and easier. They also observed that Fe_3O_4-C18 composite nanoparticles is recyclable up to ten times with negligible loss of properties [30]. In a similar study, Moliner-Martinez *et al.* incorporated Fe_3O_4 magnetic nanoparticles in a silica matrix for extraction and pre-concentration of pharmaceutical compounds, such as aspirin, acetaminophen, diclofenac and ibuprofen from water without need of clean-up process. The recovery of this nanostructured sorbent was reported to be in the range of 80-110% with relative standard deviation less than 12%. Under the optimum conditions, the new sorbent material demonstrated suitable reusability during 20 uses with no loss in efficiency [31].

Zhu *et al.* developed graphene with strong magnetic properties composites by decorating nanoplatelets with core-shell Fe-Fe_2O_3 nanoparticles. The new nanomaterial was used for removal of arsenate from water. They observed that at optimum pH (~7), the maximum adsorption capacity is around 11.34 mg/g that is much

higher than other magnetic nanoparticles i.e. 1 mg/g [37]. Ghosh *et al.* studied the adsorption naproxen, carbamazepine and bisphenol A from aqueous solutions onto Fe_3O_4 nanoparticles that were coated with thiodiglycolic acid. They also grafted 6-deoxy-6-ethylenediamino-β-cyclodextrin onto the magnetic nanoparticles to compare the adsorption capacities. According to their results, the adsorption capacities of thiodiglycolic acid-coated nanoparticles with and without 6-deoxy-6-ethylenediamino-β-cyclodextrin graft were in the range of 0.24-0.38 mg/g and 0.90-1.30 mg/g. They suggested that Fe_3O_4 nanoparticles serve as magnetic separators and 6-deoxy-6-ethylenediamino-β-cyclodextrin provides the capability to adsorb pollutants through inclusive host–guest interactions [38].

Beside adsorption, magnetic Fe and Fe_3O_4 nanoparticles can act as catalyst in the degradation of emerging contaminants. Sun *et al.* used magnetic Fe_3O_4 nanoparticles with the average size of 30 nm for degradation of the carbamazepine and ibuprofen in aqueous suspensions. They concluded that at neutral pH, hydroxyl radical ($\cdot$OH) produced form the decomposition of H_2O_2 on the Fe_3O_4 nanoparticle surface plays the major role in the degradation of carbamazepine and ibuprofen. They also observed that the degradation of carbamazepine and ibuprofen fitted with pseudo-first-order kinetics model with the rate constants (k) of 0.182 and 0.121 hr^{-1}, respectively. In addition, the presence of montmorillonite can reduce the rate constant for carbamazepine due to adsorption at neutral pH, while it has no effect on ibuprofen due to electrostatic repulsion [23]. In another investigation carried out by Cao *et al.* Iron nanoparticles showed capability to reduce perchlorate (ClO_4^-) to chloride. Under same conditions, they reported no reduction using microscale iron powder. They observed that by increasing temperature from 25 to 75 ℃, the rate constant will increase from 0.013 to 1.52 (mg perchlorate / (g nanoparticles × hour)) [25]. Unfortunately, higher activation energy of perchlorate-iron reaction i.e. 79.02±7.75 kJ/mole is not favorable for large scale applications.

Palladium is known for its catalytic properties towards conversion of harmful gases in automobile exhaust to less harmful compounds. Also, nickel is widely used as a catalyst in organic chemistry for hydrogenation. Therefore, the idea of using these two metals in combination with iron nanoparticles for degradation of contaminants has led to interesting results. Chen et al synthesized iron/palladium (Fe/Pd) bimetallic nanoparticles to catalyze the degradation of 2, 2′, 4, 4′, 5, 5′-hexachlorobiphenyl in

deionized water. According to their results, the degradation efficiency for bimetallic nanoparticles and iron nanoparticles were 93.8% and 74.9% after 20 h of reaction. Later, they applied the results to the two soil samples collected from an electrical waste recycling area that was contaminated with polychlorinated biphenyls. They observed 53.4-81.5% removal efficiency of polychlorinated biphenyls from soil by Pd/Fe nanoparticles that was higher than 48.3-64.6% removal efficiency reported for iron nanoparticles [24].

In a similar study, Lien *et al.* produced iron nanoparticles in the size range of 1-100 nm for catalytic transformation of chlorinated methanes e.g. CCl_4, $CHCl_3$, CH_2Cl_2 and CH_3Cl. They also deposited palladium at the loading of 0.05-1% Pd by weight on the surface of iron and compared the capabilities of these two nanoparticles and also commercial iron particles with the average size of 10 μm in reaction with chlorinated methane. They observed that after one hour of reacting 0.1 mM of CCl_4 or $CHCl_3$, there was no detectable reactant in the case of palladized iron nanoparticles. In these reactions, methane and CH_2Cl_2 were the major end products at the yields of 52% and 23%, respectively. However, iron nanoparticles and commercial iron particles exhibited much slower reactions of chlorinated methanes. The kinetic analyses revealed that the surface area-normalized rate coefficients (k_{SA}) for palladized iron nanoparticles was two orders of magnitude greater than those for iron nanoparticles and commercial iron particles [42]. In another attempt, Vijayakumar *et al.* synthesized iron-nickel (Fe-Ni) nanoparticles in the size range of 36-41 nm and immobilized them on to a polysulphone support to use as a catalyst for the reduction of dichloroethane ($C_2H_4Cl_2$) and trichloroethylene (C_2HCl_3). They observed 90% removal after a 36 h reaction with the initial concentration of 26.81 and 682.81 ppb for $C_2H_4Cl_2$ and trichloroethylene C_2HCl_3 respectively. According to their study, in alkaline pH, Fe–Ni nanoparticles lose their catalytic properties and cannot get involved in the hydrodechlorination of target compounds [43]. Shirazi *et al.* used iron nanoparticles in the size range of 8-18 nm for degradation of carbamazepine in water in the presence of H_2O_2. They obtained 78.5% total organic carbon removal after only 5 min in the presence of 10 ppm iron nanoparticles and 25 ppm H_2O_2. In contrast to their result for TiO_2/ultraviolet process, no difference in performance was observed when water source was changed from distilled water to groundwater [20].

Precious metal nanosystems

Gold (Au) and Silver (Ag) nanoparticles are widely used in different applications, such as sensors, catalysis, electronics and medicals. Removal of emerging contaminants from water sources is another application of precious metals that has attracted the attention of researchers. For example, Das *et al.* produced gold nanoparticles with 10 nm in diameter through biosynthesis and used them for adsorption of organophosphorous pesticide, such as malathion and parathion from aqueous solutions. They observed that synthesized nanoparticles could remove almost all of the tested pesticides after 30 min [44]. In another study, Suman *et al.* produced Ag nanoparticles and embedded them within the porous concrete pebble particles. They also synthesized nanocellulose by acid hydrolysis of cellulose and used these two nanoparticles for removal of microbes (*Escherichia coli*) from water. They used a column with two beds of nano embedded Ag nanoparticles and one bed of nanocellulose in between for continuous purification of water and observed 99% decontamination of microbes at pH 6. According to their proposed mechanism, Ag nanoparticles kill microorganisms and prevent formation of biofilm and nanocellulose can adsorb dye and heavy metals and the column can be reused up to 5 cycles with no loss in performance [45].

Li *et al.* observed that the gold Au-coated TiO_2 nanotube arrays show recyclability as a substrate for surface-enhanced Raman spectroscopy. Interestingly, this new system can clean itself through photocatalytic degradation under ultraviolet light. However, recycling process is time consuming (30 min), and only highly trained staff can performed test with this new substrate [46]. Yu *et al.* developed a nanosystem by modification of TiO_2 nanotube film with Au and Pd (Au-Pd-TiO_2) to degrade malathion, which is an organophosphorus pesticide, through photocatalytic process in the presence of ultraviolet light. Their experiments showed that Au and Pd can increase the degradation rate by 172% compared to naked TiO_2 nanotube film and attributed this behavior to effective separation of generated charge carriers and also the higher generation rate of H_2O_2 [26]. Han *et al.* formed Ag nanoparticles with a diameter of 5.9±1.2 nm on TiO_2 aggregates to use for the photocatalytic degradation of the antibiotic oxytetracycline under ultraviolet -visible light irradiation. They observed that by increasing the load of Ag, the absorption in the visible light region increased. However, under both ultraviolet -visible light and visible light illumination, the highest

photocatalytic activity for the degradation of oxytetracycline was observed at 1.9 wt% of Ag loading so that it took 2 h for ultraviolet -visible and 3 h for visible light to reach below the detection limit of gas chromatography analysis [47].

Carbon nanotubes

Carbon nanotubes are categorized into single-walled carbon nanotubes and multi-walled carbon nanotubes according to their atom layers in the walls of carbon nanotubes. The diameter of single-walled carbon nanotubes range from 0.3 to 3 nm, whereas the multi-walled carbon nanotubes have concentric arrangement of cylinders and their diameters can reach up to 100 nm [48]. Carbon nanotubes have attracted attention of many researchers due to their outstanding structural, chemical and mechanical properties [49, 50]. Besides application in electronics, sensors, catalysis, and composite materials, carbon nanotubes showed a promising application as adsorbent material for different contamination due to their large surface area and also tubular structure [48, 51]. However, there are different parameters including surface chemistry of carbon nanotubes, the chemical properties of contaminants, and the chemistry of aqueous solution including pH, ionic strength and presence of other compounds that can affect the adsorption of contaminants onto carbon nanotubes.

Zhou fabricated a column of multi-walled carbon nanotubes as a sorbent for atrazine and simazine in the pre-concentration process for measuring these compounds using HPLC in water samples. The recovery of two compounds were in the range of 82.6-103.7% in spiked samples [52]. Shao *et al.* used multi-walled carbon nanotubes grafted with β-cyclodextrin to remove polychlorinated biphenyls from water under ambient conditions. In their experiments, multi-walled carbon nanotubes grafted with β-cyclodextrin showed higher adsorption capacity (95% removal) compared to multi-walled carbon nanotubes (90% removal) [40]. In a similar study, Salipira *et al.* tried to adsorb *p*-nitrophenol from water using a copolymer of cyclodextrin cross linked by 5% 0f functionalized carbon nanotubes. The new material could remove 99% of model compounds from 10 ppm spiked samples, whereas granular activated carbon and native cyclodextrin could remove only 47 and 58%, respectively. The new nanomaterial could maintain its adsorption capacity after at least 18 cycles [53]. In another study, they used the new copolymer to adsorb trichloroethylene and achieved 98% removal efficiency [54].

Chen *et al.* combined TiO$_2$ nanoparticles with multi-walled carbon nanotubes to enhance the photocatalytic degradation of atrazine under microwave irradiation rather than ultraviolet light. According to their results, the new composite material showed 20-30% higher efficiency compared to TiO$_2$ alone. They attributed this improvement to the strong capability of the new material to absorb microwaves [55]. Cho *et al.* studied the adsorption of ibuprofen and triclosan by single-walled, multi-walled and oxidized multi-walled carbon nanotubes from water under conditions close to natural environment and water treatment systems. They concluded that for hydrophobic compounds, single-walled carbon nanotubes have higher adsorption capacity than multi-walled ones due to larger specific surface area, while oxidized multi-walled carbon nanotubes showed lower capacity compared to not oxidized 0nes due to higher surface oxygen. They also indicated that for pHs below pKa, adsorption capacity was higher due to lack of electrostatic repulsion [41].

Zhang *et al.* studied the sorption kinetics of tetrabromobisphenol A onto raw and functionalized multi-walled carbon nanotubes in aqueous solutions using a pseudo-second-order model, an intraparticle diffusion model and Boyd model. According to their results, both types of multi-walled carbon nanotubes showed rapid binding for tetrabromobisphenol A within 20 min and the kinetics could be described by the pseudo-second-order model. Also, the external diffusion (boundary layer diffusion) was considered as the rate-limiting step [56].

Xu *et al.* developed a new adsorbent by self-assembling carbon nanotubes onto CaCO$_3$ micro-particles in shell-core structure and studied its capacity for removing 2-naphthol, naphthalene and 4-chlorophenol) from aqueous solutions. They observed that with increasing carbon nanotubes loading, the adsorption coefficient (K_f) increased but the normalized adsorption coefficient (K_{fCNT}) decreased [35]. Srivastava *et al.* fabricated carbon nanotube filter that consisted of hollow cylinders with radially aligned carbon nanotubes walls and used it for removal of bacterial pathogens (*Escherichia coli* and *Staphylococcus aureus*) and Poliovirus sabin 1 from water. This new filter was easily re-usable by ultrasonication or autoclaving [57].

Graphene nanoplatelets

Graphene is a new member of the carbonaceous nanomaterials group that has a 2D (Figure 2.2.3) honeycomb structure (sp^2-hybridization) with a thickness of one carbon

atom. Graphene can be considered as a building block for other carbonaceous nanomaterials, such as fullerene and nanotubes. Due to large theoretical specific surface area and especially highly hydrophobic surface, graphene shows strong adsorption affinity to hydrophobic organic pollutants, such as polycyclic aromatic hydrocarbons, chlorobenzenes, antibiotics, pesticides and phenols [58, 59]. After increasing awareness about the potential threats of emerging contaminants, researchers considered graphene as a promising solution to address the problem of removing these contaminants at lower concentrations.

For example, Al-Khateeb *et al.* studied the removal of aspirin, acetaminophen, and caffeine from aqueous solution by graphene nanoplatelets. Their results showed that pH 8 is the optimum pH and more than 94% of all compounds can be removed within 10 min at the graphene loading of 1 g/L. They also calculated the thermodynamic parameters (ΔG, ΔH and ΔS) of adsorption process and concluded that for the studied compounds, the process is spontaneous at all temperatures [61].

Several researchers tried to compare the performance of graphene with other adsorbent materials, such as granular activated carbon, carbon nanotubes and also other graphene based nanomaterials. For example, Rizzo *et al.* coupled conventional sand filtration with graphene adsorption system to remove pharmaceutical compounds from municipal wastewater. Using this system, they achieved more than 95% removal for caffeine, carbamazepine, ibuprofen and diclofenac while in same conditions, granular activated carbon showed only 63% removal for mixture of pharmaceutical compounds. They also observed that graphene treatment can decrease toxicity towards *Daphnia magna* with 0-50% immobilization [62]. In a similar investigation, Zhu *et al.* compared graphene with granular activated carbon system for adsorption of ciprofloxacin and observed 77% greater adsorption capacity for graphene (323 mg/g) compared to granular activated carbon (180 mg/g). According to the FTIR spectroscopy, they suggested that adsorption of ciprofloxacin on graphene primarily occurred through π-π interaction. Interestingly, they observed that ionic strength, presence of natural organic matter, and different water sources were less important for graphene than granular activated carbon [63]. In another study, Balamurugan and Subramanian compared the adsorption of the homologues series of chlorobenzenes with the molecular formula of $C_6H_mCl_n$ where m & n = 0-6, and m + n = 6 onto graphene sheet and single-walled carbon nanotube. They found that graphene has higher

adsorption capacity for chlorobenzenes compared to single-walled carbon nanotube that is due to planar geometry of graphene that facilitates the surface adsorption of compounds [64]. Also, Liu *et al.* compared three different graphene with single-walled carbon nanotube to remove ketoprofen, carbamazepine, and bisphenol A from water under different solution conditions. They observed that the adsorption isotherms were consistent with the orders of the surface areas and micropore volumes of adsorbents and therefore in all cases, single-walled carbon nanotube showed the best performance. Their results also suggested incomplete occupation onto adsorption sites of graphene as a result of the aggregation of sheets and the presence of remaining oxygen-containing functionalities [58].

Some researchers attached oxygen containing groups to graphene using strong oxidizers to enhance the functionality of graphene as adsorbent. These new nanomaterials are called "graphene oxide", however in several cases; they are reported to have lower adsorption capacity compared to pristine graphene. For example, Wang *et al.* synthesized graphene and graphene oxide nanosheets and compared their performance for adsorption of naphthalene from water. They observed that attaching oxygen-containing groups to graphene can severely decrease the affinity of polycyclic aromatic hydrocarbons to graphene which is dominated by π-π interactions and the sieving effect formed by wrinkles on graphene surfaces. In fact, by attaching the new groups, the grooves on the graphene surface disappeared and π-π interactions will be restricted [59]. Also, Yan *et al.* synthesized graphene oxide for the removal of aniline, nitrobenzene, and chlorobenzene, from water. They concluded that hydrophobic interactions (π-π stacking and hydrophobic effects) between graphene oxide and adsorbates played major role in the whole adsorption process. Also, they studied the effect of oxidizing extent of graphene on adsorption capacity and observed that moderately oxidized graphene with around 50% graphitic zone had the best adsorption performance due to good dispersibility and enough activated adsorption sites [36]. Kyzas *et al.* synthesized a nanocomposite from graphite oxide, which is the precursor of graphene, and modified chitosan for the removal of dorzolamide, that is a pharmaceutical compound, from biomedical synthetic wastewaters. They suggested that the reactive groups of graphite oxide and chitosan have interaction with the amino groups in dorzolamide molecule which enhanced adsorption capacity. The maximum adsorption at optimum pH (~3) was 334 mg/g

which was superior compared to graphite oxide (175 mg/g) and chitosan (229 mg/g) [65].

Polymeric nanosponge

Mhlanga *et al.* produced cyclodextrin polymer with nanosponge structure using bifunctional isocyanate linkers to remove a series of chlorinated disinfection by-products and an odor-causing compound, in water 2-methylisoborneol. The as-synthesized polymer could adsorb the pollutants with more than 99% efficiency at ng/l level which was superior to granular activated carbon [66]. Later, they reported the removal of n-nitrosodimethylamine from drinking water, using this nanosponge polymer with 80% efficiency [67]. The high efficiency of this polymer was due to the inclusive host–guest interactions between polymer and contaminants which is shown in Figure 2.2.4. However, nanosponge structures will be saturated after sometime and researchers should also investigate their recyclability.

Arkas *et al.* impregnated TiO_2 porous ceramic filter with nanosponge made from functionalized poly (propylene imine) dendrimer, poly (ethylene imine) hyperbranched polymer, and β-cyclodextrin derivatives to remove contaminants from water at ppb level. Their results showed that by using this new class of filter system, polycyclic aromatic hydrocarbons can be removed efficiently (higher than 95%) and other contaminants, such as trihalogen methanes, monoaromatic hydrocarbons, and pesticides were also removed efficiently (higher than 80%) [68, 69]

Nanofiltration membranes

Separation processes through nanofiltration membranes have been increasingly considered as an affordable and reliable technology for the purification of water from unconventional sources, such as contaminated surface water, brackish water, and secondary effluent of wastewater treatment plants where micropollutants should be removed according to regulations. Nanofiltration membrane has pore size of less than 2 nm or molecular weight cut-off in the range of 200-500 Da. Therefore, nanofiltration membranes are capable of removing pollutants having molecular weights larger than molecular weight cut-off of membrane. In Figure 2.2.5, the performance of different filtration technologies is illustrated. According to this figure, reverse osmosis membrane retained all the solutes, even monovalent ions, which was not necessary

and their operational costs are also high. On the other hand, ultrafiltration membranes can only retain microorganisms and proteins and they are not capable of filtering molecules with MW of less than 2000. Therefore, nanofiltration membranes could fill this gap with reasonable cost and reliable performance. At the present time, nanofiltration membrane modules are working in some water treatment plants in the world for removing or reducing contaminants. For example, in Cooper city, Florida, a drinking water treatment plant was upgraded in 1998 with nanofiltration membrane module with the capacity of 11000 m^3/day and is capable of producing high quality drinking water.

In some cases, the removal efficiency for certain compounds with nanofiltration membranes is more than 98%. However, besides size exclusion, there are several parameters, such as electrostatic charge repulsion, hydrophobic interaction and membrane fouling that can increase or decrease the rejection of contaminants. In recent years, many researchers tried to understand the mechanisms of solute transport in nanofiltration membranes so that they could select the best option for remediation of specific water source [70-75]. For example, Verliefde *et al.* studied the removal of different emerging contaminants using a nanofiltration system with negatively charged surface. They concluded that the size exclusion is the dominants mechanism for rejection of neutral compound such as carbamazepine, but for negatively and positively charged compounds such as ibuprofen and atenolol, electrostatic repulsions and attractions can affect the rejection [76, 77]. Interestingly, Nghiem *et al.* observed by increasing the pH to above the pKa of the compounds, they transform from neutral to negatively charged species and therefore the rejection of the compounds will be higher through nanofiltration membranes with negatively charged surface [73, 78].

Zhang *et al.* used nanofiltration membrane to remove bisphenol A from drinking water and observed that at the beginning of filtration the rejection rate was more than 90% but after several hours, due to the saturation of membrane, the rejection rate decreased to 50% [75]. Tepus *et al.* studied the effect of pressure on rejection rate of atrazine through nanofiltration membrane and observed that by increasing the pressure from 2 bar to 12 bar, the rejection rate will decrease from 60% to 50% [34]. Also Yuksel *et al.* used nanofiltration membrane for removal of bisphenol A from water and achieved 80% removal during 4 h of filtration [79]. In another study, Ahmad *et al.*

investigated the performance of four different nanofiltration membranes for removal of atrazine and observed that the rejection rate was in the range of 60%-95% for different membranes. They also observed that increasing the transmembrane pressure can lead to enhanced solute rejection and permeate flux [80]. Therefore, the characteristics of membranes including material, molecular weight cut-off and surface charge are very important in determining the rejection rate of membrane for each compound.

To sum up, nanofiltration membranes can show high rejection efficiency for a wide range of emerging contaminants, although their performances are impacted by different parameters. But as a rule of thumb, bigger molecules with negative charge and higher hydrophilicity are rejected more efficiently.

Conclusion

Emerging contaminants are going to become a big challenge to the environment and human health in the near future and therefore, to prevent from their adverse effects, having efficient methods for their removal from different media, especially water and wastewater is of higher importance. Conventional wastewater treatment plants are not able to remove these contaminants from wastewater or they only shift them to soil through biosolids. Hence, novel methods are necessary to remove them at maximum level. Meanwhile, nanotechnology is the most likely tool to develop the solutions for contaminated media and there are numerous research works in this field. Generally there are physical methods, such as adsorption systems and chemical methods, such as photocatalytic degradation which enhance their performance through nanostructured materials. For example, carbon nanotubes with their large specific surface areas showed a promising performance in adsorbing contaminants even at low concentrations and TiO_2 nanophotocatalyst proved to be capable of near complete mineralization of contaminants. Also, nanofiltration membranes showed the ability to filter some emerging contaminants with more than 95% efficiency. However, there are several drawbacks including the high cost of nanomaterials production, limited recyclability, sensitivity to interferences and toxicity of by-products that should be addressed before commercialization. Therefore, further research may result in better understanding of the mechanisms controlling emerging contaminants removal in different processes and finding solutions for current issues. Also, developing

combinational systems which integrate physical separation and chemical transformation into one solution may attract the attention of researchers in future due to their potential to overcome the drawbacks of single process methods.

Acknowledgement(s):

References

1. Englert, B.C., Nanomaterials and the environment: uses, methods and measurement. Journal of Environmental Monitoring, 2007. 9(11): p. 1154-1161.

2. Farre, M., Perez, S., Kantiani, L., and Barceló, D., Fate and toxicity of emerging pollutants, their metabolites and transformation products in the aquatic environment. TrAC Trends in Analytical Chemistry, 2008. 27(11): p. 991-1007.

3. Deblonde, T., Cossu-Leguille, C., and Hartemann, P., Emerging pollutants in wastewater: A review of the literature. International Journal of Hygiene and Environmental Health, 2011. 214(6): p. 442-448.

4. Spina, F., Cordero, C., Sgorbini, B., Schiliro, T., Gilli, G., Bicchi, C., and Varese, G.C., Endocrine Disrupting Chemicals (EDCs) in Municipal Wastewaters: Effective Degradation and Detoxification by Fungal Laccases. Chemical Engineering Transactions, 2013. 32: p. 391-397.

5. Siddiqi, M.A., Laessig, R.H., and Reed, K.D., Polybrominated Diphenyl Ethers (PBDEs): New Pollutants–Old Diseases. Clinical Medicine & Research, 2003. 1(4): p. 281-290.

6. Chirag, M.P.N., Nanotechnology: Future of Environmental Pollution Control. International Journal on Recent and Innovation Trends in Computing and Communication, 2015. 3(2): p. 079-081.

7.   Masciangioli, T. and Zhang, W.X., Peer Reviewed: Environmental Technologies at the Nanoscale. Environmental Science & Technology, 2003. 37(5): p. 102A-108A.

8.   Savage, N. and Diallo, M., Nanomaterials and Water Purification: Opportunities and Challenges. Journal of Nanoparticle Research, 2005. 7(4-5): p. 331-342.

9.   Bottero, J.Y., Rose, J., and Wiesner, M.R., Nanotechnologies: Tools for sustainability in a new wave of water treatment processes. Integrated Environmental Assessment and Management, 2006. 2(4): p. 391-395.

10.   Theron, J., Walker, J.A., and Cloete, T.E., Nanotechnology and Water Treatment: Applications and Emerging Opportunities. Critical Reviews in Microbiology, 2008. 34(1): p. 43-69.

11.   Rickerby, D.G. and Morrison, M., Nanotechnology and the environment: A European perspective. Science and Technology of Advanced Materials, 2007. 8(1-2): p. 19-24.

12.   Vaseashta, A., Vaclavikova, M., Vaseashta, S., Gallios, G., Roy, P., and Pummakarnchana, O., Nanostructures in environmental pollution detection, monitoring, and remediation. Science and Technology of Advanced Materials, 2007. 8(1-2): p. 47-59.

13.   Qu, X., Alvarez, P.J.J., and Li, Q., Applications of nanotechnology in water and wastewater treatment. Water Research, 2013. 47(12): p. 3931-3946.

14.   Pelaez, M., Cruz, A.A.d.l., Stathatos, E., Falaras, P., and Dionysiou, D.D., Visible light-activated N-F-codoped TiO2 nanoparticles for the photocatalytic degradation of microcystin-LR in water. Catalysis Today, 2009. 144(1–2): p. 19-25.

15.   Dasgupta, N., Ranjan, S., Mundekkad, D., Ramalingam, C., Shanker, R., and Kumar, A., Nanotechnology in agro-food: From field to plate. Food Research International, 2015. 69: p. 381-400.

16. Nakata, K. and Fujishima, A., TiO_2 photocatalysis: Design and applications. Journal of Photochemistry and Photobiology C: Photochemistry Reviews, 2012. 13(3): p. 169-189.

17. Mahmoodi, N.M. and Arami, M., Immobilized titania nanophotocatalysis: Degradation, modeling and toxicity reduction of agricultural pollutants. Journal of Alloys and Compounds, 2010. 506(1): p. 155-159.

18. Hu, A., Zhang, X., Oakes, K.D., Peng, P., Zhou, Y.N., and Servos, M.R., Hydrothermal growth of free standing TiO_2 nanowire membranes for photocatalytic degradation of pharmaceuticals. Journal of Hazardous Materials, 2011. 189(1-2): p. 278-285.

19. Liang, R., Hu, A., Li, W., and Zhou, Y.N., Enhanced degradation of persistent pharmaceuticals found in wastewater treatment effluents using TiO_2 nanobelt photocatalysts. Journal of Nanoparticle Research, 2013. 15(10): p. 1-13.

20. Shirazi, E., Torabian, A., and Bidhendi, G.N., Carbamazepine Removal from Groundwater: Effectiveness of the TiO_2/UV, Nanoparticulate Zero-Valent Iron, and Fenton ($NZVI/H_2O_2$) Processes. CLEAN - Soil, Air, Water, 2013. 41(11): p. 1062-1072.

21. Hossaini, H., Moussavi, G., and Farrokhi, M., The investigation of the LED-activated $FeFNS-TiO_2$ nanocatalyst for photocatalytic degradation and mineralization of organophosphate pesticides in water. Water Research, 2014. 59(0): p. 130-144.

22. Barndõk, H., Peláez, M., Han, C., Platten, W.E., Campo, P., Hermosilla, D., Blanco, A., and Dionysiou, D.D., Photocatalytic degradation of contaminants of concern with composite $NF-TiO_2$ films under visible and solar light. Environmental Science and Pollution Research, 2013. 20(6): p. 3582-3591.

23. Sun, S.P., Zeng, X., and Lemley, A.T., Nano-magnetite catalyzed heterogeneous Fenton-like degradation of emerging contaminants carbamazepine and ibuprofen in aqueous suspensions and montmorillonite

clay slurries at neutral pH. Journal of Molecular Catalysis A: Chemical, 2013. 371(0): p. 94-103.

24.   Chen, X., Yao, X., Yu, C., Su, X., Shen, C., Chen, C., Huang, R., and Xu, X., Hydrodechlorination of polychlorinated biphenyls in contaminated soil from an e-waste recycling area, using nanoscale zerovalent iron and Pd/Fe bimetallic nanoparticles. Environmental Science and Pollution Research, 2014. 21(7): p. 5201-5210.

25.   Cao, J., Elliott, D., and Zhang, W., Perchlorate Reduction by Nanoscale Iron Particles. Journal of Nanoparticle Research, 2005. 7(4-5): p. 499-506.

26.   Yu, H., Wang, X., Sun, H., and Huo, M., Photocatalytic degradation of malathion in aqueous solution using an Au-Pd-TiO$_2$ nanotube film. Journal of Hazardous Materials, 2010. 184(1–3): p. 753-758.

27.   Wang, X., Tang, Y., Leiw, M.Y., and Lim, T.T., Solvothermal synthesis of Fe–C codoped TiO2 nanoparticles for visible-light photocatalytic removal of emerging organic contaminants in water. Applied Catalysis A: General, 2011. 409–410(0): p. 257-266.

28.   Hristovski, K., Baumgardner, A., and Westerhoff, P., Selecting metal oxide nanomaterials for arsenic removal in fixed bed columns: From nanopowders to aggregated nanoparticle media. Journal of Hazardous Materials, 2007. 147(1-2): p. 265-274.

29.   Hristovski, K., Westerhoff, P., and Crittenden, J., An approach for evaluating nanomaterials for use as packed bed adsorber media: A case study of arsenate removal by titanate nanofibers. Journal of Hazardous Materials, 2008. 156(1–3): p. 604-611.

30.   Shen, H.Y., Zhu, Y., Wen, X., and Zhuang, Y.M., Preparation of Fe3O4-C18 nano-magnetic composite materials and their cleanup properties for organophosphorous pesticides. Analytical and Bioanalytical Chemistry, 2007. 387(6): p. 2227-2237.

31.   Martínez, Y.M., Ribera, A., Coronado, E., and Falcó, P.C., Preconcentration of emerging contaminants in environmental water samples by using silica supported Fe3O4 magnetic nanoparticles for improving mass detection in capillary liquid chromatography. Journal of Chromatography A, 2011. 1218(16): p. 2276-2283.

32.   Desta, M.B., Batch Sorption Experiments: Langmuir and Freundlich Isotherm Studies for the Adsorption of Textile Metal Ions onto Teff Straw (Eragrostis tef) Agricultural Waste. Journal of Thermodynamics, 2013. 2013: p. 6.

33.   Hristovski, K., Westerhoff, P., Möller, T., Sylvester, P., Condit, W., and Mash, H., Simultaneous removal of perchlorate and arsenate by ion-exchange media modified with nanostructured iron (hydr)oxide. Journal of Hazardous Materials, 2008. 152(1): p. 397-406.

34.   Tepus, B., Simonic, M., and Petrinic, I., Comparison between nitrate and pesticide removal from ground water using adsorbents and NF and RO membranes. Journal of Hazardous Materials, 2009. 170(2-3): p. 1210-1217.

35.   Xu, L., Li, J., and Zhang, M., Adsorption Characteristics of a Novel Carbon-Nanotube-Based Composite Adsorbent toward Organic Pollutants. Industrial & Engineering Chemistry Research, 2015. 54(8): p. 2379-2384.

36.   Yan, H., Wu, H., Li, K., Wang, Y., Tao, X., Yang, H., Li, A., and Cheng, R., Influence of the Surface Structure of Graphene Oxide on the Adsorption of Aromatic Organic Compounds from Water. ACS Applied Materials & Interfaces, 2015. 7(12): p. 6690-6697.

37.   Zhu, J., Sadu, R., Wei, S., Chen, D.H., Haldolaarachchige, N., Luo, Z., Gomes, J.A., Young, D.P., and Guo, Z., Magnetic Graphene Nanoplatelet Composites toward Arsenic Removal. ECS Journal of Solid State Science and Technology, 2012. 1(1): p. M1-M5.

38.   Ghosh, S., Badruddoza, A., Hidajat, K., and Uddin, M.S., Adsorptive removal of emerging contaminants from water using superparamagnetic Fe_3O_4

nanoparticles bearing aminated β-cyclodextrin. Journal of Environmental Chemical Engineering, 2013. 1(3): p. 122-130.

39.   Pan, J., Yao, H., Xu, L., Ou, H., Huo, P., Li, X., and Yan, Y., Selective Recognition of 2,4,6-Trichlorophenol by Molecularly Imprinted Polymers Based on Magnetic Halloysite Nanotubes Composites. The Journal of Physical Chemistry C, 2011. 115(13): p. 5440-5449.

40.   Shao, D., Sheng, G., Chen, C., Wang, X., and Nagatsu, M., Removal of polychlorinated biphenyls from aqueous solutions using β-cyclodextrin grafted multiwalled carbon nanotubes. Chemosphere, 2010. 79(7): p. 679-685.

41.   Cho, H.H., Huang, H., and Schwab, K., Effects of Solution Chemistry on the Adsorption of Ibuprofen and Triclosan onto Carbon Nanotubes. Langmuir, 2011. 27(21): p. 12960-12967.

42.   Lien, H.L. and Zhang, W.X., Transformation of Chlorinated Methanes by Nanoscale Iron Particles. Journal of Environmental Engineering, 1999. 125(11): p. 1042-1047.

43.   Vijayakumar, N.S., Flower, N.A.L., Brabu, B., Gopalakrishnan, C., and Raja, S.V.K., Degradation of DCE and TCE by Fe–Ni nanoparticles immobilised polysulphone matrix. Journal of Experimental Nanoscience, 2012. 8(7-8): p. 890-900.

44.   Das, S.K., Das, A.R., and Guha, A.K., Gold Nanoparticles: Microbial Synthesis and Application in Water Hygiene Management. Langmuir, 2009. 25(14): p. 8192-8199.

45.   Suman, Kardam, A., Gera, M., and Jain, V.K., A novel reusable nanocomposite for complete removal of dyes, heavy metals and microbial load from water based on nanocellulose and silver nano-embedded pebbles. Environmental Technology, 2014. 36(6): p. 706-714.

46.   Li, X., Chen, G., Yang, L., Jin, Z., and Liu, J., Multifunctional Au-Coated TiO2 Nanotube Arrays as Recyclable SERS Substrates for Multifold Organic

Pollutants Detection. Advanced Functional Materials, 2010. 20(17): p. 2815-2824.

47.   Han, C., Likodimos, V., Khan, J.A., Nadagouda, M., Andersen, J., Falaras, P., Lombardi, P.R., and Dionysiou, D., UV–visible light-activated Ag-decorated, monodisperse TiO2 aggregates for treatment of the pharmaceutical oxytetracycline. Environmental Science and Pollution Research, 2014. 21(20): p. 11781-11793.

48.   Balasubramanian, K. and Burghard, M., Chemically Functionalized Carbon Nanotubes. Small, 2005. 1(2): p. 180-192.

49.   Popov, V.N., Carbon nanotubes: properties and application. Materials Science and Engineering: R: Reports, 2004. 43(3): p. 61-102.

50.   Miyagawa, H., Misra, M., and Mohanty, A.K., Mechanical Properties of Carbon Nanotubes and Their Polymer Nanocomposites. Journal of Nanoscience and Nanotechnology, 2005. 5(10): p. 1593-1615.

51.   Polizu, S., Savadogo, O., Poulin, P., and Yahia, L., Applications of Carbon Nanotubes-Based Biomaterials in Biomedical Nanotechnology. Journal of Nanoscience and Nanotechnology, 2006. 6(7): p. 1883-1904.

52.   Zhou, Q., Xiao, J., Wang, W., Liu, G., Shi, Q., and Wang, J., Determination of atrazine and simazine in environmental water samples using multiwalled carbon nanotubes as the adsorbents for preconcentration prior to high performance liquid chromatography with diode array detector. Talanta, 2006. 68(4): p. 1309-1315.

53.   Salipira, K.L., Mamba, B.B., Krause, R.W., Malefetse, T.J., and Durbach, S.H., Carbon nanotubes and cyclodextrin polymers for removing organic pollutants from water. Environmental Chemistry Letters, 2007. 5(1): p. 13-17.

54.   Salipira, K.L., Mamba, B.B., Krause, R.W., Malefetse, T.J., and Durbach, S.H. Cyclodextrin polyurethanes polymerised with carbon nanotubes for the removal of organic pollutants in water. 2008. 34, 113-118.

55. Chen, H., Yang, S., Yu, K., Ju, Y., and Sun, C., Effective Photocatalytic Degradation of Atrazine over Titania-Coated Carbon Nanotubes (CNTs) Coupled with Microwave Energy. The Journal of Physical Chemistry A, 2011. 115(14): p. 3034-3041.

56. Zhang, Y., Liu, G., Yu, S., Zhang, J., Tang, Y., Li, P., and Ren, Y., Kinetics and Interfacial Thermodynamics of the pH-Related Sorption of Tetrabromobisphenol A onto Multiwalled Carbon Nanotubes. ACS Applied Materials & Interfaces, 2014. 6(23): p. 20968-20977.

57. Srivastava, A., Srivastava, O.N., Talapatra, S., Vajtai, R., and Ajayan, P.M., Carbon nanotube filters. Nat Mater, 2004. 3(9): p. 610-614.

58. Liu, F.F., Zhao, J., Wang, S., Du, P., and Xing, B., Effects of Solution Chemistry on Adsorption of Selected Pharmaceuticals and Personal Care Products (PPCPs) by Graphenes and Carbon Nanotubes. Environmental Science & Technology, 2014. 48(22): p. 13197-13206.

59. Wang, J., Chen, Z., and Chen, B., Adsorption of Polycyclic Aromatic Hydrocarbons by Graphene and Graphene Oxide Nanosheets. Environmental Science & Technology, 2014. 48(9): p. 4817-4825.

60. Bonaccorso, F., Colombo, L., Yu, G., Stoller, M., Tozzini, V., Ferrari, A.C., Ruoff, R.S., and Pellegrini, V., Graphene, related two-dimensional crystals, and hybrid systems for energy conversion and storage. Science, 2015. 347(6217).

61. Al-Khateeb, L.A., Almotiry, S., and Salam, M.A., Adsorption of pharmaceutical pollutants onto graphene nanoplatelets. Chemical Engineering Journal, 2014. 248(0): p. 191-199.

62. Rizzo, L., Fiorentino, A., Grassi, M., Attanasio, D., and Guida, M., Advanced treatment of urban wastewater by sand filtration and graphene adsorption for wastewater reuse: Effect on a mixture of pharmaceuticals and toxicity. Journal of Environmental Chemical Engineering, 2015. 3(1): p. 122-128.

63.   Zhu, X., Tsang, D.C.W., Chen, F., Li, S., and Yang, X., Ciprofloxacin adsorption on graphene and granular activated carbon: kinetics, isotherms, and effects of solution chemistry. Environmental Technology, 2015: p. 1-9.

64.   Balamurugan, K. and Subramanian, V., Adsorption of Chlorobenzene onto (5,5) Armchair Single-Walled Carbon Nanotube and Graphene Sheet: Toxicity versus Adsorption Strength. The Journal of Physical Chemistry C, 2013. 117(41): p. 21217-21227.

65.   Kyzas, G.Z., Bikiaris, D.N., Seredych, M., Bandosz, T.G., and Deliyanni, E.A., Removal of dorzolamide from biomedical wastewaters with adsorption onto graphite oxide/poly(acrylic acid) grafted chitosan nanocomposite. Bioresource Technology, 2014. 152(0): p. 399-406.

66.   Mhlanga, S.D., Mamba, B.B., Krause, R.W., and Malefetse, T.J., Removal of organic contaminants from water using nanosponge cyclodextrin polyurethanes. Journal of Chemical Technology & Biotechnology, 2007. 82(4): p. 382-388.

67.   Mhlongo, S.H., Mamba, B.B., and Krause, R.W., Monitoring the prevalence of nitrosamines in South African waters and their removal using cyclodextrin polyurethanes. Physics and Chemistry of the Earth, Parts A/B/C, 2009. 34(13–16): p. 819-824.

68.   Arkas, M., Allabashi, R., Tsiourvas, D., Mattausch, E.M., and Perfler, R., Organic/Inorganic Hybrid Filters Based on Dendritic and Cyclodextrin "Nanosponges" for the Removal of Organic Pollutants from Water. Environmental Science & Technology, 2006. 40(8): p. 2771-2777.

69.   Arkas, M., Eleades, L., Paleos, C.M., and Tsiourvas, D., Alkylated hyperbranched polymers as molecular nanosponges for the purification of water from polycyclic aromatic hydrocarbons. Journal of Applied Polymer Science, 2005. 97(6): p. 2299-2305.

70.   Nghiem, L.D., Coleman, P.J., and Espendiller, C., Mechanisms underlying the effects of membrane fouling on the nanofiltration of trace organic contaminants. Desalination, 2010. 250: p. 682-687.

71.   Simon, A., Price, W.E., and Nghiem, L.D., Effects of chemical cleaning on the nanofiltration of pharmaceutically active compounds (PhACs). Separation and Purification Technology 2012. 88: p. 208–215.

72.   Verliefde, A.R.D., Cornelissen, E., Amy, G., Bruggen, B.V.D., and Dijk, H.V., Priority organic micropollutants in water sources in Flanders and the Netherlands and assessment of removal possibilities with nanofiltration. Environmental Pollution 2007. 146: p. 281-289.

73.   Nghiem, L.D., Schafer, A.I., and Elimelech, M., Pharmaceutical Retention Mechanisms by Nanofiltration Membranes. Environ. Sci. Technol. , 2005. 39: p. 7698-7705.

74.   Yüksel, S., Kabay, N., and Yüksel, M., Removal of bisphenol A (BPA) from water by various nanofiltration(NF) and reverse osmosis (RO) membranes. Journal of Hazardous Materials, 2013. 263(2): p. 307-310.

75.   Zhang, Y., Causserand, C., Aimar, P., and Cravedi, J.P., Removal of bisphenol A by a nanofiltration membrane in view of drinking water production. Water Research, 2006. 40(20): p. 3793-3799.

76.   Verliefde, A.R.D., Heijman, S.G.J., Cornelissen, E.R., Amy, G., Bruggen, B.V.D., and Dijk, J.C.V., Influence of electrostatic interactions on the rejection with NF and assessment of the removal efficiency during NF/GAC treatment of pharmaceutically active compounds in surface water. Water Research, 2007. 41: p. 3227-3240.

77.   Chellam, S.J. and Taylor, S., Simplified analysis of contaminant rejection during ground- and surface water nanofiltration under the information collection rule. Water Research, 2001. 35(10): p. 2460-2474.

78.	Nghiem, L.D., Schafer, A.I., and Elimelech, M., Role of electrostatic interactions in the retention of pharmaceutically active contaminants by a loose nanofiltration membrane. Journal of Membrane Science 2006. 286(-): p. 52-59.

79.	Yuksel, S., Kabay, N., and Yuksel, M., Removal of bisphenol A (BPA) from water by various nanofiltration (NF) and reverse osmosis (RO) membranes. Journal of Hazardous Materials, 2013. 263, Part 2: p. 307-310.

80.	Ahmad, A.L., Tan, L.S., and Shukor, S.R.A., Dimethoate and atrazine retention from aqueous solution by nanofiltration membranes. Journal of Hazardous Materials, 2008. 151(1): p. 71-77.

Table 2.2.1 Classification of different emerging contaminants. Since 1998, US Environmental Protection Agency updated the list of emerging contaminants four times and the below list is in accordance to the draft of latest list prepared in 2015.

Class of emerging contaminants	Examples	Definition
Antibiotics	Tetracycline Erythromycin	Medications that fight bacterial infections, inhibiting or stopping bacterial growth
Disinfectants	Alcohols Aldehydes	A chemical agent used on non-living surfaces to destroy, neutralize, or inhibit the growth of disease-causing microorganisms
Disinfection by-products	Chloroform Nitrosodimethylamine	Chemical substances resulting from the interaction of organic matter in water with disinfection agents, such as chlorine
Drugs of abuse	Amphetamine Cocaine Tetrahydrocannabinol	Drugs are addictive and have long-lasting changes in the brain.
Hormone mimicking agents	Bisphenol A	Natural or synthetic chemicals that can elicit an estrogenic response
Fire or flame retardants	Polybrominated diphenyl ethers Tetrabromo bisphenol A Tris (2-chloroethyl) phosphate	Any of several materials or coatings that inhibit or resist the spread of fire
Fragrances	Galaxolide Polycyclic Macrocyclic musks	Chemical substances that impart a sweet or pleasant odor
Gasoline additives	Dialkyl ethers Methyl-t-butyl ether	Chemicals that raise gasoline octane number or act as corrosion inhibitors or lubricants
Insect repellants	N, N-diethyl-meta-toluamide	Chemical substances applied to skin or other surfaces to discourage insects from coming in contact with the surface
Poly-aromatic hydrocarbons	Benzo(a) pyrene Fluoranthene Naphthalene	A large group of chemical substances usually found in the environment as a result of incomplete burning of carbon-containing materials like fossil fuels, wood, or garbage
Personal care products	Para-hydroxybenzoate Benzophenone N,N-diethyltoluamide Methylbenzylidene	Chemical substances used in a diverse group of personal items including toiletries and cosmetics
Pesticides or insecticides	Permethrin Fenitrothion Bacillus Thuringiensis israelensis	Chemical substances or microbiological agents that kill, incapacitate or otherwise prevent pests from causing damage
Pharmaceuticals	Carbamazepine Acetaminophen Diclofenac Diazepam	Chemical substances used in the prevention or treatment of physiological conditions
Plasticizers	Dioctyl Phthalate	Chemical additives that increase the plasticity or fluidity of a material
Reproductive hormones	Dihydrotestosterone Progesterone Estrone Estradiol	A group of chemical substances, usually steroids, whose purpose is to stimulate certain reproductive functions
Other hormones	Cholesterol Coprostanol Progesterone Diethylstilbestrol	A large group of fat-soluble organic compounds with a characteristic molecular structure, which includes many natural and synthetic hormones
Solvents	Ethanol Kerosene	Chemical solutions, other than water, capable of dissolving another substance

Class of emerging contaminants	Examples	Definition
Surfactants and metabolites	Sodium lauryl sulfate Alkylphenol ethoxylates Alkylphenols (nonylphenol and octylphenol) Alkylphenol carboxylates	Chemical substances that affect the surface tension of a liquid

Table 2.2.2 Current and potential applications of nanotechnology in water and wastewater treatment [13]

Application	Representative nanomaterials	Desirable nanomaterial properties	Enabled technologies	Investigated emerging contaminants
Photocatalysis	Nano-TiO$_2$	Photocatalytic activity under ultraviolet and visible light range Low human toxicity High stability Low cost	Photocatalytic reactors Solar disinfection systems	Alachlor Fenitrothion Trimethoprim
	Fullerene derivatives	Photocatalytic activity in solar spectrum High selectivity	Photocatalytic reactors Solar disinfection systems	
Adsorption	Nanoscale metal oxide	High specific surface area Short intraparticle diffusion distance More adsorption sites Compressible without significant surface area reduction Easy reuse Superparamagnetic properties	Adsorptive media filters Slurry reactors	Aspirin Acetaminophen Diclofenac Arsenate Polychlorinated biphenyls Trichloroethylene
	Nanofibers with core shell structure	Tailored shell surface chemistry for selective adsorption Reactive core for degradation Short internal diffusion distance	Reactive nano-adsorbents	
	Carbon nanotubes	High specific surface area Highly assessable adsorption sites Tunable surface chemistry Easy reuse	Contaminant preconcentration/ detection adsorption of recalcitrant contaminants	
Membranes processes	Nano-magnetite	Tunable surface chemistry Superparamagnetic properties	Forward osmosis	Trimethoprim Norfluoxetine Atorvastatin *Escherichia coli*
	Nano-TiO$_2$	Photocatalytic activity Hydrophilicity High chemical stability	Reactive membranes High performance thin film nanocomposite membranes	
	Nano-zeolites	Molecular sieve Hydrophilicity	High permeability thin film nanocomposite membranes	
	Nano-Ag	Strong and wide-spectrum antimicrobial activity Low toxicity to humans	Anti-biofouling membranes	
	Carbon nanotubes	Antimicrobial activity (unaligned Carbon nanotubes) Small diameter Atomic smoothness of inner surface Tunable opening chemistry High mechanical and chemical stability	Aligned Carbon nanotubes membranes	
Sensing and monitoring	Quantum dots	Broad absorption spectrum, narrow, bright and stable emission which scales with the particle size and chemical component	Optical detection	Aspirin Acetaminophen Diclofenac Ibuprofen
	Noble metal nanoparticles	Enhanced localized surface plasmon resonances High conductivity	Optical and electrochemical detection	

Application	Representative nanomaterials	Desirable nanomaterial properties	Enabled technologies	Investigated emerging contaminants
	Dye-doped silica nanoparticles	High sensitivity and stability Rich silica chemistry for easy conjugation	Optical detection	
	Magnetic nanoparticles	Tunable surface chemistry Superparamagnetism	Sample pre-concentration and purification	
	Carbon nanotubes	Large surface area high mechanical strength and chemical stability Excellent electronic properties	Electrochemical detection Sample pre-concentration	
Disinfection and microbial control	Nano-TiO$_2$	Photocatalytic ROS generation High chemical stability Low human toxicity and cost	Point of use to full scale decontamination	*Escherichia coli Staphylococcus aureus*
	Nano-Ag	Strong and wide-spectrum antimicrobial activity Low toxicity to humans Ease of use	Point of use water disinfection Anti-biofouling surface	
	Carbon nanotubes	Antimicrobial activity Fiber shape Conductivity	Point of use water disinfection Anti-biofouling surface	

Table 2.2.3 Chemical transformation systems which follow a Pseudo-first-order kinetic model. The highest rate constant was reported for degradation of Norfluoxetine by TiO$_2$ nanobelts and the lowest one was for Polychlorinated biphenyls by zero-valent iron nanoparticles.

Nanomaterials (conc. g/L)	Emerging contaminants	K$_1$	Water matrices	References
TiO$_2$ (4 g/L)	Alachlor	0.0017-0.0152	Distilled	[17]
	Fenitrothion	0.0015-0.0230		
TiO$_2$ nanowire membranes (1.25 g/L)	Trimethoprim	0.0269	Milli Q	[18]
	Norfluoxetine	0.1239		
	Atorvastatin	0.0688		
TiO$_2$ nanobelts (0.2 g/L)	Naproxen	0.0616	Milli Q	[19]
	Carbamazepine	0.0291		
	Theophylline	0.0912		
TiO$_2$ nanoparticles (0.02 g/L)	Carbamazepine	0.017	Groundwater	[20]
		0.050	Distilled	
FeFNS-doped TiO$_2$ (0.03-0.3 g/L)	Diazinon	0.0162	Deionized	[21]
Nitrogen and fluorine codoped TiO$_2$ (5 g/L)	Caffeine	0.0146	Milli Q	[22]
	Carbamazepine	0.0125		
	Atrazine	0.0109		
Nano-magnetite (Fe$_3$O$_4$) (1-1.8 g/L)	Carbamazepine	0.00303	Distilled	[23]
	Ibuprofen	0.00201		
Nanoscale zero valent iron (10 g/L)	Polychlorinated biphenyls	0.00183	Deionized	[24]
Pd-Fe nanoparticles (10 g/L)	Polychlorinated biphenyls	0.002	Deionized	[24]
Nanoscale iron particles (10 g/L)	Perchlorate	0.0253	Deionized	[25]
Au-Pd-TiO$_2$ nanotube film (n.d.)	Malathion	0.0158	Twice-distilled	[26]

The Pseudo-first-order equation can be expressed as:

$$Ln\ (C_t/C_0) = -k_1 t$$

Where: C_0 and C_t (mol/L) are concentrations of contaminant at different time, t (min) and k_1 (1/min) is reaction constant.

Table 2.2.4 Physical adsorption systems which follow Freundlich isotherm model. In Freunlich model. If n<1, then adsorption is a chemical process and if n>1, then adsorption is a physical process [32]. Therefore all of the processes in this table are physical except carbon nanotubes.

Nanomaterials	Emerging contaminants	K_F*	1/n	Water matrices	References
TiO_2, Fe_2O_3, ZrO_2 and NiO nanopowders	Arsenic	1.37-12.09	0.21-0.52	10 mM $NaHCO_3$ nanopure water**	[28]
Titanate nanofibers	Arsenic	5-26	0.51-0.66	10mM $NaHCO_3$ buffered nanopure water	[29]
Nanostructured iron hydroxide	Perchlorate Arsenate	2.5-34.7	< 0.6	Distilled	[33]
Nanofiltration	Atrazine	0.04-11.58	0.5633-1.1196	Groundwater	[34]
	Deethylatrazin	0.05-0.75	0.5825-0.8387		
Carbon nanotubes	2-naphthol	0.128-0.222	1.1988-1.5193	Milli-Q	[35]
Graphene oxide	Aniline	5.2-14.4	0.526-0.7519	Distilled	[36]
	Nitrobenzene	6.8-11.1	0.4386-0.4673		
	Chlorobenzene	0.78-1.80	0.7407-0.8130		
Magnetic graphene nanoplatelets	Arsenic	4.32	0.3584	Deionized	[37]

*: The freundlich isotherm model can be expressed as:
$$Q_e = K_F C_e^{1/n}$$
Where: C_e (mg/L) and Q_e (mg/g) are the equilibrium concentration of adsorbate in liquid and solid phase, n and K_F (mg/g)(L/mg)$^{1/n}$ are the adsorption equilibrium constant.
**: conductivity <1μS cm^{-1}

Table 2.2.5 Physical adsorption systems which followed Langmuir or Polanyi-Manes isotherm models. The maximum adsorption capacity was reported for Triclosan on single-walled carbon nanotubes and the lowest one was reported for Trichlorophenol on magnetic nanoparticle.

Nanomaterials	Emerging contaminants	Adsorption model	Maximum adsorption capacity	K_L or log K	Water matrices	References
Magnetic nanoparticles	2,4,6-Trichlorophenol	Langmuir	75.49	n.d.	n.d.	[39]
MWCNT[A]	Polychlorinated biphenyls	Langmuir	235-261	n.d.	Milli-Q	[40]
SWCNT[B]	Ibuprofen	Polanyi-Manes	231.5	5.61	Milli-Q	[41]
	Triclosan		558.2	6.52		
MWCNT[A]	Ibuprofen	Polanyi-Manes	81.6	4.43	Milli-Q	[41]
	Triclosan		434.7	6.08		
O-MWCNT[C]	Ibuprofen	Polanyi-Manes	19.4	3.89	Milli-Q	[41]
	Triclosan		105.4	5.53		

A) Multiwalled carbon nanotubes: MWCNT, B) Single-walled carbon nanotubes: SWCNT C) oxidized multiwalled carbon nanotubes: O-MWCNT.
The Langmuir isotherm model can be expressed as:
$$Q_e = (K_L Q_m C_e) / (1 + K_L C_e)$$

Where: Q_m is the maximum adsorption capacity of the sorbent (mg/g), and K_L is the affinity constant.
The Polanyi-Manes model (PMM) equation can be expressed as:
$$Q_e = Q^0_p \; exp \; (a \; (RT \; Ln \; (S_w/C_e)))^b$$

Where: Q^0_p is maximum sorption capacity (mg/g). a and b are model constants, R is the universal gas constant (8.314 $\times 10^{-3}$ kJ/mol/K), T is absolute temperature (K), and Sw is the solubility of the adsorbate in water at 20 ℃.
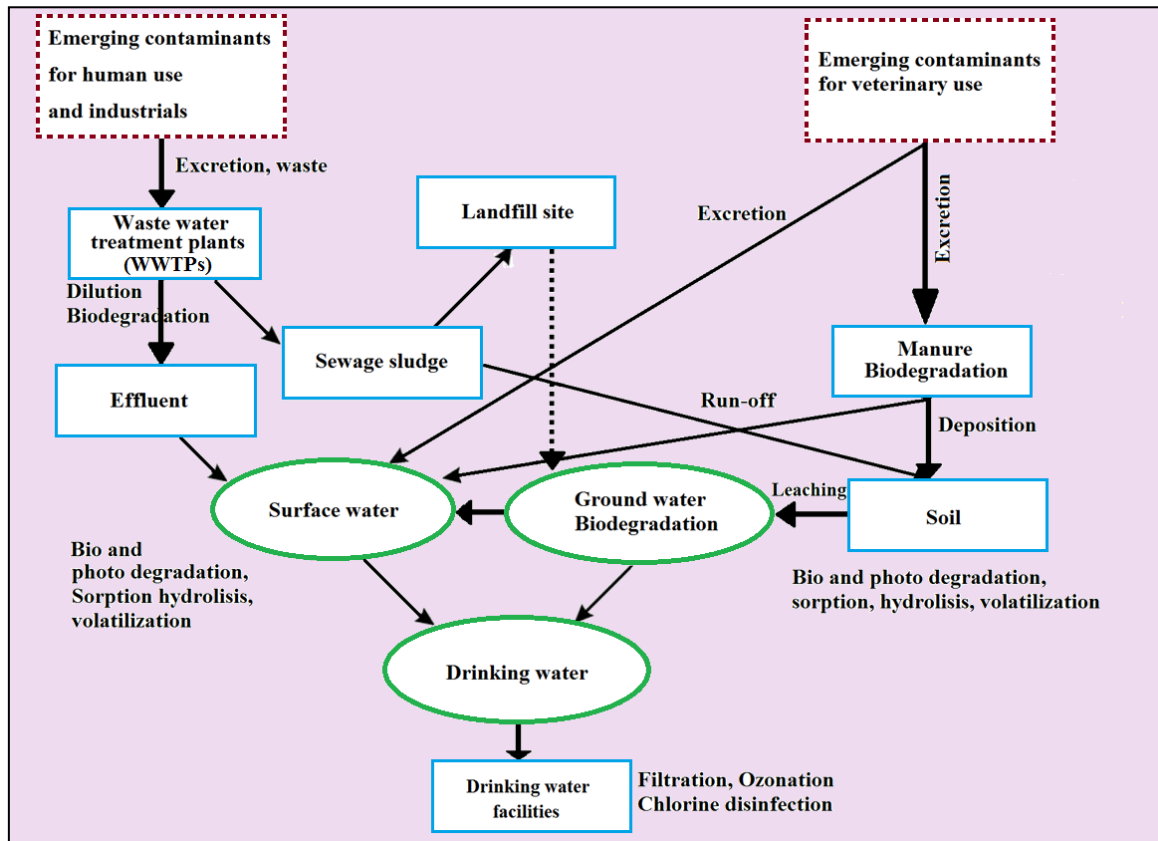
Figure 2.2.1 Distribution of emerging contaminants in the environment. Subsequent to human, veterinary and industrial use and then releasing into wastewater, emerging contaminants can easily find their ways into soil, ground water, surface water and finally drinking water.
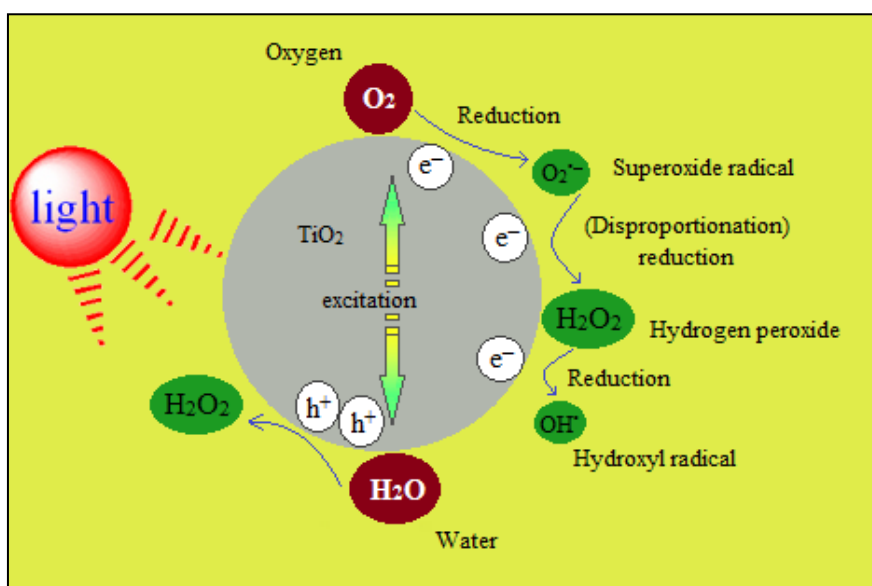
Figure 2.2.2 Formation of reactive species as a result of light absorption by TiO$_2$ photocatalyst. O$_2$ is reduced by one electron to form superoxide radical (O$_2^{\cdot-}$) that can react with a hydroperoxyl radical (HO$_2^{\cdot}$) to form hydrogen peroxide (H$_2$O$_2$). One-electron reduction of H$_2$O$_2$ produces hydroxyl radical (OH$^{\cdot}$).
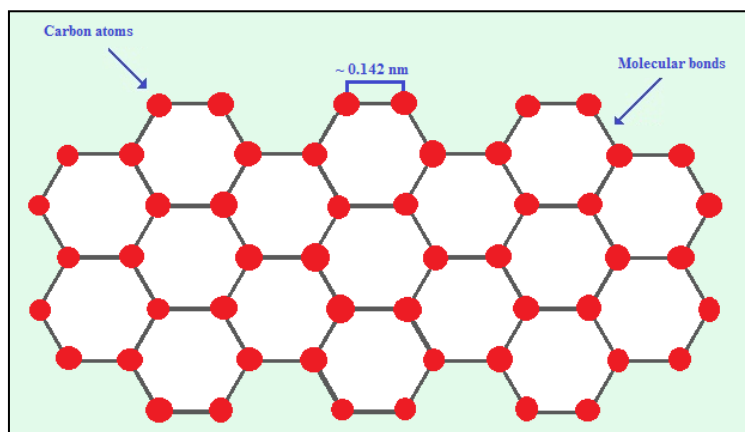
Figure 2.2.3 Schematic of the structure of graphene nanoplatelets. The carbon–carbon bond length in graphene is around 0.142 nanometers and Graphene sheets stack to form graphite with an interplanar spacing of 0.335 nm. Owing to its 2wo-dimentional structure, Graphene has a theoretical specific surface area of more than 2600 m^2/g which is much larger than that reported to date for carbon black or carbon nanotubes [60].
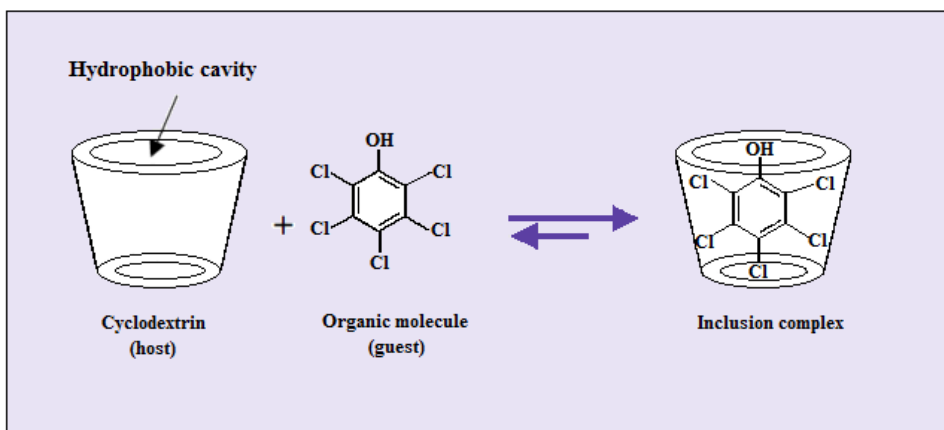
Figure 2.2.4 A schematic for host-guest interaction. In this mechanism, the host material has free spaces in its structure which is perfect for retaining the guest molecules through non-covalent forces including hydrogen bonds, ionic bonds, van der Waals forces, and hydrophobic interactions.
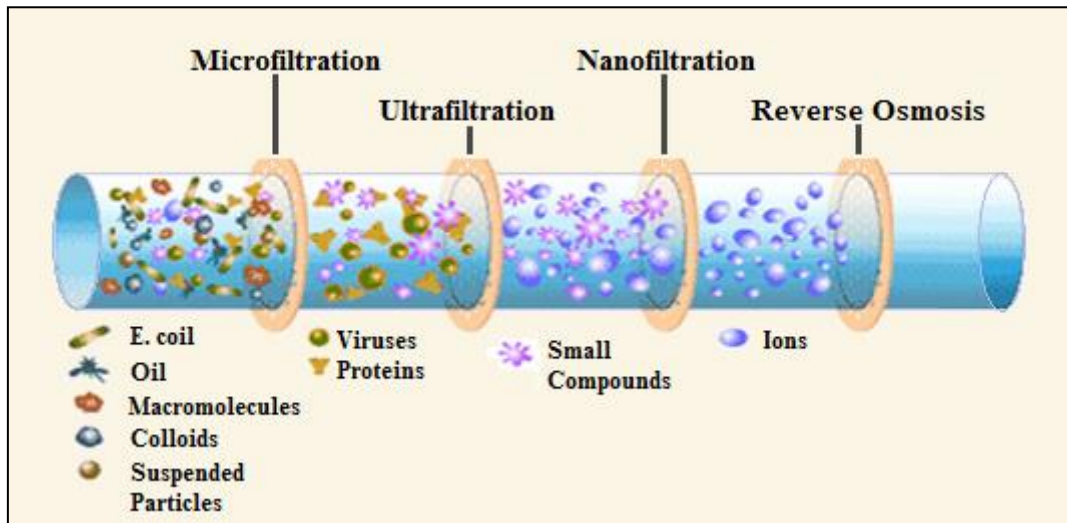
Figure 2.2.5 Performance of nanofiltration membrane compared to other filtration technology. Nanofiltration can retain up to 98% of the organic contaminants but let the ions pass through the membrane. Therefore it can be implemented for drinking water decontamination.

Part 3

A Green Method for Production of Nanobiochar by Ball Milling- Optimization and Characterization

Mitra Naghdi[1], Mehrdad Taheran[1], Satinder Kaur Brar[*1], Tarek Rouissi[1], Mausam Verma[2], Rao Yadagiri Surampalli[3] and Joseph Rene Valero[1]

[1]INRS-ETE, Université du Québec, 490, Rue de la Couronne, Québec G1K 9A9, Canada,

[2]CO$_2$ Solutions Inc., 2300, rue Jean-Perrin, Québec, Québec G2C 1T9 Canada and

[3]Department of Civil Engineering, University of Nebraska-Lincoln, N104 SEC PO Box 886105, Lincoln, NE 68588-6105, USA

(*Phone: 1 418 654 3116; Fax: 1 418 654 2600; E-mail: satinder.brar@ete.inrs.ca)

153

Résumé

Les considérations environnementales et les défis technologiques ont conduit à la recherche de procédés écologiques et à faible consommation en énergie pour les matériaux nanostructurés avancés. Dans cette étude, le nanobiochar a été produit à partir de biochar de pin à l'aide d'un broyeur à billes planétaire. Une méthodologie de conception expérimentale composite et de surface de réponse a été utilisée pour optimiser les paramètres de broyage à billes, y compris le temps, la vitesse de rotation et le rapport massique billes / poudre pour obtenir des nanoparticules en peu de temps. Les résultats de l'ANOVA ont montré que les estimations de l'effet linéaire et quadratique du temps et de l'effet d'interaction du temps et de la vitesse de rotation étaient des facteurs significatifs de la taille des particules pendant la mouture ($p <$ 0,05). Sur la base du modèle statistique développé, les conditions optimales pour obtenir les particules les plus petites, environ 60 nm, se sont révélées être de 1,6 h, 575 rpm et 4,5 g/g. Cependant, les mesures de taille ont indiqué que les particules avaient une forte tendance à s'agglomérer. D'autres études ont montré que le conditionnement du biochar à des températures cryogéniques avant le broyage inhibe l'agglomération des nanoparticules, ce qui est essentiel dans les procédés industriels. Le test d'adsorption a prouvé que le nanobiochar produit en utilisant la méthode verte est prometteur dans l'élimination des micropolluants des milieux aqueux en éliminant jusqu'à 95% de la carbamazépine de l'eau. Aux conditions optimales de broyage et de conditionnement pendant 24 h à -80 °C, on a obtenu du nanobiochar d'une taille moyenne d'environ 60 nm. Le nanobiochar produit a été caractérisé par porosimétrie au gaz de Brunauer-Emmett-Teller (BET), microscopie électronique à balayage (SEM) et spectroscopie infrarouge à transformée de Fourier (FTIR). En outre, les propriétés physiques et chimiques, telles que la capacité de rétention d'eau, la matière organique, le potentiel d'oxydoréduction (ORP), la composition élémentaire, les hydrocarbures aromatiques polycycliques (PAHs) et les métaux lourds ont été analysées.

Mots clés

Nanobiochar, Broyage à billes, Design expérimental, Propriétés physico-chimiques

Chapter 2. Study of the green production of nanoparticles…

Abstract

Environmental considerations along with the technological challenges have led to search for green and energy-efficient processes for advanced nanostructured materials. In this study, nanobiochar was produced from pine wood biochar using a planetary ball mill. A central composite experimental design and response surface methodology was employed to optimize the ball milling parameters including time, rotational speed and ball to powder mass ratio to obtain nanoparticles in short time and at lower energy consumption. ANOVA results showed that the linear and quadratic effect estimates of time and the interaction effect of time and rotational speed were significant contributors to the size of particles during milling ($p < 0.05$). Based on the developed statistical model, the optimum conditions for obtaining the smallest particles, around 60 nm, were found to be 1.6 h, 575 rpm and 4.5 g/g. However, the size measurements indicated that particles had a great tendency to agglomerate. Further study showed that the conditioning of biochar at cryogenic temperatures prior to milling inhibits the agglomeration of nanoparticles which is essential in industrial processes. The adsorption test proved that the nanobiochar produced using green method is promising in the removal of micropollutants from aqueous media by removing up to 95 % of carbamazepine from water. At the optimum milling parameters and conditioning for 24 h at -80 °C, nanobiochar with the average size of around 60 nm was obtained. The produced nanobiochar was characterized by Brunauer-Emmett-Teller (BET) gas porosimetry, scanning electron microscopy (SEM) and Fourier transform infrared spectroscopy (FTIR). Also, physical and chemical properties, such as water holding capacity, organic matter, oxidation-reduction potential (ORP), elemental composition, polycyclic aromatic hydrocarbons (PAHs) and heavy metals were analyzed.

Introduction

Biochar, a solid by-product of waste biomass pyrolysis, has recently attracted interest for both environmental protection and agricultural applications due to its unique physicochemical properties [1]. Beneficial properties include high surface area, porosity, and capability of adsorbing and exchanging different compounds such as organic contaminants, nutrients, and some gases [2]. The advantages of using biochars and especially activated biochars, in wastewater treatment processes have already been reported [3]. Furthermore, a recent study showed that biochars have superior binding capacity toward engineered nanoparticles compared to commercial activated carbons [4]. Biochars can also improve soil fertility, productivity, increase nutrients content and water holding capacity, and reduce emissions of other greenhouse gasses [5]. Production of biochar in large scale for environmental applications is feasible due to the abundance of low-cost feedstock materials. Combining biochar technology with emerging technologies, such as biotechnology and nanotechnology, might result in the creation of novel materials with enhanced capabilities for environmental applications [5, 6].

Depending on the pyrolysis technology, the particle size of the produced biochars varies in the range of hundreds of micrometers to several centimeters [7]. Reducing the particle size of biochars down to nanosized range can improve their properties for particles smaller than 100 nm, higher surface to volume ratio enhances the surface energy and hence biological effectiveness [8, 9].

There are top-down methods, such as arc discharge and laser ablation and bottom-up methods, such as chemical precipitation and microwave pyrolysis for production of carbonaceous nanoparticles. However, most of these methods require high energy input, expensive precursors and sophisticated processes [10]. Therefore, it is still essential to design a cheap, effective and green method to produce carbonaceous nanoparticles. Ball milling is a top-down approach for production of nanoparticles in which mechanical forces are used to reduce the size of particles [11]. This method has been widely studied in recent years and it has the potential for green, reproducible, low-cost and large-scale production of different classes of nanopowders [12]. For example, Awasthi *et al.* studied the ball milling of graphitic carbon at different times and constant rotational speed and reported the formation of different forms of carbon nanoparticle, such as nanotubes and nanofibers. They concluded that the formation

of small and thin graphitic sheets depends on milling time and the structure can be destroyed, if the ball-milling is done for a very long time [13]. In a similar study, Huang *et al.* reported the production of nano arches or highly curled carbon nanostructures in ball milling of graphite [14]. Also Chen *et al.* used Hexagonal graphite to produce nanoporous carbon by ball milling process at various times. Their transmission electron microscopy (TEM) micrographs confirmed the formation of the turbostatic and amorphous structures with the size around 100 nm after ball milling for 15 h. According to their observations, long milling times caused a high level of iron contamination so that the iron content in the sample was found to be about 3.5 wt % after milling for 150 h [15]. In another study, Pierard *et al.* investigated ball milling of multi-wall carbon nanotubes with the average length of 0.7 to 0.9 μm. Their TEM micrographs showed that the nanotube length decreased with increasing milling time. They also found the proper time for obtaining narrow distribution [16].

As per the results so far obtained by the researchers, there are several parameters including time, rotational speed and ball to powder mass ratio that influence the size of particles and their surface energy [17]. However, according to the literature review, there is no study on simultaneous investigation and optimization of these parameters on ball milling for the production of carbonaceous nanoparticles.

There are 12 principles in green chemistry metrics [18], among which the proposed method satisfies half of these metrics including prevention of wastes generation, high atom economy, avoiding harmful chemical process, using less toxic solvents and auxiliaries, using renewable sources and biodegradability of the product.

In this study, nanobiochars was produced using ball milling process. Considering time, rotational speed and ball to powder mass ratio, a set of experiments were planned by central composite design and the results were analyzed by response surface methodology to optimize the conditions for obtaining nanobiochar in a shorter time and at lower energy consumption rate. In fact, rather than just being optimization study, this manuscript reports about the production of nanobiochar from biochar which is a complex carbonaceous material as compared to the uniform SWCNT or MWCNT carbonaceous materials reported in the literature. The physico-chemical properties of produced nanobiochar at optimum conditions were characterized to signify its agricultural and environmental applications. Also, adsorption of carbamazepine, as a

model micropollutant, was investigated on raw and nanobiochar to evaluate the effect of size reduction on adsorption capability of biochar.

Materials and methods

Materials

Pinewood Biochar (BC-PW) was purchased from Pyrovac Inc. (Quebec (QC), Canada). BC-PW was derived from pine white wood (80 % v/v, 3 mm) obtained from Belle-Ripe in Princeville and the rest included spruce and fir (20 %). The production of BC-PW was carried out at 525±1 °C in the presence of nitrogen under atmospheric pressure for 2 min and was used as obtained from the reactor outlet. Tween 80, sodium hydroxide and ethanol was purchased from Fisher scientific (Ottawa, Canada). Milli-Q water was used throughout the work.

Sample Preparation

In a typical procedure, solid biochar and balls were weighed according to statistical plan, placed in a jar and ground until the desired time. A 5-min rest interval was considered after each 5-min grinding to prevent temperature build-up. Sampling was performed at the end of grinding.

Ball milling of biochar and optimization

In Figure 2.3.1, the factors that may affect the size of biochar through ball milling were illustrated. Among these factors, the machine setup including type, size, and material of jar and balls were fixed and all the experiments were performed at room temperature. Ball milling was performed in a planetary ball mill (PM100; Retsch Corporation) using a 500 mL stainless steel jar and stainless steel balls of 2.4 mm in size. Also, the time intervals were set to 5 min ON and 5 min OFF and this value were obtained in preliminary experiments in order to prevent overheating of biochar and balls. To optimize the milling conditions in order to reduce the size of biochar to the lowest possible value, the remaining parameters including rotational speed, ball to powder ratio and grinding time were manipulated in different experiments. The number of balls was fixed to 800 which was equal to 45 g ball, and the mass of biochar was changed accordingly to obtain the required ball to powder mass ratio.

Design of experiments

Experiments were designed using a central composite design method with 6 replicates in the center and the dependent variable was the size of biochar. Independent parameters and corresponding levels are listed in Table 2.3.1. According to these levels, 20 experiments were designed which are listed in Table 2.3.2. The levels of each parameter were selected according to the preliminary experiments performed prior to design of experiments. Optimization was carried out by applying response surface methodology (RSM) which is widely used for bioprocess optimization. RSM was known to be useful in studying of parameter interaction which allowed building models and finding optimum working ranges [19]. Independent parameters that affect the size include a period of time (h), ball to powder mass ratio (g/g) and milling speed (rpm).

Nanobiochar characterization

The characterization tests of nanobiochar as outlined in Figure 2 were performed on the optimum sample (Experiment 11 with conditioning at -80 °C).

Particle size distribution

Particle size distribution and average particle size of the ground samples were analyzed by laser beam scattering technique using a Zetasizer Nano S90 apparatus (Malvern Instruments, UK). Sample preparation was performed using two methods. In the first method, 1 mg of samples was dispersed in 200 mL of distilled water containing 1 % ethanol using magnetic stirrer for 60 min. In the second method, 1 mg of samples were dispersed in 200 mL of distilled water containing 1 % ethanol and 0.5 % Tween 80, using Vibra-Cell VCX-130 Ultrasonic Processor (Sonics & Materials, USA) for 60 min. The samples were kept cold by an external ice bath during the sonication.

Water holding capacity (WHC)

Prior to measuring WHC for optimized sample, it was dried in an oven overnight at 60±1 °C to remove absorbed water. A known amount of sample was placed in a ceramic Buchner funnel lined with Whatman filter paper. A known amount of deionized water was poured over the sample slowly and the water was drained after saturation. Considering the relative proportion of water passing through the sample and the moisture absorbed by the filter paper, the WHC was quantified by determining the moisture content of the soaked sample.

Surface area measurements

The BET specific surface areas were obtained from the N_2 adsorption isotherms recorded at 77 K ((Autsorb-1, Quantachrome Instruments) at the relative pressure range from 0.05 to 1. In this method, the sample was first degassed for 12 h by increasing the temperature to 60±1 °C and applying vacuum. Later, the amount of adsorbed N_2 gas onto the surface of a known amount of sample is measured as a function of relative pressure. Finally, from the obtained isotherm, the amount of the required N_2 gas for covering the external and the accessible internal pore surfaces of the sample with a complete monolayer of N_2 gas was determined using the BET equation.

Electron microscopy

The optimized sample was gold-coated using a sputter coater prior to scanning electron microscopy (SEM). The micrograph was captured using an EVO® 50 (Zeiss, Germany) at 10 kV accelerating voltage. One mg of sample was dispersed in 200 mL distilled water. Five small droplets of the mixture were placed on a thin aluminum foil and dried by heating at 100±1°C. Finally, the sample was gold coated with the thickness of 15 nm and used for SEM imaging. For transmission electron microscopy (TEM) imaging, one mg of nanobiochar was dispersed in methanol and a small drop was placed on a copper grid to dry at room temperature. The micrograph was captured on a JEM-1230 (JEOL, Japan) operated at 80 kV.

Organic matter, ash, volatile matter, and fixed carbon contents

The moisture content of the sample was determined gravimetrically according to ASTM D2216 prior to each test. A crucible was weighed and approximately 1 g of sample was placed in it. The crucible was then heated in the oven at 105±1°C for 2 h and placed in a desiccator for 1 h prior to weighing. Moisture was determined as a loss in weight of the sample before and after oven drying.

Organic matter content was quantified according to ASTM D 2947 by measuring loss on ignition (LOI) at 440±1 °C in presence of oxygen for 16 h. According to ASTM D 1762-84 volatile matter of air-dried biochar samples was determined by keeping them at 950±1°C for 8 h and similarly, the ash content was measured by keeping the samples at 750 ±1°C. The fixed carbon content was determined by subtraction of organic matter from the initial weight of the sample.

pH, oxidation-reduction potential (ORP) and electrical conductivity (EC)

One g of biochar sample was mixed with 10 mL of 0.01 M $CaCl_2$ aqueous solution for 3 h. Then pH, ORP (Fisher Scientific brand, accumet AR25) and EC (S230 Seven Compact™ conductivity) were measured according to ASTM D4972. All analyses were carried out in triplicate and the average results are reported. Prior to each measurement, the probes were calibrated according to the instructions provided by the manufacturer and were rinsed with distilled water before placing it in the sample. The probes were placed in the sample and readings were taken when the meter equilibrated.

Zeta potential measurements (ZP)

Zeta potential was determined in duplicate using a Zetasizer Nano S90 apparatus (MALVERN Instruments). One mg of biochar was dispersed in 50 mL deionized water with a magnetic stirrer for 60 min. A small amount of the mixture was transferred to the sample well in the ZP measurement System. For computing ZP, the velocity at which particles move toward a positive electrode is measured. The measurement was taken 15-16 times for each trial and then the average of duplicate samples was reported for nanobiochar.

CHN elemental analysis

To determine the elemental concentration of Carbon, Hydrogen, and Nitrogen, the samples was first dried at 60±1°C for 8 h and placed into a glass vial. Two sub-samples (2.0-3.0 mg each) were analyzed using a Leco-932 CHNS Analyzer in CHN mode. In CHN mode, samples are combusted in the presence of pure O_2 and the combustion gases are measured to determine initial elemental concentrations of C, H and N. The average results of each duplicate sample were reported.

2.5.9. Polycyclic aromatic hydrocarbons (PAHs) analysis

PAH analysis was performed by gas chromatography coupled with mass spectroscopy (GC-MS) (Perkin Elmer, model Clarus 500, with column type DB-5, 30 mm × 0.25 mm × 0.25 μm) according to the CEAEQ method. Samples were extracted with the ultrasonic technique in methylene chloride over a period of 30 min, followed by purification with silica [20].

Trace metal analysis

Trace metal analysis of the sample was performed by atomic emission spectrometry - inductively coupled plasma (ICP-AES). The employed device was a Vista AX Model CCO Simultaneous ICP-AES (Varian, USA). Most of the metals (Al, As, Ba, Ca, Cd,

Cr, Cu, Fe, K, Mg, Mn, Mo, Na, Ni, Pb, Se, Sn and Zn) were analyzed simultaneously after complete sample mineralization. In brief, one g of sample was placed in a 50-mL beaker and dried at 105±1 °C. Later, 4 mL of nitric acid 50 % (v/v) and 10 mL of hydrochloric acid 20 % (V/V) were added and the beaker was covered with a watch glass and refluxed for 30 minutes without stirring. Afterward, the sample was allowed to cool down. Finally, the sample was filtered in a 100-mL volumetric flask and the mixture volume was increased to 100 mL with deionized water.

Fourier transform infrared (FT-IR) spectroscopy

FT-IR spectra were recorded using a Nicole IS50 FT-IR Spectrometer (Thermo Scientific, USA) through attenuated total reflectance (ATR) using 4 cm^{-1} resolution and 32 scans per spectrum in the range of 400-4000 cm^{-1}. For taking the spectra, enough sample was placed on the diamond crystal and the gripper plate was placed on the sample to ensure that consistent contact was achieved between the crystal and the sample. The measurement was taken 16 times for each trial and their average was plotted.

Cation Exchange Capacity (CEC)

CEC describes the holding capacity of the sample for positively-charged elements (cations). The CEC is calculated from the levels of potassium, magnesium, calcium and sodium which were measured using ICP analysis [21].

Specific gravity

The specific gravity of the optimized sample was measured according to ASTM D 854. An empty clean and dry pycnometer were weighed (W_P) and 10 g of dry sample was placed in the pycnometer and weighed again (W_{PS}). Distilled water was added to fill about half to three-fourth of the pycnometer and the sample was soaked for 10 minutes. Later, the pycnometer was filled with distilled water and the contents were weighed (W_B). An empty, clean and dry pycnometer was filled with distilled water and weighed (W_A). Finally, the specific gravity of the solid sample was calculated using the following equation:

$$\text{Specific Gravity, G} = \frac{W_0}{W_0 + (W_A - W_B)} \qquad (1)$$

Where:

W_0 = weight of sample (g) = W_{PS} - W_P

W_A = weight of pycnometer filled with water

W_B = weight of pycnometer filled with water and sample

X-Ray diffraction (XRD)

Powder X-ray diffraction patterns of ground biochar with and without precooling (at -80 °C) were collected using a D5000 diffractometer (Siemens, Germany). The diffractometer was operated at 40 kV and 40 mA using Cu Kα radiation source. Diffractograms were in the range of 4° to 70° (2θ scale) at a step size of 0.02° and a counting time of 1.2 s per step.

Statistical analyses

The design of experiments and statistical analysis were performed using STATISTICA, STAT SOFT trial version 10 (StatSoft Inc., USA). Analysis of variance (ANOVA) was used to test the significance of the difference between average sizes of biochar samples. The difference was considered significant at $p < 0.05$ (significance level or α was fixed to 0.05).

Adsorption study

Adsorption study of carbamazepine on produced nanobiochar was performed to evaluate the performance of nanobiochar in one of the promising applications i.e. removal of micropollutants from water and wastewater. For this test, 5 mg of nanobiochar was added to flasks containing 100 mL of 5 ppb carbamazepine in Milli-Q water. During 24 hours, samples were taken at different intervals and after centrifugation at 11000 *x g* for 20 min, the concentration of carbamazepine in supernatants were quantified using LDTD-MS-MS (Laser Diode Thermal Desorption-Mass Spectroscopy) method. The details of the method were explained elsewhere [22]. For comparison, the same procedure was performed for raw biochar and commercial activated carbon.

Results and discussion

Particle size distributions

RSM was used along with a central composite design to model ball milling. Statistical analysis was done by ANOVA with the regression models are given below in Equation (2).

$$Y = \beta_0 + \sum_{i=1} \beta_i X_i + \sum \beta_{ii} X_i^2 + \sum_{i=1} \sum_{j=i+1} \beta_{ij} X_i X_j \qquad (2)$$

Where: Y, β_0, X_i (or X_j). β_i, β_{ii}, and β_{ij} are the predicted responses of the dependent variable, second-order reaction constant, independent variables, linear regression coefficient, the quadratic regression coefficient, and regression coefficient of interactions between two independent variables.

In order to evaluate the effect of different ball milling parameters on the average size of biochar samples, the volume mean size was selected as the input parameter for data analysis. The average of the three samples corresponding to each experiment are listed in Table 2.3.2. The volume means size values indicated that planetary ball mill can be used for the production of fine powders of biochar and at different ball milling conditions this value varied between 212.4 nm and 453.1 nm for biochar with an initial size of around 3 mm. The biggest particles were obtained in experiment 7 (7 h, 540 rpm, and 13 g), while the finest particles were observed in experiment 11 (1.6 h, 575 rpm and 10 g).

The effects of the independent variables (time, rotational speed and weight of powder) were analyzed according to the polynomial model. The standardized effects of these variables are illustrated in Figure 2.3.3. Accordingly, the time and rotational speed have a significant influence on volume mean size. The linear effect estimate of time was positive (P=0.004887) and its quadratic effect estimate was negative (P=0.008973). Also, the effect estimate of interaction between time and rotational speed was significant and negative (P=0.012327). It seems logic to have an interaction between these two parameters because increasing the rotational speed results in increasing the collision energy and frequency and finally decrease the required time for grinding. The weight of powder did not significantly affect the model since corresponding linear and quadratic effect estimate coefficients showed p values higher than the limit of probability acceptance (0.05). The statistical analysis of the regression coefficients showed an acceptable value (R^2=0.78259) which meant that more than 78 % of the variability can be explained by the developed model. Thus, the general model presented in Eq. (2) can be simplified considering only the significant effects (P < 0.05) and their regression coefficients and interactions into equation 3:

$$Volume\ mean = -3398.71 + 423.46\,Time - 8.25\ Time^2 - 0.60\,Time \times RPM \qquad (3)$$

The two-dimensional response surfaces are plotted in Figure 2.3.4 (a) and (b) based on the regression model given in Equation (3). In Figure 2.3.4 (a), a fitted response profile based on time is illustrated against rotational speed. Comparing the results of experiment 11 (1.6 h, 575 rpm and 10 g) and experiment 12 (8.4 h, 575 rpm and 10 g) in Table 2.3.2, at constant powder weight of 10 g and rotational speed of 575 rpm, the particles size increased from 212 nm to 436 nm when time increased from 1.6 h to 8.33 h. This trend was confirmed statistically in Figure 2.3.4 (a) indicating that shorter grinding time led to a finer particle which could be due to the agglomeration in experiments in longer grinding time. Generally, the crystalline structure of materials undergoes considerable changes, such as amorphization due to high energy input in ball milling [11]. Amorphization arises from defects accumulation in milled crystals which results in a highly defective crystalline phase. This phase is not physically stable and transforms into amorphous phase spontaneously. Increasing the amount of amorphous contents is reported to increase the surface energy which is the main reason for agglomeration. Therefore, agglomeration of particles with increasing milling cycles can be attributed to increasing surface energy of particles during milling [17]. On the other hand, according to Figure 2.3.4 (b) and comparing the results of 9 (5 h, 575 rpm, and 4.95 g) and 10 (5 h, 575 rpm and 15.1 g), it was observed that varying powder weight, had insignificant effect on particle size at shorter milling times. As a conclusion, Figure 2.3.1 illustrated the possible important parameters responsible for the size of ball milling products. These parameters were investigated separately (not all of them together) in the literature. However, in this research, three parameters that we were able to vary simultaneously, were selected. From these three parameters, time and speed were found to be very important, but the ball/powder ratio showed lower variation in size compared to others. However, the selected range was still appropriate to obtain sub-micron particles as there are reports in the literature which indicated the importance of selecting an appropriate range for ball/powder ratio. For example, Munkhbayar *et al.* reported that increasing the rotational speed from 200 rpm to 500 rpm in dry grinding shortened the lengths of the multi-walled carbon nanotubes. In the range of 300-400 rpm, the plastic deformation originated from the impact of the milling balls that broke the particles and formed rough surfaces. However, at 500 rpm, dense agglomerates were observed in multi-walled carbon nanotubes that were attributed due to the high energy grinding process. [23]. In

another study, Munkhbayar *et al.* synthesized silica nanoparticles from the remaining ash of rice husk by using high energy planetary ball mill at room temperature. The average particle size of the silica powders was around 70 nm which decreased, as milling time or rotational speed increased. However, they reported that increasing the particle sizes by milling at higher speeds (500 rpm) which indicated the start point of agglomeration [24].

To confirm the possibility of agglomeration, samples were prepared prior to size measurement via two methods (with and without sonication). According to Figure 2.3.5, the smaller particles obtained after sonication led to the agglomeration of biochar nanoparticles after grinding. The applied energy by ultrasonic apparatus caused the nanoparticles to separate from each other. However, repeating measurements in a short while (Data not shown) indicated that nanoparticles tend to agglomerate gradually again after sonication. This behavior was also reported for other nanomaterials. For example, Hong *et al.* investigated the thermal conductivity of Fe nanofluids and found that the thermal conductivity was reduced after stopping sonication which was due to agglomeration of nanoparticles. In another study, Mandzy *et al.* used ultrasonication to prepare stable dispersions of titania nanopowders. They observed that after sonication was stopped, nanoparticles reagglomerated back to 3-4 micrometer range [25, 26]. To the best of authors' knowledge, there is no reported study so far on the carbon nanoparticles and their aggregation.

According to Shah *et al.*, the surface energy of particles milled at cryogenic temperatures is lower than that of room temperature milling due to the inhibitory effect of low temperature on the formation of amorphous regions [17]. In other words, amorphous regions have more surface energy and caused nanoparticles to agglomerate after milling.

Therefore, to assess the possibility of avoiding agglomeration, two experiments were performed at same conditions as an optimum sample (experiment 11, 1.6 h, 575 rpm and 10 g) except that biochar samples were kept at -20 °C and -80 °C for 24 h prior to milling. The conditions of experiment 11 were close to those of optimum sample offered by the software. Therefore, the subsequent experiments were performed on experiment 11. As observed in the XRD patterns of biochar sample ground with and without preconditioning (at -80 °C) in Figure 2.3.6, both samples have turbostratic structure [27]. According to the analysis of diffractograms, the ratio of area under two

characteristic peaks of graphitic crystallites ($2\theta=6.4°$ and $2\theta=26.5°$) to the total area of peaks for preconditioned sample was 64% higher than that of the sample without preconditioning. This indicated that preconditioned sample maintained its crystallinity when compared to the sample without preconditioning.

The size measurements were performed without sonication step and the results were listed in Table 2.3.3. According to this table the particle size of samples, kept at -20 °C and -80 °C prior to milling process, were 102.5 and 60.1 nm. In Figure 2.3.7, the volume-based particle size distribution for the sample obtained in experiment 11 (1.6 h, 575 rpm, and 10 g) (preconditioned at - 80 °C) is illustrated. According to this histogram, almost all of the particles were in the range of 30-80 nm.

It indicates that cryogenic conditioning of samples followed by ball milling process is an efficient method for production of nanosized biochar. Due to increasing stringent laws for environmental protection, a combination of cryogenic treatment and ball milling can evolve into a green and robust method for production of different nanoparticles in a top-down approach. However, more investigation is needed to obtain knowledge for tuning and standardization of the whole process.

Physical and hydraulic properties

Water-holding capacity was determined for nanobiochar and shown along with the initial moisture content and specific gravity of the sample in Table 2.3.4. Most of the characteristics of produced nanoparticle are within the ranges reported in the literature [2, 28]. However, several parameters such as water holding capacity were superior to the reported range which is important for agricultural applications.

Surface area

A detailed BET analysis consisting of the specific surface area, average pore size and pore volume is summarized in Table 2.3.5. According to these results, the milled biochar particles showed higher surface area and pore volume compared to raw biochar. The adsorption isotherms plotting cumulative pore volume versus pore diameter and cumulative surface area versus pore diameter for raw biochar and nanobiochar are shown in Figure 2.3.8 and 2.3.9.

Higher surface area of nanobiochar was contributed by its micropores area (pore with a diameter of less than 2 nm) and it has a significant effect on water adsorption

capacity [28]. Also, a higher surface area in biochar was shown to improve the sorption affinity for a variety of organic materials including phenolic compounds, polyaromatic hydrocarbons, pesticides, herbicides and humic acids [29]. Furthermore, microporosity and high specific surface area of biochar are suggested to play a role in the inhibition of mineralization of the soil organic matter. The suggested mechanism is the diffusion and sorption of organic matters into the micropores, where they are protected against mineralization [30].

The raw biochar had fewer pores in the full test range of 0-400 Å pore size and therefore, it showed a lower cumulative pore volume. Nanobiochar possessed uniform pores with relatively small sizes below 35 Å and the average pore size was 16.3 Å. In contrast, raw biochar showed pores with sizes up to 85 Å and the average pore size of 31.6 Å. It indicated that the milling process removed large pores that existed in the original biochar. It is noteworthy that a small number of random macropores also existed in both samples. Hence, cumulative pore volume was used in Figure 2.3.8 to facilitate the comparison of pore distribution over the pore size range.

The N_2 adsorption isotherms (Figure 2.3.10) indicated that raw biochar had significantly lower N_2 adsorption capacity than nanobiochar so that at 0.99 P/P_o the total pore volume of raw biochar was 0.0062 mL/g while for nanobiochar, it was 0.0385 mL/g.

Electron microscopy analysis

SEM and TEM micrographs of produced nanobiochar at 10 KX and 40 KX magnifications are depicted in Figure 2.3.11. These micrographs indicated that biochar nanoparticles are polygonal in shape and most of them were less than 100 nm in size though there were few agglomerates with several hundred nanometers in size (Not shown in the figure). Similarly, Gnaneshwar and Sabarikirishwaran reported the irregular morphologies of sub-micron carbon particles obtained from crushing of burnt coconut shell in a mortar [31].

Organic matter, volatile matter, ash and fixed carbon content

Percentages of volatile matter, ash, fixed carbon and organic carbon of nanobiochar are given in Table 2.3.4. As shown in Table 2.3.4 the amount of volatile matter is higher

than reported range in literature. Consequently, ash content is low which is an advantage because it causes lower pollution to the environment [28].

pH, ORP, EC and zeta potential

Table 2.3.4 presents pH, ORP, EC, and zeta potential values of produced nanobiochar. EC and pH are dependent on the utilized feedstock and also the carbonization temperature. Bagreev *et al.* showed that for biochars produced between 400°C and 600°C, the pH and EC increased with increasing production temperature [32]. Typical feedstock, such as coal, wood and coconut shells produce more acidic carbons, however, biochars obtained from plant or animal waste generally possess higher pH which reflect the presence of salts of base metals [33]. The higher pH biochars have been proved to provide a positive liming effect on acidic soils and to release base cations to the soil [33, 34]. The positive ORP value of the nanobiochar indicated that it tended to gain electron and act as an oxidizing agent. The zeta potential reflects the surface charge of the particles and the higher magnitude of this parameter is in favor of preventing agglomeration. The zeta potential of nanobiochar was -31.3 ± 2.6 mV which falls on the border of instability (10-30 mV) and moderate stability (30-40 mV) [35].

Elemental composition

The elemental composition of nanobiochars was evaluated through measuring C, N and H in the sample and the weight percentages of C, H and N are given in Table 2.3.4. Also, the molar ratios of C:N and H:C are presented in this table as they represented the extent of biomass carbonization. Biochars with lower H:C ratios and higher C:N underwent higher thermal alteration as a result of greater outgassing of H and N comparing to C.

PAH and metal content

The total content of PAHs was 26.837 mg kg^{-1} in nanobiochar. Naphthalene, a highly volatile and low-weight PAH, accounted for the majority (around 68 %) of detected PAHs in the nanobiochar with a concentration of 18.204 mg kg^{-1} of the sample. It was consistent with the results obtained in previous studies, in which naphthalene was the dominant PAH in wood-based chars, especially with shorter times of pyrolysis [36, 37]. The total concentration of metals in nanobiochar was measured to be 5.92 g kg^{-1}

among which 89 % was for non-toxic and 11 % was for toxic metals. Figure 2.3.12 depicted the concentrations of toxic and non-toxic metals, and Figure 2.3.13 showed the PAH concentrations for nanobiochars. Generally, the least amounts of PAH and metals are desirable because of their leaching potential into the environment.

FTIR analysis

FTIR spectra for the raw biochar and also for the nanobiochar samples are shown in Figure 2.3.14. Generally, the FTIR spectra of the two sample were same in pattern and intensity indicating that ball milling did not affect the chemical structure of biochar. In the two spectra, there were four significant bands at 3324 cm^{-1} (alcohol, O-H stretching), 1582 (alkene/aromatic, C=C stretching), 1185 (phenolic, C-O stretching), and 872 (aromatic, C-H out of plane bending) cm^{-1}. The presence of phenolic groups in biochar suggests that the alkalinity of biochar was low since phenolic groups enhance the acidity in the biochar [38]. These results were consistent with pH measurements (pH 6.61).

Cation Exchange Capacity (CEC)

CEC was calculated to be 14.8 meq/100 g and calcium was the major contributor. Biochar with higher CEC will be able to increase the nutrient holding capacity and exchange properties of soils [39]. The CEC of produced nanobiochar is almost in the same range reported by other researchers. The CEC value is strongly dependent on type and content of functional groups such as hydroxyl, carboxyl, phenol and carbonyl. However, reducing the size of particles down to nano-region can facilitate the exchange of cations by increasing the surface area and also reducing the mass transport resistance [40].

Energy Consumption Calculation

Energy consumption for production of 10 g nanobiochar was calculated for experiment 11 (1.6 h, 575 rpm) since the best result was obtained for these conditions. The sample was examined for three different scenarios: 1) only grinding; 2) grinding plus 60 min sonication and; 3) conditioning at -80 °C plus grinding. The power of grinding was calculated by equation 4 [41].

$$P_{cal} = \frac{1}{2} P^* m_b w_p^3 R_p^2 n_b \qquad (4)$$

Where P_{cal} is the power consumption during milling predicted by the collision model, m_b and n_b are the mass and number of balls used in a given experiment, w_p and R_p the speed and the radius of the planetary mill disk. P^* is a dimensional coefficient depending on the geometry of mill and on the elasticity of collisions. P^* was obtained from the graph provided by Magini *et al.* [41]. For the freezer, it was assumed that the whole freezer was filled with biochar and the average energy consumption reported by the manufacturer (17 KWh/day) was divided by the mass of biochar (79 kg) to obtain the required energy for reducing the temperature of 1 g biochar from ambient to -80 °C and keeping it at this temperature for 24 h. For sonication system, the nominal power consumption of instrument (provided by the manufacturer) was multiplied by amplitude ratio (30%) and working time (60 min) to obtain the required energy. The details of the assumptions, equations and calculations are explained in supplementary material (S1).

Results from Table 2.3.6 showed that production of nanobiochar through cryogenic pre-conditioning not only led to more stable nanoparticles but also saved a considerable amount of energy compared to when using ultrasonic post-treatment.

Adsorption study

The adsorption curves for raw biochar, nanobiochar and commercial activated carbon are illustrated in Figure 2.3.15. Raw biochar did not adsorb more than 14 % of dissolved carbamazepine even after 24 hours of contact time at room temperature while nanobiochar could adsorb more than 98 % after 3 hours which showed the effect of size reduction and surface area enhancement. Same adsorption efficiency was obtained for activated carbon in a shorter time. Yu *et al.* studied the effectiveness of two granular activated carbons (coal-based and coconut-based) for the removal of carbamazepine from water and reported up to 97 % removal efficiency after 12 days [42]. In another work, Cai *et al.* investigated graphene oxide powders for adsorption of carbamazepine and obtained 95 % of removal efficiency after 24 h [43]. Also, Oleszczuk *et al.* employed multi-walled carbon nanotube for removal of carbamazepine from water and obtained up to 90.6 % removal after 24 h [44]. Comparing the removal efficiency of nanobiochar with the data reported by other researchers, it can be implied that nanobiochar with its green origin is capable of

competing with activated carbon or other carbonaceous materials where their production involves using chemical reagent.

Conclusion

In this study, green production of nanobiochar by using a planetary ball mill was statistically investigated. A central composite design along with response surface methodology was employed to analyze the results. The ANOVA indicated that among studied parameters, linear and quadratic effects of time and also the interaction effect of time and rotational speed were significant contributors to particle size. Further studies showed that conditioning the samples at cryogenic temperatures prior to milling inhibited nanoparticles agglomeration. Finally, at optimum milling parameters (1.6 h, 575 rpm and 4.5 g/g ball to powder ratio) and conditioning at -80 °C nanobiochar with the average particle size of 60 nm was achieved. The adsorption study of nanobiochar for removal of a model micropollutant from water showed that produced nanobiochar has higher adsorption capacity compared to raw biochar and it can compete with commercial activated carbon for removal of carbamazepine from the water.

Acknowledgements

References

1.   Oleszczuk, P., Ćwikła-Bundyra, W., Bogusz, A., Skwarek, E., and Ok, Y.S., Characterization of nanoparticles of biochars from different biomass. Journal of Analytical and Applied Pyrolysis, 2016. 121: p. 165-172.

2.   Yargicoglu, E.N., Sadasivam, B.Y., Reddy, K.R., and Spokas, K., Physical and chemical characterization of waste wood derived biochars. Waste Management, 2015. 36: p. 256-268.

3.   Zhang, M., Gao, B., Yao, Y., and Inyang, M., Phosphate removal ability of biochar/MgAl-LDH ultra-fine composites prepared by liquid-phase deposition. Chemosphere, 2013. 92(8): p. 1042-1047.

4.   Inyang, M., Gao, B., Zimmerman, A., Zhang, M., and Chen, H., Synthesis, characterization, and dye sorption ability of carbon nanotube–biochar nanocomposites. Chemical Engineering Journal, 2014. 236: p. 39-46.

5.   Yao, Y., Gao, B., Inyang, M., Zimmerman, A.R., Cao, X., Pullammanappallil, P., and Yang, L., Biochar derived from anaerobically digested sugar beet tailings: Characterization and phosphate removal potential. Bioresource Technology, 2011. 102(10): p. 6273-6278.

6.   Zhang, M., Gao, B., Yao, Y., Xue, Y., and Inyang, M., Synthesis, characterization, and environmental implications of graphene-coated biochar. Science of The Total Environment, 2012. 435: p. 567-572.

7.   Lehmann, J. and Joseph, S., Biochar for environmental management: science, technology and implementation. 2015: Routledge.

8.   Sulaiman, G.M., Mohammed, W.H., Marzoog, T.R., Al-Amiery, A.A., and Kadhum, A.H., Green synthesis, antimicrobial and cytotoxic effects of silver nanoparticles using Eucalyptus chapmaniana leaves extract. Asian Pacific Journal of Tropical Biomedicine, 2013. 3(1): p. 58-63.

9.   Kesavan, A. and Venkatraman, G., Nanotechnology and its Applications. The Scitech Journal, 2014. 1(6): p. 1-2.

10.   Xiao, D., Yuan, D., He, H., and Gao, M., Microwave assisted one-step green synthesis of fluorescent carbon nanoparticles from ionic liquids and their application as novel fluorescence probe for quercetin determination. Journal of Luminescence, 2013. 140: p. 120-125.

11.   Deguchi, S., Mukai, S.-a., Tsudome, M., and Horikoshi, K., Facile Generation of Fullerene Nanoparticles by Hand-Grinding. Advanced Materials, 2006. 18(6): p. 729-732.

12. Charkhi, A., Kazemian, H., and Kazemeini, M., Optimized experimental design for natural clinoptilolite zeolite ball milling to produce nano powders. Powder Technology, 2010. 203(2): p. 389-396.

13. Awasthi, K., Kamalakaran, R., Singh, A.K., and Srivastava, O.N., Ball-milled carbon and hydrogen storage. International Journal of Hydrogen Energy, 2002. 27(4): p. 425-432.

14. Huang, J.Y., Yasuda, H., and Mori, H., Highly curved carbon nanostructures produced by ball-milling. Chemical Physics Letters, 1999. 303(1–2): p. 130-134.

15. Chen, Y., Fitz Gerald, J., Chadderton, L.T., and Chaffron, L., Nanoporous carbon produced by ball milling. Applied Physics Letters, 1999. 74(19): p. 2782-2784.

16. Pierard, N., Fonseca, A., Konya, Z., Willems, I., Van Tendeloo, G., and B.Nagy, J., Production of short carbon nanotubes with open tips by ball milling. Chemical Physics Letters, 2001. 335(1–2): p. 1-8.

17. Shah, U.V., Wang, Z., Olusanmi, D., Narang, A.S., Hussain, M.A., Tobyn, M.J., and Heng, J.Y.Y., Effect of milling temperatures on surface area, surface energy and cohesion of pharmaceutical powders. International Journal of Pharmaceutics, 2015. 495(1): p. 234-240.

18. Naghdi, M., Taheran, M., Brar, S.K., Verma, M., Surampalli, R.Y., and Valero, J.R., Green and energy-efficient methods for the production of metallic nanoparticles. Beilstein Journal of Nanotechnology, 2015. 6: p. 2354-2376.

19. Derringer, G., Simultaneous Optimization of Several Response Variables. Journal of Quality Technology, 1980. 12(4): p. 214-219.

20. Reynier, N., Blais, J.F., Mercier, G., and Besner, S., Treatment of Arsenic-, Chromium-, Copper- and Pentachlorophenol-Polluted Soil Using Flotation. Water, Air, & Soil Pollution, 2013. 224(4): p. 1-12.

21. Ross, D.S., Recommended Methods for Determining Soil Cation Exchange Capacity. 1995: Delaware Cooperative Extension, College of Agriculture, University of Delaware: Newark, DE,.

22. Mohapatra, D.P., Brar, S.K., Tyagi, R.D., Picard, P., and Surampalli, R.Y., Carbamazepine in municipal wastewater and wastewater sludge: Ultrafast quantification by laser diode thermal desorption-atmospheric pressure chemical ionization coupled with tandem mass spectrometry. Talanta, 2012. 99: p. 247-255.

23. Munkhbayar, B., Nine, M.J., Jeoun, J., Bat-Erdene, M., Chung, H., and Jeong, H., Influence of dry and wet ball milling on dispersion characteristics of the multi-walled carbon nanotubes in aqueous solution with and without surfactant. Powder technology, 2013. 234: p. 132-140.

24. Salavati-Niasari, M., Javidi, J., and Dadkhah, M., Ball milling synthesis of silica nanoparticle from rice husk ash for drug delivery application. Combinatorial chemistry & high throughput screening, 2013. 16(6): p. 458-462.

25. Hong, K.S., Hong, T.K., and Yang, H.S., Thermal conductivity of Fe nanofluids depending on the cluster size of nanoparticles. Applied Physics Letters, 2006. 88(3): p. 031901.

26. Mandzy, N., Grulke, E., and Druffel, T., Breakage of TiO_2 agglomerates in electrostatically stabilized aqueous dispersions. Powder Technology, 2005. 160(2): p. 121-126.

27. Taheran, M., Naghdi, M., Brar, S.K., Knystautas, E.J., Verma, M., Ramirez, A.A., Surampalli, R.Y., and Valero, J.R., Adsorption study of environmentally relevant concentrations of chlortetracycline on pinewood biochar. Science of The Total Environment, 2016. 571: p. 772-777.

28. Ghani, W.A.W.A.K., Mohd, A., da Silva, G., Bachmann, R.T., Taufiq-Yap, Y.H., Rashid, U., and Al-Muhtaseb, A.a.H., Biochar production from waste rubber-wood-sawdust and its potential use in C sequestration: Chemical and physical characterization. Industrial Crops and Products, 2013. 44: p. 18-24.

29. Kasozi, G.N., Zimmerman, A.R., Nkedi-Kizza, P., and Gao, B., Catechol and Humic Acid Sorption onto a Range of Laboratory-Produced Black Carbons (Biochars). Environmental Science & Technology, 2010. 44(16): p. 6189-6195.

30. Ameloot, N., Graber, E.R., Verheijen, F.G.A., and De Neve, S., Interactions between biochar stability and soil organisms: review and research needs. European Journal of Soil Science, 2013. 64(4): p. 379-390.

31. Gnaneshwar, P.V. and Sabarikirishwaran, P., Structural and Morphological study of Carbon Nanoparticles synthesized using Oxidation, Thermal decomposition and Solvo chemical methods. International Journal of ChemTech Research, 2015. 7(3): p. 1465-1473.

32. Bagreev, A., Bandosz, T.J., and Locke, D.C., Pore structure and surface chemistry of adsorbents obtained by pyrolysis of sewage sludge-derived fertilizer. Carbon, 2001. 39(13): p. 1971-1979.

33. Mullen, C.A., Boateng, A.A., Goldberg, N.M., Lima, I.M., Laird, D.A., and Hicks, K.B., Bio-oil and bio-char production from corn cobs and stover by fast pyrolysis. Biomass and Bioenergy, 2010. 34(1): p. 67-74.

34. Fryda, L. and Visser, R., Biochar for Soil Improvement: Evaluation of Biochar from Gasification and Slow Pyrolysis. Agriculture, 2015. 5(4): p. 1076.

35. Dixit, C.K., Surface modification and conjugation strategies for bioassay/biomaterial applications. 2011, Dublin City University, Dublin 9, Ireland.

36. Kloss, S., Zehetner, F., Dellantonio, A., Hamid, R., Ottner, F., Liedtke, V., Schwanninger, M., Gerzabek, M.H., and Soja, G., Characterization of Slow Pyrolysis Biochars: Effects of Feedstocks and Pyrolysis Temperature on Biochar Properties. Journal of Environmental Quality, 2012. 41(4).

37. Hale, S.E., Lehmann, J., Rutherford, D., Zimmerman, A.R., Bachmann, R.T., Shitumbanuma, V., O'Toole, A., Sundqvist, K.L., Arp, H.P.H., and Cornelissen, G., Quantifying the Total and Bioavailable Polycyclic Aromatic Hydrocarbons

and Dioxins in Biochars. Environmental Science & Technology, 2012. 46(5): p. 2830-2838.

38.   Lopez-Ramon, M.V., Stoeckli, F., Moreno-Castilla, C., and Carrasco-Marin, F., On the characterization of acidic and basic surface sites on carbons by various techniques. Carbon, 1999. 37(8): p. 1215-1221.

39.   Inyang, M., Gao, B., Pullammanappallil, P., Ding, W., and Zimmerman, A.R., Biochar from anaerobically digested sugarcane bagasse. Bioresource Technology, 2010. 101(22): p. 8868-8872.

40.   Liang, B., Lehmann, J., Solomon, D., Kinyangi, J., Grossman, J., O'Neill, B., Skjemstad, J.O., Thies, J., Luizão, F.J., Petersen, J., and Neves, E.G., Black Carbon Increases Cation Exchange Capacity in Soils. Soil Science Society of America Journal, 2006. 70(5).

41.   Magini, M., Colella, C., Iasonna, A., and Padella, F., Power measurements during mechanical milling-II. The case of "single path cumulative" solid state reaction. Acta Materialia, 1998. 46(8): p. 2841-2850.

42.   Yu, Z., Peldszus, S., Anderson, W.B., and Huck, P.M., Adsorption of Selected Pharmaceuticals and Endocrine Disrupting Substances by GAC at Low Concentration Levels. Water Quality Technology Conference Proceedings, WQTC (2005), 2005: p. 1-16.

43.   Cai, N. and Larese-Casanova, P., Sorption of carbamazepine by commercial graphene oxides: A comparative study with granular activated carbon and multiwalled carbon nanotubes. Journal of Colloid and Interface Science, 2014. 426: p. 152-161.

44.   Oleszczuk, P., Pan, B., and Xing, B., Adsorption and Desorption of Oxytetracycline and Carbamazepine by Multiwalled Carbon Nanotubes. Environmental Science & Technology, 2009. 43(24): p. 9167-9173.

Table 2.3.1 Independent variables used for grinding optimization

Levels	Codes and values of independent variables of experimental designs for screening using response surface methodology				
	-2	-1	0	+1	+2
Period of Time (hr)	1.6364	3.3182	5	6.6818	8.3636
Powder of Biochar (g)	4.9546	7.4773	10	12.5227	15.0454
Milling Speed (rpm)	516.1373	545.56865	575	604.43135	633.8627

2.3.2 Variable parameters and their level in designed experiments

No.	Powder of Biochar (g) (Ball to Powder Mass Ratio (g/g))*	Period of Time (hr)	Milling Speed (rpm)	Volume Mean (nm)
1	7 (6.43)	3	540	343.8
2	7 (6.43)	3	610	369.1
3	7 (6.43)	7	540	385.6
4	7 (6.43)	7	610	347.1
5	13 (3.46)	3	540	257.9
6	13 (3.46)	3	610	371.8
7	13 (3.46)	7	540	453.1
8	13 (3.46)	7	610	296.8
9	4.96 (9.07)	5	575	348.1
10	15.01 (3.0)	5	575	391
11	10 (4.5)	1.64	575	212.4
12	10 (4.5)	8.37	575	436.1
13	10 (4.5)	5	516	414.6
14	10 (4.5)	5	634	386.4
15 (C)	10 (4.5)	5	575	414.1
16 (C)	10 (4.5)	5	575	414.9
17 (C)	10 (4.5)	5	575	410.2
18 (C)	10 (4.5)	5	575	414.9
19 (C)	10 (4.5)	5	575	410.2
20 (C)	10 (4.5)	5	575	410.2

* For convenience, the mass of balls was fixed to 45 g and the mass of biochar was changed in experiments.

Table 2.3.3 Grinding with different condition

Level	Volume mean (nm)	Condition
11	212.4	Grinding
11	102.5	- 20 °C + Grinding
11	60.1	- 80 °C + Grinding

Table 2.3.4 Chemical, Physical and hydraulic properties for biochars

Property	Nanobiochar (This study)	Data from Literature [2, 28]
Specific gravity	0.40 ± 0.02	0.59 to 1.65
Moisture content (%)	2.11 ± 0.07	1.98 to 66.2
WHC^A (g H$_2$O/g biochar)	9.75 ± 0.45	0.005 to 6.64
LOI^B organic matter content (%)	96.9 ± 3.4	32.3 to 97.5
Volatile matter content (%)	96.9 ± 4.2	28.0 to 74.1
Ash content (%)	2.0 ± 0.1	1.5 to 65.7
Fixed C content (%)	1.06 ± 0.07	0 to 40.3
pH	6.61 ± 0.35	6.24 to 8.86
ORP^C (mV)	132 ± 4	-120.8 to 74.2
EC^D (μscm^{-1})	1737 ± 28	7 to 4150
Zeta potential (mV)	-31.3 ± 2.6	-31.0 to -15.4
∑ PAHs^E (mg kg^{-1})	26.837 ± 3.291	0.68 to 83
CEC^F meq/100	14.8 ± 1.2	15-25
Elemental analysis:		
C (%)	83.1 ± 2.5	23.5 to 78.1
H (%)	3.5 ± 0.11	0.4 to 3.8
N (%)	< 1	0.01 to 0.4
H:C (Molar ratio)	0.5	0.12 to 0.63
C:N (Molar ratio)	> 96.9	143.4 to 5513.9

A: Water holding capacity, B: Loss on ignition, C: Oxidation-reduction potential, D: Electrical conductivity, E: Polycyclic aromatic hydrocarbons and F: Cation Exchange Capacity

Table 2.3.5 Comparison of BET analysis of pinewood biochars

Sample	BET surface area (m^2/g)	Pore volume (cm^3/g)	Average pore size (nm)
Raw biochar	3.12	0.0045	3.2
Nano biochar	47.25	0.0335	1.6

Table 2.3.6 Energy consumption for different scenarios of biochar nanoparticle production

No	Description	Energy consumption (KJ/g)
1	Grinding	71
2	Grinding + Sonication	198
3	Freezing + Grinding	72
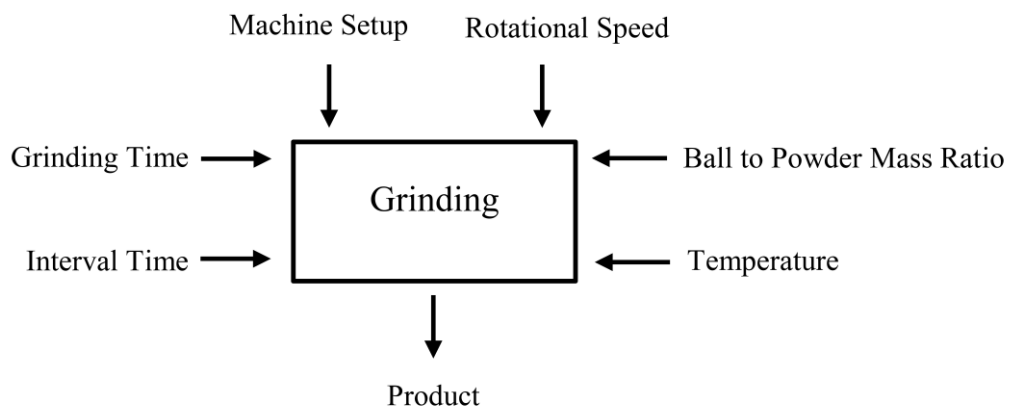
Figure 2.3.1 Factors affecting the size of ground biochar
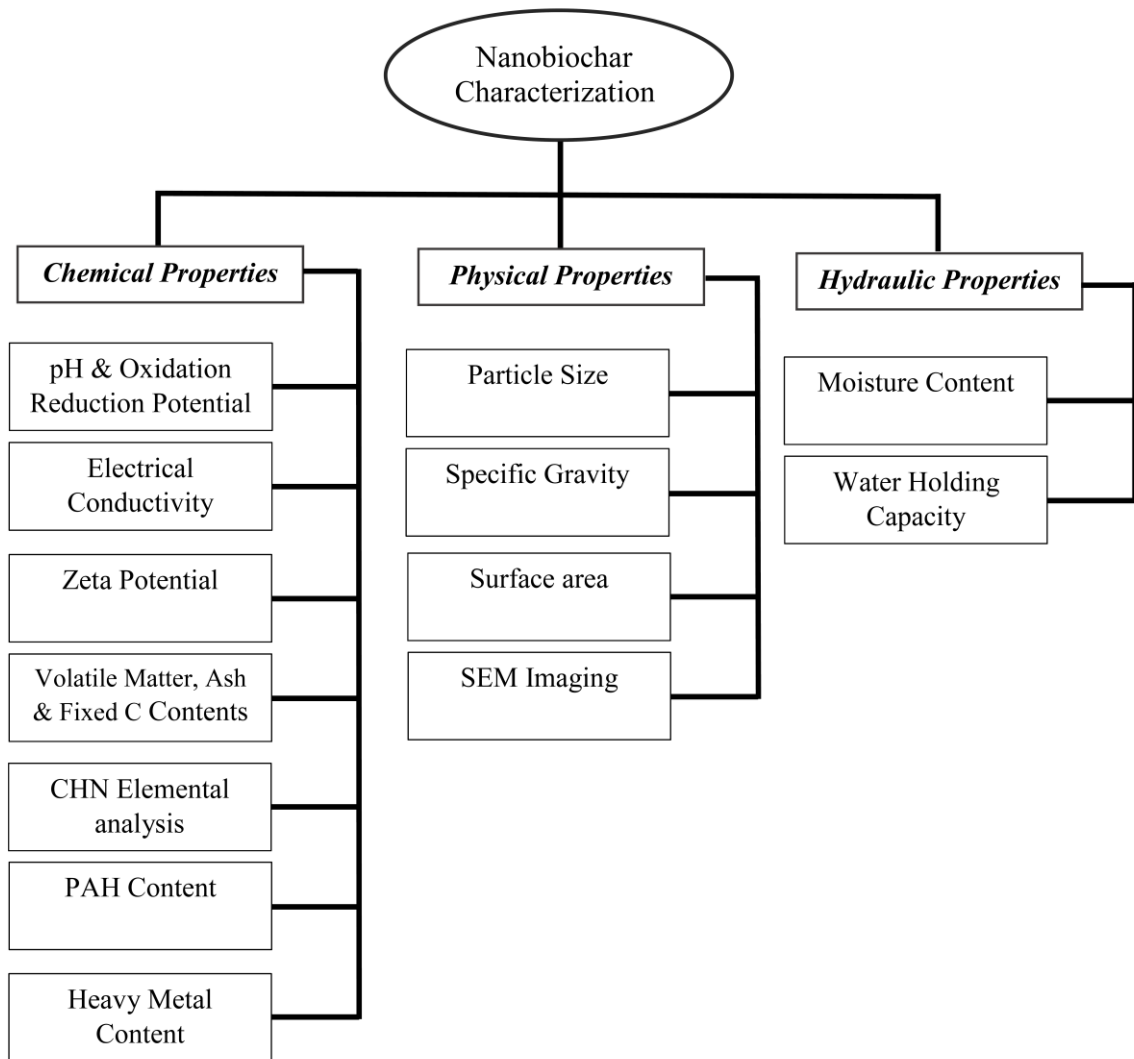
Figure 2.3.2 Characterization tests carried out for nano-biochars
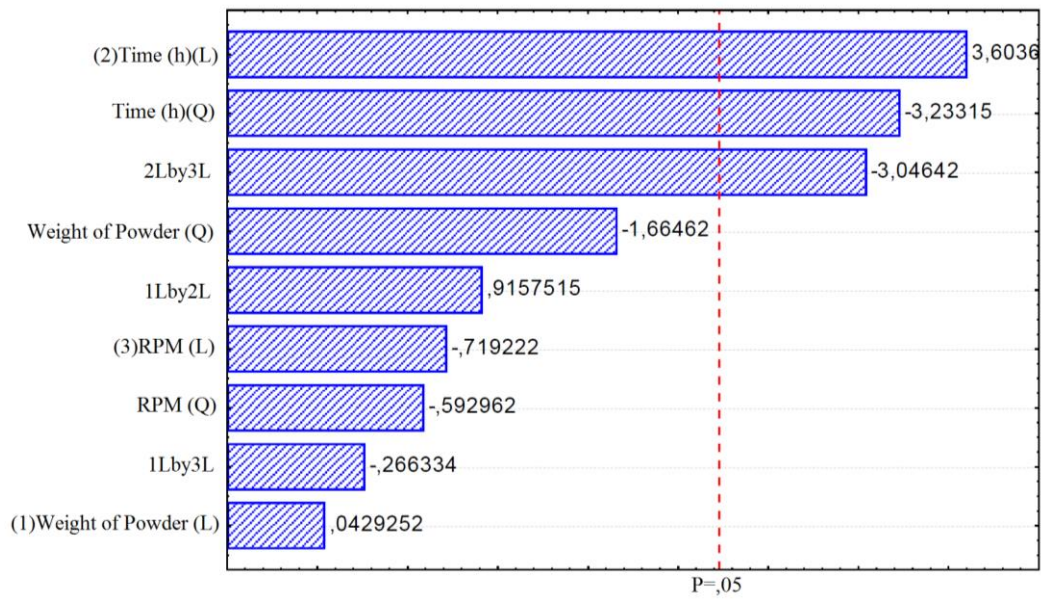
Figure 2.3.3 Pareto chart of standardized effects; variable: volume mean size (nm)
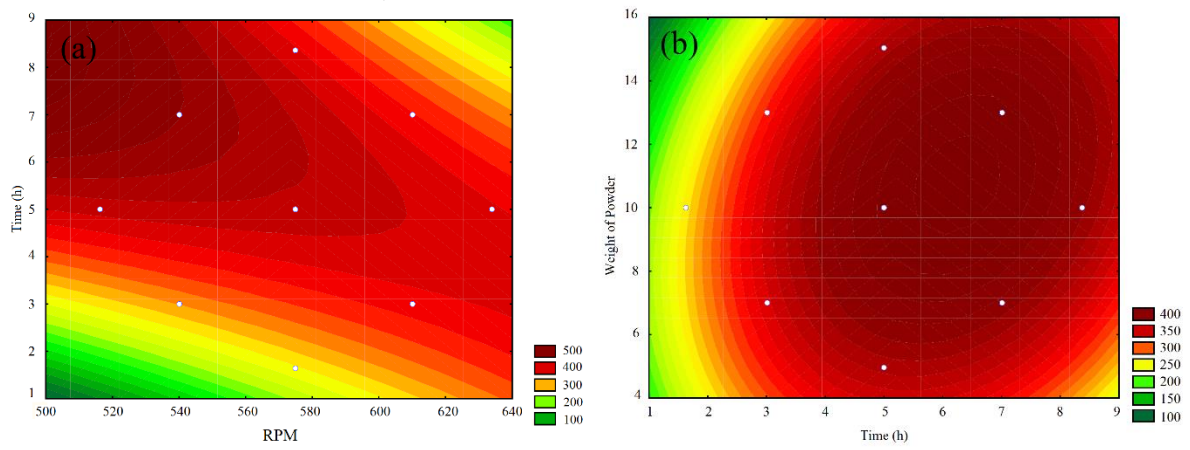
Figure 2.3.4 Effect of: (a) time of grinding and rotational speed and, (b) weight of powder and time, on the volume mean (nm) of nanobiochar
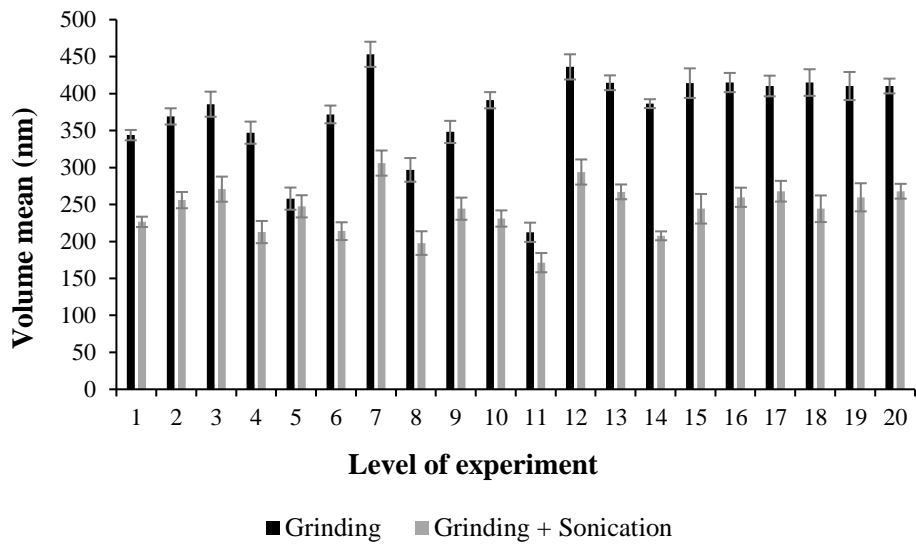
Figure 2.3.5 Volume mean diameter (nm) after grinding (black bars) and after grinding with sonication (gray bars)
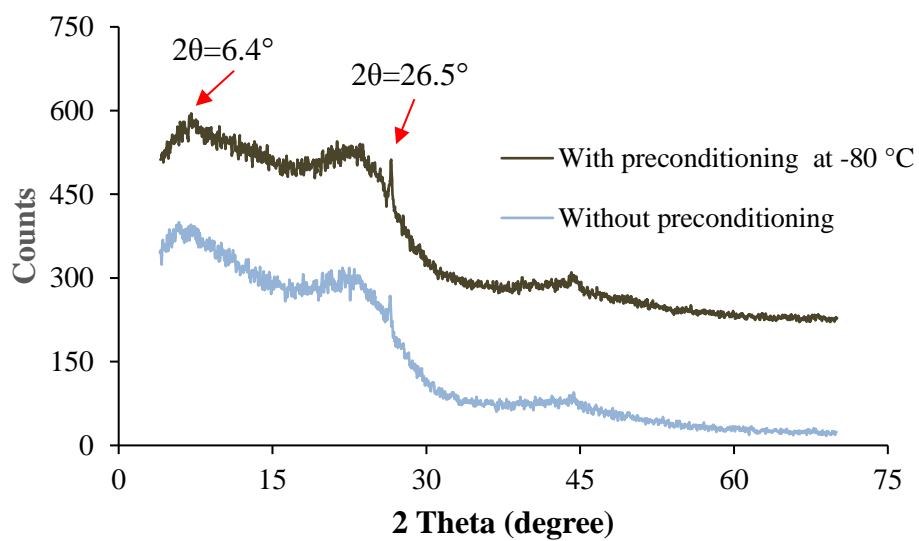
Figure 2.3.6 XRD patterns of ground biochar with and without preconditioning (pattern for preconditioned sample is shifted by +200 counts for better discrimination)
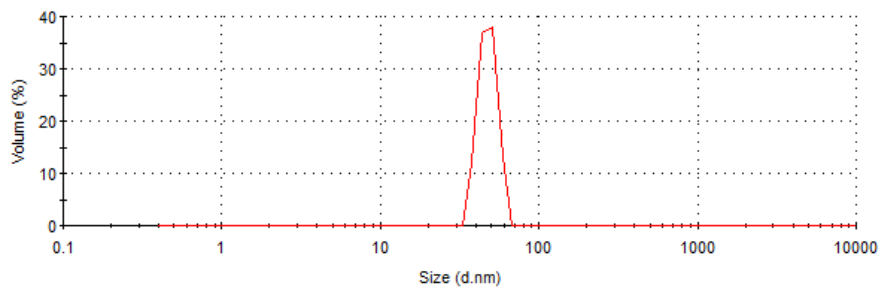
Figure 2.3.7 Size distribution by volume
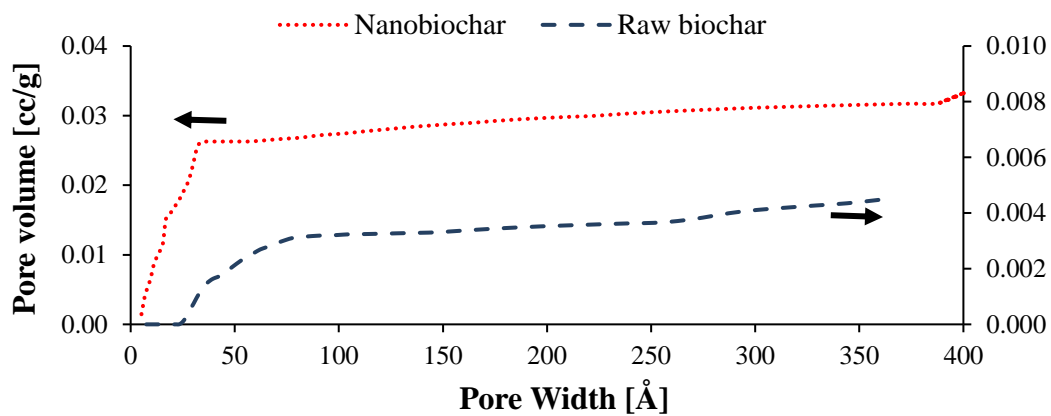
Figure 2.3.8 Cumulative pore volume vs. pore diameter for raw biochar (blue line) and nanobiochar (red line)
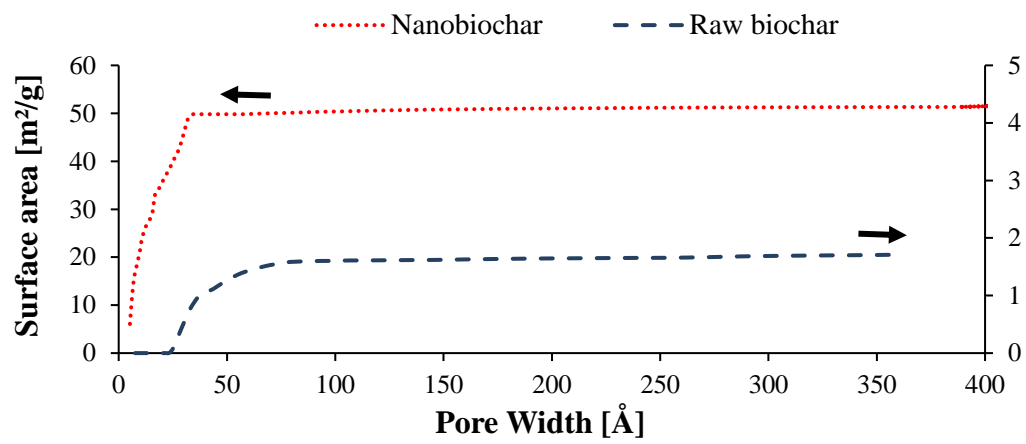
Figure 2.3.9 Cumulative surface area vs. pore diameter for raw biochar (blue line) and nanobiochar (red line)
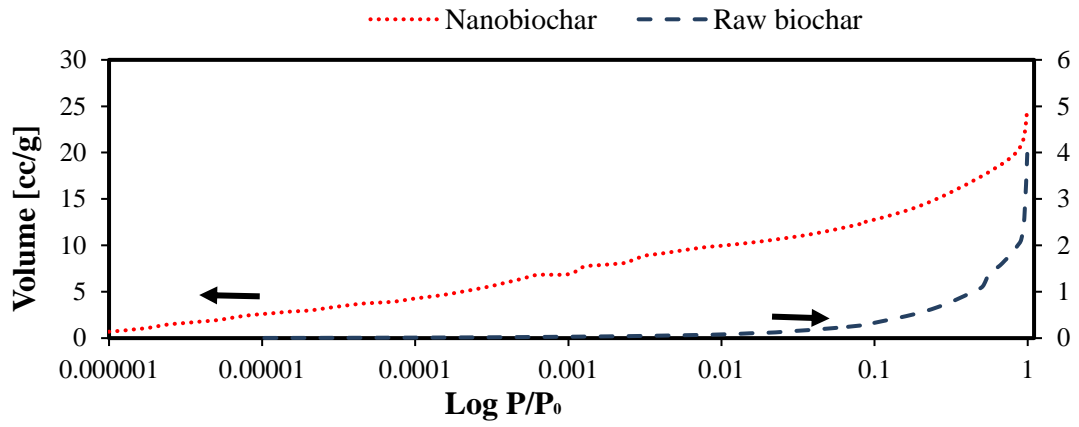
Figure 2.3.10 Nitrogen adsorption isotherms at 77 K for raw and nano-biochar (P/P0 is the partial pressure of nitrogen and the adsorbed gas onto nanobiochar is measured as a function of P/P$_0$)
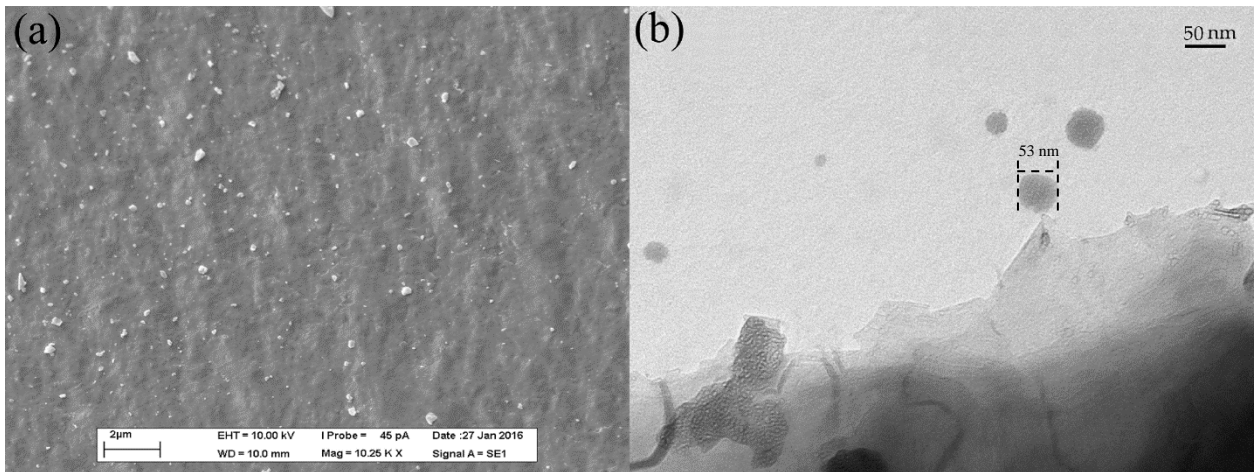
Figure 2.3.11 a: SEM and b: TEM micrographs of nanobiochar at 10 KX and 40 KX magnification, respectively
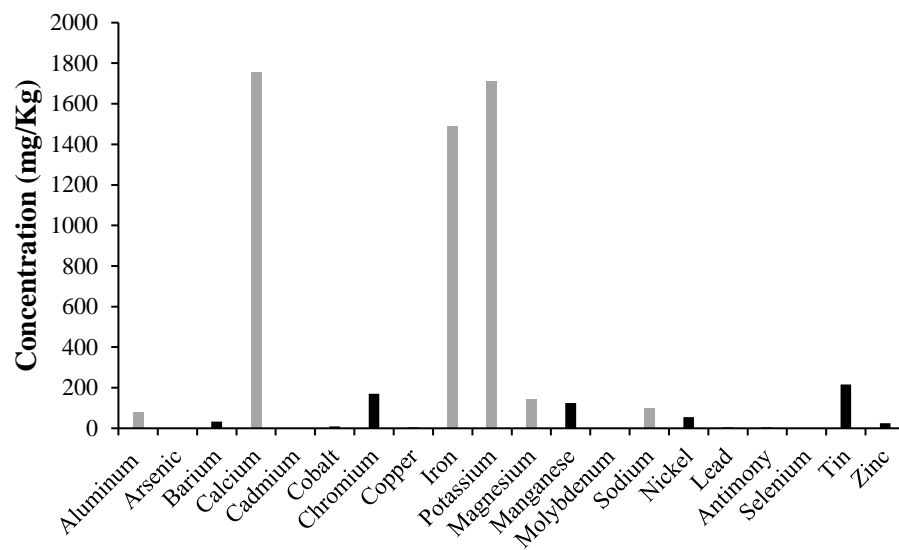
Figure 2.3.12 Toxic (black bars) and non-toxic (gray bars) metal concentrations of nanobiochar in mg kg^{-1}
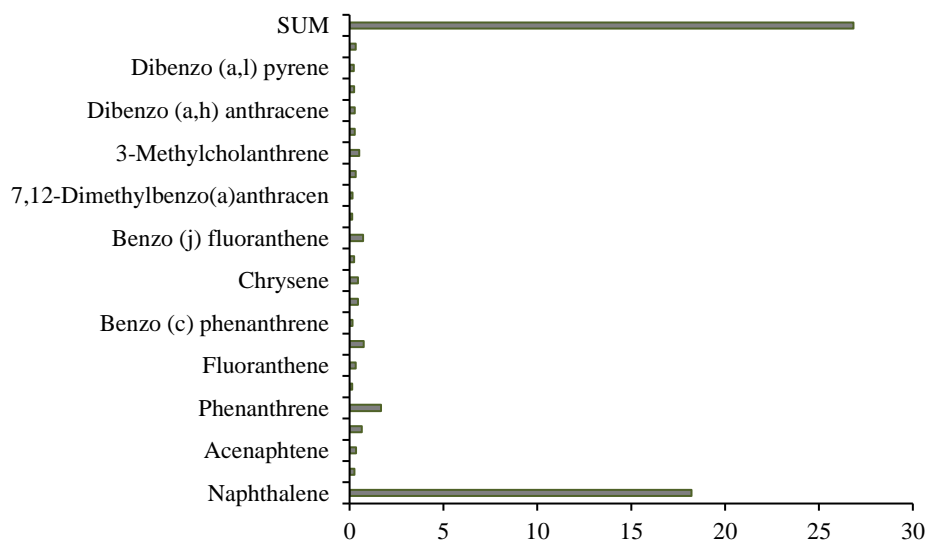
Figure 2.3.13 Polyaromatic hydrocarbons (PAHs) concentrations detected in nanobiochars in mg kg^{-1}

Note: Content of Naphthalene consists of Naphthalene, 2- Methyl Naphthalene, 1-Methyl Naphthalene, 1, 3 Dimethylnaphthalene and 2, 3, 5-Trimethyl Naphthalene
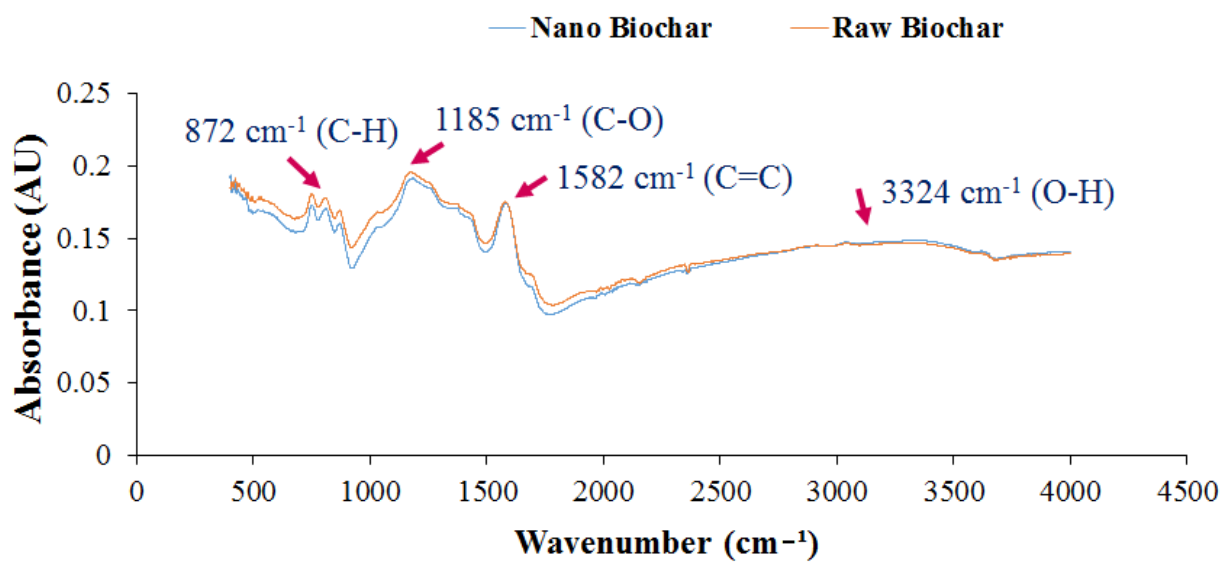
Figure 2.3.14 FT-IR spectra of raw and nano biochar (AU: Arbitrary unit)
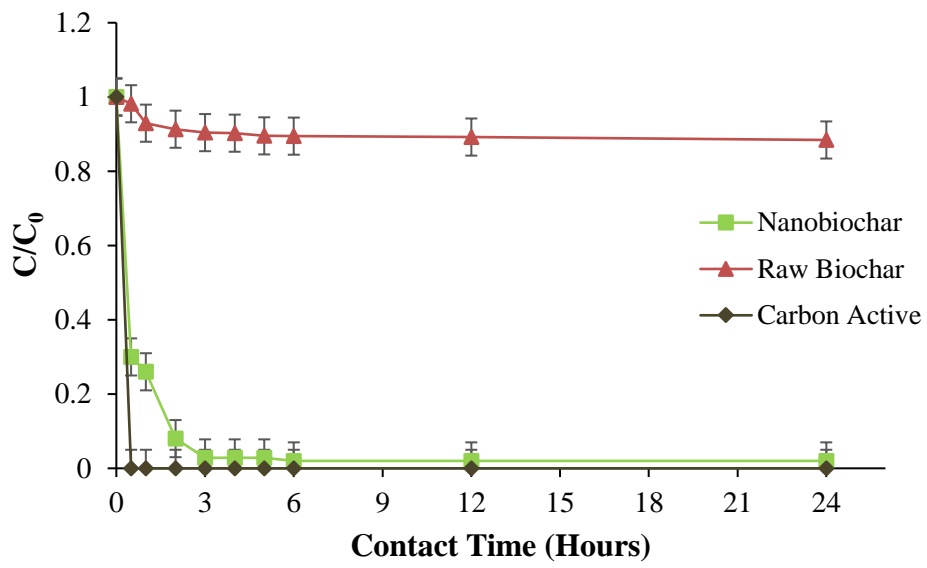
Figure 2.3.15 Residual concentration of carbamazepine versus time plot of carbamazepine adsorption onto nanobiochar, raw biochar, and activated carbon

CHAPTER 3

Application of nanobiochar for CBZ removal

Part 1

Pine-Wood derived Nanobiochar for Removal of Carbamazepine from Aqueous Media: Adsorption Behavior and Influential Parameters

Mitra Naghdi[1], Mehrdad Taheran[1], Rama Pulicharla[1], Tarek Rouissi[1], Satinder K. Brar[1*], M. Verma[2], R.Y. Surampalli[3]

[1]INRS-ETE, Université du Québec, 490, Rue de la Couronne, Québec, Canada G1K 9A9

[2]CO$_2$ Solutions Inc., 2300, rue Jean-Perrin, Québec, Québec G2C 1T9 Canada

[3]Department of Civil Engineering, University of Nebraska-Lincoln, N104 SEC PO Box 886105, Lincoln, NE 68588-6105, US

(*Phone: 1 418 654 3116; Fax: 1 418 654 2600; E-mail: satinder.brar@ete.inrs.ca)

Chapter 3. Application of nanobiochar for CBZ removal

Résumé

Ces dernières années, l'application de biochar pour l'élimination des polluants des solutions aqueuses a été intéressante en raison des propriétés physicochimiques favorables et de la disponibilité de la charge d'alimentation. Cependant, le comportement d'adsorption n'a été rapporté que pour les particules de biochar brutes et microscopiques et l'utilisation de nanoparticules de biochar, qui offrent une surface spécifique supérieure, n'a pas retenu l'attention. L'objectif de cette étude était d'étudier l'efficacité d'adsorption du nanobiochar produit à partir de la pinède. A cette fin, l'étude de l'élimination de la carbamazépine (CBZ), un médicament prescrit à l'échelle mondiale, à de très faibles concentrations (0,5-20 ppb) sur du nanobiochar produit à 60 nm a été étudiée. Les résultats ont montré que le nanobiochar peut éliminer jusqu'à 95% de la CBZ (74 μg CBZ/g de nanobiochar) après 3 h de contact. L'adsorption de la CBZ sur nanobiochar a suivi le modèle isotherme de Freundlich (R^2 = 0,9822) et le modèle cinétique de pseudo-deuxième ordre (R^2 = 0,9994). Il a été trouvé qu'une augmentation du pH de 3 à 8 peut améliorer l'efficacité d'adsorption de 2,3 fois. En outre, en raison de la présence de surfactant dans les eaux usées, l'addition de Tween 80 comme tensioactif modèle a été étudiée dans la plage de 0 à 1 (rapport molaire Tween 80 à la CBZ) et les résultats ont montré que 57% d'efficacité d'adsorption. Ainsi, le nanobiochar obtenu à partir de résidus de pin peut être un sorbant prometteur pour les micropolluants.

Mots clés :

Bois de pin, Nanobiochar, Composé pharmaceutique, Adsorption, Traitement de l'eau

Chapter 3. Application of nanobiochar for CBZ removal

Abstract

In recent years, application of biochar for removal of pollutants from aqueous solutions has been of interest due to favorable physico-chemical properties and availability of feedstock. However, adsorption behavior has been reported only for raw and micro biochar particles and taking advantage of biochar nanoparticles, which offer superior specific surface area, did not receive any attention. The objective of this study was to investigate the adsorption efficiency of produced nanobiochar from pinewood. For this purpose, removal of carbamazepine (CBZ), a globally prescribed pharmaceutical, at very low concentrations (0.5-20 ppb) on as-produced nanobiochar with average particle size of 60 nm was studied. The results showed that nanobiochar can remove up to 95% of CBZ (74 µg CBZ/g nanobiochar) after 3 hours contact time. Adsorption of CBZ on nanobiochar followed Freundlich isotherm model (R^2=0.9822) and pseudo-second order kinetic model (R^2=0.9994). It was found that increasing pH from 3 to 8 can enhance the adsorption efficiency by 2.3 folds. Also, due to the presence of surfactant in wastewater, the addition of Tween 80 as a model surfactant was studied in the range of 0 to 1 (Tween 80 to CBZ molar ratio) and the results showed that adsorption efficiency can be enhanced by 57%. Thus, the nanobiochar obtained from pinewood residues can be a promising sorbent for micropollutants.

Keywords:

Pine wood, Nanobiochar, Pharmaceutical compound, Adsorption, Water treatment

Chapter 3. Application of nanobiochar for CBZ removal

Introduction

Pharmaceutical compounds are widely used for curing or preventing human and animal diseases. The annual consumption of pharmaceuticals is estimated to be about 15 g and 50-150 g per capita in world and industrialized countries, respectively [1]. The occurrence of these compounds in the environment has attracted attention of regulatory organizations due to potential adverse effects, such as development of antibiotic resistance genes in pathogenic bacteria [2]. Carbamazepine (CBZ) is one of widely used antiepileptic/anticonvulsant drugs around the world with more than 1000 tons annual consumption. The release rate of CBZ into water bodies is estimated to be around 30 tons per year and according to several reports, it is toxic for several aquatic organisms, such as cnidarians and crustaceans [3-5]. CBZ is electrically neutral at typical pH values of drinking water and its log K_{ow} (2.45) shows that CBZ is relatively hydrophilic [6]. CBZ has been among most frequently detected pharmaceutical compounds in wastewater treatment plant (WWTP) effluent and rivers in Europe and North America [6-8]. For example, the presence of CBZ in wastewaters (up to 6.3 µg L^{-1}), surface waters (up to 1.1 µg L^{-1}), and drinking water (up to 30 ng L^{-1}) was reported in Canada and Germany [9]. However, the CBZ removal efficiency of WWTP did not exceed 7% [10]. Therefore, developing new method for effective removal of this compound is necessary prior to effluent discharge or drinking water distribution [11, 12]. Accordingly, novel treatment processes are being examined for treatment of micropollutants-containing water sources with a focus on adsorption processes considering hydrophobicity of targeted compounds, or on advanced oxidation methods considering susceptibility of compounds to oxidative processes [8, 13]. In the case of CBZ, advanced oxidation methods do not necessarily lead to complete mineralization and sometimes the transformation products such as acridine are still harmful to the environment [9, 14]. Thus, they still need further development to offer complete mineralization of micropollutants.

Carbonaceous nanomaterials showed high chemical and thermal stability and found many applications in industrial and medical devices. Due to their high specific surface area, they can act as adsorbents with high capacity and affinity for micropollutants [15-17]. For example, Cai *et al.* studied the adsorption of CBZ on graphene oxide powder and their isotherms fitted well with Freundlich model with 95% of removal efficiency [8]. In a similar study, Lerman *et al.* used single-walled carbon nanotubes (SWCNTs)

as adsorbent for removal of CBZ and their calculations showed incomplete monolayer coverage of SWCNTs which suggested that CBZ might interact with preferably polar sites on SWCNTs [18]. Oleszczuk *et al.* investigated the adsorption of CBZ on multi-walled carbon nanotubes (MWCNTs) and their isotherm and kinetic data fitted well the Polanyi-Manes model (PMM) and pseudo-second-order kinetic model. According to their observations, up to 90.6% of CBZ was adsorbed after 24 h depending on the outer diameter of MWCNT [19].

Recently biochar, which is a waste biomass pyrolysis product, has attracted a great interest for purification of water sources due to their properties, such as porosity and capability of adsorbing and exchanging different organic and inorganic contaminants [20-23]. The advantages of employing biochars for treatment of wastewater have already been reported [24-26]. Nielsen *et al.* used biochar produced from sewage sludge, aquaculture waste and their mixtures for adsorption of CBZ from water. Their results showed that equilibrium was reached within 5 hours and adsorption capacity of 90% sewage sludge and 10% aquaculture waste was 37.2 mg/g at an equilibrium concentration of 50 mg/L CBZ [10].

Meanwhile, depending on the pyrolysis conditions, the particle size of the biochars ranged from hundreds of micrometers to several centimeters [27]. In our previous works, we studied the physicochemical and adsorption properties of biochar in micro-sized range (10-600 μm) and reported that the reduction of biochar size led to increased adsorption capacity due to increasing available sites for adsorption [28, 29]. However, reducing the particle size of biochar to nanosize range i.e. smaller than 100 nm can further improve its properties, especially surface to volume ratio which can enhance the adsorption potential and surface energy [30-36]. To the best of our knowledge, nanobiochar has not been applied for investigation of adsorption micropollutants. In this work, nanobiochar was produced for the first time from pinewood biochar through a simple physical method. Also, the adsorption behavior of pharmaceutically active compound, CBZ, at low concentration levels from aqueous phase on produced nanobiochar was investigated. In the first part of the work, different isotherms and kinetics models were fitted for the obtained data to find the appropriate models for adsorption behavior. In the second part, the effects of several important parameters including solution pH, adsorbent dosage, rotational speed and surfactant concentration were studied.

Chapter 3. Application of nanobiochar for CBZ removal

Material and methods

Materials

Pinewood Biochar (BC-PW) was obtained from Pyrovac Inc. (Quebec, Canada). BC-PW was derived from pine white wood (80% v/v, 3 mm) obtained from Belle-Ripe in Princeville and the rest included spruce and fir (20%). The production of BC-PW was carried out at 525±1 °C by increasing the temperature of biomass at the rate of 25 °C/min in the presence of nitrogen under atmospheric pressure for 20 min and the produced BC-PW was used as obtained from the reactor outlet. Carbamazepine (CBZ ≥ 99%) was purchased from Sigma-Aldrich (Oakville, Canada). Carbamazepine (D10) was purchased from CDN Isotopes (Pointe-Claire, Canada). Tween 80 and methanol were purchased from Fisher scientific (Ottawa, Canada). Ultrapure water was prepared in the laboratory using Milli-Q/Milli-Ro Milli pore system (Massachusetts, USA) and it was used for preparation of CBZ stock solutions and related samples for adsorption tests.

Nanobiochar production

Nanobiochar with the average size of 60±20 nm was produced in laboratory using a planetary ball mill (PM100; Retsch Corporation) at ambient conditions. Briefly, 10 g of pinewood biochar were kept at -80 °C for 24 h prior to grinding. Ball milling was performed at 575 rpm for 100 min in a 500 mL stainless steel jar using stainless steel balls of 2.4 mm in diameter (800 balls with total weight of 45 g). The physicochemical properties of produced nanobiochar are listed in Table 3.1.1.

Equilibrium time

To determine equilibrium time for adsorption of CBZ onto nanobiochar, 5 mg nanobiochar was added to 20 ml of CBZ solution (C_0 = 5 ng/mL) in 50 mL flasks. All flasks were shaken at 150 rpm and 25±1 °C for 15 days. The samples were taken at different intervals of 1 h, 2 h,… 6 h, 12 h, 1 day, 2 days,…15 days, centrifuged for 10 min at 11,000 x g (14,000 rpm) and then analyzed for residual CBZ. In all the experiments, one sample containing only nanobiochar and one sample containing only CBZ were considered as negative and positive controls, respectively. The CBZ concentration in negative and positive controls was 0 (below detection limit) and 5 ppb, respectively. All experiments were done in duplicate and average was reported.

Chapter 3. Application of nanobiochar for CBZ removal

Isotherm test

About 20 mL of aqueous CBZ solutions with different concentrations (0.5, 1, 3, 5, 7, 10, 15 and 20 ng/mL) along with 5 mg nanobiochar were added to 50 mL flasks. The pH of all samples was adjusted to 6 and then all the flasks were tightly sealed and incubated at 150 rpm and 25±1 °C for two days (the time was determined using equilibrium test). The samples were centrifuged for 10 min at 11,000 x g (14,000 rpm) to remove the nanobiochar and the supernatants were analyzed for residual CBZ. Subsequently, three models were used to fit the adsorption isotherms of CBZ into nanobiochar (Table 3.1.2). All experiments were performed in duplicate and average values were reported. The results of isotherm tests and kinetic tests were analyzed by SigmaPlot 12 (Systat Software, Inc.) to fit in the suggested models.

Kinetics study

To study the adsorption kinetics, 5 mg nanobiochar was added to 500 mL CBZ solution (5 ng/mL). The solution pH was adjusted to 6 and stirred at 150 rpm and room temperature. Samples were taken after 1, 2, 3, 6, 9, 12, 15, 18, 21, 24, 27 and 30 min of adsorption. Later, the samples were withdrawn at different intervals times and centrifuged at 11,000 x g (14,000 rpm) for 2 min, filtered with Whatman paper (0.2 micron pore size) and analyzed for CBZ in supernatants. Different kinetic models were used to fit the adsorption kinetics of CBZ on nanobiochar (Table 3.1.3). All experiments were performed in duplicates and average values were reported.

Adsorption energy

The Dubinin-Radushkevich empirical model was used to determine the energy of adsorption. The non-linear form of this model can be expressed as Equations (8) and (9):

$$q_e = q_s \exp(-K_{ad}\varepsilon^2) \qquad (8)$$

$$Ln\ q_e = Ln\ q_s - K_{ad}\varepsilon^2 \qquad (9)$$

Where q_e is the equilibrium concentration of adsorbate in solid phase (mg/g); q_s is the theoretical isotherm saturation capacity (mg/g); K_{ad} (mol^2/kJ^2) is Dubinin-Radushkevich isotherm constant and ε is potential energy that can be related to the equilibrium concentration through following equation.

$$\varepsilon = RT\ Ln\left(1 + \frac{1}{C_e}\right) \qquad (10)$$

Where R, T and Ce represent the universal gas constant (8.314 J/mol K), absolute temperature (K) and equilibrium concentration of adsorbate in aqueous phase (mg/L), respectively. This approach can be applied to determine if the adsorption is physical or chemical by calculating the mean free energy E using the following equation:

$$E = \frac{1}{\sqrt{2 \times K_{ad}}} \qquad (11)$$

This parameter represents the amount of energy (kJ) for removing one mole of adsorbate from its location in adsorbent to the infinity. If E < 8 KJ/mol, physical forces were dominant in adsorption. If E is in the range of 8-16 KJ/mol, ion exchange mechanism governed adsorption and in the case of E > 16 KJ/mol, particle diffusion dominated adsorption [37].

Effect of operational parameters

Surfactant concentration

The effect of four different concentrations of Tween 80 (0, 25, 50, 75 and 100 ng/mL) on adsorption of CBZ onto nanobiochar was studied. The required amount of Tween 80 along with 10 mg nanobiochar was added to 18 mL of ultrapure water (adjusted to pH 6 using 0.2 M solution of HCl) and mixed for 10 min on a vortex mixer. Subsequently, the required CBZ (10 ng/mL) was added from stock solution and the volume was increased to 20 mL using ultrapure water with pH 6. For all the samples, rotational speed (150 rpm) and time (1 h) were fixed during experiments.

pH

The effect of six different pHs (3, 4, 5, 6, 7 and 8) which are typical of different water sources (rivers, lakes, groundwater or wastewater) on adsorption of CBZ onto nanobiochar was investigated. About 10 mL ultrapure water containing 10 mg nanobiochar and 1 μg Tween 80 and 10 mL ultrapure water containing 0.2 μg CBZ was prepared separately and their pH was adjusted to the required level using 0.2 M solution of NaOH or HCl. Later, they were mixed to reach CBZ concentration of 10 ng/mL and surfactant concentration of 50 ng/mL. For all the samples, the rotational speed (150 rpm) and time (1 h) were fixed during experiments.

Rotational speed

The effect of different rotational speeds (90, 120, 150, 180, 210 and 240 rpm) on adsorption of CBZ onto nanobiochar was studied. About 10 mL ultrapure water

containing 10 mg nanobiochar and 1 μg Tween 80 and 10 mL ultrapure water containing 0.2 μg CBZ were prepared separately and their pH was adjusted to 6 using 0.2 M solution of HCl. Later, they were mixed to reach CBZ concentration of 10 ng/mL and surfactant concentration of 50 ng/mL. Eventually, each sample was mixed at required rotational speed for 1 h.

Adsorbent dose

Effect of different concentration of nanobiochar (4, 7, 10, 13, 17 and 20 mg in 20 mL of solution) on adsorption of CBZ was studied. About 10 mL ultrapure water containing 1 μg Tween 80 and desired amount of nanobiochar and 10 mL ultrapure water containing 0.2 μg CBZ were prepared separately and their pH was adjusted to 6 using 0.2 M solution of HCl. For all experiments, the rotational speed (150 rpm) and time (1 h) were fixed during experiments.

Quantification of CBZ

Quantification of CBZ was performed using Laser Diode Thermal Desorption (LDTD) (Phytronix technologies, Canada) coupled with a LCQ Duo ion trap tandem mass spectrometer (Thermo Finnigan, USA). The daughter ions identified for CBZ in LDTD were 194 and 192 Da. The method reporting limit was 10 ng/L. A calibration curve of CBZ concentration was developed with six standard solutions and with R^2 no less than 0.99. The details of quantification process were described elsewhere [6]. All the experiments were performed in triplicates and the average results were reported.

Fourier transform infrared (FT-IR) spectroscopy

FT-IR spectrum in the range of 400-4000 cm^{-1} was recorded using a Nicolet IS50 FT-IR Spectrometer (Thermo Scientific, USA) through attenuated total reflectance (ATR) using 4 cm^{-1} resolution and 32 scans per spectrum. For taking the spectrum, enough sample was placed on the diamond crystal and to ensure that consistent contact, the gripper plate was placed on the sample. The average of 16 times measurement was plotted.

Results and discussion

Equilibrium time of CBZ adsorption on nanobiochar

The evolution of CBZ residual concentration (C/C_0) in aqueous phase during first 4 days is plotted in Figure 3.1.1. According to this plot, equilibrium was reached after 2

days (C/C_0=0.00001). Consequently, for isotherm experiments, 2 days was considered as required time to reach equilibrium since no changes in C/C_0 was observed after 2 days. In literature, 12 days was identified as equilibrium time for adsorption of 94% of CBZ on coal-based and coconut-based granular activated carbons [2, 38]. It is noteworthy that more than 95% of CBZ (equivalent to 74 µg CBZ/g nanobiochar) was removed in less than 3 hours which indicated rapid mass transfer of CBZ onto nanobiochar compared to other carbonaceous materials. For example, Oleszczuk *et al.* investigated the adsorption of CBZ on MWCNTs and observed that after 24 h, around 91% of CBZ was adsorbed onto MWCNT [19]. Likewise, Cai *et al.* reported 95% of removal efficiency for CBZ using graphene oxide powder after 24 hours [8]. Adsorption property of biochar is dominated by biochar surface chemical composition and physico-chemical properties which in turn is affected by the pyrolysis conditions [39, 40]. For mass transfer rate during adsorption, several properties including pore structure, pore size and surface affinity towards target compound play key role and therefore rapid equilibration of CBZ adsorption on nanobiochar compared to commercial adsorbents indicates its superior physicochemical properties to be a promising adsorbent.

Isotherm analysis

The isotherm tests were performed to obtain equilibrium concentrations of CBZ in aqueous media that were in contact with nanobiochar. The results showed that nanobiochar can remove 70-99% (56-79 µg CBZ/g nanobiochar) of CBZ from aqueous media. Three known isotherm models (Table 3.1.4), namely Freundlich, Langmuir and partition-adsorption were examined in their linear and non-linear forms to fit the experimental data obtained in isotherms tests and their linearized forms are shown in Figure 3.1.2. The calculated fitting parameters are listed in Table 3.1.4 and accordingly, Freundlich model in its linear and non-linear forms showed the best correlation coefficients (R^2>0.98) with experimental data. In Freunlich model, K_f is an approximate indicator of adsorption capacity and $1/n$ is heterogeneity parameter. Since the value of the exponent n was greater than 1 for nanobiochar, it indicated favorable adsorption with little heterogeneity and major contribution of physical binding forces [37, 41]. The results obtained for adsorption energy of CBZ on nanobiochar in section "kinetic studies" confirmed physical adsorption.

Dickenson *et al.* studied the adsorption of CBZ to powdered activated carbon and fitted the data with Freundlich isotherm model [42]. Also, Yu *et al.* used the Freundlich, Langmuir and three-parameter Langmuir-Freundlich (LF) models to evaluate the behavior of granulated activated carbon samples for the adsorption of CBZ from water and observed that Freundlich offered better fit for experimental data [2]. Likewise, Cai *et al.* examined Freundlich, Langmuir, and PMM isotherm models for adsorption of CBZ onto graphene oxide powder, granular activated carbon, and carbon nanotubes and observed better fit with Freunlich isotherm [8].

Kinetic studies

Kinetics of adsorption is important for understanding of contaminants removal, since it gives information on the transport mechanisms between two phases. In Figure 3.1.3, the obtained data from kinetic tests were plotted in linearized forms of three common kinetics models, namely pseudo first-order, pseudo second-order and intra-particle diffusion models. CBZ molecules were adsorbed very rapidly during the early time interval (71% within 30 min) that can be attributed to the small size of particles and presence of a large number of free adsorption sites. Zhao *et al.* reported similar rapid initial adsorption of CBZ on MWCNTs (74% within 30 min) and attributed to the fast mass transfer into the boundary layers near surface of carbon nanotubes [17]. In Table 3.1.5, the fitting parameters and related R^2 for different models in linear and non-linear form are listed. Based on the fitting parameters, pseudo first-order kinetic model in its linear and non-linear forms was the least probable model ($R^2 < 0.85$) which indicated that adsorption capacity could not be the major factor dominating the adsorption mechanisms of CBZ on nanobiochar [43]. Similarly, the intra-particle kinetic models (Table 3.1.3, Equation 7) in which adsorption rate is proportional to square root of time did not fit well into the experimental data ($R^2 < 0.910$). Also, two other models including liquid film diffusion and second order were tested and the obtained R^2 were less than 0.8 (data not shown). On the other hand, pseudo second-order equation with $R^2 = 0.999$ in its linear form and $R^2 = 0.946$ in its non-linear form fitted the experimental data very well. However, the experimental qe was 18.4 mg/g while the calculated qe for nonlinear pseudo-second order and linear pseudo-second order were 1.39 and 14.05 mg/g, respectively which confirmed better fitting of linear pseudo-second order kinetic model for CBZ adsorption. Although pseudo-second indicated that the adsorption

kinetics may be dominated by chemisorption [44] but employing equations 9, 10 and 11 rejected this possibility since the mean free energy (E) of CBZ adsorption on nanobiochar was calculated to be 5.5 KJ/mol which is consistent with physiosorption processes [37].

Effects of different parameters on CBZ adsorption on Nanobiochar

pH

The effects of variation of pH on adsorption of CBZ on nanobiochar is presented in Figure 3.1.5. The adsorption efficiency of CBZ was enhanced as pH increased from 3 to 6 and from 6 to 8 the effect of pH was insignificant. The solubility, ionization and hydrophilicity of many organic chemicals is increased by pH and therefore lowered adsorption on carbonaceous materials is expected. However, CBZ is a neutral compound in the whole pH range and its adsorption behavior is different from ionizable compounds which can be affected by electrostatic forces [17]. The NH_2 functional group in CBZ can interact with oxygen-containing functional groups of nanobiochar, such as OH and C=O through hydrogen bonding [45]. In the FTIR spectrum of nanobiochar (Figure 3.1.4), the significant bands at 3324 cm^{-1} (alcohol, O-H stretching) and 1185 cm^{-1} (phenolic, C-O stretching) confirmed the presence of oxygen-containing groups in nanobiochar.

Variation of solution pH may affect the properties of these functional groups on both adsorbate and adsorbent [46]. At lower pH value, functional groups on nanobiochar and CBZ can interact with H^+ more easily due to the abundance of H^+ in the solution that decrease hydrogen bonding between nanobiochar and CBZ and consequently decrease adsorption efficiency. In contrast, as concentration of H^+ is reduced at higher pH levels, hydrogen bonding donor groups on CBZ can interact with hydrogen bonding acceptors or π-donors in nanobiochar and therefore the adsorption efficiency is expected to be enhanced [17, 47-49].

Rotational speed

Adsorption of CBZ at different rotational speeds (90 to 240 rpm) was studied and the results are presented in Figure 3.1.6. CBZ adsorption was increased from 29% to 67% while increasing the rotational speed of the shaker from 90 rpm to 210 rpm and further increasing of rotational speed did not show any considerable changes in adsorption efficiency. Walker *et al.* and Zarra suggested that increasing agitation rate can

increase the magnitude of the external mass transfer coefficient [50, 51]. Per mass transfer principles, there is thin layer of fluid at the immediate vicinity of adsorbent surface where the viscous forces resist against fluid movement and play a key role in impeding mass transfer. Since the adsorbate molecules should pass through this layer to reach adsorbent surface, the thinner boundary layer results in higher rate of mass transfer. The thickness of boundary layer is inversely proportional to the square of water velocity [52] and therefore the enhancement of adsorption efficiency by rotational speed can be attributed to the increasing mass transfer rate as a result of reduction in resistance of surface film [53].

Adsorbent dose

The effect of adsorbent dose on removal of CBZ through adsorption on nanobiochar is illustrated in Figure 3.1.7. Based on the results, removal efficiency of CBZ increased from 53 to 87% when the adsorbent dose of solution was increased from 200 mg/L to 1000 mg/L. Increasing adsorbent dose is equal to increasing surface and the number of adsorption sites, which enhances the collision frequency of target compounds with adsorbent and consequently results in a higher removal of CBZ [54]. However, after a certain dose, further increasing of adsorbent dose did not show any improvement which can be due to the overlapping of adsorption sites and also possibility of particles aggregation [55].

Surfactant concentration

Surfactants are widely used in daily life products, such as detergents and food stabilizers. They find their way into wastewater and due to their amphiphilic properties, they can affect the removal of micropollutants through adsorptive systems [56, 57]. In this work, the effect of addition of a widely-used surfactant (Tween 80) on adsorption of CBZ on nanobiochar was investigated and the results are illustrated in Figure 3.1.8. It was found that with increasing Tween 80 to CBZ molar ratio from 0 to 1, the adsorption efficiency increased from 42 to 66%. It is in agreement with the results of Hari *et al.* who related this enhancement to the strong affinity of compounds for adsorbed surfactant aggregates [58]. Also, there is another report on improvement of CBZ adsorption onto modified zeolite with surfactant [59].

Tween 80 is a nonionic surfactant which in comparison with its ionic counterparts is less sensitive to the widely found divalent cations in water and wastewater [60]. Each molecule of Tween 80 has several hydrophilic functional groups and one hydrophobic

tail and therefore it can link carbamazepine to nanobiochar. The possible interactions between CBZ, nanobiochar and Tween 80 are illustrated in Figure 3.1.9. Oxygen and nitrogen in amide group of CBZ can form a hydrogen bonding with the hydrophilic head of Tween 80 and its hydrophobic tail can enter a hydrophobic interaction with graphite-like structure of nanobiochar.

Conclusions

CBZ is a pharmaceutically active compound present in water sources at very low concentration (up to several µg/L) and its removal is difficult through conventional water treatment technologies in water and wastewater treatment plants. In this paper, removal of CBZ at environmentally relevant concentration range (0.5-20 ppb) was studied through adsorption on as-produced pinewood nanobiochar that can be obtained from low-cost resources using a green production technique. The results showed that nanobiochar can remove up to 74% and 95% of CBZ after 1 and 6 hours contact time, respectively. It indicated that nanobiochar has a faster adsorption compared to other carbonaceous materials, such as activated carbons, carbon nanotubes and graphene oxides. Among examined isotherms and kinetic models, adsorption of CBZ on nanobiochar showed better fitting parameters with Freundlich isotherm model (R^2=0.9822) and pseudo-second order kinetic model (R^2=0.9994). Calculation of adsorption energy showed that adsorption of CBZ on nanobiochar is a physical process. Increasing pH from 3 to 6 and enhanced the adsorption efficiency by 2.3 folds. The addition of Tween 80 as a model surfactant was studied in the range of 0 to 1 (Tween 80 to CBZ molar ratio) and the results showed that adsorption efficiency can be enhanced by 57%. It indicated that nanobiochar can have better performance in wastewater containing surfactants. Thus, nanobiochar can be a promising adsorbent for removal of micropollutants from aqueous media and compete with conventional activated carbon filters in terms of production cost, equilibration time and environmental friendliness.

Acknowledgements

References

1.   Benotti, M.J., Trenholm, R.A., Vanderford, B.J., Holady, J.C., Stanford, B.D., and Snyder, S.A., Pharmaceuticals and Endocrine Disrupting Compounds in U.S. Drinking Water. Environmental Science & Technology, 2009. 43(3): p. 597-603.

2.   Yu, Z., Peldszus, S., and Huck, P.M., Adsorption characteristics of selected pharmaceuticals and an endocrine disrupting compound-Naproxen, carbamazepine and nonylphenol-on activated carbon. Water Research, 2008. 42(12): p. 2873-2882.

3.   Zhang, Y., Geißen, S.-U., and Gal, C., Carbamazepine and diclofenac: Removal in wastewater treatment plants and occurrence in water bodies. Chemosphere, 2008. 73(8): p. 1151-1161.

4.   Vernouillet, G., Eullaffroy, P., Lajeunesse, A., Blaise, C., Gagné, F., and Juneau, P., Toxic effects and bioaccumulation of carbamazepine evaluated by biomarkers measured in organisms of different trophic levels. Chemosphere, 2010. 80(9): p. 1062-1068.

5.   Martin-Diaz, L., Franzellitti, S., Buratti, S., Valbonesi, P., Capuzzo, A., and Fabbri, E., Effects of environmental concentrations of the antiepilectic drug carbamazepine on biomarkers and cAMP-mediated cell signaling in the mussel Mytilus galloprovincialis. Aquatic Toxicology, 2009. 94(3): p. 177-185.

6.   Mohapatra, D.P., Brar, S.K., Tyagi, R.D., Picard, P., and Surampalli, R.Y., Carbamazepine in municipal wastewater and wastewater sludge: Ultrafast quantification by laser diode thermal desorption-atmospheric pressure

chemical ionization coupled with tandem mass spectrometry. Talanta, 2012. 99: p. 247-255.

7.   Chng, E.L.K. and Pumera, M., Nanographitic impurities are responsible for electrocatalytic activity of carbon nanotubes towards oxidation of carbamazepine. Electrochemistry Communications, 2011. 13(8): p. 781-784.

8.   Cai, N. and Larese-Casanova, P., Sorption of carbamazepine by commercial graphene oxides: A comparative study with granular activated carbon and multiwalled carbon nanotubes. Journal of Colloid and Interface Science, 2014. 426: p. 152-161.

9.   Kosjek, T., Andersen, H.R., Kompare, B., Ledin, A., and Heath, E., Fate of Carbamazepine during Water Treatment. Environmental Science & Technology, 2009. 43(16): p. 6256-6261.

10.   Nielsen, L., Zhang, P., and Bandosz, T.J., Adsorption of carbamazepine on sludge/fish waste derived adsorbents: Effect of surface chemistry and texture. Chemical Engineering Journal, 2015. 267: p. 170-181.

11.   Westerhoff, P., Yoon, Y., Snyder, S., and Wert, E., Fate of Endocrine-Disruptor, Pharmaceutical, and Personal Care Product Chemicals during Simulated Drinking Water Treatment Processes. Environmental Science & Technology, 2005. 39(17): p. 6649-6663.

12.   Huerta-Fontela, M., Galceran, M.T., and Ventura, F., Occurrence and removal of pharmaceuticals and hormones through drinking water treatment. Water Research, 2011. 45(3): p. 1432-1442.

13.   Basile, T., Petrella, A., Petrella, M., Boghetich, G., Petruzzelli, V., Colasuonno, S., and Petruzzelli, D., Review of Endocrine-Disrupting-Compound Removal Technologies in Water and Wastewater Treatment Plants: An EU Perspective. Industrial & Engineering Chemistry Research, 2011. 50(14): p. 8389-8401.

14.   Wiegman, S., Barranguet, C., Spijkerman, E., Kraak, M.H.S., and Admiraal, W., The role of ultraviolet-adaptation of a marine diatom in photoenhanced toxicity of acridine. Environmental Toxicology and Chemistry, 2003. 22(3): p. 591-598.

15.   Ahmed, M.B., Zhou, J.L., Ngo, H.H., and Guo, W., Adsorptive removal of antibiotics from water and wastewater: Progress and challenges. Science of The Total Environment, 2015. 532: p. 112-126.

16.   Chen, K. and Zhou, J.L., Occurrence and behavior of antibiotics in water and sediments from the Huangpu River, Shanghai, China. Chemosphere, 2014. 95: p. 604-612.

17.   Zhao, H., Liu, X., Cao, Z., Zhan, Y., Shi, X., Yang, Y., Zhou, J., and Xu, J., Adsorption behavior and mechanism of chloramphenicols, sulfonamides, and non-antibiotic pharmaceuticals on multi-walled carbon nanotubes. Journal of Hazardous Materials, 2016. 310: p. 235-245.

18.   Lerman, I., Chen, Y., Xing, B., and Chefetz, B., Adsorption of carbamazepine by carbon nanotubes: Effects of DOM introduction and competition with phenanthrene and bisphenol A. Environmental Pollution, 2013. 182: p. 169-176.

19.   Oleszczuk, P., Pan, B., and Xing, B., Adsorption and Desorption of Oxytetracycline and Carbamazepine by Multiwalled Carbon Nanotubes. Environmental Science & Technology, 2009. 43(24): p. 9167-9173.

20.   Yargicoglu, E.N., Sadasivam, B.Y., Reddy, K.R., and Spokas, K., Physical and chemical characterization of waste wood derived biochars. Waste Management, 2015. 36: p. 256-268.

21.   Reddy, K., Xie, T., and Dastgheibi, S., Evaluation of Biochar as a Potential Filter Media for the Removal of Mixed Contaminants from Urban Storm Water Runoff. Journal of Environmental Engineering, 2014. 140(12): p. 04014043.

22. Krika, F., Azzouz, N., and Ncibi, M.C., Adsorptive removal of cadmium from aqueous solution by cork biomass: Equilibrium, dynamic and thermodynamic studies. Arabian Journal of Chemistry.

23. Aljeboree, A.M., Alshirifi, A.N., and Alkaim, A.F., Kinetics and equilibrium study for the adsorption of textile dyes on coconut shell activated carbon. Arabian Journal of Chemistry.

24. Inyang, M., Gao, B., Zimmerman, A., Zhang, M., and Chen, H., Synthesis, characterization, and dye sorption ability of carbon nanotube–biochar nanocomposites. Chemical Engineering Journal, 2014. 236: p. 39-46.

25. Inyang, M., Gao, B., Yao, Y., Xue, Y., Zimmerman, A.R., Pullammanappallil, P., and Cao, X., Removal of heavy metals from aqueous solution by biochars derived from anaerobically digested biomass. Bioresource Technology, 2012. 110: p. 50-56.

26. Zhang, M., Gao, B., Yao, Y., and Inyang, M., Phosphate removal ability of biochar/MgAl-LDH ultra-fine composites prepared by liquid-phase deposition. Chemosphere, 2013. 92(8): p. 1042-1047.

27. Lehmann, J. and Joseph, S., Biochar for environmental management: science, technology and implementation. 2015: Routledge.

28. Lonappan, L., Rouissi, T., Das, R.K., Brar, S.K., Ramirez, A.A., Verma, M., Surampalli, R.Y., and Valero, J.R., Adsorption of methylene blue on biochar microparticles derived from different waste materials. Waste Management, 2016. 49: p. 537-544.

29. Taheran, M., Naghdi, M., Brar, S.K., Knystautas, E.J., Verma, M., Ramirez, A.A., Surampalli, R.Y., and Valero, J.R., Adsorption study of environmentally relevant concentrations of chlortetracycline on pinewood biochar. Science of The Total Environment, 2016.

30. Sulaiman, G.M., Mohammed, W.H., Marzoog, T.R., Al-Amiery, A.A., and Kadhum, A.H., Green synthesis, antimicrobial and cytotoxic effects of silver

nanoparticles using Eucalyptus chapmaniana leaves extract. Asian Pacific Journal of Tropical Biomedicine, 2013. 3(1): p. 58-63.

31.   Song, J.Y. and Kim, B.S., Rapid biological synthesis of silver nanoparticles using plant leaf extracts. Bioprocess and Biosystems Engineering 2009. 32(1): p. 79-84.

32.   Deguchi, S., Mukai, S.-a., Tsudome, M., and Horikoshi, K., Facile Generation of Fullerene Nanoparticles by Hand-Grinding. Advanced Materials, 2006. 18(6): p. 729-732.

33.   Darroudi, M., Ahmad, M.B., Abdullah, A.H., and Ibrahim, N.A., Green synthesis and characterization of gelatin-based and sugar-reduced silver nanoparticles. International Journal of Nanomedicine, 2011. 6: p. 569-574.

34.   Kumar, V.V., Nithya, S., Shyam, A., Subramanian, N.S., Anthuvan, J.T., and Anthony, S.P., Natural Amino Acid Based Phenolic Derivatives for Synthesizing Silver Nanoparticles with Tunable Morphology and Antibacterial Studies. Bulletin of the Korean Chemical Society, 2013. 34(9): p. 2702-2706.

35.   Kesavan, A. and Venkatraman, G., Nanotechnology and its Applications. The Scitech Journal, 2014. 1(6): p. 1-2.

36.   Shameli, K., Ahmad, M.B., Jazayeri, S.D., Sedaghat, S., Shabanzadeh, P., Jahangirian, H., Mahdavi, M., and Abdollahi, Y., Synthesis and Characterization of Polyethylene Glycol Mediated Silver Nanoparticles by the Green Method. International Journal of Molecular Sciences, 2012. 13(6): p. 6639-6650.

37.   Dada, A., Olalekan, A., Olatunya, A., and Dada, O., Langmuir, Freundlich, Temkin and Dubinin–Radushkevich isotherms studies of equilibrium sorption of Zn2+ unto phosphoric acid modified rice husk. Journal of Applied Chemistry, 2012. 3(1): p. 38-45.

38.   Yu, Z., Peldszus, S., Anderson, W.B., and Huck, P.M., Adsorption of Selected Pharmaceuticals and Endocrine Disrupting Substances by GAC at Low

Concentration Levels. Water Quality Technology Conference Proceedings, WQTC (2005), 2005: p. 1-16.

39.   Pintor, A.M.A., Ferreira, C.I.A., Pereira, J.C., Correia, P., Silva, S.P., Vilar, V.J.P., Botelho, C.M.S., and Boaventura, R.A.R., Use of cork powder and granules for the adsorption of pollutants: A review. Water Research, 2012. 46(10): p. 3152-3166.

40.   Tan, X., Liu, Y., Zeng, G., Wang, X., Hu, X., Gu, Y., and Yang, Z., Application of biochar for the removal of pollutants from aqueous solutions. Chemosphere, 2015. 125: p. 70-85.

41.   Cheng, G., Sun, L., Jiao, L., Peng, L.X., Lei, Z.H., Wang, Y.X., and Lin, J., Adsorption of methylene blue by residue biochar from copyrolysis of dewatered sewage sludge and pine sawdust. Desalination and Water Treatment, 2013. 51(37-39): p. 7081-7087.

42.   Dickenson, E.R.V. and Drewes, J.E., Quantitative structure property relationships for the adsorption of pharmaceuticals onto activated carbon. Water Science and Technology, 2010. 62(10): p. 2270-2276.

43.   Jung, C., Application of Various Adsorbents to Remove Micro-Pollutants in Aquatic System. 2014, University of South Carolina: Columbia. p. 1-164.

44.   Ho, Y.S. and McKay, G., Pseudo-second order model for sorption processes. Process Biochemistry, 1999. 34(5): p. 451-465.

45.   Teixidó, M., Pignatello, J.J., Beltrán, J.L., Granados, M., and Peccia, J., Speciation of the Ionizable Antibiotic Sulfamethazine on Black Carbon (Biochar). Environmental Science & Technology, 2011. 45(23): p. 10020-10027.

46.   Wu, W., Jiang, W., Xia, W., Yang, K., and Xing, B., Influence of pH and surface oxygen-containing groups on multiwalled carbon nanotubes on the transformation and adsorption of 1-naphthol. Journal of Colloid and Interface Science, 2012. 374(1): p. 226-231.

47.   Yang, W., Lu, Y., Zheng, F., Xue, X., Li, N., and Liu, D., Adsorption behavior and mechanisms of norfloxacin onto porous resins and carbon nanotube. Chemical Engineering Journal, 2012. 179: p. 112-118.

48.   Lu, C. and Su, F., Adsorption of natural organic matter by carbon nanotubes. Separation and Purification Technology, 2007. 58(1): p. 113-121.

49.   Peng, H., Pan, B., Wu, M., Liu, R., Zhang, D., Wu, D., and Xing, B., Adsorption of ofloxacin on carbon nanotubes: Solubility, pH and cosolvent effects. Journal of Hazardous Materials, 2012. 211–212: p. 342-348.

50.   Walker, G.M., Hansen, L., Hanna, J.A., and Allen, S.J., Kinetics of a reactive dye adsorption onto dolomitic sorbents. Water Research, 2003. 37(9): p. 2081-2089.

51.   Zarraa, M.A., A Study on the Removal of Chromium(VI) from Waste Solutions by Adsorption on to Sawdust in Stirred Vessels. Adsorption Science & Technology, 1995. 12(2): p. 129-138.

52.   Srivastava, V., Weng, C.H., Singh, V.K., and Sharma, Y.C., Adsorption of Nickel Ions from Aqueous Solutions by Nano Alumina: Kinetic, Mass Transfer, and Equilibrium Studies. Journal of Chemical & Engineering Data, 2011. 56(4): p. 1414-1422.

53.   Saruchi, Kumar, V., Vikas, P., Kumar, R., Kumar, B., and Kaur, M., Low cost natural polysaccharide and vinyl monomer based IPN for the removal of crude oil from water. Journal of Petroleum Science and Engineering, 2016. 141: p. 1-8.

54.   Amarasinghe, B.M.W.P.K. and Williams, R.A., Tea waste as a low cost adsorbent for the removal of Cu and Pb from wastewater. Chemical Engineering Journal, 2007. 132(1-3): p. 299-309.

55.   Garg, V.K., Gupta, R., Bala Yadav, A., and Kumar, R., Dye removal from aqueous solution by adsorption on treated sawdust. Bioresource Technology, 2003. 89(2): p. 121-124.

56. Kibbey, T.C.G. and Hayes, K.F., Partitioning and UV absorption studies of phenanthrene on cationic surfactant-coated silica. Environmental Science & Technology, 1993. 27(10): p. 2168-2173.

57. Shiau, B.J., Sabatini, D.A., and Harwell, J.H., Properties of Food Grade (Edible) Surfactants Affecting Subsurface Remediation of Chlorinated Solvents. Environmental Science & Technology, 1995. 29(12): p. 2929-2935.

58. Hari, A.C., Paruchuri, R.A., Sabatini, D.A., and Kibbey, T.C.G., Effects of pH and Cationic and Nonionic Surfactants on the Adsorption of Pharmaceuticals to a Natural Aquifer Material. Environmental Science & Technology, 2005. 39(8): p. 2592-2598.

59. Cabrera-Lafaurie, W.A., Román, F.R., and Hernández-Maldonado, A.J., Removal of salicylic acid and carbamazepine from aqueous solution with Y-zeolites modified with extraframework transition metal and surfactant cations: Equilibrium and fixed-bed adsorption. Journal of Environmental Chemical Engineering, 2014. 2(2): p. 899-906.

60. Stellner, K.L. and Scamehorn, J.F., Hardness tolerance of anionic surfactant solutions. 2. Effect of added nonionic surfactant. Langmuir, 1989. 5(1): p. 77-84.

Table 3.1.1 Physico-chemical properties of produced nanobiochar

Property	Nanobiochar
Specific gravity	0.40 ± 0.02
Moisture content (%)	2.11 ± 0.07
WHC[A] (g H_2O/g biochar)	9.75 ± 0.45
LOI[B] organic matter content (%)	96.9 ± 3.4
Volatile matter content (%)	96.9 ± 4.2
Ash content (%)	2.0 ± 0.1
Fixed C content (%)	1.06 ± 0.07
pH	6.61 ± 0.35
ORP[C] (mV)	132 ± 4
EC[D] (μscm^{-1})	1737 ± 28
Zeta potential (mV)	-31.3 ± 2.6
∑ PAHs[E] (mg kg^{-1})	26.837 ± 3.291
CEC[F] meq/100	14.8 ± 1.2
Particle size (nm)	60 ± 5
Surface area (m^2/g)	47.25
Elemental analysis:	
C (%)	83.1 ± 2.5
H (%)	3.5 ± 0.11
N (%)	< 1
H:C (Molar ratio)	0.5
C:N (Molar ratio)	> 96.9

A: Water holding capacity, B: Loss on ignition, C: Oxidation-reduction potential, D: Electrical conductivity, E: Polycyclic aromatic hydrocarbons and F: Cation Exchange Capacity

Table 3.1.2 Models used for good fitting of isotherms

Name	Equation	Term definition[a]
Freundlich model	$Non\text{-}Linear: q_e = K_F C_e^{1/n}$ $Linear: \log q_e = \log K_F + \frac{1}{n} \log C_e$ (1)	K_f [(mg/g)/(mg/L)$^{1/n}$]: Freundlich affinity coefficient 1/n: Freundlich exponential coefficient
Langmuir model	$Non\text{-}Linear: q_e = Q^0 C_e/(K_L + C_e)$ $Linear: \dfrac{1}{q_e} = \left(\dfrac{K_L}{Q^0}\right)\dfrac{1}{C_e} + \dfrac{1}{Q^0}$ (2)	K_L [mg/L]: affinity coefficient
Partition-adsorption model	$q_e = K_P C_e + Q^0 C_e / (K_L + C_e)$ (3)	K_P [L/g]: partition coefficient K_L [mg/L]: affinity coefficient

Note: [a]: qe [mg/g] is the equilibrium concentration of adsorbate in solid; Ce [mg/L] is the equilibrium aqueous concentration of adsorbate; Q^0 [mg/g] is the maximum sorption capacity for adsorbate;

Table 3.1.3 Models used for fitting of kinetics data

Name	Equation[1]	Term definition[a]
Pseudo first-order model	$Non\text{-}Linear: q_t = q_e\,(1 - exp^{-k_1 t})$ $Linear: \log(q_e - q_t) = \log q_e - \dfrac{k_1}{2.303}t \quad (4)$	k_1[min^{-1}]: adsorption rate constant
Pseudo second-order model	$Non\text{-}Linear: q_t = \dfrac{k_2 q_e^2 t}{1 + k_2 q_e t}$ $Linear: \dfrac{t}{q_t} = \dfrac{1}{k_2 q_e^2} + \dfrac{1}{q_e}\,t \quad (5)$ $V_0 = k_2 q_e^2 \qquad (6)$	V_0 [mg/g.h]: initial adsorption rate k_2 [g/mg.h]: pseudo second-order rate constant
Intra-particle diffusion model	$Non\text{-}Linear: q_t = k_p t^{0.5} \qquad (7)$	K_p [mg/g.h$^{0.5}$]: rate constant for intra-particle diffusion
q_t represent the adsorption capacity (mg/g) at time t		

Table 3.1.4 Isotherm parameters estimated using three different models (p-value <0.05)

Linear Regression									
Langmuir Model			*Freundlich Model*			*Partition-adsorption model*			
Q^0 (ng/mg)	K_L (ng/L)	R^2	K_f (ng/mg)(L/ng)$^{1/n}$	1/n	R^2	Q^0 (ng/mg)	K_L (ng/L)	K_P (L/mg)	R^2
40	521	0.968	0.082	0.914	0.982	36	461	282	0.970
Non-Linear Regression									
Q^0 (ng/mg)	K_L (ng/L)	R^2	K_f (ng/mg)(L/ng)$^{1/n}$	1/n	R^2	Q^0 (ng/mg)	K_L (ng/L)	K_P (L/mg)	R^2
116	1440	0.889	0.068	0.963	0.985	1.06	10.2	0.049	0.976

Table 3.1.5 Kinetic parameters for Lagergren and intra-particle diffusion models (p-value <0.05)

Pseudo first-order			Pseudo second-order			Intra-particle diffusion	
Linear Regression							
k_1 (h^{-1})	qe (µg/g)	R^2	k_2 (g/mg.min)	qe (µg/g)	R^2	K (mg/g.hr$^{0.5}$)	R^2
1.202	6.7	0.856	95.21	14.05	0.999	0.048	0.910
Non-Linear Regression							
k_1 (h^{-1})	qe (µg/g)	R^2	k_2 (g/mg.min)	qe (µg/g)	R^2	K (mg/g.hr$^{0.5}$)	R^2
79.8	13.4	0.759	1.85	1.39	0.946	0.18	0.906
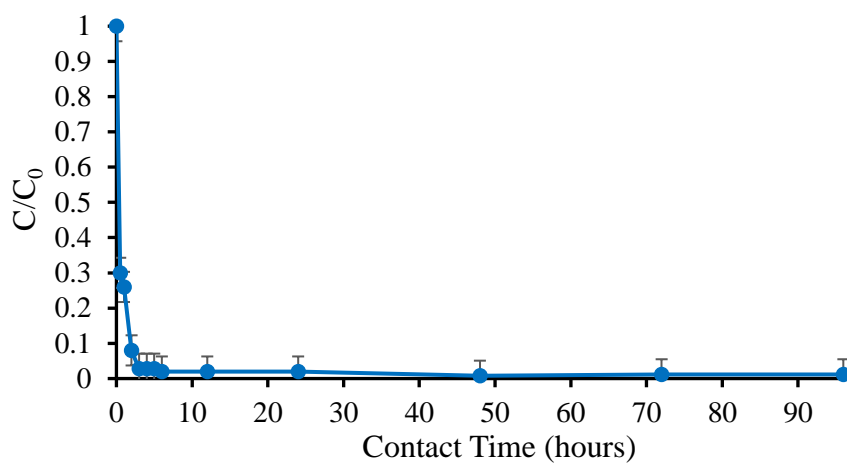
Figure 3.1.1 Aqueous concentration profile of carbamazepine with time (C_0 = 5 ng/mL, 0.25 mg/mL nanobiochar, 25 °C, pH 6 and 150 rpm)
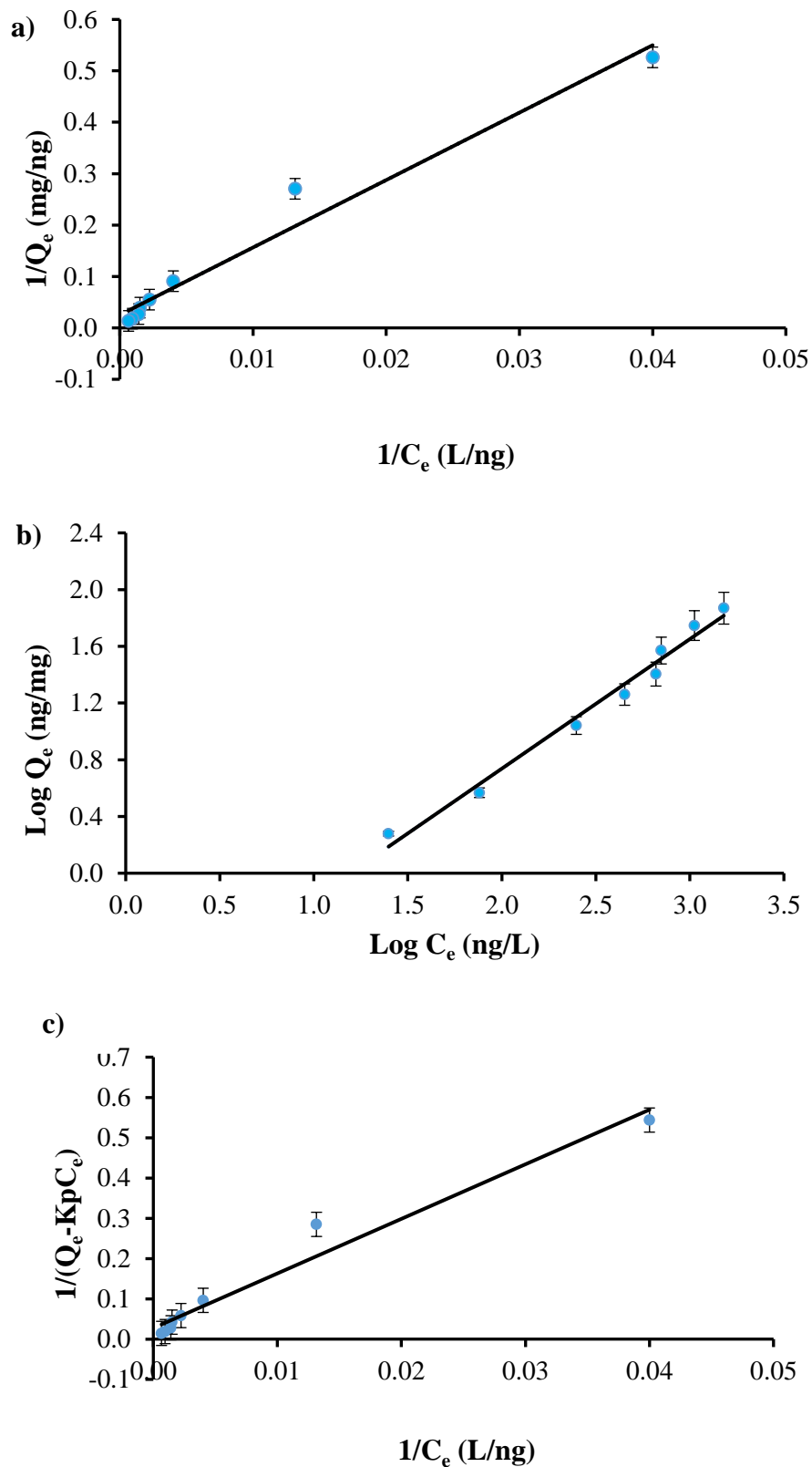
Figure 3.1.2 a) Linearized Langmuir isotherm b) Linearized Freundlich isotherm and; c) Partition-adsorption model for carbamazepine adsorption on nanobiochar (C_0 = 0.5-20 ng/mL, 0.25 mg/mL nanobiochar, 25 °C, pH 6 and 150 rpm)
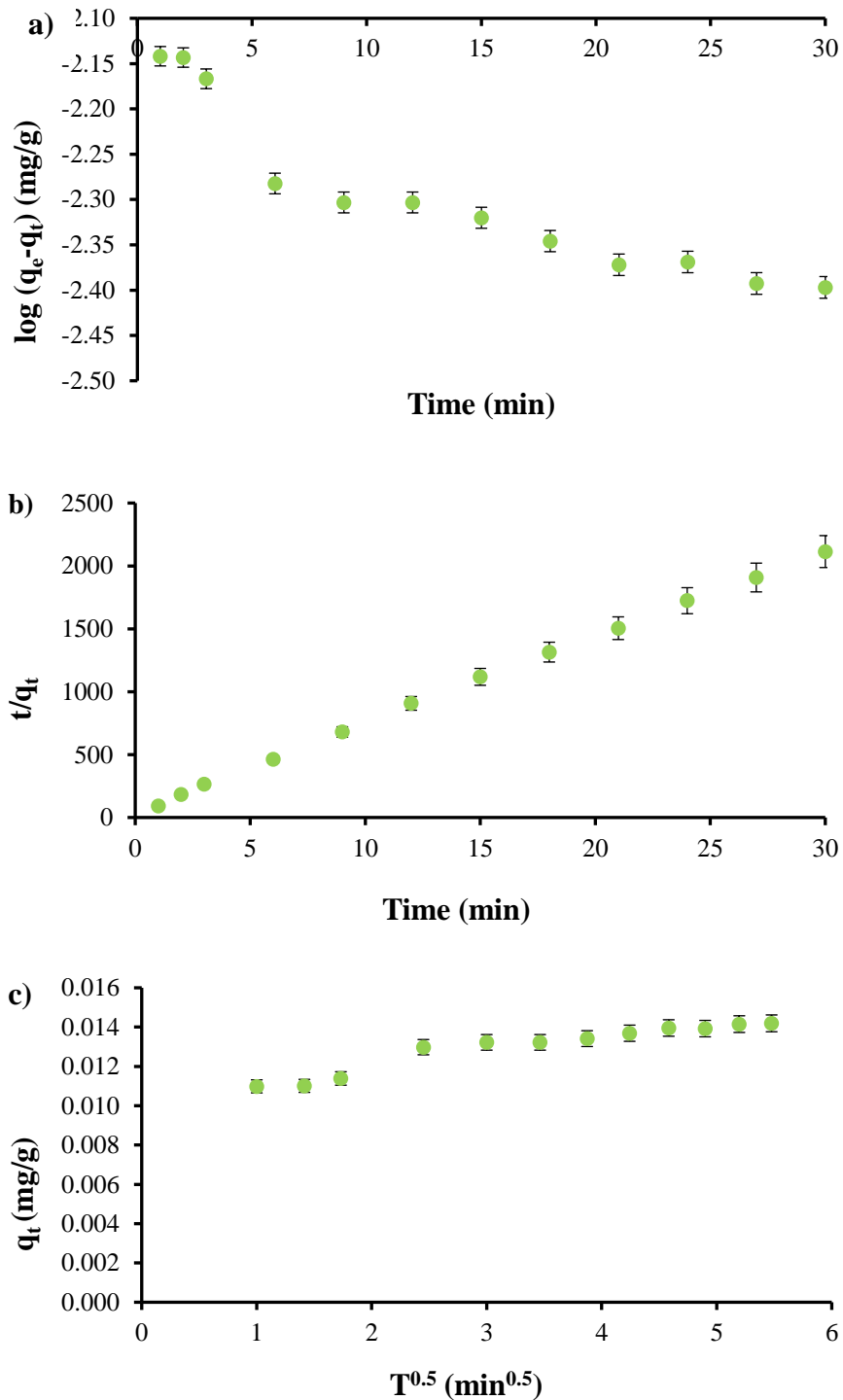
Figure 3.1.3 Fitting of three kinetic models: (a) pseudo-first order, (b) pseudo-second order, and (c) intra-particle diffusion model (C_0 = 5 ng/ml; 0.01 mg/mL nanobiochar; time = 30 min; pH = 6; T = 25 °C and 150 rpm).
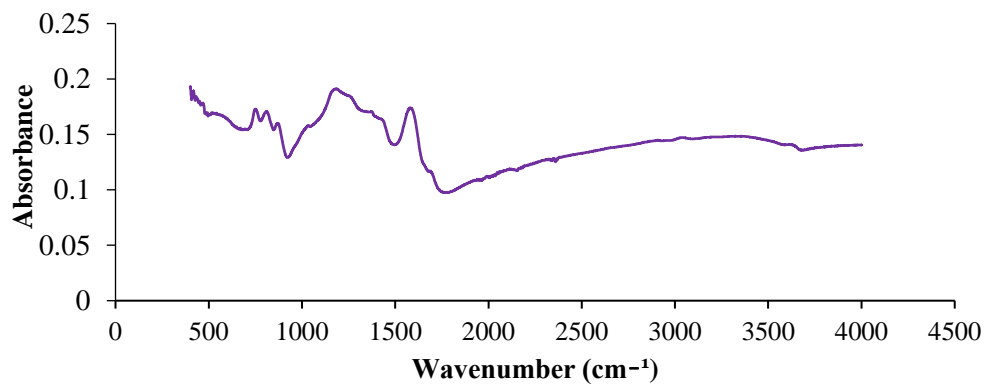
Figure 3.1.4 FTIR spectrum of produced nanobiochar
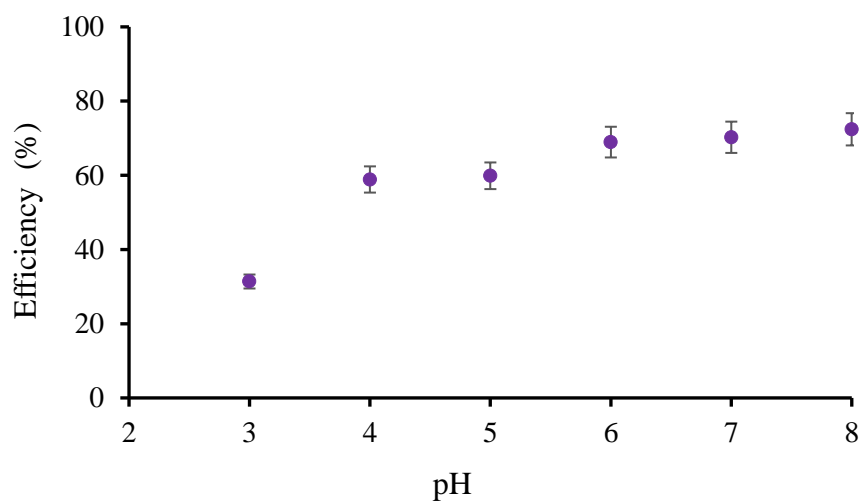
Figure 3.1.5 Effect of pH on adsorption efficiency of carbamazepine on nanobiochar
(C_0 = 10 ng/mL, 0.5 mg/mL nanobiochar, 25 °C and 150 rpm)
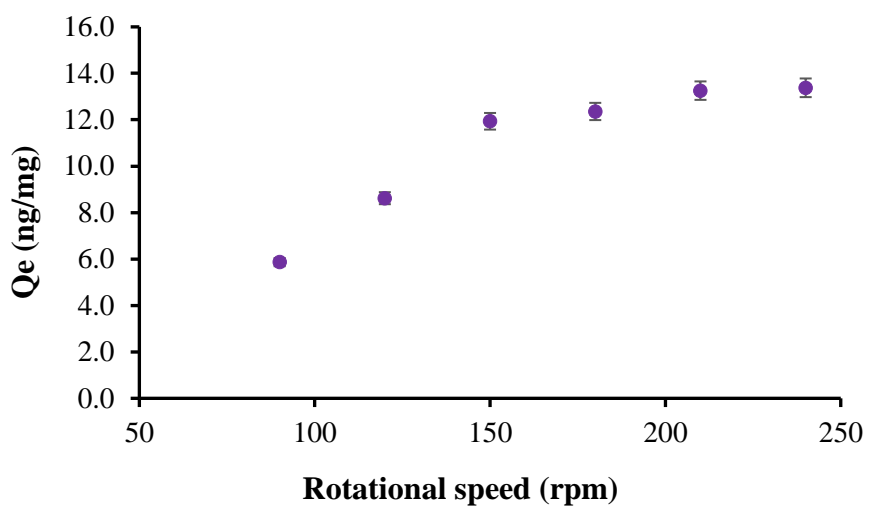
Figure 3.1.6 Effect of rotational speed on adsorption of carbamazepine on nanobiochar (C_0 = 10 ng/mL, 0.5 mg/mL nanobiochar, 25 °C and pH 6)
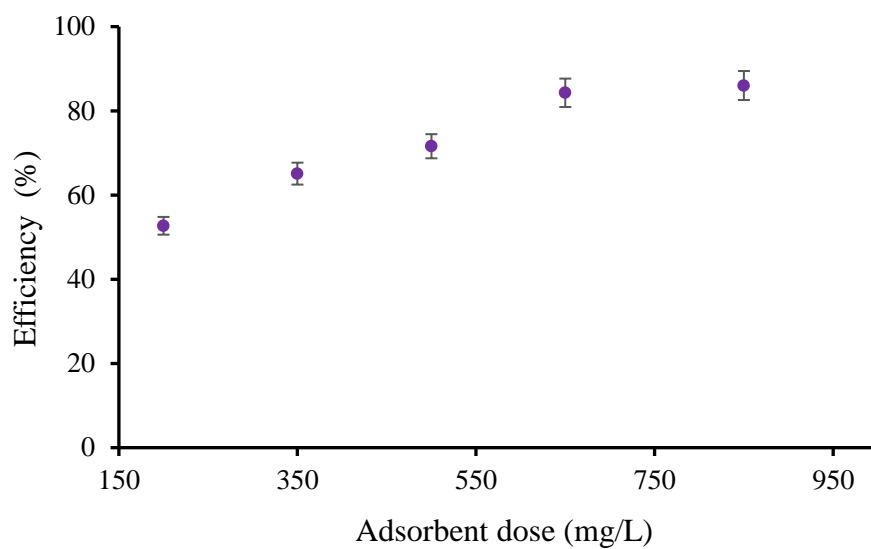
Figure 3.1.7 Effect of adsorbent dose on adsorption of carbamazepine (C_0 = 10 ng/mL, 25 °C, pH 6 and 150 rpm)
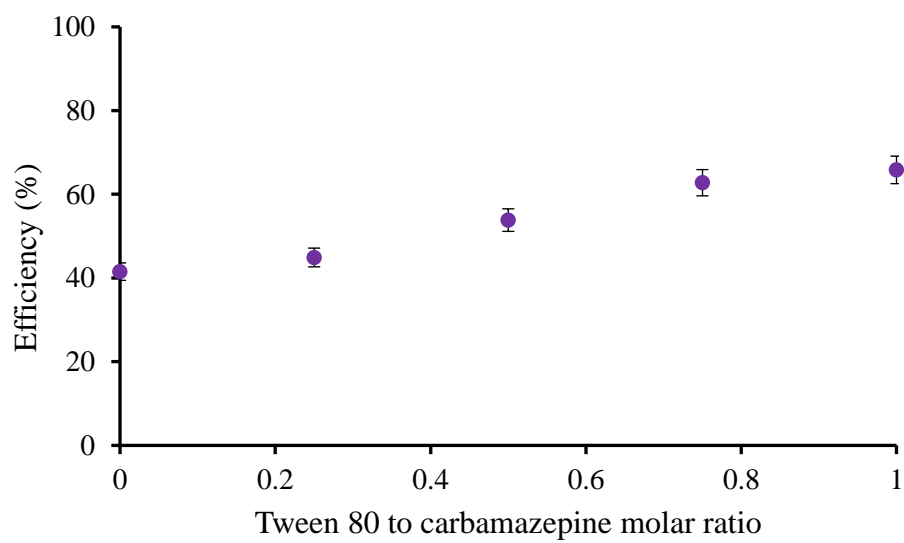
Figure 3.1.8 Effect of surfactant concentration on adsorption of carbamazepine (C_0 = 10 ng/mL, 0.5 mg/mL nanobiochar, 25 °C, pH 6 and 150 rpm)
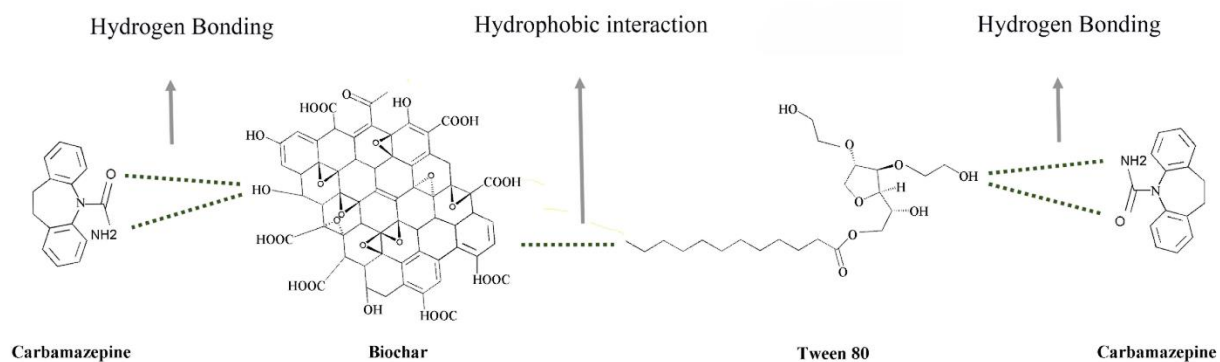
Figure 3.1.9 Illustration of possible interaction between Tween 80, nanobiochar and carbamazepine

CHAPTER 4

Study the performance of oxidoreductase enzymes for the removal of micropollutants

Part 1

Removal of Pharmaceutical Compounds in Water and Wastewater Using Fungal Oxidoreductase Enzymes

Mitra Naghdi[1], Mehrdad Taheran[1], Satinder Kaur Brar[1*], Azadeh Kermanshahi-pour[2], Mausam Verma[1] and R.Y. Surampalli[4]

[1]INRS-ETE, Université du Québec, 490, Rue de la Couronne, Québec, Canada G1K 9A9

[2]Biorefining and Remediation Laboratory, Department of Process Engineering and Applied Science, Dalhousie University, 1360 Barrington Street, Halifax, Nova Scotia, Canada, B3J 1Z1

[3]Department of Civil Engineering, University of Nebraska-Lincoln, N104 SEC PO Box 886105, Lincoln, NE 68588-6105, US

(*Phone: 1 418 654 3116; Fax: 1 418 654 2600; E-mail: satinder.brar@ete.inrs.ca)

Résumé

En raison de la récalcitrantes de certains composés pharmaceutiquement actifs (PhACs), le traitement des eaux usées conventionnelles n'est pas capable de les éliminer efficacement. Par conséquent, leur présence dans les eaux de surface et leur impact potentiel sur l'environnement ont soulevé de graves préoccupations à l'échelle mondiale. La transformation biologique de ces contaminants à l'aide de champignons de la pourriture blanche (WRF) et de leurs enzymes oxydoréductases a été proposée comme solution économique et écologique pour le traitement de l'eau. La performance d'élimination des PhACs par une culture fongique dépend de plusieurs facteurs, tels que les espèces fongiques, les enzymes sécrétées, la structure moléculaire des composés cibles, la composition du milieu de culture, etc. Ces 20 dernières années, de nombreux chercheurs ont tenté d'élucider les mécanismes d'élimination et les effets de paramètres opérationnels importants tels que la température et le pH sur le traitement enzymatique des PhACs. Cette revue résume et analyse les études réalisées sur l'élimination des PhACs à partir d'eau pure dopée et des eaux usées réelles en utilisant des enzymes oxydoréductases et les données relatives aux efficacités de dégradation des composés les plus étudiés. La revue offre également un aperçu de l'immobilisation des enzymes, des réacteurs fongiques, des médiateurs, des mécanismes de dégradation et des produits de transformation (TPs) des PhACs. En bref, une hydrophobie plus élevée et ayant des groupes donneurs d'électrons, tels que les groupes amine et hydroxyle dans la structure moléculaire, conduit à une dégradation plus efficace des PhACs par des cultures fongiques. Pour les composés récalcitrants, l'utilisation de médiateurs redox, tels que le syringaldéhyde, augmente l'efficacité de la dégradation, cependant, ils peuvent provoquer une toxicité dans l'effluent et désactiver l'enzyme. L'immobilisation d'enzymes sur des supports peut améliorer les performances de l'enzyme en termes de réutilisabilité et de stabilité. Cependant, la stratégie d'immobilisation doit être soigneusement sélectionnée pour réduire le coût et permettre la régénération. Cependant, d'autres études sont nécessaires pour élucider les mécanismes impliqués dans la dégradation enzymatique et les niveaux de toxicité des TPs et aussi pour optimiser la stratégie de traitement dans son ensemble pour avoir une compétitivité économique et technique.

Mots clés

Traitement enzymatique, Composés pharmaceutiques, Champignons de pourriture blanche, Biodégradation, Eaux usées

Abstract

Due to recalcitrance of some pharmaceutically active compounds (PhACs), conventional wastewater treatment is not able to remove them effectively. Therefore, their occurrence in surface water and potential environmental impact has raised serious global concern. Biological transformation of these contaminants using white-rot fungi (WRF) and their oxidoreductase enzymes has been proposed as a low cost and environmentally friendly solution for water treatment. The removal performance of PhACs by a fungal culture is dependent on several factors, such as fungal species, the secreted enzymes, molecular structure of target compounds, culture medium composition, etc. In recent 20 years, numerous researchers tried to elucidate the removal mechanisms and the effects of important operational parameters such as temperature and pH on the enzymatic treatment of PhACs. This review summarizes and analyzes the studies performed on PhACs removal from spiked pure water and real wastewaters using oxidoreductase enzymes and the data related to degradation efficiencies of the most studied compounds. The review also offers an insight into enzymes immobilization, fungal reactors, mediators, degradation mechanisms and transformation products (TPs) of PhACs. In brief, higher hydrophobicity and having electron-donating groups, such as amine and hydroxyl in molecular structure leads to more effective degradation of PhACs by fungal cultures. For recalcitrant compounds, using redox mediators, such as syringaldehyde increases the degradation efficiency, however they may cause toxicity in the effluent and deactivate the enzyme. Immobilization of enzymes on supports can enhance the performance of enzyme in terms of reusability and stability. However, the immobilization strategy should be carefully selected to reduce the cost and enable regeneration. Still, further studies are needed to elucidate the mechanisms involved in enzymatic degradation and the toxicity levels of TPs and also to optimize the whole treatment strategy to have economical and technical competitiveness.

Keywords

Introduction

Agricultural and industrial activities result in release of variety of chemicals into the environment, leading to serious concerns over the health and environmental impact of these chemicals and their associated degradation metabolites [1, 2]. Moreover, population increase and disposal of municipal sewage contributed to the pollution of waterways and almost 70-80% of rivers and streams around the world carry polluted water [3]. Beside the potential adverse effects on human health, the released pollutants into waterways may have chronic and acute toxicity to the organisms in aquatic ecosystem and may lead to loss of biodiversity and habitats [4].

Pharmaceutically active compounds (PhACs), are among water pollutants that have been frequently detected in the effluents of wastewater treatment plants (WWTPs) [5]. PhACs are widely used as prescription or non-prescription medicines and after their usage, they find their way into wastewater through urine and feces either as intact substances or metabolites [6]. It is a matter of concern that WWTPs are not able to efficiently remove these pollutants due to their persistent nature, resulting in their discharge into surface water [7]. Due to the persistence and high lipid solubility of some of the organic pollutants, they can bioaccumulate in the fatty tissues of living organisms [8]. Recently, some evidences have been found that a few pharmaceutical compounds can mobilize towards the food chain, and hence their concentration is increased [9]. The presence of PhACs in waterways may lead to several issues in the environment, such as male fish feminization as a result of exposure to steroidal hormones and development of antibiotic-resistant genes due to released non-metabolized antibiotics into water [10, 11].

The worldwide annual consumption of PhACs is estimated to be 100,000 tons or more and the trend is increasing due to the diseases and aging population [12]. For instance, about 877 tons of diclofenac, listed as 12th best-selling generics in the world [13], and 942 tons of carbamazepine, listed as 8th bestselling psychiatric drugs worldwide [14], were sold in 2007 in 76 countries. A significant portion of these PhACs are released into the environment in intact or metabolized form. The increasing concern over the accumulation of micropollutants in the aquatic media triggered many research works to evaluate their biodegradation in wastewater treatment systems [15]. The results implied that unlike traditional wastewater treatment processes, such as conventional activated sludge, recently-developed methods for wastewater treatment including

membrane separation, advanced oxidation processes (AOPs) and adsorption onto activated carbon, are able to achieve high efficiency for PhACs removal [16-19]. However, still, challenges remained with these technologies including the formation of more toxic by-products during AOPs [20], the disposal of the concentrated stream in membrane separation [21] and the regeneration of absorbents [22]. Therefore, development of effective treatment processes to remove PhACs from wastewater is always of high importance. In Table 4.1.1, the information about physicochemical properties of the most studied compounds has been presented as they are helpful in the prediction of the efficiency of enzymatic treatment. In the following sections, removal efficiencies of PhACs by different forms of the enzyme (whole-cell culture, crude extracts and immobilized) are also discussed.

Biocatalytic conversion is an environmentally benign alternative method, which involves the use of living organisms or their enzymes. This treatment method requires lower energy input, works under moderate conditions and produces less or no toxic by-products compared to other conventional technologies [25]. Additionally, the specificity of enzymes towards substrate facilitates minimizing the unfavorable side reactions, where required [26]. Therefore, enzymes are promising options for the selective removal of pollutants from water and wastewater [27]. In recent years, numerous researchers studied the treatment of wastewater with the enzymatic approach, especially with oxidoreductase enzymes due to their known potential for oxidizing recalcitrant pollutants. The ligninolytic enzymes obtained from WRF are relatively non-specific towards organic compounds and they use the free radical mechanism to catalyze the degradation of a wide range of micropollutants [28, 29]. The capability of these enzymes was first employed in 1980s to degrade different organic compounds, such as pesticides, dyes, polyaromatic hydrocarbons, etc. [30] and in 1990s, the researchers showed the applicability of these enzymes for degradation of pharmaceutical compounds [31, 32].

Many review papers have been recently published to cover the occurrence and fate of micropollutants in the aquatic environment as well as their removal by conventional and advanced treatment processes i.e. adsorption, AOPs and membrane separations [24, 25, 33]. However, there is no comprehensive review to cover the approaches of biocatalytic treatment of pollutants including whole fungal culture, crude/pure enzyme, immobilized enzyme, and the combination of enzymatic treatment with other

technologies. The aim of this work is to review the performance of ligninolytic enzymes for removal of PhACs from aqueous media. Different types of fungi and their intracellular and extracellular enzymes in free and immobilized forms used to treat micropollutants as well as the effects of operating conditions on removal efficiencies are discussed.

Enzymatic treatment for removal of PhACs

Enzymes are biologically-made catalysts that mediate biochemical reactions at a rapid rate and can play a crucial role in preventing pollution through cleaner methods for production of substances [34]. For some commercial processes, such as synthesis of enantiomerically pure intermediates [35], enzymes have been used and they showed advantages over synthetic catalysts with respect to substrate specificity, working under mild conditions, energy input and posing no toxicity.

Recently, enzymes were employed for transformation of pollutants in different effluents into other less harmful compounds in lab scale reactors [34, 36, 37]. A biological promising alternative to conventional treatment in WWTPs may be developed based on the use of living cultures or extracted enzymes of fungi such as WRF. These microorganisms have been reported to be able to degrade a wide spectrum of xenobiotics due to the action of extracellular oxidoreductase enzymes, such as lignin peroxidase (LiP), manganese peroxidase (MnP), versatile peroxidase (VP) and laccase (Lac). This consortium of oxidoreductase enzymes is also known as ligninolytic enzymes since they have produced by the fungi for decomposing the lignin-rich biomass into nutrients [38]. LiP (EC 1.11.1.14) catalyzes the depolymerization of lignin through the H_2O_2-based oxidative process. LiP showed the capability to degrade several recalcitrant aromatic pollutants [37]. The molecular mass and optimum temperature and pH of LiP fall within 37-50 kDa, 35-55 °C and 2-5, respectively [39-41]. MnP (EC 1.11.1.13) is a heme glycoprotein enzyme that can catalyze the oxidation of organic molecules in the presence of H_2O_2 [42]. The molecular mass and optimum temperature and pH of MnP fall within 32-62.5 kDa, 40-60 °C, and 4-7 respectively. The different isoforms of MnP are secreted in nitrogen and carbon-limited media supplemented with VEA and Mn^{2+} [43, 44]. VP (EC 1.11.1.16) combines the substrate-specificity of MnP and LiP and is able to oxidize different types of molecular structures such as low- and high-redox-potential dyes, phenolic/non-phenolic

compounds as given in Table 4.1.1 and hydroquinones [45]. Lac (EC 1.10.3.2) is a member of multicopper enzymes family with low-specificity. It can catalyze the oxidation of hydrogen-donating compounds such as phenol, lignin, or acrylamines through the reduction of O_2 to H_2O [42, 46]. The molecular mass, optimum temperature and pH of Lac fall within 58-90 kDa, 40 to 65 °C and 2-10, respectively [47, 48]. Among oxidoreductase enzymes, Lac is of great interest since it only needs gaseous oxygen as a co-substrate [49]. Therefore, low specificity, ability to use atmospheric oxygen as the electron acceptor and good yields make Lac attractive for environmental applications [50-52]. In Table 4.1.2, the properties of mostly used oxidoreductase enzymes in degradation of PhACs are summarized.

The hydrophobicity of PhACs that can be expressed by log K_{ow}, (Table1) is a key parameter that governs the sorption onto biomass and can enhance the removal of some compounds. For instance, Yang *et al.* investigated the contribution of biodegradation by extracellular enzymes and biosorption and reported that the removal of hydrophobic compounds (log K_{ow} > 4) was highly impacted by both mechanisms. They also found that the biosorption of hydrophobic compounds facilitated their biodegradation [53]. On the other hand, the role of biosorption in the removal of the hydrophilic compounds (log K_{ow} < 3) is limited so that for some compounds, the effect of biosorption was reported to be negligible compared to the biodegradation. Since whole-cell fungal treatment involves extracellular, intracellular, and mycelium-bound enzymes, there are significant differences in treatment by whole-cell WRF and extracted enzymes. The complete removal of some compounds in whole-cell fungal reactors indicates the important role of intracellular and mycelium-bound enzymes and their synergistic effect with extracellular enzymes [54-56].

Laccase, as illustrated in Figure 4.1.1A, has four 4 copper atoms divided into three types (1, 2 and 3) at the catalytic center of each monomer. The type 1 atom (T1) imparts the color of the enzyme and catalyzes the oxidation of the substrate. Afterwards, the donated electron from the substrate is internally transferred from T1 to the T2 and T3 copper sites where the reduction of oxygen to water takes place [26, 57]. The oxidation in T1 is a one-electron reaction that generates a radical, and the reduction in T2 and T3 sites is a four-electron reaction that produces two molecules of water. The initial free radical is fairly unstable and may be transformed to a quinone by spontaneous disproportionation or in a second enzyme-catalyzed step. For

phenolic polymers, such as humic acids, further non-enzymatic radical reactions are also possible that may result in their partial degradation [50].

LiP has a high redox potential and therefore it can oxidize the compounds that are not oxidized by other enzymes. It can attack both phenolic and non-phenolic structures and lead to hydroxylation, carbon-carbon cleavage, phenolic oxidation, methylation, aromatic ring fission, demethoxylation and dimerization reactions. LiP follows a well-known peroxidase catalytic mechanism in which native enzyme is oxidized by hydrogen peroxide and forms LiP-I with two electron deficiencies. LiP-I oxidizes the target compound and reduces to one electron deficient LiP-II. When LiP-II oxidizes another target molecule, it returns to the native form of LiP. Due to low mobility and accessibility of enzyme active sites for target compounds, the involvement of low molecular weight redox mediator plays an important role. Veratryl alcohol (VEA) is naturally produced by WRF and serves as a mediator to facilitate oxidation of substrates. VEA can be oxidized by LiP to a cationic radical species (VEA$^{\bullet+}$) which is responsible for the oxidation of target compounds [58, 59].

MnP, as illustrated in Figure 4.1.1B, oxidizes Mn^{2+} to Mn^{3+} that can be stabilized by chelators, such as organic acids and acts as a redox mediator to attack organic compounds and oxidize them through abstraction of one hydrogen and one electron. Similar to LiP, MnP first reacts with hydrogen peroxide and form MnP-I with two electron deficiency. MnP-I oxidizes the target compounds and is transformed to MnP-II which is slowly reduced to native MnP and needs Mn^{2+} to complete the catalytic cycle [60].

A single fungal species is not able to produce all four extracellular enzymes and the combination of ligninolytic enzymes varies from one WRF species to another. Even the secretion profile of enzymes varies among WRF species. Furthermore, the nutrient composition e.g. carbon and nitrogen and conditions of growth media e.g. temperature and pH can influence the secretion of enzymes [53]. Apart from the mentioned enzymes, an intracellular enzyme system in WRF i.e. cytochrome P450 (CYP450) was found to play a significant role in the degradation of some pollutants [61]. Therefore, employing these fungi for removal of PhACs can be divided into three categories of: (i) using whole-cell culture; (ii) using crude culture extract or pure enzyme; and (iii) using immobilized enzymes [5, 62, 63].

Whole-cell fungal culture

Among fungal species, WRF is able to efficiently remove a wide range of organic compounds that are resistant to bacterial degradation [65]. This capability comes from the action of the intracellular system i.e. CYP450 and extracellular ligninolytic enzymes i.e. LiP, MnP and Lac [54, 65]. Because of the combined effect of intracellular/extracellular enzymes and sorption of PhACs on the biomass, whole-cell fungal treatment can remove a wider spectrum of PhACs, such as antibiotics, anti-inflammatories and antiepileptics compared to the case of using a single enzyme [5, 66, 67]. Several properties of WRF make them attractive for application in removal of PhACs, such as: (1) non-specificity of their produced enzyme which enables the degradation of a wide range of micropollutants; (2) the fast colonization through hyphal growth which enables WRF to access pollutants; (3) production and secretion of enzymes to degrade compounds with low water solubility; and (4) the ability to degrade compounds in nutrient deficient media over a wide pH range of 3 to 9. It is noteworthy that the degradation of persistent pollutant by WRF is a co-metabolic process which means it happens in the presence of a readily degradable substrate [68, 69]. The necessity of co-substrate addition, typically glucose, is a drawback which increases the cost but simultaneously increases the degradation efficiency [70]. An illustration of pollutant removal with the fungal cell, as discussed earlier, is presented in Figure 4.1.2. Accordingly, the target pollutants can be adsorbed on the surface of fungi or into the cell and later degraded by extracellular and intracellular enzymes.

The removal efficiency of pollutants by WRF can be affected by sorption, which is significant for compounds with a high octanol/water (K_{ow}) partition coefficient [53]. For example, Guo *et al.* studied the degradation of SMX by the fungus, *Phanerochaete chrysosporium* (PC) in whole fungal culture and also with extracted crude Lac. In the case of whole fungal culture with Lac activity of around 1500 U/L, they reported 53% degradation efficiency of SMX after 24 h when initial SMX concentration was 10 mg/L and less than 3% removal efficiency due to biosorption. While in the case of using crude enzyme at 6076 U/L of Lac activity, they observed SMX degradation of 42%, in 24 h [71]. It is indicated that the sorption of pollutants into the cell and the action of the intracellular enzyme increased the degradation efficiency. However, systematic investigation on the contribution of biosorption and biodegradation during fungal removal of PhACs will be useful for designing an efficient and stable fungal reactor for

removal of micropollutants [53]. For example, Yang *et al.* studied the removal of DCF by whole-cell of the WRF *Trametes versicolor* (TV). DCF showed high initial sorption (44±13%) and high removal efficiency (> 90%). Lucas *et al.* reported that the contribution of the sorption process to overall removal depends on the fungal strain and the interactions between PhACs and the components of fungal surface. Among the six fungal strains, they related the minimum and maximum removal by sorption to *Stropharia rugosoannulata* (4%) and *Ganoderma lucidum* (26%) [72]. According to Table 4.1.1, the relatively hydrophobic nature of DCF (K_{ow}= 4.51) plays an important role in DCF sorption to fungal cells. Comparison between the whole fungal culture and extracted enzyme (30 % degradation efficiency) indicated that a pathway independent of extracellular Lac was responsible for removal of DCF [53].

The removal mechanisms involved in treatment with WRF whole-culture can be divided into three steps including sorption onto biomass, biodegradation by extracellular enzymes e.g. Lac and degradation by intracellular or mycelium-bound enzymes (Figure 4.1.2). In addition to biosorption, there are other factors, including pollutant structure, fungal species, enzyme systems, culture medium, pH, temperature and enhancing methods e.g. the presence of mediators that affects the removal performance of a WRF [66, 73]. For instance, TV, which seems to have a good potential for the degradation of micropollutants, secretes three types of ligninolytic enzymes i.e. Lac, LiP and MnP among which Lac is the predominant one in some strains [74, 75]. This fungi showed better performance in aqueous media than solid matrices that can be due to the better mass transport in liquid media. As an instance, DCF, IBP, and NPX were almost completely removed in liquid media of TV [5, 66] while their removal efficiencies in solid media of TV were 64%, 75% and 47%, respectively [76]. Furthermore, the degradation ability of different species of WRFs and even different strains of one species is not similar. Similar behavior is not expected for one kind of crude enzyme extracted from different fungi. For example, LiP from *Phanerochaete sordida* (PS) showed higher efficiency for removal of some pollutants compared to LiP from PC [77]. Fungi other than WRF also showed capability to degrade PhACs. For example, *Pestalotiopsis guepini* strain P-8 showed 67.7% and 68.9% removal efficiency for CPF and NOR after 18 days with initial concentration of 300 μM and 313 μM, respectively [78]. In another study, three strains of *Mucor ramannianus* grown on the malt/sucrose medium were used for biodegradation of antimalarial drug

248

artemisinin. These strains transformed the artemisinin into 7β-6β-hydroxyartemisinin at 51% yield and hydroxyartemisinin at 88% yield [79]. Recent studies showed that the hydroxylated derivatives of this compound possess higher anti-malarial activity and water solubility [80]. Also, the saprobic fungus, *Mucor ramannianus*, demonstrated 89.1% removal efficiency for CPF (initial concentration of 100 mg/L) after 14 days [81].

Role of intracellular and extracellular enzymes

The role of mycelium-related enzymes and intracellular systems especially CYP450 in biodegradation of PhACs have been intensely studied for compounds, such as CTL, SMX, DCF, IBP, CBZ, SMZ, NPX and KEP [73, 75, 82, 83]. For example, Hata *et al.* demonstrated that the WRF PS YK-624 can degrade and remove the acute lethal toxicity of MFA and DCF towards *Thamnocephalus platyurus* (the freshwater crustacean) within 6 days. They suggested that catalytic hydroxylation by CYP450 is responsible for detoxification of MFA and DCF [67]. Also, Golan-Rozen *et al.* studied three strains of *Pleurotus ostreatus* (PO) and noticed the significance of CYP450 and MnP in degradation of CBZ [61]. Their results implied that when both MnP and CYP450 systems were involved, 99% of the CBZ was transformed to 10,11 Epoxy-CBZ. This end-product is an active pharmaceutical compound and its presence in waterways is not desirable [84]. However, when both MnP and CYP450 were inactivated, less than 30% CBZ removal was achieved [61]. In a related study, Marco-Urrea *et al.* studied the degradation of IBP and CBZ at 10 mg/L by four WRF i.e. TV, *Irpex lacteus*, *Ganoderma lucidum* and PC within 7 days. Accordingly, all strains except PC almost completely degraded IBP. The *in vitro* tests showed that although intracellular systems play a major role in degradation of IBP, CYP450 did not affect this process. In contrast, inhibition of CYP450 reduced the degradation efficiency of CBZ by more than 57% [5]. Later, they studied the degradation of NPX at two different concentrations (10 mg/L and 55 µg/L) in a liquid medium of TV and achieved > 99% and 95% of degradation after 6 and 5 hours, respectively. In this case, they observed that Lac and the CYP450 system was responsible for degradation of NPX [85]. Similarly, Prieto *et al.* reported the inhibition of NOR and CPF degradation by addition of CYP450 inhibitor to TV grown on malt extract liquid medium which indicated the important role of CYP450 in degradation of the two antibiotics [86]. However, Rodriguez-Rodriguez *et al.* studied the removal of NPX in sewage sludge samples

with TV and observed that NPX values did not necessarily correlate with CYP450 or Lac amounts though in most cases, over 30% degradation happened [87]. They also found that addition of CYP450 inhibitor to the TV culture partially suppresses the degradation STZ but has no effect was on degradation of SPY [88]. To sum up, both intra-cellular and extracellular enzymes play key roles in the degradation of PhACs, but depending on the compounds, they act differently. The intracellular enzymes may advance the first step of PhACs oxidation, while, extracellular enzymes do not intervene in the first step of degradation.

Bioreactors

Developing an effective setup to facilitate preparation, handling and implementation of reactor system is essential for wide application of bioremediation with WRF. Different reactor configurations have been studied for the treatment of PhACs with enzymes [89, 90] and the data on degradation efficiencies of different systems are listed in Table 4.1.3. The performance of WRF for removal of PhACs has been often studied on synthetic wastewater containing high concentrations of contaminants (up to several mg/L) under sterile conditions to avoid contamination with bacterial strains [33]. Contamination with bacteria in the fungal bioreactor has adverse effects on removal efficiency of PhACs since they compete with fungi for substrate, disrupt the growth of fungi and damage the mycelium [91]. Hence, it is essential to develop methods for an uninterrupted fungal growth. Some possible strategies to avoid contamination with bacterial are reducing reaction pH to acidic range, immobilization of fungi, limiting nitrogen in feed, using disinfecting agents and pretreatment of wastewater [92, 93]. In few cases, fungal bioreactors were operated under non-sterile conditions for a short period of time and above strategies were investigated [74, 94]. For example Li *et al*. used a continuous bioreactor packed with a mixture of WRF mycelia pellets under non-sterile condition for 28 days for removal of NPX and CBZ at 1.0 mg/L. They observed 60-80% removal efficiency of CBZ and complete removal of NPX in the beginning, but the removal efficiencies dropped to less than 20% by the 14th day due to the contamination. Addition of sodium hypochlorite into the influent tank increased the removal efficiency to initial level for NPX by inhibiting contamination, but it did not work for CBZ [95]. Cruz-Morato *et al.* monitored the degradation of 10 PhACs in urban wastewater in a non-sterile batch fluidized bed bioreactor inoculated with TV culture

at fixed pH level of 4.5. According to their observations, TV can remain active in the presence of bacteria and contaminants and addition of nutrients such as nitrogen and glucose can maintain a significant biological activity. They reported that in 8 days, 7 out of the 10 PhACs, such as IBP, ACT and KEP were removed completely, 2 of them were removed partially and only one of them (CBZ) showed higher concentration due to deconjugation of compound intermediates [74]. Also, they compared the operation in sterile and non-sterile modes for treatment of hospital wastewater containing more than 8 mg/L of PhACs and observed 83.2% and 53.3% degradation efficiency, respectively. They also employed Microtox test to demonstrate that both treatment can reduce the toxicity of wastewater [96]. In another study, Yang *et al.* compared the removal of DCF in a sterile TV fungal reactor operated in batch mode (three months of reaction time) and continuous mode (two days of retention time). They observed complete removal in batch mode and 55% removal efficiency in continuous mode [97]. This huge difference can be due to the shorter contact time and loss of enzyme in the continuous reactor.

Despite the lack of Lac and VP, the removal performance of PC towards pharmaceuticals has also been studied [98]. For instance, Zhang and Geißen grew PC on polyether foam under non-sterile conditions in a plate bioreactor to remove CBZ in continuous mode for 100 days. They found that the supply of nutrients is essential for effective elimination of CBZ. They achieved around 80% removal efficiency with synthetic wastewater and around 60% with the real effluent [99]. Also, Rodarte-Morales *et al.* studied the degradation of DCF and IBP and NPX with PC in a fed-batch reactor with continuous air supply over 30 days. They observed the complete removal of IBP and DCF after 23 h in aerated reactors. These observations implied that the oxidative capacity of PC for the anti-inflammatory PhACs is not limited to an oxygen environment since the fungal reactor could remove them under aerated conditions [89]. In a related study, they found that working in a continuous reactor with aged PC culture (more than 20 days) is in favor of removal of CBZ (>90%). But compared to the fed-batch reactor with fresh PC culture, it reduced the removal efficiency for anti-inflammatory drugs i.e. DCF, IBP, and NPX from > 99% to less than 50% [100]. It can be due to wash-out of the enzyme in a continuous system and also the fact that the aged culture of fungi had less enzyme production compared to fresh culture.

As mentioned earlier, most of the researchers worked with synthetic wastewater or spiked wastewater with high concentrations (up to 20 mg/L) of PhACs and the results cannot be satisfactorily extrapolated to environmentally relevant concentrations (ng/L to µg/L). For example, Jelic *et al.* performed the aerobic degradation of CBZ in Erlenmeyer flask by TV. At 9 mg/L of CBZ, they observed 94% removal after 6 days, while at initial CBZ concentration of 50 µg/L, they observed only 61% removal after 7 days. Also, they performed degradation of CBZ in an air pulsed fluidized bioreactor in batch and continuous modes and observed 96% and 54% degradation efficiency, respectively [94]. Comparing the performance of fungi in batch and continuous tests, two inherent restrictions were reported as the main reasons for lowering the removal efficiency from batch to continuous mode i.e. washout of extracellular enzymes with effluent and destabilization of fungal activity by bacteria [101, 102]. However, Ferrando-Clement *et al.* reported that the degradation efficiency of TV towards CPF in hospital wastewater is higher in non-sterile compared to sterile conditions. They attributed it to the synergistic degrading contribution by fungi and fecal bacterial [103]. To sum up, it is still required to work on real wastewater containing environmentally-relevant concentrations of different contaminants (ng/L to µg/L) under non-sterile conditions in continuous mode to investigate the performance and feasibility of fungal reactors for the treatment of contaminated water and wastewater.

Metabolite and toxicity assays

Degradation of PhACs by enzymes take place through different pathways and several intermediates and end-products are generated during the reaction. In most of the studies, researchers predominantly focused on the disappearance of the parent compounds rather than degradation pathways and toxicity of the TPs [109-111]. However, the properties of TPs are of high importance for releasing into the environment. In this section, the degradation pathways of some PhACs are discussed and the most observed TPs for widely-used PhACs are illustrated in Table 4.1.4.

There are several instruments for investigation of degradation products. Direct inlet-mass spectrometry (DI-MS, electron impact), gas chromatography-mass spectrometry [65, 67, 90], ^{1}H nuclear magnetic resonance (^{1}H NMR) and ^{13}C NMR [5, 67, 112] are the widely used instruments for identification of TPs. Liquid chromatography electrospray time-of-flight mass spectrometry (LC-ESI-TOF-MS) in negative and

positive mode [113, 114] and high-performance liquid chromatography-diode array detection-electrospray ionization mass spectrometry (HPLC-DAD-MS) are also used for compounds that are not possible to be handled by gas chromatography [82, 115]. Recently, newly developed and rapid laser diode thermal desorption-mass spectroscopy (LDTD-MS) was used for identification of TPs [116].

To detect the formation of toxic TPs, most researchers used a standard procedure called bioluminescence inhibition test or Microtox assay (ISO 11348-3, 2007), that employs bacterium *Aliivibrio fischeri* [85, 94, 110, 112, 117] or *Photobacterium phosphoreum* [5]. They are marine luminescent bacteria that emit visible light (λ_{max} = 490 nm). Effluent toxicity is expressed as units of Equitox/m^3 (determined as $100/EC_{50}$). The Equitox values are directly proportional to toxicity level, while EC_{50} is inversely related to toxicity. Counting the number of living freshwater crustacean *Thamnocephalus platyurus* and defining the relative acute lethal toxicity (%) as the percentage of lethality of fungal-treated influent compared to that of untreated sample is another method employed by Hata *et al.* [67]. In addition, the toxicity of treated and untreated solutions can be assessed based on their inhibitory effect towards the growth of Gram-positive and Gram-negative bacterial species e.g. *Bacillus subtilis, Bacillus megaterium*, *Escherichia coli*, and *Saccharomyces*. In this case, microorganisms are exposed to the media and the number of viable cells is monitored over a period of time [110, 111]. Moreover, the Yeast Estrogen Screen assay (YES) can confirm the estrogenic activity of environmental samples, such as wastewater effluent [118]. In this assay, the human estrogen receptor (hER) is expressed in yeast to make it responsive against estrogens [119]. The recombinant yeast hosts plasmids carrying lac-Z (the b-galactosidase-encoding reporter gene). In the presence of estrogenic compounds, the lac-Z gene is activated and b-galactosidase degrades a specific substrate that causes a color change from yellow to red as an indicator of compound estrogenicity [120].

Fungal mediated degradation of DCF starts with the introduction of the hydroxyl group in its structure and formation of hydroxy diclofenac. This reaction facilitates further biodegradation [67, 112]. *In vitro* and *in vivo* experiments using purified Lac and the CYP450 inhibitor, suggested that TV employed two different mechanisms to initiate degradation of DCF. Two TPs namely 4'-hydroxydiclofenac and 5-hydroxydiclofenac (Table 4.1.4) were identified which disappeared in 24 h resulting in a decrease in

ecotoxicity according to Microtox test [112]. Hata *et al.* reported that DCF degradation by fungus PS produced the hydroxylated metabolites that were found in the degradation by TV, and also they found 4,5-dihydroxydiclofenac as transformation product [65]. These hydroxylated products disappear at the end of the treatment with decreasing trend in toxicity that suggests mineralization [114]. However, according to Stadlmair *et al.*, polymerization occurred after degradation of DCF by horseradish peroxidase (HRP). TPs showed lower toxicity compared to the parent compound [113]. Hydroxylation is also the predominant start point for conversion of IBP to its TPs. In degradation of IBP by TV, it was reported to transform to 1-hydroxy ibuprofen and 2-hydroxy ibuprofen intermediates. These species were finally transformed to 1,2-dihydroxy ibuprofen (Table 4.1.4) during 7 days of incubation. However, Microtox bioassay revealed an increase in the toxicity after 7 days which was related to the presence of 1,2-hydroxy ibuprofen [5]. This finding emphasizes the significance of the identification of TPs in any treatment since they might be more toxic than their original compound [121]. Likewise, hydroxylation reaction played an important role in the degradation of KEP with TV. 2-[3-(4-hydroxybenzoyl)phenyl]-propanoic acid, 2-[(3-hydroxy(phenyl)methyl)phenyl]-propanoic acid and 2-(3-benzyl-4-hydroxyphenyl)-propanoic acid were detected as main intermediates of TV activity. However, none of the mentioned intermediates was detected at the final stage which suggested KEP mineralization. It was also observed that extracellular enzyme (Lac) had a negligible effect on the degradation of KEP [82]. Hata *et al.* found four hydroxylated TPs in degradation of MFA by PS. Their results showed that CYP450 catalyzed the hydroxylation which finally resulted in complete removal of acute lethal toxicity of MFA after 6 days of treatment [65].

Both CYP450 and Lac can mediate the degradation of NPX in whole-cell WRF treatment. 1-(6-methoxynaphthalen-2-yl) ethanone and 2-(6-hydroxynaphthalen-2-yl) propanoic acid were detected as intermediates of NPX which disappear after 6 h of incubation without remaining toxicity [85]. Also, 6-O-desmethyl-naproxen, was reported as the major degradation products of the NPX in a bioreactor of PC [90].

Degradation pathways of CBZ by whole-cell WRFs, such as TV and PO was reported to result in the formation of 10,11-dihydro-10,11-epoxycarbamazepine while pure Lac resulted in the formation of 9(10H)-acridone as TPs after 48 h [65]. Microtox test showed that the toxicity of these two TPs is higher than the toxicity of CBZ [94].

Similarly, fungi other than WRFs, such as *Umbelopsis ramanniana* and *Cunninghamella elegans* produce 10,11-epoxycarbamazepine as the major TPs but they also produce (2-and 3-hydroxy carbamazepine) [122]. Extracellular MnP and intracellular CYP450 were identified to affect the CBZ oxidation. It is noteworthy that at high initial CBZ concentration (10 mg/L), 10,11-epoxycarbamazepine was the major stable TP, but at an environmentally relevant concentration (1 µg/L), further transformation of 10,11-epoxycarbamazepine to 10,11 trans-diol was carried out by PO fungus [61]. It seems that the major TP of CBZ degradation with fungi is 10,11-epoxycarbamazepine though other TPs, especially hydroxylated derivatives were also identified. However, the toxicity of the TPs seemed to be more than CBZ.

Sulfonamides are sometimes desulfonated as a result of biodegradation with WRFs [83]. For example, aniline and 4-(2-imino-1-pyridyl)aniline were identified as TPs of SPY and 4-(6-imino-2,4-dimethoxypyrimidin-1-yl)aniline was determined for SDM [115]. Also, desamino-sulfamethazine and hydroxyl-sulfamethazine were identified for SMZ and for the transformation of SPY and STZ, a formyl intermediate was observed after the loss of the thiazole/pyrimidine group [83, 88]. In another study, anions, such as sulfate, nitrate, and nitrite were detected as an intermediate of SMX degradation with crude VP obtained from *Bjerkandera adusta* [114]. Rahmani *et al.* showed that the growth inhibition property of a solution containing SMX and STZ against bacteria was remarkably decreased after treatment with laccase [111]. Although many metabolites of sulfonamides degradation with enzymes were identified, the pathways and mechanisms still need to be studied.

In the case of CPF degradation with *Gloeophyllum striatum* after 90 h, reduction in antibacterial activity and production of CO_2 was reported along with eleven metabolites including hydroxylated congeners and TPs indicating the degradation of the piperazinyl moiety [123]. Using extracted Lac resulted in the identification of new TPs that were obtained from the breakdown of piperazinyl moiety, hydroxylation, and removal of a cyclopropyl group [86]. There are also other acetylated derivatives identified as TPs for degradation of CPF using different fungi, such as *Pestalotiopsis guepini* [78]*, Mucor ramannianus* [81] and *Trichoderma viride* [124]. Similarly, in degradation of EFC by *Gloeophyllum striatum* hydroxylated congeners, an isatin-type compound (obtained by cleavage of the heterocyclic core of EFC) and an anthranilic acid derivative was identified [125]. TPs with hydroxylated aromatic rings undergo ring

cleavage to transform to one catechol-type and four potential oxidizable *o*-aminophenol intermediates [126]. Degradation of EFC with *Mucor ramannianus*, resulted in the formation of EFC N-oxide, N-acetylciprofloxacin, and desethylene-enrofloxacin as TPs [127]. Parshikov *et al.* demonstrated that the intermediates and TPs of degradation of NOR with *Pestalotiopsis guepini* and *Trichoderma viride* were analogous to those derived from CPF by the same fungi [78, 124]. Gros *et al.* studied the degradation of antibiotic ofloxacin by TV in sterile and unsterile hospital wastewater as well as synthetic wastewater. They reported that TPs of ofloxacin are obtained mainly through hydroxylation, oxidation, and cleavage of the piperazine ring. Their toxicity tests showed a reduction of the toxicity in the synthetic medium and in the batch bioreactor [117]. Llorca *et al.* investigated the TPs formed by enzymatic degradation of antibiotic TC. They attributed the formation of major TPs to (bi) demethylation, dehydroxylation and oxidation of the rings C and A [128].

To sum up, few researchers have paid attention to the evaluation of toxicity of TPs until the date and it should be considered in future investigations. According to the few published research works, in some cases, the TPs of enzymatic processes were found to be more toxic than their parent compounds. Therefore, the major TPs of enzymatic processes should be identified for the majority of present compounds in the waste streams and their toxicity should be determined prior to the decision for system scale-up.

Crude enzyme

Extraction of enzymes from microorganisms and using them instead of using live cultures for removal of pollutant from aqueous media has several advantages. Extracted enzymes do not need the continuous addition of nutrients or compete with bacteria and they can reach high reaction kinetics in mild temperature and pH conditions [27, 130, 131]. Enzymatic treatment consumes less energy and chemicals and produce fewer wastes compared to other bioprocesses [33, 132]. Enzymatic treatment is particularly an attractive technology for the treatment of PhACs that are resistant to conventional treatment. The performance of individual ligninolytic enzymes has been studied for the removal of a broad range of micropollutants and the results are summarized in Table 4.1.5. In addition, the capacity of crude and purified extracellular ligninolytic enzymes for PhACs removal in batch and continuous mode

has been extensively investigated [49, 53, 55, 66, 133, 134]. For instance, Li *et al.* reported more than 90% removal of NPX in two days of reaction with crude enzyme obtained from PC at an initial concentration of 10 mg/L. This level of degradation efficiency was higher than the performance in whole-cell cultivation in which 68% removal efficiency was achieved after two days [95]. Margot *et al.* compared the ability of extracted Lac from bacterium *Streptomyces cyaneus* and TV for degradation of DCF and MFA. They reported that fungal Lac was more active than bacterial Lac in normal conditions of municipal wastewater (neutral pH and 10-25 °C) and showed faster kinetics for degradation of DCF and MFA. Complete removal of DCF and MFA was achieved during 12 days of incubation with fungal Lac, while around 50% of both pollutants were removed by bacterial Lac within the same incubation time [135]. Llorca *et al.* reported that degradation efficiency of Lac towards TC after 18 h and EreB esterase towards ETM after 16 h were ~78% and ~50%, respectively [128].

Purified enzyme

Purification of the enzyme is a costly process that can be performed through different methods, such as membrane separation, size exclusion chromatography, etc. [136]. Purified oxidoreductase enzymes, obtained from different strains of WRF, have been used for removal of pollutants from aqueous media in both continuous and batch reactors [112]. Purified oxidoreductase enzymes demonstrated degradation potential towards a wide range of micropollutants, however, crude enzyme demonstrated better removal performance for some compounds, such as NPX and DCF (Table 4.1.5). It was related to the natural mediators that exist in the crude enzyme [137]. For instance, Tran *et al.* observed complete removal (> 99%) of several compounds, such as IBP, DCF and IDM and related them to the natural mediators in crude Lac obtained from TV grown in basal liquid medium [66] whereas purified laccase obtained from TV and *Aspergillus oryzae* achieved only 20-50% removal efficiency for these compounds [133, 136]. Although utilization of crude enzyme is more economical and in some cases leads to higher removal efficiency compared to the purified enzyme, the crude solution contains remarkable levels of the unspent nutrients that can increase the organic loading of wastewater to be treated [56]. Therefore, still more research is needed to simultaneously take advantage of natural mediators and rejection of nutrients.

Mediator effect

Lac catalyzes the mono-electronic oxidation of PhACs through copper active sites. However, the oxidation-reduction potential (ORP) of the enzyme affects the extent of removal [139]. Poor degradation of non-phenolic PhACs is generally attributed to the presence of strong electron withdrawing groups (EWGs), such as amide (-CONR$_2$), carboxylic (-COOH), halogen (-X) and nitro (-NO$_2$) in the molecular structure and higher ORP of non-phenolic compounds compared to Lac [139].

Degradation efficiency of pollutants with Lac can be enhanced by the addition of mediators that work as electron shuttles between the target compounds and enzyme [140]. The low molecular weight mediators, such as syringaldazine (SA) and 1-hydroxybenzotriazole (HBT) are oxidized by the enzyme, they diffuse and oxidize the substrate that cannot enter the enzymatic pocket due to its size. The generated radicals serve as a shuttle for electron transfer between PhACs and Lac and consequently facilitate the degradation of recalcitrant compounds. Also, they can enhance the degradation of non-phenolic compounds by generating highly reactive radicals as a result of mediator oxidation by the enzyme. Therefore, the mediator can extend the range of substrates degradable by the enzyme [141]. In Table 4.1.6, the most studied redox mediator for Lac with their structure and related information are listed. The mediators follow three mechanisms for oxidation i.e. ionic mechanisms, hydrogen atom transfer, and electron transfer [25]. For instance, HBT and SA tend to follow hydrogen atom transfer, while 2,2'-azino-bis(3-ethylbenzothiazoline-6-sulphonic acid) (ABTS) and 2,2,6,6-tetramethylpiperidinyloxyl (TEMPO) were reported to follow electron transfer and ionic mechanisms, respectively [142, 143]. The type and concentration of mediator and the properties of target compound affect the performance of a mediator. For instance, violuric acid (VLA) and HBT were reported to work better for non-phenolic PhACs, while SA and ABTS showed better performance for phenolic compounds [56, 133, 134, 144].

Lloret *et al.* investigated the effects of SA on the degradation of DCF by commercial Lac from *Myceliophthora thermophila* (MT). They found that removal of DCF was improved from 40 to 80% by increasing the SA concentration from 0.1 to 0.5 mM [136]. Similarly, Nguyen *et al.* obtained 35% improvement in the removal of DCF by increasing the concentration of SA from 0.01 to 0.1 mM in an enzymatic reactor [56]. Increasing the mediator concentration beyond a threshold level, may not affect the

removal of PhAC. For example, Ashe *et al.* reported that NPX can be efficiently removed by Lac in the presence of VA or HBT mediators but increasing the VA concentration from 0.5 to 1 mM caused no improvement in the removal of NPX [142]. The small aminoxyl radicals formed by reaction of HBT and Lac can abstract hydrogen atom from the O-H bond in substrates and form the phenoxyl radicals which are able to react with the substrate [145]. Suda *et al.* investigated the degradation of several tetracycline antibiotics (TC, CTC, DC, and OTC) with a Lac mediated by HBT. Their results showed complete elimination of DC and CTC in 15 min, and complete removal of CTC and TC in 1 h [146]. Nguyen *et al.* observed that coupling HBT with laccase in a fungal membrane bioreactor (MBR) can eliminate DCF (70-95%) and NPX (20-98%) that are resistant to bacterial degradation but cannot degrade compounds such as IBP, GFZ and AMP that are perfectly removed by activated sludge treatment [54]. This finding indicates that WRF and activated sludge would be a complementary system in WWTPs. However, the high loading of mediator required for the treatment casts doubts on the applicability of enzyme-mediator systems. Margot *et al.* investigated the removal of SMX with Lac mediated by ABTS, SA, and acetosyringone (ACE). They observed that mediators were consumed at the mediator to pollutant molar ratio of 1.1 to 16 [147].

Another issue with using mediators is the compromising of enzymatic activity after the addition of mediators though they can improve the kinetics of the reaction. For instance, Hata *et al.* reported 90% reduction in Lac activity 8 hours after the addition of HBT [65]. Likewise, rapid reduction in activity of laccase was reported after the addition of ABTS, VA, or HBT but the rate of inactivation depends on the stability of the generated radicals [142]. If there is no enzyme inhibitor in the medium, rapid inactivation of enzyme in presence of mediator can be due to the blocking of enzyme active sites by metabolites and charged radicals and also the reaction of enzyme-active sites with metabolites and form non-productive complexes [25, 148]. Nevertheless, the periodic enzyme replenishment will be required to maintain the removal efficiency of PhACs which increases the operational cost.

Although the use of mediators can improve the removal of micropollutant, these compounds are toxic and their release into the environment may pose chronic problems [33]. As a result, increasing the toxicity of treated wastewater with enzyme-mediator system leads to another environmental problem. For example, Nguyen *et al.*

found that effluent of enzymatic treatment mediated with SA was more toxic than control sample for all dosages applied, while the addition of HBT did not increase the toxicity at concentrations lower than 0.5 mM [55]. Therefore, to develop an effective removal strategy, selecting the appropriate mediator and determination of its optimum concentration are critical. Furthermore, it has to be ensured that use of mediator does not result in increasing the toxicity of the effluent.

Operational parameters

The performance of ligninolytic enzymes in wastewater treatment plants depends on operational conditions and physiochemical properties of PhACs and wastewater. Briefly, the properties of wastewater, such as temperature, pH, salinity and the presence of metals and dissolved organic/inorganic matter may influence the performance of fungal cultures or their extracted enzyme [46]. In the following sections, the effects of different parameters have been summarized.

The temperature of wastewater affects both the stability of biocatalytic systems and the rate of reaction. It is assumed that the reaction rate increases to some extent when the temperature is increased [62]. However, depending on the strain of fungi, thermal denaturation of enzymes is expected at a temperature higher than 40 °C [152, 153]. Few studies investigated the effect of temperature on the activity of ligninolytic enzymes [154, 155]. The optimal temperature to obtain the highest degradation efficiency of ligninolytic enzymes differ from one compound to another. For instance, Wen *et al.* studied the degradation of TC and OTC by crude LiP obtained from PC and observed that in the range of 30-37 °C, TC was totally removed while the degradation efficiency of OTC was about 90% at 30 °C and increased with the temperature, until it was 37 °C [28]. In a related study, Margot *et al.* used purified Lac from TV to degrade DCF and observed that by increasing the temperature from 10 °C to 25 °C, degradation efficiency was increased and further temperature increase resulted in a plateau [156]. Similarly, Naghdi *et al.* showed that Lac obtained from TV has its highest stability at 30 °C with 66% of its initial activity and between 50-70 °C, Lac could not retain more than 11% of its initial activity [6].

The performance of enzyme and several properties of substrates can be highly impacted by pH of the reaction medium, which subsequently affects the extent of PhACs removal. The effects of pH on degradation efficiency are caused by the stability

of target compounds at different pH levels and the pH dependency of the enzyme activity. The latter is because of the fact that the pH changes the ionization status of enzyme and each enzyme can be active only in a special ionization status [28].

The optimum pH for DCF removal (60-100%) by purified Lac obtained from TV and MT and LiP obtained from PC was reported to be in the range of 3.0-4.5 [62, 134, 136, 156]. Zhang and Geißen found that crude LiP obtained from PC can completely degrade DCF at pH 3.0-4.5 while only 10% degradation happened at pH 6.0. They indicated that this decline in removal efficiency was due to the inactivation of LiP at higher pH [62]. Wen *et al.* studied the degradation of TC and OTC with crude MnP obtained from PC and observed that pH range of 2.96-4.80 was the optimum range for treatment [155]. In another study, it was found that pH 4.2 was the optimum value for degradation of TC and OTC with LiP. They also observed no degradation for pH values below 2.8 or above 5.4. Interestingly, for pH values higher than 4.2, the degradation efficiency of TC decreased more rapidly than that of OTC [28]. In a related study, Weng *et al.* observed that Lac activity decreased when pH was pushed toward alkaline values and related it to the binding of hydroxide anion to the copper element of laccase, which subsequently interrupted the electron transfer pathway [157].

Besides temperature and pH, the constituents of wastewater matrix, such as surfactants, natural organic matter, various organic/inorganic compounds and heavy metal ions need to be evaluated in the case of removal of PhACs [158]. The effects of dissolved organic and inorganic compounds on the activity of Lac and removal of PhACs has been discussed by several studies. Accordingly, compounds such as heavy metals, halides, sulfides and natural/synthetic organics can inhibit the activity of Lac [159-161]. Each compound may inhibit the enzyme via a different mechanism. For instance, fatty acids inhibit the catalytic potential of Lac by blocking the enzyme binding sites for phenolic substrates [162]. Also, the catalytic voltammetry analysis indicated that anionic inhibitors, such as sulfides and halides could block the access of substrates to the active copper sites in Lac [163]. Among anionic inhibitors, azide and fluoride are known as the most effective inhibitors that can rapidly reduce the activity of Lac by 50% even at very low concentrations [164]. The inhibition of Lac by halides can follow this order: fluoride > chloride > bromide, however, the halides concentration required to inhibit Lac varies and no correlation with their inhibition potential have been found [165, 166].

Lu *et al.* investigated the effect of natural organic matter on biodegradation of ACT with Lac and found that dissolved natural organic matter can inhibit self-coupling of the ACT and enhance its removal. It can be due to the cross-coupling between ACT and dissolved natural organic matter [167]. Cross-coupling between pharmaceuticals and natural organic matter may play a more important role than self-coupling of pharmaceuticals in degradation of micropollutants due to a higher concentration of natural organic matter [168]. Cross-coupling of the pollutants with molecules of natural organic matter through the oxidative action of enzymes can deactivate their biological effects. Also, the cross-coupling of natural organic matter molecules to each other as a result of enzymatic reaction can enhance the removal of natural organic matter. Therefore, using enzymatic treatment can simultaneously remove micropollutants and natural organic matter [168, 169].

Although oxidoreductase enzymes act non-specifically towards pollutants, they follow the "one electron oxidation" mechanism and therefore the substrates need to have electron donor properties in this reaction. The essential criteria for substrates of these enzymes are the presence of the heterocyclic or aromatic ring, easily oxidized substitutions, such as hydroxyl groups and electron donor substituent such as phenyl, alkyl, etc. [66]. Hydrophobicity and the presence of electron donating groups (EDGs) or EWGs are important factors affecting the biodegradation of trace organic contaminants in WWTPs [170]. EWGs, such as an amide ($-CONR_2$) and carboxylic ($-COOH$) groups cause the compounds to be less susceptible to oxidative catabolism while EDGs such as an amine ($-NH_2$) and hydroxyl ($-OH$) groups facilitate the electrophilic attack by oxygenase produced in aerobic treatment [16]. As a consequence, high removal efficiency was observed for hydrophilic and hydrophobic compounds, which possess EDGs while low removal efficiency was observed for hydrophilic compounds bearing EWGs. It is noteworthy that some compounds, such as DCF and NPX contain both EDGs and EWGs and the overall influence of these groups on biodegradability is complex. In this case, an extensive study on the structure-activity relationship is required [46, 139].

Immobilized enzyme

Using batch reactors with free enzymes is not economically viable for wastewater treatment due to the high volume of wastewater to be treated, high quantities of

required enzyme and necessity for removal of the enzyme at the end of treatment [171]. Since enzymes are expensive, the economic viability of the whole process needs to be demonstrated. To overcome the cost of large amount of free enzyme needed for real applications (due to enzyme losses during the treatment), different strategies that have been adopted include: (i) immobilization of the enzymes on supports to separate enzymes from the effluent and reuse them several times [57], (ii) using ultrafiltration membranes to prevent the release of enzyme with effluent and (iii) production of the enzyme during treatment using microorganisms grown on cost-effective substrates. Using immobilized enzymes is a potential solution for industrial-scale application since it enables reusing of biocatalyst and continuous operation and reduces the operational costs [172]. Furthermore, immobilization of enzyme improves the stability of enzyme during storage, against organic solvents and variations in temperature and pH. Immobilization of enzymes also increases the contact surface and helps to avoid too much shear stress which inactivates enzymes [131, 171, 173]. However, the immobilized enzyme may have less activity compared to free one due to conformational alterations of the enzyme and its heterogeneity on the support [57, 174, 175]. The immobilization process influences the properties of the biocatalyst and therefore the selection of an immobilization method determines the process specifications of an enzyme such as cost, catalytic activity, effectiveness and deactivation kinetics [57, 176]. Also, the toxicity of reagents used for immobilization should be considered for waste disposal and specific application of the biocatalyst [176].

In Table 4.1.7, the data on the efficiencies of immobilized enzymes for removal of PhACs obtained by different researchers have been summarized. Immobilization of enzymes has been performed on different types of inert (e.g., aluminum oxide pellets and alginate beads) and active (e.g., activated carbon and silica gel) carrier materials. The selection criteria for support materials are being cost-effective and having non-toxic nature, high surface area and mechanical strength [177, 178]. Several immobilization methods have been developed so far i.e. covalent attachment, crosslinking, entrapment in pores or spun fibers, encapsulation, ionic interaction and adsorption [177-180].

Immobilization methods that involved chemical reaction with enzyme provided stable attachment and reduced enzyme inactivation rates, however, they tend to reduce the

activity of the biocatalyst because the covalent bonds can perturb the native structure of enzyme [181]. By contrast, physical immobilization and entrapment methods typically have fewer effects on the structure of the enzyme and provide less stability during the reaction [176]. The appropriate selection of immobilization method depends on several parameters. Normally, an immobilized enzyme with a lower initial activity but long-time stability is preferred to the one with a high initial activity but with less stability [176, 181, 182].

Among these methods, physical adsorption on carriers is a simple and economical approach [6]. To improve the stability and enzyme loading, the carrier surfaces should be properly modified to create functional groups with affinity for protein [183]. Naghdi *et al.* immobilized Lac on functionalized nanobiochar through acidic treatment and observed an improvement in storage, pH, and thermal stability. The immobilized Lac preserved 70% of its initial activity after 3 cycles of reaction with ABTS [6]. Similarly, Nguyen *et al.* immobilized Lac onto functionalized granular activated carbon through acid treatment and observed more than 90% residual activity after three oxidation cycles using 2, 6-dimethoxy phenol as substrate [184]. In another study, Ji *et al.* immobilized Lac on carbon nanotubes via physical adsorption and observed 60% activity retention after three cycles of ABTS oxidation [185]. Therefore, still, physical methods need to be improved since losing 30-40% of activity in 3 cycles is not economically viable.

Covalently immobilized enzymes showed high performance in removal of PhACs. For example, Kumar *et al.* used covalently immobilized Lac on electrospun poly(lactic-co-glycolic acid) nanofibers and observed the almost complete removal of DCF in a batch reactor after 5 h. Also, they reported similar degradation efficiency after 3 cycles [186]. Likewise, Xu *et al.* immobilized Lac on polyvinyl alcohol/chitosan nanofibers through covalent bonding for degradation of DCF and observed complete removal after 6 h in batch mode [187]. Also, they employed immobilized HRP on Poly(vinyl alcohol)/poly(acrylic acid)/SiO_2 nanofibers for degradation of paracetamol and obtained more than 80% removal after 90 min. Around 20% reduction in degradation efficiency was reported after 3 cycles [188]. However, in the mentioned research the initial concentrations of compounds (>10 ppm) were far beyond their environmentally relevant concentration i.e. several ppb.

Cross-linking of enzyme molecules to each other and formation of insoluble enzyme aggregates is another approach to enhance stability. In this method, it is possible to work with or without support. Due to the small size of aggregates, different methods such as microfiltration and using magnetic particles are proposed for separation of the enzyme from effluent [189, 190]. Lac cross-linking enzyme aggregates and Lac-grafted particles have been used for the degradation of PhACs in different reactor configurations e.g. fluidized-bed reactors and fixed-bed reactors [191]. For example, Ba *et al.* used Lac cross-linked aggregates for degradation of the ACT, CBZ, and MFA and observed 99%, nearly 100% and up to 85% degradation efficiency respectively after 8 hours in a batch reactor. In continuous experiments, complete removal of ACT and MFA within 24 h and 93% removal for CBZ after 72 h was achieved [192]. In another study, a combination of Lac and Tyr were crosslinked to form aggregates and this combined system was used to degrade ACT in municipal wastewaters in batch mode. They observed more than 80%-100% removal for the ACT in municipal wastewater and more than 90% removal in hospital wastewater [193]. Nair *et al.* immobilized Lac on silica spheres in a two-step adsorption-crosslinking process and achieved more than 30% of DCF removal in continuous mode [194]. There are also other research papers that reported different removal efficiency (up to 95%) while using enzyme aggregates [190, 195, 196].

Enzymatic membrane reactors (EMRs)

Application of enzymatic treatment in continuous mode still remained a technical challenge since the enzyme is washed out with the treated effluent [199]. Using membranes with a pore size smaller than the size of enzyme macromolecules is a potential approach to solve this issue [200]. In this, so-called enzymatic membrane reactor (EMR), the enzyme remains in the reactor while continuous feeding and effluent withdrawal are enabled. Compared to the enzyme immobilization approach, EMR has advantages, such as better enzyme dispersion in the reactor, more effective enzyme retention and easier replenishment of fresh enzymes. There are few studies in which continuous PhACs degradation by EMRs is investigated [25, 201]. Two types of EMRs have been already distinguished (Figure 4.1.3) [132]. In the first case (Figure 4.1.3A), which is also called "stirred-tank membrane reactors" the membrane acts as a barrier against escape of free enzyme from the reactor, while transformation

products (TPs) are able to cross the membrane along with effluent. In this design, separated devices for reaction and separation are deployed in series and independently controlled in terms of operating conditions [131]. One of the challenges for this type of EMR is adjusting the tangential flow to avoid concentration polarization, to prevent enzyme inactivation and to achieve a feasible filtration rate. Stirred-tank membrane reactors have been already studied for hydrolysis reactions, but such reactors were also studied for environmental applications. Recent investigations have focused on the removal of DCF, CBZ, and SMX from water and wastewater. For instance, Nguyen *et al.* studied the effect of the addition of granular activated carbon (GAC) to Lac-based stirred-tank membrane reactors on the removal of CBZ, DCF, and SMX. They observed that dosing of 3 g/L GAC caused 14-25% improvement in biodegradation of the PhACs and reduced membrane fouling. They also found that the removal of DCF increased from 30% in a batch reactor (8 h contact time) to 60% in EMR continuous operation (8 h retention time) [49]. In a related study, they observed that addition of SA as a mediator at 5 µM can increase the removal efficiency from 60% to 80% under DCF loading rate of 480 µg/L.d. They also found that DCF was trapped into the gel layer of enzyme formed on the membrane surface, which helped in its biodegradation [133, 134]. They also found that a higher concentration of SA increased the toxicity of effluent, due to the presence of generated radicals and unconsumed SA [56]. A gradual depletion of the enzymatic activity has been reported even with properly selected molecular weight cut-off, which indicates enzyme denaturation during operation. Depletion of enzymatic activity is caused by both natural activity decay of free enzymes and inactivation due to shear stresses. Therefore, the periodic addition of enzyme to the reactor will be required to maintain the level of enzymatic activity [49, 134].

In the second type of EMRs (Figure 4.1.3B), the membrane is a selective barrier, which was already used as a support for immobilization of enzyme. Therefore, the biocatalytic reaction happens at many places where the enzyme is immobilized i.e. the external/internal surface of the membrane. This configuration offers several advantages, such as lower energy consumption compared to packed bed reactors, enzyme stability and reducing the blockage of the membrane and forcing the pollutants to pass over the active sites during filtration. The latter is considered as the main benefit of this process [202]. In this type of EMRs, the collision between enzyme and

substrate occurs during the mass transfer process through the membrane. Therefore, the biocatalytic reaction takes place during the mass transfer process and the TPs are released into the permeate. This concept enables better control of the process by reducing the distance between the substrate and catalyst and increasing the probability of reaction. The membrane is an assembly of pores, which can be considered as micro-reactors. In these micro-reactors, the contact between reactants is improved since the path for mass transfer is reduced and simultaneously the retention time can be adjusted by manipulating the flux rate [132, 203].

The selection of immobilization method is based on membrane properties, enzyme properties, and cost. There are three main techniques for preparation of active membranes: attachment through covalent or physical bonds on the membrane, entrapment in the pores and deposition of a gel layer of enzymes on the surface of the membrane [204, 205].

Attachment through covalent bonding methods such as the formation of carbodiimides, diazonium salts, etc. is advantageous in terms of enzyme stability and leaching prevention. De Cazes *et al.* covalently immobilized Lac onto the ceramic membrane and degraded TC at 56% efficiency after 24 h whereas the efficiency was only 30% with free Lac. Furthermore, their EMR reached a constant degradation rate during 10 days [206, 207]. However covalent bonding to support is not a preferred method due to reduction of activity, high cost and regeneration problems [173, 208-212]. On the other hand, entrapping enzyme in the pores and formation of gel on the surface of membrane are simple, cheap and offer the possibility of regeneration and their leaching can be overcome by forming enzymes clusters inside the membrane pores [213-215]. Also, the stability of the enzyme layer can be improved by covalent bonding of enzyme molecules to each other [216]. It is obvious that further studies are needed to advance in EMR design, particularly to verify their viability at large scales and their potential challenges such as fouling. A mathematical study by Abejon *et al.* on immobilized Lac for degradation of antibiotics showed that this process is still far from economic competitiveness due to the costs of membrane conditioning. They concluded that some improvements on the lifetime of the reactors, enzymatic activity, and membrane conditioning or regeneration costs need to be made to achieve competitive economical [217].

Hybrid methods

The combination and enzymatic degradation with other treatment methods attracted the attention of researchers due to the potential of overcoming the drawbacks of single process approaches. For example, placing fungal reactor and activated sludge system in series can combine the benefits of both systems, namely the oxidative activities with fungi and decreasing chemical oxygen demand (COD) by activated sludge [218]. Also, a combination of sonication with oxidation by Lac enzyme improves the degradation efficiency and reduces reaction time [109, 219]. Ultrasonication produces radicals that independently attack and oxidize the contaminant molecules [220]. Combination of fungal media with Fenton system is another strategy studied for degradation of PhACs. In this system, the degradation efficiency of recalcitrant CBZ was reported to reach 80% after addition of 2,6-dimethoxy-1,4-benzoquinone and Fe^{3+}-oxalate to fungal culture [221]. Yang studied the augmentation of an MBR with TV to take the advantage of both fungi and bacteria for removal of DCF. Initially, they observed the high removal of DCF, which gradually dropped from 80% to 40% after three weeks of operation in continuous mode. Their mass balance showed that 66% of adsorbed DCF onto sludge underwent biodegradation that reveals a successful combination. However, the loss of extracellular laccase through membrane should be mentioned as a drawback [144].

Conclusion and future outlook

Over the past 20 years, numerous researchers have investigated the performance of different processes to remove PhACs from water and wastewaters. Treatment systems based on WRFs and their related oxidoreductase enzyme systems offer a promising and environmentally friendly solution for removing such pollutants. This method has advantages over other treatment methods, such as the production of less toxic by-products and producing no concentrated stream.

The reviewed literature showed that a variety of pharmaceuticals are efficiently removed by both crude/purified enzymes and whole-cell fungi. Treatment with whole-cell fungi showed superior performance for many compounds due to the synergistic effects of intracellular and extracellular enzymes coupled with sorption onto fungal biomass. However, in these systems, the washing out of enzymes with effluent and constant supply of different nutrients to keep fungi active increase the organic loading of final effluent. Furthermore, the bacterial contamination of fungal culture should be

considered for large-scale applications since in real water and wastewater, there are different consortia of microorganisms that can compete with fungal activity. Also, there are factors including temperature, pH, aeration, and dissolved constituents that affect the removal performance in enzymatic treatment system and this needs to be investigated. Based on the data obtained from the effects of different factors, the limitations of enzymatic treatment in terms of influent characteristics, operational conditions and effluent quality will be elucidated. Performing the enzymatic treatment in pilot scale is needed f the operational problems and to estimate the capital and operational costs for large-scale applications.

While using extracted enzymes, the lower stability of enzyme and its loss with the effluent urged researchers to insolubilize or immobilize the free enzyme through different methods. Although immobilization can increase the stability and enable reusability, most of the immobilization methods have significant drawbacks, such as being highly expensive, loss of enzyme activity and regeneration problems. Low molecular weight redox mediators can enhance the kinetic and degradation efficiency of enzymes, however, they deplete the enzyme activity and may pose toxicity to the final effluents.

Although ligninolytic enzymes and especially laccases were already commercialized for applications, such as denim bleaching, still there are significant hurdles in the commercialization of these enzymes for waste stream bioremediation. Large amounts of required enzyme, the high cost of mediators, production of toxic compounds and losing enzyme activity as a result of inhibitors in the waste stream are among the most important hurdles that need to be addressed in research phase before proceeding to commercialization phase.

According to the performed studies on by-products of enzymatic treatment of PhACs till date, final TPs are less toxic as compared to the parent compounds in many cases. However, there are several examples of enzymatic treatment by-products, such as hydroxylated IBP, which is more toxic compared to IBP. Therefore, the major TPs of enzymatic treatment can be identified for the majority of present compounds in the waste streams and their toxicity should be determined through standard methods prior to the decision for the system scale-up.

Recent investigations suggested using immobilized enzymes in hybrid processes to improve pollutant degradation. These complementary processes, such as adsorption,

Fenton oxidation, and ultrasonication can improve the degradation of recalcitrant compounds, such as CBZ. Further investigation is required to evaluate the technical, economical and environmental aspects of different process combinations to obtain a reliable and robust strategy for degradation of micropollutants.

Acknowledgements

References

1.   Kim, S.D., Cho, J., Kim, I.S., Vanderford, B.J., and Snyder, S.A., Occurrence and removal of pharmaceuticals and endocrine disruptors in South Korean surface, drinking, and waste waters. Water research, 2007. 41(5): p. 1013-1021.

2.   Deblonde, T., Cossu-Leguille, C., and Hartemann, P., Emerging pollutants in wastewater: a review of the literature. International journal of hygiene and environmental health, 2011. 214(6): p. 442-448.

3.   Husain, M. and Husain, Q., Applications of redox mediators in the treatment of organic pollutants by using oxidoreductive enzymes: a review. Critical Reviews in Environmental Science and Technology, 2007. 38(1): p. 1-42.

4.   Alexander, J.T., Hai, F.I., and Al-aboud, T.M., Chemical coagulation-based processes for trace organic contaminant removal: Current state and future potential. Journal of environmental management, 2012. 111: p. 195-207.

5.   Marco-Urrea, E., Pérez-Trujillo, M., Vicent, T., and Caminal, G., Ability of white-rot fungi to remove selected pharmaceuticals and identification of degradation products of ibuprofen by Trametes versicolor. Chemosphere, 2009. 74(6): p. 765-772.

6.   Naghdi, M., Taheran, M., Brar, S.K., Kermanshahi-pour, A., Verma, M., and Surampalli, R., Immobilized laccase on oxygen functionalized nanobiochars through mineral acids treatment for removal of carbamazepine. Science of The Total Environment, 2017.

7.   Lienert, J., Güdel, K., and Escher, B.I., Screening method for ecotoxicological hazard assessment of 42 pharmaceuticals considering human metabolism and excretory routes. Environmental science & technology, 2007. 41(12): p. 4471-4478.

8.   Burkhardt-Holm, P., Linking water quality to human health and environment: The fate of micropollutants. Inst. Water Policy Natl. Univ. Singapore, 2011: p. 1-62.

9.   Lagesson, A., Fahlman, J., Brodin, T., Fick, J., Jonsson, M., Byström, P., and Klaminder, J., Bioaccumulation of five pharmaceuticals at multiple trophic levels in an aquatic food web - Insights from a field experiment. Science of The Total Environment, 2016. 568(Supplement C): p. 208-215.

10.   Nazaret, S. and Aminov, R., Role and prevalence of antibiosis and the related resistance genes in the environment. Frontiers in microbiology, 2013. 5: p. 520-520.

11.   De García, S.O., Pinto, G.P., García-Encina, P.A., and Mata, R.I., Ranking of concern, based on environmental indexes, for pharmaceutical and personal care products: an application to the Spanish case. Journal of environmental management, 2013. 129: p. 384-397.

12.   Kümmerer, K., Pharmaceuticals in the environment–a brief summary, in Pharmaceuticals in the Environment. 2008, Springer. p. 3-21.

13.   Lonappan, L., Brar, S.K., Das, R.K., Verma, M., and Surampalli, R.Y., Diclofenac and its transformation products: Environmental occurrence and toxicity-A review. Environment international, 2016. 96: p. 127-138.

14.   Mohapatra, D.P., Brar, S.K., Tyagi, R.D., Picard, P., and Surampalli, R.Y., Carbamazepine in municipal wastewater and wastewater sludge: Ultrafast quantification by laser diode thermal desorption-atmospheric pressure chemical ionization coupled with tandem mass spectrometry. Talanta, 2012. 99: p. 247-255.

15.   Stackelberg, P.E., Gibs, J., Furlong, E.T., Meyer, M.T., Zaugg, S.D., and Lippincott, R.L., Efficiency of conventional drinking-water-treatment processes in removal of pharmaceuticals and other organic compounds. Science of the Total Environment, 2007. 377(2): p. 255-272.

16.   Tadkaew, N., Hai, F.I., McDonald, J.A., Khan, S.J., and Nghiem, L.D., Removal of trace organics by MBR treatment: the role of molecular properties. Water research, 2011. 45(8): p. 2439-2451.

17.   Suárez, S., Carballa, M., Omil, F., and Lema, J.M., How are pharmaceutical and personal care products (PPCPs) removed from urban wastewaters? Reviews in Environmental Science and Bio/Technology, 2008. 7(2): p. 125-138.

18.   Ikehata, K., Jodeiri Naghashkar, N., and Gamal El-Din, M., Degradation of aqueous pharmaceuticals by ozonation and advanced oxidation processes: a review. Ozone: Science and Engineering, 2006. 28(6): p. 353-414.

19.   Radjenović, J., Petrović, M., Ventura, F., and Barceló, D., Rejection of pharmaceuticals in nanofiltration and reverse osmosis membrane drinking water treatment. Water Research, 2008. 42(14): p. 3601-3610.

20.   Kosjek, T., Andersen, H.R., Kompare, B., Ledin, A., and Heath, E., Fate of carbamazepine during water treatment. Environmental science & technology, 2009. 43(16): p. 6256-6261.

21.   Westerhoff, P., Moon, H., Minakata, D., and Crittenden, J., Oxidation of organics in retentates from reverse osmosis wastewater reuse facilities. Water research, 2009. 43(16): p. 3992-3998.

22.   Bathen, D., Physical waves in adsorption technology-an overview. Separation and Purification Technology, 2003. 33(2): p. 163-177.

23.   Nghiem, L.D., Coleman, P.J., and Espendiller, C., Mechanisms underlying the effects of membrane fouling on the nanofiltration of trace organic contaminants. Desalination, 2010. 250(2): p. 682-687.

24.   Taheran, M., Brar, S.K., Verma, M., Surampalli, R.Y., Zhang, T.C., and Valéro, J.R., Membrane processes for removal of pharmaceutically active compounds (PhACs) from water and wastewaters. Science of The Total Environment, 2016. 547: p. 60-77.

25.   Asif, M.B., Hai, F.I., Singh, L., Price, W.E., and Nghiem, L.D., Degradation of Pharmaceuticals and Personal Care Products by White-Rot Fungi-a Critical Review. Current Pollution Reports, 2017: p. 1-16.

26.   Senthivelan, T., Kanagaraj, J., and Panda, R., Recent trends in fungal laccase for various industrial applications: An eco-friendly approach-A review. Biotechnology & Bioprocess Engineering, 2016. 21(1).

27.   Demarche, P., Junghanns, C., Nair, R.R., and Agathos, S.N., Harnessing the power of enzymes for environmental stewardship. Biotechnology advances, 2012. 30(5): p. 933-953.

28.   Wen, X., Jia, Y., and Li, J., Degradation of tetracycline and oxytetracycline by crude lignin peroxidase prepared from Phanerochaete chrysosporium-a white rot fungus. Chemosphere, 2009. 75(8): p. 1003-1007.

29.   Rodrıguez, E., Nuero, O., Guillén, F., Martınez, A., and Martınez, M., Degradation of phenolic and non-phenolic aromatic pollutants by four Pleurotus species: the role of laccase and versatile peroxidase. Soil Biology and Biochemistry, 2004. 36(6): p. 909-916.

30.   Bumpus, J., Tien, M., Wright, D., and Aust, S., Oxidation of persistent environmental pollutants by a white rot fungus. Science, 1985. 228(4706): p. 1434-1436.

31.   Bauer, C.G., Kühn, A., Gajovic, N., Skorobogatko, O., Holt, P.-J., Bruce, N.C., Makower, A., Lowe, C.R., and Scheller, F.W., New enzyme sensors for morphine and codeine based on morphine dehydrogenase and laccase. Fresenius' Journal of Analytical Chemistry, 1999. 364(1): p. 179-183.

32.   Martens, R., Wetzstein, H.G., Zadrazil, F., Capelari, M., Hoffmann, P., and Schmeer, N., Degradation of the fluoroquinolone enrofloxacin by wood-rotting fungi. Applied and Environmental Microbiology, 1996. 62(11): p. 4206-9.

33.   Grandclément, C., Seyssiecq, I., Piram, A., Wong-Wah-Chung, P., Vanot, G., Tiliacos, N., Roche, N., and Doumenq, P., From the conventional biological wastewater treatment to hybrid processes, the evaluation of organic micropollutant removal: A review. Water Research, 2017.

34.   Arora, D.S. and Sharma, R.K., Ligninolytic fungal laccases and their biotechnological applications. Applied biochemistry and biotechnology, 2010. 160(6): p. 1760-1788.

35.   Carvalho, A., Fonseca, T., Mattos, M., Oliveira, M., Lemos, T., Molinari, F., Romano, D., and Serra, I., Recent Advances in Lipase-Mediated Preparation of Pharmaceuticals and Their Intermediates. International Journal of Molecular Sciences, 2015. 16(12): p. 26191.

36.   Duran, N. and Esposito, E., Potential applications of oxidative enzymes and phenoloxidase-like compounds in wastewater and soil treatment: a review. Applied catalysis B: environmental, 2000. 28(2): p. 83-99.

37.   Christian, V., Shrivastava, R., Shukla, D., Modi, H.A., and Vyas, B.R.M., Degradation of xenobiotic compounds by lignin-degrading white-rot fungi: Enzymology and mechanisms involved. Indian Journal of Experimental Biology, 2005. 43(04): p. 301-312.

38.   Garcia-Ruiz, E., Mate, D.M., Gonzalez-Perez, D., Molina-Espeja, P., Camarero, S., Martínez, A.T., Ballesteros, A.O., and Alcalde, M., Directed evolution of ligninolytic oxidoreductases: From functional expression to stabilization and beyond. Cascade Biocatalysis, 2014: p. 1-22.

39.   Asgher, M., Asad, M.J., Bhatti, H.N., and Legge, R.L., Hyperactivation and thermostabilization of Phanerochaete chrysosporium lignin peroxidase by immobilization in xerogels. World Journal of Microbiology and Biotechnology, 2007. 23(4): p. 525-531.

40.   Hirai, H., Sugiura, M., Kawai, S., and Nishida, T., Characteristics of novel lignin peroxidases produced by white-rot fungus Phanerochaete sordida YK-624. FEMS microbiology letters, 2005. 246(1): p. 19-24.

41.   Christian, V., Shrivastava, R., Shukla, D., Modi, H., and Vyas, B.R.M., Mediator role of veratryl alcohol in the lignin peroxidase-catalyzed oxidative decolorization of Remazol Brilliant Blue R. Enzyme and microbial technology, 2005. 36(2): p. 327-332.

42.   Wong, D.W.S., Structure and Action Mechanism of Ligninolytic Enzymes. Applied Biochemistry and Biotechnology, 2009. 157(2): p. 174-209.

43.   CHENG, X.B., Rong, J., Ping-Sheng, L., Qin, Z., Shi-Qian, T., and Wen-Zhong, T., Studies on the properties and co-immobilization of manganese peroxidase. Chinese Journal of Biotechnology, 2007. 23(1): p. 90-96.

44.   Baborová, P., Möder, M., Baldrian, P., Cajthamlová, K., and Cajthaml, T., Purification of a new manganese peroxidase of the white-rot fungus Irpex lacteus, and degradation of polycyclic aromatic hydrocarbons by the enzyme. Research in Microbiology, 2006. 157(3): p. 248-253.

45.   Camarero, S., Sarkar, S., Ruiz-Dueñas, F.J., Martínez, M.a.J., and Martínez, Á.T., Description of a versatile peroxidase involved in the natural degradation of lignin that has both manganese peroxidase and lignin peroxidase substrate interaction sites. Journal of Biological Chemistry, 1999. 274(15): p. 10324-10330.

46.   Yang, S., Hai, F.I., Nghiem, L.D., Price, W.E., Roddick, F., Moreira, M.T., and Magram, S.F., Understanding the factors controlling the removal of trace organic contaminants by white-rot fungi and their lignin modifying enzymes: a critical review. Bioresource technology, 2013. 141: p. 97-108.

47.   Quaratino, D., Federici, F., Petruccioli, M., Fenice, M., and D'Annibale, A., Production, purification and partial characterisation of a novel laccase from the white-rot fungus Panus tigrinus CBS 577.79. Antonie van Leeuwenhoek, 2007. 91(1): p. 57-69.

48.   Zouari-Mechichi, H., Mechichi, T., Dhouib, A., Sayadi, S., Martínez, A.T., and Martínez, M.J., Laccase purification and characterization from Trametes trogii isolated in Tunisia: decolorization of textile dyes by the purified enzyme. Enzyme and Microbial Technology, 2006. 39(1): p. 141-148.

49.   Nguyen, L.N., Hai, F.I., Price, W.E., Leusch, F.D., Roddick, F., Ngo, H.H., Guo, W., Magram, S.F., and Nghiem, L.D., The effects of mediator and granular activated carbon addition on degradation of trace organic contaminants by an enzymatic membrane reactor. Bioresource technology, 2014. 167: p. 169-177.

50.   Strong, P. and Claus, H., Laccase: a review of its past and its future in bioremediation. Critical Reviews in Environmental Science and Technology, 2011. 41(4): p. 373-434.

51.   Lundell, T.K., Mäkelä, M.R., and Hildén, K., Lignin-modifying enzymes in filamentous basidiomycetes-ecological, functional and phylogenetic review. Journal of basic microbiology, 2010. 50(1): p. 5-20.

52.   Martínková, L., Kotik, M., Marková, E., and Homolka, L., Biodegradation of phenolic compounds by Basidiomycota and its phenol oxidases: A review. Chemosphere, 2016. 149: p. 373-382.

53.   Yang, S., Hai, F.I., Nghiem, L.D., Roddick, F., and Price, W.E., Removal of trace organic contaminants by nitrifying activated sludge and whole-cell and crude enzyme extract of Trametes versicolor. Water Science and Technology, 2013. 67(6): p. 1216-1223.

54.   Nguyen, L.N., Hai, F.I., Yang, S., Kang, J., Leusch, F.D., Roddick, F., Price, W.E., and Nghiem, L.D., Removal of trace organic contaminants by an MBR comprising a mixed culture of bacteria and white-rot fungi. Bioresource technology, 2013. 148: p. 234-241.

55. Nguyen, L.N., Hai, F.I., Kang, J., Leusch, F.D., Roddick, F., Magram, S.F., Price, W.E., and Nghiem, L.D., Enhancement of trace organic contaminant degradation by crude enzyme extract from Trametes versicolor culture: Effect of mediator type and concentration. Journal of the Taiwan Institute of Chemical Engineers, 2014. 45(4): p. 1855-1862.

56. Nguyen, L.N., van de Merwe, J.P., Hai, F.I., Leusch, F.D., Kang, J., Price, W.E., Roddick, F., Magram, S.F., and Nghiem, L.D., Laccase-syringaldehyde-mediated degradation of trace organic contaminants in an enzymatic membrane reactor: Removal efficiency and effluent toxicity. Bioresource technology, 2016. 200: p. 477-484.

57. Fernández-Fernández, M., Sanromán, M.Á., and Moldes, D., Recent developments and applications of immobilized laccase. Biotechnology advances, 2013. 31(8): p. 1808-1825.

58. Kersten, P.J., Glyoxal oxidase of Phanerochaete chrysosporium: its characterization and activation by lignin peroxidase. Proceedings of the National Academy of Sciences, 1990. 87(8): p. 2936-2940.

59. Gold, M.H., Wariishi, H., and Valli, K., Extracellular peroxidases involved in lignin degradation by the white rot basidiomycete Phanerochaete chrysosporium. 1989, ACS Publications.

60. Christian, V., Shrivastava, R., Shukla, D., Modi, H., and Vyas, B., Degradation of xenobiotic compounds by lignin-degrading white-rot fungi: enzymology and mechanisms involved. 2005.

61. Golan-Rozen, N., Chefetz, B., Ben-Ari, J., Geva, J., and Hadar, Y., Transformation of the recalcitrant pharmaceutical compound carbamazepine by Pleurotus ostreatus: role of cytochrome P450 monooxygenase and manganese peroxidase. Environmental science & technology, 2011. 45(16): p. 6800-6805.

62.   Zhang, Y. and Geißen, S.U., In vitro degradation of carbamazepine and diclofenac by crude lignin peroxidase. Journal of Hazardous Materials, 2010. 176(1-3): p. 1089-1092.

63.   Taheran, M., Naghdi, M., Brar, S.K., Knystautas, E.J., Verma, M., and Surampalli, R.Y., Covalent Immobilization of Laccase onto Nanofibrous Membrane for Degradation of Pharmaceutical Residues in Water. ACS Sustainable Chemistry & Engineering, 2017.

64.   Asgher, M., Bhatti, H.N., Ashraf, M., and Legge, R.L., Recent developments in biodegradation of industrial pollutants by white rot fungi and their enzyme system. Biodegradation, 2008. 19(6): p. 771.

65.   Hata, T., Shintate, H., Kawai, S., Okamura, H., and Nishida, T., Elimination of carbamazepine by repeated treatment with laccase in the presence of 1-hydroxybenzotriazole. Journal of Hazardous Materials, 2010. 181(1–3): p. 1175-1178.

66.   Tran, N.H., Urase, T., and Kusakabe, O., Biodegradation characteristics of pharmaceutical substances by whole fungal culture Trametes versicolor and its laccase. Journal of Water and Environment Technology, 2010. 8(2): p. 125-140.

67.   Hata, T., Kawai, S., Okamura, H., and Nishida, T., Removal of diclofenac and mefenamic acid by the white rot fungus Phanerochaete sordida YK-624 and identification of their metabolites after fungal transformation. Biodegradation, 2010. 21(5): p. 681-689.

68.   Pointing, S., Feasibility of bioremediation by white-rot fungi. Applied microbiology and biotechnology, 2001. 57(1): p. 20-33.

69.   Rouches, E., Herpoël-Gimbert, I., Steyer, J., and Carrere, H., Improvement of anaerobic degradation by white-rot fungi pretreatment of lignocellulosic biomass: a review. Renewable and Sustainable Energy Reviews, 2016. 59: p. 179-198.

70.   González, L.F., Sarria, V., and Sánchez, O.F., Degradation of chlorophenols by sequential biological-advanced oxidative process using Trametes pubescens and TiO 2/UV. Bioresource technology, 2010. 101(10): p. 3493-3499.

71.   Guo, X.I., Zhu, Z.W., and Li, H.I., Biodegradation of sulfamethoxazole by Phanerochaete chrysosporium. Journal of Molecular Liquids, 2014. 198: p. 169-172.

72.   Lucas, D., Castellet-Rovira, F., Villagrasa, M., Badia-Fabregat, M., Barceló, D., Vicent, T., Caminal, G., Sarrà, M., and Rodríguez-Mozaz, S., The role of sorption processes in the removal of pharmaceuticals by fungal treatment of wastewater. Science of The Total Environment, 2018. 610-611(Supplement C): p. 1147-1153.

73.   Rodarte-Morales, A., Feijoo, G., Moreira, M., and Lema, J., Degradation of selected pharmaceutical and personal care products (PPCPs) by white-rot fungi. World Journal of Microbiology and Biotechnology, 2011. 27(8): p. 1839-1846.

74.   Cruz-Morató, C., Ferrando-Climent, L., Rodriguez-Mozaz, S., Barceló, D., Marco-Urrea, E., Vicent, T., and Sarrà, M., Degradation of pharmaceuticals in non-sterile urban wastewater by Trametes versicolor in a fluidized bed bioreactor. Water research, 2013. 47(14): p. 5200-5210.

75.   Nguyen, L.N., Hai, F.I., Yang, S., Kang, J., Leusch, F.D.L., Roddick, F., Price, W.E., and Nghiem, L.D., Removal of pharmaceuticals, steroid hormones, phytoestrogens, UV-filters, industrial chemicals and pesticides by Trametes versicolor: Role of biosorption and biodegradation. International Biodeterioration & Biodegradation, 2014. 88: p. 169-175.

76.   Rodríguez-Rodríguez, C.E., Jelić, A., Llorca, M., Farré, M., Caminal, G., Petrović, M., Barceló, D., and Vicent, T., Solid-phase treatment with the fungus Trametes versicolor substantially reduces pharmaceutical concentrations and toxicity from sewage sludge. Bioresource technology, 2011. 102(10): p. 5602-5608.

77. Wang, J., Majima, N., Hirai, H., and Kawagishi, H., Effective removal of endocrine-disrupting compounds by lignin peroxidase from the white-rot fungus Phanerochaete sordida YK-624. Current microbiology, 2012. 64(3): p. 300-303.

78. Parshikov, I., Heinze, T., Moody, J., Freeman, J., Williams, A., and Sutherland, J., The fungus Pestalotiopsis guepini as a model for biotransformation of ciprofloxacin and norfloxacin. Applied microbiology and biotechnology, 2001. 56(3): p. 474-477.

79. Parshikov, I.A., Miriyala, B., Muraleedharan, K.M., Illendula, A., Avery, M.A., and Williamson, J.S., Biocatalysis of the Antimalarial Artemisinin by Mucor ramannianus. Strains. Pharmaceutical biology, 2005. 43(7): p. 579-582.

80. Zhan, Y., Wu, Y., Xu, F., Bai, Y., Guan, Y., Williamson, J.S., and Liu, B., A novel dihydroxylated derivative of artemisinin from microbial transformation. Fitoterapia, 2017. 120: p. 93-97.

81. Parshikov, I.A., Freeman, J.P., Lay, J.O., Beger, R.D., Williams, A.J., and Sutherland, J.B., Regioselective transformation of ciprofloxacin to N-acetylciprofloxacin by the fungus Mucor ramannianus. FEMS microbiology letters, 1999. 177(1): p. 131-135.

82. Marco-Urrea, E., Pérez-Trujillo, M., Cruz-Morató, C., Caminal, G., and Vicent, T., White-rot fungus-mediated degradation of the analgesic ketoprofen and identification of intermediates by HPLC–DAD–MS and NMR. Chemosphere, 2010. 78(4): p. 474-481.

83. García-Galán, M.J., Rodríguez-Rodríguez, C.E., Vicent, T., Caminal, G., Díaz-Cruz, M.S., and Barceló, D., Biodegradation of sulfamethazine by Trametes versicolor: Removal from sewage sludge and identification of intermediate products by UPLC-QqTOF-MS. Science of The Total Environment, 2011. 409(24): p. 5505-5512.

84. Buchicchio, A., Bianco, G., Sofo, A., Masi, S., and Caniani, D., Biodegradation of carbamazepine and clarithromycin by Trichoderma harzianum and Pleurotus ostreatus investigated by liquid chromatography – high-resolution tandem mass

spectrometry (FTICR MS-IRMPD). Science of The Total Environment, 2016. 557: p. 733-739.

85.   Marco-Urrea, E., Pérez-Trujillo, M., Blánquez, P., Vicent, T., and Caminal, G., Biodegradation of the analgesic naproxen by Trametes versicolor and identification of intermediates using HPLC-DAD-MS and NMR. Bioresource technology, 2010. 101(7): p. 2159-2166.

86.   Prieto, A., Möder, M., Rodil, R., Adrian, L., and Marco-Urrea, E., Degradation of the antibiotics norfloxacin and ciprofloxacin by a white-rot fungus and identification of degradation products. Bioresource technology, 2011. 102(23): p. 10987-10995.

87.   Rodríguez-Rodríguez, C.E., Marco-Urrea, E., and Caminal, G., Naproxen degradation test to monitor Trametes versicolor activity in solid-state bioremediation processes. Journal of Hazardous materials, 2010. 179(1): p. 1152-1155.

88.   Rodríguez-Rodríguez, C.E., García-Galán, M.J., Blánquez, P., Díaz-Cruz, M.S., Barceló, D., Caminal, G., and Vicent, T., Continuous degradation of a mixture of sulfonamides by Trametes versicolor and identification of metabolites from sulfapyridine and sulfathiazole. Journal of hazardous materials, 2012. 213: p. 347-354.

89.   Rodarte-Morales, A., Feijoo, G., Moreira, M., and Lema, J., Biotransformation of three pharmaceutical active compounds by the fungus Phanerochaete chrysosporium in a fed batch stirred reactor under air and oxygen supply. Biodegradation, 2012. 23(1): p. 145-156.

90.   Rodarte-Morales, A., Feijoo, G., Moreira, M., and Lema, J., Operation of stirred tank reactors (STRs) and fixed-bed reactors (FBRs) with free and immobilized Phanerochaete chrysosporium for the continuous removal of pharmaceutical compounds. Biochemical engineering journal, 2012. 66: p. 38-45.

91.   Espinosa-Ortiz, E.J., Rene, E.R., Pakshirajan, K., van Hullebusch, E.D., and Lens, P.N., Fungal pelleted reactors in wastewater treatment: applications and perspectives. Chemical Engineering Journal, 2016. 283: p. 553-571.

92.   Van Leeuwen, J., Hu, Z., Yi, T., Pometto III, A., and Jin, B., Kinetic model for selective cultivation of microfungi in a microscreen process for food processing wastewater treatment and biomass production. Engineering in Life Sciences, 2003. 23(2-3): p. 289-300.

93.   Mir-Tutusaus, J., Sarrà, M., and Caminal, G., Continuous treatment of non-sterile hospital wastewater by Trametes versicolor: How to increase fungal viability by means of operational strategies and pretreatments. Journal of Hazardous Materials, 2016. 318: p. 561-570.

94.   Jelic, A., Cruz-Morató, C., Marco-Urrea, E., Sarrà, M., Perez, S., Vicent, T., Petrović, M., and Barcelo, D., Degradation of carbamazepine by Trametes versicolor in an air pulsed fluidized bed bioreactor and identification of intermediates. Water research, 2012. 46(4): p. 955-964.

95.   Li, X., de Toledo, R.A., Wang, S., and Shim, H., Removal of carbamazepine and naproxen by immobilized Phanerochaete chrysosporium under non-sterile condition. New biotechnology, 2015. 32(2): p. 282-289.

96.   Cruz-Morató, C., Lucas, D., Llorca, M., Rodriguez-Mozaz, S., Gorga, M., Petrovic, M., Barceló, D., Vicent, T., Sarrà, M., and Marco-Urrea, E., Hospital wastewater treatment by fungal bioreactor: removal efficiency for pharmaceuticals and endocrine disruptor compounds. Science of The Total Environment, 2014. 493: p. 365-376.

97.   Yang, S., Hai, F.I., Nghiem, L.D., Nguyen, L.N., Roddick, F., and Price, W.E., Removal of bisphenol A and diclofenac by a novel fungal membrane bioreactor operated under non-sterile conditions. International Biodeterioration & Biodegradation, 2013. 85: p. 483-490.

98.   Hatakka, A., Lignin-modifying enzymes from selected white-rot fungi: production and role from in lignin degradation. FEMS microbiology reviews, 1994. 13(2-3): p. 125-135.

99.   Zhang, Y. and Geißen, S.-U., Elimination of carbamazepine in a non-sterile fungal bioreactor. Bioresource technology, 2012. 112: p. 221-227.

100.   Rodarte-Morales, A.I., Feijoo, G., Moreira, M.T., and Lema, J.M., Evaluation of Two Operational Regimes: Fed-Batch and Continuous for the Removal of Pharmaceuticals in a Fungal Stirred Tank Reactor. CHEMICAL ENGINEERING, 2012. 27.

101.   Hai, F.I., Yamamoto, K., Nakajima, F., and Fukushi, K., Factors governing performance of continuous fungal reactor during non-sterile operation–the case of a membrane bioreactor treating textile wastewater. Chemosphere, 2009. 74(6): p. 810-817.

102.   Gao, D., Zeng, Y., Wen, X., and Qian, Y., Competition strategies for the incubation of white rot fungi under non-sterile conditions. Process Biochemistry, 2008. 43(9): p. 937-944.

103.   Ferrando-Climent, L., Cruz-Morató, C., Marco-Urrea, E., Vicent, T., Sarrà, M., Rodriguez-Mozaz, S., and Barceló, D., Non conventional biological treatment based on Trametes versicolor for the elimination of recalcitrant anticancer drugs in hospital wastewater. Chemosphere, 2015. 136: p. 9-19.

104.   Sahar, E., Ernst, M., Godehardt, M., Hein, A., Herr, J., Kazner, C., Melin, T., Cikurel, H., Aharoni, A., Messalem, R., Brenner, A., and Jekel, M., Comparison of two treatments for the removal of selected organic micropollutants and bulk organic matter: conventional activated sludge followed by ultrafiltration versus membrane bioreactor. Water Science and Technology, 2011. 63(4): p. 733-740.

105.   Vergeynst, L., Haeck, A., De Wispelaere, P., Van Langenhove, H., and Demeestere, K., Multi-residue analysis of pharmaceuticals in wastewater by liquid chromatography-magnetic sector mass spectrometry: Method quality

assessment and application in a Belgian case study. Chemosphere, 2015. 119(Supplement): p. S2-S8.

106. Zuehlke, S., Duennbier, U., Lesjean, B., Gnirss, R., and Buisson, H., Long-Term Comparison of Trace Organics Removal Performances Between Conventional and Membrane Activated Sludge Processes. Water Environment Research, 2006. 78(13): p. 2480-2486.

107. Rosal, R., Rodríguez, A., Perdigón-Melón, J.A., Petre, A., García-Calvo, E., Gómez, M.J., Agüera, A., and Fernández-Alba, A.R., Occurrence of emerging pollutants in urban wastewater and their removal through biological treatment followed by ozonation. Water Research, 2010. 44(2): p. 578-588.

108. Tiwari, B., Sellamuthu, B., Ouarda, Y., Drogui, P., Tyagi, R.D., and Buelna, G., Review on fate and mechanism of removal of pharmaceutical pollutants from wastewater using biological approach. Bioresource Technology, 2017. 224(Supplement C): p. 1-12.

109. Sutar, R.S. and Rathod, V.K., Ultrasound assisted enzymatic degradation of diclofenac sodium: Optimization of process parameters and kinetics. Journal of Water Process Engineering, 2016. 9: p. e1-e6.

110. Becker, D., Della Giustina, S.V., Rodriguez-Mozaz, S., Schoevaart, R., Barceló, D., de Cazes, M., Belleville, M.P., Sanchez-Marcano, J., de Gunzburg, J., and Couillerot, O., Removal of antibiotics in wastewater by enzymatic treatment with fungal laccase–Degradation of compounds does not always eliminate toxicity. Bioresource Technology, 2016. 219: p. 500-509.

111. Rahmani, K., Faramarzi, M.A., Mahvi, A.H., Gholami, M., Esrafili, A., Forootanfar, H., and Farzadkia, M., Elimination and detoxification of sulfathiazole and sulfamethoxazole assisted by laccase immobilized on porous silica beads. International Biodeterioration & Biodegradation, 2015. 97: p. 107-114.

112. Marco-Urrea, E., Pérez-Trujillo, M., Cruz-Morató, C., Caminal, G., and Vicent, T., Degradation of the drug sodium diclofenac by Trametes versicolor pellets

and identification of some intermediates by NMR. Journal of Hazardous Materials, 2010. 176(1): p. 836-842.

113. Stadlmair, L.F., Letzel, T., Drewes, J.E., and Graßmann, J., Mass spectrometry based in vitro assay investigations on the transformation of pharmaceutical compounds by oxidative enzymes. Chemosphere, 2017. 174(Supplement C): p. 466-477.

114. Eibes, G., Debernardi, G., Feijoo, G., Moreira, M.T., and Lema, J.M., Oxidation of pharmaceutically active compounds by a ligninolytic fungal peroxidase. Biodegradation, 2011. 22(3): p. 539-550.

115. Schwarz, J., Aust, M.O., and Thiele-Bruhn, S., Metabolites from fungal laccase-catalysed transformation of sulfonamides. Chemosphere, 2010. 81(11): p. 1469-1476.

116. Lonappan, L., Rouissi, T., Laadila, M.A., Brar, S.K., Hernández-Galán, L., Verma, M., and Surampalli, R.Y., Agro-industrial produced laccase for degradation of diclofenac and identification of transformation products. ACS Sustainable Chemistry & Engineering, 2017.

117. Gros, M., Cruz-Morato, C., Marco-Urrea, E., Longrée, P., Singer, H., Sarrà, M., Hollender, J., Vicent, T., Rodriguez-Mozaz, S., and Barceló, D., Biodegradation of the X-ray contrast agent iopromide and the fluoroquinolone antibiotic ofloxacin by the white rot fungus Trametes versicolor in hospital wastewaters and identification of degradation products. Water Research, 2014. 60(Supplement C): p. 228-241.

118. Spengler, P., Körner, W., and Metzger, J.W., Substances with estrogenic activity in effluents of sewage treatment plants in southwestern Germany. 1. Chemical analysis. Environmental Toxicology and Chemistry, 2001. 20(10): p. 2133-2141.

119. Routledge, E.J. and Sumpter, J.P., Estrogenic activity of surfactants and some of their degradation products assessed using a recombinant yeast screen. Environmental Toxicology and Chemistry, 1996. 15(3): p. 241-248.

120. Bistan, M., Podgorelec, M., Marinšek Logar, R., and Tišler, T., Yeast estrogen screen assay as a tool for detecting estrogenic activity in water bodies. Food Technology and Biotechnology, 2012. 50(4): p. 427-433.

121. Cruz-Morató, C., Rodríguez-Rodríguez, C., Marco-Urrea, E., Sarrà, M., Caminal, G., Vicent, T., Jelić, A., García-Galán, M., Pérez, S., and Díaz-Cruz, M., Biodegradation of pharmaceuticals by fungi and metabolites identification, in Emerging organic contaminants in sludges. 2012, Springer. p. 165-213.

122. Kang, S.I., Kang, S.Y., and Hur, H.G., Identification of fungal metabolites of anticonvulsant drug carbamazepine. Applied microbiology and biotechnology, 2008. 79(4): p. 663.

123. Wetzstein, H.G., Stadler, M., Tichy, H.V., Dalhoff, A., and Karl, W., Degradation of Ciprofloxacin by Basidiomycetes and Identification of Metabolites Generated by the Brown Rot FungusGloeophyllum striatum. Applied and environmental microbiology, 1999. 65(4): p. 1556-1563.

124. Parshikov, I.A., Moody, J.D., Freeman, J.P., Lay Jr, J.O., Williams, A.J., Heinze, T.M., and Sutherland, J.B., Formation of conjugates from ciprofloxacin and norfloxacin in cultures of Trichoderma viride. Mycologia, 2002. 94(1): p. 1-5.

125. Wetzstein, H.G., Schmeer, N., and Karl, W., Degradation of the fluoroquinolone enrofloxacin by the brown rot fungus Gloeophyllum striatum: identification of metabolites. Applied and Environmental Microbiology, 1997. 63(11): p. 4272-4281.

126. Wetzstein, H.G., Schneider, J., and Karl, W., Patterns of metabolites produced from the fluoroquinolone enrofloxacin by basidiomycetes indigenous to agricultural sites. Applied microbiology and biotechnology, 2006. 71(1): p. 90-100.

127. Parshikov, I.A., Freeman, J.P., Lay, J.O., Beger, R.D., Williams, A.J., and Sutherland, J.B., Microbiological transformation of enrofloxacin by the fungus Mucor ramannianus. Applied and environmental microbiology, 2000. 66(6): p. 2664-2667.

128. Llorca, M., Rodríguez-Mozaz, S., Couillerot, O., Panigoni, K., de Gunzburg, J., Bayer, S., Czaja, R., and Barceló, D., Identification of new transformation products during enzymatic treatment of tetracycline and erythromycin antibiotics at laboratory scale by an on-line turbulent flow liquid-chromatography coupled to a high resolution mass spectrometer LTQ-Orbitrap. Chemosphere, 2015. 119: p. 90-98.

129. Golan-Rozen, N., Seiwert, B., Riemenschneider, C., Reemtsma, T., Chefetz, B., and Hadar, Y., Transformation pathways of the recalcitrant pharmaceutical compound carbamazepine by the white-rot fungus Pleurotus ostreatus: Effects of growth conditions. Environmental science & technology, 2015. 49(20): p. 12351-12362.

130. Baldrian, P., Fungal laccases-occurrence and properties. FEMS microbiology reviews, 2006. 30(2): p. 215-242.

131. De Cazes, M., Abejón, R., Belleville, M.-P., and Sanchez-Marcano, J., Membrane bioprocesses for pharmaceutical micropollutant removal from waters. Membranes, 2014. 4(4): p. 692-729.

132. Jochems, P., Satyawali, Y., Diels, L., and Dejonghe, W., Enzyme immobilization on/in polymeric membranes: status, challenges and perspectives in biocatalytic membrane reactors (BMRs). Green chemistry, 2011. 13(7): p. 1609-1623.

133. Nguyen, L.N., Hai, F.I., Price, W.E., Kang, J., Leusch, F.D., Roddick, F., van de Merwe, J.P., Magram, S.F., and Nghiem, L.D., Degradation of a broad spectrum of trace organic contaminants by an enzymatic membrane reactor: Complementary role of membrane retention and enzymatic degradation. International Biodeterioration & Biodegradation, 2015. 99: p. 115-122.

134. Nguyen, L.N., Hai, F.I., Price, W.E., Leusch, F.D., Roddick, F., McAdam, E.J., Magram, S.F., and Nghiem, L.D., Continuous biotransformation of bisphenol A and diclofenac by laccase in an enzymatic membrane reactor. International Biodeterioration & Biodegradation, 2014. 95: p. 25-32.

135. Margot, J., Bennati-Granier, C., Maillard, J., Blánquez, P., Barry, D.A., and Holliger, C., Bacterial versus fungal laccase: potential for micropollutant degradation. AMB Express, 2013. 3(1): p. 63.

136. Lloret, L., Eibes, G., Lú-Chau, T.A., Moreira, M.T., Feijoo, G., and Lema, J.M., Laccase-catalyzed degradation of anti-inflammatories and estrogens. Biochemical Engineering Journal, 2010. 51(3): p. 124-131.

137. Wang, J. and Wang, S., Removal of pharmaceuticals and personal care products (PPCPs) from wastewater: A review. Journal of Environmental Management, 2016. 182: p. 620-640.

138. Lu, J., Huang, Q., and Mao, L., Removal of acetaminophen using enzyme-mediated oxidative coupling processes: I. Reaction rates and pathways. Environmental science & technology, 2009. 43(18): p. 7062-7067.

139. D'Acunzo, F., Galli, C., Gentili, P., and Sergi, F., Mechanistic and steric issues in the oxidation of phenolic and non-phenolic compounds by laccase or laccase-mediator systems. The case of bifunctional substrates. New Journal of Chemistry, 2006. 30(4): p. 583-591.

140. Kim, Y.J. and Nicell, J.A., Laccase-catalysed oxidation of aqueous triclosan. Journal of Chemical Technology and Biotechnology, 2006. 81(8): p. 1344-1352.

141. Fabbrini, M., Galli, C., and Gentili, P., Comparing the catalytic efficiency of some mediators of laccase. Journal of Molecular Catalysis B: Enzymatic, 2002. 16(5–6): p. 231-240.

142. Ashe, B., Nguyen, L.N., Hai, F.I., Lee, D.-J., van de Merwe, J.P., Leusch, F.D., Price, W.E., and Nghiem, L.D., Impacts of redox-mediator type on trace organic contaminants degradation by laccase: Degradation efficiency, laccase stability and effluent toxicity. International Biodeterioration & Biodegradation, 2016. 113: p. 169-176.

143. Astolfi, P., Brandi, P., Galli, C., Gentili, P., Gerini, M.F., Greci, L., and Lanzalunga, O., New mediators for the enzyme laccase: mechanistic features

and selectivity in the oxidation of non-phenolic substrates. New journal of chemistry, 2005. 29(10): p. 1308-1317.

144. Yang, S., Removal of micropollutants by a fungus-augmented membrane bioreactor. 2012, University of Wollongong.

145. Coniglio, A., Galli, C., Gentili, P., and Vadala, R., Oxidation of amides by laccase-generated aminoxyl radicals. Journal of Molecular Catalysis B: Enzymatic, 2008. 50(1): p. 40-49.

146. Suda, T., Hata, T., Kawai, S., Okamura, H., and Nishida, T., Treatment of tetracycline antibiotics by laccase in the presence of 1-hydroxybenzotriazole. Bioresource technology, 2012. 103(1): p. 498-501.

147. Margot, J., Copin, P.J., von Gunten, U., Barry, D.A., and Holliger, C., Sulfamethoxazole and isoproturon degradation and detoxification by a laccase-mediator system: Influence of treatment conditions and mechanistic aspects. Biochemical Engineering Journal, 2015. 103: p. 47-59.

148. Purich, D.L., Enzyme kinetics: catalysis and control: a reference of theory and best-practice methods. 2010: Elsevier.

149. Lloret, L., Eibes, G., Moreira, M., Feijoo, G., and Lema, J., On the use of a high-redox potential laccase as an alternative for the transformation of non-steroidal anti-inflammatory drugs (NSAIDs). Journal of Molecular Catalysis B: Enzymatic, 2013. 97: p. 233-242.

150. Weng, S.-S., Ku, K.L., and Lai, H.T., The implication of mediators for enhancement of laccase oxidation of sulfonamide antibiotics. Bioresource technology, 2012. 113: p. 259-264.

151. Sathishkumar, P., Mythili, A., Hadibarata, T., Jayakumar, R., Kanthimathi, M., Palvannan, T., Ponraj, M., Salim, M.R., and Yusoff, A.R.M., Laccase mediated diclofenac transformation and cytotoxicity assessment on mouse fibroblast 3T3-L1 preadipocytes. RSC Advances, 2014. 4(23): p. 11689-11697.

152. Mukhopadhyay, A., Dasgupta, A.K., and Chakrabarti, K., Enhanced functionality and stabilization of a cold active laccase using nanotechnology based activation-immobilization. Bioresource technology, 2015. 179: p. 573-584.

153. Sampaio, L.M., Padrão, J., Faria, J., Silva, J.P., Silva, C.J., Dourado, F., and Zille, A., Laccase immobilization on bacterial nanocellulose membranes: Antimicrobial, kinetic and stability properties. Carbohydrate polymers, 2016. 145: p. 1-12.

154. Bosco, F., Capolongo, A., and Ruggeri, B., Effect of temperature, pH, ionic strength, and sodium nitrate on activity of LiPs: Implications for bioremediation. Bioremediation journal, 2002. 6(1): p. 65-76.

155. Wen, X., Jia, Y., and Li, J., Enzymatic degradation of tetracycline and oxytetracycline by crude manganese peroxidase prepared from Phanerochaete chrysosporium. Journal of Hazardous Materials, 2010. 177(1-3): p. 924-928.

156. Margot, J., Maillard, J., Rossi, L., Barry, D.A., and Holliger, C., Influence of treatment conditions on the oxidation of micropollutants by Trametes versicolor laccase. New biotechnology, 2013. 30(6): p. 803-813.

157. Weng, S.S., Liu, S.M., and Lai, H.T., Application parameters of laccase–mediator systems for treatment of sulfonamide antibiotics. Bioresource technology, 2013. 141: p. 152-159.

158. Hu, X., Wang, C., Wang, L., Zhang, R., and Chen, H., Influence of temperature, pH and metal ions on guaiacol oxidation of purified laccase from Leptographium qinlingensis. World Journal of Microbiology and Biotechnology, 2014. 30(4): p. 1285-1290.

159. Wan, J., Zeng, G., Huang, D., Huang, C., Lai, C., Li, N., Wei, Z., Xu, P., He, X., and Lai, M., The oxidative stress of Phanerochaete chrysosporium against lead toxicity. Applied biochemistry and biotechnology, 2015. 175(4): p. 1981-1991.

160. Sondhi, S., Sharma, P., Saini, S., Puri, N., and Gupta, N., Purification and characterization of an extracellular, thermo-alkali-stable, metal tolerant laccase from Bacillus tequilensis SN4. PloS one, 2014. 9(5): p. e96951.

161. D'Souza-Ticlo, D., Sharma, D., and Raghukumar, C., A thermostable metal-tolerant laccase with bioremediation potential from a marine-derived fungus. Marine biotechnology, 2009. 11(6): p. 725-737.

162. Gianfreda, L., Sannino, F., Filazzola, M., and Leonowicz, A., Catalytic behavior and detoxifying ability of a laccase from the fungal strain Cerrena unicolor. Journal of Molecular Catalysis B: Enzymatic, 1998. 4(1-2): p. 13-23.

163. Blanford, C.F., Foster, C.E., Heath, R.S., and Armstrong, F.A., Efficient electrocatalytic oxygen reduction by the 'blue'copper oxidase, laccase, directly attached to chemically modified carbons. Faraday discussions, 2009. 140: p. 319-335.

164. Bento, I., Martins, L.O., Lopes, G.G., Carrondo, M.A., and Lindley, P.F., Dioxygen reduction by multi-copper oxidases; a structural perspective. Dalton Transactions, 2005(21): p. 3507-3513.

165. Xu, F., Oxidation of phenols, anilines, and benzenethiols by fungal laccases: correlation between activity and redox potentials as well as halide inhibition. Biochemistry, 1996. 35(23): p. 7608-7614.

166. Rodgers, C.J., Blanford, C.F., Giddens, S.R., Skamnioti, P., Armstrong, F.A., and Gurr, S.J., Designer laccases: a vogue for high-potential fungal enzymes? Trends in biotechnology, 2010. 28(2): p. 63-72.

167. Lu, J. and Huang, Q., Removal of acetaminophen using enzyme-mediated oxidative coupling processes: II. Cross-coupling with natural organic matter. Environmental science & technology, 2009. 43(18): p. 7068-7073.

168. Piccolo, A., Cozzolino, A., Conte, P., and Spaccini, R., Polymerization of humic substances by an enzyme-catalyzed oxidative coupling. Naturwissenschaften, 2000. 87(9): p. 391-394.

169. Cozzolino, A. and Piccolo, A., Polymerization of dissolved humic substances catalyzed by peroxidase. Effects of pH and humic composition. Organic Geochemistry, 2002. 33(3): p. 281-294.

170. Joutey, N.T., Bahafid, W., Sayel, H., El Ghachtouli, N., Chamy, R., and Rosenkranz, F., Biodegradation: involved microorganisms and genetically engineered microorganisms. Biodegradation-life of science. InTech, Rijeka, 2013. 289320.

171. Majeau, J.-A., Brar, S.K., and Tyagi, R.D., Laccases for removal of recalcitrant and emerging pollutants. Bioresource Technology, 2010. 101(7): p. 2331-2350.

172. Cabana, H., Jones, J., and Agathos, S., Elimination of endocrine disrupting chemicals using white rot fungi and their lignin modifying enzymes: a review. Engineering in Life Sciences, 2007. 7(5): p. 429-456.

173. Mateo, C., Palomo, J.M., Fernandez-Lorente, G., Guisan, J.M., and Fernandez-Lafuente, R., Improvement of enzyme activity, stability and selectivity via immobilization techniques. Enzyme and microbial technology, 2007. 40(6): p. 1451-1463.

174. Davis, S. and Burns, R.G., Covalent immobilization of laccase on activated carbon for phenolic effluent treatment. Applied microbiology and biotechnology, 1992. 37(4): p. 474-479.

175. Ji, C., Hou, J., Wang, K., Zhang, Y., and Chen, V., Biocatalytic degradation of carbamazepine with immobilized laccase-mediator membrane hybrid reactor. Journal of Membrane Science, 2016. 502: p. 11-20.

176. Durán, N., Rosa, M.A., D'Annibale, A., and Gianfreda, L., Applications of laccases and tyrosinases (phenoloxidases) immobilized on different supports: a review. Enzyme and microbial technology, 2002. 31(7): p. 907-931.

177. Daâssi, D., Rodríguez-Couto, S., Nasri, M., and Mechichi, T., Biodegradation of textile dyes by immobilized laccase from Coriolopsis gallica into Ca-alginate beads. International Biodeterioration & Biodegradation, 2014. 90: p. 71-78.

178. Cabana, H., Alexandre, C., Agathos, S.N., and Jones, J.P., Immobilization of laccase from the white rot fungus Coriolopsis polyzona and use of the immobilized biocatalyst for the continuous elimination of endocrine disrupting chemicals. Bioresource technology, 2009. 100(14): p. 3447-3458.

179. Cristóvão, R.O., Tavares, A.P., Brígida, A.I., Loureiro, J.M., Boaventura, R.A., Macedo, E.A., and Coelho, M.A.Z., Immobilization of commercial laccase onto green coconut fiber by adsorption and its application for reactive textile dyes degradation. Journal of Molecular Catalysis B: Enzymatic, 2011. 72(1): p. 6-12.

180. Cabana, H., Jones, J.P., and Agathos, S.N., Preparation and characterization of cross-linked laccase aggregates and their application to the elimination of endocrine disrupting chemicals. Journal of Biotechnology, 2007. 132(1): p. 23-31.

181. Sheldon, R.A., Enzyme immobilization: the quest for optimum performance. Advanced Synthesis & Catalysis, 2007. 349(8-9): p. 1289-1307.

182. Turło, J. and Turło, A., Application of mushroom cultures and isolated enzymes for biodegradation of organic environmental pollutants. Military Pharmacy and Medicine, 2013. 3: p. 27-36.

183. Lloret, L., Hollmann, F., Eibes, G., Feijoo, G., Moreira, M., and Lema, J., Immobilisation of laccase on Eupergit supports and its application for the removal of endocrine disrupting chemicals in a packed-bed reactor. Biodegradation, 2012. 23(3): p. 373-386.

184. Nguyen, L.N., Hai, F.I., Dosseto, A., Richardson, C., Price, W.E., and Nghiem, L.D., Continuous adsorption and biotransformation of micropollutants by granular activated carbon-bound laccase in a packed-bed enzyme reactor. Bioresource Technology, 2016. 210(Supplement C): p. 108-116.

185. Ji, C., Hou, J., and Chen, V., Cross-linked carbon nanotubes based biocatalytic membranes for micro-pollutants degradation: Performance, stability, and regeneration. Journal of Membrane Science, 2016.

186. Sathishkumar, P., Chae, J.C., Unnithan, A.R., Palvannan, T., Kim, H.Y., Lee, K.J., Cho, M., Kamala-Kannan, S., and Oh, B.T., Laccase-poly (lactic-co-glycolic acid)(PLGA) nanofiber: highly stable, reusable, and efficacious for the transformation of diclofenac. Enzyme and microbial technology, 2012. 51(2): p. 113-118.

187. Xu, R., Tang, R., Zhou, Q., Li, F., and Zhang, B., Enhancement of catalytic activity of immobilized laccase for diclofenac biodegradation by carbon nanotubes. Chemical Engineering Journal, 2015. 262: p. 88-95.

188. Xu, R., Si, Y., Li, F., and Zhang, B., Enzymatic removal of paracetamol from aqueous phase: horseradish peroxidase immobilized on nanofibrous membranes. Environmental Science and Pollution Research, 2015. 22(5): p. 3838-3846.

189. Arca-Ramos, A., Kumar, V., Eibes, G., Moreira, M., and Cabana, H., Recyclable cross-linked laccase aggregates coupled to magnetic silica microbeads for elimination of pharmaceuticals from municipal wastewater. Environmental Science and Pollution Research, 2016. 23(9): p. 8929-8939.

190. Kumar, V.V. and Cabana, H., Towards high potential magnetic biocatalysts for on-demand elimination of pharmaceuticals. Bioresource technology, 2016. 200: p. 81-89.

191. Cao, L., Immobilised enzymes: science or art? Current Opinion in Chemical Biology, 2005. 9(2): p. 217-226.

192. Ba, S., Jones, J.P., and Cabana, H., Hybrid bioreactor (HBR) of hollow fiber microfilter membrane and cross-linked laccase aggregates eliminate aromatic pharmaceuticals in wastewaters. Journal of hazardous materials, 2014. 280: p. 662-670.

193. Ba, S., Haroune, L., Cruz-Morató, C., Jacquet, C., Touahar, I.E., Bellenger, J.P., Legault, C.Y., Jones, J.P., and Cabana, H., Synthesis and characterization of combined cross-linked laccase and tyrosinase aggregates transforming

acetaminophen as a model phenolic compound in wastewaters. Science of the Total Environment, 2014. 487: p. 748-755.

194. Nair, R.R., Demarche, P., and Agathos, S.N., Formulation and characterization of an immobilized laccase biocatalyst and its application to eliminate organic micropollutants in wastewater. New biotechnology, 2013. 30(6): p. 814-823.

195. Shi, L., Ma, F., Han, Y., Zhang, X., and Yu, H., Removal of sulfonamide antibiotics by oriented immobilized laccase on Fe 3 O 4 nanoparticles with natural mediators. Journal of Hazardous materials, 2014. 279: p. 203-211.

196. Touahar, I.E., Haroune, L., Ba, S., Bellenger, J.P., and Cabana, H., Characterization of combined cross-linked enzyme aggregates from laccase, versatile peroxidase and glucose oxidase, and their utilization for the elimination of pharmaceuticals. Science of the Total Environment, 2014. 481: p. 90-99.

197. Arca-Ramos, A., Ammann, E., Gasser, C., Nastold, P., Eibes, G., Feijoo, G., Lema, J., Moreira, M., and Corvini, P.-X., Assessing the use of nanoimmobilized laccases to remove micropollutants from wastewater. Environmental Science and Pollution Research, 2016. 23(4): p. 3217-3228.

198. Taheran, M., Naghdi, M., Brar, S.K., Knystautas, E.J., Verma, M., and Surampalli, R.Y., Degradation of chlortetracycline using immobilized laccase on Polyacrylonitrile-biochar composite nanofibrous membrane. Science of The Total Environment, 2017. 605-606: p. 315-321.

199. Hai, F.I., Yamamoto, K., Nakajima, F., and Fukushi, K., Application of a GAC-coated hollow fiber module to couple enzymatic degradation of dye on membrane to whole cell biodegradation within a membrane bioreactor. Journal of membrane science, 2012. 389: p. 67-75.

200. Lloret, L., Eibes, G., Feijoo, G., Moreira, M., and Lema, J.M., Continuous biotransformation of estrogens by laccase in an enzymatic membrane reactor. Chemical Engineering, 2012. 27.

201. Cabana, H., Jones, J.P., and Agathos, S.N., Utilization of cross-linked laccase aggregates in a perfusion basket reactor for the continuous elimination of endocrine-disrupting chemicals. Biotechnology and bioengineering, 2009. 102(6): p. 1582-1592.

202. Sanchez Marcano, J.G. and Tsotsis, T.T., Membrane Bioreactors, in Catalytic Membranes and Membrane Reactors. 2004, Wiley-VCH Verlag GmbH & Co. KGaA. p. 133-168.

203. Rios, G., Belleville, M., Paolucci, D., and Sanchez, J., Progress in enzymatic membrane reactors-a review. Journal of Membrane Science, 2004. 242(1): p. 189-196.

204. Kanwar, L. and Goswami, P., Isolation of a Pseudomonas lipase produced in pure hydrocarbon substrate and its application in the synthesis of isoamyl acetate using membrane-immobilised lipase. Enzyme and Microbial Technology, 2002. 31(6): p. 727-735.

205. Hilal, N., Nigmatullin, R., and Alpatova, A., Immobilization of cross-linked lipase aggregates within microporous polymeric membranes. Journal of membrane science, 2004. 238(1): p. 131-141.

206. De Cazes, M., Belleville, M.-P., Petit, E., Llorca, M., Rodríguez-Mozaz, S., De Gunzburg, J., Barceló, D., and Sanchez-Marcano, J., Design and optimization of an enzymatic membrane reactor for tetracycline degradation. Catalysis Today, 2014. 236: p. 146-152.

207. de Cazes, M.d., Belleville, M.-P., Mougel, M., Kellner, H., and Sanchez-Marcano, J., Characterization of laccase-grafted ceramic membranes for pharmaceuticals degradation. Journal of Membrane Science, 2015. 476: p. 384-393.

208. Xu, J., Wang, Y., Hu, Y., Luo, G., and Dai, Y., Immobilization of lipase by filtration into a specially designed microstructure in the CA/PTFE composite membrane. Journal of Molecular Catalysis B: Enzymatic, 2006. 42(1): p. 55-63.

209. Belleville, M., Lozano, P., Iborra, J., and Rios, G., Preparation of hybrid membranes for enzymatic reaction. Separation and purification technology, 2001. 25(1): p. 229-233.

210. Durante, D., Casadio, R., Martelli, L., Tasco, G., Portaccio, M., De Luca, P., Bencivenga, U., Rossi, S., Di Martino, S., and Grano, V., Isothermal and non-isothermal bioreactors in the detoxification of waste waters polluted by aromatic compounds by means of immobilised laccase from Rhus vernicifera. Journal of molecular catalysis B: Enzymatic, 2004. 27(4): p. 191-206.

211. Chea, V., Paolucci-Jeanjean, D., Belleville, M., and Sanchez, J., Optimization and characterization of an enzymatic membrane for the degradation of phenolic compounds. Catalysis today, 2012. 193(1): p. 49-56.

212. Hou, J., Dong, G., Ye, Y., and Chen, V., Laccase immobilization on titania nanoparticles and titania-functionalized membranes. Journal of Membrane Science, 2014. 452: p. 229-240.

213. Sakaki, K., Giorno, L., and Drioli, E., Lipase-catalyzed optical resolution of racemic naproxen in biphasic enzyme membrane reactors. Journal of Membrane Science, 2001. 184(1): p. 27-38.

214. Trusek-Holownia, A. and Noworyta, A., An integrated process: Ester synthesis in an enzymatic membrane reactor and water sorption. Journal of biotechnology, 2007. 130(1): p. 47-56.

215. Paiva, A.L., Balcao, V.M., and Malcata, F.X., Kinetics and mechanisms of reactions catalyzed by immobilized lipases☆. Enzyme and microbial technology, 2000. 27(3): p. 187-204.

216. Yujun, W., Jian, X., Guangsheng, L., and Youyuan, D., Immobilization of lipase by ultrafiltration and cross-linking onto the polysulfone membrane surface. Bioresource technology, 2008. 99(7): p. 2299-2303.

217. Abejón, R., Belleville, M.P., and Sanchez-Marcano, J., Design, economic evaluation and optimization of enzymatic membrane reactors for antibiotics

degradation in wastewaters. Separation and Purification Technology, 2015. 156, Part 2: p. 183-199.

218. Anastasi, A., Spina, F., Romagnolo, A., Tigini, V., Prigione, V., and Varese, G.C., Integrated fungal biomass and activated sludge treatment for textile wastewaters bioremediation. Bioresource technology, 2012. 123: p. 106-111.

219. Sutar, R.S. and Rathod, V.K., Ultrasound assisted enzyme catalyzed degradation of Cetirizine dihydrochloride. Ultrasonics sonochemistry, 2015. 24: p. 80-86.

220. Sutar, R.S. and Rathod, V.K., Ultrasound assisted Laccase catalyzed degradation of Ciprofloxacin hydrochloride. Journal of Industrial and Engineering Chemistry, 2015. 31: p. 276-282.

221. Marco-Urrea, E., Radjenović, J., Caminal, G., Petrović, M., Vicent, T., and Barceló, D., Oxidation of atenolol, propranolol, carbamazepine and clofibric acid by a biological Fenton-like system mediated by the white-rot fungus Trametes versicolor. Water research, 2010. 44(2): p. 521-532.

Table 4.1.1 Physical-chemical properties and therapeutic functions of selected pharmaceuticals [23, 24]

Compound	Acronym	Molecular weight (g/mol)	Molecular formula	Classification	Water solubility (mg/L)	Log K_{ow}	pKa
Acetaminophen	ACT	151	$C_8H_9NO_2$	Analgesic, antipyretic	14000	0.46	9.5
Amitriptyline	AMP	277.403	$C_{20}H_{23}N$	Antidepressant	9.71	4.92	9.4
Atenolol	ATL	266.336	$C_{14}H_{22}N_2O_3$	Antihypertensive agent	13300	0.16	9.6
Bezafibrate	BFB	361.82	$C_{19}H_{20}ClNO_4$	Lipid regulator	Slight	4.25	3.44
Caffeine	CAF	194.19	$C_8H_{10}N_4O_2$	Stimulant drug	21600	-0.07	14
Carbamazepine	CBZ	236.27	$C_{15}H_{12}N_2O$	Anti-epileptic	17.7	2.45	13.9
Cetirizine	CET	388.89	$C_{21}H_{25}ClN_2O_3$	Antihistamine	101	1.70	$P_1 = 2.70$ $P_2 = 3.57$ $P_3 = 7.56$
Chlortetracycline	CTC	478.882	$C_{22}H_{23}ClN_2O_8$	Antibiotic	8.6	-0.68	$P_1 = 3.30$ $P_2 = 7.55$ $P_3 = 9.33$
Ciprofloxacine	CPF	331.346	$C_{17}H_{18}FN_3O_3$	Antibiotic	30000	0.28	6.09
Citalopram	CTL	324.392	$C_{20}H_{21}FN_2O$	Antidepressant	5.88	3.5	9.78
Diazepam	DZP	284.70	$C_{16}H_{13}ClN_2O$	Tranquilizers	50	2.82	3.4
Diclofenac	DCF	296.15	$C_{14}H_{11}C_{l2}NO_2$	Anti-inflammatory, analgesic	2.37	4.51	4.08
Doxycycline	DC	444.43	$C_{22}H_{24}N_2O_8$	Antibiotic	630	3.5	$P_1 = 3.4$ $P_2 = 7.7$ $P_3 = 9.7$
Enrofloxacin	EFC	359.4	$C_{19}H_{22}FN_3O_3$	Antibiotic	146	3.48	$P_1 = 5.94$ $P_2 = 8.70$
Erythromycin	ETM	733.93	$C_{37}H_{67}NO_{13}$	Antibiotic	2000	3.06	8.9
Fenofibrate	FEF	360.831	$C_{20}H_{21}ClO_4$	Anti-hyperlipidemic	250	5.19	-4.9
Fenoprofen	FEP	242	$C_{15}H_{14}O_3$	Anti-inflammatory	Slight	3.9	4.21
Fluoxetine	FLX	309.30	$C_{17}H_{18}F_3NO$	Anti-depressants	50	4.05	8.7
Gemfibrozil	GFZ	250.34	$C_{15}H_{22}O_3$	Lipid regulator	11	4.77	4.45
Ibuprofen	IBP	206.29	$C_{13}H_{18}O_2$	Anti-inflammatory, analgesic	21	3.97	4.47
Indomethacin	IDM	357.78	$C_{19}H_{16}ClNO_4$	Anti-inflammatory	0.937	4.23	3.8
Ketoprofen	KEP	254.28	$C_{16}H_{14}O_3$	Anti-inflammatory, analgesic	51	3.12	4.29
Mefenamic acid	MFA	241.285	$C_{15}H_{15}NO_2$	Anti-inflammatory	20	5.12	3.8
Naproxen	NPX	230	$C_{14}H_{14}O_3$	Anti-inflammatory, analgesic	15.9	3.18	4.2
Norfloxacin	NOR	319.331	$C_{16}H_{18}FN_3O_3$	Antibiotic	178000	0.46	$P_1 = 6.34$ $P_2 = 8.75$
Oseltamivir	OST	312.40	$C_{16}H_{28}N_2O_4$	Antiviral	1600	0.95	7.7
Oxytetracycline	OTC	460.434	$C_{22}H_{24}N_2O_9$	Antibiotic	313	-0.90	$P_1 = 3.3$ $P_2 = 7.3$ $P_3 = 9.1$

Paracetamol	PCT	151.163	$C_8H_9NO_2$	Analgesic, antipyretic	13000	0.34	9.5
Propranolol	PPL	259.34	$C_{16}H_{21}NO_2$	Beta-blocker	61.7	3.48	9.6
Propyphenazone	PPZ	230.306	$C_{14}H_{18}N_2O$	Anti-pyretic, anti-inflammatory	2400	1.94	0.8
Sulfadimethoxine	SDM	310.33	$C_{12}H_{14}N_4O_4S$	Antibacterial	343	1.63	5.9
Sulfamethazine	SMZ	278.33	$C_{12}H_{14}N_4O_2S$	Antibacterial	1500	0.14	$P_1 = 2.65$ $P_2 = 7.65$
Sulfamethoxazole	SMX	253.3	$C_{10}H_{11}N_3O_3S$	Antibiotic	610	0.89	$P_1 = 1.7$ $P_2 = 5.6$
Sulfamonomethoxine	SMM	280.302	$C_{11}H_{12}N_4O_3S$	Antibiotic	10000	-0.04	5.9
Sulfapyridine	SPY	249.29	$C_{11}H_{11}N_3O_2S$	Antibiotic	268	0.35	8.43
Sulfathiazole	STZ	255.319	$C_9H_9N_3O_2S_2$	Antibacterial	373	0.05	$P_1 = 2.2$ $P_2 = 7.24$
Sulfonamides sulfanilamide	SAA	172.20	$C_6H_8N_2O_2S$	Antibacterial	7500	-0.62	$P_1 = 10.43$ $P_2 = 11.63$
Tetracycline	TC	444.435	$C_{22}H_{24}N_2O_8$	Antibiotic	231	-1.37	3.3
Trimethoprim	TMP	290.32	$C_{14}H_{18}N_4O_3$	Antibacterial	400	0.91	7.2

Table 4.1.2 Enzyme properties and some of their application [3, 36, 64]

Enzymes	Acronym	Source	Molecular weight (kDa)	Optimum condition	Co-substrate	Applications
Laccase	Lac	*Funalia trogii* *Fomas annosus* *Cerrena unicolor* *Trametes hispida* *Daedalea quercina* *Coriolus versicolor* *Trametes versicolor* *Pycnoporus cinnabarinus*	58-90	Temperature: 40-65 °C pH: 2-10	O_2	Dyes decoloration and degradation
Tyrosinase	Tyros	*Agaricus bisporus*	119.5-133	Temperature: 20-40 °C pH: 5-8	O_2	Phenols and amines degradation
Lignin peroxidase	LiP	*Phanerochaete chrysosporium*	37-50	Temperature: 35-55 °C pH: 2-5	H_2O_2	Phenolic and Aromatic compounds degradation
Versatile peroxidase	VP	*Pleurotus eryngii* *Bjerkandera adusta*	38-45	Temperature: 15-50 °C pH: 3-5	H_2O_2	Textile effluent degradation
Manganese peroxidase	MnP	*Phlebia radiata* *Lentinula edodes* *Pleurotus ostreatus* *Phanerochaete chrysosporium*	32-62.5	Temperature: 40-60 °C pH: 4-7	H_2O_2	Phenols, lignins and dyes degradation

Table 4.1.3 Removal (%) of PhACs by different species of white rot fungi using different operating conditions

Compound	Matrix	Fungal species	Reactor type	Conditions	Initial concentration (µg/L)	Removal efficiency (%)	Removal by CAS* (%)	References
Acetaminophen	Non-sterile urban wastewater	*Trametes versicolor*	Fluidized bed (Batch-fed)	Reactor volume: 10 L Total time: 8 days Temperature: 25 °C Speed: 135 rpm pH: 4.5	1.56	100	90	[74]
	Hospital wastewater		Fluidized bed (Continuous)	Reactor volume: 10 L Total time: 8 days Temperature: 25 °C pH: 4.5	109	100		[96]
Amitriptyline	Synthetic wastewater	*Trametes versicolor*	Membrane Bioreactor (Continuous)	Reactor volume: 5.5 L Total time: 110 days Temperature: 27 °C pH: 4.5	5	85	90	[54]
Azithromycin	Non-sterile urban wastewater	*Trametes versicolor*	Fluidized bed (Batch-fed)	Reactor volume: 10 L Total time: 8 days Temperature: 25 °C Speed: 135 rpm pH: 4.5	4.31	100	50	[74]
	Hospital wastewater		Fluidized bed (Continuous)	Reactor volume: 10 L Total time: 8 days Temperature: 25 °C pH: 4.5	1.37	26		[96]
Carbamazepine	Spiked water	*Phanerochaete chrysosporium*	Stirred tank (Continuous)	Reactor volume: 1.5 L Total time: 50 days Temperature: 30 °C pH: 4.5	500	25-60	< 25	[90]
	Synthetic wastewater		Batch reactor	Reactor volume: 3 L Total time: 7 days	20000	34		[95]

Compound	Matrix	Fungal species	Reactor type	Conditions	Initial concentration (µg/L)	Removal efficiency (%)	Removal by CAS[*] (%)	References
				Temperature: 30 °C Speed: 90 rpm pH: 4.5				
	Spiked water		Fluidized bed (Batch-fed)	Reactor volume: 1.5 L Total time: 15 days Temperature: 25 °C pH: 4.5	200	61-94		[94]
	Hospital wastewater	*Trametes versicolor*	Fluidized bed (Continuous)	Reactor volume: 10 L Total time: 8 days Temperature: 25 °C pH: 4.5	0.056	0		[96]
	Synthetic wastewater		Membrane Bioreactor (Continuous)	Reactor volume: 5.5 L Total time: 110 days Temperature: 27 °C pH: 4.5	5	20		[54]
Ciprofloxacine	Non-sterile urban wastewater		Fluidized bed (Batch-fed)	Reactor volume: 10 L Total time: 8 days Temperature: 25 °C Speed: 135 rpm pH: 4.5	84.71	35	-	[74]
	Hospital wastewater	*Trametes versicolor*	Fluidized bed (Continuous)	Reactor volume: 10 L Total time: 8 days Temperature: 25 °C pH: 4.5	13	99		[96]
	Hospital wastewater		Fluidized bed (Batch-fed)	Reactor volume: 10 L Total time: 8 days Temperature: 25 °C Speed: 135 rpm pH: 4.5	7	84		[103]
	Spiked water	*Phanerochaete chrysosporium*	Sequence batch reactor	Reactor volume: 2 L Total time: 5 days	5000	60-80		[99]

Compound	Matrix	Fungal species	Reactor type	Conditions	Initial concentration (µg/L)	Removal efficiency (%)	Removal by CAS* (%)	References
				Temperature: 35 °C pH: 4.5				
Clarithromycin	Hospital wastewater	*Trametes versicolor*	Fluidized bed (Continuous)	Reactor volume: 10 L Total time: 8 days Temperature: 25 °C pH: 4.5	2.2	80	63	[96]
Diazepam	Spiked water	*Phanerochaete chrysosporium*	Stirred tank (Continuous)	Reactor volume: 1.5 L Total time: 50 days Temperature: 30 °C pH: 4.5	250	0	-	[90]
Diclofenac	Spiked water	*Phanerochaete chrysosporium*	Stirred tank (Batch-fed)	Reactor volume: 2 L Total time: 30 days Temperature: 30 °C Speed: 200 rpm pH: 4.5	0.8	> 99	50	[89]
	Spiked water		Stirred tank (Continuous)	Reactor volume: 1.5 L Total time: 50 days Temperature: 30 °C pH: 4.5	1000	92		[90]
	Hospital wastewater		Fluidized bed (Continuous)	Reactor volume: 10 L Total time: 8 days Temperature: 25 °C pH: 4.5	0.477	100		[96]
	Synthetic wastewater	*Trametes versicolor*	Membrane Bioreactor (Continuous)	Reactor volume: 5.5 L Total time: 90 days Temperature: 27 °C pH: 5.4	345	55		[97]
	Synthetic wastewater		Membrane Bioreactor (Continuous)	Reactor volume: 5.5 L Total time: 110 days Temperature: 27 °C	5	50		[54]

Compound	Matrix	Fungal species	Reactor type	Conditions	Initial concentration (µg/L)	Removal efficiency (%)	Removal by CAS* (%)	References
				pH: 4.5				
Gemfibrozil	Synthetic wastewater	*Trametes versicolor*	Membrane Bioreactor (Continuous)	Reactor volume: 5.5 L Total time: 110 days Temperature: 27 °C pH: 4.5	5	95	-	[54]
Ibuprofen	Spiked water	*Phanerochaete chrysosporium*	Stirred tank (Batch-fed)	Reactor volume: 2 L Total time: 30 days Temperature: 30 °C Speed: 200 rpm pH: 4.5	0.9	75-90	90	[89]
	Spiked water		Stirred tank (Continuous)	Reactor volume: 1.5 L Total time: 50 days Temperature: 30 °C pH: 4.5	1000	95		[90]
	Non-sterile urban wastewater	*Trametes versicolor*	Fluidized bed (Batch-fed)	Reactor volume: 10 L Total time: 8 days Temperature: 25 °C Speed: 135 rpm pH: 4.5	2.34	100		[74]
	Hospital wastewater		Fluidized bed (Continuous)	Reactor volume: 10 L Total time: 8 days Temperature: 25 °C pH: 4.5	35.5	100		[96]
	Synthetic wastewater		Membrane Bioreactor (Continuous)	Reactor volume: 5.5 L Total time: 110 days Temperature: 27 °C pH: 4.5	5	95		[54]
	Hospital wastewater		Fluidized bed (Continuous)	Reactor volume: 1.5 L Total time: 5 days Temperature: 25 °C pH: 4.5	20000	90		[93]

Compound	Matrix	Fungal species	Reactor type	Conditions	Initial concentration (µg/L)	Removal efficiency (%)	Removal by CAS* (%)	References
Ketoprofen	Non-sterile urban wastewater	*Trametes versicolor*	Fluidized bed (Batch-fed)	Reactor volume: 10 L Total time: 8 days Temperature: 25 °C Speed: 135 rpm pH: 4.5	0.08	100	50	[74]
	Hospital wastewater		Fluidized bed (Continuous)	Reactor volume: 10 L Total time: 8 days Temperature: 25 °C pH: 4.5	2.17	95		[96]
	Synthetic wastewater		Membrane Bioreactor (Continuous)	Reactor volume: 5.5 L Total time: 110 days Temperature: 27 °C pH: 4.5	5	90		[54]
	Hospital wastewater		Fluidized bed (Continuous)	Reactor volume: 1.5 L Total time: 5 days Temperature: 25 °C pH: 4.5	20000	70		[93]
Metronidazole	Hospital wastewater	*Trametes versicolor*	Fluidized bed (Continuous)	Reactor volume: 10 L Total time: 8 days Temperature: 25 °C pH: 4.5	0.912	85	38.7	[96]
	Synthetic wastewater		Membrane Bioreactor (Continuous)	Reactor volume: 5.5 L Total time: 110 days Temperature: 27 °C pH: 4.5	5	40		[54]
Naproxen	Spiked water	*Phanerochaete chrysosporium*	Stirred tank (Batch-fed)	Reactor volume: 2 L Total time: 30 days Temperature: 30 °C Speed: 200 rpm pH: 4.5	1	> 99	94	[89]
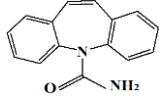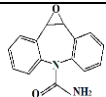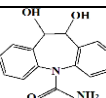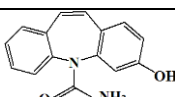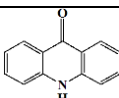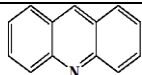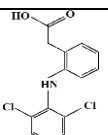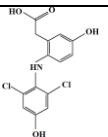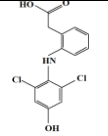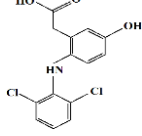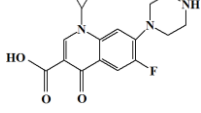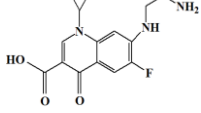
Compound	Matrix	Fungal species	Reactor type	Conditions	Initial concentration (μg/L)	Removal efficiency (%)	Removal by CAS[*] (%)	References
	Spiked water		Stirred tank (Continuous)	Reactor volume: 1.5 L Total time: 50 days Temperature: 30 °C pH: 4.5	1000	95		[90]
	Hospital wastewater	*Trametes versicolor*	Fluidized bed (Continuous)	Reactor volume: 10 L Total time: 8 days Temperature: 25 °C pH: 4.5	1.62	100		[96]
	Synthetic wastewater		Membrane Bioreactor (Continuous)	Reactor volume: 5.5 L Total time: 110 days Temperature: 27 °C pH: 4.5	5	95		[54]
Phenazone	Hospital wastewater	*Trametes versicolor*	Fluidized bed (Continuous)	Reactor volume: 10 L Total time: 8 days Temperature: 25 °C pH: 4.5	0.497	96	15	[96]
Propranolol	Non-sterile urban wastewater	*Trametes versicolor*	Fluidized bed (Batch-fed)	Reactor volume: 10 L Total time: 8 days Temperature: 25 °C Speed: 135 rpm pH: 4.5	0.06	100	1	[74]
Sulfamethoxazole	Hospital wastewater	*Trametes versicolor*	Fluidized bed (Continuous)	Reactor volume: 10 L Total time: 8 days Temperature: 25 °C pH: 4.5	1.41	100	51.9	[96]
Tetracycline	Hospital wastewater	*Trametes versicolor*	Fluidized bed (Continuous)	Reactor volume: 10 L Total time: 8 days Temperature: 25 °C pH: 4.5	0.011	0		[96]

* Conventional activated sludge
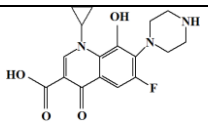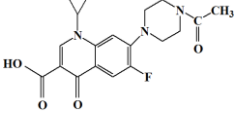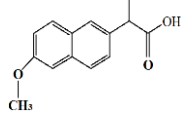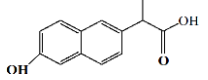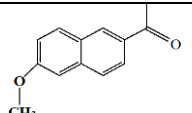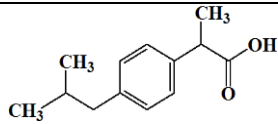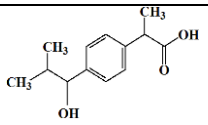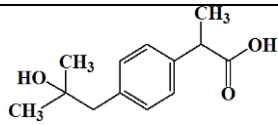
The data for removal by CAS (%) are extracted from the following references [33, 104-108].

Table 4.1.4 Structures of most studied micropollutants and proposed transformation products formed during biodegradation

Compounds	Acronym	Compound mass (Da)	Formula	Chemical structure	Reference
Carbamazepine	CBZ	236.269	$C_{15}H_{12}N_2O$		[61, 65, 94, 129]
10,11-epoxycarbamazepine	CBZ-EP	253.0983	$C_{15}H_{12}N_2O_2$		
10,11-dihydroxycarbamazepine	DiOH-CBZ	293.091	$C_{15}H_{14}N_2O_3$		
2-and 3- and 4-hydroxy carbamazepine	2-OH-CBZ 3-OH-CBZ 4-OH-CBZ	252.27	$C_{15}H_{12}N_2O_2$		
Acridone	Acridone	196.0762	$C_{13}H_9NO$		
Acridine	Acridine	179.222	$C_{13}H_9N$		
Diclofenac	DCF	296.149	$C_{14}H_{11}Cl_2NO_2$		[67, 112, 114, 116]
4,5-dihydroxydiclofenac	4',5-diOH-DCF	328.147	$C_{14}H_{11}Cl_2NO_4$		
4'-hydroxydiclofenac	4'-OH-DCF	312.148	$C_{14}H_{11}Cl_2NO_3$		
5-hydroxydiclofenac	5-OH-DCF	312.148	$C_{14}H_{11}Cl_2NO_3$		
Ciprofloxacin	CPF	331.341	$C_{17}H_{18}FN_3O_3$		[78, 81, 86]
Ciprofloxacin-7-ethylenediamine	CPF-1	305.309	$C_{15}H_{16}FN_3O_3$		

Compounds	Acronym	Compound mass (Da)	Formula	Chemical structure	Reference
Ciprofloxacin N-Oxide	CPF-3	347.346	$C_{17}H_{18}FN_3O_4$		
N-acetylciprofloxacin	N-acetyl-CPF	373	$C_{19}H_{20}FN_3O_5$		
Naproxen	NPX	230.259	$C_{14}H_{14}O_3$		[85]
2-(6-hydroxynaphthalen-2-yl)propanoic acid	-	216.236	$C_{13}H_{12}O_3$		
1-(6-methoxynaphthalen-2-yl)ethanone	-	200.237	$C_{13}H_{12}O_2$		
Ibuprofen	IBP	206.281	$C_{13}H_{18}O_2$		[5, 121]
1-Hydroxyibuprofen	1-OH-IBP	222.284	$C_{13}H_{18}O_3$		
2-Hydroxyibuprofen	2-OH-IBP	222.284	$C_{13}H_{18}O_3$		

Table 4.1.5 Biodegradation of PhACs by crude and purified enzymes

Compound	Enzyme source	Condition	Concentration of PhACs[*] (mg/L)	Scale	Conversion (%)	References
Acetaminophen	Not mentioned	Purified laccase	7.55	25 °C, 47 min, 50 mL	50	[138]
Carbamazepine	*Trametes versicolor*	Crude laccase	0.01	30 °C, 125 rpm, 48 h, 100 mL	37	[66]
	Phanerochaete chrysosporium	Crude lignin peroxidases	5	25 °C, 120 rpm, 2 h, 10 mL	<10	[62]
	Phanerochaete chrysosporium	Purified manganese peroxidases	4.7	30 °C, 150 rpm, 24 h, 100 mL	14	[65]
Diclofenac	*Trametes versicolor*	Purified laccase	10	25 °C, 135 rpm, 4.5 h, 25 mL	95	[112]
	Bjerkandera adusta	Purified versatile peroxidase	2.5	22 °C, 25 min, 50 mL	100	[114]
	Trametes versicolor	Crude laccase	0.01	30 °C, 125 rpm, 48 h, 100 mL	100	[66]
	Myceliophthora thermophila	Purified laccase	5	22 °C, 8 h, 20 mL	65	[136]
	Phanerochaete chrysosporium	Crude lignin peroxidases	5	25 °C, 120 rpm, 2 h, 10 mL	100	[62]
Ibuprofen	*Trametes versicolor*	Crude laccase	0.01	30 °C, 125 rpm, 48 h, 100 mL	38	[66]
Naproxen	*Trametes versicolor*	Purified laccase	20	25 °C, 135 rpm, 30 h, 25 mL	10	[85]
		Crude laccase	0.01	30 °C, 125 rpm, 48 h, 100 mL	100	[66]
Sulfadimethoxine	*Trametes versicolor*	Purified laccase	310.33	21 °C, Static, 15 d, 100 mL	75.1	[115]
Sulfanilamide	*Trametes versicolor*	Purified laccase	172.20	21 °C, Static, 15 d, 100 mL	10	[115]
Sulfapyridine	*Trametes versicolor*	Purified laccase	10	25 °C, 135 rpm, 50 h, 50 mL	75	[88]
			249.29	21 °C, Static, 15 d, 100 mL	95.6	[115]
Sulfathiazole	*Trametes versicolor*	Purified laccase	10	25 °C, 135 rpm, 50 h, 50 mL	82	[88]
* Pharmaceutically active compounds						

Table 4.1.6 Physicochemical properties of redox-mediators used to improve the performance of laccase-based treatment of PhACs

Redox-mediator	Natural/ synthetic	Type of mediator	Free radicals	Oxidation mechanism	Chemical structure	Application for PhACs removal	Average removal (%)	References
HBT[A]	Synthetic	N-OH	Aminoxyl =N-O•	HAT[H]		NPX[K]	89	[66, 85, 149]
						DCF[L]	96	[55, 66, 149]
						CBZ[M]	60	[65]
ABTS[B]	Synthetic	ABTS	ABTS+• ABTS++	ET[I]		DCF	100	[66]
						NPX	100	[66]
						IDM[N]	100	[66]
						SDM[O]	100	[150]
						SMM[P]	100	[150]
TEMPO[C]	Synthetic	N-O	Oxoammonium N=O•	Ionic[J]		NPX	37	[142]
HPI[D]	Synthetic	N-OH	Aminoxyl =N-O•	HAT[H]		NPX	38	[142]
SA[E]	Natural	$C_6H_4(OH)(OCH_3)$	Phenoxyl $C_6H_5O•$	HAT[H]		DCF	64	[55, 149, 151]
						IBP[Q]	19	[56, 133]
						GFZ[R]	34	[133]
						NPX	23	[133]
						KEP[S]	17	[133]
						CBZ	32	[49, 133]
						AMP[T]	100	[56, 133]
VLA[F]	Natural	N-OH	Aminoxyl =N-O•	HAT[H]		SDM	100	[150]
						SMM	100	[150]
VAN[G]	Synthetic	$C_6H_4(OH)(OCH_3)$	Phenoxyl $C_6H_5O•$	HAT[H]		NPX	39	[142]

A:1-hydroxibenzotriazole, B:2,2-azino-nis (3-ethylbenzothiazoline-6-sulfnoic acid, C:2,2,6,6-tetramethylpiperidinyloxyl, D:N-hydroxyphthalimide, E:Syringaldehyde, F:Violuric acid, G:Vanillin, H:Hydrogen atom transfer, I:Electron transfer, J:Ionic oxidation, K:Naproxen, L:Diclofenac, M:Carbamazepine, N:Indomethacin, O:Sulfadimethoxine, P:Sulfamonomethoxine, Q:Ibuprofen, R:Gemfibrozil, S:Ketoprofen T:Amitriptyline.

Table 4.1.7 Removal efficiencies PhACs by immobilized enzyme in batch experiments

Compound	Initial PhAC concentration	Source of Fungi	Enzyme	Immobilization method	Removal conditions	Removal (%)	References
Acetaminophen	10-50 µg/L	*Trametes versicolor*	Laccase	Cross-linked enzyme aggregates	Wastewater 30 °C, 150 rpm, 6 h, 10 mL	26	[189]
	100 µg/L	*Trametes versicolor*	Laccase	Cross-linked enzyme aggregates	Wastewater 20 °C, 125 rpm, 12 h, 10 mL	97	[190]
	100 µg/L	*Trametes versicolor*	Laccase	Cross-linked enzyme aggregates	Wastewater 20 °C, 300 rpm, 120 h, 3500 mL	100	[192]
	90 µg/L	*Trametes versicolor/* Mushroom	Laccase/Tyrosinase	Cross-linked enzyme aggregates	Wastewater 20 °C, 8 h	93	[193]
Atenolol	100 µg/L	*Trametes versicolor*	Laccase	Cross-linked enzyme aggregates	Wastewater 20 °C, 125 rpm, 12 h, 10 mL	90	[190]
Diazepam	100 µg/L	*Trametes versicolor*	Laccase	Cross-linked enzyme aggregates	Wastewater 20 °C, 125 rpm, 12 h, 10 mL	68	[190]
Diclofenac	93 µg/L	*Trametes versicolor*	Laccase	Immobilized on silica nanoparticles	Wastewater 25 °C, 210 rpm, 24 h, 100 mL	0	[197]
	93 µg/L	*Myceliophthora thermophila*	Laccase	Immobilized on silica nanoparticles	Wastewater 25 °C, 210 rpm, 24 h, 100 mL	0	[197]
	2.5 mg/L	*Aspergillus oryzae*	Laccase	Immobilized on granular activated carbon	Spiked water 25 ºC, 70 rpm, 2 h, 100 mL	60	[184]
	50 mg/L	*Pleurotus florida*	Laccase	Immobilized on poly (lactic-co-glycolic acid)	Spiked water 30 °C, 100 rpm, 5 h	100	[186]
	12.5 mg/L	*Trametes versicolor*	Laccase	Immobilized on polyvinyl alcohol / chitosan/ multi-walled carbon nanotubes	Spiked water 50 °C, 6 h	100	[187]

Compound	Initial PhAC concentration	Source of Fungi	Enzyme	Immobilization method	Removal conditions	Removal (%)	References
	100 µg/L	*Trametes versicolor*	Laccase	Cross-linked enzyme aggregates	Wastewater 20 °C, 125 rpm, 12 h, 10 mL	95	[190]
	10 µM	*Coriolopsis gallica*	Laccase	Immobilized on mesoporous silica spheres	Wastewater 20 °C, 24 h, 50 mL	70	[194]
Carbamazepine	20 µg/L	*Trametes versicolor*	Laccase	Immobilized on nanobiochar	Wastewater 25 °C, 200 rpm, 24 h, 20 mL	66	[6]
	5 mg/L	*Trametes versicolor*	Laccase	ImmobilizedonTiO$_2$ nanoparticles	Wastewater 25 °C, Constant stirring, 96 h, 50 mL	60	[175]
	2.5 mg/L	*Aspergillus oryzae*	Laccase	Immobilized on granular activated carbon	Spiked water 25 ºC, 70 rpm, 2 h, 100 mL	40	[184]
	100 µg/L	*Trametes versicolor*	Laccase	Cross-linked enzyme aggregates	Wastewater 20 °C, 300 rpm, 120 h, 3500 mL	18	[192]
Chlortetracycline	200 µg/L	*Trametes versicolor*	Laccase	Immobilized on nanofibers	Spiked water 25 ºC, continuous mode (1 mL/h.cm^2)	58.3	[198]
Fenofibrate	10-50 µg/L	*Trametes versicolor*	Laccase	Cross-linked enzyme aggregates	Wastewater 30 °C, 150 rpm, 6 h, 10 mL	37	[189]
	100 µg/L	*Trametes versicolor*	Laccase	Cross-linked enzyme aggregates	Wastewater 20 °C, 125 rpm, 12 h, 10 mL	45	[190]
Ketoprofen	100 µg/L	*Trametes versicolor*	Laccase	Cross-linked enzyme aggregates	Wastewater 20 °C, 125 rpm, 12 h, 10 mL	48	[190]
Mefenamic acid	100 µg/L	*Trametes versicolor*	Laccase	Cross-linked enzyme aggregates	Wastewater 20 °C, 125 rpm, 12 h, 10 mL	99	[190]

Compound	Initial PhAC concentration	Source of Fungi	Enzyme	Immobilization method	Removal conditions	Removal (%)	References
	100 µg/L	*Trametes versicolor*	Laccase	Cross-linked enzyme aggregates	Wastewater 20 °C, 300 rpm, 120 h, 3500 mL	100	[192]
Paracetamol	20 mg/L	*Not mentioned*	Horseradish peroxidase	Immobilized on nanofibrous membranes	Spiked water 25°C, 90 min, 50 mL	98	[188]
Sulfadiazine	50 mg/L	*Echinodontium taxodii*	Laccase	Immobilized on Fe_3O_4 nanoparticles	Spiked water 25°C, 5 min	100	[195]
Sulfamethazine	50 mg/L	*Echinodontium taxodii*	Laccase	Immobilized on Fe_3O_4 nanoparticles	Spiked water 25°C, 3 min	100	[195]
Sulfamethoxazole	50 mg/L	*Trametes versicolor*	Laccase	Immobilized on CPC silica beads	Spiked water 40 °C, 50 rpm, 60 min, 5 mL	53	[111]
	2.5 mg/L	*Aspergillus oryzae*	Laccase	Immobilized on granular activated carbon	Spiked water 25 ºC, 70 rpm, 2 h, 100 mL	59	[184]
	50 mg/L	*Echinodontium taxodii*	Laccase	Immobilized on Fe_3O_4 nanoparticles	Spiked water 25°C, 5 min	100	[195]
Sulfathiazole	50 mg/L	*Trametes versicolor*	Laccase	Immobilized on CPC silica beads	Spiked water 40 °C, 50 rpm, 60 min, 5 mL	71.7	[111]
Trimethoprim	100 µg/L	Trametes versicolor	Laccase	Cross-linked enzyme aggregates	Wastewater 20 °C, 125 rpm, 12 h, 10 mL	60	[190]
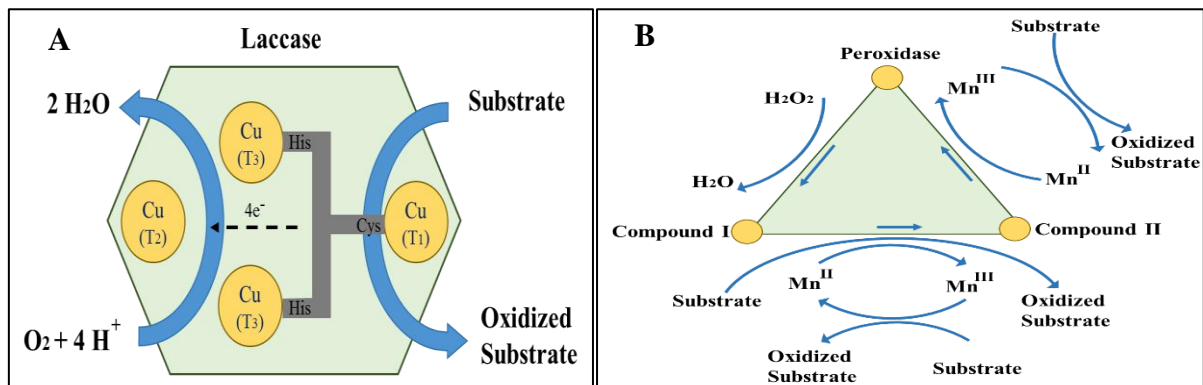
Figure 4.1.1 Mechanism of oxidation of compounds: (a) by the laccase enzyme and; (b) by peroxidase enzyme
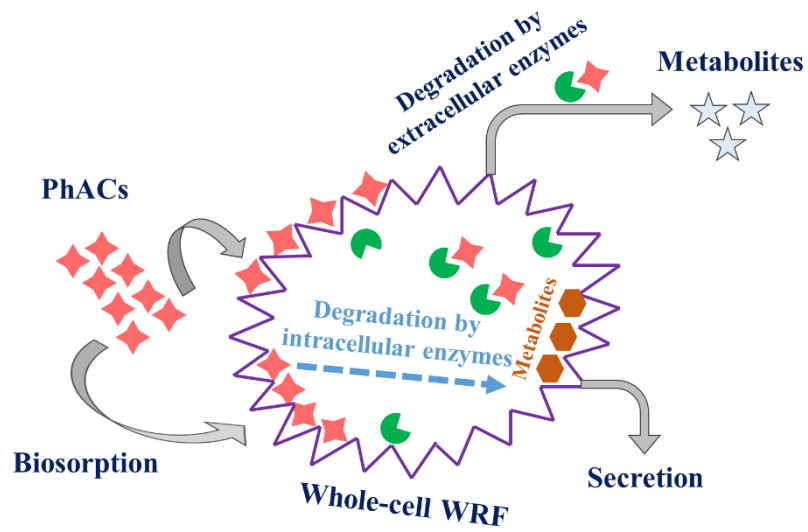
Figure 4.1.2 A schematic illustration of pollutant removal by white-rot fungi
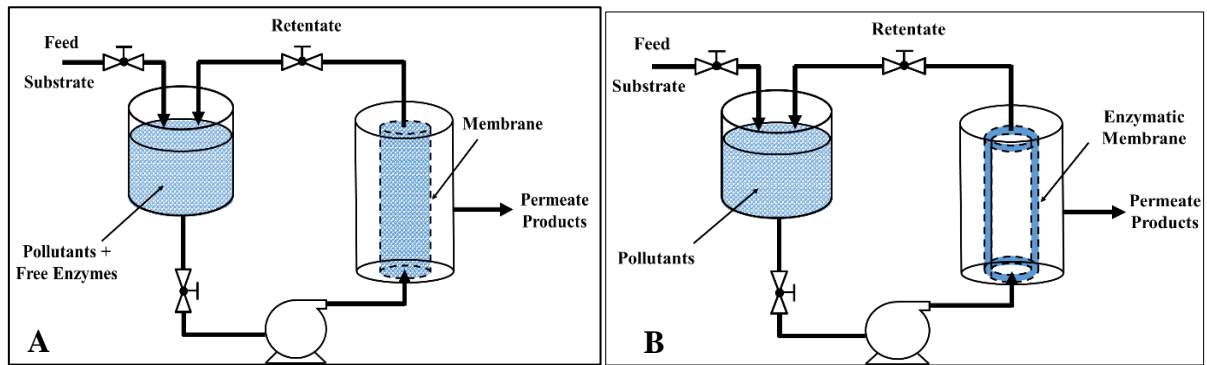
Figure 4.1.3 Enzymatic membrane reactor configurations: (A) Type one: the membrane is only used as a selective barrier to retain enzyme (B) Type two: the membrane acts as both support for biocatalyst and selective barrier

Part 2

Biotransformation of Carbamazepine by Laccase-Mediator System: Kinetics, By-products and Toxicity Assessment

Mitra Naghdi[1], Mehrdad Taheran[1], Satinder Kaur Brar[1*], Azadeh Kermanshahi-pour[2], Mausam Verma[1] and R.Y. Surampalli[4]

[1]INRS-ETE, Université du Québec, 490, Rue de la Couronne, Québec, Canada G1K 9A9

[2]Biorefining and Remediation Laboratory, Department of Process Engineering and Applied Science, Dalhousie University, 1360 Barrington Street, Halifax, Nova Scotia, Canada, B3J 1Z1

[3]Department of Civil Engineering, University of Nebraska-Lincoln, N104 SEC PO Box 886105, Lincoln, NE 68588-6105, US

(*Phone: 1 418 654 3116; Fax: 1 418 654 2600; E-mail: satinder.brar@ete.inrs.ca)

Résumé

La carbamazépine (CBZ) est l'un des composés pharmaceutiques les plus détectés dans le monde dans les effluents des eaux usées, avec des effets néfastes sur la santé humaine et animale. Récemment, la dégradation biocatalytique en utilisant des enzymes ligninolytiques telles que la laccase avec des médiateurs redox fournit une approche prometteuse pour leur élimination de la CBZ de l'eau et des eaux usées. Cependant, les effets des paramètres opérationnels sur la biotransformation doivent être étudiés afin de concevoir un processus robuste et efficace. Dans cette recherche, la conception composite centrale a été réalisée et analysée en utilisant la méthodologie de la surface de réponse pour étudier les effets de la température, du pH, de la concentration enzymatique et de la concentration du médiateur. L'adéquation du modèle développé a été confirmée par le coefficient de régression multiple (R^2 = 75,97%) indiquant un modèle raisonnable pour une mise en œuvre pratique. Les résultats ont montré que l'exécution de la biotransformation à 35 °C, pH 6, avec 60 U/L de concentration enzymatique et 18 µM de concentration du médiateur a entraîné une élimination de 95% de CBZ. La 10,11-dihydro-10,11-dihydroxy-CBZ et la 10,11-dihydro-10,11-époxy-CBZ ont été identifiées comme les principaux métabolites de l'oxydation du CBZ par la laccase. Les tests d'œstrogénicité ont indiqué que la CBZ avec une concentration initiale de 4 µM et ses produits de biotransformation n'avaient aucun effet œstrogénique. La transformation réussie de la CBZ a démontré le potentiel du système de laccase-médiateur pour l'élimination des micro-contaminants récalcitrants.

Mots clés

Carbamazépine, Biotransformation, Laccase, Sous-produits, Test d'analyse de l'œstrogénèse des levures

Abstract

Carbamazepine (CBZ) is one of the most detected pharmaceutical compounds around the world, with adverse human and animal health impacts in wastewater effluents. Recently, biocatalytic degradation using ligninolytic enzymes such as laccase along with redox mediators provides a promising approach for their removal from water and wastewater. However, the effects of operational parameters on biotransformation need to be investigated in order to design a robust and efficient process. In this research, central composite design was performed and analyzed using response surface methodology to study the effects of temperature, pH, enzyme concentration and mediator concentration. The adequacy of the developed model was confirmed by the coefficient of multiple regression (R^2=75.97%) indicating a reasonable model for practical implementation. The results showed that performing the biotransformation at 35 °C, pH 6, with 60 U/L of enzyme concentration and 18 μM of mediator concentration resulted in 95% removal of CBZ. 10,11-dihydro-10,11-dihydroxy-CBZ and 10,11-dihydro-10,11-epoxy-CBZ were identified as the major metabolites of CBZ oxidation by laccase. The estrogenicity tests indicated that the CBZ with an initial concentration of 4 μM and its biotransformation products had no estrogenic effect. The successful transformation of CBZ demonstrated the potential of the laccase-mediator system for the removal of recalcitrant micro-contaminants.

Keywords

Carbamazepine, Biotransformation, Laccase, By-products, Yeast Estrogenicity Screen Assay.

Introduction

Currently, pharmaceutically active compounds (PhACs) are routinely detected at very low concentrations in the effluents of wastewater treatment plants (WWTPs) [1, 2]. Since the PhACs can produce a biological effect at lower concentrations, the discharge of these compounds into the aquatic environment may pose adverse effects on the receiving ecosystem [3, 4]. Therefore, the removal of such compounds is beneficial to the environment and human health.

Carbamazepine (CBZ), a widely used psychiatric drug, is one of the most frequently detected compounds in the surface water and groundwater that receive wastewater effluent [5]. Around 30% of the CBZ is excreted in intact form after administration [6]. CBZ is resistant to biotransformation and adsorption to sludge [7, 8], which leads to poor removal in conventional WWTPs [9]. Clara *et al.* found that CBZ removal was negligible in conventional activated sludge plants, such as sequencing batch reactor (SBR) and a membrane bioreactor operated at different sludge retention times [10, 11]. CBZ also showed resistance against removal with chlorination, coagulation, and flocculation [1]. Although CBZ does not produce acute toxicity in the aquatic environment, the chronic and synergistic effects with other compounds cannot be excluded [12]. Therefore, many research works were performed to develop new strategies for CBZ removal from wastewater [13]. Several treatment methods, such as membrane separation, ozonation, and adsorption onto activated carbon showed high levels of CBZ removal [14, 15]. However, these methods have drawbacks, such as generation of a waste stream and formation of more toxic compounds [16, 17]. For example, Donner *et al.* analyzed the transformation products of CBZ during ultraviolet (UV) photolysis with three standard ecotoxicity assays (algae, bacteria, and crustaceans) and observed higher toxicity compared to the parent compound [18].

As an alternative to the mentioned methods, biocatalytic degradation of PhACs with enzymes may provide environmentally benign approaches that require low energy input and moderate conditions. Furthermore, the specificity of the enzymatic methods leads to minimization of the undesirable products [13, 19]. Therefore, enzymes offer a promising tool for selective and efficient removal of pollutants from water and wastewater streams [13, 19]. Among biocatalytic systems, using white-rot fungi (WRF) attracted much attention since they can degrade recalcitrant pollutants through their ligninolytic enzymes i.e. laccase [20, 21], manganese peroxidase (MnP) and lignin

peroxidase (LiP) [22]. For example, Jelic *et al.* used *Trametes versicolor* to remove CBZ with an air pulsed fluidized bioreactor in continuous mode and obtained removal efficiency of 54%. They also observed no toxicity in final culture broth [19]. Besides whole fungal culture, the use of crude or purified ligninolytic enzymes for removal of contaminants has also been investigated. Laccase is one of the most targeted ligninolytic enzymes for degradation of phenolic and non-phenolic contaminants due to its stability, low cost, feasible production and broad substrate specificity [23]. The capability of laccase to degrade different compounds, such as pesticides, dyes, and polycyclic aromatic hydrocarbons to less toxic by-products, made it attractive for wastewater bioremediation [13, 24]. Recent studies on the degradation of CBZ with laccase showed poor degradation efficiency due to the presence of an electron withdrawing group such as amide in CBZ structure. This functional group caused severe electron deficiency and made CBZ less susceptible to oxidation by laccase [25]. In this case, using redox mediators, such as 2, 2'-azino-bis (3-ethyl-benzothiazoline-6-sulfonic acid) (ABTS) and 1-hydro-xybenzotriazole (HBT) can enhance the oxidizing capability of laccase toward recalcitrant compounds [24, 26, 27]. For example, Hata *et al.* observed that addition of HBT increased the degradation efficiency of CBZ by laccase from 22% to 60 % [27].

Although the capability of laccase-mediator systems for degradation of pollutants has been already verified, production of pure laccase is cost-intensive laccase and challenges its commercial application. Likewise, the influence of operational parameters has not been statistically investigated to develop a reliable and efficient treatment method. In this work, fermentation of a cost-effective substrate i.e. apple pomace was used to produce laccase by *Trametes versicolor*. Subsequently, the effects of four parameters including enzyme concentration, mediator concentration, temperature and pH on the biotransformation rate of laccase for CBZ were studied using response surface methodology (RSM) which is an experimental approach to find the optimum conditions for a system with several variables. Finally, the CBZ biotransformation products were identified and yeast estrogenic toxicity bioassay was performed to understand the effect of biocatalytic treatment on the CBZ toxicity. To the best of our knowledge, this is the first study that investigates the performance of crude laccase-mediator for the removal of CBZ at the environmentally-related

concentrations. Working at this range is of significance since the results are more reliable and it is possible to extrapolate them to real conditions.

Materials and methods

Chemicals

Carbamazepine (CBZ) and 2, 2'-azino-bis (3-ethylbenzothiazoline-6-sulphonic acid) (ABTS) were procured from Sigma-Aldrich (Oakville, Canada) with purity of >99%. Carbamazepine (D10), as an internal standard, was purchased from CDN Isotopes (Pointe-Claire, Canada). Methanol and Tween 80 were obtained from Fisher Scientific (Ottawa, Canada). Ultrapure water was produced in the laboratory using a Milli-Q/Milli-Ro Millipore system (Massachusetts, USA). The ultrapure water was used for the preparation of stock solutions and samples for degradation tests.

Preparation of inoculum

The fungus, *Trametes versicolor* (Tv) (ATCC (American Type Culture Collection) 20869) was grown aerobically in a liquid medium (Potato dextrose broth) (2.4% w/v and 30 mL) at 30±1 °C and 150 rpm for 7 days. The inoculum was prepared by growing the fungus (100 µL from PDB (Potato dextrose broth) media) on potato dextrose agar (PDA) plates for 9 days at 30±1 °C. After incubation, the plates were stored at 4±1 °C prior to use for fermentation.

Solid-state fermentation and enzyme extraction

Apple pomace (Vergers Paul Jodoin Inc., Quebec, Canada) was used as a solid substrate for the production of laccase by the Tv. In brief, 40 grams of solid substrate (78% moisture (w/w) and pH 4.5), along with Tween 80 at 0.5% v/w in a 500 mL Erlenmeyer flasks were magnetically stirred (Isotemp™ Stirrer, Fisher Scientific) and autoclaved (3870 ELV, Heidolph) at 121±1 °C for 20 min. After inoculation, the substrate was thoroughly mixed and incubated in a static incubator (Isotemp Incubator Fisher Scientific) for 14 days at 30±1 °C. For extraction of laccase, one gram of fermented sample was added to 20 mL of 50 mM sodium phosphate buffer (pH 6.5). Then, the mixture was mixed using a shaker incubator (Multitron, Infors HT) at 150 rpm and 35±1 °C for 1 h and centrifuged (Sorvall RC 5C, Dupont) for 30 min at 4 °C and 7,000 × g. The collected supernatant was analyzed spectrophotometrically (Cary 300 Bio, Varian) for respective laccase activity expressed as activity per gram of dry

culture (Section "enzyme assay"). The supernatant was freeze-dried at - 55 °C and 5 Pa for 48 h and kept at -20 °C (Revco, Fisher Scientific) before performing the experiments.

Enzyme assay

Oxidation of ABTS was used to measure the laccase activity. 500 µL ABTS (1.5 mM) was mixed with 2.450 mL of 0.1 M citrate-phosphate buffer (pH 4) and 50 µL of enzyme sample. ABTS oxidation was monitored at 45±1 °C by recording the absorbance at 420 nm (ε_{420} = 36,000 M^{-1} cm^{-1}) for 10 minutes [28]. One activity unit of laccase was defined as the amount of required enzyme to oxidize 1 µmol of ABTS per min under the mentioned conditions. The average of the three measurements was reported as final laccase activity.

Experimental design and degradation efficiency

Central composite design (CCD) and response surface methodology (RSM) was employed to study the degradation efficiency of laccase as a function of temperature (°C), ABTS concentration (µM), enzyme concentration (U/L) and pH. The degradation efficiency for CBZ was considered as the dependent variable. Independent parameters and their corresponding levels are listed in Table 4.2.1. Design-Expert®-7 software (Stat-Ease Inc., Minneapolis, USA) was used in the formation of the experimental array which resulted in 30 experiments with 6 replicates in the center. The details of designed experiments are listed in Table 4.2.2. In each experiment, exact concentration of enzyme and ABTS along with CBZ (1 ppm) were mixed in desired pH (total volume of 10 mL). The flask was later kept at suitable respective temperature (25-45 °C) and 150 rpm. After 24 h, the reaction was stopped by addition of methanol (1:1 v/v ratio) and the sample was analyzed.

Kinetics of Laccase-Mediated CBZ Degradation

Degradation kinetics of CBZ was carried out for CBZ at an initial concentration of 1000 µg/L and enzyme activity of 60 U/L for 24 h. Sampling was performed at different time intervals (0.5, 1.5, 2, 3, 4, 6, 7, 8, 16 and 24). Also, different initial concentrations of CBZ (2 µg/L, 10 µg/L, 20 µg/L, 100 µg/L, 200 µg/L, 1000 µg/L and 2000 µg/L) was used against 60 U/L of laccase in constant reaction time of 12 h to determine the parameters of Michaelis-Menten kinetics. The parameters in Michaelis−Menten

kinetics were determined by measuring the initial degradation rate of CBZ at different CBZ concentrations (Equation 1) [29].

$$V = \frac{V_m\,[S]}{K_M + [S]} \tag{1}$$

In this equation, V (μg L^{-1}/h) is the reaction rate, V_m (μg L^{-1}/h) is the maximum reaction rate, [S] is the substrate concentration, and K_M is a constant. K_m and V_{max} values are determined by fitting the data into the Lineweaver-Burk plot, which resulted from Michaelis-Menten plot conversion.

Quantification of CBZ

Quantification of CBZ was performed on a liquid chromatography quadrupole (LCQ) Duo ion trap tandem mass spectrometer (Thermo Finnigan, USA) coupled with a Laser Diode Thermal Desorption (LDTD) (Phytronix technologies, Canada). The identified daughter ions for CBZ were 194 and 192 Da. The calibration curve of CBZ concentration comprised six standard solutions and the R^2 was greater than 0.99. The details of quantification process were described elsewhere [30]. All the experiments were performed in duplicates and the average results were reported.

Data analysis

The results obtained from experiment based on CCD were analyzed with RSM and fitted to a second-order polynomial model. The equation (Equation 2) mentioned below was employed in the RSM analysis to correlate the dependent and independent variables.

$$Y = \beta_0 + \sum_{i=1} \beta_i X_i + \sum \beta_{ii} X_i^2 + \sum_{i=1} \sum_{j=i+1} \beta_{ij} X_i X_j \tag{2}$$

In this equation Y, β_0, X_i (or X_j). β_i, β_{ii}, and β_{ij} are the predicted responses for the dependent variable, second-order constant, independent variable, the coefficient of linear regression, the coefficient of quadratic regression and coefficient of interactions regression between two independent variables, respectively.

The calculated degradation efficiency (%) for each run was chosen as the response (dependent) variable. The relationship between the independent parameters and the response variable was determined by design matrix evaluation, by taking the response

surface quadratic model for interactions into consideration. The significance of the regression was tested and models with a *p*-value higher than 0.05 were not considered. The best fit for polynomial models was evaluated from adjusted coefficient of determination (R^2 values) and final equation in terms of factors and lack of fit test (LOF) was obtained by analysis of variance (ANOVA).

By-product identification

Accurate mass of CBZ and its biotransformation products under the optimum conditions were measured by LDTD-mass spectrometry (MS) and LDTD-MS-MS in the m/z range of 10-1000. About 4 µL of each sample was placed into the 96-well plates and dried at 35 °C. The sample was desorbed by laser power and guided into Atmospheric pressure chemical ionization (APCI) module to ionize all the compounds. Later, the ionized molecules were guided into the mass spectrometer and their m/z ratio was scanned. After selecting the most probable m/z for by-products, another experiment was performed with LDTD-MS-MS to scan the daughter ions of by-products in the second mass spectrophotometer.

Yeast Estrogen Screen (YES) assay

The YES assay described by Routledge and Sumpter was employed to measure the estrogenic activity of CBZ and its degradation by-products [31]. The procedure for the determination of the total estrogenic activity was carried out by serial dilution of CBZ, its by-products and 17β-estradiol (as standard) in ethanol across 12 wells in a 96-well plate (Costar Brand, NY, and the USA). In the first row of the plate, 10 µL of ethanol was placed in each well as blank. In the second and third rows, 10 µL 17β-estradiol with different concentrations (0, 0.5 ng/L, 5 ng/L,…, 5 mg/L, 50 mg/L) was placed in duplicate. In the fourth-row, CBZ sample at 1 mg/L (4 µM) and its degradation by-products (with and without ABTS) were placed in quadruplicate. Later, the plate was conditioned under laminar flow for complete drying of the samples. 200 µL of the seeded assay medium containing chlorophenol red-β-D-galactopyranoside (CPRG) and the yeast (hER-transfected recombinant yeast) were added to the samples. The sealed plate with parafilm was incubated for 3 days at 32±1 °C. The color development of the samples was checked periodically for qualitative assessment of toxicity.

Result and Discussion

Production of crude laccase

TV is known as an excellent producer of laccase at industrial scale [32]. To have a sufficient amount of crude laccase in this study, laccase was biosynthesized by fermentation of apple pomace. Figure 4.2.1 depicts the profile of laccase production during the fermentation period. The results showed that during the first 5 days of fermentation, no laccase activity was detected in the cultures. After the 6th day, laccase production started and reached its maximum on the 13th day (1800 U/L), and then decreased. No MnP or LiP activity was found during the fermentation, which can be due to the properties of strain, substrate and the fermentation conditions [32].

Fitting the degradation model

The effect of different parameters and their interactions on the biotransformation of CBZ was investigated. The RSM design considered central points (0), low (-) and high (+) levels for the parameters (Table 4.2.1). The values of parameters for all designed experiments and the obtained results are summarized in Table 4.2.2. The obtained data were analyzed to determine the coefficients of the quadratic model. The mathematical expression of the relationship of CBZ biotransformation with variables, A, B, C and D (temperature, ABTS concentration, pH and enzyme concentration, respectively) are given below in Equation 3 in terms of coded factors:

$$Y = + 86.10 - 0.38\ A + 3.43\ B - 3.91\ C - 1.03\ D - 2.83\ AB + 0.77\ AC + 1.27\ AD +$$
$$1.48\ BC - 0.04\ BD - 2.53\ CD - 5.30\ A^2 - 2.16\ B^2 - 5.39\ C^2 - 3.48\ D^2$$

$$(3)$$

The results of ANOVA for the biotransformation of CBZ have been summarized in Table 4.2.3. The probability (P) value and the R-squared of the whole quadratic model were 0.0126 and 0.759. Therefore, the regression of the quadratic equation for CBZ biotransformation was significant and applicable for practical applications. According to Table 4.2.3, the P values of quadratic and linear coefficients are less than 0.05 which means they are generally significant through the model. Moreover, the P value for interaction coefficients was 0.528 which indicates the insignificance of interactions within this model. This observation may be related to the fact that some parameters have a negligible effect on each other for the biotransformation of CBZ. The observed

CBZ removal efficiency varied between 47% (30 °C, 6 µM ABTS, pH 7 and 80 U/L enzyme) and 95% (35 °C, 18 µM ABTS, pH 6, 60 U/L enzyme).

Based on F-value, the linear effects of ABTS concentration and pH and also the quadratic effect of temperature, pH and enzyme concentration were the most significant contributors to the efficiency of CBZ degradation. The RSM procedure predicted a convex shape for response surfaces, which means there is a unique optimum point for biotransformation efficiency. The details of parameters' role in biotransformation are discussed in the following sections.

Effect of pH and temperature on CBZ degradation

Figure 4.2.2 presents the degradation efficiency of CBZ by the laccase-ABTS system at different pH and temperatures. It is evident that pH has both quadratic and linear effects on CBZ biotransformation within the studied range of 4-8. In pH range of 5.5-6, CBZ was almost completely degraded by the laccase-ABTS system (> 95%). However, by increasing the pH to 7, the degradation efficiency significantly (p-value < 0.02) decreased to 62%. This behavior is in accordance with the reduction of laccase activity at higher pH values compared to the acidic pH range. It has been already proven that the highest oxidation level by laccase was obtained at pH range of 4-6 [24]. The reduction of laccase activity reduced the rate of generation of mediator radical and slowed down CBZ oxidation. Also, for other ligninolytic enzymes e.g. LiP, the activity decreased at pH values higher than 4.5 due to inactivation of the enzyme [33]. Cantarella *et al.* also reported a drastic reduction in laccase activity when pH was over 7 [34]. Huerta-Fontela *et al.* reported that CBZ degradation with chlorination was enhanced at higher chlorine concentrations. They concluded that CBZ removal depended on pH so that at higher pH values (> 7), the CBZ removal was lower at lower pH [1]. The enzymes were mainly stabilized by weak interactions, such as Van der Waals and hydrogen bonds. The latter is largely influenced by the medium pH and therefore increasing or decreasing the pH beyond certain range reduced the stability and activity of the enzyme [35].

Complete removal of CBZ was observed at 35 °C while the degradation efficiency was 69% and 73% at 25 °C and 45 °C, respectively. Decreased degradation efficiency at a lower temperature (25 °C) was due to the lowered activation energy of the reaction. On the other hand, decreasing the efficiency at higher temperatures was due to

inactivation of laccase [34]. Temperature played an important role in the rate of biological reactions. However, above a certain temperature (40 °C), the rate of biological reactions experienced a decrease due to the denaturation of related enzymes [35]. Furthermore, the analysis of the surface plot for the effect of pH and temperature revealed that the interaction effect of two parameters was negligible.

Effect of enzyme and mediator concentration

The effect of enzyme and ABTS concentration on CBZ biotransformation are depicted in Figure 4.2.3. According to Figure 4.2.3, increasing the enzyme concentration from 40 to 60 U/L, increased the biotransformation efficiency (from around 70% to 95%) but a further increase to 80 U/L decreased the biotransformation efficiency to the same level as observed for 40 U/L. It showed that the enzyme concentration had only a quadratic effect on biotransformation. Higher laccase activity led to a rapid generation of ABTS radicals, which attacked CBZ and caused efficient transformation of CBZ. Similar results were observed in the research work of Tran *et al.,* who reported that while increasing the laccase activity from 2000 U/L to 6000 U/L, the degradation efficiency increased 4.3 folds [32]. Further addition of enzyme to the solution increase the collisions and interactions among enzyme macromolecules and they can block each other's active sites. Therefore, at higher concentrations of enzyme, compared to the optimum level, the degradation efficiency was reduced.

On the other hand, increasing the ABTS concentration in the whole studied range (6-14 µM) enhanced the biotransformation efficiency, which is derived from the linearity of the effect. The CBZ degradation efficiency was improved from 47% to 95% by increasing the ABTS concentration from 6 µM to 14 µM. Ji *et al.* observed that less than 5% of CBZ was removed by free laccase in 96 h while the addition of a mediator (p-coumaric acid) increased the degradation efficiency to more than 60% [13]. Similarly, Hata *et al.* observed increase in the removal efficiency of CBZ from 39% to 60% after addition of HBT as redox mediator [27].

The presence of a mediator allows the enzyme to overcome a kinetic barrier [36]. Mediators can stabilize the enzyme through binding to its active site or another suitable region on the protein structure of enzyme [37]. The capability of ABTS for degradation of CBZ was evaluated in another experiment through monitoring the removal efficiency of CBZ by laccase over 24 h treatment in presence and absence of ABTS. The results

of this test were depicted in Figure 4.2.4. Accordingly, CBZ was not a highly reactive substrate for laccase and less than 30% of CBZ was degraded by free laccase after 24 h. In comparison, in the presence of ABTS, the degradation efficiency of CBZ was improved to more than 82% after 24 h. In laccase-mediator systems, laccase oxidize the mediator to form reactive radicals (ABTS$^{•+}$ with 0.61 V or perhaps ABTS^{++} 1.1 V redox potential), which can oxidize recalcitrant compounds through one electron transfer mechanism [13, 26, 34]. Free radicals can also react with compounds through radical-radical reactions and hydrogen abstraction [24]. The general theory is that the mediator carries out the oxidation of the substrate in a catalytic cycle by turning over between its natural and oxidized (Med$_{ox}$) states [34]. Also, the intervention of by-products of the Med$_{ox}$ species is possible. The non-phenolic substrate can be oxidised by reacting with mediator's by-products [38, 39].

Kinetics of degradation of CBZ

Analysis of data can lead to estimation of the dependent variable within the range of parameters and also can suggest several optimum points with maximum degradation efficiency. According to the results, by setting temperature, pH, enzyme concentration and ABTS concentration to 35 °C, 6, 60 U/L and 18 µM, respectively can increase the degradation efficiency of CBZ by laccase-ABTS system to more than 95%. These parameters' levels along with CBZ concentration of 1000 ppb were selected for kinetic study. The time evolution trends of concentration of CBZ in the optimized conditions is illustrated in Figure 4.2.5. As predicted by the software, CBZ was almost completely degraded (95%) by laccase-ABTS system after 24 h of incubation. The CBZ degradation efficiency was 60% during the first 8 h. Enzymatic processes generally follow Michaelis-Menten kinetic model according to which the degradation rate is of first order at very low substrate concentrations. Therefore, due to very low concentrations of micropollutants (µM level) in environmental compartment, degradation of these compounds can be fitted by a first order reaction rate [40]. Assuming the first-order kinetics for degradation, the constants were determined by plotting logarithmic concentrations against time (Figure 4.2.5). The kinetic constant, *K,* was determined to be 0.07 (h^{-1}) (R^2 = 0.93). At environmentally relevant concentrations, the rate of reaction is significantly lower than high concentrations. For example, in a research by Jelic *et al.*, white-rot fungus TV, eliminated 94% of CBZ at

initial concentration of 9 mg/L after 6 days while at initial concentration of 50 µg/L, 61% of CBZ was degraded in 7 days [19]. Furthermore, Lineweaver-Burk model was used to determine the Michaelis-Menten parameters i.e. K_m and V_{max}. The plot was fitted very well with an R^2 of 0.9996 and accordingly, V_{max} and K_m were found to be 29.85 µg L^{-1} h^{-1} and 498.60 µg/L (plot not shown). The results of Lineweaver-Burk model are in excellent agreement with the first order model as the ratio of V_{max} to K_m was calculated to be around 0.06 h^{-1}.

Metabolites identification of CBZ biotransformation

To identify the CBZ biotransformation products, a full-scan chromatogram for sample taken after 24 h of treatment by the laccase-ABTS system at optimal parameters was recorded over m/z range of 70-300. The protonated molecule of parent compound CBZ appeared at m/z of 237.10. Several more peaks were observed at m/z 271.10 and 253.10 which are attributed to 10,11-dihydro-10,11-dihydroxy-CBZ (DiOH-CBZ), 10,11-dihydro-10,11-epoxy-CBZ (EP-CBZ). EP-CBZ has been already reported as the major by-product of CBZ by oxidation with fungal whole cell and laccase [13, 41]. The appearance of two product ions at m/z of 236 and 210 in MS-MS spectrum (data not shown) of EP-CBZ (m/z: 253, $C_{15}H_{13}N_2O_2$) is similar to the CBZ spectrum which undergoes loss of ammonia (17 Da) or HNCO (43 Da), respectively. Likewise, DiOH-CBZ (m/z: 271.1, $C_{15}H_{15}N_2O_3$) resulted in three product ions at m/z 253, 236 and 210 through loss of a water molecule followed by the abstraction of ammonia or HNCO, respectively (See Figure 4.2.6). According to Bahlmann *et al.*, the level of concern estimated for EP-CBZ was similar to CBZ, while higher levels of concern estimated for DiOH-CBZ were higher than the parent compound [6].

Estrogenic activity of CBZ by-products

The YES test is a method in which the human estrogen receptor (hER) should be expressed in yeast so that in an estrogen-dependent manner, it can activate the transcription of a promoter carrying estrogen-responsive sequences [31]. The reproducibility and sensitivity of this assay was assessed by comparing the response of the yeast to 17β-estradiol with responses for different samples spiked with CBZ. The change in color due to addition of 17β-estradiol and different samples is presented in Figure 4.2.7. Accordingly, the estrogenicity for samples containing 17β-estradiol, as

the color turned red after 3 day of incubation. However, the samples with CBZ or its by-products did not show any changes in color. The results showed that CBZ (at 1 mg/L or 4 µM) and its by-products from treatment with laccase-ABTS system has no estrogenic activity. Therefore, this enzymatic treatment may be considered as a safe disposal strategy for wastewater disposal. Ji *et al.* employed the growth inhibition of algae using as a viability indicator for CBZ toxicity. They observed that 24 h incubation in CBZ solution (0.4 µM), resulted in 95% mortality of *C. marina* cell viability, while the effluent of a laccase-mediator system (with 20 µM initial CBZ) had no effect on viability [13]. In contrast, Jelic *et al.*, used Microtox test (*Vibrio fischeri luminescence*) to assess the toxicity of the treated CBZ with fungus, TV. According to their results, CBZ (200 µg/L) showed a 15 min EC50 of 95% while the effluent of continuous reactor showed a 15 min EC50 of 77% which meant that the by-products were more toxic than the parent compound [19]. Comparing the results in this research with the results of other researchers [13, 19] indicates that the presence of mediator helped to remove the estrogenicity of CBZ by facilitating the production of less estrogenic compounds.

Conclusion

Crude laccase was produced by growing *Trametes versicolor* and employed for degradation of CBZ in the absence and presence of the enzyme mediators, ABTS. The impacts of operational parameters along with their interactions on biotransformation of CBZ were investigated using central composite design of experiments and response surface methodology. The ANOVA results indicated that the linear effects of ABTS concentration and pH and also the quadratic effect of temperature, pH and enzyme concentration were significant contributors to the efficiency of CBZ degradation. The optimization results showed that at 35 °C, pH 6, 60 U/L of laccase concentration and 18 µM of ABTS concentration) the degradation efficiency reached to 95% within 24 h. 10,11-dihydro-10,11-dihydroxy-CBZ and 10,11-dihydro-10,11-epoxy-CBZ were identified as the major transformation products of CBZ degradation. The estrogenicity tests determined by yeast estrogenic activity assay revealed that the applied degradation treatment using laccase (with and without ABTS) had no estrogenicity effect. The data presented suggested that the laccase-ABTS system has potential for the removal of CBZ in aqueous media.

Acknowledgements

References

1.   Huerta-Fontela, M., Galceran, M.T., and Ventura, F., Occurrence and removal of pharmaceuticals and hormones through drinking water treatment. Water Research, 2011. 45(3): p. 1432-1442.

2.   Jelic, A., Gros, M., Ginebreda, A., Cespedes-Sánchez, R., Ventura, F., Petrovic, M., and Barcelo, D., Occurrence, partition and removal of pharmaceuticals in sewage water and sludge during wastewater treatment. Water Research, 2011. 45(3): p. 1165-1176.

3.   Kasprzyk-Hordern, B., Dinsdale, R.M., and Guwy, A.J., The removal of pharmaceuticals, personal care products, endocrine disruptors and illicit drugs during wastewater treatment and its impact on the quality of receiving waters. Water Research, 2009. 43(2): p. 363-380.

4.   Malchi, T., Maor, Y., Tadmor, G., Shenker, M., and Chefetz, B., Irrigation of Root Vegetables with Treated Wastewater: Evaluating Uptake of Pharmaceuticals and the Associated Human Health Risks. Environmental Science & Technology, 2014. 48(16): p. 9325-9333.

5.   Ferrari, B.t., Paxéus, N., Giudice, R.L., Pollio, A., and Garric, J., Ecotoxicological impact of pharmaceuticals found in treated wastewaters: study of carbamazepine, clofibric acid, and diclofenac. Ecotoxicology and Environmental Safety, 2003. 55(3): p. 359-370.

6.   Bahlmann, A., Brack, W., Schneider, R.J., and Krauss, M., Carbamazepine and its metabolites in wastewater: analytical pitfalls and occurrence in Germany and Portugal. Water research, 2014. 57: p. 104-114.

7.   Tixier, C., Singer, H.P., Oellers, S., and Müller, S.R., Occurrence and Fate of Carbamazepine, Clofibric Acid, Diclofenac, Ibuprofen, Ketoprofen, and Naproxen in Surface Waters. Environmental Science & Technology, 2003. 37(6): p. 1061-1068.

8.   Verlicchi, P., Al Aukidy, M., and Zambello, E., Occurrence of pharmaceutical compounds in urban wastewater: removal, mass load and environmental risk after a secondary treatment-a review. Science of the total environment, 2012. 429: p. 123-155.

9.   Radjenović, J., Petrović, M., and Barceló, D., Fate and distribution of pharmaceuticals in wastewater and sewage sludge of the conventional activated sludge (CAS) and advanced membrane bioreactor (MBR) treatment. Water Research, 2009. 43(3): p. 831-841.

10.   Clara, M., Strenn, B., Gans, O., Martinez, E., Kreuzinger, N., and Kroiss, H., Removal of selected pharmaceuticals, fragrances and endocrine disrupting compounds in a membrane bioreactor and conventional wastewater treatment plants. Water Research, 2005. 39(19): p. 4797-4807.

11.   Clara, M., Strenn, B., and Kreuzinger, N., Carbamazepine as a possible anthropogenic marker in the aquatic environment: investigations on the behaviour of Carbamazepine in wastewater treatment and during groundwater infiltration. Water Research, 2004. 38(4): p. 947-954.

12.   Jos, A., Repetto, G., Rios, J.C., Hazen, M.J., Molero, M.L., del Peso, A., Salguero, M., Fernández-Freire, P., Pérez-Martín, J.M., and Cameán, A., Ecotoxicological evaluation of carbamazepine using six different model systems with eighteen endpoints. Toxicology in Vitro, 2003. 17(5–6): p. 525-532.

13. Ji, C., Hou, J., Wang, K., Zhang, Y., and Chen, V., Biocatalytic degradation of carbamazepine with immobilized laccase-mediator membrane hybrid reactor. Journal of Membrane Science, 2016. 502: p. 11-20.

14. Ikehata, K., Jodeiri Naghashkar, N., and Gamal El-Din, M., Degradation of Aqueous Pharmaceuticals by Ozonation and Advanced Oxidation Processes: A Review. Ozone: Science & Engineering, 2006. 28(6): p. 353-414.

15. Laera, G., Chong, M.N., Jin, B., and Lopez, A., An integrated MBR–TiO2 photocatalysis process for the removal of Carbamazepine from simulated pharmaceutical industrial effluent. Bioresource Technology, 2011. 102(13): p. 7012-7015.

16. Radjenović, J., Petrović, M., Ventura, F., and Barceló, D., Rejection of pharmaceuticals in nanofiltration and reverse osmosis membrane drinking water treatment. Water Research, 2008. 42(14): p. 3601-3610.

17. Westerhoff, P., Moon, H., Minakata, D., and Crittenden, J., Oxidation of organics in retentates from reverse osmosis wastewater reuse facilities. Water Research, 2009. 43(16): p. 3992-3998.

18. Donner, E., Kosjek, T., Qualmann, S., Kusk, K.O., Heath, E., Revitt, D.M., Ledin, A., and Andersen, H.R., Ecotoxicity of carbamazepine and its UV photolysis transformation products. Science of The Total Environment, 2013. 443: p. 870-876.

19. Jelic, A., Cruz-Morató, C., Marco-Urrea, E., Sarrà, M., Perez, S., Vicent, T., Petrović, M., and Barcelo, D., Degradation of carbamazepine by Trametes versicolor in an air pulsed fluidized bed bioreactor and identification of intermediates. Water Research, 2012. 46(4): p. 955-964.

20. Shi, L., Yu, H., Dong, T., Kong, W., Ke, M., Ma, F., and Zhang, X., Biochemical and molecular characterization of a novel laccase from selective lignin-degrading white-rot fungus Echinodontium taxodii 2538. Process Biochemistry, 2014. 49(7): p. 1097-1106.

21. Bettin, F., da Rosa, L.O., Montanari, Q., Calloni, R., Gaio, T.A., Malvessi, E., da Silveira, M.M., and Dillon, A.J.P., Growth kinetics, production, and characterization of extracellular laccases from Pleurotus sajor-caju PS-2001. Process Biochemistry, 2011. 46(3): p. 758-764.

22. Kong, W., Chen, H., Lyu, S., Ma, F., Yu, H., and Zhang, X., Characterization of a novel manganese peroxidase from white-rot fungus Echinodontium taxodii 2538, and its use for the degradation of lignin-related compounds. Process Biochemistry, 2016. 51(11): p. 1776-1783.

23. Majeau, J.A., Brar, S.K., and Tyagi, R.D., Laccases for removal of recalcitrant and emerging pollutants. Bioresource Technology, 2010. 101(7): p. 2331-2350.

24. Garcia, H.A., Hoffman, C.M., Kinney, K.A., and Lawler, D.F., Laccase-catalyzed oxidation of oxybenzone in municipal wastewater primary effluent. Water Research, 2011. 45(5): p. 1921-1932.

25. Yang, S., Hai, F.I., Nghiem, L.D., Price, W.E., Roddick, F., Moreira, M.T., and Magram, S.F., Understanding the factors controlling the removal of trace organic contaminants by white-rot fungi and their lignin modifying enzymes: A critical review. Bioresource Technology, 2013. 141: p. 97-108.

26. Cañas, A.I. and Camarero, S., Laccases and their natural mediators: Biotechnological tools for sustainable eco-friendly processes. Biotechnology Advances, 2010. 28(6): p. 694-705.

27. Hata, T., Shintate, H., Kawai, S., Okamura, H., and Nishida, T., Elimination of carbamazepine by repeated treatment with laccase in the presence of 1-hydroxybenzotriazole. Journal of Hazardous Materials, 2010. 181(1–3): p. 1175-1178.

28. Gassara, F., Brar, S.K., Tyagi, R., John, R.P., Verma, M., and Valero, J., Parameter optimization for production of ligninolytic enzymes using agro-industrial wastes by response surface method. Biotechnology and Bioprocess Engineering: BBE, 2011. 16(2): p. 343.

29. Johnson, K.A. and Goody, R.S., The original Michaelis constant: translation of the 1913 Michaelis–Menten paper. Biochemistry, 2011. 50(39): p. 8264-8269.

30. Mohapatra, D.P., Brar, S.K., Tyagi, R.D., Picard, P., and Surampalli, R.Y., Carbamazepine in municipal wastewater and wastewater sludge: Ultrafast quantification by laser diode thermal desorption-atmospheric pressure chemical ionization coupled with tandem mass spectrometry. Talanta, 2012. 99: p. 247-255.

31. Routledge, E.J. and Sumpter, J.P., Estrogenic activity of surfactants and some of their degradation products assessed using a recombinant yeast screen. Environmental Toxicology and Chemistry, 1996. 15(3): p. 241-248.

32. Tran, N.H., Urase, T., and Kusakabe, O., Biodegradation Characteristics of Pharmaceutical Substances by Whole Fungal Culture Trametes versicolor and its Laccase. Journal of Water and Environment Technology, 2010. 8(2): p. 125-140.

33. Zhang, Y. and Geißen, S.U., In vitro degradation of carbamazepine and diclofenac by crude lignin peroxidase. Journal of Hazardous Materials, 2010. 176(1-3): p. 1089-1092.

34. Cantarella, G., Galli, C., and Gentili, P., Free radical versus electron-transfer routes of oxidation of hydrocarbons by laccase/mediator systems: Catalytic or stoichiometric procedures. Journal of Molecular Catalysis B: Enzymatic, 2003. 22(3-4): p. 135-144.

35. Bhattacharya, S.S. and Banerjee, R., Laccase mediated biodegradation of 2,4-dichlorophenol using response surface methodology. Chemosphere, 2008. 73(1): p. 81-85.

36. Bourbonnais, R., Leech, D., and Paice, M.G., Electrochemical analysis of the interactions of laccase mediators with lignin model compounds. Biochimica et Biophysica Acta (BBA) - General Subjects, 1998. 1379(3): p. 381-390.

37.   Ostadhadi-Dehkordi, S., Tabatabaei-Sameni, M., Forootanfar, H., Kolahdouz, S., Ghazi-Khansari, M., and Faramarzi, M.A., Degradation of some benzodiazepines by a laccase-mediated system in aqueous solution. Bioresource Technology, 2012. 125: p. 344-347.

38.   Cantarella, G., d'Acunzo, F., and Galli, C., Determination of laccase activity in mixed solvents: Comparison between two chromogens in a spectrophotometric assay. Biotechnology and Bioengineering, 2003. 82(4): p. 395-398.

39.   Fabbrini, M., Galli, C., and Gentili, P., Radical or electron-transfer mechanism of oxidation with some laccase/mediator systems. Journal of Molecular Catalysis B: Enzymatic, 2002. 18(1): p. 169-171.

40.   Eibes, G., Debernardi, G., Feijoo, G., Moreira, M.T., and Lema, J.M., Oxidation of pharmaceutically active compounds by a ligninolytic fungal peroxidase. Biodegradation, 2011. 22(3): p. 539-550.

41.   Golan-Rozen, N., Chefetz, B., Ben-Ari, J., Geva, J., and Hadar, Y., Transformation of the Recalcitrant Pharmaceutical Compound Carbamazepine by Pleurotus ostreatus: Role of Cytochrome P450 Monooxygenase and Manganese Peroxidase. Environmental Science & Technology, 2011. 45(16): p. 6800-6805.

Table 4.2.1 Independent parameters and their coded levels used for degradation optimization

Independent factor	Units	Coded levels				
Levels		-2	-1	0	+1	+2
Temperature	°C	25	30	35	40	45
ABTS concentration	µM	2	6	10	14	18
pH	-	4	5	6	7	8
Enzyme concentration	U/L	20	40	60	80	100

Table 4.2.2 Four-factor and five-level central composite designs for RSM and experimentally achieved degradation efficiency

No.	Temperature (°C)	ABTS concentration (µM)	pH	Enzyme concentration (U/L)	Degradation efficiency (%)
1	30	6	5	40	68.76
2	40	6	5	40	64.68
3	30	14	5	40	81.58
4	40	14	5	40	66.81
5	30	6	7	40	63.49
6	40	6	7	40	67.32
7	30	14	7	40	69.68
8	40	14	7	40	65.55
9	30	6	5	80	71.21
10	40	6	5	80	76.34
11	30	14	5	80	70.65
12	40	14	5	80	69.15
13	30	6	7	80	46.78
14	40	6	7	80	55.52
15	30	14	7	20	70.04
16	40	14	7	80	58.76
17	25	10	6	60	68.93
18	45	10	6	60	73.34
19	35	2	6	60	72.71
20	35	18	6	60	94.75
21	35	10	4	60	76.23
22	35	10	8	60	65.35
23	35	10	6	20	77.28
24	35	10	6	100	79.59
25 (C)	35	10	6	60	86.61
26 (C)	35	10	6	60	86.00
27 (C)	35	10	6	60	86.61
28 (C)	35	10	6	60	86.00
29 (C)	35	10	6	60	86.61
30 (C)	35	10	6	60	86.00

Table 4.2.3 ANOVA of the regression parameters of the predicted response surface model for degradation of CBZ

Regression	Degrees of freedom	Sum of squares	Mean square	F-value	Pr > F
Linear	4	677.85	169.46	3.23	0.0156
Quadratic	4	2027.36	506.84	9.65	0.0001
Interaction	6	300.84	50.14	0.96	0.5280
Residual error	15	787.72	52.51		
Lack of fit	10	787.42	78.74	1281.25	<0.0001
Pure error	5	0.31	0.061		
Total model	14	2490.80	177.91	3.39	0.0126
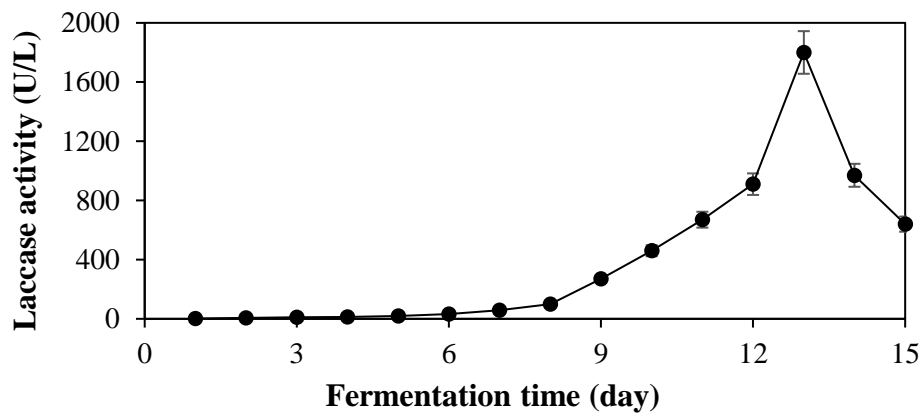
Figure 4.2.1 Production of laccase during fermentation of *T. versicolor* (Y-axis is the laccase activity in crude extract. The error bars represent standard deviation of two replicates)
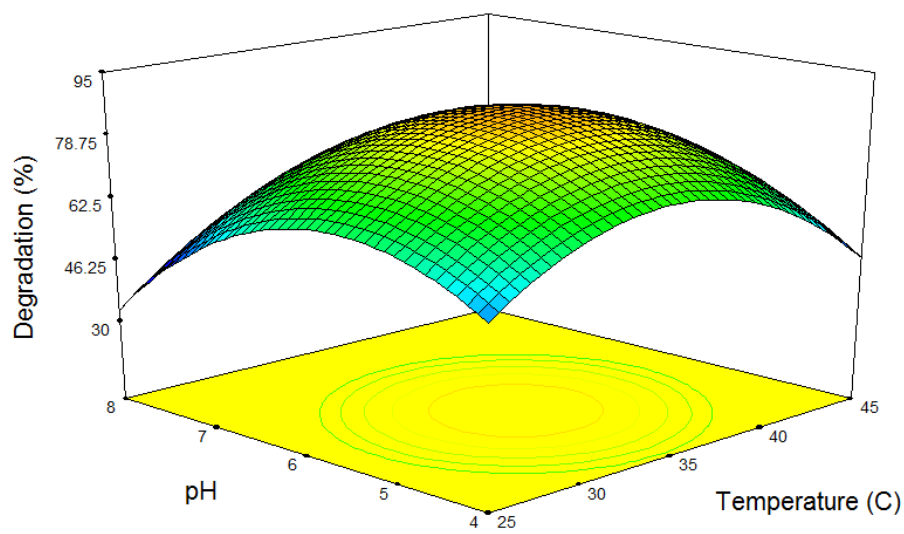
Figure 4.2.2 Influence of pH and temperature on the degradation of carbamazepine by laccase-ABTS system
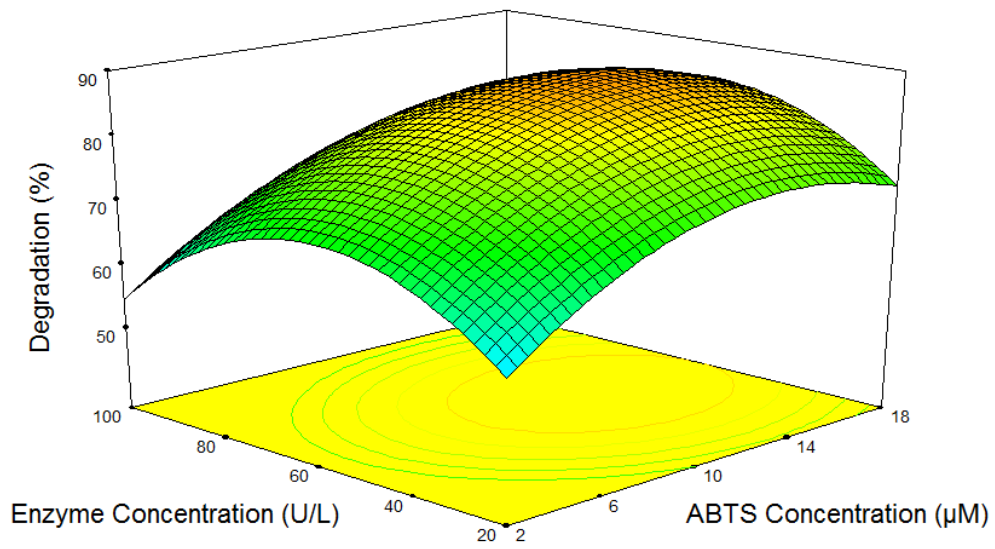
Figure 4.2.3 Response surface plot showing the effect of enzyme and ABTS concentration on the degradation of carbamazepine (%)
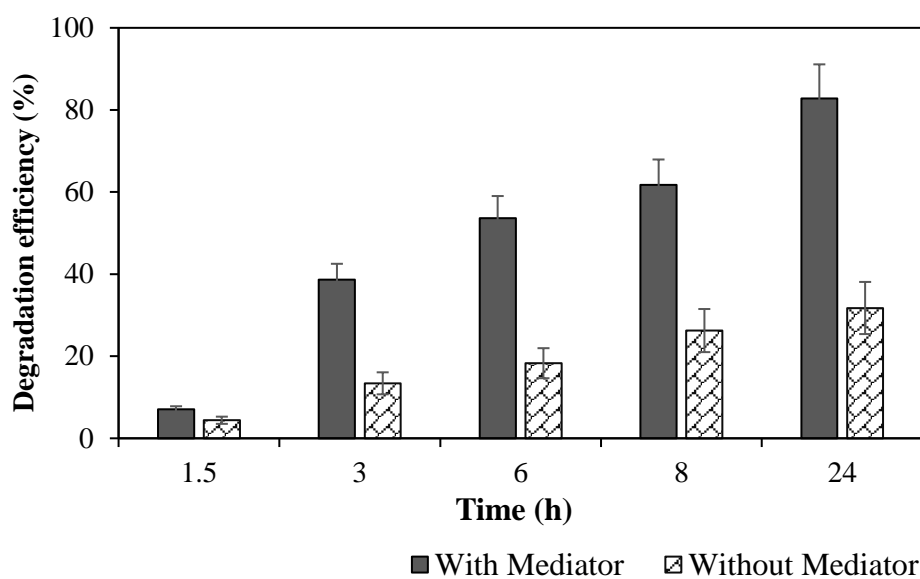
Figure 4.2.4 Carbamazepine degradation during reaction with laccase without mediator (White) and with mediator (Gray) (1 mg/L (4 µM) carbamazepine, 18 µM ABTS, pH 6, 60 U/mL initial laccase activity)

$$Y = -0.0663 \, X + 2.69$$
$$R^2 = 0.9312$$
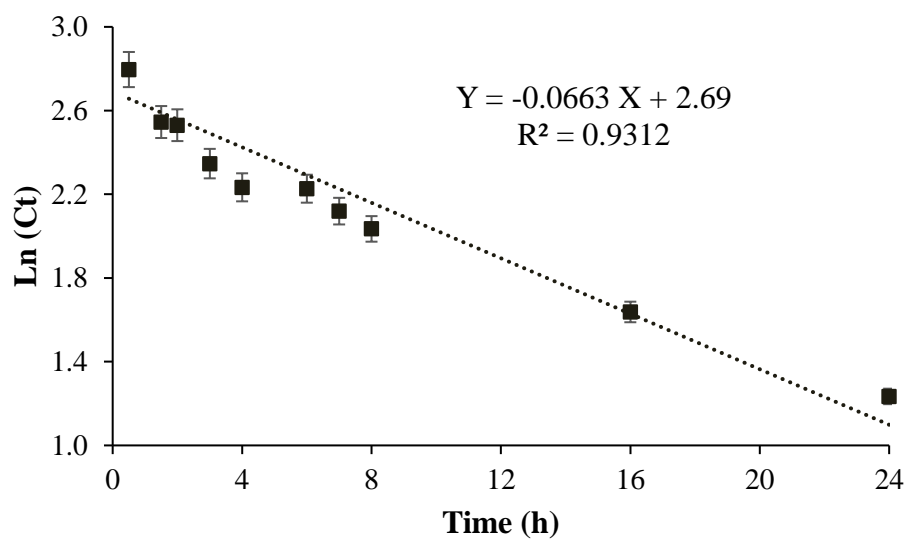
Figure 4.2.5 Plot for first-order kinetics of carbamazepine biotransformation with laccase and ABTS (C_0 = 1 mg/L, 35 °C, time = 24 h, pH = 6)
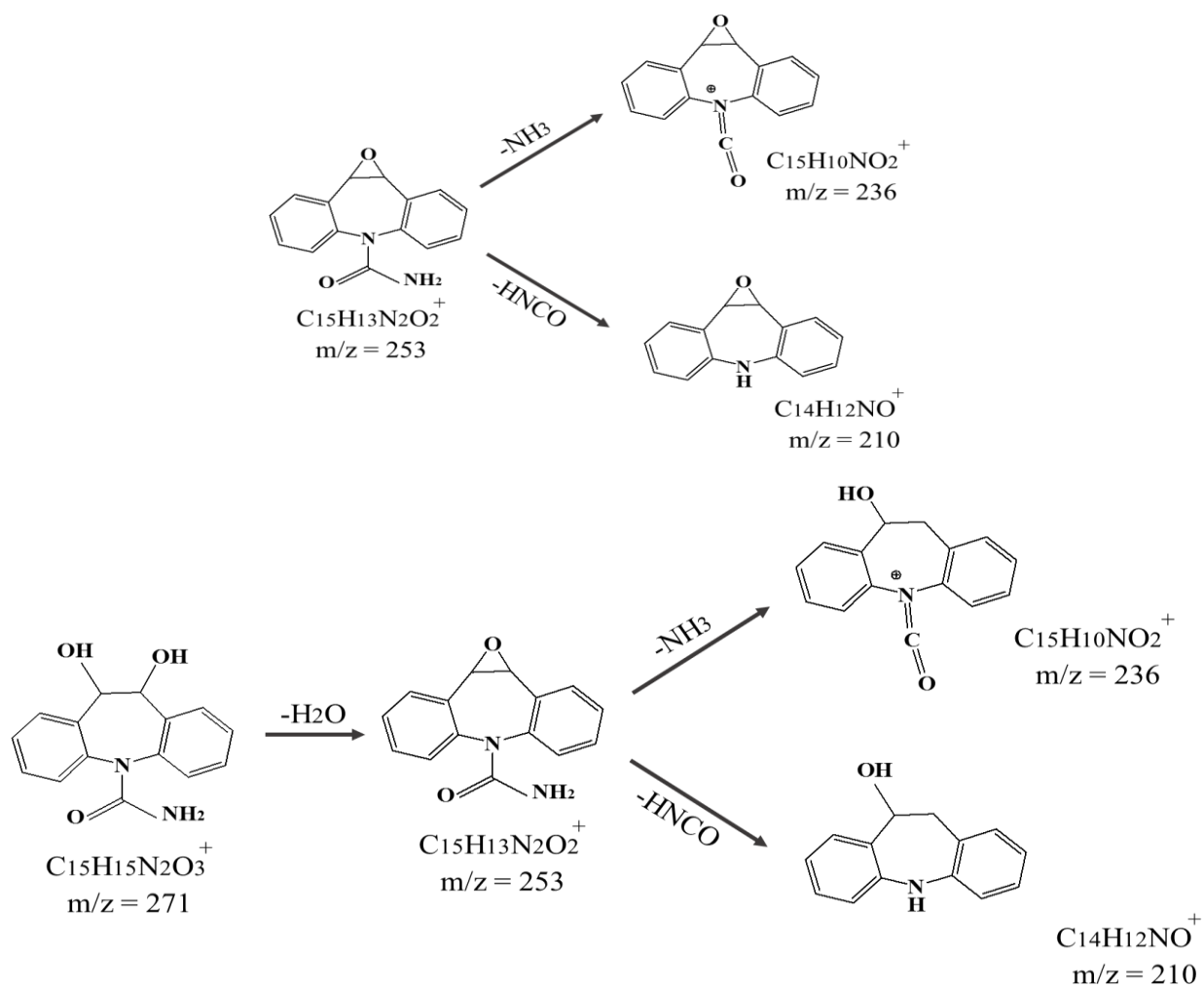
Figure 4.2.6 Two main by-products of carbamazepine biotransformation and their related daughter ions in tandem mass spectroscopy
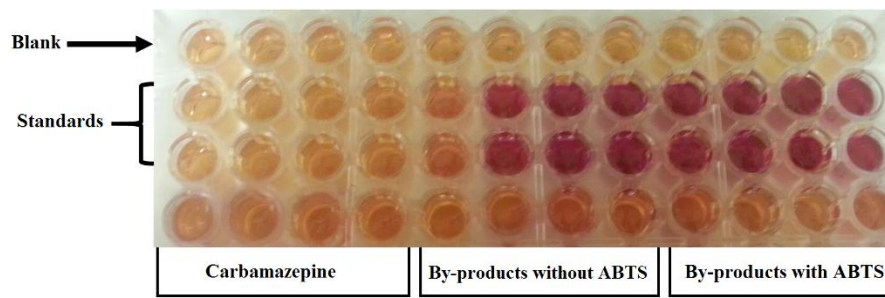
Figure 4.2.7 Yeast estrogenic activity assay of blank, E2 (17-β estradiol) and samples with carbamazepine

Part 3

Antagonistic effects of divalent metal ions and humic acid on removal of carbamazepine

Mitra Naghdi[1], Mehrdad Taheran[1], Mohamed-Amine Laadila[1], Satinder Kaur Brar[1*], R.Y. Surampalli[2] and Mausam Verma[1]

[1]INRS-ETE, Université du Québec, 490, Rue de la Couronne, Québec, Canada G1K 9A9

[2]Department of Civil Engineering, University of Nebraska-Lincoln, N104 SEC PO Box 886105, Lincoln, NE 68588-6105, US

(*Phone: 1 418 654 3116; Fax: 1 418 654 2600; E-mail: satinder.brar@ete.inrs.ca)

Résumé

La présence de certains composés pharmaceutiquement actifs dans les eaux de surface a suscité des préoccupations à l'échelle mondiale. La laccase est une option prometteuse pour éliminer ces composés en solution aqueuse. Cependant, il y a des informations limitées pour indiquer comment des constituants importants des solutions aqueuses, comme les cations métalliques divalents et la matière organique naturelle, influencent le devenir des contaminants cibles pendant l'oxydation de la laccase. Dans cette étude, la dégradation de la carbamazépine (CBZ) en présence de différentes concentrations d'ions métalliques divalents, y compris Fe^{2+}, Cu^{2+}, Mg^{2+} et Ca^{2+} et l'acide humique a été étudiée. Nous avons observé que la laccase de *Trametes versicolor* peut éliminer jusqu'à 32% de la CBZ en l'absence des métaux et de la matière organique. Les résultats ont montré que Cu^{2+} et Ca^{2+} peuvent augmenter l'efficacité de dégradation de la CBZ de 18%, mais Fe^{2+} et Mg^{2+} diminuent l'efficacité de la dégradation de 40%. En outre, il a été observé que l'augmentation de la concentration en acide humique diminuait de 42% l'efficacité de dégradation de la CBZ en raison de la liaison covalente / non covalente avec les polluants. La présence d'ions métalliques et d'acide humique a diminué l'efficacité globale de la dégradation de 15%. Nos résultats indiquent que la présence de cations métalliques et de matière organique naturelle peut avoir un effet négatif ($p < 0,05$) sur l'élimination de la CBZ par l'enzyme.

Mots clés

Carbamazépine, Activité de la laccase, Dégradation, Ions métalliques, Matière organique naturelle

Abstract

The occurrence of some pharmaceutically active compounds in surface water has raised global concern. Laccase is a promising option to remove these compounds in aqueous solution. However, there is limited information to indicate how do the important constituents of aqueous solutions, namely divalent metal ions and natural organic matter influence the fate of the target contaminants during laccase oxidation. In this study, the degradation of carbamazepine (CBZ) in the presence of different concentrations of divalent metal ions including Fe^{2+}, Cu^{2+}, Mg^{2+} and Ca^{2+} and humic acid was investigated. We observed that the laccase from *Trametes versicolor* can remove CBZ up to 32% in the absence of metals and organic matter. The results showed that Cu^{2+} and Ca^{2+} can increase the degradation efficiency of CBZ by 18%, but Fe^{2+} and Mg^{2+} decrease the degradation efficiency by 40%. Furthermore, it was observed that increase in the concentration of humic acid decreased the degradation efficiency of CBZ by 42% due to covalent/noncovalent binding with pollutants. The presence of both metal ions and humic acid decreased the overall degradation efficiency by 15%. Our results indicated that the presence of metal cations and natural organic matter can have a negative effect ($p < 0.05$) on the removal of CBZ by the enzyme.

Keywords

Carbamazepine, Laccase activity, Degradation, Metal ions, Natural organic matter

Introduction

Pharmaceutical compounds are widely used for curing the diseases in human and animal [1]. The excess amounts of these compounds find their way into the environment through wastewater treatment plants (WWTPs). The potential adverse effects of such compounds on different organisms, such as the development of antibiotic resistance genes in pathogenic bacteria, has attracted the attention of researchers and regulatory organizations in recent years [2]. Currently, one of the promising approaches for biodegradation of pharmaceutical compounds in aqueous systems is the use of white-rot fungi and their related ligninolytic enzymes which can oxidize a wide spectrum of organic substrates [3].

Carbamazepine (CBZ) is one of the widely used antiepileptic drugs with more than 1000 tons of annual consumption around the world. The rate of CBZ release into water bodies is around 30 tons per year and according to several reports, it can be toxic for several aquatic organisms, such as crustaceans and cnidarians [4]. Laccases (EC 1.10.3.2), belonging to the multi-copper oxidases family, can oxidize various organic pollutants, using molecular oxygen as the electron acceptor [5]. The low specificity, being able to use atmospheric oxygen and high yield rendered laccase an attractive option for environmental applications [6]. However, for practical application of laccases, the operational stability of the enzyme in different conditions is of the question. Wastewaters and their treated effluents typically contain divalent metal ions and organic compounds at different concentrations which may decrease laccase activity [7].

Divalent metal ions are present in aquatic ecosystems and they can have a high influence on the abiotic reactions of phenolic contaminants. Shankar and Nill investigated decolorization of synthetic dyes with crude laccase from *Peniophora sp.* They observed that the presence of Ca^{2+} increased decolorization of Amido Black and Methylene Blue up to 14.5% compared to control [8]. In another study, Si *et al.* reported that the time for complete decolorization of azo dye Congo red by laccase from *Trametes pubescens* was reduced from 78 h to 21 h in the presence of Cu^{2+} [9]. Moreover, natural organic matter are present in aquatic ecosystems and play key roles in fate of compounds in these media. He *et al.* demonstrated that the natural organic matter from different sources could influence the removal of contaminants in oxidation processes [10]. For instance, Sun *et al.* observed that humic acid significantly

suppressed transformation of triclosan during laccase oxidation, and the inhibitory effect was enhanced with increasing the humic acid concentration from 0 to 50 mg/L [7].

Although several studies have been done on the laccase-catalyzed degradation of pharmaceutical compounds, little attention has been paid to the effect of metal ions and natural organic matters on the degradation of pharmaceutical compounds by laccase. Therefore, the objective of this study was to investigate the effects of several metal ions in wastewater effluents and natural organic matter on CBZ transformation in aqueous solution by laccase. We initially examined the reactions of CBZ mediated by laccase from *Trametes versicolor.* Then, we evaluated the effects of metal ions (Cu^{2+}, Ca^{2+}, Mg^{2+}, and Fe^{2+}) and natural organic matter on CBZ transformation by batch experiments. Our results provide a novel insight into the transformation of CBZ in natural aquatic environments by laccase enzyme in the presence of metal ions and natural organic matter.

2. Material and methods

2.1. Materials

Carbamazepine (CBZ) and 2, 2'-azino-bis (3-ethylbenzothiazoline-6-sulphonic acid) (ABTS) were purchased from Sigma-Aldrich (Oakville, Canada) with a purity of > 99%. Carbamazepine (D10), as an internal standard, was provided by CDN Isotopes (Pointe-Claire, Canada). Copper (II) sulfate, Calcium chloride, Magnesium chloride, Iron (II) sulfate, methanol and Tween 80 were obtained from Fisher Scientific (Ottawa, Canada). Ultrapure water was produced in the laboratory using a Milli-Q/Milli-Ro Millipore system (Massachusetts, USA). The ultrapure water was used for the preparation of stock solutions and samples for degradation tests.

2.2. Preparation of inoculum

The fungus, *Trametes versicolor* (ATCC 20869) was grown aerobically in potato dextrose broth (PDB, 2.4% w/v and 30 mL) at 30±1 °C and 150 rpm for 7 days. Then, the fungus was grown by adding 100 μL aliquots of PDB media to potato dextrose agar (PDA) plates for 9 days at 30±1 °C. After incubation, the plates were stored at 4±1 °C prior to being utilized for solid fermentation.

2.3 Laccase production and extraction

Around 40 g of apple pomace (pH 4.5 and 78% w/w moisture) was mixed with Tween 80 (0.5% v/w) in 500 mL Erlenmeyer flasks and sterilized for 20 min at 121±1 °C. Then, the mixture was inoculated with *T. versicolor* and incubated at 30±1 °C for 14 days. For extraction of the enzyme, one gram of fermented sample was mixed with 20 mL of 50 mM sodium phosphate buffer (pH 6.5). The mixture was mixed for 1 h on an incubator shaker at 35±1 °C and 150 rpm and then centrifuged for 30 min at 7000 × g. The supernatant was analyzed for laccase activity and dried for 48 h using Scanvac Coolsafe freeze drier (LaboGen, Denmark).

2.4 Degradation of pharmaceutical compounds

To study the effect of natural organic matter on the removal of pharmaceutical compounds from pure water using laccase, CBZ (40 ppb) were spiked into 15 mL milli-Q water containing 3.0 U/mL laccase and 5, 15 and 30 ppm of humic acid. The flasks were shaken at 25±1 °C in an incubator shaker at 150 rpm and samples were taken at different interval times. Likewise, for the effect of metal ions on the removal of CBZ, Fe^{2+} and Cu^{2+} were added at the concentrations of 0.1, 0.5 and 1 ppm, and Mg^{2+} and Ca^{2+} were added at the concentrations of 1, 5 and 10 ppm, to the solution. Moreover, the effect of both metal ions and humic acid on the removal of CBZ was investigated.

2.5 Quantification of CBZ

Quantification of CBZ was performed with a Laser Diode Thermal Desorption (LDTD) (Phytronix technologies, Canada) coupled with an LCQ Duo ion trap tandem mass spectrometer (Thermo Finnigan, USA). The identified daughter ions for CBZ were 194 and 192 Da. The calibration curve of CBZ concentration comprised six standard solutions and the R^2 was greater than 0.99. The details of the quantification process were described elsewhere [11]. All experiments were carried out in duplicates and the average values were reported for analysis.

2.6 Enzyme assay

Laccase activity was quantified by monitoring the rate of ABTS oxidation to its radical form in aqueous solution. One unit of laccase activity was considered as the amount of required enzyme for oxidizing one µmol of ABTS per min at 45 °C. In brief, a mixture containing 500 µL of ABTS (1.5 mM), 2.450 mL of 0.1 M citrate-phosphate buffer (pH 3.5) and 50 µL of laccase sample was prepared. Then the increase in absorbance at

the wavelength of 420 nm (ε_{420} = 36.000 M^{-1} cm^{-1}) was monitored [12] using a Cary 100 UV-VIS spectrophotometer (Varian, Australia).

2.7 Statistical analyses

All the experiments were performed in triplicates, and the averages and standard deviation were calculated. Analysis of variance (ANOVA) was carried out for the data using Microsoft Excel 2013 and the results which have P < 0.05 were reported as significant.

3. Result and discussion

3.1 Influence of divalent metal ions on CBZ transformation

Laccase enzyme is proved to be able to degrade different pharmaceutical compounds in aqueous solution. For instance, in our previous work, we observed that laccase from *T. versicolor* with 60 U/L can remove 30% of CBZ after 24 h [13]. In most cases, laccase capability was studied in pure water while in real surface water and wastewater, there are metals and organic matter that can affect the activity of laccase. For example, some of the metal ions have been proved to have an inhibiting effect on laccase by binding and destabilizing the protein structure [14]. Generally, the kind of metal ions in wastewater depends on the nature of the upstream process. For example, textile wastewater contains a high concentration of Cu^{2+} which comes from the dye molecules [15]. Also, the municipal wastewater contains Fe^{2+}, Cu^{2+}, $Mg^{2+,}$ and Ca^{2+} and they could be derived from both natural sources, such as ore deposits and erosion of bed rocks and anthropogenic sources such as industries, mining, wastewater irrigation and agricultural activities [16].. The presence of metal ions can also influence the environmental fate of contaminants in aquatic ecosystems [7]. In this study, the influence of different concentrations of Fe^{2+}, Cu^{2+}, Mg^{2+} and Ca^{2+} on CBZ removal with laccase were evaluated. Compared to the metal-free control, the removal rates of CBZ did not change significantly ($P < 0.05$) (Figure 4.3.1). The highest removal of CBZ was with Cu^{2+} (1 ppm) and Ca^{2+} (10 ppm) by laccase mediated system after 24 h of incubation, which was around 40%. The presence of divalent metal ions affected the degradation of CBZ in laccase system, by changing the enzyme activity. Anipsitakis and Dionysiou observed that the addition of Cu^{2+} rapidly enhanced laccase activity, which consequently formed more radicals for pollutants removal [17]. Copper

is an essential component for the active site of laccase as copper-dioxygen complexes play crucial role in the oxidation. Lorenzo *et al.* reported that Cu^{2+} had a positive effect on laccase production and activity in *T. versicolor* [18]. Also, Tran *et al.* reported that the Ca^{2+} can increase enzyme activity, indicating the role of Ca^{2+} in biocatalytic mechanism [19]. Chmelova and Ondrejovic observed that laccase from *T. versicolor* was tolerant to metal ions present in wastewater, such as Cu^{2+} and Ca^{2+}. Their results showed that up to 1 mmol/L, most of the metals did not inhibit the activity of laccase [14]. Figure 4.3.1 shows the removal efficiency of CBZ at different concentrations of metal ions by laccase. Increasing the concentration of Cu^{2+} and Ca^{2+} increased the degradation efficiency of CBZ. Nagai *et al.* and Baldrian and Gabriel reported that laccase showed up to 40% higher activity in the presence of Cu^{2+} [20, 21]. Lu *et al.* investigated the effect of Cu^{2+} on the rate of degradation of 4-nitrophenol by laccase and observed 8.5 times higher degradation in the presence of Cu^{2+}. They attributed this behavior to the catalytic activity of copper [22]. Murugesan *et al.* reported that the presence of Ca^{2+} and Cu^{2+} can enhance the laccase activity at low concentrations (1 mM). Their results suggested that the decolorization level decreased by increasing the concentration of metal ions to values higher than 1 mM [23]. The oxidation of substrates by the laccase can happen through different mechanisms that may be influenced by the interaction of divalent metal ion in the solution with copper atoms in the enzyme and with the substrate. Increasing the concentrations of the divalent metal ions (such as Ca^{+2}) may change its competition with Cu^{2+} into a cooperative relationship and therefore enhance the degradation of the substrate [22].

On the contrary, the removal efficiency of CBZ in the presence of Fe^{2+} and Mg^{2+} was lower than the control and it was around 28%. The inhibiting effect was probably due to the binding of metal cations to the active site of the enzyme, which consequently blocks the electron transfer system [23, 24]. Fang *et al.* found that ions act as competitive inhibitors of electron donors by blocking the access of the T1 site to the substrate [25]. Murugesan *et al.* reported that Fe^{2+} at 0.4 mM inhibited 50% of dye decolorization during 1 h incubation. They attributed this behavior to the inactivation of laccase by Fe^{2+} [23]. Also, increasing the concentration of Fe^{+2} and Mg^{+2} decreased the degradation efficiency of CBZ. In this case, Shankar *et al.* suggested that the wastewaters should be diluted which challenges the feasibility of treatment [8].
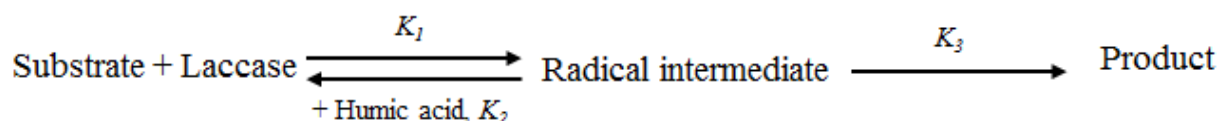
Generally, divalent ions showed a positive effect on laccase activity. However, several metal ions may cause conformational changes in the enzyme and reduce the activity [14]. The competition of these divalent ions with Cu^{2+} of the laccase catalytic site can be turned into a cooperative relationship in a way that divalent metal ions act as inorganic redox mediators [26]. In conclusion, two theories explain the effect of metals on laccase activity. One theory implies that the binding of metal ions can induce conformational changes to the enzyme and stimulates decomposition of the trimer complex including metal ion, substrate, and enzyme, as proved by noncompetitive inhibition model [9]. Laccase has three types of copper sites (type I, II, and III), and its catalytic site includes a cluster of four copper atoms, which is able to perform monoelectronic oxidation [27]. The second theory is that binding the metal ion near the TI copper atom in laccase cause a competitive inhibition of electron donors by blocking the access of TI site to substrates or by inhibiting the electron transfer at the TI active site. This theory justifies the inhibition of laccase activity at a high concentration of divalent metal ions [25]. Therefore, one should consider these synergistic and antagonistic effects into account for designing the treatment systems based on laccase oxidation.

Role of humic acid in CBZ transformation

The natural organic matter has different functional groups, such as carboxyl, ketone and hydroxyl groups and its main constituent is humic acid. Therefore, humic acid was widely used as a representative model of natural organic matter. The mentioned functional groups can inhibit the degradation of target contaminants since they act as substrates for laccase [7]. Also, the reaction of free radicals, generated from the contaminant-enzyme reaction, is possible [28]. In this study, the presence of humic acid decreased the degradation efficiency of CBZ during 24 h of incubation (Figure 4.3.2). Increasing the concentration of humic acid from 0 to 30 ppm led to decrease in the degradation efficiency from 32% to 18% after 24 h. The humic acid may form covalent and/or noncovalent binding with target compounds and therefore reduce the apparent concentration in the active sites of laccase [29]. According to Zavarzina *et al.* humic acid inhibits laccase activity and the inhibitory effect increases with increasing humic acid concentration. The inhibitory effect may be due to: (1) functional groups, such as carboxylic groups on humic acid that may affect the active site of

laccase by formation of complex with copper ions and; (2) the different contents of hydrophilic and hydrophobic fragments in humic acid [30]. The first step of CBZ transformation by laccase is the oxidation of the substrate by enzyme. This step takes place at the catalytic center of enzyme where CBZ loses an electron to form a radical. This radical is released in to the solution. The radical intermediate can be reduced through reaction with humic acid and reverse the oxidation. As a result, inhibition of substrate transformation can occur in the presence of humic acid [31]. The reaction scheme is shown as follows:

$$\text{Substrate} + \text{Laccase} \underset{+ \text{ Humic acid, } K_2}{\overset{K_1}{\rightleftharpoons}} \text{Radical intermediate} \xrightarrow{K_3} \text{Product}$$

Gulkowska *et al.* indicated that laccase can catalyze the formation of stable bonds between sulfonamide antibiotics and quinones in humic acid through nucleophilic addition reactions [29]. Also, Lorenzo *et al.* reported that organic compounds can inhibit laccase activity by forming complex compounds with its copper ions [18]. Therefore, despite the fact that the natural organic matter can increase the apparent removal through sorption and covalent bonding, they can decrease the efficiency of degradation by decreasing the concentration of target compounds near active sites of the enzyme and also by reducing the enzyme activity.

We further examined the degradation of CBZ in the presence of both humic acid and metal ions. The data are presented in Figure 4.3.3. According to the results in previous sections, the presence of copper and calcium ions was expected to increase the degradation efficiency but on the other hand, the presence of iron and magnesium ions and also natural organic matter was expected to decrease the degradation efficiency. However, the resultant effect reduced the degradation efficiency from 32% to 27% after 24 h. Humic acid is negatively charged due to the presence of phenolic and carboxylic groups. Binding with metals can neutralize the negative charge of humic acid and render it more accessible for the enzyme and thus increasing the chances to react with the radical intermediate. The more the metal cations in the solution, more the binding and neutralization of humic acid is expected [31].

Conclusion

The transformation of oxidation of contaminants by laccase is not only governed by enzyme activity, but also by the presence of metal ions and natural organic matters. The results showed that as compared to the control sample, Cu^{2+} and Ca^{2+} can increase the degradation efficiency of CBZ by 18%, but Fe^{2+} and Mg^{2+} can decrease the degradation efficiency by 40%. Also, the presence of humic acid decreased the degradation efficiency of CBZ by 42% due to covalent/non-covalent binding with pollutants. The presence of metal ions and humic acid decreased the degradation efficiency by 15%. These insights are not only important in evaluating the significance of key factors on oxidation of pollutants, but also have values in the design of bioprocesses based on laccase oxidation since the engineers need to identify theses synergistic and antagonistic effects for designing an appropriate and stable treatment system.

Acknowledgment

Reference

1.   Benotti, M.J., Trenholm, R.A., Vanderford, B.J., Holady, J.C., Stanford, B.D., and Snyder, S.A., Pharmaceuticals and Endocrine Disrupting Compounds in U.S. Drinking Water. Environmental Science & Technology, 2009. 43(3): p. 597-603.

2.   Yu, Z., Peldszus, S., and Huck, P.M., Adsorption characteristics of selected pharmaceuticals and an endocrine disrupting compound-Naproxen, carbamazepine and nonylphenol-on activated carbon. Water Research, 2008. 42(12): p. 2873-2882.

3.   Naghdi, M., Taheran, M., Brar, S.K., Kermanshahi-pour, A., Verma, M., and Surampalli, R.Y., Removal of pharmaceutical compounds in water and

wastewater using fungal oxidoreductase enzymes. Environmental Pollution, 2018. 234: p. 190-213.

4.   Zhang, Y., Geißen, S.U., and Gal, C., Carbamazepine and diclofenac: Removal in wastewater treatment plants and occurrence in water bodies. Chemosphere, 2008. 73(8): p. 1151-1161.

5.   Yang, S., Hai, F.I., Nghiem, L.D., Price, W.E., Roddick, F., Moreira, M.T., and Magram, S.F., Understanding the factors controlling the removal of trace organic contaminants by white-rot fungi and their lignin modifying enzymes: a critical review. Bioresource technology, 2013. 141: p. 97-108.

6.   Martínková, L., Kotik, M., Marková, E., and Homolka, L., Biodegradation of phenolic compounds by Basidiomycota and its phenol oxidases: A review. Chemosphere, 2016. 149: p. 373-382.

7.   Sun, K., Kang, F., Waigi, M.G., Gao, Y., and Huang, Q., Laccase-mediated transformation of triclosan in aqueous solution with metal cations and humic acid. Environmental Pollution, 2017. 220: p. 105-111.

8.   Shankar, S. and Nill, S., Effect of metal ions and redox mediators on decolorization of synthetic dyes by crude laccase from a novel white rot fungus Peniophora sp.(NFCCI-2131). Applied biochemistry and biotechnology, 2015. 175(1): p. 635-647.

9.   Si, J., Peng, F., and Cui, B., Purification, biochemical characterization and dye decolorization capacity of an alkali-resistant and metal-tolerant laccase from Trametes pubescens. Bioresource technology, 2013. 128: p. 49-57.

10.   He, D., Guan, X., Ma, J., Yang, X., and Cui, C., Influence of humic acids of different origins on oxidation of phenol and chlorophenols by permanganate. Journal of hazardous materials, 2010. 182(1-3): p. 681-688.

11.   Mohapatra, D.P., Brar, S.K., Tyagi, R.D., Picard, P., and Surampalli, R.Y., Carbamazepine in municipal wastewater and wastewater sludge: Ultrafast quantification by laser diode thermal desorption-atmospheric pressure

chemical ionization coupled with tandem mass spectrometry. Talanta, 2012. 99: p. 247-255.

12.   Faramarzi, M.A. and Forootanfar, H., Biosynthesis and characterization of gold nanoparticles produced by laccase from Paraconiothyrium variabile. Colloids and Surfaces B: Biointerfaces, 2011. 87(1): p. 23-27.

13.   Naghdi, M., Taheran, M., Brar, S.K., Kermanshahi-pour, A., Verma, M., and Surampalli, R.Y., Biotransformation of carbamazepine by laccase-mediator system: Kinetics, by-products and toxicity assessment. Process Biochemistry, 2018. 67: p. 147-154.

14.   Chmelová, D. and Ondrejovič, M., Effect of metal ions on triphenylmethane dye decolorization by laccase from Trametes versicolor. Nova Biotechnologica et Chimica, 2015. 14(2): p. 191-200.

15.   Yan, J., Niu, J., Chen, D., Chen, Y., and Irbis, C., Screening of Trametes strains for efficient decolorization of malachite green at high temperatures and ionic concentrations. International Biodeterioration & Biodegradation, 2014. 87: p. 109-115.

16.   Muhammad, S., Shah, M.T., and Khan, S., Health risk assessment of heavy metals and their source apportionment in drinking water of Kohistan region, northern Pakistan. Microchemical Journal, 2011. 98(2): p. 334-343.

17.   Anipsitakis, G.P. and Dionysiou, D.D., Radical generation by the interaction of transition metals with common oxidants. Environmental science & technology, 2004. 38(13): p. 3705-3712.

18.   Lorenzo, M., Moldes, D., Couto, S.R., and Sanromán, M., Inhibition of laccase activity from Trametes versicolor by heavy metals and organic compounds. Chemosphere, 2005. 60(8): p. 1124-1128.

19.   Tran, T.T., Hashim, S.O., Gaber, Y., Mamo, G., Mattiasson, B., and Hatti-Kaul, R., Thermostable alkaline phytase from Bacillus sp. MD2: effect of divalent

metals on activity and stability. Journal of inorganic biochemistry, 2011. 105(7): p. 1000-1007.

20.   Nagai, M., Sato, T., Watanabe, H., Saito, K., Kawata, M., and Enei, H., Purification and characterization of an extracellular laccase from the edible mushroom Lentinula edodes, and decolorization of chemically different dyes. Applied Microbiology and Biotechnology, 2002. 60(3): p. 327-335.

21.   Baldrian, P. and Gabriel, J., Copper and cadmium increase laccase activity in Pleurotus ostreatus. FEMS Microbiology letters, 2002. 206(1): p. 69-74.

22.   Lu, C., Cao, L., Liu, R., Lei, Y., and Ding, G., Effect of common metal ions on the rate of degradation of 4-nitrophenol by a laccase-Cu^{2+} synergistic system. Journal of environmental management, 2012. 113: p. 1-6.

23.   Murugesan, K., Kim, Y.-M., Jeon, J.-R., and Chang, Y.-S., Effect of metal ions on reactive dye decolorization by laccase from Ganoderma lucidum. Journal of hazardous materials, 2009. 168(1): p. 523-529.

24.   Paterson, R.R., Meon, S., Abidin, M.Z., and Lima, N., Prospects for inhibition of lignin degrading enzymes to control Ganoderma white rot of oil palm. Current Enzyme Inhibition, 2008. 4(4): p. 172-179.

25.   Fang, Z.M., Li, T.L., Chang, F., Zhou, P., Fang, W., Hong, Y.Z., Zhang, X.C., Peng, H., and Xiao, Y.Z., A new marine bacterial laccase with chloride-enhancing, alkaline-dependent activity and dye decolorization ability. Bioresource technology, 2012. 111: p. 36-41.

26.   Liu, W., Chao, Y., Yang, X., Bao, H., and Qian, S., Biodecolorization of azo, anthraquinonic and triphenylmethane dyes by white-rot fungi and a laccase-secreting engineered strain. Journal of Industrial Microbiology and Biotechnology, 2004. 31(3): p. 127-132.

27.   Frasconi, M., Favero, G., Boer, H., Koivula, A., and Mazzei, F., Kinetic and biochemical properties of high and low redox potential laccases from fungal and

plant origin. Biochimica et Biophysica Acta (BBA)-Proteins and Proteomics, 2010. 1804(4): p. 899-908.

28.   Feng, Y., Colosi, L.M., Gao, S., Huang, Q., and Mao, L., Transformation and removal of tetrabromobisphenol A from water in the presence of natural organic matter via laccase-catalyzed reactions: reaction rates, products, and pathways. Environmental science & technology, 2013. 47(2): p. 1001-1008.

29.   Gulkowska, A., Sander, M., Hollender, J., and Krauss, M., Covalent binding of sulfamethazine to natural and synthetic humic acids: assessing laccase catalysis and covalent bond stability. Environmental science & technology, 2013. 47(13): p. 6916-6924.

30.   Zavarzina, A.G., Leontievsky, A.A., Golovleva, L.A., and Trofimov, S.Y., Biotransformation of soil humic acids by blue laccase of Panus tigrinus 8/18: an in vitro study. Soil Biology and Biochemistry, 2004. 36(2): p. 359-369.

31.   Lu, J., Shi, Y., Ji, Y., Kong, D., and Huang, Q., Transformation of triclosan by laccase catalyzed oxidation: The influence of humic acid-metal binding process. Environmental pollution, 2017. 220: p. 1418-1423.
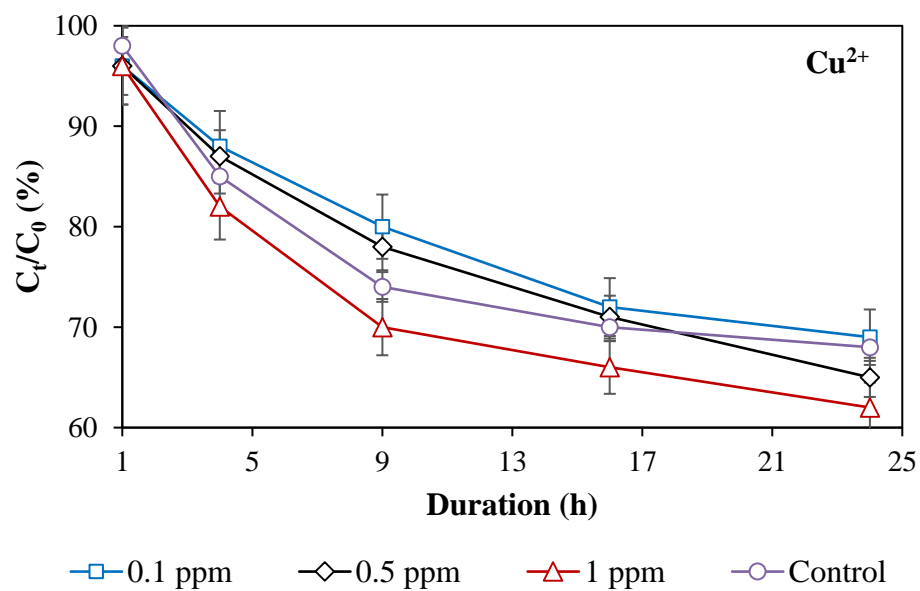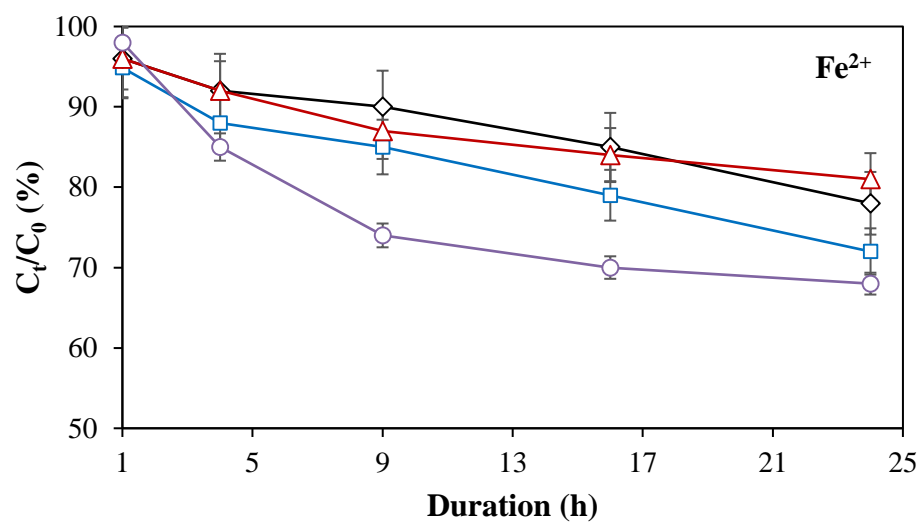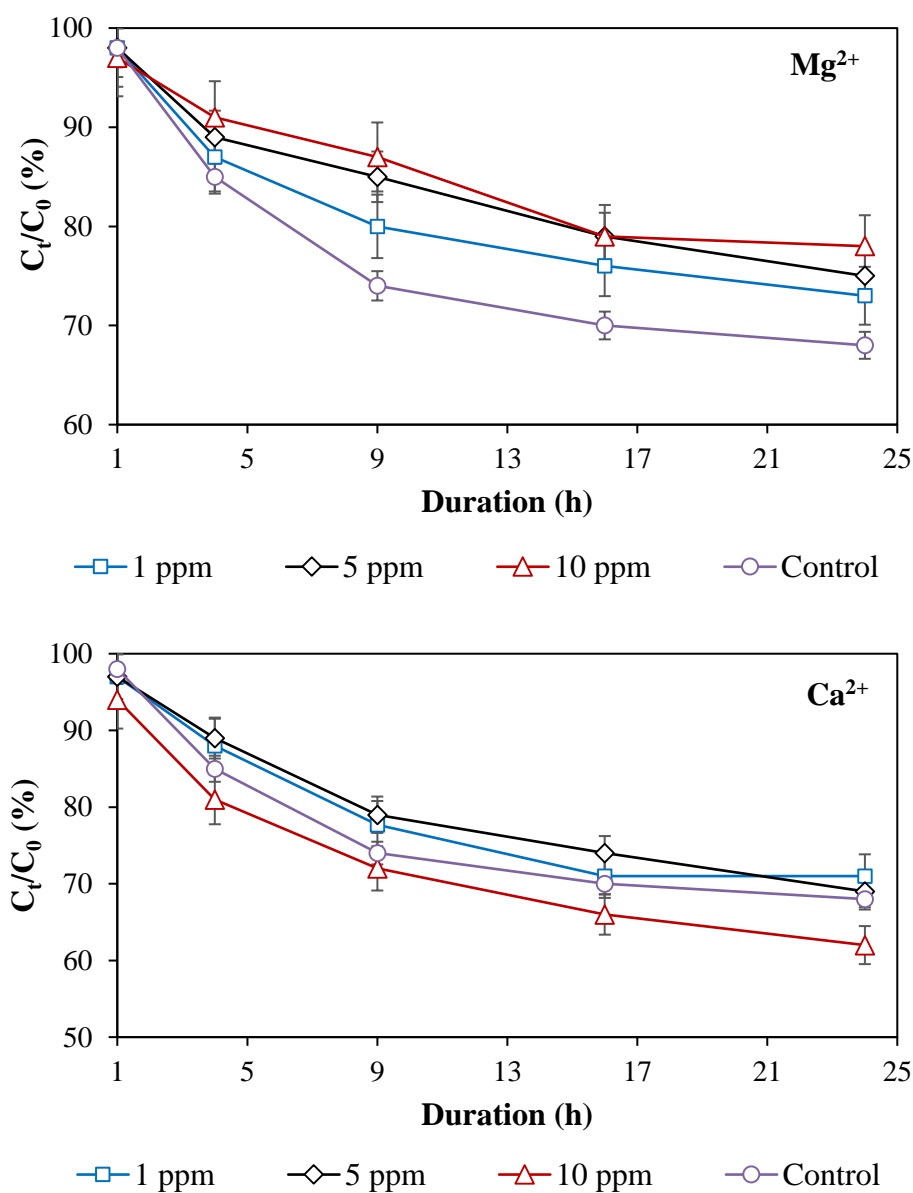
Figure 4.3.1 Removal of carbamazepine in the presence of different concentration of metal ions: a) Fe²⁺, b) Cu²⁺, c) Mg²⁺ and; d) Ca²⁺ by laccase from *Trametes versicolor* during 24 h, pH 6.0 and 25 °C.
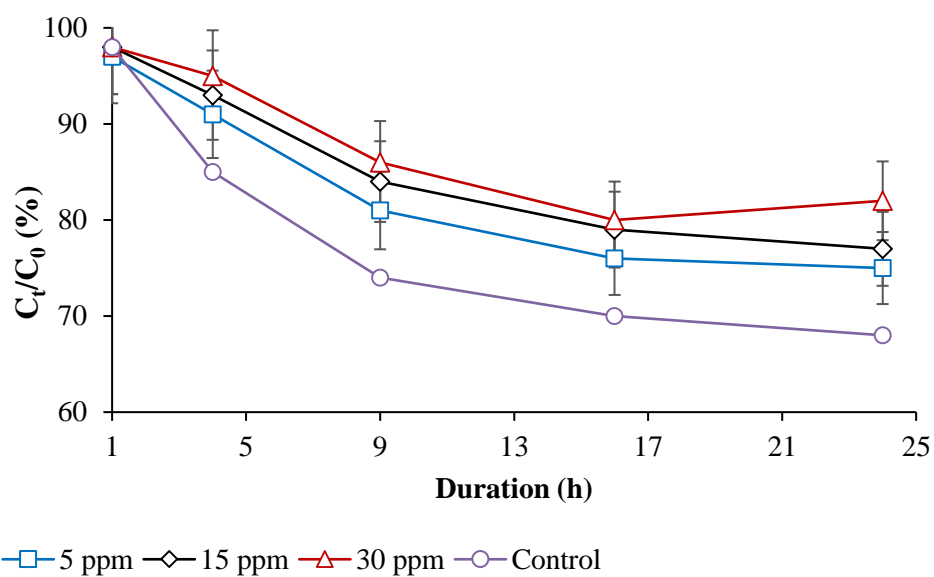
Figure 4.3.2 Carbamazepine transformation rates for laccase in the presence of different humic acid concentrations by laccase from *Trametes versicolor* for 24 h, pH 6.0 and 25 °C

Figure 4.3.3 Influence of divalent metal ions (Fe^{+2}, Cu^{+2}, Mg^{+2} and Ca^{+2}) and humic acid on carbamazepine removal by laccase from *Trametes versicolor* for 24 h, pH 6.0 and 25 °C

CHAPTER 5

Investigating different techniques for immobilization of laccase onto nanobiochar

Part 1

Pinewood Nanobiochar: a Unique Carrier for the Immobilization of Crude Laccase by Covalent Bonding

Mitra Naghdi[1], Mehrdad Taheran[1], Satinder Kaur Brar[1*], Azadeh Kermanshahi-pour[2], Mausam Verma[1] and R.Y. Surampalli[4]

[1]INRS-ETE, Université du Québec, 490, Rue de la Couronne, Québec, Canada G1K 9A9

[2]Biorefining and Remediation Laboratory, Department of Process Engineering and Applied Science, Dalhousie University, 1360 Barrington Street, Halifax, Nova Scotia, Canada, B3J 1Z1

[3]Department of Civil Engineering, University of Nebraska-Lincoln, N104 SEC PO Box 886105, Lincoln, NE 68588-6105, US

(*Phone: 1 418 654 3116; Fax: 1 418 654 2600; E-mail: satinder.brar@ete.inrs.ca)

Résumé

Les systèmes biocatalytiques inspirés par les nanotechnologies ont attiré l'attention sur de nombreuses applications notamment les supports nanométriques utilisés pour l'immobilisation des enzymes. Ce genre de supports est capable d'améliorer les facteurs déterminant l'efficacité, par ex. améliorer la surface et la capacité de chargement et réduire la résistance de transfert de masse. Parmi ces nanomatériaux, on peut compter le nanobiochar. Il possède des caractéristiques uniques en tant que support pour l'immobilisation enzymatique, à savoir un rapport surface/volume élevé, une structure poreuse et la présence de groupes fonctionnels sur sa surface. Cependant, la performance de l'immobilisation dépend fortement des conditions d'immobilisation et des propriétés de l'enzyme et du matériau de support. Dans cette recherche, la laccase brute a été immobilisée par covalence sur du nanobiochar fonctionnalisé en utilisant une méthode en deux étapes d'amidation activée par le diimide. L'effet de différents paramètres a été étudié. Les conditions optimales se sont révélées être 14 mg/mL de concentration de laccase, 5 mg/mL de nanobiochar, 8,2 mM d'agent de liaison et 3 h de temps de contact. Pour étudier le pH, la température, le stockage et la stabilité opérationnelle, l'échantillon obtenu à partir des conditions optimisées a été utilisé. Les résultats ont montré la plus grande stabilité de la laccase immobilisée par rapport à la variation de température et de pH par rapport à la laccase libre. De plus, la laccase immobilisée a maintenu sa performance catalytique jusqu'à sept cycles d'utilisation et a montré plus de 50% de l'activité initiale après deux mois de stockage à température ambiante.

Mots clés

Nanobiochar, Laccase, Immobilisation

Abstract

Nanotechnology-inspired biocatalytic systems attracted attention for many applications since nanosized supports for enzyme immobilization can improve efficiency-determining factors e.g. enhancing the surface area and loading capacity and reducing the mass transfer resistance. Among the nanomaterials, nanobiochar has unique features as a support for enzyme immobilization i.e. high surface to volume ratio, porous structure, and presence of functional groups on its surface. However, the performance of the immobilization is highly dependent on the immobilization conditions and the properties of the enzyme and the support material. In this research, crude laccase was covalently immobilized onto functionalized nanobiochar using a two-step method of diimide-activated amidation. The effect of different parameters were investigated. The optimal conditions were found to be 14 mg/mL of laccase concentration, 5 mg/mL of nanobiochar, 8.2 mM of cross-linker and 3 h of contact time. For investigating the pH, thermal, storage, and operational stability, the sample obtained from the optimized conditions was used. The results showed the higher stability of immobilized laccase against temperature and pH variation compared to free laccase. In addition, immobilized laccase maintained its catalytic performance up to seven cycles of utilization and showed more than 50% of initial activity after two months of room temperature storage.

Keywords

Nanobiochar, Laccase, Immobilization

Introduction

Application of enzymes as catalysts has gained significant attention due to their biodegradability, high selectivity and ability to operate in a wide range of pH, temperature, and salinity. Laccase (EC 1.10.3.2) is an oxidoreductase enzyme that can catalyze the oxidation of phenolic compounds with reduction of oxygen to water without requiring hydrogen peroxide as a co-substrate [1-3]. Laccase has attracted attention for different applications, from delignification of pulp to remediation of water and soil because of its capability of catalyzing the oxidation of various compounds [1, 4, 5]. It has the immense potential for industrial processes since it requires only air as a co-substrate and releases water as a by-product so that it can be classified as a green catalyst [6].

However, utilization of free enzymes in industrial processes has encountered some limitations including non-reusability, poor stability, inactivation by inhibitors and the high cost of isolation and purification [2, 4]. In contrast, immobilized enzymes exhibited advantages, such as stability against pH and thermal variations and easy separation of the enzyme from reaction medium [5]. Selection of suitable support for enzyme immobilization is very important since it affects enzyme loading, operational stability, and cost of the process [1, 4]. A varied spectrum of materials has been employed for the immobilization of enzymes as well as whole cell microorganisms and among them, carbonaceous materials showed superior textural properties and higher water stability [7, 8]. For example, charcoal has attracted much attention for enzyme immobilization due to its application in many areas, such as biotechnology, medicine, biology, and food processing [9].

Conversion of the agro-forestry residues by thermochemical and biological conversion for compost and biofuel production is a potential strategy for conserving natural resources, saving costs, and production of added-value products [10]. Pyrolysis of agro-forestry residual biomass is considered as a promising strategy for value-addition of these residues. In this treatment, residues are heated in the absence of oxygen to produce synthesis gas, bio-oil, and biochar [11]. The latter has a large surface area, enriched surface functional groups, porous structure, slow biological decay and moderate content of essential elements [12]. Biochar showed the excellent capability to remove contaminants, such as organic pollutants and heavy metals from aqueous solutions [12]. Soil amendment, nutrients retention, and bioremediation of

contaminated soils and water are among applications of biochar [13]. Recently, biochar has been employed by numerous researchers in a new application i.e. as a support for enzyme immobilization [14]. Using biochar for such a purpose can increase the product value and improve the cost to benefit ratio of the enzyme immobilization. Cea *et al.* evaluated the capability of biochar samples obtained from pyrolysis of oats husk at 300 °C (BCA 300) and 450 °C (BCA 450) and pretreated or not with 99% ethanol for immobilization of lipase. They found that the treatment with ethanol had no effect on biochar prepared at 300 °C, but the immobilized enzyme onto the treated biochar prepared at 450 °C showed 22.4 % more activity compared to untreated sample [14]. Davis and Burns covalently immobilized laccase onto activated carbon using four different derivatization methods. The highest immobilized activity was obtained using coupling of diimide to carboxyl groups in laccase. The immobilized laccase showed improved stability against pH and temperature variations [15]. Similar behavior in the enhancement of stability of the enzyme was observed in the research of Bezerra *et al.* who activated fibers obtained from green coconut husk with glyoxyl or glutaraldehyde to immobilize laccase. The thermal stability was higher with increments of 6.8-fold (with glutaraldehyde) up to 16.5-fold (with glyoxyl) compared to the free enzyme [16]. In a similar study, Cristovao *et al.* covalently immobilized commercial laccase on green coconut fiber activated with 3-glycidoxy propyl trimethoxysilane, which led to improved thermal and operational stabilities of the enzyme, but the biocatalyst showed a lower activity and affinity [4]. Modification of different agro-forestry residues for immobilization of enzyme is reported in several studies. However, there is significant knowledge gap on the effect of parameters including the reaction time, enzyme concentration, coupling reagent concentration, on the activity, stability, and recyclability of the biocatalyst.

In this work, nanobiochar obtained from residues of pinewood was modified and used to immobilize laccase through covalent bonding. To the best of our knowledge, this is the first effort for modification of pinewood-derived biochar nanoparticles for covalent immobilization of laccase. Biochar use as support and apple pomace as a substrate for enzyme production provides a waste management option for protecting the environment. The effect of important parameters on immobilization of laccase onto functionalized nanobiochar (FNBC) including FNBC dosage (mg/mL), the concentration of the coupling reagent (mM), and laccase concentration in solution

(mg/mL) were investigated and optimized since the optimization is critical for application of this nanobiocatalyst in the wastewater or water treatment plants. Additionally, pH, temperature and storage stability of free and immobilized laccase, as well as the reusability of immobilized laccase, were investigated.

Material and methods

Material

Pinewood biochar was supplied by Pyrovac Inc. (Quebec, Canada). This biochar was derived from pine white wood (80% w/w, size: 3 mm) and the rest 20% w/w was fir and spruce. The carbonization process was performed in the presence of nitrogen under atmospheric pressure at 525±1 °C by increasing the temperature at the rate of 25 °C/min for 20 min. 2, 2'-azino-bis (3-ethylbenzothiazoline-6-sulphonic acid) (ABTS), 2-(N-Morpholino) ethanesulfonic acid (MES), N-hydroxysuccinimide (NHS), N-ethyl-N'-(3-dimethylaminopropyl) carbodiimide hydrochloride (EDAC) were purchased from Sigma-Aldrich (Oakville, Canada). Tween-80, sulfuric acid and nitric acid were purchased from Fisher Scientific (Ottawa, Canada). Apple pomace, provided by Vergers Paul Jodoin Inc. (Quebec, Canada), was used as substrate for *Trametes versicolor* (ATCC 20869) for laccase production. Ultrapure water was produced in the laboratory using Milli-Q/Milli-Ro Millipore system (Massachusetts, USA).

Nanobiochar production and functionalization

Nanobiochar with the average size of 60±20 nm and specific surface area of 47.3 m^2/g was produced using a planetary ball mill (PM100; Retsch Corporation) at ambient conditions. Briefly, 10 g of pinewood biochar was preconditioned at -80 °C for 24 h and then ball milling was carried out at 575 rpm for 100 min using stainless steel balls of 2.4 mm in diameter (800 balls with total weight of 45 g) in a 500 mL stainless steel jar. The physicochemical properties of produced nanobiochar are described elsewhere [17]. For functionalization of nanobiochar through acidic treatment, the procedure of Naghdi *et al.* was employed with some modification [18]. About 4 g of produced nanobiochar was dispersed in 500 mL of H_2SO_4/HNO_3 mixture (5 M, 3:1 V/V) and mixed at 200 rpm and room temperature for 48 h. Subsequently, the functionalized nanobiochar (FNBC) suspension was washed several times with milli-

Q water to remove residual acids and to reach pH 7. The treated nanobiochar was then freeze-dried and stored at room temperature as a dry powder.

Laccase production and extraction

About 40 grams of apple pomace (pH 4.5, 78% (w/w) moisture), was mixed with Tween 80 at 0.5% v/w in several 500 mL Erlenmeyer flasks and autoclaved at 121±1 °C for 20 min. Then, the substrate was inoculated with *Trametes versicolor* strain and kept at 30±1 °C in a static incubator for 15 days. For extraction of enzyme, each gram of fermented apple pomace was mixed with 20 mL of 50 mM sodium phosphate buffer (pH 6.5). The mixture was agitated on a shaker at 150 rpm and 35±1 °C for 1 h and then the mixture was centrifuged for 30 min at 7000 ×g. The collected supernatant was dried at -55 °C, 5 Pa, for 48 h using freeze dryer (FD-1000, Eyela, Japan).

Covalent immobilization of laccase

Central composite design (CCD) and response surface methodology (RSM) were used to study the effects of FNBC concentration, enzyme concentration and EDAC concentration on the activity of immobilized laccase, which was considered as the dependent variable. RSM was employed for optimization of enzymatic activity as this method is widely used for bioprocess optimization, studying parameters interaction and building mathematical models [19]. Independent parameters and their levels are listed in Table 5.1.1. Design-Expert®-7 software (Stat-Ease Inc., Minneapolis, USA) was employed to create the experimental array composed of 20 experiments with 6 replicates in the center. The details of proposed experiments by software are listed in Table 5.1.2. Laccase was chemically attached to FNBC through diimide-activated amidation in two-steps. In the first step, different concentrations of FNBC (see Table 5.1.2) was prepared in MES buffer (50 mM, pH 6.2) and an equal volume of 400 mM NHS (prepared in MES buffer (50 mM, pH 6.2) was added to the solution and the mixture was sonicated for 30 min in an ultrasonication bath. Also, different concentrations of EDAC (see Table 5.1.2) was prepared in MES buffer (50 mM, pH 6.2) and then they were added to initiate the linking of NHS to the carboxylic groups on the FNBC and the mixture was sonicated for 2 h. Then, the FNBC mixture was centrifuged and rinsed thoroughly with MES buffer to remove excess EDC and NHS. In the second step, the activated FNBC was transferred to a solution of laccase in 10

mM phosphate buffer, pH 8.0 (see Table 5.1.2) and sonicated for 1 min to re-disperse the FNBC. The mixture was incubated at 200 rpm and at room temperature for 3 h. The immobilization time was optimized by performing a set of experiments at different contact times (1, 2, 3, 4, 5, 6, 12, 18, 24, 36, 48 and 72 h). The FNBC-laccase suspension was centrifuged and washed several times with ultrapure water to remove any unbound enzyme and freeze-dried at -55 °C, 5 Pa, for 48 h. A control experiment was performed using an identical procedure except using EDC and NHS. The activity of immobilized laccase on FNBC was measured through the method explained in 2.7.

Data analysis

The obtained experimental data were analyzed through RSM and fitted into a second-order polynomial model. The following function (Equation 1) was employed in the analysis of response surface to correlate the independent and dependent factors.

$$Y = \beta_0 + \sum_{i=1} \beta_i X_i + \sum \beta_{ii} X_i^2 + \sum_{i=1} \sum_{j=i+1} \beta_{ij} X_i X_j \tag{1}$$

Where: Y, β_0, X_i (or X_j). β_i, β_{ii}, and β_{ij} are the predicted responses, second-order constant, independent variables, the linear coefficient of regression, the quadratic coefficient of regression, and interaction coefficient of regression between every two independent variables, respectively.

Stability of immobilized laccase

The effect of pH on the stability of immobilized laccase at optimum conditions (5 mg/mL of functionalized nanobiochar, 14 mg/mL of laccase and 8.2 mM of EDC) was investigated by incubating immobilized and free laccase in buffer solutions over a pH range of 3 to 10 at 200 rpm and 25 °C. Briefly, 10 mg of immobilized laccase and 50 µL of free laccase (with an initial laccase activity of 1.2 U/mL) were added to separate tubes containing 2 mL of respective buffers. After 8 h of incubation, the residual laccase activity for free laccase was measured. For immobilized laccase, all samples were incubated for 8 h and centrifuged for 20 min at 11, 000 × g before activity measurement. The thermal stability was assessed by incubating free and immobilized laccase at different temperatures (20-70 °C) for 8 h and measuring the residual activity, in the same way, explained for pH stability. For evaluating the storage stability of free and immobilized laccase, samples were stored at room temperature for up to 30 days and their activity was measured at intervals. For evaluation of the operational

stability, about 50 mg of immobilized laccase on FNBC was dispersed in 1 mL of citrate-phosphate buffer (pH 4) containing 1.5 mM ABTS and incubated at room temperature and 200 rpm for 10 min. Then, the sample was centrifuged for 10 min at 11,000 × g and the concentration of transformed ABTS in the supernatant was measured. The immobilized laccase on FNBC was washed with Milli-Q water, decanted and the procedure was repeated for 7 cycles.

Analytical methods

Enzyme assay

Oxidation of ABTS was used to determine the laccase activity by spectrophotometry. About 50 µL of enzyme sample was mixed with 500 µL of 1.5 mM ABTS and 2.450 mL of 50 mM citrate-phosphate buffer (pH 3.5). Oxidation of ABTS was monitored by an increase in the absorbance at 420 nm (ε_{420} = 36,000 M^{-1} cm^{-1}) [20] using a Cary 50 UV-visible spectrophotometer (Varian, Australia). One unit of laccase activity was defined as the amount of required enzyme for oxidizing one µmol of ABTS per min under the assay conditions. For immobilized laccase, 10 mg of sample was mixed with one mL of 1.5 mM ABTS and 2 mL of citrate phosphate buffer (pH 3.5). After 10 min of incubation at 45 °C, the sample was centrifuged for 10 min at 11, 000 × g and the absorbance at 420 nm was recorded. The final activity of immobilized laccase onto FNBC was expressed in U/g nanobiochar.

Fourier transform infrared (FT-IR) spectroscopy

FT-IR spectra were recorded in attenuated total reflectance (ATR) mode with 4 cm^{-1} resolution in the range of 400-4000 cm^{-1} using a Nicole IS50 FT-IR Spectrometer (Thermo Scientific, USA). Briefly, the sample was placed on the diamond crystal and consistent contact between the crystal and the sample was achieved with the gripper plate. The measurement was taken 16 times for each spectrum and their average was used for plotting.

Results and discussions

Covalent immobilization of laccase onto FNBC

Covalent and non-covalent bonding have been reported for the immobilization of various types of enzymes [21]. Non-covalent bonding retains the unique features of both supports and enzymes material, but the enzyme is lost during the repeated usage

of the support-enzyme system [22]. Covalent bonding provides durable attachment between enzyme and support, but it can significantly disrupt the enzyme structure. For efficient immobilization, chemical modifications of support are required to create reactive groups, such as carboxylic groups for covalent bonding [23, 24]. The carboxylic groups on the nanobiochar surface provide anchoring points for the covalent attachment of enzyme using EDAC cross-linker. This method was employed by many researchers in recent years for functionalization of different support materials [25-27]. The results of laccase immobilization in this work indicated that the activity of covalently immobilized laccase onto FNBC using EDAC was 16 times more than the immobilized laccase onto nanobiochar without acid treatment and without using EDAC and NHS as cross-linker (4.95 U/g compared to 0.31 U/g). Also, it was 4.8 times more than immobilized laccase onto FNBC without using EDAC and NHS (noncovalent interactions). Lee *et al.* reported that the activity of the immobilized horseradish peroxidase on carboxylated multi-wall carbon nanotubes was three times higher than that on un-functionalized multi-wall carbon nanotubes, indicating the critical role of carboxyl groups on carbon in the immobilization of enzyme [28]. These results indicated that laccase was immobilized on FNBC by multiple modes of binding including physical adsorption, specific interactions between carboxyl groups on FNBC and polar or ionic groups of laccase and covalent coupling of the enzyme molecules by EDAC.

Fourier transform infrared (FT-IR) spectroscopy analysis

Figure 5.1.1a illustrate the mechanism of immobilization of laccase onto functionalized nanobiochar through diimide-activated amidation and Figure 5.1.1b presents the FTIR spectra of FNBCs, laccase, and laccase immobilized on FNBCs samples. Five main peaks were observed in the spectrum of laccase including: (i) a strong band centered at 3332 cm^{-1} attributed to OH and NH vibrations; (ii) a weak band at around 2930 cm^{-1} attributed to CH bonds; (iii) a band at 1610 cm^{-1} corresponding to CONH linkage; (iv) a band at 1240 cm^{-1} corresponding to CN stretching vibration of amines; and finally (v) a sharp band at 1037 cm^{-1} due to COC groups. The band at 3000-3500 cm^{-1} in untreated FNBCs was due to phenol groups or OH groups in the adsorbed moisture. For functionalized FNBC, the band at 1707 cm^{-1} corresponded to C=O stretching bond in carboxylic acid functional groups. After the reaction of FNBC with laccase, the bands

at 3000-3500 cm^{-1} and 1610 cm^{-1} ascribed to OH vibration and CONH, respectively showed higher intensity which indicated the immobilization of enzyme molecules on the surface of FNBC [8]. Further, an additional broad peak appeared after immobilization of laccase onto FNBCs at 1586 cm^{-1} which can be mostly attributed to the Amide I in the proteins [29].

Optimization of covalently immobilized laccase

The experiments designed by CCD were carried out and their results have been presented in Table 5.1.2. The RSM design considered central points (0), low (-) and high (+) levels for each parameter (Table 5.1.1) and the obtained results were analyzed to determine the coefficients of the quadratic model. A mathematical expression obtained for the relationship of the activity of immobilized laccase onto FNBC with variables A, B, and C (concentration of FNBC, enzyme concentration and EDAC concentration, respectively) are given below in Equation 2 in terms of coded factors:

$$Y = + 3.58 + 0.62\,A + 0.70\,B + 0.82\,C + 0.13\,AB - 0.052\,AC + 0.19\,BC - 0.22\,A^2 - 0.26\,B^2 - 0.36\,C^2$$

$$(2)$$

The results of Analysis of variances (ANOVA) for the activity of immobilized laccase showed that the probability (P) value and the R-squared of the quadratic model were 0.0004 and 0.9095. Therefore, the regression of the quadratic equation for immobilized laccase activity was significant and applicable for practical applications. The P values for quadratic enzyme and EDAC concentration and linear coefficients of all studied parameters of the model were less than 0.05, which meant they were significant. On the other hand, the P value for interaction coefficients was greater than 0.05 which indicated the insignificance of interactions among the parameters. The observed activity of immobilized laccase varied between 0.71 (U/g) (obtained at 4 mg/mL FNBC, 2 mg/mL laccase and 7.5 mM EDAC) and 4.95 (U/g) (obtained at 5 mg/mL FNBC, 14 mg/mL laccase and 8.2 mM EDAC). Furthermore, the control sample (untreated FNBC) showed no oxidation of ABTS (laccase substrate).

EDAC is expected to accelerate the covalent bonding of amino-groups on the enzyme molecules with carboxyl groups (COOH) on the surface of FNBC [28]. Figure 5.1.2

shows the effect of EDAC concentration in the range from 5.7 to 9 mM on the activity of immobilized laccase on FNBC. As seen, increasing the concentration of EDAC enhanced the activity of immobilized laccase. Similar behavior was observed in the work of Lee *et al.* when they immobilized horseradish peroxidase on carboxylated multi-wall carbon nanotubes using EDAC concentration of up to 10 mM [28]. Tastan *et al.* changed the EDAC/carboxylic group (mol/mol) ratios in the range of 0.05 to 0.6 and observed the maximum activity of immobilized laccase at the ratio of 0.1. At EDAC/carboxylic group ratio higher than 0.4, they observed no activity, which was attributed to a negative effect on the enzyme at high concentrations of the cross-linker [30]. In addition, Figure 5.1.2 shows that the immobilization activity of laccase increases rapidly when the initial concentration of laccase in the immobilization mixture increases up to 10 mg/mL, then increases steadily upon further increase in the laccase concentration. Hu *et al.* immobilized laccase on silica nanoparticles by physical adsorption and covalence bonding in which the nanoparticles were functionalized by concentrated HNO_3 and then activated by glutaraldehyde. They reported that covalent coupling enhanced activity than the physical adsorption [31]. Likewise, Ji *et al.* covalently immobilized *P. ostreatus* crude laccase onto the functionalized TiO_2 nanoparticles by glutaraldehyde. They reported that the apparent activity increased 8 times for purified laccase compared to crude laccase [32]. However, using cross-linkers, such as glutaraldehyde at high concentrations can result in distortion of structure, aggregation, precipitation, and loss of enzyme activity [33]. In addition, glutaraldehyde is a toxic and hazardous cross-linking agent which can induce different adverse effects on living organisms [34].

The effect of laccase concentration on the enzymatic activity of final product is shown in Figure 5.1.2. For concentrations in the range of 2-14 mg/mL, the enzymatic activity of the immobilized laccase increased with increasing enzyme concentration and beyond this range, enzymatic activity was independent of the enzyme concentration. This suggested that up to 14 mg/mL, the enzyme molecules were covalent-bonded as a monolayer at the surface of the nanoparticles. Later, the surface of the FNBC is occupied by enzyme molecules and there is no possibility for more enzyme molecules to attach despite increasing the concentration of the enzyme [8]. Similarly, Silva *et al.* immobilized laccase on functionalized spent grains and reported that by increasing enzyme concentrations up to 5 mg/mL, the enzymatic activity increased faster, while

beyond this concentration, enzymatic activity did not differ significantly [35]. In a related study, Salis *et al.* showed that enzymatic activity increased linearly with the enzyme concentration, but higher loadings resulted in decreased laccase activity. They attributed this behavior to the limitations of substrates diffusion inside the support pores before reaching the active site of the enzyme [36]. However, Cristovao *et al.* observed two slopes in the activity trend of laccase immobilized on coconut fiber when they changed the enzyme concentration from 8 to 67 mg/mL and then to 260 mg/mL. They concluded that the enzyme adsorption was not restricted to a monolayer on the support, and adsorption of secondary layers was possible [37]. Also, Tastan *et al.* observed a gradual increase in the activity of the immobilized enzyme with increasing initial enzyme concentration [30].

The effect of incubation time was investigated after setting the other parameters at their optimum levels. Figure 5.1.3 illustrates the effects of incubation time on the enzymatic activity of biocatalyst, which reaches to a maximum value at 3 h and then decreases slightly for longer incubation times. The results indicated that the adsorption of laccase over FNBC was faster and 3 h was enough to attain the maximum enzyme immobilization. At longer incubation time, two or more layers of the enzyme were possibly formed over the carrier that reduces the number of free enzymes [35]. Silva *et al.* reported 3.5 h of incubation time as the optimum value for immobilization of laccase on spent grains [35]. Similarly, Cristovao *et al.* observed that the activity increased until 3.5 h, remained constant until 5-6 h and decreased after 6 h. They attributed this behavior to desorption of some enzyme or adsorption of the enzyme as the second monolayer, which ceased the availability of the enzymes [37]. Thus, the longer contact time between the support and enzyme had no advantages nevertheless more molecules were immobilized on a support. In literature, different incubation times were reported as the optimal value for different supports, such as 48 h for Eupergit® C [38]; 24 h for chitosan [39]; 24 h for activated carbon [38]; 5 h for silica [40]; 3.5 h for spent grain [1]; 1.6 h for mesoporous silica [36]; and 30 min for MWCNTs [8]. The difference among supports can be explained by the fact that the adsorption of a macromolecule onto a porous support involved complex steps including diffusion from solution to the surface of the support, diffusion inside the pores and attachment of protein. Therefore, the rate of adsorption depended on every single step, which, in turn, depended on the nature and structure of the support and the enzyme [36, 41].

The above results indicated the higher potential of FNBC as support for immobilization of laccase so that at the optimum conditions, i.e., FNBC of 5 mg/mL, initial laccase concentration of 14 mg/mL, and EDAC concentration of 8.2 and a contact time of 180 min, 5 Unit/g of activity toward ABTS oxidation was achieved. These optimized conditions were maintained for further studies on the thermal, pH, operational and storage stability of free and immobilized laccase.

Characteristics of the activity of immobilized laccase

Immobilization of enzyme has propounded effects on the enzyme's activity and performance. In this research, the effect of immobilization on the pH dependency of activity of free and covalently immobilized laccase on FNBC was investigated in the pH range of 3.0 to 10.0 (Figure 5.1.4) and the results were compared with the previously reported literature (Table 5.1.3). Accordingly, the free and covalently immobilized laccase exhibited their maximal activities at pH 4.0 and pH 3.0, respectively. Other researchers reported the same level of optimum pH shift for immobilized laccase on poly (4 vinyl pyridine) [42] and magnetic bimodal mesoporous carbon [43]. This behavior was attributed to the influence of support microenvironment on electrostatic interaction. Therefore, the activity of the immobilized enzyme is significantly impacted by the characteristics of the support and the link between the enzyme and the support. In a related research, Misra *et al.* observed same profile for free and immobilized enzyme but the immobilized laccase higher sensitivity to pH variation [29]. Similarly, Tastan *et al.* immobilized laccase on PTFE membranes through entrapment into gelatin and covalent immobilization. Their results showed optimum pH values of 5, 4 and 6 for free laccase, immobilized laccase through entrapment and immobilized laccase through covalent bonding [30]. Also, the immobilized laccase showed a broader profile for pH-activity than the free laccase as well as higher activity at pH 8-10, indicating that immobilization retained the enzyme activity in a broader pH range [44]. Similarly, Wang *et al.* showed that the immobilized laccase demonstrated higher pH stability than free enzyme, especially in the pH range of 3-7 [45]. Also, Jolivalt *et al.* reported higher stability of immobilized laccase onto PVDF membrane, though the pH activity profiles for the immobilized and the free enzymes were similar [46].

Determining the optimum temperature to achieve the maximum activity of the enzyme is very important since it can determine the maximum efficiency of a biocatalytic system. Immobilization of enzyme alter the activity profile of an enzyme within its working temperature range and may shift the optimum temperature [29] and affect the stability against high temperatures by limiting the conformational changes of the enzyme [4]. To assess the thermal stability of free and covalently immobilized laccase onto FNBC experiments, the samples were incubated at different temperature values ranging from 20 to 70 °C for 8 h. The measured activity of samples after incubation is illustrated in Figure 5.1.5. Accordingly, the enzymatic activity of both free and immobilized enzyme was significantly dependent on temperature and both exhibited their maximal activity at 30 °C. However, the immobilized laccase showed a broader temperature profile compared to the free laccase. The attachment of laccase to FNBC results in its thermostabilization, as reflected by both elevated activity at low temperature and decreased deactivation extent at high temperatures. After 8 h of incubation at 30 °C, the free laccase showed around 30% deactivation while the immobilized ones lost less than 15% of its initial activity. Also, as shown in Figure 5.1.5, at a temperature range of 40-50 °C, immobilized laccase on FNBC showed higher stability compared to free laccase. Increasing the thermal stability resulted in retaining the enzymatic activity at high temperatures, so that the residual activity of immobilized laccase was ~ 6-fold higher than that for the free laccase at 60 °C. Similarly, Asuri *et al.* observed an increase in the thermal stability of soybean peroxidase immobilized on MWNT at high temperatures compared to free enzyme so that the maximal initial reaction rate for the immobilized enzyme at 90 °C was 2.5-fold higher than that for the free enzyme at 75 °C [27]. Also, the immobilized laccase onto coconut fiber was reported to be 6.86-fold more stable than the free enzyme at 60 °C [5]. Increasing the thermal stabilization can be attributed to the multi-point attachment of the enzyme macromolecule to the support and/or decreased protein-protein interactions [31, 48, 49].

The storage stability of the immobilized laccase on FNBC was evaluated by incubating the samples at room temperature and the results were compared with the results of similar research previously reported in the literature (Table 5.1.3). According to Figure 5.1.6, after 5 and 30 days, the immobilized laccase on FNBC lost around 33% and 50% of its initial activity after 30 days, whereas free laccase lost 58% and 100% activity

during the same period. Asuri *et al.* reported that immobilized soybean peroxidase on MWNT retained 70% of its initial activity after 30 days of incubation at room temperature, while the native enzyme retained only ~ 30% of its activity [27]. Compared to other reports, the immobilized enzyme on nanosized biochar showed higher stability than immobilized enzyme on different supports. For instance, 60% of activity loss was observed after 25 days for immobilized laccase on TiO_2-montmorillonite complexes [45], 60% activity loss after 34 days for immobilized laccase on multi-walled carbon nanotubes at 4 °C [8] and 40% activity loss for laccase immobilized on poly(vinyl alcohol) cryogel after 2 days [50]. In addition, Misra *et al.* immobilized laccase on epoxy functionalized polyethersulfone and observed 12% loss in the initial activity of free laccase after 20 days, while immobilized laccase retained almost all its activity during the same period [29]. Also, Pezzella *et al.* immobilized laccase on perlite and observed 98% and 81% of activity loss for free and immobilized laccase after 27 days storage at room temperature [47].

Reusability of immobilized laccase on FNBC

The reusability of the biocatalyst in a batch or continuous system is an important factor in assessing the value of immobilization. Stabilization of laccase due to attachment to FNBC enabled the facile reuse of the immobilized laccase. To assess this property, the immobilized laccase was repeatedly incubated with ABTS and the catalytic activity was measured, and the results are illustrated in Figure 5.1.7. The FNBC-laccase conjugates retained around 30% and 5% of its initial activity after four and seven cycles. In related studies, laccase immobilized on different supports showed similar activities, for example: 30% residual activity after 7 cycles for Amberlite IR-120 [33], 10-30% after 7 cycles for activated carbon [15]; 87% after 10 cycles for digested spent grain [1]; and 55% for green coconut fiber [37]. However, several researchers reported higher reusability for immobilized laccase. For example, the immobilized laccase on carbon-based magnetic mesoporous composites was reported to retain above 70% and 50% of its initial activity after 5 and 10 cycles of ABTS oxidation [43]. One reason for higher reusability was using ABTS with lower concentrations and for shorter reaction time. Tavares *et al.* observed that the immobilization of laccase onto MWCNTs increased the enzymatic activity up to cycle 4. They related the decrease in the activity after the fourth cycle of leaching from the support [8].

Conclusion

Enhancing the conformational stability of an enzyme through immobilization is one of the most important steps for implementing the enzymatic technology. In this research, laccase was covalently attached to functionalized nanobiochar via diimide-activated amidation under mild conditions. The two-step process was carried out at room temperature in buffer solutions in a short time (3 h), and the activity of the immobilized enzyme reached a maximum at 5 Unit/g. The characterization results showed that the proteins were intimately associated with the nanobiochar. The optimum conditions for covalently immobilized laccase were determined to be FNBC of 5 mg/mL, initial laccase concentration of 14 mg/mL, and EDAC concentration of 8.2 and a contact time of 180 min. The thermal and pH stabilities of the immobilized laccase were improved as compared to the free laccase. Also, the immobilized laccase showed good reusability so that it retained 70% of initial activity after 4 consecutive cycles.

Acknowledgments

References

1.   Da Silva, A.M., Tavares, A.P.M., Rocha, C.M.R., Cristóvão, R.O., Teixeira, J.A., and Macedo, E.A., Immobilization of commercial laccase on spent grain. Process Biochemistry, 2012. 47(7): p. 1095-1101.

2.   Guo, L.Q., Lin, S.X., Zheng, X.B., Huang, Z.R., and Lin, J.F., Production, purification and characterization of a thermostable laccase from a tropical white-rot fungus. World Journal of Microbiology and Biotechnology, 2011. 27(3): p. 731-735.

3.   Baldrian, P., Fungal laccases-occurrence and properties. FEMS microbiology reviews, 2006. 30(2): p. 215-242.

4.   Cristóvão, R.O., Silvério, S.C., Tavares, A.P.M., Brígida, A.I.S., Loureiro, J.M., Boaventura, R.A.R., Macedo, E.A., and Coelho, M.A.Z., Green coconut fiber: a novel carrier for the immobilization of commercial laccase by covalent attachment for textile dyes decolourization. World Journal of Microbiology and Biotechnology, 2012. 28(9): p. 2827-2838.

5.   de Souza Bezerra, T.M., Bassan, J.C., de Oliveira Santos, V.T., Ferraz, A., and Monti, R., Covalent immobilization of laccase in green coconut fiber and use in clarification of apple juice. Process Biochemistry, 2015. 50(3): p. 417-423.

6.   Riva, S., Laccases: blue enzymes for green chemistry. Trends in Biotechnology, 2006. 24(5): p. 219-226.

7.   Quirós, M., García, A.B., and Montes-Morán, M.A., Influence of the support surface properties on the protein loading and activity of lipase/mesoporous carbon biocatalysts. Carbon, 2011. 49(2): p. 406-415.

8.   Tavares, A.P.M., Silva, C.G., Dražić, G., Silva, A.M.T., Loureiro, J.M., and Faria, J.L., Laccase immobilization over multi-walled carbon nanotubes: Kinetic, thermodynamic and stability studies. Journal of Colloid and Interface Science, 2015. 454: p. 52-60.

9.   Thomas, T.D., The role of activated charcoal in plant tissue culture. Biotechnology Advances, 2008. 26(6): p. 618-631.

10.   Kang, B.S., Lee, K.H., Park, H.J., Park, Y.-K., and Kim, J.-S., Fast pyrolysis of radiata pine in a bench scale plant with a fluidized bed: Influence of a char separation system and reaction conditions on the production of bio-oil. Journal of Analytical and Applied Pyrolysis, 2006. 76(1–2): p. 32-37.

11.   González, M.E., Cea, M., Sangaletti, N., González, A., Toro, C., Diez, M.C., Moreno, N., Querol, X., and Navia, R., Biochar Derived from Agricultural and Forestry Residual Biomass: Characterization and Potential Application for

Enzymes Immobilization. Journal of Biobased Materials and Bioenergy, 2013. 7(6): p. 724-732.

12.   Tan, X., Liu, Y., Zeng, G., Wang, X., Hu, X., Gu, Y., and Yang, Z., Application of biochar for the removal of pollutants from aqueous solutions. Chemosphere, 2015. 125: p. 70-85.

13.   Beesley, L., Moreno-Jiménez, E., Gomez-Eyles, J.L., Harris, E., Robinson, B., and Sizmur, T., A review of biochars' potential role in the remediation, revegetation and restoration of contaminated soils. Environmental Pollution, 2011. 159(12): p. 3269-3282.

14.   Cea, M., Sangaletti, N., González, M.E., and Navia, R., Candida rugosa lipase immobilization on biochar derived from agricultural residues. 2nd International Workshop "Advances in Science and Technology of Natural Resources, 2010(Pucón-Chile).

15.   Davis, S. and Burns, R.G., Covalent immobilization of laccase on activated carbon for phenolic effluent treatment. Applied Microbiology and Biotechnology, 1992. 37(4): p. 474-479.

16.   Bezerra, T.M.d.S., Bassan, J.C., Santos, V.T.d.O., Ferraz, A., and Monti, R., Covalent immobilization of laccase in green coconut fiber and use in clarification of apple juice. Process Biochemistry, 2015. 50(3): p. 417-423.

17.   Naghdi, M., Taheran, M., Brar, S.K., Rouissi, T., Verma, M., Surampalli, R.Y., and Valero, J.R., A green method for production of nanobiochar by ball milling-optimization and characterization. Journal of Cleaner Production, 2017. 164: p. 1394-1405.

18.   Naghdi, M., Taheran, M., Brar, S.K., Kermanshahi-pour, A., Verma, M., and Surampalli, R.Y., Immobilized laccase on oxygen functionalized nanobiochars through mineral acids treatment for removal of carbamazepine. Science of The Total Environment, 2017. 584: p. 393-401.

19.	Derringer, G., Simultaneous Optimization of Several Response Variables. Journal of Quality Technology, 1980. 12(4): p. 214-219.

20.	Faramarzi, M.A. and Forootanfar, H., Biosynthesis and characterization of gold nanoparticles produced by laccase from Paraconiothyrium variabile. Colloids and Surfaces B: Biointerfaces, 2011. 87(1): p. 23-27.

21.	Feng, W. and Ji, P., Enzymes immobilized on carbon nanotubes. Biotechnology Advances, 2011. 29(6): p. 889-895.

22.	Gao, Y. and Kyratzis, I., Covalent Immobilization of Proteins on Carbon Nanotubes Using the Cross-Linker 1-Ethyl-3-(3-dimethylaminopropyl)carbodiimide-a Critical Assessment. Bioconjugate Chemistry, 2008. 19(10): p. 1945-1950.

23.	Wong, S.S., Joselevich, E., Woolley, A.T., Cheung, C.L., and Lieber, C.M., Covalently functionalized nanotubes as nanometre- sized probes in chemistry and biology. Nature, 1998. 394(6688): p. 52-55.

24.	Labus, K., Gancarz, I., and Bryjak, J., Immobilization of laccase and tyrosinase on untreated and plasma-treated cellulosic and polyamide membranes. Materials Science and Engineering: C, 2012. 32(2): p. 228-235.

25.	Huang, W., Taylor, S., Fu, K., Lin, Y., Zhang, D., Hanks, T.W., Rao, A.M., and Sun, Y.-P., Attaching Proteins to Carbon Nanotubes via Diimide-Activated Amidation. Nano Letters, 2002. 2(4): p. 311-314.

26.	Jiang, K., Schadler, L.S., Siegel, R.W., Zhang, X., Zhang, H., and Terrones, M., Protein immobilization on carbon nanotubes via a two-step process of diimide-activated amidation. Journal of Materials Chemistry, 2004. 14(1): p. 37-39.

27.	Asuri, P., Karajanagi, S.S., Sellitto, E., Kim, D.-Y., Kane, R.S., and Dordick, J.S., Water-soluble carbon nanotube-enzyme conjugates as functional biocatalytic formulations. Biotechnology and Bioengineering, 2006. 95(5): p. 804-811.

28. Lee, Y.-M., Kwon, O.-Y., Yoon, Y.-J., and Ryu, K., Immobilization of Horseradish Peroxidase on Multi-Wall Carbon Nanotubes and its Electrochemical Properties. Biotechnology Letters, 2006. 28(1): p. 39-43.

29. Misra, N., Kumar, V., Goel, N.K., and Varshney, L., Laccase immobilization on radiation synthesized epoxy functionalized polyethersulfone beads and their application for degradation of acid dye. Polymer, 2014. 55(23): p. 6017-6024.

30. Tastan, E., Önder, S., and Kok, F.N., Immobilization of laccase on polymer grafted polytetrafluoroethylene membranes for biosensor construction. Talanta, 2011. 84(2): p. 524-530.

31. Hu, X., Zhao, X., and Hwang, H.-m., Comparative study of immobilized Trametes versicolor laccase on nanoparticles and kaolinite. Chemosphere, 2007. 66(9): p. 1618-1626.

32. Ji, C., Nguyen, L.N., Hou, J., Hai, F.I., and Chen, V., Direct immobilization of laccase on titania nanoparticles from crude enzyme extracts of P. ostreatus culture for micro-pollutant degradation. Separation and Purification Technology, 2017. 178: p. 215-223.

33. Spinelli, D., Fatarella, E., Di Michele, A., and Pogni, R., Immobilization of fungal (Trametes versicolor) laccase onto Amberlite IR-120 H beads: Optimization and characterization. Process Biochemistry, 2013. 48(2): p. 218-223.

34. Lam, P.L., Gambari, R., Kok, S.L., Lam, K.H., Tang, J.O., Bian, Z.X., Lee, K.H., and Chui, C.H., Non-toxic agarose/gelatin-based microencapsulation system containing gallic acid for antifungal application. International journal of molecular medicine, 2015. 35(2): p. 503-510.

35. Da Silva, A.M., Tavares, A.P., Rocha, C.M., Cristóvão, R.O., Teixeira, J.A., and Macedo, E.A., Immobilization of commercial laccase on spent grain. Process biochemistry, 2012. 47(7): p. 1095-1101.

36. Salis, A., Pisano, M., Monduzzi, M., Solinas, V., and Sanjust, E., Laccase from Pleurotus sajor-caju on functionalised SBA-15 mesoporous silica:

Immobilisation and use for the oxidation of phenolic compounds. Journal of Molecular Catalysis B: Enzymatic, 2009. 58(1): p. 175-180.

37.   Cristóvão, R.O., Tavares, A.P.M., Brígida, A.I., Loureiro, J.M., Boaventura, R.A.R., Macedo, E.A., and Coelho, M.A.Z., Immobilization of commercial laccase onto green coconut fiber by adsorption and its application for reactive textile dyes degradation. Journal of Molecular Catalysis B: Enzymatic, 2011. 72(1): p. 6-12.

38.   Brandi, P., D'Annibale, A., Galli, C., Gentili, P., and Pontes, A.S.N., In search for practical advantages from the immobilisation of an enzyme: the case of laccase. Journal of Molecular Catalysis B: Enzymatic, 2006. 41(1): p. 61-69.

39.   Yang, W.Y., Min, D.Y., Wen, S.X., Jin, L., Rong, L., Tetsuo, M., and Bo, C., Immobilization and characterization of laccase from Chinese Rhus vernicifera on modified chitosan. Process Biochemistry, 2006. 41(6): p. 1378-1382.

40.   Areskogh, D. and Henriksson, G., Immobilisation of laccase for polymerisation of commercial lignosulphonates. Process Biochemistry, 2011. 46(5): p. 1071-1075.

41.   Peralta-Zamora, P., Pereira, C.M., Tiburtius, E.R., Moraes, S.G., Rosa, M.A., Minussi, R.C., and Durán, N., Decolorization of reactive dyes by immobilized laccase. Applied Catalysis B: Environmental, 2003. 42(2): p. 131-144.

42.   Bayramoğlu, G., Yilmaz, M., and Yakup Arica, M., Reversible immobilization of laccase to poly(4-vinylpyridine) grafted and Cu(II) chelated magnetic beads: Biodegradation of reactive dyes. Bioresource Technology, 2010. 101(17): p. 6615-6621.

43.   Liu, Y., Zeng, Z., Zeng, G., Tang, L., Pang, Y., Li, Z., Liu, C., Lei, X., Wu, M., Ren, P., Liu, Z., Chen, M., and Xie, G., Immobilization of laccase on magnetic bimodal mesoporous carbon and the application in the removal of phenolic compounds. Bioresource Technology, 2012. 115: p. 21-26.

44.   Bayramoğlu, G. and Yakup Arıca, M., Immobilization of laccase onto poly(glycidylmethacrylate) brush grafted poly(hydroxyethylmethacrylate) films: Enzymatic oxidation of phenolic compounds. Materials Science and Engineering: C, 2009. 29(6): p. 1990-1997.

45.   Wang, Q., Peng, L., Li, G., Zhang, P., Li, D., Huang, F., and Wei, Q., Activity of laccase immobilized on TiO2-montmorillonite complexes. International journal of molecular sciences, 2013. 14(6): p. 12520-12532.

46.   Jolivalt, C., Brenon, S., Caminade, E., Mougin, C., and Pontié, M., Immobilization of laccase from Trametes versicolor on a modified PVDF microfiltration membrane: characterization of the grafted support and application in removing a phenylurea pesticide in wastewater. Journal of Membrane Science, 2000. 180(1): p. 103-113.

47.   Pezzella, C., Russo, M.E., Marzocchella, A., Salatino, P., and Sannia, G., Immobilization of a Pleurotus ostreatus laccase mixture on perlite and its application to dye decolourisation. BioMed research international, 2014. 2014.

48.   Asuri, P., Karajanagi, S.S., Dordick, J.S., and Kane, R.S., Directed Assembly of Carbon Nanotubes at Liquid−Liquid Interfaces: Nanoscale Conveyors for Interfacial Biocatalysis. Journal of the American Chemical Society, 2006. 128(4): p. 1046-1047.

49.   Rekuć, A., Jastrzembska, B., Liesiene, J., and Bryjak, J., Comparative studies on immobilized laccase behaviour in packed-bed and batch reactors. Journal of Molecular Catalysis B: Enzymatic, 2009. 57(1): p. 216-223.

50.   Stanescu, M.D., Fogorasi, M., Shaskolskiy, B.L., Gavrilas, S., and Lozinsky, V.I., New potential biocatalysts by laccase immobilization in PVA cryogel type carrier. Applied biochemistry and biotechnology, 2010. 160(7): p. 1947-1954.

Table 5.1.1 Independent variables used for optimization of covalent immobilization of laccase onto functionalized nanobiochar

Independent factor	Units	Coded levels				
Levels		-2	-1	0	+1	+2
FNBC	(mg/mL)	2	3	4	5	6
Laccase	(mg/mL)	2	6	10	14	18
EDAC	mM	5.7	6.7	7.5	8.2	8.9

Table 5.1.2 Variable parameters and their level in designed experiments

No	FNBC (mg/mL)	Enzyme (mg/mL)	EDAC (mM)	Laccase activity (U/g)
1	3	6	6.7	1.13
2	5	6	6.7	1.66
3	3	14	6.7	1.35
4	5	14	6.7	2.54
5	3	6	8.2	2.96
6	5	6	8.2	3.42
7	3	14	8.2	4.10
8	5	14	8.2	4.95
9	2	10	7.5	0.97
10	6	10	7.5	4.43
11	4	2	7.5	0.71
12	4	18	7.5	4.39
13	4	10	5.7	1.03
14	4	10	8.9	3.23
15 (C)	4	10	7.5	3.59
16 (C)	4	10	7.5	3.57
17 (C)	4	10	7.5	3.59
18 (C)	4	10	7.5	3.57
19 (C)	4	10	7.5	3.59
20 (C)	4	10	7.5	3.57

Table 5.1.3 Properties of immobilized laccase

Property	Immobilized laccase (This study)	Data from Literature	
		Value	Reference
pH stability	3-5	3-7	[30, 45, 46]
Temperature stability	30-50 °C	30-60 °C	[5, 27]
Storage stability	30 days	25-40 days	[27, 45, 47]
Reusability	7 cycles	5-10 cycles	[1, 33, 37]
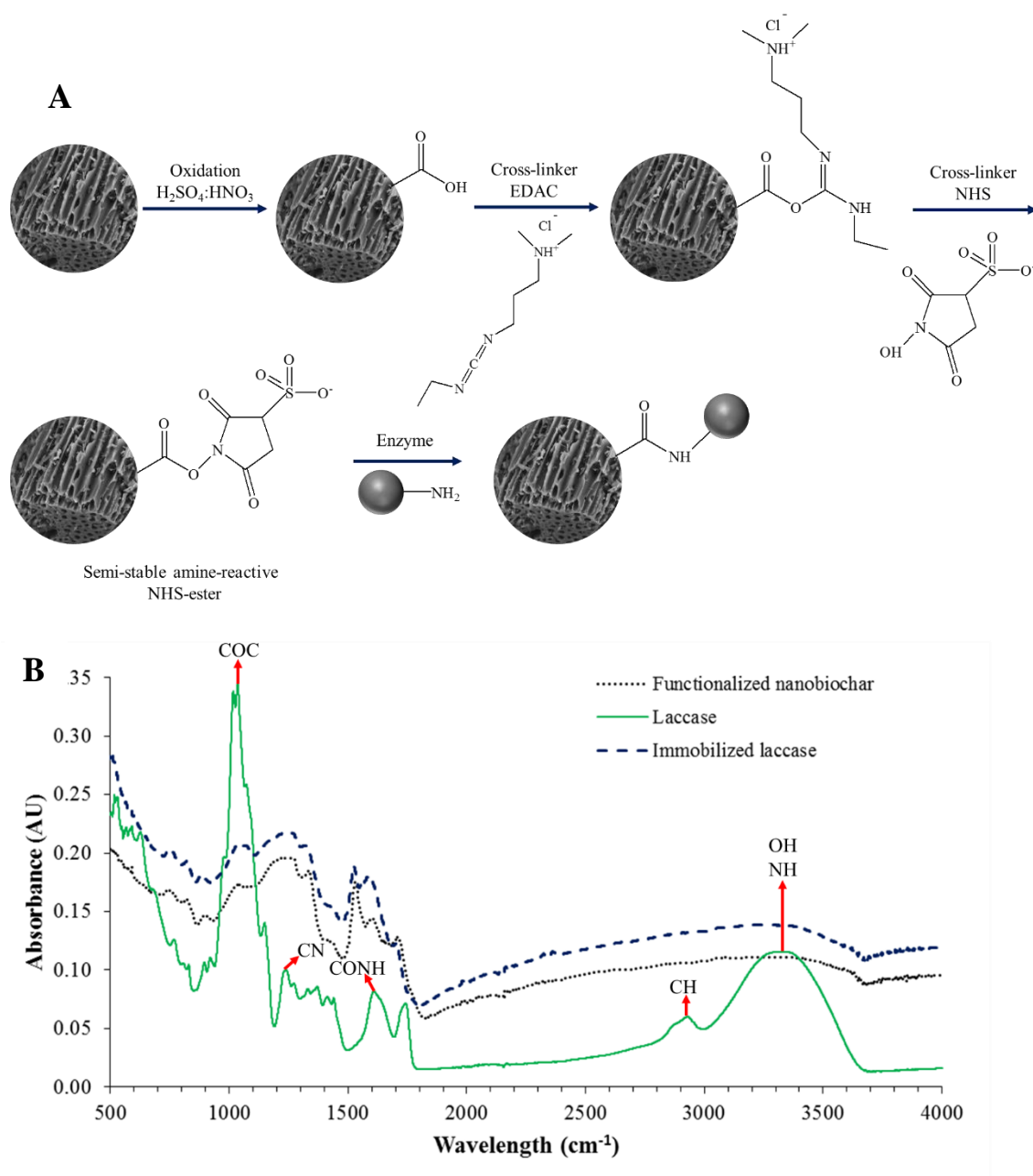
Figure 5.1.1 a) Mechanism of immobilization of laccase onto functionalized nanobiochar and; b) FTIR spectra of laccase (solid line), neat functionalized nanobiochars (short-dash line) and laccase immobilized over functionalized nanobiochars (dash line)
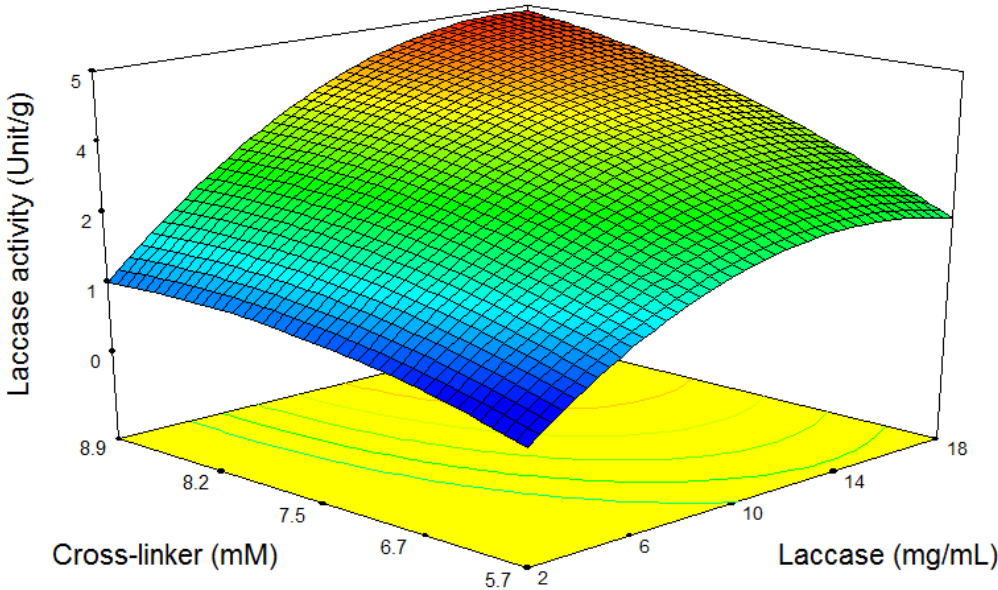
Figure 5.1.2 Effects of cross-linker concentration and laccase concentration on the immobilization activity of laccase on functionalized nanobiochar
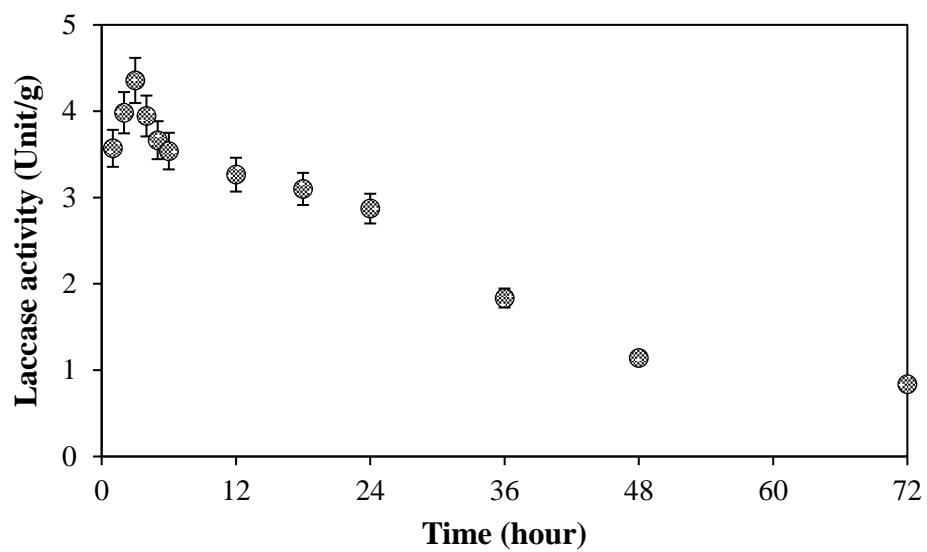
Figure 5.1.3 Effect of incubation period on the immobilization activity laccase on functionalized nanobiochar at 4 °C
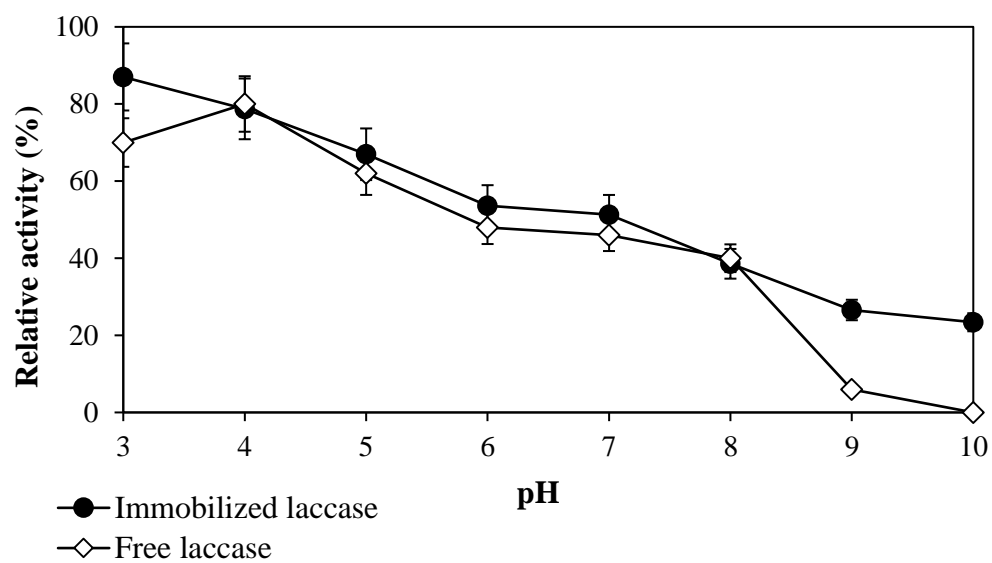
Figure 5.1.4 The effect of pH on the activity of free laccase and immobilized laccase
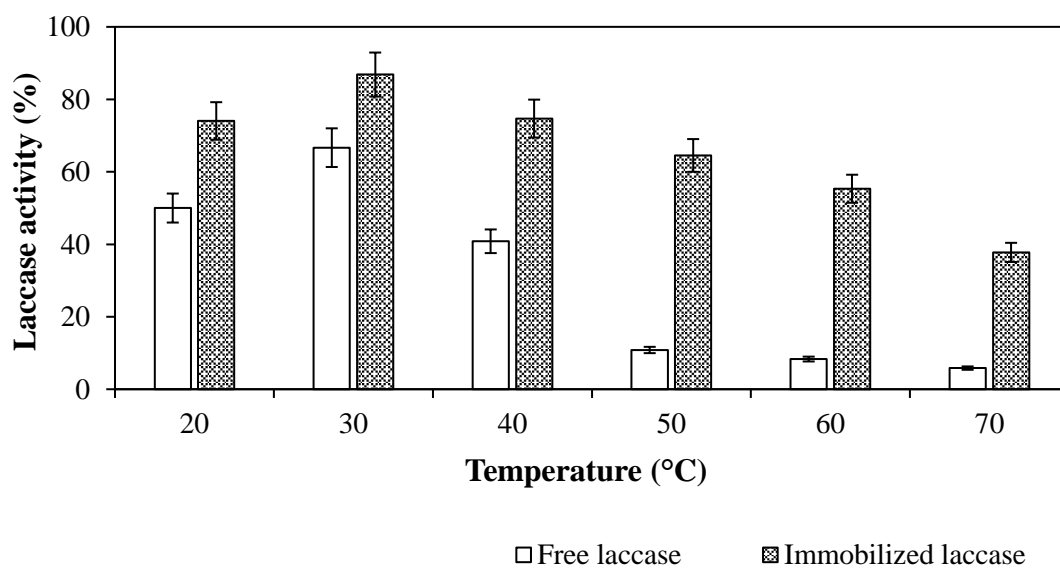
Figure 5.1.5 Influence of temperature on the activity of free and immobilized laccase after 8 h of incubation at a desired temperature
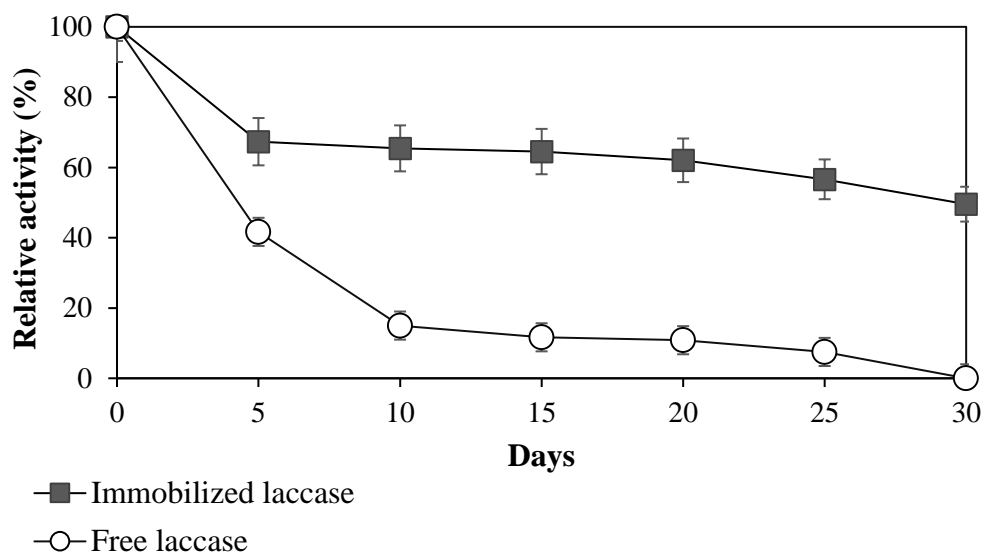
Figure 5.1.6 Retention of enzymatic activity at room temperature for free laccase and immobilized laccase on functionalized nanobiochar
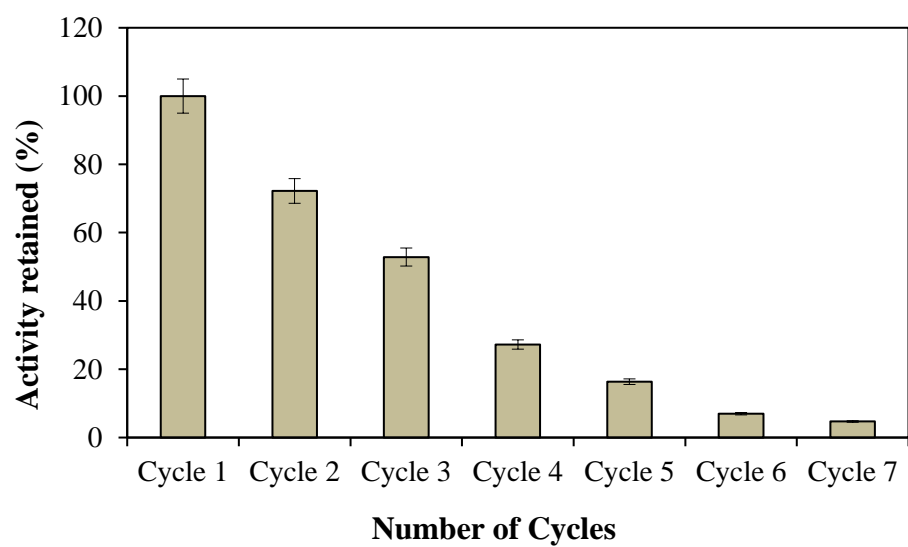
Figure 5.1.7 Reusability of functionalized nanobiochar-immobilized laccase during seven cycles of incubation

Part 2

Fabrication of Nanobiocatalyst Using Encapsulated Laccase onto Chitosan-Nanobiochar composite

Mitra Naghdi[1], Mehrdad Taheran[1], Satinder Kaur Brar[1*], Azadeh Kermanshahi-pour[2], Mausam Verma[1] and R.Y. Surampalli[4]

[1]INRS-ETE, Université du Québec, 490, Rue de la Couronne, Québec, Canada G1K 9A9

[2]Biorefining and Remediation Laboratory, Department of Process Engineering and Applied Science, Dalhousie University, 1360 Barrington Street, Halifax, Nova Scotia, Canada, B3J 1Z1

[3]Department of Civil Engineering, University of Nebraska-Lincoln, N104 SEC PO Box 886105, Lincoln, NE 68588-6105, US

(*Phone: 1 418 654 3116; Fax: 1 418 654 2600; E-mail: satinder.brar@ete.inrs.ca)

Résumé

La laccase est l'une des enzymes les plus utilisées pour les procédés en biotechnologie. L'immobilisation des enzymes est une approche universellement acceptée pour augmenter leur réutilisabilité et leur stabilité. Dans cette étude, l'enzyme laccase de *Trametes versicolor* a été encapsulée pour la première fois dans une matrice de chitosane-nanobiochar. La technique de formation de gel de chitosane-tripolyphosphate a été utilisée pour produire des nanoparticules de biocatalyseur homogènes, avec 35% d'efficacité de liaison efficace et 3,5 unités/g d'activité apparente dans la meilleure configuration. La réutilisabilité de la laccase encapsulée a été démontrée vers l'oxydation du 2,2'-azinobis-(3-éthylbenzothiazoline-6-sulfonate) (ABTS) pendant plusieurs cycles consécutifs, présentant 30% de l'activité initiale après 5 cycles. La laccase encapsulée a montré une augmentation modérée de la stabilité de l'enzyme vis-à-vis du pH et de la variation de température par rapport à l'enzyme libre. De plus, la stabilité durant le stockage de la laccase à 4 °C et 25 °C a augmenté après l'immobilisation. Seulement 2% de la laccase a fui pendant une période de 5 jours à partir du biocatalyseur. La laccase sous sa forme libre n'a montré aucune activité antibactérienne contre les micro-organismes modèles Gram positif et Gram négatif, tandis que la laccase encapsulée a montré une activité antibactérienne vis-à-vis des bactéries Gram-positives. Ainsi, l'encapsulation de la laccase est une méthode efficace pour maintenir l'enzyme active et stable pour différentes applications.

Mots clés

Laccase, Chitosan, Nanobiochar, Nanoencapsulation, Réticulation Glutaraldéhyde, Stabilité, Bactéries

Abstract

Laccase is one of the widely used enzymes for biotechnological processes. Immobilization of enzymes is a universally accepted approach to increase their reusability and stability. In this study, laccase enzyme from *Trametes versicolor* was encapsulated for the first time in a chitosan-nanobiochar matrix. The chitosan-tripolyphosphate gel formation technique was employed to produce homogeneous biocatalyst nanoparticles, with 35% of effective binding efficiency and 3.5 Units/g apparent activity under the best configuration. The reusability of the encapsulated laccase was demonstrated towards the oxidation of 2,2'-azinobis-(3-ethylbenzothiazoline-6-sulfonate) (ABTS) for several consecutive cycles, exhibiting 30% of the initial activity after 5 cycles. The encapsulated laccase showed a moderate increase in enzyme stability against pH and temperature variation compared to the free enzyme. Moreover, the storage stability of laccase at both 4 °C and 25 °C was increased after immobilization. Only 2% of laccase was leaked during a 5-day period from biocatalyst. Laccase in its free form showed no antibacterial activity against Gram positive and Gram negative model microorganisms, while encapsulated laccase showed antibacterial activity towards Gram-positive ones. Thus, the encapsulation of the laccase is an efficient method to keep the enzyme active and stable for different applications.

Keywords

Introduction

Enzymes have potential to be used in different biochemical processes, but their application is challenged due to their unstable nature and low stability against variation in pH and temperature [1]. Immobilization of enzymes is a widely used approach to enable repeated use of enzymes in industrial applications [2]. Immobilization can also enhance the stability and durability of the enzymes which leads to economical operations [3, 4]. Among different immobilization methods, encapsulation of enzymes into polymers has been proved to be successful since the entrapment can protect the enzyme structure from harsh conditions [5].

Although different synthetic polymers can be used for immobilization of enzymes, natural polymers have advantages such as biocompatibility, nontoxic and appropriate interactions with enzymes due to their functional groups [6]. Chitosan (Cs) is a natural cationic polymer with primary amines and can be obtained from crustacean shells [7]. Cs exhibits interesting properties, such as availability, biocompatibility and having reactive functional groups [8]. Due to its non-toxic nature and tensile strength, Cs has been widely used to encapsulate active ingredients in different industries [9].

Laccase (Lac, EC 1.10.3.2) is a member of multicopper oxidases enzymes with the capability of oxidizing the hydrogen-donating compounds such as lignin and phenol through the reduction of O_2 to H_2O [10, 11]. Lac is recognized for removal of micropollutants from water and wastewater. There are several reports on conjugation of laccase (Lac) with Cs through cross-linking of the primary amines that exist in Cs and enzyme [12, 13]. Glutaraldehyde (Glu) is the widely used cross-linker between enzymes and Cs [14]. The polycationic nature of Cs can be transformed into cross-linked beads or films through polycondensation in the presence of anionic molecules such as tripolyphosphate (TPP) which is nontoxic and has quick gelling ability [15]. In fact, the positively charged amino groups on Cs bind with the negatively charged phosphates groups on TPP through electrostatic attraction [16].

On the other hand, biochar, which is a by-product of waste biomass pyrolysis, holds promise due to its unique physicochemical properties for both agricultural applications and environmental protection [17, 18]. The beneficial properties are porosity, high surface area, and capability for adsorbing various compounds, such as organic contaminants and cations [19]. Biochar can be used in biotechnological and nanotechnological processes to develop novel materials with enhanced capabilities

for environmental applications [20]. We have already reported the production of nano-sized biochar to enhance the adsorption capacity of biochar towards different pharmaceutically active compounds [21].

There are several reports on the conjugation of laccase with chitosan. The idea of encapsulation of laccase into the chitosan-nanobiochar matrix can provide an innovative laccase preparation for the practical application of biocatalyst. In this system, nanobiochar can act as a suitable support for adsorption of pollutants and provide enough contact time for degradation by immobilized laccase. The objective of this study was to encapsulate the laccase in a chitosan-nanobiochar matrix in order to understand the performance of this immobilized biocatalyst system with respect to removal efficiency, enzyme stability and recyclability. The properties of encapsulated laccase including the stability at different pHs and temperatures, the potential reusability of immobilized enzyme, antibacterial activity, leakage and storage time were studied.

Material and methods

Materials

Pinewood biochar with an average particle size of 3 mm was obtained by Pyrovac Inc. (Quebec, Canada). The biochar was derived from pine white wood (80% v/v) and the rest 20% was spruce and fir. For the production of this biochar, the temperature of biomass was increased to 525±1 °C at the rate of 25 °C/min in the presence of nitrogen and kept for 20 min. 2, 2′-azino-bis (3-ethylbenzothiazoline-6-sulphonic acid) (ABTS) was purchased from Sigma-Aldrich (Oakville, Canada). Sulfuric acid, Tween 80, nitric acid (analytical grades) tripolyphosphate (TPP), glutaraldehyde (Glu) solution (50%) and chitosan (Cs) (molecular weight 150-200 KDa, degree of deacetylation 85%) were purchased from Fisher Scientific (Ottawa, Canada). Apple pomace was obtained from Vergers Paul Jodoin Inc. (Quebec, Canada) and used as a solid substrate for Lac production using *Trametes versicolor* (ATCC 20869). All bacterial strains (*Bacillus Subtilis*, *Enterobacter Aerogenes* and *Escherichia coli)* were obtained from USDA culture collection. Ultrapure water was produced in the laboratory using Milli-Q/Milli-RO-Milli pore system (Massachusetts, USA).

Nanobiochar production and functionalization

Nanobiochar with a specific surface area of 47.3 m^2/g and average particle size of 60±20 nm was produced using a PM-100 planetary ball mill (Retsch Corporation, Germany) in the laboratory at ambient conditions [17]. Briefly, 10 g of pinewood biochar was preconditioned at -80 °C for 24 h and ball milling was performed in a 500 mL stainless steel jar for 100 min at 575 rpm using 45 g steel balls of 2.4 mm in diameter. The physicochemical properties of the produced nanobiochar are discussed elsewhere [17]. For functionalization through acidic treatment, the procedure of Naghdi *et al.* was employed with little modification [22]. Briefly, 4 g nanobiochar was dispersed in 500 mL of acidic solution (5 M H$_2$SO$_4$/HNO$_3$, 3:1 v/v) and stirred at 200 rpm and room temperature for 48 h. Subsequently, the suspension was washed with milli-Q water several times in order to remove acids and reach neutral pH. The functionalized nanobiochar (FNBC) was then freeze-dried and stored at room temperature as a dry powder.

Laccase production and extraction

About 40 g of apple pomace (78% w/w moisture and pH 4.5) was mixed with Tween 80 (0.5% v/w) in 500 mL Erlenmeyer flasks and autoclaved for 20 min at 121±1 °C. Then, the mixture was inoculated with *Trametes versicolor* (ATCC 20869) and incubated for 15 days at 30±1 °C. For enzyme extraction, the fermented sample was mixed with 50 mM sodium phosphate buffer (pH 6.5) at 1:20 V/V ratio. The mixture was then homogenized for 1 h on an incubator shaker at 150 rpm and 35±1 °C and then centrifuged for 30 min at 7000 ×g. The collected supernatant was analyzed for enzymatic activity and dried for 48 h using FD-1000 freeze drier (Eyela, Japan).

Preparation of encapsulated laccase

Six different procedures for the addition of the solutions were tried and the order of the addition is listed in Table 5.2.1. Stock solutions of required chemicals were prepared and kept at 4±1 °C prior to use. For this purpose, 1% w/v of Cs was dissolved in 1% v/v of aqueous acetic acid at a room temperature, ultrasonicated for 30 min and left overnight in the shaker at 250 rpm. The pH of Cs solution was adjusted to 6±0.5 by adding 1.0 M NaOH solution. Lac solution was prepared in phosphate buffer (pH 4) and centrifuged to remove solid particles. Stocks of 0.5% (v/v) aqueous Glu and 0.4% (w/v) aqueous TPP were prepared in milli-Q water and phosphate buffer pH 7,

respectively. For each run of experiments, 10 mg FNBC, 4 mL of Cs solution, 10 mL of Glu, 8 mL of Lac solution and 10 mL of TPP were used. After each step, the solution was mixed on a magnetic stirrer for 5 h at 20±1 °C and 150 rpm. All the chemicals were added dropwise into solution using a 10 mL plastic syringe with a 22 gauge needle. At the end of each run, the formed hydrogel was centrifuged at 11, 000 ×g for 30 min at room temperature to separate the gel particles. Later, the samples were washed twice using 10 mL of 0.05 mM buffer (pH 7.2). Initial Lac activity, residual activity of Lac in supernatant and activity of encapsulated Lac were measured. The best procedure was selected based on Lac loading and the samples were freeze-dried at -55 °C, 5 Pa, for 48 h using for further studies. In addition, the stability tests (pH, temperature and storage stability), leaching and reusability were carried out for both fresh and freeze-dried samples. A similar method was used for the preparation of a control sample i.e. Cs beads without Lac.

Stability assessment

pH, temperature and storage stability

For pH stability test, 50 µL of free Lac (0.8 Unit/mL) and 10 mg of encapsulated Lac in freeze-dried form and 100 mg of encapsulated Lac in fresh form were added to separate tubes containing 2 mL of buffers (pH range of 3 to 10) and kept at 200 rpm and 25±1 °C for 8 h. Then, the Lac activity of free and encapsulated samples was spectrophotometrically measured based on the method explained in Section "enzyme assay". For thermal stability, the procedure was similar to the one for pH stability except that the samples were incubated at different temperatures (4, 10, 20, 30, 40, 50, 60 and 70 °C) for 8 h at constant pH 7.0. For storage stability test, the free and encapsulated Lac samples were stored at 4 and 25±1 °C for up to 30 days and Lac activities were determined at 5-day intervals.

Reusability in terms of using ABTS

Around 50 mg of freeze-dried and 500 mg of fresh encapsulated Lac on nanobiochar were dispersed in 1 mL of citrate-phosphate buffer (pH 4) containing 1.5 mM ABTS and incubated for 10 min at 45 °C and 150 rpm. The samples were centrifuged (10 min, 11,000 × g) and the concentration of formed ABTS radical in the supernatant were measured. The encapsulated Lac on nanobiochar (freeze-dried and fresh)

samples were washed with Milli-Q water, decanted and the procedure was repeated for 7 cycles.

Leaching test of encapsulated laccase

The leaching of encapsulated lac from functionalized nanobiochar in aqueous media has been studied. 50 mg freeze-dried and 500 mg fresh encapsulated nanobiocatalysts were incubated individually in 10 mL of aqueous solution of the buffer at room temperature and pH 3.5. Samples were taken at specific time intervals (0, 8, 16, 24, 32, 40, 48, 72, 96 and 120 h) and activity of the leached enzyme was analyzed using lac assay.

Bacterial strains, culture media, and antibacterial test

The antibacterial performance of free and encapsulated Lac were compared by well diffusion method using three bacterial strains, *Bacillus Subtilis* (BS, Gram-positive), *Enterobacter aerogenes* (EA, Gram-negative) and *Escherichia coli* (EC, Gram-negative). BS was grown in a liquid medium containing 3 g/L yeast extract, 30 g/L tryptic soya broth, and 5 g/L NaCl. EA was grown in a liquid medium containing 50 g/L casein peptone, 50 g/L glucose, 20 g/L KH_2PO_4 and 5 g/L yeast extract. EC was grown in a liquid medium containing 1 g/L beef extract, 5 g/L peptone, 2 g/L yeast extract and 5 g/L NaCl. The incubation conditions were 37±1 °C for 12 hours (BS), 30±1 °C for 24 hours (EA) and 30±1 °C for 24 hours (EC) and the rotational speed was 150 rpm for all strains. The prepared cultures were preserved at 4±1 °C for future use. One mL of each bacterial suspension was mixed with 19 mL of molten solid media before transferring to the Petri plate. Wells of 8 mm in diameter were prepared on the agar plates using a sterile micropipette tip. Aliquots of free and encapsulated Lac were delivered into the prepared wells. After incubation at 30 ±1 °C for 24 hours, the radius of inhibition zones around the wells was measured in millimeters using calipers.

Enzyme assay

Lac activity was measured by monitoring the rate of ABTS oxidation to $ABTS^+$ in aqueous solution. One unit of Lac activity was defined as the amount of enzyme required for oxidizing one µmol of ABTS per min under the assay conditions. For free enzyme, the mixture contained 500 µL of ABTS (1.5 mM), 2.450 mL of 0.1 M citrate-phosphate buffer (pH 3.5) and 50 µL of Lac sample. The rate of ABTS oxidation at 45

°C was quantified by monitoring the increase in absorbance at the wavelength of 420 nm (ε_{420} = 36.000 M^{-1} cm^{-1}) [23] using a Cary 100 UV-VIS spectrophotometer (Varian, Australia). For encapsulated Lac, 10 mg of freeze-dried and 100 mg of fresh samples were reacted for 10 min with one mL ABTS (1.5 mM, pH 4) at 45 °C and 200 rpm. Later, the samples were centrifuged for 10 min at 11,000 × g and the absorbance of supernatants was determined at 420 nm. The final activity of encapsulated Lac on functionalized nanobiochar was expressed as Unit/g nanobiochar.

Statistical analyses

All the experiments were performed in triplicates, and the average of replicates and standard deviation were determined. Analysis of variance (ANOVA) was performed for the data using Microsoft Excel 2013 and the results which have P < 0.05 were considered as significant.

Results and discussion

Preliminary studies

To find the best order for sample preparation (Table 5.2.1), the performance of each experiment was evaluated in preliminary studies. The capability of each combination in terms of enzymatic activity was studied and the immobilization yield of the prepared samples was evaluated. Table 5.2.1 lists the laccase activity, the binding yield, and the effective binding yield of encapsulated Lac on FNBCs through different combinations. The crosslinking of Glu is a two-step reaction in which the amino groups of Cs react with Glu and provide terminal aldehydes which subsequently react with the amino group in Lac [24]. The highest Lac activity (3.50 Unit/g) was obtained for a fresh sample of combination # 5 (Cs→ En→ Glu→ FNBC→ TPP) and the effective binding yield was calculated to be 35%. The purpose of studying the effective binding yield was to examine the ability of the support as well as the manufacturing process to entrap the enzyme and preserve its activity. According to Table 5.2.1, the binding yields for samples prepared by procedure #1 (Cs→ En→ Glu→ TPP→ FNBC) and #5 (Cs→ En→ Glu→ FNBC→ TPP) are not significantly different (P < 0.01). However, their effective binding yields are completely different (27% for #1 versus 35% for #5). The highest enzyme loading (3.5 Unit/g) was observed for procedure #5 in which, crude Lac 10 Units/g was entrapped into FNBC but only 35% of it remained active.

During the immobilization reaction, the impendent aldehyde groups on Cs surface react with amino groups in Lac and form imino group (-CH=N-) [25]. In acidic pH range, the amino groups in Cs can be protonated and form polycations. Also, carboxylic acid groups were already created on nanobiochar through acidic treatment. Therefore, positively charged Cs molecules can be adsorbed on the surface of negatively charged FNBCs by electrostatic interaction. Using nanobiochar provides two important advantages for the enzyme immobilization. The first advantage is reducing the effect of mass transfer resistance between enzyme and substrate due to the small size of particles [22]. The second advantage is the capability for separation of the enzyme from the reaction medium for the purpose of reuse, which in turn reduce the capital and operational costs.

In the following context, the stability of nanobiocatalyst against variations in pH, temperature, and storage, as well as reusability and leaching, were evaluated for fresh and freeze-dried samples prepared through combination #5.

pH and thermostability profiles

A small change in temperature and pH of the reaction medium may cause enzyme denaturation and loss of activity. The conditions for maximum enzyme stability differ for free and immobilized enzymes depending on the method of immobilization, carrier type and activation method [26]. The pH stability was determined for free Lac, fresh and freeze-dried nanobiocatalyst, within a pH range from 3-10 at 25±1 °C and the relative activities are presented in Figure 5.2.1A. Lac activity in free and fresh immobilized samples showed their optimum activity at pH 4.0 while the freeze-dried sample showed its optimum activity at pH 5.0 and pH increase towards alkaline or pH reduction towards acidic conditions declined the activity. Koyani and Vazquez-Duhalt reported that pH activity profile of encapsulated Lac into Cs nanoparticles became wider compared to free enzyme due to the effect of the charge on the surface of support [12]. Yamak *et al.* reported 0.5 or 1 unit shift to higher pH for entrapped Lac in hydrogel structures. They reported optimum pH at 5.0 and 5.5-6.0 for free and immobilized Lac, respectively. Entrapment in hydrogel change the microenvironment and causes the kind of envelopment to the enzyme. Therefore a shift in maximum activity towards higher pH values is expected [3]. Vazquez-Duhalt *et al.* also reported that soluble Lac-Cs conjugate loses activity more slowly compared to free Lac over 2-

7 pH range. They attributed this behavior to multiple points attachment between enzyme and Cs, which improve the stabilization of conjugate system [27].

Thermostability of free Lac and encapsulated Lac (fresh and freeze-dried) were evaluated at different temperatures (Figure 5.2.1B). In the range of 4-70±1 °C, the optimum temperatures for all systems were found to be 20±1 °C. Free Lac lost around 14% and 78% of the activity at 4 and 60±1 °C, respectively, while fresh encapsulated Lac lost 11% and 71% and freeze-dried sample lost 16% and 70%, respectively. Entrapment into particles creates a kind of protection against temperature changes for the encapsulated enzymes and leads to higher stability compared to free enzyme. Enhancing this property makes the systems suitable for industrial applications in the operational temperature ranges [28]. As the temperature was increased to 70±1 °C, relative activity decreased down to 5% for free Lac; to 26% and 24% for fresh and freeze-dried nanobiocatalysts, respectively. Generally, enzyme immobilization improves the thermostability of enzymes due to interactions between enzyme and support, which increase the molecular rigidity [29-31]. This hypothesis is especially valid for solid supports. Cs particles seem to remain flexible and thus they are not able to induce rigidity to the enzyme. Therefore, better performance of encapsulated Lac can be attributed to the presence of nanobiochar in the sample.

Storage stability

Storage stability is one of the most significant parameters to be considered in enzyme immobilization since it affects productivity. Storage stability of free laccase, fresh and freeze-dried nanobiocatalyst at 4±1 °C and 25±1 °C is shown in Figure 5.2.2. In order to check the storage stability, free and encapsulated Lac were stored at 4±1°C and 25±1 °C for a certain period and their related activities were determined periodically. At the end of 35 days of storage at 4±1 °C, the retained activity of the free enzyme was 16%, while the entrapped enzyme in fresh and freeze-dried samples, retained about 31% and 29% of their original activities, respectively (Figure 5.2.2). Also, at 25±1 °C, the retained activity of the free enzyme, fresh and freeze-dried samples were 10%, 17%, and 13%, respectively. It should be noted that enzymes require some water in their structures to maintain their conformation which allows them to deliver full functionality after storage [8]. According to Figure 5.2.2, the activities of encapsulated Lac decreased with a slower rate and exhibited higher storage stability than that of

free Lac. It was reported that free and the immobilized Lac from *Trametes versicolor* can retain 42% and 79-91% of their initial activities after 56 days of storage at 4±1 °C, respectively [3]. In similar research works, it was observed that the encapsulation of the enzymes with agents, such as Cs, Arabic gum, and alginate protects the encapsulated enzyme's activity and hence increase their stability [8, 32]. In a controlled release system, the most important parameter is the equilibration with water. Encapsulation of enzyme in Cs provides a swelling-controlled system for release control, in which Cs agent protects the enzyme activity by controlling the release of the enzyme [8, 33].

Reusability of the encapsulated enzyme

Reusability of immobilized enzymes is an important aspect of industrial applications since it can decrease the cost of production [3, 22]. In this study, the reusability of immobilized Lac was examined in a batch reactor by using the samples in 7 consecutive cycles in one day and residual activities were measured and are presented in Figure 5.2.3. After 7th cycle, the retained activities for fresh and freeze-dried nanobiocatalyst were found to be 12% and 19%, respectively. Encapsulated Lac activities decreased continuously in usage cycles. Other researchers observed similar behavior [3, 34]. For example, Zhou *et al.* reported that 61% of the activity loss after six cycles for hybrid alginate-chitosan beads [35]. The lower value obtained for the freeze-dried sample can be attributed to the chemical structure of the matrix as freeze-drying may cause difficulty in the diffusion of the substrate and product in the matrix. This limitation may cause a decrease in the maximum activity of Lac entrapped in dry form by repeated use [1]. Immobilization improves the efficiency and the catalytic properties of Lac so that immobilized systems provide useful indications for practical applications.

Leakage of nanobiocatalyst into the buffer

The ability to retain the Lac onto the surface of Cs-FNBC over time was studied to consider the potential reuse of the biocatalyst in a long-term process. For this purpose, the activity of Lac in a buffer solution at room temperature was measured and the leaching of Lac from fresh and freeze-dried samples are shown in Figure 5.2.4. According to the results, only 2% of the enzyme leached out even after 120 hours of

incubation in both fresh and freeze-dried forms. This might be due to the presence of physically adsorbed enzyme on the FNBC. It is important to mention that the covalent bonds between Lac and Cs lead to strong attachment, and therefore leaching occurs to a negligible extent [2].

Hong *et al.* compared leakage of entrapped and covalently bonded Lac on a mixture of polyethylene glycol and gelatine. The leakages were 14.5% and 13.9% after 32 days for covalent bonded and entrapped Lac enzyme, respectively. They attributed the low leakage level to the application of optimum storage temperature i.e. 4±1 °C and restriction of the enzyme within a matrix or with a covalent bond to support [36]. Similarly, Zhou *et al.* used hybrid alginate-Cs beads with Glu to immobilize *Saccharomyces cerevisiae* alcohol dehydrogenase and reported very compact and stable beads and low level of enzyme leakage [35]. Bayramoglu *et al.* covalently immobilized Lac on the magnetic Cs and observed no leakage in the medium, even after long-term storage (6 weeks) [37]. The freeze-dried encapsulated Lac showed higher leakage at the beginning, which is probably the result of the migrated enzyme to the surface in the freeze drying process [1]. It is hypothesized that during the initial process of freezing the major part of the enzyme was lost since the water freezes and keeps the enzyme on the surface [1, 38].

Antibacterial activity studies

Antibacterial performance of free and encapsulated Lac was investigated towards three different bacterial strains (Gram-positive and Gram-negative bacteria). No significant inhibition was observed in many cases (BS, EA, and EC) for free Lac (data does not show). However, encapsulated Lac showed the antibacterial activity against only BS (Gram-positive) and the mean diameter of growth inhibition per well was 6 mm. The capability of encapsulated laccase into Cs to inhibit the growth of the BS on solid media is shown in Figure 5.2.5. The antibacterial mechanism of Cs is attributed to the cationic form of the amino group at the C-2 position of the glucosamine residue [39]. In a similar research, Chung et al. reported that the cationic form of Cs (amino groups, NH_3^+) had higher antibacterial activity towards Gram-positive strains, such as *Staphylococcus aureus* compared to Gram-negative strains, such as *Escherichia coli* [40]. Also, Benhabiles *et al.* reported that the Cs flocculates the bacteria and kill them by preventing nutrients and oxygen (i.e. mass transfer limitation) [41]. Furthermore, it

is proposed that Cs can be bonded with DNA of bacteria and penetrate into the nuclei and thus inhibit the mRNA and protein synthesis. In this hypothesis, Cs molecules are assumed to be able to pass through the cell wall and reach the plasma membrane [42]. However, Chung *et al.* mentioned that Cs with positive charges increases intermolecular electric repulsion, which leads to a longer persistence and prevents Cs from passing through bacterial cell wall [43].

Conclusion

A successful laccase encapsulation in the chitosan-nanobiochar matrix has been achieved. Compared with free laccase, the encapsulated laccase showed less sensitivity to changes in pH and temperature, as well as significantly improved stability. The optimum pH and temperature for storage of the encapsulated laccase were found to be 4-5 and 20±1 °C. Furthermore, stability test showed that encapsulated laccase kept more than 30% of its initial activity after 35 days. Encapsulated laccase showed antibacterial activity towards Gram-positive strain bacterium *Bacillus subtilis*. The encapsulation of laccase in chitosan and nanobiochar protected the enzyme against inactivation. The increased stability and the high activity of the encapsulated laccase could make this approach an attractive choice for biotechnology applications. Particularly, this biocatalyst can be a promising candidate for removal of micropollutants from water and wastewater since laccase already proved its capability for transformation of organic pollutants to less toxic compounds. Evaluation and optimization of this system for a real application will reveal its advantages and drawbacks.

Acknowledgements

References

1. Betigeri, S.S. and Neau, S.H., Immobilization of lipase using hydrophilic polymers in the form of hydrogel beads. Biomaterials, 2002. 23(17): p. 3627-3636.

2. Moreira, M.T., Moldes-Diz, Y., Feijoo, S., Eibes, G., Lema, J.M., and Feijoo, G., Formulation of Laccase Nanobiocatalysts Based on Ionic and Covalent Interactions for the Enhanced Oxidation of Phenolic Compounds. Applied Sciences, 2017. 7(8): p. 851.

3. Yamak, O., Kalkan, N.A., Aksoy, S., Altinok, H., and Hasirci, N., Semi-interpenetrating polymer networks (semi-IPNs) for entrapment of laccase and their use in Acid Orange 52 decolorization. Process Biochemistry, 2009. 44(4): p. 440-445.

4. Ansari, S.A. and Husain, Q., Potential applications of enzymes immobilized on/in nano materials: a review. Biotechnology advances, 2012. 30(3): p. 512-523.

5. Lu, L., Zhao, M., and Wang, Y., Immobilization of laccase by alginate–chitosan microcapsules and its use in dye decolorization. World Journal of Microbiology and Biotechnology, 2007. 23(2): p. 159-166.

6. Wang, Y. and Caruso, F., Mesoporous silica spheres as supports for enzyme immobilization and encapsulation. Chemistry of Materials, 2005. 17(5): p. 953-961.

7. Burrs, S., Vanegas, D., Bhargava, M., Mechulan, N., Hendershot, P., Yamaguchi, H., Gomes, C., and McLamore, E., A comparative study of graphene-hydrogel hybrid bionanocomposites for biosensing. Analyst, 2015. 140(5): p. 1466-1476.

8. Amid, M., Manap, Y., and Zohdi, N.K., Microencapsulation of purified Amylase enzyme from Pitaya (Hylocereus polyrhizus) peel in Arabic Gum-Chitosan using freeze drying. Molecules, 2014. 19(3): p. 3731-3743.

9.   Miao, Y. and Tan, S., Amperometric hydrogen peroxide biosensor with silica sol-gel/chitosan film as immobilization matrix. Analytica Chimica Acta, 2001. 437(1): p. 87-93.

10.   Wong, D.W.S., Structure and Action Mechanism of Ligninolytic Enzymes. Applied Biochemistry and Biotechnology, 2009. 157(2): p. 174-209.

11.   Yang, S., Hai, F.I., Nghiem, L.D., Price, W.E., Roddick, F., Moreira, M.T., and Magram, S.F., Understanding the factors controlling the removal of trace organic contaminants by white-rot fungi and their lignin modifying enzymes: a critical review. Bioresource technology, 2013. 141: p. 97-108.

12.   Koyani, R.D. and Vazquez-Duhalt, R., Laccase encapsulation in chitosan nanoparticles enhances the protein stability against microbial degradation. Environmental Science and Pollution Research, 2016. 23(18): p. 18850-18857.

13.   Cabana, H., Ahamed, A., and Leduc, R., Conjugation of laccase from the white rot fungus Trametes versicolor to chitosan and its utilization for the elimination of triclosan. Bioresource technology, 2011. 102(2): p. 1656-1662.

14.   Mirzaei B, E., Ramazani SA, A., Shafiee, M., and Danaei, M., Studies on glutaraldehyde crosslinked chitosan hydrogel properties for drug delivery systems. International Journal of Polymeric Materials and Polymeric Biomaterials, 2013. 62(11): p. 605-611.

15.   Huang, H. and Yang, X., Synthesis of chitosan-stabilized gold nanoparticles in the absence/presence of tripolyphosphate. Biomacromolecules, 2004. 5(6): p. 2340-2346.

16.   Sun, P., Li, P., Li, Y.M., Wei, Q., and Tian, L.H., A pH-sensitive chitosan-tripolyphosphate hydrogel beads for controlled glipizide delivery. Journal of Biomedical Materials Research Part B: Applied Biomaterials, 2011. 97B(1): p. 175-183.

17.   Naghdi, M., Taheran, M., Brar, S.K., Rouissi, T., Verma, M., Surampalli, R.Y., and Valero, J.R., A green method for production of nanobiochar by ball milling-

optimization and characterization. Journal of Cleaner Production, 2017. 164: p. 1394-1405.

18.   Oleszczuk, P., Ćwikła-Bundyra, W., Bogusz, A., Skwarek, E., and Ok, Y.S., Characterization of nanoparticles of biochars from different biomass. Journal of Analytical and Applied Pyrolysis, 2016. 121: p. 165-172.

19.   Yargicoglu, E.N., Sadasivam, B.Y., Reddy, K.R., and Spokas, K., Physical and chemical characterization of waste wood derived biochars. Waste Management, 2015. 36: p. 256-268.

20.   Zhang, M., Gao, B., Yao, Y., Xue, Y., and Inyang, M., Synthesis, characterization, and environmental implications of graphene-coated biochar. Science of The Total Environment, 2012. 435: p. 567-572.

21.   Naghdi, M., Taheran, M., Pulicharla, R., Rouissi, T., Brar, S.K., Verma, M., and Surampalli, R.Y., Pine-wood derived nanobiochar for removal of carbamazepine from aqueous media: Adsorption behavior and influential parameters. Arabian Journal of Chemistry, 2017.

22.   Naghdi, M., Taheran, M., Brar, S.K., Kermanshahi-pour, A., Verma, M., and Surampalli, R.Y., Immobilized laccase on oxygen functionalized nanobiochars through mineral acids treatment for removal of carbamazepine. Science of The Total Environment, 2017. 584: p. 393-401.

23.   Faramarzi, M.A. and Forootanfar, H., Biosynthesis and characterization of gold nanoparticles produced by laccase from Paraconiothyrium variabile. Colloids and Surfaces B: Biointerfaces, 2011. 87(1): p. 23-27.

24.   Xiao, H.Y., Huang, J., Liu, C., and Jiang, D.S., Immobilization of laccase on amine-terminated magnetic nano-composite by glutaraldehyde crosslinking method. Transactions of Nonferrous Metals Society of China, 2006. 16(Supplement 1): p. s414-s418.

25. Jiang, D.S., Long, S.Y., Huang, J., Xiao, H.Y., and Zhou, J.Y., Immobilization of Pycnoporus sanguineus laccase on magnetic chitosan microspheres. Biochemical Engineering Journal, 2005. 25(1): p. 15-23.

26. Demirel, G., Özçetin, G., Şahin, F., Tümtürk, H., Aksoy, S., and Hasirci, N., Semi-interpenetrating polymer networks (IPNs) for entrapment of glucose isomerase. Reactive and Functional Polymers, 2006. 66(4): p. 389-394.

27. Taheran, M., Naghdi, M., Brar, S.K., Knystautas, E.J., Verma, M., and Surampalli, R.Y., Degradation of chlortetracycline using immobilized laccase on Polyacrylonitrile-biochar composite nanofibrous membrane. Science of The Total Environment, 2017. 605: p. 315-321.

28. Vazquez-Duhalt, R., Tinoco, R., D'Antonio, P., Topoleski, L.T., and Payne, G.F., Enzyme conjugation to the polysaccharide chitosan: smart biocatalysts and biocatalytic hydrogels. Bioconjugate Chemistry, 2001. 12(2): p. 301-306.

29. Gassara-Chatti, F., Brar, S.K., Ajila, C.M., Verma, M., Tyagi, R.D., and Valéro, J.R., Encapsulation of ligninolytic enzymes and its application in clarification of juice. Food chemistry, 2013. 137(1): p. 18-24.

30. Xu, R., Zhou, Q., Li, F., and Zhang, B., Laccase immobilization on chitosan/poly (vinyl alcohol) composite nanofibrous membranes for 2, 4-dichlorophenol removal. Chemical engineering journal, 2013. 222: p. 321-329.

31. Kunamneni, A., Ghazi, I., Camarero, S., Ballesteros, A., Plou, F.J., and Alcalde, M., Decolorization of synthetic dyes by laccase immobilized on epoxy-activated carriers. Process Biochemistry, 2008. 43(2): p. 169-178.

32. Osma, J.F., Toca-Herrera, J.L., and Rodríguez-Couto, S., Biodegradation of a simulated textile effluent by immobilised-coated laccase in laboratory-scale reactors. Applied Catalysis A: General, 2010. 373(1): p. 147-153.

33. DeGroot, A.R. and Neufeld, R.J., Encapsulation of urease in alginate beads and protection from α-chymotrypsin with chitosan membranes. Enzyme and Microbial Technology, 2001. 29(6): p. 321-327.

34. Leonard, M., De Boisseson, M.R., Hubert, P., Dalencon, F., and Dellacherie, E., Hydrophobically modified alginate hydrogels as protein carriers with specific controlled release properties. Journal of controlled release, 2004. 98(3): p. 395-405.

35. Lloret, L., Eibes, G., Feijoo, G., Moreira, M., Lema, J., and Hollmann, F., Immobilization of laccase by encapsulation in a sol–gel matrix and its characterization and use for the removal of estrogens. Biotechnology progress, 2011. 27(6): p. 1570-1579.

36. Li, G.Y. and Li, Y.J., Immobilization of Saccharomyces cerevisiae alcohol dehydrogenase on hybrid alginate-chitosan beads. International Journal of Biological Macromolecules, 2010. 47(1): p. 21-26.

37. Hong, C.S., Lau, C.C.Y., Leong, C.Y., Chua, G.K., and Chin, S.Y., A comparison of entrapped and covalently bonded laccase: Study of its leakage, reusability, and the catalytic efficiency in TEMPO-mediated glycerol oxidation. Biocatalysis and Biotransformation, 2017: p. 1-10.

38. Bayramoglu, G., Yilmaz, M., and Yakup Arica, M., Preparation and characterization of epoxy-functionalized magnetic chitosan beads: laccase immobilized for degradation of reactive dyes. Bioprocess and Biosystems Engineering, 2010. 33(4): p. 439-448.

39. Tal, Y., Van Rijn, J., and Nussinovitch, A., Improvement of Structural and Mechanical Properties of Denitrifying Alginate Beads by Freeze-Drying. Biotechnology Progress, 1997. 13(6): p. 788-793.

40. Xie, W., Xu, P., Wang, W., and Liu, Q., Preparation and antibacterial activity of a water-soluble chitosan derivative. Carbohydrate Polymers, 2002. 50(1): p. 35-40.

41. Chung, Y.C., Su, Y.P., Chen, C.C., Jia, G., Wang, H.L., Wu, J.G., and Lin, J.G., Relationship between antibacterial activity of chitosan and surface characteristics of cell wall. Acta Pharmacologica Sinica, 2004. 25(7): p. 932-936.

42.   Benhabiles, M.S., Salah, R., Lounici, H., Drouiche, N., Goosen, M.F.A., and Mameri, N., Antibacterial activity of chitin, chitosan and its oligomers prepared from shrimp shell waste. Food Hydrocolloids, 2012. 29(1): p. 48-56.

43.   Goy, R.C., Britto, D.d., and Assis, O.B.G., A review of the antimicrobial activity of chitosan. Polímeros, 2009. 19: p. 241-247.

44.   Chung, Y.C., Wang, H.L., Chen, Y.M., and Li, S.L., Effect of abiotic factors on the antibacterial activity of chitosan against waterborne pathogens. Bioresource Technology, 2003. 88(3): p. 179-184.

Table 5.2.1 Different configurations of encapsulated laccase and their immobilization yields

No	Step I	Step II	Step III	Step IV	Step V	Laccase activity (U/g)^F	Binding yield (%)	Effective binding yield (%)
1	Cs^A	Lac^B	Glu^C	TPP^D	FNBC^E	2.69	48	27
2	Cs	Glu	Lac	TPP	FNBC	1.92	56	19
3	FNBC	Cs	Glu	Lac	TPP	1.83	39	18
4	Cs	Glu	Lac	FNBC	TPP	1.73	41	17
5	Cs	Lac	Glu	FNBC	TPP	3.50	49	35
6	FNBC	Cs	Lac	Glu	TPP	2.62	59	26

A: Chitosan, B: Laccase, C: Glutaraldehyde, D: Tripolyphosphate, E: Functionalized nanobiochar, F: The activity of immobilized laccase on nanobiochars.
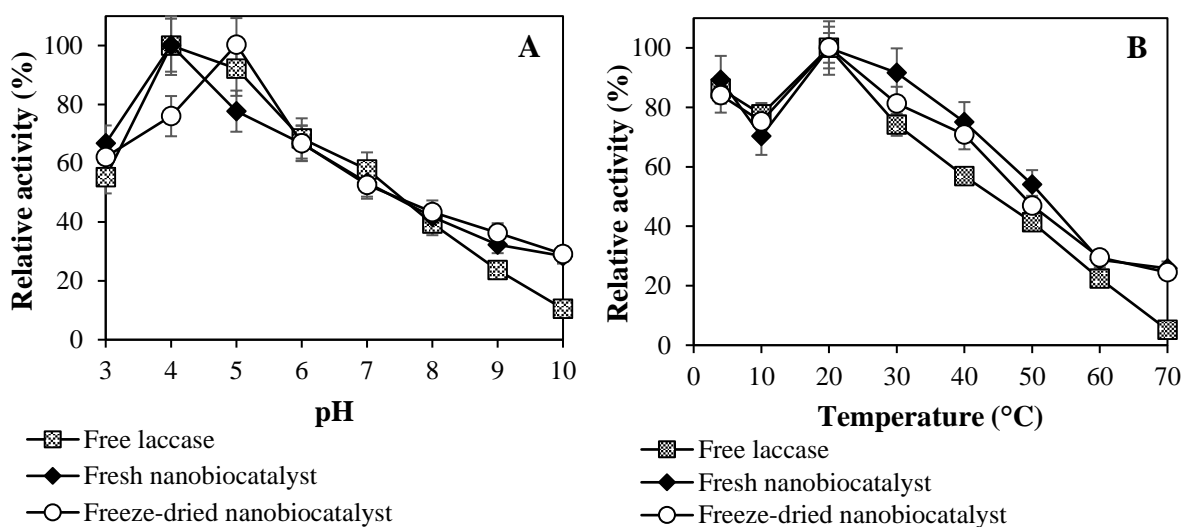
Figure 5.2.1 a) Influence of pH and; b) effect of temperature on the catalytic activity of free laccase, fresh and freeze-dried nanobiocatalyst
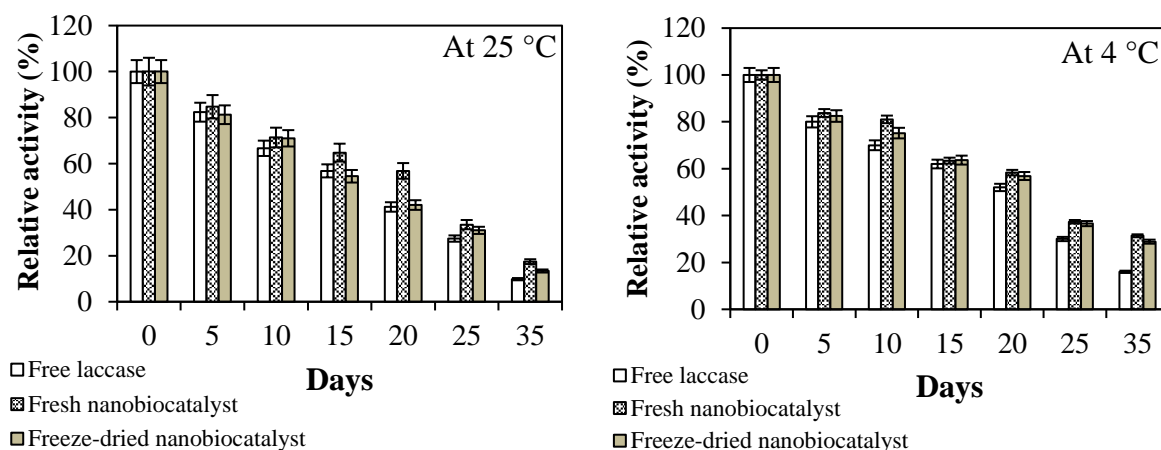
Figure 5.2.2 Effect of storage time on the activities of free laccase, fresh and freeze-dried nanobiocatalyst at 4±1 °C and 25±1 °C
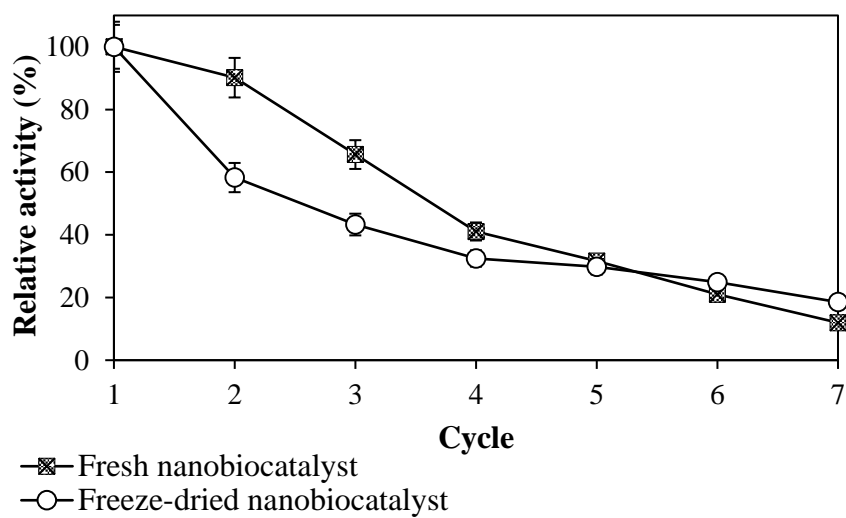
Figure 5.2.3 Effect of the reuse number of activities of immobilized laccases (reaction conditions: in the batch reactor, 25±1 °C, pH 3.5, 1.5 mM ABTS)
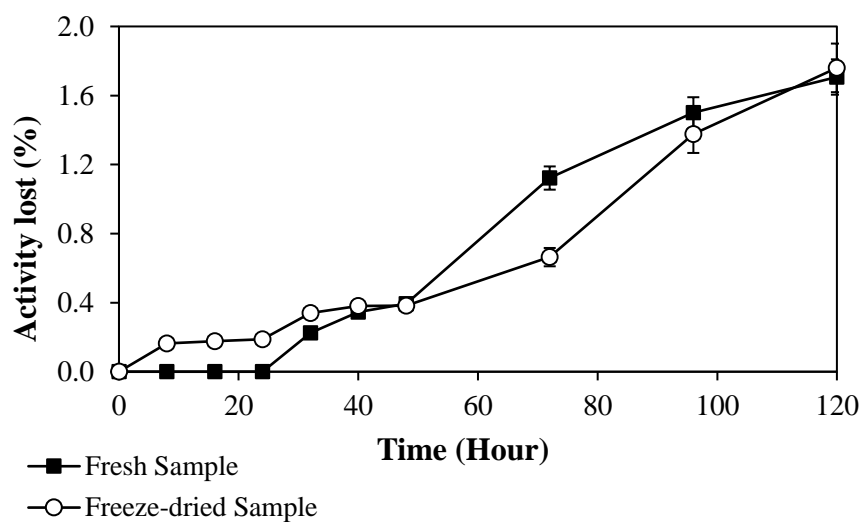
Figure 5.2.4 Leaching profile of encapsulated laccase on functionalized nanobiochar

Before growth   Before growth   After growth

6 mm

No bacterial growth
(Zone of inhibition)

Figure 5.2.5 Antibacterial activity of encapsulated laccase against *Bacillus subtilis*: a) after making the holes in the media, B) after filling the holes with bacterial suspension and; C) after 12 h incubation at 30±1 °C

CHAPTER 6

Investigating the degradation of carbamazepine with immobilized laccase

Part 1

Immobilized Laccase on Oxygen Functionalized Nanobiochars through Mineral Acids Treatment for Removal of Carbamazepine

Mitra Naghdi[1], Mehrdad Taheran[1], Satinder Kaur Brar[1*], Azadeh Kermanshahi-pour[2], Mausam Verma[1] and R.Y. Surampalli[4]

[1]INRS-ETE, Université du Québec, 490, Rue de la Couronne, Québec, Canada G1K 9A9

[2]Biorefining and Remediation Laboratory, Department of Process Engineering and Applied Science, Dalhousie University, 1360 Barrington Street, Halifax, Nova Scotia, Canada, B3J 1Z1

[3]Department of Civil Engineering, University of Nebraska-Lincoln, N104 SEC PO Box 886105, Lincoln, NE 68588-6105, US

(*Phone: 1 418 654 3116; Fax: 1 418 654 2600; E-mail: satinder.brar@ete.inrs.ca)

Chapter 6. Investigating the degradation of carbamazepine …

Résumé

Le traitement biocatalytique avec des enzymes oxydoréductases, en particulier les laccases, est une méthode respectueuse de l'environnement pour la biodégradation de composés pharmaceutiques, tels que la carbamazépine pour des composés moins nocifs. Cependant, les enzymes doivent être immobilisées sur des supports pour être réutilisables et maintenir leur activité. La fonctionnalisation du support avant l'immobilisation de l'enzyme est très importante en raison de l'interface biomolécule-support sur l'activité enzymatique et la stabilité. Dans ce travail, l'effet de l'oxydation du nanobiochar, en utilisant HCl, H_2SO_4, HNO_3 et leurs mélanges sur l'immobilisation de la laccase a été étudié. La microscopie électronique à balayage a indiqué que la structure des nanobiochars restait intacte après oxydation et que la spectroscopie infrarouge à transformée de Fourier confirmait la formation de groupes carboxyliques en raison du traitement à l'acide. Les mesures de titrage ont montré que l'échantillon traité avec H_2SO_4/HNO_3 (50:50, v/v) avait le plus grand nombre de groupes carboxyliques (4,7 mmol/g) et par conséquent l'efficacité la plus élevée pour l'immobilisation de la laccase. De plus, il a été observé que le stockage, le pH et la stabilité thermique de la laccase immobilisée sur le nanobiochar fonctionnalisé étaient améliorés par rapport à la laccase libre, montrant son potentiel pour des applications continues. Les essais de réversibilité vis-à-vis de l'oxydation de l'acide 2, 2'-azino-bis (3-éthylbenzothiazoline-6-sulfonique) (ABTS) ont montré que la laccase immobilisée conservait 70% de l'activité initiale après 3 cycles. Enfin, l'utilisation de laccase immobilisée pour la dégradation de la carbamazépine a montré une élimination de 83% et 86% dans l'eau enrichie et l'effluent secondaire, respectivement.

Mots clés

Nanobiochar, Fonctionnalisation, Acide, Oxydation, Immobilisation, Enzyme et effluent secondaire

Abstract

Biocatalytic treatment with oxidoreductase enzymes, especially laccases are an environmentally benign method for biodegradation of pharmaceutical compounds, such as carbamazepine to less harmful compounds. However, enzymes are required to be immobilized on supports to be reusable and maintain their activity. Functionalization of support prior to immobilization of enzyme is highly important because of biomolecule-support interface on enzyme activity and stability. In this work, the effect of oxidation of nanobiochar, a carbonaceous material produced by biomass pyrolysis, using HCl, H_2SO_4, HNO_3 and their mixtures on immobilization of laccase has been studied. Scanning electron microscopy indicated that the structure of nanobiochars remained intact after oxidation and Fourier transform infrared spectroscopy confirmed the formation of carboxylic groups because of acid treatment. Titration measurements showed that the sample treated with H_2SO_4/HNO_3 (50:50, v/v) had the highest number of carboxylic groups (4.7 mmol/g) and consequently the highest efficiency for laccase immobilization. Additionally, it was observed that the storage, pH and thermal stability of immobilized laccase on functionalized nanobiochar was improved compared to free laccase showing its potential for continuous applications. The reusability tests towards oxidation of 2, 2'-azino-bis (3-ethylbenzothiazoline-6-sulphonic acid) (ABTS) showed that the immobilized laccase preserved 70% of the initial activity after 3 cycles. Finally, using immobilized laccase for degradation of carbamazepine exhibited 83% and 86% removal in spiked water and secondary effluent, respectively.

Keywords

Nanobiochar, Functionalization, Acid, Oxidation, Immobilization, Enzyme and Secondary effluent

Introduction

Detection of pharmaceutically active compounds in the aquatic environment has raised concerns over their potential adverse effects on the environment [1]. Among them, carbamazepine (CBZ), a well-known antiepileptic compound, has been frequently detected in the wastewater effluent all over the world due to its chemical stability. It is classified as a harmful compound to aquatic organisms per European legislations [2, 3]. Due to low performance of conventional wastewater treatment technologies in removing CBZ, developing optimal strategies for removal of such compounds is crucial [4, 5]. Technologies, such as oxidation, reverse osmosis and adsorption are available that can efficiently remove CBZ. However, the main disadvantages of these technologies include formation of toxic by-products, large amount of retentate flow and need for regeneration of adsorbents [5, 6]. Employing oxidoreductase enzymes, such as laccase is an environmentally friendly alternative, which does not have the challenges of other methods besides its lower energy consumption [7-10]. However, using laccase in its free form leads to continuous loss of enzyme with treated effluent, which increases the operational cost. Immobilization of laccase onto solid support is a potential approach to overcome this challenge [11]. There is plenty of research reporting the benefits of immobilization of laccase including longer storage stability, reusability, temperature and pH stability on supports, such as SiO_2, TiO_2 and polymeric nanofibers and through different methods for degradation of micropollutants [5, 12-14].

Physical adsorption is a straightforward method for immobilization of enzymes onto supports, which does not involve using expensive and toxic compounds. However, the limited adsorption capacity and the possibility of enzyme leaching challenges the enzyme immobilization technology [10]. In this method, the support should have higher surface area and chemical stability. Therefore, carbonaceous materials, such as carbon nanotubes, graphene and activated carbon are appropriate choices for this application.

Biochar is a new class of carbonaceous material produced from pyrolysis of biomass, such as wood chips and manure in the absence of oxygen [15, 16]. Using biochar in soil amendment is considered as a waste management strategy which is beneficial to the environment in terms of mitigation of global warming and carbon sequestration [17, 18]. Also, the specific properties of biochar, such as low cost, porous structure, high

surface area and surface functional groups attracted researcher's interest to use it as adsorbent for removal of pollutants, such as organic pollutants and heavy metals from aqueous solutions [9, 19-21]. Furthermore, the choice of using nanobiochar (biochar with particle size less than 100 nm) can offer higher surface area, which is beneficial to the overall adsorption efficiency. Nanobiochar can efficiently adsorb micropollutants but, like other adsorbents, it will eventually be saturated and regeneration of nanobiochar is necessary to maintain the system performance [10]. Therefore, pre-adsorption of laccase onto nanobiochar could be a solution for in-situ regeneration of nanobiochar since immobilized laccase can degrade the adsorbed micropollutants and liberate occupied sites. Moreover, co-adsorption of micropollutants and laccase on carbonaceous material can increase contact time which may improve the biodegradation [22].

However, the weak physical bonding between support and laccase support results in leaching of laccase. Therefore, the surface of supports should be properly modified to form functional groups with stronger protein binding [13]. Mineral acids, such as HCl, H_2SO_4, HNO_3 and their mixtures are the common chemicals used to form carboxylic (COOR) and phenolic (C-OR) groups, resulting in increasing the affinity of carbonaceous materials with organic compounds [23-27]. There are many reports on using functionalized carbonaceous materials for different industrial applications, but only few of them are related to immobilization of enzymes. For example Gomez *et al.* functionalized multi walled carbon nanotubes by nitric acid at 120 °C and formed carboxylic acid and phenolic hydroxyl groups on the surface of the carbon nanotubes. They reported that new functional groups led to formation of stronger link between the surface of the support and enzyme through electrostatic interactions [28]. In a related research, Nguyen *et al.* functionalized activated carbon with HCl at 60 °C and used it for enzyme immobilization [10]. It seems that the role and efficiency of acidic treatment in functionalization of carbonaceous supports for immobilization of enzymes is not exhaustively studied and never applied for removal of ultra-trace contaminants (μg/L-ng/L).

To the best of our knowledge, this is the first report on functionalization of pinewood nanobiochar through acidic treatment for immobilization of enzymes. The main objective of this study was to evaluate three mineral acids including HCl, H_2SO_4, HNO_3, as well their binary and ternary mixtures in terms of carboxylic group formation.

The secondary objective was to immobilize the laccase on functionalized nanobiochar and assess its stability and reusability and examine the performance of immobilized laccase for the removal of CBZ.

Material and Methods

Material

Pinewood Biochar (BC-PW) was provided by Pyrovac Inc. (Quebec, Canada). The BC-PW was derived from pine white wood (80% v/v, size: 3 mm) obtained from Belle-Ripe in Princeville and the rest 20% was spruce and fir. The carbonization process was performed at 525±1 °C under nitrogen gas at atmospheric pressure for 2 min. 2, 2'-azino-bis (3-ethylbenzothiazoline-6-sulphonic acid) (ABTS) and carbamazepine (CBZ) with ≥ 99% purity were purchased from Sigma-Aldrich (Oakville, ON, Canada). Tween 80, sulfuric acid, hydrochloric acid and nitric acid (analytical grades) were obtained from Fisher scientific (Ottawa, Canada). Carbamazepine (D10), as internal standard in mass spectroscopy, was purchased from CDN Isotopes (Pointe-Claire, Canada). Apple pomace (Vergers Paul Jodoin Inc., Quebec, Canada) was used as solid substrate for laccase production using *Trametes versicolor* (TV). Secondary effluent samples were collected from Quebec wastewater treatment plant (Beauport, Quebec City, Canada). The characteristics of the secondary effluent are listed in Table 6.1.1. Ultrapure (double distilled) water was produced in the laboratory using Milli-Q/Milli-Ro Milli pore system (Massachusetts, USA).

Production of nanobiochar

Nanobiochar was produced in laboratory using ball mill. Briefly, 10 g raw biochar samples were kept at -80 °C for 24 h before milling at ambient conditions using a planetary ball mill (PM100; Retsch Corporation). Milling was performed at 575 rpm for 100 min in a stainless-steel jar (500 mL) using stainless steel balls of 2.4 mm in size (800 balls with total weight of 45 g). Nanobiochar with specific surface area of 47.3 m^2/g and average size of 60±10 nm was achieved.

Laccase production and extraction

Forty grams of apple pomace (78% (w/w) moisture and pH 4.5), was mixed with Tween 80 (0.5% v/w) in 500 mL Erlenmeyer flasks and autoclaved at 121±1 °C for 20 min. Later, the substrate was inoculated with *Trametes versicolor* (ATCC 20869) and

incubated at 30±1 °C for 15 days. For extraction of enzyme, one gram of fermented sample was mixed with 20 mL of 50 mM sodium phosphate buffer (pH 6.5). The mixture was homogenized on incubator shaker at 35±1 °C and 150 rpm for 1 h and then the mixture was centrifuged at 7,000 × g for 30 min. The collected supernatant was analyzed for enzyme activity and dried at - 55 °C, 5 Pa, for 48 h using freeze dryer (FD-1000, Eyela, Japan).

Functionalization of nanobiochar

Three types of acidic treatments were employed to functionalize nanobiochar. In type-1, 200 mg of nanobiochar was dispersed in 25 mL, 5 M of H_2SO_4/HNO_3/HCl (1:1:1 v) mixture and kept at room temperature and 200 rpm for 48 h. Subsequently, the nanobiochar suspension was repeatedly washed with milli-Q water to remove acids and reach pH 7. The treated nanobiochar was then lyophilized and stored at room temperature as a dry powder. In treatment-2, HNO_3/H_2SO_4 (1:1 v/v), HNO_3/HCl (1:1 v/v) and H_2SO_4/HCl (1:1 v/v) mixtures and in treatment-3, HNO_3, H_2SO_4 and HCl in their pure forms were used as functionalizing agent through the same procedure as treatment-1. To understand the effect of different treatments on functionalization, a nanobiochar sample without any treatment was considered as control.

Titration

All the acid treated nanobiochar samples were examined by titration to measure the amount of formed carboxylic groups (COOH) on their surfaces. About 50 mg of acid treated nanobiochar was stirred in 30 mL milli-Q water containing NaOH (0.01 M) for 48 h. The excess amount of NaOH in solution was determined through titration by 0.01 M aqueous HCl [29].

The required amount of NaOH to react with one gram of acid treated sample was calculated and reported as mmol of COOH per gram nanobiochar.

Laccase immobilization

In 50 mL flasks, 100 mg of acid treated nanobiochars were suspended in 10 mL of citrate-phosphate buffer (pH 3.5) containing laccase (2.3 Unit). The mixtures were incubated at 25 °C and 200 rpm in a rotary shaker. Immobilization of laccase was performed also on a nanobiochar without acid treatment as a control sample. The samples were centrifuged, decanted and the laccase activity in supernatant and also

in immobilized laccase were determined. The best pre-treatment method was selected based on laccase loading and stability tests (pH, temperature and storage stability), reusability and performance for CBZ removal was carried out on this sample.

Stability assessment

pH, temperature and storage stability

For pH stability, aliquots of 50 µL of free laccase (0.23 Unit/mL) and 10 mg of immobilized laccase were added to separate tubes containing 2 mL of buffers (pH range of 3 to 10) and kept for 8 h at 25 ºC and 200 rpm. The residual laccase activity of free and immobilized samples was measured (see section "enzyme assay"). For thermal stability, the procedure was similar to the one for pH stability except that the samples were kept at different temperatures (20-70 °C) for 8 h at constant pH 4. For storage stability, the free and immobilized laccase samples were stored at room temperature for up to 30 days and residual activities were determined at 5 day intervals.

Reusability in terms of using ABTS

About 50 mg of immobilized laccase on nanobiochar was dispersed in 1 mL of citrate-phosphate buffer (pH 4) containing 1.5 mM ABTS and incubated at room temperature and 200 rpm for 10 min. The sample was centrifuged (10 min, 11,000 × g) and the concentration of transformed ABTS in the supernatant was measured. The immobilized laccase on nanobiochar was washed with Milli-Q water, decanted and the procedure was repeated for 7 cycles.

CBZ degradation by laccase immobilized system

Repeated use of immobilized laccase

The performance of immobilized laccase on nanobiochar for removal of CBZ from aqueous media was evaluated in batch tests in both Milli-Q water and secondary effluent of municipal wastewater treatment plant. In a 50-mL flask, 50 mg immobilized laccase on nanobiochar was dispersed in 20 mL of CBZ solution (20 ng/mL) and the reaction mixture was stored for 24 h at 200 rpm and 25 ºC. The reaction time was selected according to the preliminary tests which indicated that after 24 h, the removal rate was negligible. The supernatant was decanted (10 min and 11, 000 × g) and CBZ removal efficiency was measured based on its initial and final aqueous phase

concentrations. The immobilized laccase on nanobiochar was washed with Milli-Q water, decanted and the procedure was repeated.

Contribution of adsorption and biodegradation to removal

The removal of CBZ by the immobilized laccase on nanobiochar is due to a combination of CBZ adsorption onto the nanobiochar and its degradation by laccase. To reveal the role of biodegradation in CBZ removal, an experiment was performed with nanobiochar and immobilized laccase on nanobiochar. Two test solutions contained 30 mL milli-Q water, 20 mg nanobiochar or immobilized laccase on nanobiochar and CBZ at 20 ng/mL were incubated at 25 °C and 200 rpm for 24 h. After incubation, the concentration of CBZ in aqueous phases was measured. To determine the amount of CBZ adsorbed on nanobiochar and immobilized laccase on nanobiochar, freeze-dried samples were mixed with 5 mL of methanol, sonicated for 10 min and incubated for 8 h at room temperature and 200 rpm to desorb CBZ. The mixture was then decanted and the concentration of CBZ in methanol phase was measured [30].

Analytical methods

Enzyme assay

Laccase activity was determined through monitoring the rate of oxidation of ABTS. One unit of laccase activity was defined as the amount of required enzyme to oxidize one μmol of ABTS per min under the assay conditions. For free enzyme, the reaction mixture contained 2.450 mL mM citrate phosphate buffer (pH 4), 500 μL ABTS (1.5 mM) and 50 μL of laccase sample. The oxidation of ABTS at room temperature was monitored by an increase in absorbance at the wavelength of 420 nm (ε_{420} = 36,000 M^{-1} cm^{-1}) [31] using a Cary 50 UV-visible spectrophotometer (Varian, Australia). For immobilized laccase, 10 mg of sample was reacted for 10 min with one mL ABTS (1.5 mM, pH 4) at room temperature and 200 rpm. Later, the sample was centrifuged for 10 min at 11, 000 × g and the absorbance of supernatant was measured at 420 nm. The final activity of laccase immobilized on nanobiochar was expressed as Unit/g nanobiochar.

Scanning electron microscopy

Scanning electron microscopy (SEM) imaging was carried out to characterize nanobiochars, before and after functionalization of nanobiochar. One mg of sample was dispersed in 200 ml distillated water. Small droplets of mixture were placed on an aluminum foil and dried at room temperature. The sample was gold-coated (15 nm thickness) using a sputter coater prior to imaging. Micrographs were captured at 10 kV accelerating voltage on a scanning electron microscope (Zeiss EVO® 50 Smart SEM system).

Fourier transform infrared (FT-IR) spectroscopy

FT-IR spectra was recorded in the range of 400-4000 cm^{-1} using a Nicole IS50 FT-IR Spectrometer (Thermo Scientific, USA) in attenuated total reflectance (ATR) mode with 4 cm^{-1} resolution. Briefly, sample was placed on the diamond crystal and the gripper plate was placed on the sample to achieve consistent contact between the crystal and the sample. The measurement was taken 16 times for each spectrum and their average was used for plotting.

Quantification of CBZ

Quantification of CBZ was performed with a Laser Diode Thermal Desorption (LDTD) (Phytronix technologies, Canada) coupled with a LCQ Duo ion trap tandem mass spectrometer (Thermo Finnigan, USA). The daughter ions identified for CBZ in LDTD were 194 and 192 Da. A calibration curve of CBZ concentration was developed with six standard solutions and with R^2 no less than 0.99. The details of quantification process were described elsewhere [32]. All the experiments were performed in triplicates and the average results were reported.

Surface area measurements

The Brunauer-Emmett-Teller (BET) specific surface area of the samples were determined from the N_2 adsorption isotherms recorded at 77 K ((Autsorb-1, Quantachrome Instruments) at the relative pressure range from 0.05 to 1. In this method, the sample was first heated to 60±1 °C and degassed by applying vacuum for 12 h. Later, the amount of adsorbed N_2 gas onto the surface of the sample was measured at different relative pressure. The amount of the required N_2 gas for monolayer coverage, the accessible internal pore and external surface of the sample was determined using the BET equation. Finally, taking the cross-sectional area of N_2 as 0.162 nm^2, the specific surface area was estimated.

Particle size measurement

Average particle size of the biochar sample was analyzed by laser beam scattering technique using a Zetasizer Nano-ZS apparatus (Malvern Instruments, UK). For sample preparation, 1 mg of sample was dispersed in 200 mL of distilled water containing 1% ethanol using magnetic stirrer for 60 min.

Results and discussion

Characterization of functionalized nanobiochars

Figure 6.1.1a shows the FTIR spectra of nanobiochars treated with different acid combinations. Infrared spectrum measures the quantity of radiation absorbed by atoms at different frequency. When a compound is exposed to an infrared radiation, the difference of charge between carbon atoms causes the formation of an electric dipole, which generates detectable signals [33]. The nanobiochar without acid treatment showed weak infrared signals due to the weak difference of charge between its carbon atoms, which consequently led to weak electric dipole.

As observed in Figure 6.1.1a, the spectra for nanobiochar samples treated with HCl, H_2SO_4 and H_2SO_4/HCl are almost the same as the spectrum for untreated nanobiochar. It means that these acids and their combinations had negligible effects on formation of functional groups on surface of nanobiochar. The broad bands at 1680-1730 cm^{-1} corresponded to C=O stretching bond in carboxylic acid functional group formed by surface oxidation [27]. In functionalization process, the structure of carbons breaks and therefore the generation of induced electric dipoles is enhanced. Comparing the spectra, nanobiochar samples treated with HNO_3 and other acid combinations containing HNO_3 showed stronger peaks for carboxylic acid functional group among which H_2SO_4/HNO_3 showed the peak with highest intensity. This behavior can be explained by the bonding of carboxyl groups onto the surfaces of nanobiochars and multiplication of defects by oxidation of mixed acid [25]. Also, the titration tests confirmed that the nanobiochar sample treated with H_2SO_4/HNO_3 had the highest level of carboxylic acid functional group (see section "carboxylic group concentration"). The FTIR spectra related to untreated nanobiochar and sample with the highest peak intensity for carboxylic groups (nanobiochar treated by H_2SO_4/HNO_3) are illustrated in Figure 6.1.1b. The broad band at around 3400 cm^{-1} in both spectra is a characteristic peak of O-H stretching that can be attributed to either carboxylic or alcoholic groups (O=C-OH and C-OH) [34]. The strong peak at around 1280 cm^{-1}

which corresponds to the C-O stretching of carboxylic acids, confirms the formation of carboxylic groups as a result of surface oxidation [33]. Furthermore, two bands observed at 1330-1380 cm^{-1} and 1520-1550 cm^{-1} can be attributed to $C-NO_2$ group which was formed as a result of nitration of aromatic rings [35].

The BET analysis showed that the pristine nanobiochar has surface area equal to 47.25 m^2/g and pore volume equal to 38.47 mm^3/g. Also, the surface area of acid treated nanobiochar and immobilized laccase onto acid treated nanobiochar were 52.11 and 20.68 m^2/g and their pore volumes were 40.39 and 18.17 mm^3/g, respectively. These parameters are calculated from nitrogen adsorption/desorption isotherms using BET theory and the results indicated that treating nanobiochar with HNO_3/H_2SO_4 increased N_2-accessible surface and pore volume by 10% and 5%, respectively. In a similar study, Nguyen *et al.* treated granular activated carbon with hydrochloric acid and reported 8% of increase in N_2-accessible surface [10]. On the other hand, during immobilization, laccase macromolecules occupied 60% of the surface area of functionalized nanobiochar and reduced it from 52.11 m^2/g to 20.68 m^2/g. Badgujar *et al.* immobilized lipase on a polymeric composite and observed that the N_2-accessible surface was reduced from 0.8047 m^2/g to 0.4373 m^2/g (45% reduction) [36]. Likewise, Pirozzi *et al.* entrapped lipase into ZrO_2 porous structure and observed that the surface area of the support was reduced from 316 m^2/g to 219 m^2/g (31% reduction) [37]. Similar behavior has been reported in research performed by He *et al.* [38] and Yunyu *et al.* [39].

Accordingly, still 40% of the surface area is accessible for adsorption to retain micropollutants and provide enough time for degradation as further discussed in Section "operational stability".

Carboxylic group concentration

The formation of carboxylic functional groups on the surface of carbonaceous materials provide ideal anchoring points for physical attachment and covalent bonding of enzymes on their surface [40]. It is due to the fact that, carboxylic group is easily formed via oxidizing treatment and can undergo a variety of reactions [41]. A back titration using NaOH and HCl were performed for this purpose [29]. The amount of functional groups per gram of nanobiochar (equivalent to the amount of used NaOH) were 3.3, 3.3, 3.5, 3.5, 4.0, 4.0 and 4.7 mmol/g for samples treated with HCl, H_2SO_4,

HNO_3, H_2SO_4/HCl, HNO_3/HCl, $H_2SO_4/HCl/HNO_3$ and H_2SO_4/HNO_3 respectively. The value for control sample was 3.0 mmol/g. According to the results, oxidation of nanobiochar by chemical reaction led to an increase in the concentration of acidic functional groups on the surface, from 3.0 mmol/g for untreated nanobiochar to 4.7 mmol/g (1.6 times increase) for nanobiochar treated with H_2SO_4/HNO_3 solution. In a similar study, Datsyuk *et al.* treated multiwalled carbon nanotubes with nitric acid and reported that the concentration of acidic functional groups on the surface increased 2.1 times more compared to untreated carbon. [42]. Marshall *et al.* functionalized single-walled carbon nanotubes by using sonication in a mixture of H_2SO_4/HNO_3 acids. They found that sonication for 14 h helped to cut nanotubes and enhance the concentration of COOH groups from 0.91 mmol/g to 6.4 mmol/g [43].

Nanobiochar morphology

Scanning electron microscopy (SEM) was employed to observe possible morphological changes on nanobiochar samples after acid treatment with a H_2SO_4/HNO_3 mixture. According to the micrographs presented in Figure 6.1.2, no alteration of the structural integrity of nanobiochars are observed. It can be attributed to the mild acidic treatment conditions that caused the functional group modification on the edges of graphitic structure of biochar to lesser extent and therefore the morphology changes are not remarkable. Xia *et al.* reported that no morphological changes was observed after 15 h of treating carbon nanotubes with HNO_3 vapor at 200 °C [44]. Also, Rosca *et al.* reported that no visual changes happened after oxidation of multiwall carbon nanotubes in concentrated nitric acid for 6-9 h. But after 24 h of oxidation, they observed that smaller nanotubes were destroyed [45]. Similarly, Datsyuk *et al.* reported that oxidation of multiwalled carbon nanotubes with nitric acid for 48 h led to shorter tubes with a large population of disordered sites [42].

Immobilization efficiency

Laccase was immobilized onto nanobiochar treated with different acid combinations through direct adsorption in the absence of any coupling reagents. Table 6.1.2 lists the laccase activity, the binding yield, and the effective binding yield of immobilized laccase on treated nanobiochars. As expected, the highest laccase activity (1.48 Unit/g) was obtained for nanobiochar sample treated with H_2SO_4/HNO_3 mixture

compared to untreated nanobiochar (0.44 Unit/g), which is due to the highest concentration of COOH functional groups. The improved adsorption of laccase on acid treated nanobiochars could be due to both functionalization and the removal of impurities on the nanobiochar during the acid treatment [10]. Park *et al.* immobilized laccase from *Trametes versicolor* on raw multiwalled carbon nanotubes and its functionalized form with HNO_3 at 120 °C for 12 h. They reported 0.24 U/mg and 0.32 U/mg laccase loading for multiwalled carbon nanotubes, respectively [8]. Also, Gomez *et al.* functionalized multi walled carbon nanotubes by HNO_3 at 120 °C for 3 h and immobilized β-glucosidase at loading rate 400 U/g [28]. However, they did not evaluate the effect of functionalization, considering the enzyme loading on pristine support.

In Table 6.1.2, the binding yield represents the theoretical activity of the bound laccase to the support divided by the initial laccase activity and the effective binding yield is defined as the apparent activity of the produced biocatalyst divided by the initial laccase activity during immobilization. The theoretical activity of the bound laccase represents the difference between the activities in liquid phase before immobilization and after washing step [14]. According to this table, using hydrochloric acid, sulfuric acid and their combination for functionalization of nanobiochar did not have considerable effect on effective binding yield. It can be attributed to the poor efficiency of these two acids during oxygen atom transferring reaction. It is reported that only nitric acid and its mixture with sulfuric acid has enough oxidizing ability to attack disordered carbon [42, 44]. Due to superior effective binding yield of nanobiochar treated with H_2SO_4/HNO_3 acids, this pre-treatment was employed for laccase immobilization in the rest of the study.

Stability of free and immobilized laccase

Storage stability

Generally, the enzyme in its free form is not stable during storage and gradually loose its activity [46]. Rapid depletion of catalytic activity during storage and problems in recovery after reactions restricted applications of enzymes in free form. Therefore, versatile solid supports were studied for immobilization of enzymes to overcome these obstacles [47]. High storage stability of the immobilized enzyme is one of the important criteria to assess the performance of enzyme, which causes the solid biocatalyst to be more advantageous compared to free enzyme. The free and immobilized laccase were

kept at room temperature for up to 30 days and their activities were determined periodically to evaluate their storage stability. The results are illustrated in Figure 6.1.3 and indicated that the immobilized laccase on functionalized nanobiochar had better storage stability than the free laccase during one month storage. During the first 5 days of storage period, 31% activity reduction was observed for immobilized laccase while free laccase showed 58% reduction. After 30 days, free laccase showed no activity while immobilized laccase still had 15% of its initial activity. Xu *et al.* observed 40% activity reduction for immobilized laccase on polymeric nanofibers after 10 days storage at room temperature while free laccase showed almost no activity after same period [48]. Similar increase in storage stability have been reported by Lloret *et al.* and Gupta *et al* after immobilization of laccase and β-glucosidase on Eupergit and alginate [13, 49]. The deactivation constant (K_d) of free and immobilized laccase, considering a first-order deactivation rate [50], were determined to be 0.12 day^{-1} and 0.07 day^{-1}. In a similar study, Cristovao *et al.* immobilized laccase onto coconut fibers through adsorption process and obtained high value for deactivation constant i.e. 835.2 day^{-1} and 135.3 day^{-1} for free and immobilized laccase. In contrast, Patel *et al.* employed covalent bonding for immobilization of laccase onto SiO_2 nanoparticles and reported K_d to be 1.8 day^{-1} and 0.216 day^{-1} for free and immobilized laccase. [51]. It showed that by functionalization of biochar, comparable results with covalent bonding can be obtained. The observed increase in storage stability can be attributed to the stabilization of the enzyme on support, structural rigidness and protection of enzyme from unfolding and denaturation [52, 53].

pH Stability

The solution pH can significantly affect the activity and structure of enzymes because it determines the ionization state of amino acids [54]. Subsequently, the ionization state of amino acids influences the 3-D shape of the enzyme and may lead to its deactivation [10]. The stability of free and immobilized laccase on functionalized nanobiochar was studied in the solution pH range of 3 to 10 and the results are depicted in Figure 6.1.4. According to this figure, at pH 4, both free and immobilized forms of laccase showed maximum stability. However, free laccase lost 20% to 60% of its activity in acidic and natural pH range (3-7) and almost all its activity at pH >8. On the other hand, immobilized laccase not only showed higher stability in acidic

region (5 to 30 % activity loss in pH 3-6) but also maintained around 36% of its activity at pH >8. The stability of immobilized laccase in basic region may be of interest for treatment of basic wastewater. The enhanced pH stability suggested that nanobiochar may confer protection to the immobilized laccase against pH variation. It can be attributed to the multi-point attachment of protein on the support, which can improve the rigidification of the enzyme and protect it from denaturation [10]. The result is in agreement with other studies which reported the pH effect on activity profile of free and immobilized laccase. Jordaan *et al.* self-immobilized laccase into particles and reported 1.38-fold stability enhancement at pH 4 compared to free laccase [54]. Also, Jiang *et al.* immobilized laccase onto magnetic chitosan microspheres and observed that the immobilized laccase exhibited maximal enzyme stability at pH 6 and retained 70% activity at pH>8 [55]. Lloret *et al.* immobilized laccase on Eupergit and reported pH 3 as the optimum value for storage of free and immobilized laccase. Also, they reported that in pH range of 4-7, immobilized laccase exhibited slightly higher activity (10%) compared to free laccase [13].

Thermostability

The thermal stability of immobilized enzymes is one of the most important factors concerning their application as biocatalyst [56]. The thermostability of the free and immobilized laccase on functionalized nanobiochar was compared over a temperature range of 20 to 70 ºC. As can be seen in Figure 6.1.5, immobilized laccase was generally more stable than free one. Both free and immobilized laccase showed their highest stability at 30 ºC so that immobilized laccase showed 96% of its initial activity while free laccase showed only 66%. Furthermore, between 50-70 ºC, the immobilized laccase maintained 35-42% of its initial activity while free laccase could not retain more than 11% of its initial activity. The results are in agreement with the previous studies, which attributed the high stability towards denaturation by high temperatures to increase enzyme rigidity and decreasing conformational flexibility of the enzyme [13, 57]. For example, Jiang *et al.* determined the activity of free and immobilized laccase after storage at 60 °C and reported that within 210 min, free and immobilized enzymes retained 19.4% and 74% of their initial activity, respectively [55]. Also, the higher thermal stability can be related to the physical bond between the supports and enzyme or a lower restriction of substrate diffusion at higher temperatures [12, 48]. The

enhanced thermal stability of immobilized laccase is advantageous to its industrial application due to the commonly found high temperatures in the industrial processes [58].

Operational stability

To evaluate the industrial benefits of biocatalytic systems, their operational stability is an important factor to determine the processing costs. For this purpose, several consecutive reaction/separation cycles in batch experiments were carried out using a standard substrate (ABTS) to assess the operating stability of the immobilized laccase. The results presented in Figure 6.1.6, showed that the immobilized laccase on functionalized nanobiochar lost 30% and 89% of its activity after 3 and 7 cycles, respectively. The physical adsorption method for immobilization is known for having weak bonds between enzyme and support and therefore the activity loss can be due to the enzyme leaching during washings stages. The observed activity loss in this work was in agreement with other data reported by other researchers. For example, Cristovao *et al.* immobilized laccase on green coconut fibers and reported that their biocatalyst lost 30% of its initial activity after 5 cycles of ABTS oxidation [56]. In a similar work, Sathishkumar *et al.* immobilized laccase on cellulose nanofibers and observed 33% activity loss after 10 ABTS oxidation cycles [12]. Also, Spinelli *et al.* immobilized laccase on Amberlite beads and reported 30% residual activity after 7 cycles. They attributed the decrease in laccase activity to leaching and/or denaturation of the enzyme during the reaction cycles [58].

In order to evaluate the operational stability of the immobilized laccase for industrial applications, the removal of the pharmaceutical compound, CBZ from ultrapure and secondary effluent of wastewater treatment plant was investigated and the results are illustrated in Figure 6.1.7. The removal efficiency gradually decreased from 83 to 6% and 86 to 4% for ultrapure and secondary effluent, respectively after 7 cycles. Ji *et al.* observed same decreasing behavior using immobilized laccase on TiO_2 nanoparticles so that after 5 cycles, CBZ degradation efficiency decreased from 61 % to 15% [5]. Also, Ji *et al.* used immobilized laccase on carbon nanotubes for degradation of CBZ and reported that the removal efficiency decreased from 56% to 21% after 4 consecutive cycles [4]. Since there are biodegradation (laccase) and adsorption sites on nanobiochar (40% as per section "stability of free and immobilized laccase'), two

mechanisms can be proposed for removal of CBZ. In the first mechanism, it is assumed that adsorption on free sites of nanobiochar is the only removal process and there is no degradation. However, according to our previous tests (data not shown), the maximum adsorption capacity towards CBZ was 1.2 µg for 50 mg biocatalyst and therefore no removal should have been observed after the third cycle. In the second mechanism, CBZ was adsorbed onto free sites of biocatalyst and after initiation of biodegradation by laccase, the occupied sites were liberated and sorption-biodegradation cycle could begin anew. To assess the second mechanism, the contributions of degradation and adsorption in the first cycle were determined.

As depicted in Figure 6.1.8, the contribution of biodegradation in both matrices (ultrapure water and secondary effluent) is higher than 45% while adsorption accounted for less than 30% of the total removal. The higher CBZ degradation performance of biocatalyst in secondary effluent in the first three cycles can be attributed to the fact that the presence of ions in effluent (TDS = 414 ppm compared to TDS = 0 ppm for Milli-Q water) is in favor of electron transfer in electrochemical reactions. Also, the reduction of catalytic performance in following cycles in secondary effluent could be due to the occupation of adsorption sites with non-degradable compounds and inactivation of enzyme by unknown compounds in effluent. Therefore, it can be inferred that immobilized laccase actively degraded CBZ and prevented the saturation of adsorption sites on nanobiochar, which is essential for continuous operation. Also, the decreasing trend in removal efficiency (Figure 6.1.7) can be attributed to leaching and denaturation of enzyme as same behavior was observed for ABTS oxidation [58, 59]. Such a degradation system is promising to be implemented as a part of tertiary treatment stage in the wastewater treatment plant to prevent the release of pharmaceutically active compounds into the environment. However, the economy of the whole process should be analyzed and the operational parameters need to be tuned for a broad range of PhACs through further investigation prior to proceeding to scale up level.

Conclusion

Chemical functionalization of the nanobiochar surface was investigated using mineral acids including HCl, H_2SO_4, HNO_3 and their mixtures to form carboxylic functional groups for stronger bonding. The mixture of H_2SO_4 and HNO_3 (50:50, v/v) showed the

best performance on the surface of carbon by formation of 4.7 mmol/g carboxylic groups. The formation of carboxyl and hydroxyl groups was confirmed by Fourier Transform infrared spectroscopy. The storage, pH and thermal stabilities of immobilized laccase on functionalized nanobiochar was improved compared to free laccase. The reusability tests toward oxidation of ABTS showed that the immobilized laccase maintained 70% of the initial activity after 3 cycles. Finally, using immobilized laccase for degradation of carbamazepine exhibited 83% and 86% removal in spiked water and secondary effluent, respectively.

Acknowledgements

References

1.   Flaherty, C.M. and Dodson, S.I., Effects of pharmaceuticals on Daphnia survival, growth, and reproduction. Chemosphere, 2005. 61(2): p. 200-207.

2.   Jos, A., Repetto, G., Rios, J.C., Hazen, M.J., Molero, M.L., del Peso, A., Salguero, M., Fernández-Freire, P., Pérez-Martín, J.M., and Cameán, A., Ecotoxicological evaluation of carbamazepine using six different model systems with eighteen endpoints. Toxicology in Vitro, 2003. 17(5-6): p. 525-532.

3.   Marco-Urrea, E., Radjenović, J., Caminal, G., Petrović, M., Vicent, T., and Barceló, D., Oxidation of atenolol, propranolol, carbamazepine and clofibric acid by a biological Fenton-like system mediated by the white-rot fungus Trametes versicolor. Water Research, 2010. 44(2): p. 521-532.

4.   Ji, C., Hou, J., and Chen, V., Cross-linked carbon nanotubes based biocatalytic membranes for micro-pollutants degradation: Performance, stability, and regeneration. Journal of Membrane Science, 2016.

5.   Ji, C., Hou, J., Wang, K., Zhang, Y., and Chen, V., Biocatalytic degradation of carbamazepine with immobilized laccase-mediator membrane hybrid reactor. Journal of Membrane Science, 2016. 502: p. 11-20.

6.   Taheran, M., Brar, S.K., Verma, M., Surampalli, R.Y., Zhang, T.C., and Valero, J.R., Membrane processes for removal of pharmaceutically active compounds (PhACs) from water and wastewaters. Science of The Total Environment, 2016. 547: p. 60-77.

7.   Bunte, C., Prucker, O., König, T., and Rühe, J., Enzyme Containing Redox Polymer Networks for Biosensors or Biofuel Cells: A Photochemical Approach. Langmuir, 2010. 26(8): p. 6019-6027.

8.   Park, J.H., Xue, H., Jung, J.S., and Ryu, K., Immobilization of laccase on carbon nanomaterials. Korean Journal of Chemical Engineering, 2012. 29(10): p. 1409-1412.

9.   Taheran, M., Naghdi, M., Brar, S.K., Knystautas, E.J., Verma, M., Ramirez, A.A., Surampalli, R.Y., and Valero, J.R., Adsorption study of environmentally relevant concentrations of chlortetracycline on pinewood biochar. Science of The Total Environment, 2016. 571: p. 772-777.

10.   Nguyen, L.N., Hai, F.I., Dosseto, A., Richardson, C., Price, W.E., and Nghiem, L.D., Continuous adsorption and biotransformation of micropollutants by granular activated carbon-bound laccase in a packed-bed enzyme reactor. Bioresource Technology, 2016. 210: p. 108-116.

11.   Ansari, S.A. and Husain, Q., Potential applications of enzymes immobilized on/in nano materials: A review. Biotechnology Advances, 2012. 30(3): p. 512-523.

12.   Sathishkumar, P., Kamala-Kannan, S., Cho, M., Kim, J.S., Hadibarata, T., Salim, M.R., and Oh, B.T., Laccase immobilization on cellulose nanofiber: The catalytic efficiency and recyclic application for simulated dye effluent treatment. Journal of Molecular Catalysis B: Enzymatic, 2014. 100: p. 111-120.

13. Lloret, L., Hollmann, F., Eibes, G., Feijoo, G., Moreira, M.T., and Lema, J.M., Immobilisation of laccase on Eupergit supports and its application for the removal of endocrine disrupting chemicals in a packed-bed reactor. Biodegradation, 2012. 23(3): p. 373-386.

14. Cabana, H., Alexandre, C., Agathos, S.N., and Jones, J.P., Immobilization of laccase from the white rot fungus Coriolopsis polyzona and use of the immobilized biocatalyst for the continuous elimination of endocrine disrupting chemicals. Bioresource Technology, 2009. 100(14): p. 3447-3458.

15. Sohi, S.P., Carbon Storage with Benefits. Science, 2012. 338(6110): p. 1034-1035.

16. Xu, X., Cao, X., and Zhao, L., Comparison of rice husk- and dairy manure-derived biochars for simultaneously removing heavy metals from aqueous solutions: Role of mineral components in biochars. Chemosphere, 2013. 92(8): p. 955-961.

17. Verheijen, F.G.A., Graber, E.R., Ameloot, N., Bastos, A.C., Sohi, S., and Knicker, H., Biochars in soils: new insights and emerging research needs. European Journal of Soil Science, 2014. 65(1): p. 22-27.

18. Tan, X., Liu, Y., Zeng, G., Wang, X., Hu, X., Gu, Y., and Yang, Z., Application of biochar for the removal of pollutants from aqueous solutions. Chemosphere, 2015. 125: p. 70-85.

19. Meyer, S., Glaser, B., and Quicker, P., Technical, Economical, and Climate-Related Aspects of Biochar Production Technologies: A Literature Review. Environmental Science & Technology, 2011. 45(22): p. 9473-9483.

20. Zhang, M., Gao, B., Yao, Y., Xue, Y., and Inyang, M., Synthesis of porous MgO-biochar nanocomposites for removal of phosphate and nitrate from aqueous solutions. Chemical Engineering Journal, 2012. 210: p. 26-32.

21. Yang, Y., Lin, X., Wei, B., Zhao, Y., and Wang, J., Evaluation of adsorption potential of bamboo biochar for metal-complex dye: equilibrium, kinetics and

artificial neural network modeling. International Journal of Environmental Science and Technology, 2014. 11(4): p. 1093-1100.

22.   Zille, A., Tzanov, T., Gübitz, G.M., and Cavaco-Paulo, A., Immobilized laccase for decolourization of Reactive Black 5 dyeing effluent. Biotechnology Letters, 2003. 25(17): p. 1473-1477.

23.   Song, W., Zheng, Z., Tang, W., and Wang, X., A facile approach to covalently functionalized carbon nanotubes with biocompatible polymer. Polymer, 2007. 48(13): p. 3658-3663.

24.   Kitano, H., Tachimoto, K., and Anraku, Y., Functionalization of single-walled carbon nanotube by the covalent modification with polymer chains. Journal of Colloid and Interface Science, 2007. 306(1): p. 28-33.

25.   Men, X.H., Zhang, Z.Z., Song, H.J., Wang, K., and Jiang, W., Functionalization of carbon nanotubes to improve the tribological properties of poly(furfuryl alcohol) composite coatings. Composites Science and Technology, 2008. 68(3-4): p. 1042-1049.

26.   Shen, J., Huang, W., Wu, L., Hu, Y., and Ye, M., Study on amino-functionalized multiwalled carbon nanotubes. Materials Science and Engineering: A, 2007. 464(1-2): p. 151-156.

27.   Tao, Y., Lin, Z.J., Chen, X.-M., Huang, X.L., Oyama, M., Chen, X., and Wang, X.-R., Functionalized multiwall carbon nanotubes combined with bis(2,2′-bipyridine)-5-amino-1,10-phenanthroline ruthenium(II) as an electrochemiluminescence sensor. Sensors and Actuators B: Chemical, 2008. 129(2): p. 758-763.

28.   Gomez, J., Romero, M., and Fernandez, T., Immobilization of β-Glucosidase on carbon nanotubes. Catalysis Letters, 2005. 101(3-4): p. 275-278.

29.   Hu, H., Bhowmik, P., Zhao, B., Hamon, M.A., Itkis, M.E., and Haddon, R.C., Determination of the acidic sites of purified single-walled carbon nanotubes by acid-base titration. Chemical Physics Letters, 2001. 345(1-2): p. 25-28.

30. Wijekoon, K.C., Fujioka, T., McDonald, J.A., Khan, S.J., Hai, F.I., Price, W.E., and Nghiem, L.D., Removal of N-nitrosamines by an aerobic membrane bioreactor. Bioresource Technology, 2013. 141: p. 41-45.

31. Faramarzi, M.A. and Forootanfar, H., Biosynthesis and characterization of gold nanoparticles produced by laccase from Paraconiothyrium variabile. Colloids and Surfaces B: Biointerfaces, 2011. 87(1): p. 23-27.

32. Mohapatra, D.P., Brar, S.K., Tyagi, R.D., Picard, P., and Surampalli, R.Y., Carbamazepine in municipal wastewater and wastewater sludge: Ultrafast quantification by laser diode thermal desorption-atmospheric pressure chemical ionization coupled with tandem mass spectrometry. Talanta, 2012. 99: p. 247-255.

33. Osorio, A.G., Silveira, I.C.L., Bueno, V.L., and Bergmann, C.P., $H_2SO_4/HNO_3/HCl$-Functionalization and its effect on dispersion of carbon nanotubes in aqueous media. Applied Surface Science, 2008. 255(5, Part 1): p. 2485-2489.

34. Atieh, M.A., Bakather, O.Y., Al-Tawbini, B., Bukhari, A.A., Abuilaiwi, F.A., and Fettouhi, M.B., Effect of carboxylic functional group functionalized on carbon nanotubes surface on the removal of lead from water. Bioinorganic chemistry and applications, 2011. 2010.

35. Olah, G.A., Kuhn, S.J., Flood, S.H., and Evans, J.C., Aromatic Substitution. XIII.1a Comparison of Nitric Acid and Mixed Acid Nitration of Alkylbenzenes and Benzene with Nitronium Salt Nitrations. Journal of the American Chemical Society, 1962. 84(19): p. 3687-3693.

36. Badgujar, K.C., Dhake, K.P., and Bhanage, B.M., Immobilization of Candida cylindracea lipase on poly lactic acid, polyvinyl alcohol and chitosan based ternary blend film: Characterization, activity, stability and its application for N-acylation reactions. Process Biochemistry, 2013. 48(9): p. 1335-1347.

37. Pirozzi, D., Fanelli, E., Aronne, A., Pernice, P., and Mingione, A., Lipase entrapment in a zirconia matrix: Sol–gel synthesis and catalytic properties. Journal of Molecular Catalysis B: Enzymatic, 2009. 59(1-3): p. 116-120.

38. He, J., Song, Z., Ma, H., Yang, L., and Guo, C., Formation of a mesoporous bioreactor based on SBA-15 and porcine pancreatic lipase by chemical modification following the uptake of enzymes. Journal of Materials Chemistry, 2006. 16(44): p. 4307-4315.

39. Yi, Y., Neufeld, R., and Kermasha, S., Controlling sol-gel properties enhancing entrapped membrane protein activity through doping additives. Journal of Sol-Gel Science and Technology, 2007. 43(2): p. 161-170.

40. Gao, Y. and Kyratzis, I., Covalent Immobilization of Proteins on Carbon Nanotubes Using the Cross-Linker 1-Ethyl-3-(3-dimethylaminopropyl)carbodiimide-a Critical Assessment. Bioconjugate Chemistry, 2008. 19(10): p. 1945-1950.

41. Jiang, K., Schadler, L.S., Siegel, R.W., Zhang, X., Zhang, H., and Terrones, M., Protein immobilization on carbon nanotubes via a two-step process of diimide-activated amidation. The Royal Society of Chemistry, 2004. 14: p. 37-39.

42. Datsyuk, V., Kalyva, M., Papagelis, K., Parthenios, J., Tasis, D., Siokou, A., Kallitsis, I., and Galiotis, C., Chemical oxidation of multiwalled carbon nanotubes. Carbon, 2008. 46(6): p. 833-840.

43. Marshall, M.W., Popa-Nita, S., and Shapter, J.G., Measurement of functionalised carbon nanotube carboxylic acid groups using a simple chemical process. Carbon, 2006. 44(7): p. 1137-1141.

44. Xia, W., Jin, C., Kundu, S., and Muhler, M., A highly efficient gas-phase route for the oxygen functionalization of carbon nanotubes based on nitric acid vapor. Carbon, 2009. 47(3): p. 919-922.

45. Rosca, I.D., Watari, F., Uo, M., and Akasaka, T., Oxidation of multiwalled carbon nanotubes by nitric acid. Carbon, 2005. 43(15): p. 3124-3131.

46.   De Queiroz, A.A., Passos, E.D., De Brito Alves, S., Silva, G.S., Higa, O.Z., and Vítolo, M., Alginate-poly (vinyl alcohol) core–shell microspheres for lipase immobilization. Journal of Applied Polymer Science, 2006. 102(2): p. 1553-1560.

47.   Guzik, U., Hupert-Kocurek, K., and Wojcieszyńska, D., Immobilization as a strategy for improving enzyme properties-application to oxidoreductases. Molecules, 2014. 19(7): p. 8995-9018.

48.   Xu, R., Zhou, Q., Li, F., and Zhang, B., Laccase immobilization on chitosan/poly(vinyl alcohol) composite nanofibrous membranes for 2,4-dichlorophenol removal. Chemical Engineering Journal, 2013. 222: p. 321-329.

49.   Gupta, A., Kumar, V., Dubey, A., and Verma, A., Kinetic characterization and effect of immobilized thermostable β-glucosidase in alginate gel beads on sugarcane juice. ISRN biochemistry, 2014. 2014.

50.   Bassetti, F.J., Bergamasco, R., Moraes, F.F., and Zanin, G.M., Thermal stability and deactivation energy of free and immobilized invertase. Brazilian Journal of Chemical Engineering, 2000. 17: p. 867-872.

51.   Patel, S., Kalia, V.C., Choi, J.H., Haw, J.R., Kim, I.W., and Lee, J.K., Immobilization of laccase on SiO2 nanocarriers improves its stability and reusability. J Microbiol Biotechnol, 2014. 24(5): p. 639-47.

52.   Bhushan, B., Pal, A., and Jain, V., Improved enzyme catalytic characteristics upon glutaraldehyde cross-linking of alginate entrapped xylanase Isolated from Aspergillus flavus MTCC 9390. Enzyme research, 2015. 2015.

53.   Li, J., Jiang, Z., Wu, H., Long, L., Jiang, Y., and Zhang, L., Improving the recycling and storage stability of enzyme by encapsulation in mesoporous CaCO3–alginate composite gel. Composites Science and Technology, 2009. 69(3-4): p. 539-544.

54.   Jordaan, J., Mathye, S., Simpson, C., and Brady, D., Improved chemical and physical stability of laccase after spherezyme immobilisation. Enzyme and Microbial Technology, 2009. 45(6-7): p. 432-435.

55.   Jiang, D.S., Long, S.Y., Huang, J., Xiao, H.Y., and Zhou, J.Y., Immobilization of Pycnoporus sanguineus laccase on magnetic chitosan microspheres. Biochemical Engineering Journal, 2005. 25(1): p. 15-23.

56.   Cristóvão, R.O., Tavares, A.P., Brígida, A.I., Loureiro, J.M., Boaventura, R.A., Macedo, E.A., and Coelho, M.A.Z., Immobilization of commercial laccase onto green coconut fiber by adsorption and its application for reactive textile dyes degradation. Journal of Molecular Catalysis B: Enzymatic, 2011. 72(1): p. 6-12.

57.   Hu, X., Zhao, X., and Hwang, H.M., Comparative study of immobilized Trametes versicolor laccase on nanoparticles and kaolinite. Chemosphere, 2007. 66(9): p. 1618-1626.

58.   Spinelli, D., Fatarella, E., Di Michele, A., and Pogni, R., Immobilization of fungal (Trametes versicolor) laccase onto Amberlite IR-120 H beads: Optimization and characterization. Process Biochemistry, 2013. 48(2): p. 218-223.

59.   Lloret, L., Eibes, G., Feijoo, G., Moreira, M.T., Lema, J.M., and Hollmann, F., Immobilization of laccase by encapsulation in a sol-gel matrix and its characterization and use for the removal of estrogens. Biotechnology Progress, 2011. 27(6): p. 1570-1579.

Table 6.1.1 Characteristics of the secondary effluent used in experiments

Parameters	Value (Wastewater)
Chemical oxygen demand (COD, mg/L)	68±1.5
Biochemical oxygen demand (5 days) (BOD$_5$, mg/L)	23±1.2
Suspended solids (SS, mg/L)	18.6±0.5
Volatile suspended solids (VSS, mg/L)	16±0.0
Ammonia (NH$_3$-NH$_4$, mg/L)	12.3±0.5
Total Kjeldahl nitrogen (TKN, mg/L)	15.8±0.3
Nitrate-nitrite (NO$_2$-NO$_3$, mg/L)	1.16±0.3
Total solids (TS, mg/L)	510±12
Total dissolved solids (TDS, mg/L)	414±1
pH	7.1±0.1
CBZ (ng/mL)	0.283±0.01

Table 6.1.2 Immobilization yields of laccase on nanobiochars prepared using different acid treatments

Acid/ Combinations	Laccase activity (U/g)[*]	Binding yield (%)	Effective binding yield (%)
HNO_3	0.52	40	5
HCl	0.44	13	4
H_2SO_4	0.43	14	4
H_2SO_4/HCl	0.42	35	4
H_2SO_4/HNO_3	1.48	26	15
HNO_3/HCl	0.56	41	6
H_2SO_4/HCl/HNO_3	0.55	29	5
No-treatment	0.44	18	4

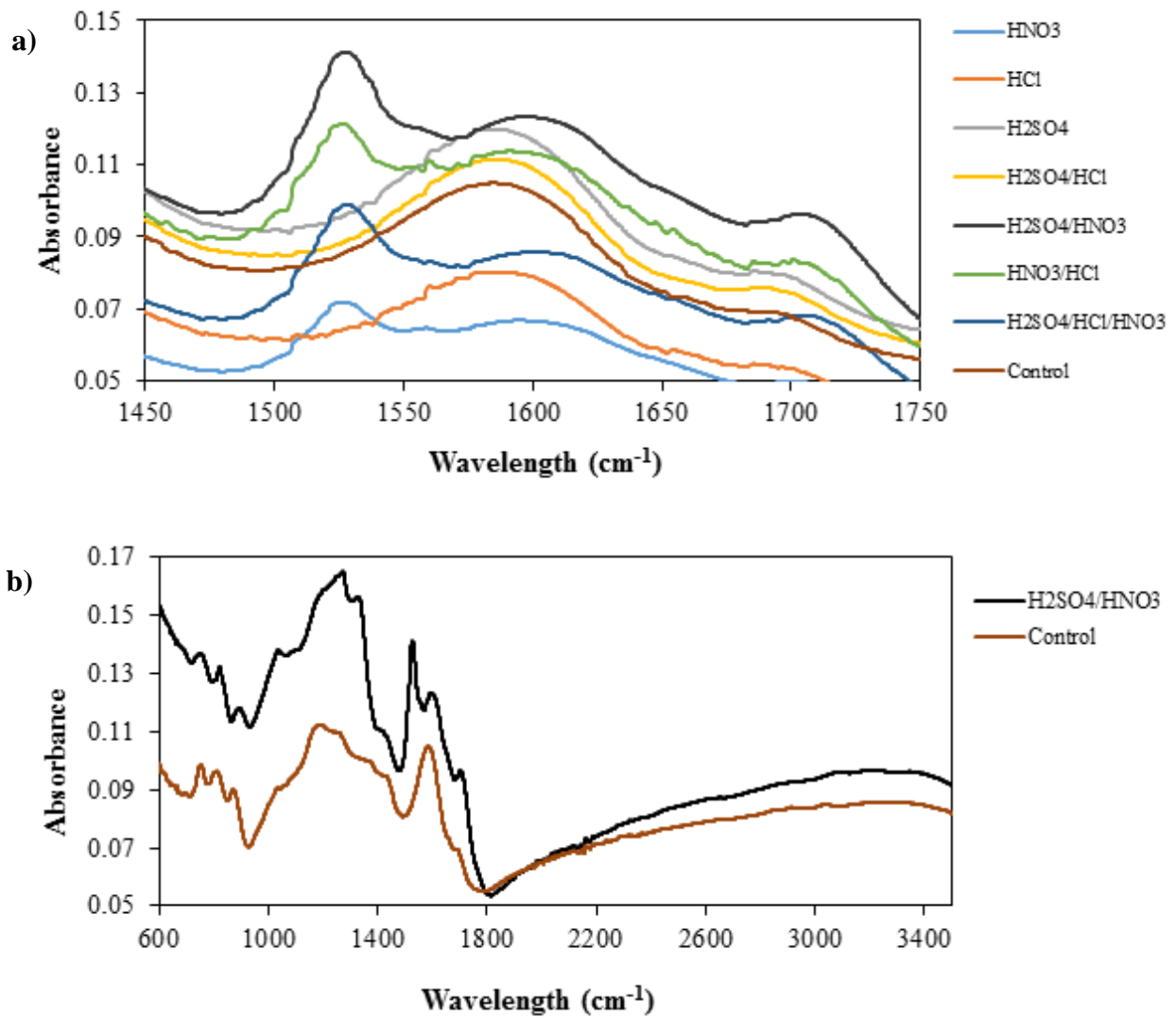[*]: the activity of immobilized laccase on nanobiochars

Figure 6.1.1 FT-IR spectra of nanobiochar treated with: a) mineral acids and their combinations and; b) H$_2$SO$_4$/HNO$_3$ versus control sample
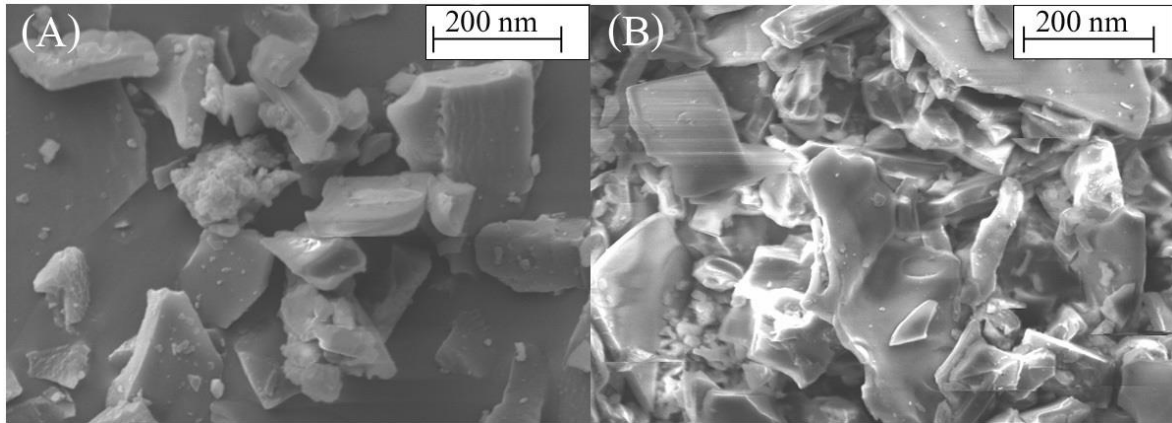
Figure 6.1.2 SEM images of nanobiochars treated with: (a) H$_2$SO$_4$/HNO$_3$ for 24 h at 25 °C and; (b) as-produced nanobiochars
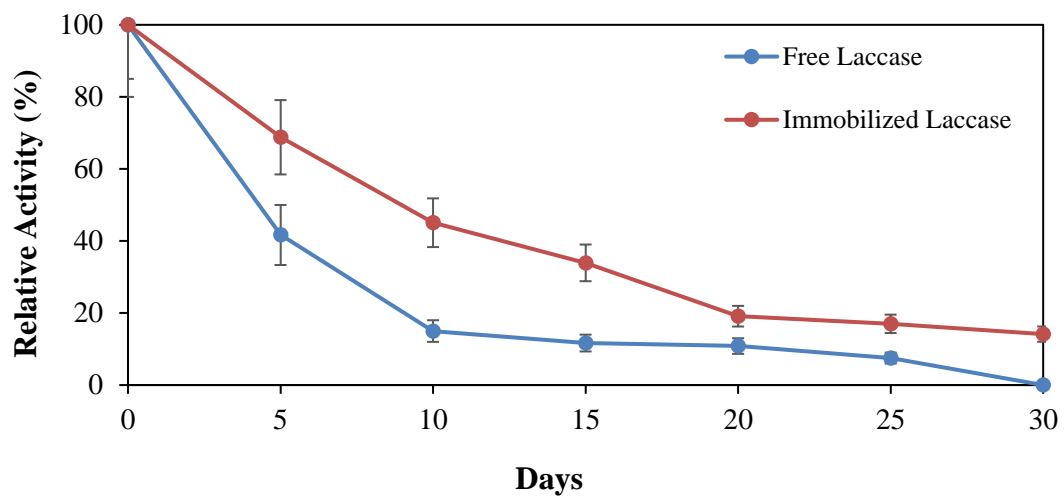
Figure 6.1.3 Storage stability of free and immobilized laccase on functionalized nanobiochar
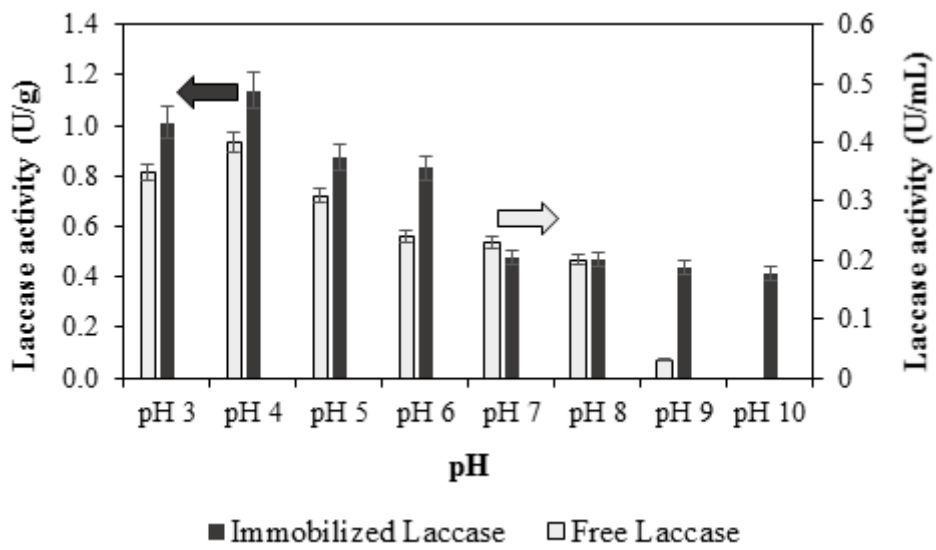
Figure 6.1.4 Effect of pH of storage solution on the activity of: free laccase (with 0.5 U/mL initial activity) and; immobilized laccase on functionalized nanobiochars (with 1.2 U/g initial activity)
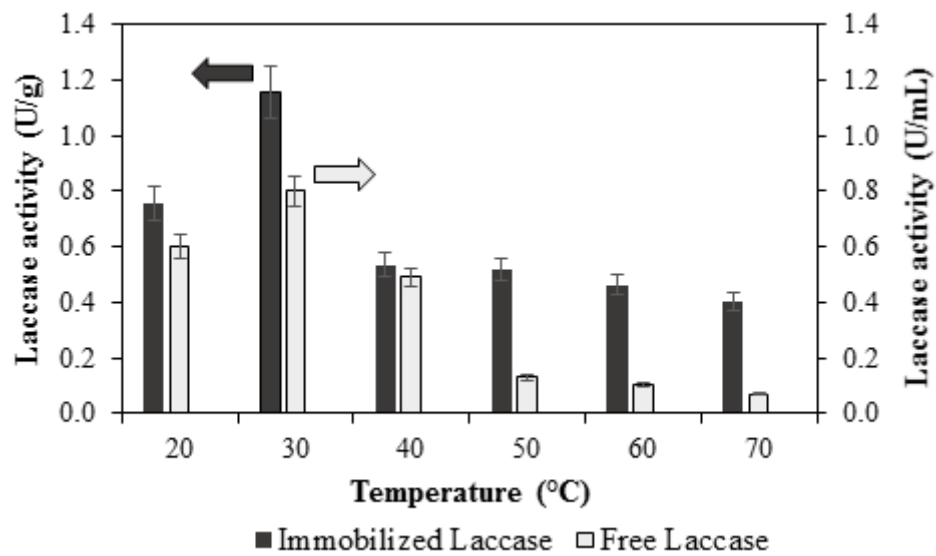
Figure 6.1.5 Effect of temperature on the stability of: free laccase (with 1.2 U/mL initial activity) and; immobilized laccase on functionalized nanobiochar (with 1.2 U/g initial activity)
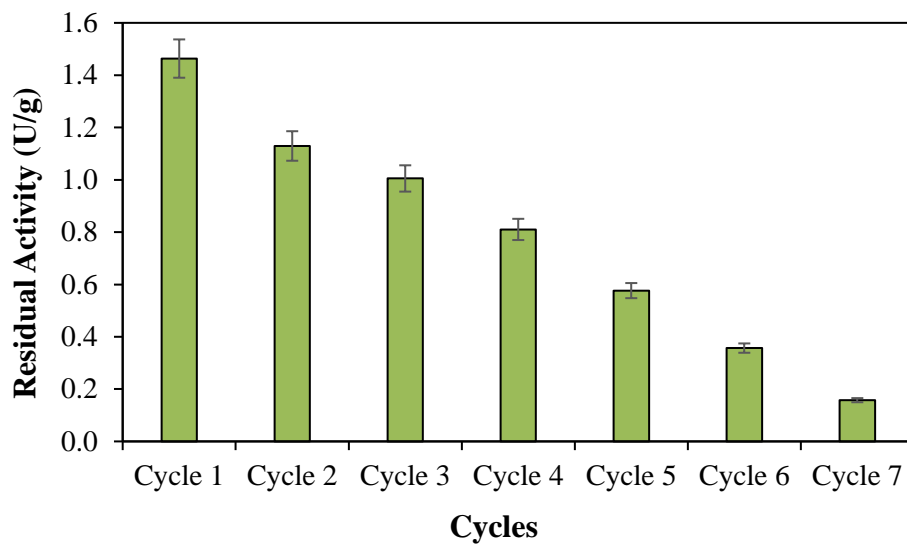
Figure 6.1.6 Reusability of the immobilized laccase on functionalized nanobiochar towards oxidation of ABTS

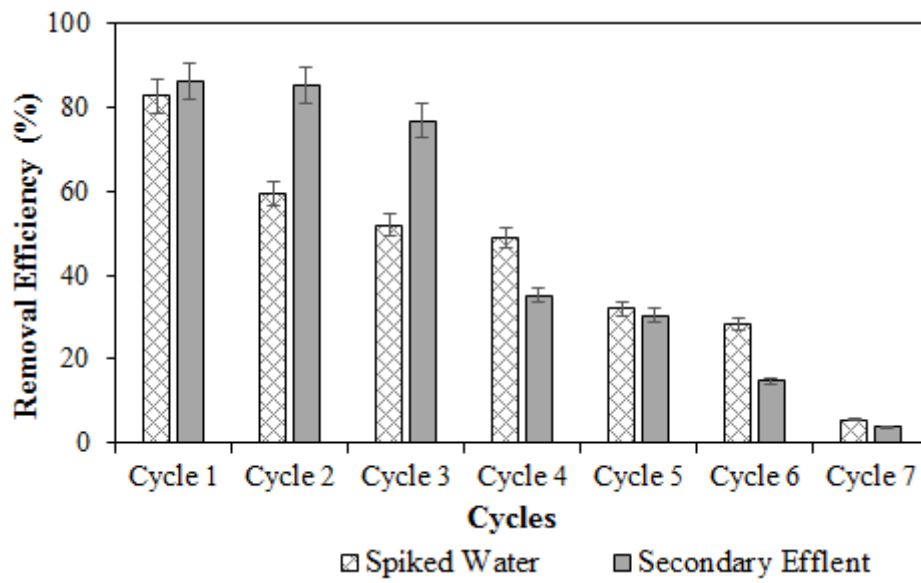**Figure 6.1.7 Removal of carbamazepine during reuse of the immobilized laccase on functionalized nanobiochar**
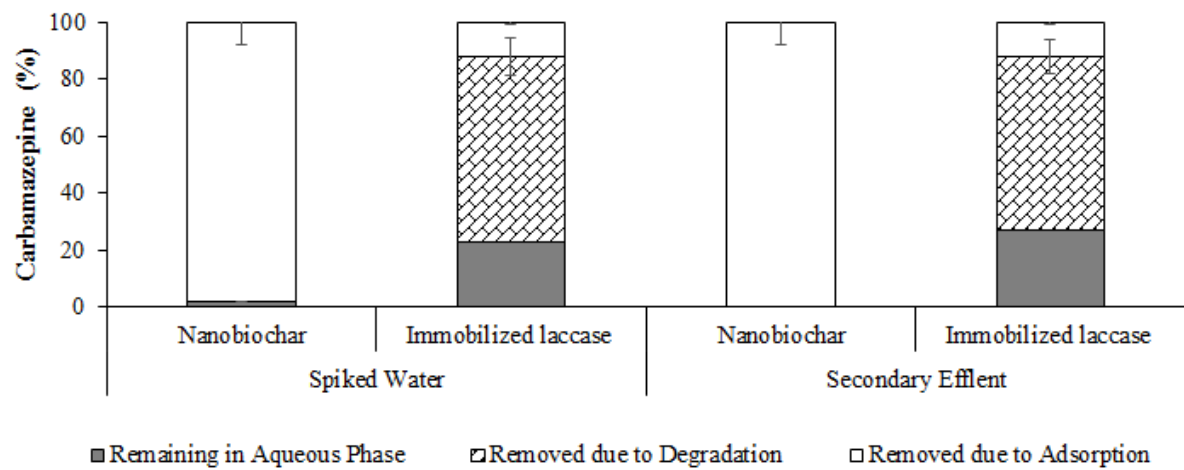
Figure 6.1.8 Overall fate of carbamazepine following treatment (24 h) via nanobiochar and immobilized laccase on functionalized nanobiochar

Part 2

Biodegradation of Carbamazepine by Covalently Immobilized Enzyme Using Nanobiochar and Crude Laccase in Batch and Continuous Mode

Mitra Naghdi[1], Alexandre Mateos[2], Mehrdad Taheran[1], Satinder K. Brar[1*], M. Verma[3], R.Y. Surampalli[4]

[1]INRS-ETE, Université du Québec, 490, Rue de la Couronne, Québec, Canada G1K 9A9

[2]Université Clermont Auvergne, 63000 Clermont Ferrand, France

[3]IRDA, 2700 Rue Einstein, Québec, QC G1P 3W8, Canada

[4]Department of Civil Engineering, University of Nebraska-Lincoln, N104 SEC PO Box 886105, Lincoln, NE 68588-6105, US

(*Phone: 1 418 654 3116; Fax: 1 418 654 2600; E-mail: satinder.brar@ete.inrs.ca)

Résumé

Le traitement enzymatique peut efficacement dégrader les micropolluants dans des milieux aqueux. Cependant, l'enzyme doit être immobilisée sur un support approprié afin de faciliter sa séparation des milieux de réaction et de réduire le coût d'opération. Ce travail a présenté une technique chimique pour l'immobilisation directe des extraits de laccase brute (de Trametes versicolor) sur la surface fonctionnalisée du nanobiochar. La capacité de dégradation des micropolluants par des nanoparticules biocatalytiques a été démontrée avec un micropolluant fréquemment trouvé dans l'environnement, à savoir la carbamazépine (CBZ). L'effet de différentes conditions opérationnelles (pH, température, concentration de CBZ et temps de contact) sur l'élimination de la CBZ par la laccase immobilisée a été étudié en mode discontinu. L'élimination la plus élevée a été obtenue à pH 4, 20 °C, 5 µg/L de concentration de la CBZ et 24 h de temps de contact. La contribution de l'adsorption et de la dégradation à l'efficacité d'élimination pour la CBZ dans l'eau pure était d'environ 33% et 63%, respectivement, après 24 h de réaction. L'efficacité du nanobiocatalyseur en mode continu a été étudiée dans une colonne garnie à lit fixe sous-alimentation continue d'une solution enrichie. Plus de 45% et 60% d'élimination de la CBZ ont été obtenus le premier jour dans l'eau pure et l'effluent secondaire, respectivement. Cependant, les efficacités d'élimination pour les deux échantillons sont tombées soudainement à 25% et 45%, respectivement au deuxième jour, peut-être en raison de la désactivation de l'enzyme dans le réacteur. L'immobilisation efficace de la laccase sur le nanobiochar fonctionnalisé peut ainsi constituer un candidat prometteur pour un traitement rentable des eaux usées polluées par des micropolluants.

Mots clés

Laccase brute, Immobilisation enzymatique, Nanobiochar, Dégradation des micropolluants

Abstract

Enzymatic treatment can efficiently degrade micropollutants in aqueous media. However, enzyme need to be immobilized on proper support in order to facilitate its separation from reaction media and reducing the cost of operation. This work introduced a chemical technique for direct immobilization of the crude laccase extracts (from *Trametes versicolor*) onto the functionalized nanobiochar surface. The micropollutant degradation capability of the biocatalytic nanoparticles was demonstrated with a frequently found micropollutant in the environment, namely, carbamazepine (CBZ). The effect of different operational conditions (pH, temperature, CBZ concentration and contact time) on removal of CBZ by immobilized laccase was investigated in batch mode. The highest removal was achieved in pH 4, 20 °C, 5 µg/L of CBZ concentration and 24 h of contact time. The contribution of adsorption and degradation to removal efficiency for CBZ in pure water was around 33% and 63%, respectively after 24 h of reaction. The efficiency of the nanobiocatalyst in continuous mode was investigated in a fixed-bed packed column under continuous feeding of spiked solution. More than 45% and 60% removal of CBZ was obtained on the first day in pure water and secondary effluent, respectively. However, the removal efficiencies for both samples suddenly dropped to 25% and 45%, respectively by second day, possibly due to the deactivation of enzyme in the reactor. The efficient laccase immobilization on functionalized nanobiochar can thus provide a promising candidate for cost-effective treatment of wastewater polluted with micropollutants.

Introduction

Currently, pharmaceutically active compounds (PhACs) are detected in aquatic environments [1]. As the PhACs are designed to generate a biological effect, the discharge of these compounds may impose significant impacts on receiving organisms [2]. Carbamazepine (CBZ) is a widely used antiepileptic drug frequently detected in the wastewater effluents. Approximately one-third of the administered CBZ is excreted in its original form [3, 4]. The CBZ concentration in the environment reaches up to 647 ng/L in surface water, 30 ng/L for drinking water and up to 610 ng/L for groundwater [5]. Considering wastewater as the important point source of CBZ, collecting and treating the wastewater in treatment plants can manage the issue. However, previous studies have shown that the current technologies of wastewater treatment plants failed to remove PhACs [4, 6]. Jos *et al.* found that CBZ can have chronic and synergistic effects with other chemicals [7]. Based on European classification and labeling of chemicals (92/32/EEC), CBZ is harmful to aquatic organisms and may pose long-term effects in aquatic environment [1]. Therefore, developing novel technologies to efficiently remove the PhACs, such as CBZ from wastewater effluents is important.

Laccases (EC 1.10.3.2) are multicopper oxidases enzymes that are known for catalyzing the oxidation of different organic compounds by reduction of oxygen to water without requiring co-substrate or any cofactor [8, 9]. Laccases have been studied for various applications, such as the discoloration of dyes, treatment of industrial effluents and contaminated soils, ethanol production, wine clarification and production of biosensors [10]. The application of enzymes is of interest in industrial processes if the enzyme can be immobilized on an inert support to facilitate its separation from the reaction medium and reducing the cost of the process by enhancing its stability [8, 11, 12]. One of the important challenges of this area is an exploration of new supports with appropriate structures and compositions to improve the catalytic efficiency [9]. Recently, a series of nanomaterials have been developed immobilizing the enzymes due to their large surface to volume ratio [11, 13, 14].

Carbonization of biomass and production of biochar is an approach to avoid the negative impacts of global warming [15]. The unique properties of biochar, such as large specific surface area, porous structure, and functional groups make it a proper adsorbent removal of pollutants from aqueous solutions [16]. Furthermore, the choice of using nanobiochar (biochar with a particle size less than100 nm) can offer higher

surface area, which is beneficial to the overall adsorption efficiency [17]. Biochar is a promising candidate for use in the immobilization of enzymes and can be a potential strategy for reducing the costs [18]. For instance, Cea *et al.* showed that biochar from oats husk is an excellent support for immobilization of lipase [19]. Similarly Bezerra *et al.* used green coconut husk as solid support for immobilization of laccase and reported higher thermal stability for immobilized laccase compared to free laccase [8]. In this study, a novel biocatalyst was developed based on nanobiochar for remediation of the released effluents of wastewater treatment plants (WWTPs) to the environment. For this purpose, laccase was covalently bonded on functionalized nanobiochar (FNBC) to prepare nanobiocatalyst. Later, the performance of the prepared nanobiocatalyst for removal of CBZ was investigated and the effects of different parameters such as pH, temperature, CBZ concentration and contact time on its removal were studied. Moreover, the reusability of the immobilized laccase to degrade CBZ in both Milli-Q water and secondary effluent of WWTP were evaluated. In the last step, the removal of CBZ in a continuous mode was investigated.

Material and methods

Material

Pinewood biochar was donated by Pyrovac Inc. (Quebec, Canada). This biochar consists of pine white wood (80% v/v, size: 3 mm) and spruce and fir (20% v/v). 2, 2'-azino-bis (3-ethylbenzothiazoline-6-sulphonic acid) (ABTS), 2-(N-Morpholino) ethanesulfonic acid (MES), N-hydroxysuccinimide (NHS), N-ethyl-N'-(3-dimethylaminopropyl) carbodiimide hydrochloride (EDAC) were purchased from Sigma-Aldrich (Oakville, Canada). Tween-80, sulfuric acid and nitric acid were purchased from Fisher Scientific (Ottawa, Canada). Apple pomace, provided by Vergers Paul Jodoin Inc., (Quebec, Canada), was utilized as a substrate for laccase production. The secondary effluent sample was collected from Quebec wastewater treatment plant (Quebec, Canada). The characteristics of the secondary effluent were listed somewhere else [17]. Ultrapure water was prepared in the laboratory using Milli-Q/Milli-RO Millipore system (Massachusetts, USA).

Production and functionalization of nanobiochar

Nanobiochar with the average size of 60±20 nm and specific surface area of 47.3 m^2/g was produced using a ball mill (PM100; Retsch Corporation) at ambient conditions [20]. Briefly, 10 g of pinewood biochar was kept at -80 °C for 24 h and then ball milling was performed at 575 rpm for 100 min using stainless steel balls of 2.4 mm in diameter (total weight of 45 g). The physicochemical properties of produced nanobiochar were discussed elsewhere [20]. For functionalization of nanobiochar through acidic treatment, the procedure of Naghdi *et al.* was used with some modification [17]. Briefly, 4 g nanobiochar was dispersed in 500 mL of 5 M H_2SO_4/HNO_3 (3:1 v/v) mixtures and kept at room temperature and 200 rpm for 48 h. Subsequently, the suspension was washed repeatedly with milli-Q water to remove acids and until it reached pH 7. The treated nanobiochar was then lyophilized (at 5 Pa and -55 °C) and kept at -20 °C before performing the experiments.

Production and extraction of laccase

Forty grams of apple pomace (pH 4.5 and 78% (w/w) moisture) was mixed with Tween-80 (0.5% v/w) in a 500 mL flask and autoclaved at 121±1 °C for 20 min. Then, the sterilized substrate was inoculated with *Trametes versicolor* (ATCC 20869) and incubated at 30±1 °C for 14 days. For extraction of the enzyme, one gram of fermented sample was mixed with 20 mL of 50 mM sodium phosphate buffer (pH 6.5). The mixture was homogenized on incubator shaker at 150 rpm and 35±1 °C for 1 h and then centrifuged at 7000 × g for 30 min. The collected supernatant was passed through 30 kDa membrane to concentrate the enzyme and partially remove the impurities. The sample was then analyzed for the enzyme activity and kept at -20 °C, prior to use.

Covalent immobilization of laccase

Laccase was covalently attached to FNBC through a two-step process of diimide-activated amidation. In the first step, 5 g of FNBC was dispersed in 1 L of MES buffer (50 mM, pH 6.2) and then an equal volume of 400 mM NHS (prepared in same MES buffer) was added to the solution. The mixture was sonicated for 30 min in an ultrasonication bath and then 1.4 L of 8.2 mM of EDAC (prepared in same MES buffer) was added to initiate the coupling of NHS to the carboxylic groups. After sonication for 2 h, the mixture was centrifuged and rinsed thoroughly with MES buffer to remove excess EDC and NHS. In the second step, the activated FNBC was transferred to a

solution of laccase (15 mg/mL in 10 mM phosphate buffer, pH 8.0) and sonicated for 1 min to re-disperse the FNBC. The mixture was then shaken on an orbital shaker at 200 rpm and room temperature for 3 h. The FNBC-laccase suspension was centrifuged and washed three times with ultrapure water to remove excess enzyme and dried at -55 °C, 5 Pa, for 48 h using freeze dryer. A control experiment was performed using an identical procedure except using EDC and NHS. The activity of immobilized laccase on FNBC was 5 U/g.

Removal of CBZ

Effect of pH

The effect of pH solution on the removal of CBZ by covalently immobilized laccase was investigated by incubating solutions containing CBZ (20 µg/L) and immobilized laccase (5 mg/mL) in buffer solutions over a pH range of 3 to 10 on a rotary shaker (200 rpm) at 20 ºC for 24 h. After incubation, samples were centrifuged for 20 min at 11, 000 ×g and then the residual laccase activity and removal of CBZ were measured.

Effect of temperature

The effect of the temperature on the removal of CBZ was studied by incubating solutions containing CBZ (20 µg/L) and immobilized laccase (5 mg/mL) at different temperature (5, 10, 15, 20, 25, 30, 35, 40 and 50 °C) on a rotary shaker (200 rpm) at pH 7 for 24 h. Then samples were centrifuged for 20 min at 11, 000 ×g and then the residual laccase activity and removal of CBZ were measured.

Effect of CBZ Concentration

Removal of CBZ was determined studied by incubating solutions containing immobilized laccase (5 mg/mL) and different concentrations of CBZ (1, 3, 5, 8, 12, 16, 20 and 50 µg/L) on a rotary shaker (200 rpm) at pH 7 and 20 ºC. After 24 h of incubation, samples were centrifuged for 20 min at 11, 000 ×g and then the residual laccase activity and removal of CBZ were determined.

Effect of Contact time

Effect of different contact time (1, 2, 3, 4, 5, 6, 9, 12, 15, 18, 21, 24, 48 and 72 hours) on removal of CBZ was studied by incubating solutions containing immobilized laccase (5 mg/mL) and CBZ (20 µg/L) on a rotary shaker (200 rpm) at pH 7 and 20 ºC. After desired time of incubation, the samples were centrifuged for 20 min at 11, 000 ×g and then the residual laccase activity and removal of CBZ were determined.

Reusability

The reusability of immobilized laccase on FNBC was tested in terms of CBZ degradation, during repeated cycles in both Milli-Q water and secondary effluent of municipal wastewater treatment plant. The tests were performed in optimum conditions as obtained in section "removal of CBZ" (pH 4, 20 µg/L of CBZ, 20 °C and 24 h). The reaction mixture contained 50 mg immobilized laccase on FNBC and 20 mL of CBZ solution (20 µg/L) in a 50 mL flask. The reaction mixture was incubated in a rotary shaker at 200 rpm and 20 ºC for 24 h. CBZ removal efficiency was determined based on its initial and final aqueous phase concentrations. After each run, the supernatant was decanted (10 min and 11, 000 ×g) and then fresh CBZ solution was added to start the next cycle.

Continuous removal of CBZ

Two Econo-Column® glass columns (Bio-Rad Company, Philadelphia, USA) were filled with 1.5 g of nanobiochar and immobilized laccase onto FNBC. The columns had an internal diameter of 2.5 cm and a length of 10 cm. The remaining volume of the columns were filled by glass beads and the bottom and top ends of the column were plugged with glass fibers to prevent any loss of samples. The feed solution was pumped through the column in downward mode at a flow rate of 50 mL/min using a syringe pump (New Era Pump Systems, NE-1000, USA). The feed solution containing 20 µg/L of CBZ was prepared in both Milli-Q water and secondary effluent (in separate experiments). The columns were operated for 48 h at room temperature and the concentration of CBZ in feed and effluent were determined at different time intervals.

Analytical methods

Enzyme assay

Oxidation of ABTS (as a substrate of laccase) was used to determine the laccase activity. The reaction mixture consisted of 500 µL ABTS (1.5 mM) dissolved in 2.450 mL of 50 mM citrate-phosphate buffer (pH 3.5) and 50 µL of enzyme sample. ABTS oxidation was quantified by recording the increase in absorbance at 420 nm (ε_{420} = 36,000 M^{-1} cm^{-1}) [21] using a Cary 50 UV-visible spectrophotometer (Varian, Australia). One unit of laccase activity was considered as the amount of required enzyme to transform one µmol of product per min under the assay conditions. For the

assay of the immobilized laccase on FNBC, 10 mg of sample was used along with one mL ABTS. After 10 min of incubation at 45 °C, the sample was centrifuged for 10 min at 11, 000 ×g and the amount of transformed ABTS was measured at 420 nm in simple read mode. The final activity of immobilized laccase on FNBC was expressed in U/g nanobiochar.

CBZ Quantification

The concentration of CBZ was determined using a Laser Diode Thermal Desorption (LDTD) (Phytronix technologies, Canada) coupled with a LCQ Duo ion trap tandem mass spectrometer (Thermo Finnigan, USA). The daughter ions identified for CBZ in mass spectrometer were 194 and 192 Da. A calibration curve with R^2 no less than 0.99 was developed with six standard solutions containing different concentrations of CBZ. The details of quantification process were described elsewhere [22]. All the experiments were performed in triplicates and the average results were reported.

Surface area measurements

The specific surface area of the samples was determined using Brunauer-Emmett-Teller (BET) theory from the nitrogen adsorption isotherms recorded at 77 K (Autsorb-1, Quantachrome Instruments) at the relative pressure range from 0.05 to 1. In brief, the sample was first heated to 60±1 °C and degassed by applying vacuum for 12 h. Then, the amount of adsorbed nitrogen gas onto the surface of the sample was measured at different relative pressure. The amount of the required nitrogen gas for monolayer coverage, the accessible internal pore and external surface area were determined using the BET equation. Finally, considering the cross-sectional area of nitrogen molecule as 0.162 nm^2, the specific surface area was estimated.

Results and discussion

Characterization of covalently immobilized laccase onto FNBC

The laccase was covalently attached onto FNBC in the presence of coupling reagents (EDC and NHS) through a two-step process of diimide-activated amidation under ambient conditions. This two-step process helps avoid the intermolecular attachment of proteins, and guarantees the uniform immobilization of proteins on supports [23]. It also provides stable enzyme attachment and decreases the conformational changes or enzyme desorption when exposed to some medium variations [11]. The maximum

enzymatic activity of immobilized laccase onto FNBC with and without crosslinkers was calculated to be 5 Units/g and 1 Units/g, respectively.

Chemical modifications of the support can increase the efficiency of immobilization by creating reactive groups on the surface [24]. A popular method for carbonaceous materials is reacting with a highly oxidizing mixture of sulfuric acid and nitric acid (typically 3:1 v/v). This treatment leads to creation of carboxylic groups (COOH) at the surface and defect sites [25]. Prior to laccase immobilization, the FNBC was subjected to pre-treatment by acid washing. The activity of covalently immobilized laccase onto acid-washed nanobiochar was 16 times higher than immobilized laccase onto untreated nanobiochar. In this work, the BET analysis showed that the untreated nanobiochar has pore volume of 38.47 mm^3/g and surface area of 47.25 m^2/g. Also, the pore volumes of acid treated nanobiochar and covalently immobilized laccase onto FNBC were 40.77 mm^3/g and 21.20 mm^3/g and their surface area were 52.11 m^2/g and 24.49 m^2/g, respectively. These results indicated that acidic treatment of nanobiochar increased accessible pore volume and surface area by 6%, and 10%, respectively. In a similar study, Nguyen *et al.* treated granular activated carbon with hydrochloric acid and reported 8% of increase in accessible surface area [26]. The carboxylic groups on the nanobiochar act as anchoring points for the covalent attachment of enzyme using the cross-linker. Many researchers preferred this method due to its effect on efficiency of immobilization [23, 27-29]. During immobilization, laccase macromolecules occupied 53% of the surface area of FNBC and reduced it from 52.11 m^2/g to 24.49 m^2/g. Badgujar *et al.* and Pirozzi *et al.* reported 45% and 31% reduction in the surface area after immobilization of lipase on a support [30, 31]. Reduction of surface area by enzyme immobilization is also reported by other researchers [32, 33]. Accordingly, still 47% of the surface area is accessible for adsorbing and retaining micropollutants to provide enough time for degradation as further discussed in Section "reusability of nanobiocatalyst".

CBZ removal with the nanobiocatalyst

Effect of pH and temperature

The influence of pH on the degradation of CBZ was explored by adjusting the solution pH from 3 to 10. Figure 6.2.1 describes the fate of CBZ at different pH levels in pure water. Variation of the pH values can affect the removal of pharmaceuticals through

influencing the enzyme molecular structure. As shown in Figure 6.2.1, the removal of CBZ by covalently immobilized system was more efficient under the acidic condition compared to basic conditions. After desired incubation time, the CBZ removal at pH 4 was 91% (32% adsorption and 59% degradation). The removal rate was decreased to 17% (16% adsorption and 1% degradation) when the pH was increased to 10. The degradation of CBZ is more efficient at acidic conditions due to the higher laccase activity at acidic conditions or the inactivation of laccase at higher pH values. The result is in agreement with other studies which reported that in pH range of 4-7, immobilized laccase exhibited higher activity compared to pH > 8 [34-38]. Cantarella *et al.* also reported remarkable reduction in laccase activity when pH was over 7 [39]. Also, for other ligninolytic enzymes e.g. lignin peroxidase, inactivation of enzyme decreased the activity at pH values higher than 4.5 [40]. In fact, increasing or decreasing the pH beyond certain range decreases the stability and activity of the enzymes [41].

Removal of CBZ was investigated at different temperatures (5-50 °C). Figure 6.2.2 depicts the evolution of the CBZ removal at different temperatures (5-50 °C). The best removal of CBZ was 71.6% (20% adsorption and 51.6% degradation) and 81.5% (33.2% adsorption and 48.2% degradation) for 20 °C and 25 °C, respectively. Observing lower degradation efficiency at a lower temperature (20 °C) was due to the lower energy to meet the activation energy of the reaction. On the other hand, decreasing the efficiency at higher temperatures was due to inactivation of laccase [39]. Temperature plays an important role in the rate of enzymatic based biochemical reactions. However, above a certain value, the rate of these reactions experienced a decrease due to the denaturation of related enzymes [41].

Effect of CBZ concentration on the CBZ removal

Typical concentration of CBZ in the effluents of wastewater treatment plant from 1 µg/L to 46 µg/L [42], so that lowest concentrations was reported in Germany (1-7 µg/L) [43], Canada (up to 2.3 µg/L) and Austria (ca. 1.5 µg/L) [44]. The effect of the initial CBZ concentration on the removal of CBZ is of interest for the present investigations (Figure 6.2.3). In this study, the removal of CBZ reached 79-84% within 24 h for the initial concentration range of 1-3 µg/L. For a higher initial concentration of CBZ (40 µg/L and 50 µg/L) the removal was observed to be 74% to 72% within 24 h. With increasing initial concentration of CBZ, the removal tends to decrease. Similar behavior was

reported for oxidations of contaminants in aqueous systems [42]. Increasing the initial CBZ concentration potentially decreases the available FNBC surface for adsorption, and consequently decreases the removal efficiency. Moreover, at higher CBZ concentrations, the competitive reaction between laccase and intermediates or transformation products can decrease the degradation efficiency [5]. Luis Sotelo *et al.* reported that for lower concentrations of CBZ, the surface of the adsorbent is saturated after a long time whereas, for higher CBZ concentration, the saturation occurred in a shorter time [45]. Also, a higher surface coverage increases the activation energy and consequently making it more difficult for the remaining molecules to adsorb onto the surface and be degraded by enzyme [46].

Effect of contact time on the CBZ removal

The effect of contact time on the removal of CBZ (adsorption and degradation) by immobilized laccase onto FNBC is depicted in Figure 6.2.4 over a time period of 1-72 h. It can be seen that CBZ was adsorbed very fast at the early stage of reaction so that the removal of CBZ by adsorption was 90% and 30% after 3 h and 72 h, respectively. Hasan *et al.* also reported that the adsorption of pollutant was rapid at the initial stages of the contact time due to the presence of a huge number of available sites for adsorption and then it approached to an equilibrium [47]. According to our previous research work, after 3 h of contact time, the adsorbed amount of CBZ reaches its equilibrium value [48]. The reduction in the contribution of adsorption in total removal is due to the degradation of adsorbed CBZ by biocatalyst. On the contrary, as shown in Figure 6.2.4, the effect of degradation is not initially significant due to the slow nature of enzymatic reactions. However, removal of CBZ due to degradation increased over time and reached to a maximum of 63% after 24 h. Jelic *et al.* also reported that with increasing the reaction time, degradation was increased [49]. Degradation of CBZ at 48 h and 72 h were almost the same as 24 h, perhaps due to lower collision frequency or occupation of adsorption sites by transformation products. This observation suggests that, over the course of reactions, the adsorbed CBZ on FNBC was degraded by immobilized laccase over time. Therefore, it can be stated that contact time is the critical parameter for beginning the degradation.

Reusability of nanobiocatalyst

Immobilized enzymes are more interesting for commercial applications compared to free enzymes because they are easily recycled and can be used in continuous reaction processes. Therefore, characterization of the operational stability and reusability of the biocatalyst is important [17]. The efficiency of laccase-FNBC systems was evaluated over several consecutive cycles of CBZ removal and the results are illustrated in Figure 6.2.5. The results indicate that the removal efficiency decreased gradually with a number of cycles. This decrease in enzyme activity could be due to inactivation and loss of enzyme. Similar results from a number of research groups have been reported for other nanobiocatalysts [2, 50]. The removal of CBZ by nanobiocatalyst was decreased from 84% to 31% during 7 repeated cycles. It is reported that the co-adsorption of micropollutants and enzyme can enhance the interaction of micropollutants with active sites of enzyme and facilitate the degradation of micropollutants [26, 51]. Ji *et al.* covalently immobilized laccase on TiO_2 nanoparticles for CBZ removal. They reported that within 24 hours, 40% of CBZ was degraded by immobilized laccase and background adsorption of CBZ on TiO_2 was less than 2% [1].

Removal of CBZ in continuous mode

Continuous removal of CBZ was performed in four columns filled with laccase-FNBC biocatalyst and untreated nanobiochar (as control) and fed with Milli-Q water and secondary effluent for 48 h. At the beginning of the operation, around 65% and 73% of CBZ removal were achieved in columns fed by Milli-Q water and secondary effluent, respectively (Figure 6.2.6). The removal efficiency was decreased with fast rate for nanobiochar compared to laccase-FNBC due to saturation of nanobiochar free sites [52]. On the other hand, the column filled with immobilized laccase onto FNBC experienced steady removal of CBZ until 24 h, and then the removal efficiency started to decline. After 48 h of contact time, the removal efficiency was 25% and 45% for immobilized laccase in milli-Q water and secondary effluents, respectively. The higher CBZ degradation performance of biocatalyst in secondary effluent compared to Milli-W water can be attributed to the presence of ions in effluent (TDS = 414 ppm compared to TDS = 0 ppm for Milli-Q water) which is in favor of electron transfer in electrochemical reactions. Unlike for untreated nanobiochar, the removal of CBZ by the laccase-FNBC can occur in different stages: 1) extensive adsorption on free available sites FNBC and negligible degradation by laccase; 2) adsorption on

nanobiochar and degradation by laccase at equilibrium phase, and 3) declining degradation by immobilized laccase due to the dislodgement of enzyme from nanobiochar surface and denaturation [17, 53]. Similar results were reported by Cabana *et al.* who investigated the elimination of several pollutants such as nonylphenol and triclosan for five consecutive batch cycles in a packed-bed reactor by laccase covalently immobilized on diatomaceous earth [54].

The current study demonstrated the advantages of immobilized laccase onto FNBC over free enzyme including better stability of laccase and regeneration of FNBC through enzymatic degradation of adsorbed CBZ. In overall, simultaneous adsorption and laccase degradation prolonged the lifetime of the immobilized laccase onto FNBC column.

Conclusion

In the present study, crude laccase from *Trametes versicolor* was immobilized onto FNBC and employed for removal of CBZ in batch and continues modes. The effect of operational parameters for removal of CBZ was investigated in batch tests and the results showed that the highest removal can be obtained at pH 4, 20 °C, CBZ concentration of 5 µg/L and contact time of 24 h. A fixed-bed column packed with immobilized laccase onto FNBC was fed continuously with spiked pure water and secondary effluent of sewage treatment for two days. The results showed that adsorption played an important role at the beginning but biodegradation with enzyme remained as the major removal mechanism for CBZ. The removal efficiencies for CBZ in both pure water and secondary effluent dropped to 25% and 45% by the end of two days. In general, the nanobiochar in this work showed a significant potential to immobilize crude enzyme extracts for cost-effective practical applications.

Acknowledgments

References

1.   Ji, C., Hou, J., Wang, K., Zhang, Y., and Chen, V., Biocatalytic degradation of carbamazepine with immobilized laccase-mediator membrane hybrid reactor. Journal of Membrane Science, 2016. 502: p. 11-20.

2.   Liu, Y., Zeng, Z., Zeng, G., Tang, L., Pang, Y., Li, Z., Liu, C., Lei, X., Wu, M., Ren, P., Liu, Z., Chen, M., and Xie, G., Immobilization of laccase on magnetic bimodal mesoporous carbon and the application in the removal of phenolic compounds. Bioresource Technology, 2012. 115: p. 21-26.

3.   Tixier, C., Singer, H.P., Oellers, S., and Müller, S.R., Occurrence and fate of carbamazepine, clofibric acid, diclofenac, ibuprofen, ketoprofen, and naproxen in surface waters. Environmental science & technology, 2003. 37(6): p. 1061-1068.

4.   Kasprzyk-Hordern, B., Dinsdale, R.M., and Guwy, A.J., The removal of pharmaceuticals, personal care products, endocrine disruptors and illicit drugs during wastewater treatment and its impact on the quality of receiving waters. Water research, 2009. 43(2): p. 363-380.

5.   Im, J.K., Son, H.S., Kang, Y.M., and Zoh, K.D., Carbamazepine Degradation by Photolysis and Titanium Dioxide Photocatalysis. Water Environment Research, 2012. 84(7): p. 554-561.

6.   Lin, A.Y.C., Yu, T.H., and Lateef, S.K., Removal of pharmaceuticals in secondary wastewater treatment processes in Taiwan. Journal of hazardous materials, 2009. 167(1-3): p. 1163-1169.

7.   Jos, A., Repetto, G., Rios, J., Hazen, M., Molero, M., Del Peso, A., Salguero, M., Fernández-Freire, P., Pérez-Martín, J., and Cameán, A., Ecotoxicological evaluation of carbamazepine using six different model systems with eighteen endpoints. Toxicology in Vitro, 2003. 17(5-6): p. 525-532.

8.   Guo, L.Q., Lin, S.X., Zheng, X.B., Huang, Z.R., and Lin, J.F., Production, purification and characterization of a thermostable laccase from a tropical

white-rot fungus. World Journal of Microbiology and Biotechnology, 2011. 27(3): p. 731-735.

9.   Skoronski, E., Souza, D.H., Ely, C., Broilo, F., Fernandes, M., Fúrigo, A., and Ghislandi, M.G., Immobilization of laccase from Aspergillus oryzae on graphene nanosheets. International Journal of Biological Macromolecules, 2017. 99: p. 121-127.

10.   Whiteley, C.G. and Lee, D.J., Enzyme technology and biological remediation. Enzyme and Microbial Technology, 2006. 38(3): p. 291-316.

11.   Cristóvão, R.O., Silvério, S.C., Tavares, A.P.M., Brígida, A.I.S., Loureiro, J.M., Boaventura, R.A.R., Macedo, E.A., and Coelho, M.A.Z., Green coconut fiber: a novel carrier for the immobilization of commercial laccase by covalent attachment for textile dyes decolourization. World Journal of Microbiology and Biotechnology, 2012. 28(9): p. 2827-2838.

12.   Bornscheuer, U.T., Immobilizing Enzymes: How to Create More Suitable Biocatalysts. Angewandte Chemie International Edition, 2003. 42(29): p. 3336-3337.

13.   Kim, J., Grate, J.W., and Wang, P., Nanostructures for enzyme stabilization. Chemical Engineering Science, 2006. 61(3): p. 1017-1026.

14.   Tsang, S.C., Yu, C.H., Gao, X., and Tam, K., Silica-encapsulated nanomagnetic particle as a new recoverable biocatalyst carrier. The Journal of Physical Chemistry B, 2006. 110(34): p. 16914-16922.

15.   Giri, B., Goswami, M., and Singh, R., Review on Application of Agro-Waste Biomass Biochar for Adsorption and Bioremediation Dye. Chemosphere, 2017. 99: p. 19-33.

16.   Tan, X., Liu, Y., Zeng, G., Wang, X., Hu, X., Gu, Y., and Yang, Z., Application of biochar for the removal of pollutants from aqueous solutions. Chemosphere, 2015. 125: p. 70-85.

17.	Naghdi, M., Taheran, M., Brar, S.K., Kermanshahi-pour, A., Verma, M., and Surampalli, R.Y., Immobilized laccase on oxygen functionalized nanobiochars through mineral acids treatment for removal of carbamazepine. Science of The Total Environment, 2017. 584: p. 393-401.

18.	Kang, B.-S., Lee, K.H., Park, H.J., Park, Y.-K., and Kim, J.-S., Fast pyrolysis of radiata pine in a bench scale plant with a fluidized bed: Influence of a char separation system and reaction conditions on the production of bio-oil. Journal of Analytical and Applied Pyrolysis, 2006. 76(1-2): p. 32-37.

19.	Cea, M., Sangaletti, N., González, M.E., and Navia, R., Candida rugosa lipase immobilization on biochar derived from agricultural residues. 2nd International Workshop "Advances in Science and Technology of Natural Resources, 2010(Pucón-Chile).

20.	Naghdi, M., Taheran, M., Brar, S.K., Rouissi, T., Verma, M., Surampalli, R.Y., and Valero, J.R., A green method for production of nanobiochar by ball milling-optimization and characterization. Journal of Cleaner Production, 2017. 164: p. 1394-1405.

21.	Faramarzi, M.A. and Forootanfar, H., Biosynthesis and characterization of gold nanoparticles produced by laccase from Paraconiothyrium variabile. Colloids and Surfaces B: Biointerfaces, 2011. 87(1): p. 23-27.

22.	Mohapatra, D.P., Brar, S.K., Tyagi, R.D., Picard, P., and Surampalli, R.Y., Carbamazepine in municipal wastewater and wastewater sludge: Ultrafast quantification by laser diode thermal desorption-atmospheric pressure chemical ionization coupled with tandem mass spectrometry. Talanta, 2012. 99: p. 247-255.

23.	Jiang, K., Schadler, L.S., Siegel, R.W., Zhang, X., Zhang, H., and Terrones, M., Protein immobilization on carbon nanotubes via a two-step process of diimide-activated amidation. Journal of Materials Chemistry, 2004. 14(1): p. 37-39.

24. Wong, S.S., Joselevich, E., Woolley, A.T., Cheung, C.L., and Lieber, C.M., Covalently functionalized nanotubes as nanometre- sized probes in chemistry and biology. Nature, 1998. 394(6688): p. 52-55.

25. Gao, Y. and Kyratzis, I., Covalent Immobilization of Proteins on Carbon Nanotubes Using the Cross-Linker 1-Ethyl-3-(3-dimethylaminopropyl)carbodiimide-a Critical Assessment. Bioconjugate Chemistry, 2008. 19(10): p. 1945-1950.

26. Nguyen, L.N., Hai, F.I., Dosseto, A., Richardson, C., Price, W.E., and Nghiem, L.D., Continuous adsorption and biotransformation of micropollutants by granular activated carbon-bound laccase in a packed-bed enzyme reactor. Bioresource Technology, 2016. 210(Supplement C): p. 108-116.

27. Huang, W., Taylor, S., Fu, K., Lin, Y., Zhang, D., Hanks, T.W., Rao, A.M., and Sun, Y.-P., Attaching Proteins to Carbon Nanotubes via Diimide-Activated Amidation. Nano Letters, 2002. 2(4): p. 311-314.

28. Lee, Y.-M., Kwon, O.-Y., Yoon, Y.-J., and Ryu, K., Immobilization of Horseradish Peroxidase on Multi-Wall Carbon Nanotubes and its Electrochemical Properties. Biotechnology Letters, 2006. 28(1): p. 39-43.

29. Asuri, P., Karajanagi, S.S., Sellitto, E., Kim, D.-Y., Kane, R.S., and Dordick, J.S., Water-soluble carbon nanotube-enzyme conjugates as functional biocatalytic formulations. Biotechnology and Bioengineering, 2006. 95(5): p. 804-811.

30. Badgujar, K.C., Dhake, K.P., and Bhanage, B.M., Immobilization of Candida cylindracea lipase on poly lactic acid, polyvinyl alcohol and chitosan based ternary blend film: Characterization, activity, stability and its application for N-acylation reactions. Process Biochemistry, 2013. 48(9): p. 1335-1347.

31. Pirozzi, D., Fanelli, E., Aronne, A., Pernice, P., and Mingione, A., Lipase entrapment in a zirconia matrix: Sol-gel synthesis and catalytic properties. Journal of Molecular Catalysis B: Enzymatic, 2009. 59(1): p. 116-120.

32.	He, J., Song, Z., Ma, H., Yang, L., and Guo, C., Formation of a mesoporous bioreactor based on SBA-15 and porcine pancreatic lipase by chemical modification following the uptake of enzymes. Journal of Materials Chemistry, 2006. 16(44): p. 4307-4315.

33.	Yi, Y., Neufeld, R., and Kermasha, S., Controlling sol-gel properties enhancing entrapped membrane protein activity through doping additives. Journal of Sol-Gel Science and Technology, 2007. 43(2): p. 161-170.

34.	Jordaan, J., Mathye, S., Simpson, C., and Brady, D., Improved chemical and physical stability of laccase after spherezyme immobilisation. Enzyme and Microbial Technology, 2009. 45(6): p. 432-435.

35.	Jiang, D.S., Long, S.Y., Huang, J., Xiao, H.Y., and Zhou, J.Y., Immobilization of Pycnoporus sanguineus laccase on magnetic chitosan microspheres. Biochemical Engineering Journal, 2005. 25(1): p. 15-23.

36.	Lloret, L., Hollmann, F., Eibes, G., Feijoo, G., Moreira, M., and Lema, J., Immobilisation of laccase on Eupergit supports and its application for the removal of endocrine disrupting chemicals in a packed-bed reactor. Biodegradation, 2012. 23(3): p. 373-386.

37.	Garcia, H.A., Hoffman, C.M., Kinney, K.A., and Lawler, D.F., Laccase-catalyzed oxidation of oxybenzone in municipal wastewater primary effluent. Water Research, 2011. 45(5): p. 1921-1932.

38.	Huerta-Fontela, M., Galceran, M.T., and Ventura, F., Occurrence and removal of pharmaceuticals and hormones through drinking water treatment. Water Research, 2011. 45(3): p. 1432-1442.

39.	Cantarella, G., Galli, C., and Gentili, P., Free radical versus electron-transfer routes of oxidation of hydrocarbons by laccase/mediator systems: Catalytic or stoichiometric procedures. Journal of Molecular Catalysis B: Enzymatic, 2003. 22(3-4): p. 135-144.

40.   Zhang, Y. and Geißen, S.-U., In vitro degradation of carbamazepine and diclofenac by crude lignin peroxidase. Journal of Hazardous Materials, 2010. 176(1-3): p. 1089-1092.

41.   Bhattacharya, S.S. and Banerjee, R., Laccase mediated biodegradation of 2,4-dichlorophenol using response surface methodology. Chemosphere, 2008. 73(1): p. 81-85.

42.   Braeutigam, P., Franke, M., Schneider, R.J., Lehmann, A., Stolle, A., and Ondruschka, B., Degradation of carbamazepine in environmentally relevant concentrations in water by Hydrodynamic-Acoustic-Cavitation (HAC). Water Research, 2012. 46(7): p. 2469-2477.

43.   Ternes, T.A., Occurrence of drugs in German sewage treatment plants and rivers. Water research, 1998. 32(11): p. 3245-3260.

44.   Zhang, Y., Geißen, S.U., and Gal, C., Carbamazepine and diclofenac: Removal in wastewater treatment plants and occurrence in water bodies. Chemosphere, 2008. 73(8): p. 1151-1161.

45.   Sotelo, J.L., Ovejero, G., Rodríguez, A., Álvarez, S., and García, J., Adsorption of carbamazepine in fixed bed columns: Experimental and modeling studies. Separation Science and Technology, 2013. 48(17): p. 2626-2637.

46.   Andersson, K.I., Eriksson, M., and Norgren, M., Lignin removal by adsorption to fly ash in wastewater generated by mechanical pulping. Industrial & Engineering Chemistry Research, 2012. 51(8): p. 3444-3451.

47.   Hasan, Z., Jeon, J., and Jhung, S.H., Adsorptive removal of naproxen and clofibric acid from water using metal-organic frameworks. Journal of Hazardous Materials, 2012. 209-210: p. 151-157.

48.   Naghdi, M., Taheran, M., Pulicharla, R., Rouissi, T., Brar, S.K., Verma, M., and Surampalli, R.Y., Pine-wood derived nanobiochar for removal of carbamazepine from aqueous media: Adsorption behavior and influential parameters. Arabian Journal of Chemistry, 2017.

49.   Jelic, A., Cruz-Morató, C., Marco-Urrea, E., Sarrà, M., Perez, S., Vicent, T., Petrović, M., and Barcelo, D., Degradation of carbamazepine by Trametes versicolor in an air pulsed fluidized bed bioreactor and identification of intermediates. Water Research, 2012. 46(4): p. 955-964.

50.   Bayramoğlu, G., Yilmaz, M., and Yakup Arica, M., Reversible immobilization of laccase to poly(4-vinylpyridine) grafted and Cu(II) chelated magnetic beads: Biodegradation of reactive dyes. Bioresource Technology, 2010. 101(17): p. 6615-6621.

51.   Zille, A., Tzanov, T., Gübitz, G.M., and Cavaco-Paulo, A., Immobilized laccase for decolourization of Reactive Black 5 dyeing effluent. Biotechnology letters, 2003. 25(17): p. 1473-1477.

52.   Nguyen, L.N., Hai, F.I., Kang, J., Price, W.E., and Nghiem, L.D., Coupling granular activated carbon adsorption with membrane bioreactor treatment for trace organic contaminant removal: Breakthrough behaviour of persistent and hydrophilic compounds. Journal of Environmental Management, 2013. 119: p. 173-181.

53.   Russo, M.E., Giardina, P., Marzocchella, A., Salatino, P., and Sannia, G., Assessment of anthraquinone-dye conversion by free and immobilized crude laccase mixtures. Enzyme and Microbial Technology, 2008. 42(6): p. 521-530.

54.   Cabana, H., Alexandre, C., Agathos, S.N., and Jones, J.P., Immobilization of laccase from the white rot fungus Coriolopsis polyzona and use of the immobilized biocatalyst for the continuous elimination of endocrine disrupting chemicals. Bioresource Technology, 2009. 100(14): p. 3447-3458.
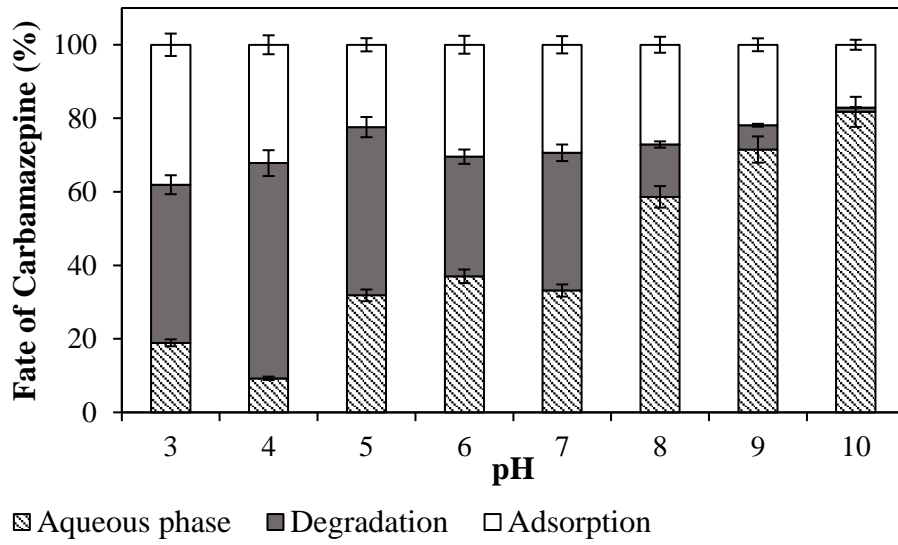
Figure 6.2.1 Effect of solution pH on the removal of carbamazepine within 24 h (C_o = 20 µg/L, T = 20 °C, laccase activity = 3.3 Units/g)
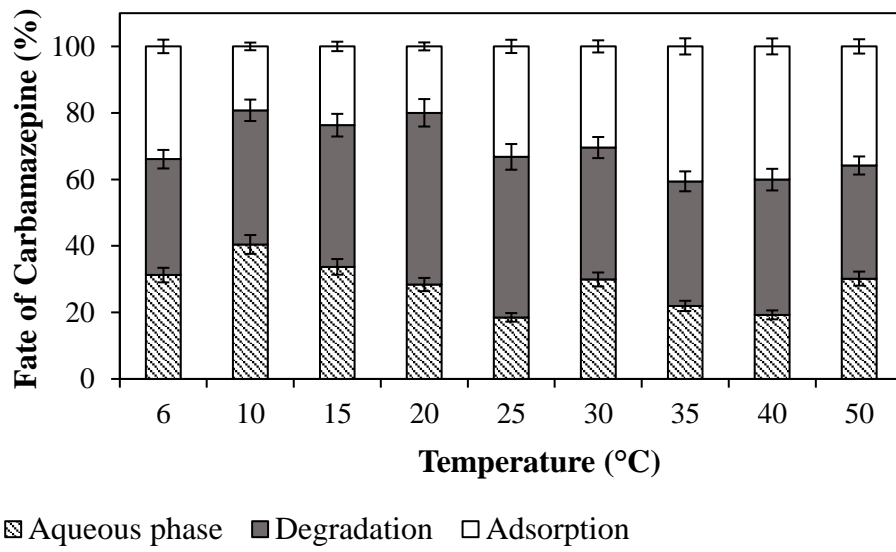
Figure 6.2.2 Effect of temperature on the removal of carbamazepine within 24 h (C_o = 20 µg/L, pH = 7, laccase activity = 3.3 Units/g)
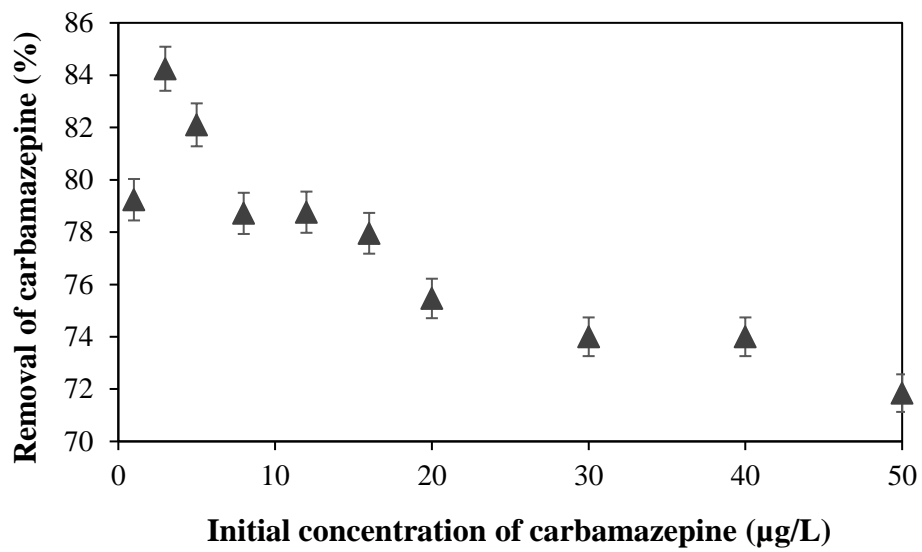
Figure 6.2.3 Effect of initial carbamazepine concentration on its removal within 24 h (T = 20 °C, pH = 7, laccase activity = 3.3 Units/g)

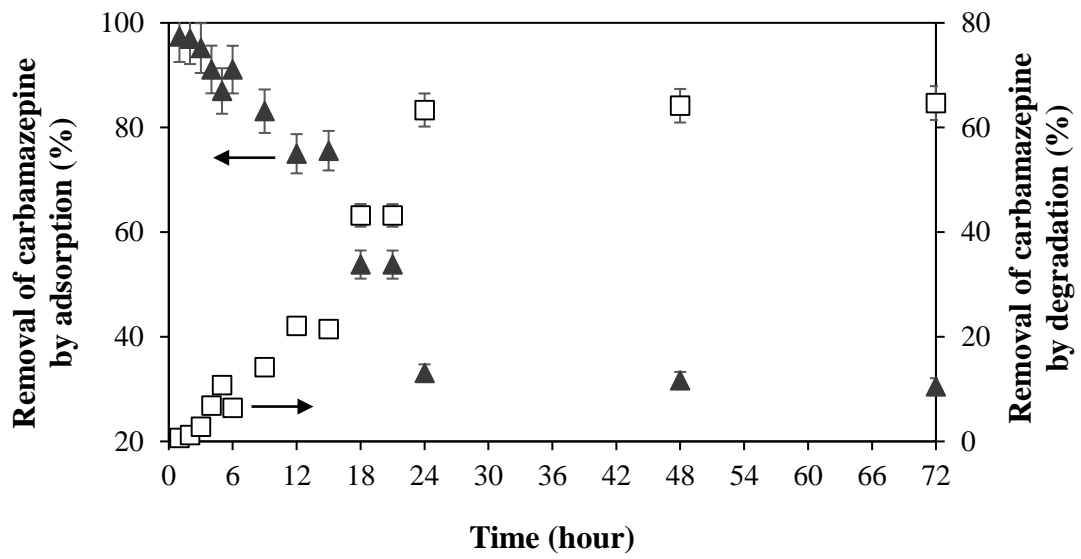**Figure 6.2.4 Effect of contact time on CBZ removal (C$_o$ = 20 µg/L, T = 20 °C, pH = 7, laccase activity = 3.3 Units/g)**

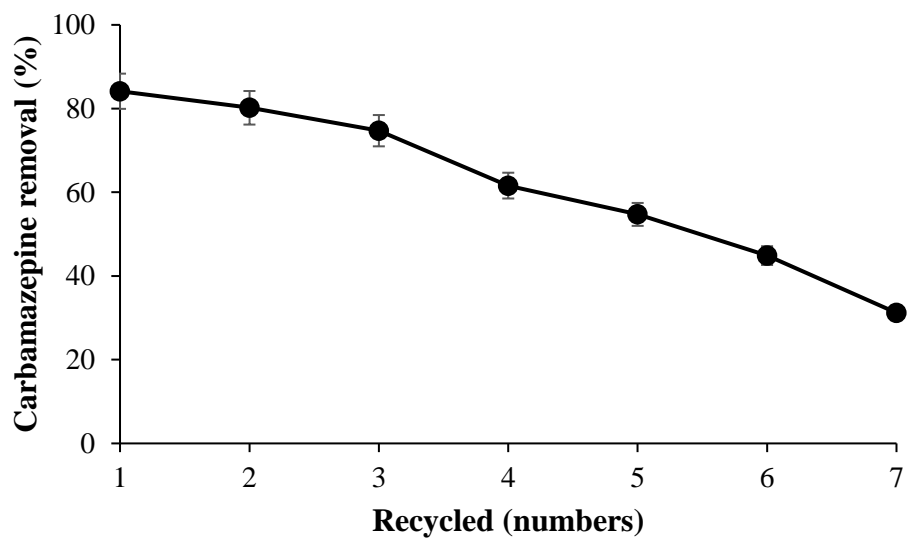**Figure 6.2.5 Operational stability of immobilized laccase for removal of carbamazepine (C$_0$ = 20 µg/L, pH = 7, T = 20 °C)**
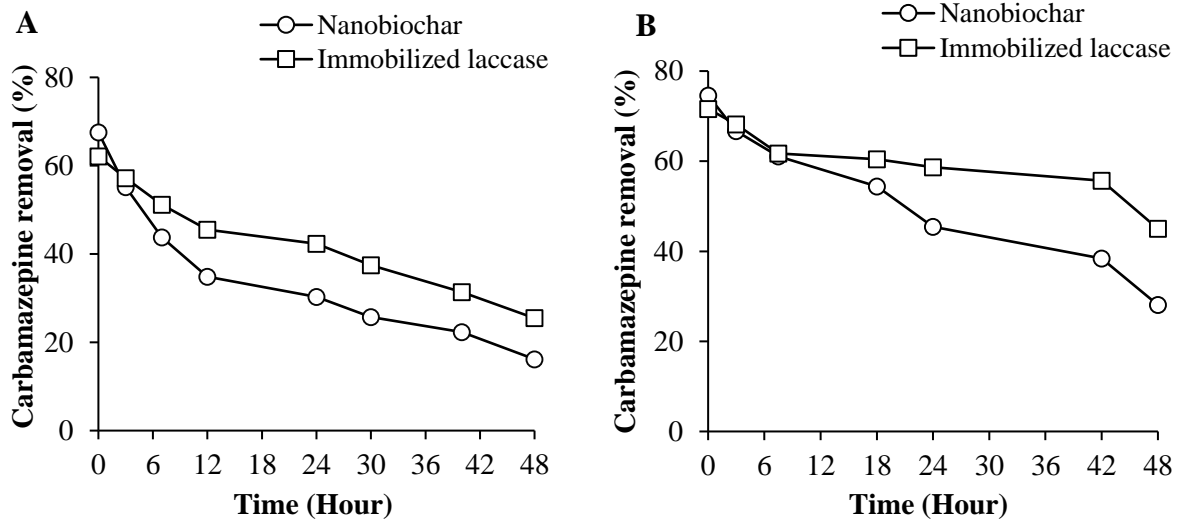
Figure 6.2.6 Removal efficiency of carbamazepine by continuous flow columns of nanobiochar and immobilization laccase onto functionalized nanobiochar for a) Milli-Q water and b) secondary effluent

CHAPITRE 7

Conclusions et Recommandations

Chapitre 7. Conclusions et Recommandations

Conclusions

Les conclusions suivantes peuvent être tirées du travail accompli:

1) Les conditions optimales pour obtenir les plus petites particules de biochar, environ 60 nm, se sont révélées être de 100 min, 575 rpm et 4,5 g/g. La surface spécifique a été portée de 3,12 m^2/g à 47,25 m^2/g. Le temps et la vitesse de rotation ont grandement contribué à la taille des particules pendant le broyage à billes. Les spectres de la spectroscopie infrarouge à transformée de Fourier (FTIR) des échantillons bruts de biochar et de nanobiochar étaient identiques en termes de modèle et d'intensité, indiquant que le *broyage à billes n'affectait pas la structure chimique du biochar.*

2) L'adsorption de la CBZ sur nanobiochar a suivi le modèle isotherme de Freundlich et le modèle cinétique de pseudo-deuxième ordre. L'efficacité d'élimination du biochar vis-à-vis de la CBZ peut être améliorée de 14% à 98% en réduisant la taille des particules de 3 mm à 60 nm, ce qui le rend compétitif avec le charbon actif commercial. *L'augmentation du pH de 3 à 8 a amélioré l'efficacité d'adsorption de 2,3 fois.*

3) La laccase libre peut dégrader la CBZ jusqu'à 30% en 24 heures de réaction et le transformer en produits moins nocifs. En utilisant ABTS, la laccase peut augmenter l'efficacité de dégradation à plus de 95%. La température, le pH et la concentration de la laccase sont les paramètres clés dans la dégradation enzymatique de la CBZ. *La 10,11-dihydro-10,11-dihydroxy-CBZ et la 10,11-dihydro-10,11-époxy-CBZ ont été identifiées comme les principaux métabolites de l'oxydation du CBZ par la laccase.*

4) La fonctionnalisation chimique de la surface du nanobiochar avec un mélange de H_2SO_4 et HNO_3 (50:50, v/v) a montré la meilleure performance à la surface du carbone par la formation de 4,7 mmol/g de groupes carboxyliques. Laccase physiquement immobilisée sur nanobiochar fonctionnalisé a montré une meilleure stabilité au stockage (45% après 10 jours) et réutilisabilité (60% après 5 cycles) par rapport à la laccase libre montrant son potentiel pour des applications continues. *L'utilisation de la laccase immobilisée en mode discontinu a montré une élimination de 83% et 86% de la CBZ dans l'eau pure enrichie et l'effluent secondaire, respectivement.*

5) L'activité de la laccase immobilisée dans la méthode covalente était de 5 U/g dans des conditions optimales, qui étaient de 14 mg/mL de concentration de laccase, 5 mg/mL de nanobiochar, 8,2 mM de réticulant et 3 h de temps de contact. *Laccase*

immobilisée par covalence sur nanobiochar fonctionnalisé a montré une stabilité au stockage élevée (50% après 60 jours) et réutilisabilité (53% après 3 cycles).

6) L'immobilisation covalente de la laccase sur du nanobiochar fonctionnalisé a montré 96% d'élimination de la CBZ. Les conditions optimales se sont avérées être pH 4, 20 °C, 5 µg/L de concentration de la CBZ et 24 h de temps de contact. La contribution de l'efficacité d'élimination pour la CBZ dans l'eau pure a été atteinte à 33% et 63% pour l'adsorption et la dégradation en 24 h, respectivement. L'élimination de la CBZ en mode continu a montré plus de 45% et 60% dans l'eau pure et l'effluent secondaire, respectivement, après 24 heures de réaction. Le taux d'élimination plus élevé dans l'effluent d'eaux usées peut être attribué à la présence de cofacteurs de laccase, c'est-à-dire de cuivre ou d'autres acides organiques qui peuvent jouer le rôle de médiateur pour l'enzyme. *De 84% à 31% de la CBZ ont été éliminés après un et sept cycles consécutifs.*

Recommandations

À partir des résultats obtenus, les recommandations suivantes peuvent être considérées:

1) La propriété d'interaction et d'adsorption de toutes les classes de contaminants émergents sur le nanobiochar devrait être étudiée.

2) En raison de la résistance de certains composés pharmaceutiquement actifs, il est nécessaire de développer un nouveau traitement tertiaire pour traiter les effluents d'eaux usées avant de les relâcher dans l'environnement.

3) Les biochars provenant d'autres sources telles que la paille de blé, la paille de maïs, la coquille d'arachide, le bois et la balle de riz doivent être étudiés afin de fournir une charge enzymatique plus élevée pouvant réduire l'empreinte et améliorer l'efficacité du retrait.

4) Le nanobiocatalyseur produit peut également être étudié pour l'assainissement des sols contaminés.

5) Différentes méthodes de fonctionnalisation, telles que l'utilisation de l'oxygène atmosphérique peuvent être étudiées pour créer des groupes carboxyliques sur la surface du biochar.

Chapitre 7. Conclusions et Recommandations

6) L'effet de différents médiateurs tels que la syringaldazine et le 1-hydroxybenzotriazole, le 2,2,6,6-tétraméthylpipéridinyloxyle et autres doit être étudié afin d'améliorer l'efficacité de l'élimination.

7) Des recherches supplémentaires sont nécessaires sur les méthodes combinées / hybrides pour améliorer leur efficacité par leurs effets synergiques et les rendre écologiquement et économiquement viables. La combinaison du système enzyme-nanobiochar avec des processus d'oxydation avancés tels que l'ultrasonication peut être un système potentiel.
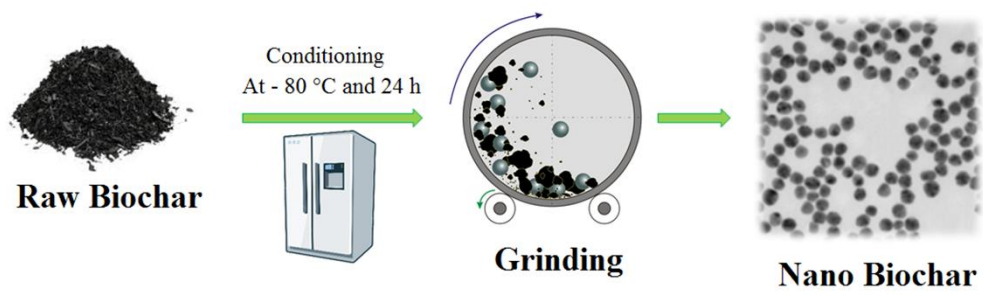
ANNEXES

ANNEXE I

CHAPTER 1 PART 3

Data 1: Production of nanobiochar through ball milling and effect of cryogenic temperature

ANNEXE II

CHAPTER 1 PART 3

Data: Calculation of energy consumption

1. Planetary Ball Mill

Planetary ball mill is a high-energy mill used for energy-intensive processes like the chemo-mechanical process and mechanical alloying. As shown in Figure 1, the grinding jars which rotate around axis X_2 with a rotation speed W_J, are mounted on a disk which revolves around axis X_1 with a revolution speed W_ρ. The rotation direction of the revolving disk is counteractive to jars in order to generate higher impact energy for balls [1]. Unlike traditional ball mills, each ball in the jars is not just subjected to the gravitational force and additional coriolis and centrifugal force lead to increase the kinetic energy of the components up to 100 times the gravitational force [2]. Therefore, materials in the mill are effectively and quickly comminuted by frictional, impact and shear forces from ball-to-ball and ball-to wall collisions.
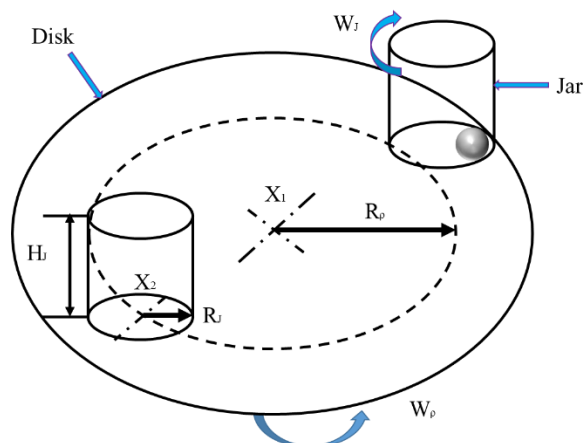

Figure 1: Schematic of the planetary disk with movement in a counter direction of jars in which W_ρ and R_ρ are revolution speed and radius, W_J and R_J are rotation speed and radius, H_J: jar height.

Processing variables of ball milling are divided into three groups:

The milling machine:

Kinetic factor (W_J/W_ρ), geometrical factor (R_ρ/R_J), jar diameter (D_J), jar height (H_J)

Operation:

milling time (t), Milling speed (W_ρ), milling frequency (f), ball type (ρ_b), ball size (d_b), the number of balls (N_b), the filling ratio (n_J), Ball-to-powder mass ratio (BPR)

Others:

Process control agent, milling atmosphere, temperature

Rojac *et al.* used nine parameters to find a relation for milling energy in a planetary ball mill (Figure 2). They established a mathematical model to correlate the milling parameters with the ball-impact energy

and frequencies of ball-to-ball and ball-to-wall collisions and thereby the relation of processing variables and the milling energy can be calculated [3].
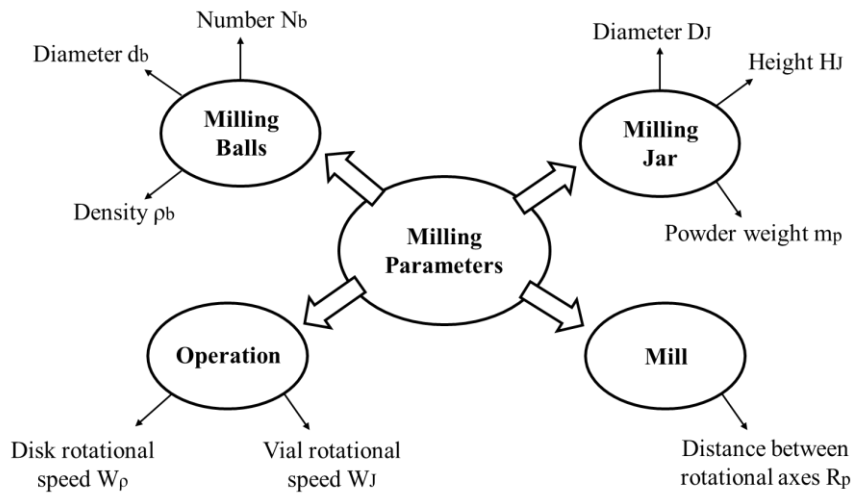

Figure 2: Parameters of a planetary ball mill

The particle is ground when two balls collide and/or a ball collides against the jar wall. The Equation for calculating the absolute velocity of the ball is:

$$v_b = \left[(W_\rho R_\rho)^2 + W_J^2 \left(R_J - {d_b}/{2} \right)^2 \left(1 - 2 {W_J}/{W_\rho} \right) \right]^{1/2} \tag{1}$$

According to this equation, kinetic factor (W_J/W_ρ) and geometrical factor (R_ρ/R_J) are the significant contributors to the absolute velocity. For a certain ball mill with given geometry, the absolute velocity of a ball impacting the jar wall:

$$v_b = K_b W_\rho R_\rho \tag{2}$$

K_b is a geometrical coefficient which depends on the geometry of the mill. For a planetary ball mill, K_b is ~ 0.90 for a ball with a diameter of 10 mm and ~ 1.06 for a point ball. Due to the simplicity of the Equation (2), it is usually employed for calculation of the kinetic energy in ball milling. The kinetic energy of a non-rotating ball is ½ mv². So the kinetic energy in the collision is then given by:

$$\Delta E = (1/2) K_a m_b v_b^2 \tag{3}$$

Where m_b is the ball mass and K_a describes the collision property. K_a varies from zero for perfect elastic (no energy transfer) to 1 for perfect inelastic collisions. If the balls are covered with a layer of powder, the collisions are almost inelastic, so that K_a is considered 1. Even in the early stages of milling, the portion of transferred kinetic energy to the powder is practically equal to the total energy of the collision. The transferred energy to the powder per ball in a collision event is given by:

$$\Delta E = K_c m_b W_\rho^2 R_\rho^2 \; [joule/hit] \tag{4}$$

Where R_ρ [m], W_ρ [rpm = 2π/60 rads/sec.], m_b [kg] and $K_c = (1/2) K_a K_b^2$
This equation shows that because the disk radius (R_ρ) is fixed for a certain milling machine, the transferred energy to the powder depends on the mass of the ball and the rotation speed of the mill.

Annexes

The described analysis of the collision let us assume that in a real milling process, as long as the collision is considered to be inelastic, the Equation (4) represent the given energy to the powder. Equation (4) should be modified in order to consider the degree of filling of the jar, by inserting a yield coefficient ϕ_b < 1 that relates the energy dissipated (ΔE_b^*) by one ball in a system with N_b ball:

$$\Delta E_b^* = \emptyset_b \Delta E_b \qquad (5)$$

The ϕ_b should be defined by accurate mathematical modeling or by experimental measurements. ϕ_b can be expressed as a function of a parameter n_J:

$$\emptyset_b = \left(1 - n_J^\varepsilon\right)$$

The details were described in [4], ϕ_b is almost 1 for 1/3 filling of the jar and ε depends on the ball diameter. The degree of filling, n_J, defined as $n_J = N_b/N_{b, max}$. Where $N_{b, max}$ is the required number of balls to fill the jar completely so that no movement is possible.

1.1. Power consumption

The transferred energy to the powder during a single collision is determined by Equation (4). By multiplying this energy by the collision frequency, we determine the power absorption. For a single ball, the collision frequency, f, can be determined as follows [4].

$$f = \frac{K\left(W_\rho - W_J\right)}{2\pi} = \frac{K\,W_\rho\left(1 - {W_J}\big/{W_\rho}\right)}{2\pi} = Kk W_\rho = K_J W_\rho \qquad (6)$$

The value of K depends on the ball diameter. In the experiments low level of jar filling, the reciprocal hindering of the balls is negligible and therefore the total collision frequency f_t is given by:

$f_t = f\,N_b$

The power consumption is calculated by:

$Pcal = \Delta E\,f_t$

$$P_{cal} = \left(\frac{1}{2}\right) P^* m_b W_\rho^3 R_\rho^2 N_b, [W] \qquad (7)$$

With P^* includes $K_a\,K_b\,K_J$. In the case that K_a, K_b and K_J are not available, P^* can also be obtained from Fig. 9 in Ref. [5].

If the jar was filled at a high level, the hindering coefficient of the N_b balls, ϕ_b, need to be considered:

$Pcal = \phi_b\,\Delta E\,f_t$

However, in this research work, we did not consider it since the jar was not filled at a high level. Equation (7) gives the power consumption during milling according to the collision model.

1.2. Energy consumption

To obtain the energy required for the production of 1 gram powder, the following equation is used:

$$E_{cal} = \frac{P_{cal} \times t}{1000 \times m_s}, [KJ/g] \qquad (8)$$

In which, t is the grinding time (s) and m_s is the mass of sample (g). In Table 1, the values of different parameters and the result of a calculation based on Equation 7 and Equation 8 are listed.

Annexes

Table 1: summary of parameters value and calculation

Parameters	Value
P^*	1.12^*
m_b	0.056 g
W_ρ	60.2 Rad/s
R_ρ	0.148 m
N_b	800
P_{cal}	118.3 Wat
m_s	10 g
t	6000 s
E_{cal}	71 KJ (for 1 g)
*Obtained from Fig.9 in [5]	

2. Freezer

We required calculating the energy for reduction of the temperature from 25 °C to -80 °C (W_1) and the energy for keeping the sample at this temperature for 24 hours (W_2). The total energy is calculated by:

$$W = W_1 + W_2 \ (KJ) \qquad\qquad (9)$$

For W_1, we used the basic rules of classic physic for calculation and for W_2, it was assumed that the whole freezer was filled with biochar and the average energy consumption reported by the manufacturer was divided by the mass of biochar to obtain the required energy for keeping the sample at -80 °C for 24 h.

2.1 Calculation of W_1

Heat capacity is defined as the amount of energy needed to increase one unit of mass (Kg or lb) one unit in temperature (K or °F). The heat capacity of wood depends on the temperature and moisture content of the wood but is practically independent of density or species. The heat capacity of dry wood C_p (KJ/Kg K) is approximately related to temperature T (K) [6].

$$C_p = 0.1031 + 0.003867\,T \qquad\qquad (10)$$

$$dQ = m \times C_p \times dT \qquad\qquad (11)$$

$$Q_C = m \int_{T_1}^{T_2} (0.1031 + 0.003867\,T)dT \qquad (12)$$

The coefficient of performance (COP) relates the work load (W_1) of the freezer to the heat (Q_C) to be removed.

$$COP = \frac{Q_C}{W_1} \qquad\qquad (13)$$

COP is between 0.5 to 1.5 depending on the cooling fluid, compressor efficiency, etc. Here we assumed the average value for it (COP = 1). Therefore, W1 can be calculated using equations 10 to 13.

2.1 Calculation of W_2

In this research study, Thermo Scientific™ Forma™ 900 Series -86°C Upright Ultra-Low Temperature Freezers was used. The average energy consumption of this freezer is 17 KWh/day and its capacity is 79 kg. Therefore, the energy consumption to maintain the temperature of 1 g sample for 24 hours can be obtained by dividing the average energy consumption of freezer per day by the freezer capacity. In

Annexes

Table 2, the values of different parameters and the result of a calculation based on Equation 10 and Equation 14 are listed.

Table 2: summary of parameters value and calculation

Parameters	Value
T_1	25 °C
T_2	-80 °C
Capacity of freezer*	79 Kg
Qc	0.1319 KJ (for 1 g)
W_1	0.1319 KJ (for 1 g)
W_2	0.7746 KJ (for 1 g)
W	0.9065 KJ
*Provided by manufacture	

2. Sonication

In this research work, Vibra-Cell VCX-130 Ultrasonic Processor (Sonics & Materials, USA) was used to disaggregate the particles. The nominal power of this instrument was 130 W and it was used at 30% of its intensity. Therefore the energy used for this instrument can be obtained from the following equation:

$$E_s = \frac{P_n \times t \times I}{1000 \times m_{max}} \qquad (14)$$

In which, E_s is required energy for sonication (KJ/g), P_n is the nominal power (W), t is the working time (s), I is intensity and m_{max} is the maximum mass of powder (g) that can be dispersed in the working volume. In Table 3, the values of different parameters and the result of a calculation based on Equation 14 are listed.

Table 3: Summary of parameters value and calculation

Parameters	Value
P_n*	130 W
t	3600 s
I	0.3
m_{max}	1.1 g
E_s	127 KJ (for 1 g)
*Provided by manufacture	

Reference

1. Watanabe, R., H. Hashimoto, and G.G. Lee, *Computer simulation of milling ball motion in mechanical alloying (overview).* Materials Transactions, JIM, 1995. **36**(2): p. 102-109.

2. Khoa, H.X., et al., *Planetary Ball Mill Process in Aspect of Milling Energy.* Journal of Korean Powder Metallurgy Institute, 2014. **21**(2): p. 155-164.

3. Rojac, T., et al., *The application of a milling map in the mechanochemical synthesis of ceramic oxides.* Journal of the European Ceramic society, 2006. **26**(16): p. 3711-3716.

4. Burgio, N., et al., *Mechanical alloying of the Fe− Zr system. Correlation between input energy and end products.* Il nuovo cimento D, 1991. **13**(4): p. 459-476.
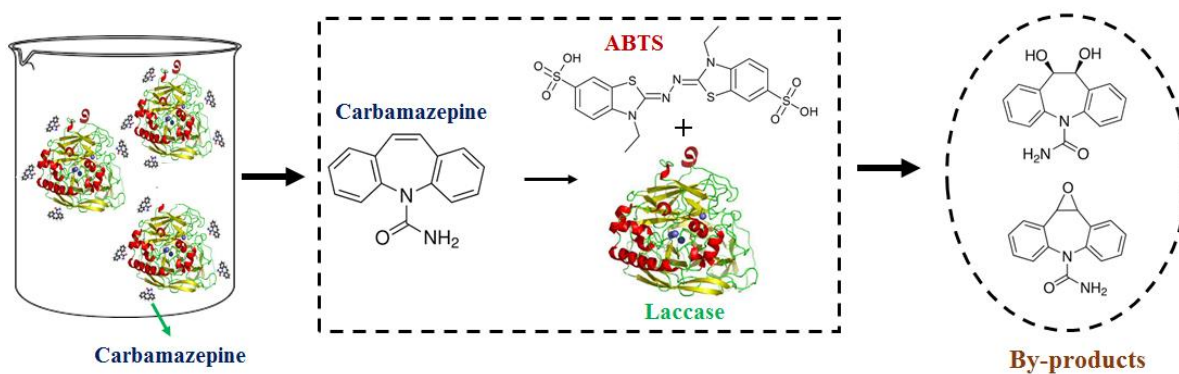
Annexes

5.   Magini, M., et al., *Power measurements during mechanical milling—II. The case of "single path cumulative" solid state reaction.* Acta materialia, 1998. **46**(8): p. 2841-2850.

6.   Matsuda, K., et al., *Advanced energy saving and its applications in industry*. 2012: Springer Science & Business Media.
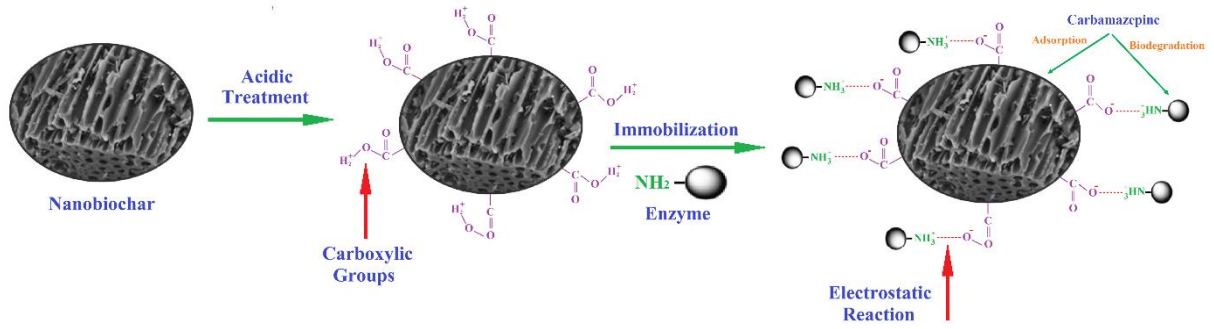
ANNEXE III

CHAPTER 4 PART 2

Data: Interaction of carbamazepine, laccase and mediator

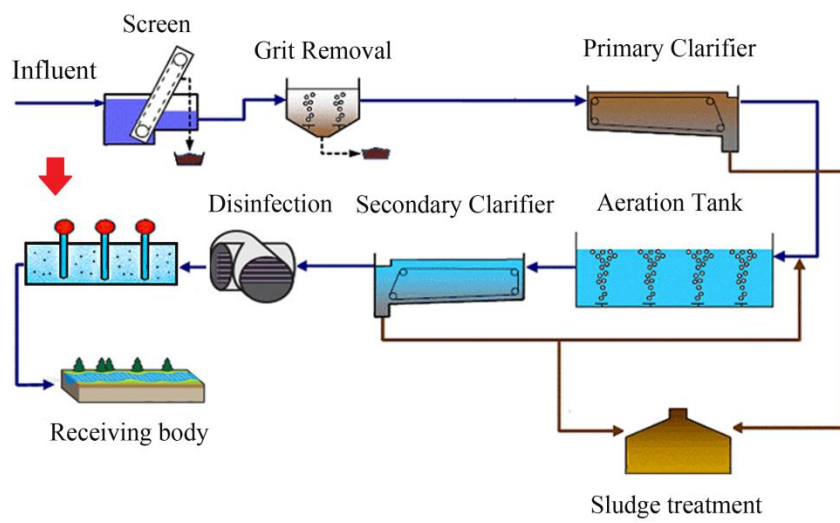# ANNEXES IV

CHAPTER 6 PART 1

Data: Surface modification of nanobiochar and interaction with enzyme

ANNEXES V

CHAPTER 6 PART 2

Data: Proposed stage for incorporation of BENS B

ANNEXES VI

Conclusion

Data: Approximate cost calculation for biochar enzyme impregnated nanosystems (BENS)

Approximate cost-estimation has been carried out per kilogram of immobilized laccase onto functionalized nanobiochar. Operational expenses (OPEX) are not presented here since pilot scale study data is not available until now.

I: Cost Calculations for BENS Production

1) Laccase production

Apple pomace is used as a substrate for fermentation using white-rot fungi. After fermentation, the biomass is mixed with buffer (1:20 ratio, substrate: buffer), centrifuged and the supernatant is separated. Then the crude laccase is subjected to concentration through ultrafiltration process to reduce the volume to 5%.

Apple pomace costs about $100/ton and it can produce 50×10^6 IU (International unit) of laccase.

Potato dextrose agar (PDA) can be considered as the standard media for fungal production (*Trametes versicolor*), which costs about $1000/ton for bulk purchase (Alibaba.com). For the production of 1 L of laccase extract, we need 5 Petri dishes of fungi (consist of 20 mL of media with a concentration of 39 g/L). Therefore, the cost of PDA for production of 1 L laccase will be $0.39.

Other expenses related to laccase production including energy, chemicals, sterilization, incubation, centrifugation, maintenance, analysis, and labor can be approximately calculated to be **$400** and therefore the total cost will be **$500** for production laccase (50×10^6 IU). For enzyme concentration, through ultrafiltration, we need around **$100** per 1 ton of the apple pomace.

As a result, per one ton of apple pomace, we will have 1000 L of a crude extract containing 50000 IU/L of laccase at the cost of $600. In other words, 1 L of concentrated enzyme costs **$0.6**.

Per kilogram of biochar, 5 L concentrated laccase is required. The Cost per 5 L of laccase will be $3.

2) Production of functionalized nanobiochar

Commercially biochar can be procured for $0.50-$2.5/Kg (from international biochar initiative website) in Canada. For this study, $1.5 has been used. The cost of converting raw biochar to nanobiochar will be $2. Pretreatment with acids will be $0.6/Kg (25 L of 98% sulfuric acid and 10 L of 70% nitric acid from Alibaba.com). Other laboratory related expenses are estimated to be $0.5/Kg. The total cost will be $4.6 per Kg of biochar.

3) Immobilization of laccase onto functionalized nanobiochar

2-(N-Morpholino) ethanesulfonic acid (MES, 50 mM), N-hydroxysuccinimide (NHS, 400 mM) and N-ethyl-N'-(3-dimethylaminopropyl) carbodiimide hydrochloride (EDC, 20 mM) were used for the immobilization of laccase onto functionalized nanobiochar.

Annexes

MES, NHS and EDC cost is about $1 per 1 Kg of each product. For immobilization of laccase onto 1 Kg of functionalized nanobiochar, 6 Kg, 9 Kg and 1 Kg of MES, NHS and EDC are required. Therefore, per Kg of functionalized nanobiochar is $16. Considering energy and labor the cost will be around $1. The total cost of immobilization will be $17.

The total expenses for 1 Kg of immobilization of laccase onto functionalized nanobiochar will be the summation of items 1, 2 and 3 which is equal to $24.6 (3+4.6+17).

II. Removal efficiencies

Basis:

Removal of Carbamazepine (CBZ) from wastewater at 20 µg/L concentration with 1 g of laccase immobilized biochar.

The efficiency of nano biocatalyst for removal of CBZ

Cycle No	Removal (µg CBZ)
1	367
2	343
3	294
4	221
5	213
6	95
7	55
Total	**1588**

Note 1: Per 1 g of immobilized laccase on functionalized nanobiochar

Note 2: One cycle lasts for 24 hours and therefore 7 cycles take 7 days

Note 3: Total removal is 1588 µg of CBZ by 1 g of immobilized laccase on functionalized nanobiochar Therefore, considering CBZ concentration of 20 µg/L; 1 g of immobilized laccase on functionalized nanobiochar can treat 1588/20 = 79.4 L of effluent of wastewater treatment plant (WWTP) in seven days. 1 Kg of immobilized laccase on functionalized nanobiochar can treat 79.4 × 1000 = 79,400 L of wastewater.

Therefore the cost per 1 m^3 of WWTP effluent with 1 Kg of immobilized laccase on functionalized nanobiochar will be 24.6/79.4 = $0.31

III. Remarks

- Excluding the operational costs, the produced nanobiocatalyst approximately costs $0.31 for the treatment of 1 m^3 of WWTP effluent.
- This system will be an **add-on process to the conventional treatment scheme**.
- For the production of this biocatalyst, two waste materials including apple pomace and biochar are valorized.
- This nanosystem will be promising as a green option for the treatment of pharmaceutical residues.

Annexes

- Moreover, even after the application for the treatment of CBZ, used laccase-immobilized biochar can be used as a fertilizer on the agricultural lands and which further expands the application potential of BENS.
- The cost of wastewater treatment is up to $1.13/m^3 ($ 0.7 /m^3 in Quebec) based on energy cost, requirements and treatment efficiency. Therefore using BENS system as a complementary system in WWTPs will increase the cost of operation by 40% but increase the quality of effluent.